



UNIVERSITY OF  
BIRMINGHAM

Investigating a Novel Role for the IL-36 / IL-36R Pathway in Mediating Inflammation in the Adult and Aged Murine Heart after Ischaemia-Reperfusion Injury

By

Juma El-Awaisi

A thesis submitted to the University of Birmingham for the degree of  
DOCTOR OF PHILOSOPHY

Institute of Cardiovascular Sciences  
College of Medical and Dental Sciences  
University of Birmingham

June 2022

# UNIVERSITY OF BIRMINGHAM

**University of Birmingham Research Archive**

**e-theses repository**

This unpublished thesis/dissertation is copyright of the author and/or third parties. The intellectual property rights of the author or third parties in respect of this work are as defined by The Copyright Designs and Patents Act 1988 or as modified by any successor legislation.

Any use made of information contained in this thesis/dissertation must be in accordance with that legislation and must be properly acknowledged. Further distribution or reproduction in any format is prohibited without the permission of the copyright holder.

## Abstract

**Introduction:** Whilst blood flow restoration is critical following myocardial infarction (MI), ischaemia-reperfusion injury (IRI) accounts for ~50% of the final infarct size. The newly discovered cytokine, interleukin-36 (IL-36), could potentially mediate these disturbances. However, its role in myocardial IRI is not known. Although several anti-inflammatory therapies have been successful in pre-clinical models of MI, they have failed in the clinical setting. This translational failure may be linked to a lack of inclusion of comorbidities and/or risk factors, as well as an early benefit at the level of the coronary microcirculation. We firstly investigated if IL-36 cytokines and its receptor (IL-36R) were present in the heart, and whether their expression varied in an injury-, age-, and sex-related manner. We then determined whether coronary microcirculatory disturbances and infarct size post-IRI were modified by age and sex, and whether IL-36Ra could confer vasculoprotection.

**Methods:** Myocardial IRI was induced in adult (3-months) and aged (>18-months) female mice, with sex differences assessed in adult male and female mice. Myocardial IL-36R/ $\alpha/\beta$ , VCAM-1 expression, and oxidative stress were investigated by immunostaining, flow cytometry, and/or using Western blot. Expression on human heart tissue samples of varying ages was also determined. IL-36R/ $\alpha/\beta$  expression was also determined on stimulated vena cava endothelial cells (VCECs). The beating heart coronary microcirculation was imaged *in vivo* intravitaly for neutrophils, platelets, and functional capillary density, and also *ex vivo* using multiphoton microscopy. Laser speckle contrast imaging was used to determine overall left ventricular perfusion. The effects of topical IL-36 cytokine application was also observed intravitaly. In some studies, recombinant mouse IL-36Ra (15 $\mu$ g/mouse) was injected intra-arterially at 5 minutes pre-reperfusion and 60 minutes post-reperfusion. Infarct size was measured using dual TTC/Evans Blue staining.

**Results:** Expression of IL-36 cytokine and its receptor was predominantly on the vasculature and cardiomyocytes of both the murine and human hearts, and their expression increased with age and injury. Expression was significantly higher in healthy and injured adult female hearts compared to male hearts. Basal VCEC surface expression of IL-36R increased after cytokine stimulation in a concentration-dependent manner. Intravital imaging of the beating heart demonstrated heightened basal and injury-induced neutrophil recruitment and poorer blood flow in the aged coronary microcirculation when compared with adult hearts. These events were mirrored in deeper myocardial layers when imaged using multiphoton microscopy. A greater burden of thrombotic disease was noted in adult injured male coronary microvessels, whilst a greater neutrophil presence was identified in adult injured female coronary microvessels. Infarct size was significantly larger in injured adult female hearts when compared to males. All IL-36 cytokines were able to induce an inflammatory response when topically applied to the adult and aged hearts. An IL-36R antagonist (IL-36Ra) decreased neutrophil recruitment, improved blood flow and ventricular perfusion, and reduced infarct size in both adult and aged mice. This may be mechanistically explained by attenuated endothelial oxidative damage and VCAM-1 expression in IL-36Ra-treated mice.

**Conclusion:** These novel results are the first to demonstrate myocardial presence of IL-36 and its receptor and how expression changes with age and sex. Our findings of enhanced coronary microcirculatory perturbations associated with age may explain the poorer outcomes in elderly MI patients. The cellular nature of the thromboinflammatory response may explain the sex-related differences in outcomes after MI. Importantly, we are the first to demonstrate that targeting IL-36/IL-36R pathway may be a potential novel therapy for treatment of myocardial IRI.

*“God loves someone who when works, he performs it in a perfect manner (itqan).”*

Prophet of God

*“Everything is theoretically impossible, until it is done.”*

Robert A. Heinlein.

*“What you learn from a life in science is the vastness of our ignorance.”*

David Eagleman

## Acknowledgments

First and foremost, I would like to praise God the Almighty, the Most Gracious, and the Most Merciful for giving me the blessing, strength, and endurance to complete this study.

I owe a great deal of appreciation to a number of people for their support and encouragement during my PhD. Firstly, my heartfelt gratitude goes to Dr. Neena Kalia, without whom none of this would have been possible. I honestly could not have asked for a better supervisor. You have truly made this a once in a lifetime ecstatic experience, and I feel honoured to have been supervised by you. I must also extend this to Dr. Dean Kavanagh, whose continued support and advice have proven to be invaluable. Your ability to turn anything around is phenomenal and just one of a kind. Thank you also to Mr. Nigel Drury, whose feedback and support was immensely helpful throughout. I'd also want to express my gratitude to the British Heart Foundation for supporting this research.

To everyone else I met on this journey, whether office friends, fellow PhD students or institute colleagues, a BIG thank you. You have all made this a journey to remember in your own unique, beautiful way. Honestly, I had a great time with you all through every high and low. I wish you all the best in your future. A HUGE thank you to all my friends for your encouragement and support throughout and for keeping me sane. My deepest gratitude must go to Pan for his continued support and encouragement.

Ultimately, my deepest gratitude must go to my mother and father for their unconditional support and loving kindness. For them, this thesis is dedicated. I wish to extend this gratitude to my siblings, nieces, nephews, and the rest of my family. Throughout everything, you have supported me and kept me going, I owe you all so much.

## Publications arising from this Thesis

### Papers:

**El-awaisi J**, Kavanagh D, Rink M, Weston C, Drury N, Kalia N (2022) Targeting IL-36 improves age-related coronary microcirculatory dysfunction and attenuates myocardial ischaemia-reperfusion injury in mice. Journal of Clinical Investigation Insight: doi.org/10.1172/jci.insight.155236

**El-awaisi J**, Kavanagh D, Kalia (2021) Intravital investigations of the role of IL-36 in mediating age and gender specific changes in the injured beating coronary microcirculation. Heart 2021;107:A162. (Published Conference Proceedings)

### Oral Presentations:

Mechanisms of Inflammation – October 2019 - **El-Awaisi J**, Kavanagh D, Rink M, Weston C, Drury N, Kalia N. Investigating A Novel Role For The IL-36 / IL-36R Pathway In Mediating Inflammation In The Adult And Aged Murine Heart After Ischaemia-Reperfusion Injury.

British Microcirculation Society Conference – June 2020 – Best communication winner. **El-Awaisi J**, Kavanagh D, Rink M, Weston C, Drury N, Kalia N. Investigating A Novel Role For The IL-36 / IL-36R Pathway In Mediating Inflammation In The Adult And Aged Murine Heart After Ischaemia-Reperfusion Injury.

British Microcirculation and Vascular Biology Conference – April 2021 - Best communication winner. **El-Awaisi J**, Kavanagh D, Rink M, Weston C, Drury N, Kalia N. Intravital investigations of the role of IL-36 in mediating age and gender specific changes in the injured beating heart coronary microcirculation.

European Society for Microcirculation – May 2021 - Best communication winner. **El-Awaisi J**, Kavanagh DPJ, Rink M, Weston C, Drury N, Kalia N. Intravital investigations of the role of IL-36 in mediating age and gender specific changes in the injured beating heart coronary microcirculation.

Neutrophil 2021 International Conference – May/June 2021 – Plenary session. **El-Awaisi J**, Kavanagh DPJ, Kalia N. Age, and gender specific changes in the neutrophil response to myocardial Infarction – intravital investigations in the injured beating coronary microcirculation.

British Society for Cardiovascular Research (BAS/BSCR at BCS) – June 2021 - Finalist in the 4 Best-of-the-Best oral communications. **El-Awaisi J**, Kavanagh D, Rink M, Weston C, Drury N, Kalia N. Intravital investigations of the role of IL-36 in mediating age and gender specific changes in the injured beating heart microcirculation.

Three-minute thesis – June 2021 – Runner up. **El-Awaisi J**. Getting to the heart of the matter.

Birmingham Inflammation, Repair and Ageing Conference – July 2021 – Elevated short talk.

**El-Awaisi J**, Kavanagh DPJ, Rink M, Weston C, Drury N, Kalia N. Intravital investigations of the role of IL-36 in mediating age specific changes in the injured beating heart coronary microcirculation.

North American Vascular Biology Organization summer camp – July 2021 - **El-Awaisi J**, Kavanagh D, Rink M, Weston C, Drury N, Kalia N. Investigating A Novel Role For The IL-36 / IL-36R Pathway In Mediating Inflammation In The Adult And Aged Murine Heart After Ischaemia-Reperfusion Injury.

Frontiers in Cardiovascular Biomedicine – April 2022 – Young investigator Award (Silver Award Winner) - **El-Awaisi J**, Kavanagh D, Drury N, Kalia N. Intravital & laser speckle investigations of the role of interleukin36 in myocardial ischaemia reperfusion injury; a new therapeutic target for the aged heart.

Joint meeting between the German Society for Microcirculation and Vascular Biology and the British Microcirculation and Vascular Biology Society. July 2022 - **El-Awaisi J**, Kavanagh D, Drury N, Kalia N. Differences in the response of male and female mouse coronary microcirculation to myocardial IR injury with inhibition of IL-36 pathway being vasculoprotective in both sexes.

12<sup>th</sup> World Congress for Microcirculation – September 2023 – Invited symposium presentation – **El-Awaisi J**. Getting to the Heart of the Matter: Intravital and laser speckle Imaging of the coronary microcirculation in the injured and aged beating heart.

## Table of Contents

Chapter 1: General Introduction .....	1
1.1. Cardiovascular Disease.....	2
1.1.1. Ischaemic Heart Disease and Atherosclerosis.....	2
1.2. Myocardial Infarction .....	4
1.2.1. Current Treatment of Myocardial Infarction .....	6
1.2.1.1. Pharmacological Agents to Prevent another MI .....	9
1.2.1.2. Thrombolytics and PCI to Reperfuse the Ischaemic Heart.....	10
1.2.2. Myocardial Ischaemia-Reperfusion Injury .....	11
1.3. Coronary Microcirculation .....	15
1.3.1. Role of the Coronary Microcirculation in Ischaemia-Reperfusion Injury.....	15
1.3.2. MINOCA and Microvascular Angina .....	16
1.4. Inflammation during Myocardial Infarction.....	21
1.4.1. Pro-inflammatory Response in a Myocardial Infarction .....	22
1.4.2. DAMPS, TLRs, and the Inflammasome .....	23
1.4.3. Pro-inflammatory Cytokines and Chemokines.....	26
1.4.5. Pro-inflammatory Chemokines .....	27
1.4.6. Pro-inflammatory Cell Adhesion Molecules.....	28
1.4.7. Role of Inflammatory Cells in Myocardial Infarction .....	30
1.4.7.1. Role of Neutrophils in Myocardial Infarction.....	30
1.4.7.2. Role of Monocytes, Macrophages, and Lymphocytes in MI .....	33
1.4.7.3. Role of Platelets in a Myocardial Infarction .....	36
1.5. Therapeutic Targets for Inflammation in a Myocardial Infarction.....	36
1.5.1.1. Targeting Interleukin-1 in Myocardial Infarction .....	37
1.5.1.2. Targeting Neutrophils in Myocardial Infarction .....	39
1.5.2. Need for a New Anti-inflammatory Target in Myocardial Infarction.....	40
1.6. Therapeutic Targets in the Interleukin-1 Super Family.....	41
1.6.1. Interleukin-36: Characterization and Expression .....	42
1.6.2. Interleukin-36: Signalling Pathway.....	43
1.6.3. Interleukin-36: Effect on the Immune System .....	44
1.6.4. Antagonism of the Interleukin-36 Receptor .....	45
1.6.5. Interleukin-36: Role in Inflammatory Diseases .....	48
1.6.6. Interleukin-36: Role in IR Injury.....	49
1.7. Risk Factors Associated with Myocardial Infarction – Age and Sex .....	50
1.7.1. Ageing and Myocardial Infarction .....	50
1.7.1.1. Inflammaging.....	51

1.7.2.	Biological Sex and Myocardial Infarction .....	52
1.7.2.1.	Sex Hormones .....	55
1.7.2.2.	Sex Differences in Immune Responses.....	55
1.8.	Summary .....	57
1.8.1.	Imaging the Coronary Microcirculation in a Beating Heart in vivo .....	57
1.8.2.	Requirement for novel anti-inflammatory targets.....	59
1.8.3.	Inclusion of co-morbidities and risk factors .....	60
1.9.	Aims and Hypotheses .....	61
	<b>Chapter 2: Materials &amp; Methods .....</b>	<b>63</b>
2.0.	Reagents and Materials.....	64
2.1.	Animals.....	69
2.1.1.	Myocardial IR Injury .....	69
2.1.1.1.	Surgical Preparation .....	69
2.1.1.2.	Surgical Procedure.....	70
2.2.	<i>In Vivo</i> Experiments.....	73
2.2.1.	Intravital Imaging of the Coronary Microcirculation in the Mouse Beating Heart <i>in vivo</i> .....	73
2.2.1.1.	Monitoring Thromboinflammatory Cells and Microvascular Perfusion in the Coronary Microcirculation .....	74
2.2.1.2.	Imaging the Coronary Microcirculation Immediately after Ischaemia .....	75
2.2.1.3.	Topical application of IL-36 Cytokines on the Beating Heart .....	75
2.2.2.	Laser Speckle Contrast Imaging.....	76
2.2.3.	Analysis of <i>In Vivo</i> Experiments.....	79
2.2.3.1.	Analysis of Intravital Imaging of the Coronary Microcirculation.....	79
2.2.3.2.	Analysis of Laser Speckle Imaging of the Beating Heart .....	80
2.3.	<i>In Vitro</i> Experiments.....	84
2.3.1.	Immunofluorescence Assay .....	84
2.3.1.1.	Mouse Immunofluorescence Assay .....	84
2.3.1.2.	Human Immunofluorescence Assay.....	85
2.3.1.3.	Patient Samples.....	85
2.3.1.3.1.	Obtaining Right Ventricular Samples from Children .....	86
2.3.1.3.2.	Neonate Group.....	86
2.3.1.3.3.	Infant/Toddler Group .....	<b>Error! Bookmark not defined.</b>
2.3.1.3.4.	Older Children Group .....	<b>Error! Bookmark not defined.</b>
2.3.1.4.	Obtaining Older Left Ventricular Patient Samples – Left Ventricular Assist Device Implantation .....	<b>Error! Bookmark not defined.</b>

2.3.1.5.	Frozen Tissue Section Analysis of Immunofluorescence.....	88
2.3.2.	Western Blotting Analysis .....	91
2.3.3.	Expression of IL-36R, IL-36 $\alpha$ , and IL-36 $\beta$ on VCECs .....	93
2.3.3.1.	Murine VCEC Culture.....	93
2.3.3.2.	Assessing IL-36R, IL-36 $\alpha$ and IL-36 $\beta$ Expression in Stimulated VCECs.....	94
2.3.3.3.	Analysis of VCEC Culture Assay .....	95
2.3.4.	Flow Cytometry Based Experiments .....	<b>Error! Bookmark not defined.</b>
2.3.4.1.	Digestion of the Mouse Heart .....	97
2.3.4.2.	Assessing Oxidative Damage and IL-36R Expression in the Mouse Heart .....	98
2.3.4.3.	Acquisition and Analysis of Flow Cytometry Studies .....	99
2.3.5.	Myocardial Infarct Size Analysis.....	101
2.3.5.1.	Preparation of Mouse Heart Samples .....	101
2.3.5.2.	Triphenyl Tetrazolium Chloride (TTC) Staining.....	101
2.3.5.3.	Analysis of Infarct Assay .....	102
2.3.6.	Multiphoton Imaging of Heart Sections.....	104
2.4.	Statistical Analysis .....	105
<b>Chapter 3: Microcirculatory Disturbances in Adult and Aged Ischaemia - Reperfusion Injured Hearts.....</b>		<b>107</b>
3.1.	Introduction .....	108
3.1.1.	Hypotheses and Aims .....	109
3.2.	Results .....	110
3.2.1.	General Observations.....	110
3.2.2.	Laser Speckle Contrast Imaging (LSCI) Demonstrated a Decreased Overall Perfusion of the Aged Heart Post-Reperfusion <i>in vivo</i> .....	110
3.2.3.	Age Increased Thromboinflammatory Disturbances within the Healthy and IR Injured Coronary Microcirculation <i>in vivo</i> .....	116
3.2.4.	Age Increased Neutrophil Presence within the Deeper Layers of the Healthy and IR Injured Myocardium.....	118
3.2.5.	IR Injury Decreases Functional Capillary Density within the Adult and Aged Beating Heart Coronary Microcirculation <i>in vivo</i> .....	126
3.2.6.	Age and IR Injury Increase Expression of VCAM-1 and Oxidative Damage.....	127
3.2.7.	Myocardial Infarct Size does not Significantly Increase with Age.....	129
3.2.8.	Age Increases Oxidative Damage in Human Ventricular Samples .....	137
3.3.	Discussion.....	139
3.3.1.	Overall Ventricular Blood Perfusion – a false indicator of all being well? .....	139
3.3.2.	Enhanced Thromboinflammatory Response with Age Alone .....	143
3.3.3.	Additional Characteristics Noted in the Healthy Aged Heart.....	145

3.3.3.1.	Mechanisms for Neutrophil Recruitment in the Aged Heart .....	146
3.3.4.	Exacerbated Inflammatory and Perfusion Responses in Aged IR Injured Mice .....	148
3.3.5.	Immediate Aftermath of Reperfusion – Early Intervention is Critical.....	152
3.3.6.	Conclusion .....	154
<b>Chapter 4: Targeting Interleukin-36 in Myocardial Ischaemia Reperfusion Injury – A New Therapeutic Target .....</b>		<b>156</b>
4.1.	Introduction .....	157
4.1.1.	Hypotheses and Aims.....	159
4.2.	Results .....	160
4.2.1.	IL-36R is Expressed in the Murine Heart, and Expression Increases with Age and IR injury	160
4.2.2.	IL-36R Expressed on Murine VCECs.....	163
4.2.3.	IL-36 Cytokines Expressed in the Murine Heart .....	163
4.2.4.	IL-36 Cytokines Expressed on Murine VCECs .....	164
4.2.5.	Increased Expression of IL-36R/ $\alpha/\beta$ with IR Injury and Age was Observed Specifically on the Murine Coronary Microvessels .....	165
4.2.6.	Age Increase Expression of IL-36R/ $\alpha/\beta/\gamma$ in Human Ventricular Samples. ....	175
4.2.7.	IL-36 Cytokine Application Induces an Inflammatory Response <i>in vivo</i> .....	180
4.2.7.1.	Topical Application of IL-36 Cytokines Increases Neutrophil Presence on the Surface of the Healthy Myocardium .....	180
4.2.7.2.	Topical Application of IL-36 Cytokines Increases Neutrophil Presence within the Deeper Layers of the Healthy Myocardium.....	190
4.2.7.3.	Topical TNF $\alpha$ and not IL-1 $\beta$ Application Induces an Inflammatory Response	193
4.2.8.	IL-36R Inhibition Reduced Myocardial Inflammation <i>in vivo</i> in Adult and Aged IR Injured Hearts.....	197
4.2.9.	IL-36R Inhibition Increases Functional Capillary Density within the Beating Heart Coronary Microcirculation <i>in vivo</i> .....	199
4.2.10.	IL-36R Inhibition Increases Perfusion in Adult and Aged Beating Heart Coronary Circulation <i>in vivo</i> .....	208
4.2.11.	IL-36R Inhibition Decreases Infarct Size in Adult Hearts .....	209
4.2.12.	IL-36R Inhibition Reduced Endothelial and Cardiac Myocyte Oxidative Damage and VCAM-1 Expression in the IR Injured Heart .....	210
4.3.	Discussion.....	220
4.3.1.	Expression of IL-36R Increases with Age and IR Injury.....	220
4.3.2.	Expression of IL-36 also Increases with Age and IR Injury .....	222
4.3.3.	Vascular Localisation of IL-36R and IL-36.....	224
4.3.4.	Topical IL-36 Cytokine can induce an Inflammatory Response in the Beating Murine Heart <i>in vivo</i> .....	226

4.3.5.	Vasculoprotective Effect of IL-36R Inhibition.....	229
4.3.6.	Conclusion .....	232
<b>Chapter 5: Intravital Investigations of the Role of IL-36 in Mediating Sex-Specific Changes in the Injured Coronary Microcirculation .....</b>		<b>234</b>
5.1.	Introduction .....	235
5.1.1.	Hypotheses and Aims.....	237
5.2.	Results .....	237
5.2.1.	General Observations.....	237
5.2.2.	Sex-Related Differences in Thromboinflammatory Disturbances within the IR Injured Coronary Microcirculation <i>in vivo</i> .....	238
5.2.3.	No Sex-Related Differences in Functional Capillary Density within the IR Injured Coronary Microcirculation <i>in vivo</i> .....	245
5.2.4.	Sex-Related Differences in Overall Ventricular Perfusion within the IR Injured Beating Heart <i>in vivo</i> .....	247
5.2.5.	Sex-Related Differences in Myocardial Infarct Size with Females having Larger Infarcts	248
5.2.6.	Sex-Related Differences in IL-36R Expression, but not VCAM-1, with Females Having a Higher Expression both Basally and after IR injury .....	253
5.2.7.	Sex-Related Differences in IL-36 $\alpha$ and IL-36 $\beta$ Expression, with Females Having a Higher Expression Basally and after IR Injury.....	254
5.2.8.	Sex-Related Differences in DNA/RNA Oxidative Damage, with Males having Greater Oxidative Damage, Particularly on Cardiomyocytes .....	258
5.2.9.	No Sex-Related Differences in the Ability of IL-36R Inhibition to Reduce Myocardial Inflammation <i>in vivo</i> .....	260
5.2.10.	IL-36R Inhibition Increases Functional Capillary Density, with Improvements More Notable in Female Mice <i>in vivo</i> .....	261
5.2.11.	IL-36R Inhibition Increases Overall Left Ventricular Perfusion in the Adult Male Beating Heart Coronary Circulation <i>in vivo</i> .....	262
5.2.12.	IL-36R Inhibition Decreases Infarct Size in Adult Hearts .....	263
5.2.13.	IL-36R Inhibition Reduced Endothelial and Cardiac Myocyte Oxidative Damage and VCAM-1 Expression in the Male IR Injured Heart .....	275
5.3.	Discussion.....	279
5.3.1.	Sex-Related Thromboinflammatory and Perfusion Perturbations Following Myocardial IR Injury <i>in vivo</i> .....	280
5.3.1.1.	Increased Neutrophils in IR Injured Female Hearts .....	280
5.3.1.2.	Increased Platelets in IR Injured Male Hearts .....	282
5.3.2.	Sex-Related Changes in VCAM-1 and Oxidative Damage.....	284
5.3.3.	Sex-Related Changes in IL-36R and IL-36 .....	285
5.3.4.	Vasculoprotective Effect of IL-36R Inhibition.....	287

5.3.5.	Infarct Size Reduction with IL-36R Inhibition .....	289
5.3.6.	Conclusion .....	290
	<b>Chapter 6: General Discussion .....</b>	<b>292</b>
6.1.	Summary of Main Findings.....	293
6.2.	Future Work and Limitations to the Study.....	304
6.3.	Concluding Remarks.....	307
	<b>Chapter 7: References .....</b>	<b>308</b>
	Appendix – JCI insight paper .....	325

## Table of figures

Figure 1.1. Atherosclerosis is a multistep process that can lead to a cardiovascular event	7
Figure 1.2. Myocardial infarction classification	8
Figure 1.3. Mechanism of energy supply during ischaemia and reperfusion	14
Figure 1.4. Epicardial microcirculation and coronary microcirculation	19
Figure 1.5. X-ray angiography of patients with symptoms of myocardial infarction (MI) either in the presence or absence of occlusions within coronary arteries	20
Figure 1.6. Overview of the IL-1 $\beta$ inflammatory response in a myocardial infarction	25
Figure 1.7. Leucocyte adhesion cascade	32
Figure 1.8. IL-36/IL-36R pathway	47
Figure 2.1. Intravital microscopy of the mouse beating heart microcirculation in vivo	72
Figure 2.2. Intravital microscopy of the beating heart microcirculation in vivo	78
Figure 2.3. Laser speckle contrast imaging of the beating heart	83
Figure 2.4. Predefined arrangement for frozen tissue section analysis	96
Figure 2.5. Gating strategy for flow cytometry-based experiments	100
Figure 2.6. Myocardial infarct size analysis	103
Figure 2.7. Preparing the mouse LV for multiphoton imaging ex vivo	106
Figure 3.1. Laser speckle contrast imaging (LSCI) allows changes in the overall perfusion of the left ventricle to be quantitated during ischaemia and reperfusion in the (A) adult and (B) aged female beating heart coronary circulation <i>in vivo</i>	112
Figure 3.2. Laser speckle contrast imaging (LSCI) demonstrated a decreased overall perfusion of the aged female heart left ventricle post-reperfusion <i>in vivo</i>	113
Figure 3.3. Laser speckle data can be analysed to determine the inter-beat distance and subsequently the standard deviation (SD) of the inter-beat distance. The SD of the inter-beat distance can provide an indication of whether there is an irregularity in the heartbeat rhythm	114
Figure 3.4. Laser speckle contrast imaging (LSCI) demonstrated a decreased overall perfusion of the aged female heart left ventricle post-reperfusion during both systolic and diastolic phases of the cardiac cycle <i>in vivo</i> . A decreased basal perfusion in the aged hearts was also demonstrated	115
Figure 3.5. Intravital imaging demonstrated that age increased thromboinflammatory disturbances within sham and IR injured beating heart coronary microcirculation <i>in vivo</i>	119
Figure 3.6. Intravital imaging demonstrated that age increased thromboinflammatory disturbances within sham and IR injured beating heart coronary microcirculation <i>in vivo</i>	120
Figure 3.7. Intravital images showing neutrophil rolling within medium-sized blood vessels and thromboinflammatory emboli within a large coronary blood vessel <i>in vivo</i>	121
Figure 3.8. Intravital imaging demonstrated that a thromboinflammatory response was mediated as soon as reperfusion was initiated	122
Figure 3.9. Intravital imaging demonstrated that a thromboinflammatory response was mediated as soon as reperfusion was initiated	123
Figure 3.10. Multiphoton <i>ex vivo</i> imaging demonstrated that age increased inflammatory disturbances within sham and IR injured beating hearts even within the deeper layers of the myocardium	124

Figure 3.11. Multiphoton <i>ex vivo</i> imaging demonstrated that age increased inflammatory disturbances within sham and IR injured beating hearts even within the deeper layers of the myocardium	125
Figure 3.12. Intravital imaging demonstrated that IR injury decreased functional capillary density within the beating heart coronary microcirculation <i>in vivo</i>	130
Figure 3.13. Age and IR injury increases expression of VCAM-1 as determined by immunofluorescence studies on frozen heart sections	131
Figure 3.14. Age and IR injury increases oxidative damage as determined by immunofluorescence studies on frozen heart sections	132
Figure 3.15. Gating strategy for flow cytometry-based experiments on adult and aged collagenase digested hearts	133
Figure 3.16. Age and IR injury increases oxidative damage on cardiac myocytes and endothelial cells as determined by flow cytometry of digested heart tissue	134
Figure 3.17. IR injury induces oxidative damage to cardiac myocytes and endothelial cells within the first 30 minutes of reperfusion in adult and aged mice as determined by flow cytometry of digested heart tissue	135
Figure 3.18. Infarct size following IR injured is not worsened with age	136
Figure 3.19. Age increases oxidative damage in human tissue as determined by immunofluorescence studies on frozen heart sections	138
Figure 4.1. Age increases the expression of IL-36R within healthy, and IR injured heart	166
Figure 4.2. Expression of IL-36R is on both coronary macrovasculature and microvasculature	167
Figure 4.3. Cardiac expression of IL-36R confirmed using a different secondary antibody	168
Figure 4.4. Age increases expression of IL-36R within the healthy and IR injured heart	169
Figure 4.5. Age and IR injury increase IL-36R expression on cardiac myocytes and endothelial cells within the first 30 minutes of reperfusion	170
Figure 4.6. Expression of IL-36R on endothelial cells increases with TNF $\alpha$ or IL-36 cytokine stimulation	171
Figure 4.7. Age increases expression of IL-36 $\alpha$ within the healthy and IR injured heart, which can also be released from endothelial cells with TNF $\alpha$ , IL-36 $\beta$ , or IL-36 $\gamma$ cytokine stimulation	172
Figure 4.8. Age increases expression of IL-36 $\beta$ within the healthy and IR injured heart, which can also be induced released from endothelial cells with TNF $\alpha$ , or IL-36 cytokine stimulation	173
Figure 4.9. Changes in the expression of IL-36 cytokines and its receptor occurs on the coronary microvasculature and not on the large blood vessels	174
Figure 4.10. Age increases expression of IL-36R in human tissue	176
Figure 4.11. Age increases expression of IL-36 $\alpha$ in human tissue	177
Figure 4.12. Age increases expression of IL-36 $\beta$ in human tissue	178
Figure 4.13. Age increases expression of IL-36 $\gamma$ in human tissue	179
Figure 4.14. Topically applied single dose of IL-36 $\gamma$ is pro-inflammatory in the adult beating heart <i>in vivo</i>	183
Figure 4.15. Topically applied single dose of IL-36 $\gamma$ is pro-inflammatory in the aged beating heart <i>in vivo</i>	184
Figure 4.16. Topically applied IL-36 is pro-inflammatory in the adult beating heart <i>in vivo</i>	185
Figure 4.17. Topically applied IL-36 is pro-inflammatory in the aged beating heart <i>in vivo</i>	186

Figure 4.18. Topically applied IL-36 is pro-inflammatory in the adult and aged beating heart <i>in vivo</i>	187
Figure 4.19. Topical application of a single dose of IL-36 $\gamma$ does not reach maximum pro-inflammatory response in the adult beating heart <i>in vivo</i>	188
Figure 4.20. Topical application of a single dose of IL-36 $\gamma$ does not reach maximum pro-inflammatory response in the aged beating heart <i>in vivo</i>	189
Figure 4.21. Topical application of IL-36 cytokines increases neutrophil presence within the deeper layers of the healthy myocardium	191
Figure 4.22. Topical application of IL-36 cytokines increases neutrophil presence within the deeper layers of the healthy myocardium	192
Figure 4.23. Topically applied TNF $\alpha$ is pro-inflammatory in the adult beating heart <i>in vivo</i>	194
Figure 4.24. Topically applied TNF $\alpha$ is pro-inflammatory in the aged beating heart <i>in vivo</i>	195
Figure 4.25. Topically applied TNF $\alpha$ is pro-inflammatory in the adult and aged beating heart <i>in vivo</i>	196
Figure 4.26. IL-36R inhibition reduces myocardial inflammation <i>in vivo</i> in the IR injured adult heart	200
Figure 4.27. IL-36R inhibition reduces myocardial inflammation <i>in vivo</i> in the IR injured aged heart	201
Figure 4.28. IL-36R inhibition reduces neutrophil recruitment, and platelet accumulation <i>in vivo</i> in the IR injured adult and aged heart	202
Figure 4.29. IL-36R inhibition reduces neutrophil recruitment <i>in vivo</i> in the IR injured adult heart	203
Figure 4.30. IL-36R inhibition reduces neutrophil recruitment <i>in vivo</i> in the IR injured adult heart	204
Figure 4.31. IL-36R inhibition reduces myocardial inflammation <i>in vivo</i> in the IR injured adult heart	205
Figure 4.32. IL-36R inhibition reduces neutrophil presence within the deeper layers of the IR injured myocardium	206
Figure 4.33. IL-36R inhibition non significantly increases capillary density within the beating heart coronary microcirculation <i>in vivo</i>	207
Figure 4.34. IL-36R inhibition increases perfusion in adult and aged beating heart coronary circulation <i>in vivo</i>	211
Figure 4.35. IL-36R inhibition increases perfusion in adult beating heart coronary circulation <i>in vivo</i>	212
Figure 4.36. IL-36R inhibition increases perfusion in aged beating heart coronary circulation <i>in vivo</i>	213
Figure 4.37. IL-36R inhibition reduces systole and diastole anomalies following IR injury <i>in vivo</i> .	214
Figure 4.38. IL-36R inhibition decreases infarct size in adult hearts	215
Figure 4.39. IL-36R inhibition decreases infarct size in aged hearts	216
Figure 4.40. IL-36R inhibition decreases expression of DNA/RNA damage on cardiac myocytes and endothelial cells	217
Figure 4.41. IL-36R inhibition decreases expression of VCAM-1	218
Figure 5.1. Sex-related differences in thromboinflammation within the IR injured coronary microcirculation <i>in vivo</i>	240
Figure 5.2. Sex-related differences in thromboinflammation within the IR injured coronary microcirculation <i>in vivo</i>	241

Figure 5.3. IR injury induces a thromboinflammatory response immediately after reperfusion in the adult male mouse beating heart coronary microcirculation <i>in vivo</i>	242
Figure 5.4. Sex-related differences in thromboinflammation within the IR injured coronary microcirculation only become apparent after the first 30 minutes of reperfusion <i>in vivo</i>	243
Figure 5.5. Adult female IR injured mice have an increased neutrophil presence within the deeper layers of the myocardium when compared to male mice	244
Figure 5.6. No sex-related differences in functional capillary density within the IR injured coronary microcirculation <i>in vivo</i>	245
Figure 5.7. Typical LSCI readings from an adult male mouse undergoing myocardial IR injury showing perfusion not returning to baseline values after reperfusion is commenced	249
Figure 5.8. Sex-related differences in overall ventricular perfusion within the IR injured beating heart <i>in vivo</i> with adult mice having decreased overall perfusion than females	250
Figure 5.9. Sex-related differences in overall ventricular perfusion within the IR injured beating heart <i>in vivo</i> with adult mice having decreased overall perfusion than females	251
Figure 5.10. Sex-related differences in myocardial infarct size with adult injured female mice having larger infarcts	252
Figure 5.11. Sex-related differences in IL-36R expression, but not VCAM-1, with adult females having a higher expression basally and after IR injury compared to adult male hearts	255
Figure 5.12. Sex-related differences in IL-36R expression, with females having a higher expression particularly on ECs	256
Figure 5.13. Sex-related differences in IL-36a and IL-36b expression with females having a higher expression basally and after IR injury compared to adult male hearts	257
Figure 5.14. Sex-related differences in DNA/RNA Damage, with males having greater damage, particularly on cardiomyocytes	259
Figure 5.15. IL-36R inhibition reduces myocardial inflammation <i>in vivo</i> in the IR injured adult male heart	265
Figure 5.16. IL-36R inhibition reduces myocardial inflammation <i>in vivo</i> in the IR injured adult male heart	266
Figure 5.17. No Sex-related differences in the ability of IL-36R inhibition to reduce myocardial inflammation <i>in vivo</i>	267
Figure 5.18. IL-36R inhibition reduces neutrophil presence within the deeper layers of the IR injured male myocardium	268
Figure 5.19. IL-36R inhibition reduces neutrophil presence within the deeper layers of the IR injured male and female myocardium	269
Figure 5.20. IL-36R inhibition increases functional capillary density within the beating heart coronary microcirculation <i>in vivo</i> , with improvements more notable in adult injured female mice than adult injured male mice.	270
Figure 5.21. IL-36R inhibition increases perfusion in adult male beating heart coronary circulation <i>in vivo</i> .	271
Figure 5.22. IL-36R inhibition increases perfusion in adult male beating heart coronary circulation <i>in vivo</i> .	272
Figure 5.23. IL-36R inhibition reduces systole and diastole anomalies following IR injury <i>in vivo</i>	273
Figure 5.24. IL-36R inhibition decreases infarct size in adult male and female hearts	274

Figure 5.25. IL-36R inhibition decreases expression of DNA/RNA damage on cardiac myocytes and endothelial cells	276
Figure 5.26. IL-36R inhibition decreases expression of VCAM-1	277
Figure 6.1 – Schematic of a potential novel IL-36/IL-36R pathway in age and IR injury	299

## List of tables

Table 1.1. Monocyte subsets in humans and mice.	35
Table 1.2. Differences in the incidence, symptoms, and prognosis of acute myocardial infarction between men and women.	54
Table 2.1: List of reagents	65
Table 2.2: List of antibodies	67
Table 2.3: List of recombinant proteins	68
Table 2.4: Vascular perfusion point-scoring	82
Table 2.5: List of patient details	87
Table 3.1. Summary of the major observations between adult and aged sham and IR injured female mouse hearts	142
Table 4.1. Summary of the major observations on IL-36R/IL-36 expression and between IL-36Ra treated and untreated adult and aged IR injured female mouse hearts	219
Table 5.1. Summary of the major sex-related differences between adult male and female IR injured mouse hearts	278

## Abbreviations

AAR	Area at risk
ACE	Angiotensin converting enzyme
ACS	Acute coronary syndrome
AUC	Area under the curve
CAM	Cell adhesion molecules
CMR	Cardiac magnetic resonance
CMs	Cardiac myocytes
CRP	C-reactive protein
cTnT	Cardiac troponin
CVD	Cardiovascular diseases
CVD	Cardiovascular diseases
DAMPs	Damage-associated molecular patterns
ECG	Electrocardiogram
ECM	Extracellular matrix
ECs	Endothelial cells
ER	Oestrogen receptors
GTN	Glyceryl trinitrate
HFpEF	Heart failure with preserved ejection fraction
ICAM-1	Intercellular adhesion molecule 1
IFN	Interferons
IgSF	Immunoglobulin super family
IHD	Ischaemic heart disease
IRI	Ischaemia-reperfusion injury
IL	Interleukin
IVM	Intravital microscopy
LAD	Left anterior descending
LCA	Left coronary arteries
LCx	<u>Left circumflex</u>
LSCI	Laser speckle contrast imaging
LV	Left ventricle
LVESVi	LV end-systolic volume index
MCP-1	Monocyte chemoattractant protein 1
MFI	Mean florescence intensity
MI	Myocardial infarction
MINOCA	Myocardial infarction with nonobstructive coronary arteries
mPTP	Mitochondrial permeability transition pore
MRI	Magnetic resonance imaging
MyD88	Myeloid differentiation factor 88
NF-κB	Nuclear factor kappa B
NLPR3	Nucleotide-binding oligomerization domain receptor family protein 3
NO	Nitric oxide
NSTEMI	Non-ST segment elevation MI
PAMPs	Pathogen-associated molecular patterns
PCI	Percutaneous coronary intervention
PDGF	Platelet-derived growth factor
PET	Positron emission tomography
PI3K	Phosphoinositol 3-kinase

P-L	Platelet-leucocyte
PRRs	Pattern recognition receptors
RBCs	Red blood cells
RCA	Right coronary arteries
ROS	Reactive oxygen species
RV	Right ventricle
RVOT	Right ventricular outflow tract muscle resection
RV-PA	Right ventricular-pulmonary artery
SDF-1	Stromal cell-derived factor 1
SLE	Systemic lupus erythematosus
SPECT	Single-photon emission computed tomography
STEMI	Non-ST segment elevation MI
TLRs	Toll-like receptors
TNF- $\alpha$	Tumour necrosis factor- $\alpha$
tPA	Tissue plasminogen activators
VCAM-1	Vascular cell adhesion molecule 1
VCECs	Vena cava endothelial cells
WBCs	White blood cells

# **Chapter 1:**

## **General Introduction**

## 1.0. General Introduction

### 1.1. Cardiovascular Disease

The cardiovascular system is made up of the heart, blood, and blood vessels. Its main function is to transport oxygen ( $O_2$ ), nutrients and hormones to cells to meet their energy requirements, as well as remove carbon dioxide ( $CO_2$ ) and other toxic waste products of metabolism [1]. It also allows the body to maintain homeostasis, regulate temperature and pH and protect against infection and blood loss [1, 2]. Generally, the circulatory system of a healthy adult operates very effectively. However, any abnormality in any one or more of the components or mechanisms within this compartment can result in acute or chronic disease, broadly termed cardiovascular diseases (CVD) [3]. These can be generally classified into two main groups [4]; (i) diseases that affect the heart, such as heart failure, valvular heart disease, ischaemic heart disease (IHD), cardiomyopathy, and cardiac arrhythmias (ii) diseases that affect the blood vessels, also known as vascular diseases, such as peripheral arterial disease and aortic aneurysm. CVD is the leading cause of death globally, accounting for approximately 17.7 million (30%) deaths annually [5].

#### 1.1.1. Ischaemic Heart Disease and Atherosclerosis

IHD, is the leading cause of CVD and accounts for 49% of the total global burden [4, 6]. Ischaemia (isch: keep back; aemia: blood) is a term used to describe the inadequate supply of blood to bodily tissues [5]. This results in a reduction in  $O_2$  and nutrient delivery, which subsequently causes problems with cellular metabolism and allows local accumulation of

toxic waste [7]. The inability of the coronary arteries to supply O<sub>2</sub> rich blood to the tissues of the heart due to the narrowing of their lumen is the primary driver of IHD [7]. This narrowing is primarily due to atherosclerosis, a localised fatty plaque in the vessel wall, which can result in partial or complete occlusion of the artery, thus reducing or completely blocking blood flow respectively [1-3, 7]. A partial blockage of the artery may result in angina (chest pain), whereas complete blockage would usually lead to a myocardial infarction (MI), commonly called a heart attack. The latter could further develop with complications, such as arrhythmias, heart failure, and death [7].

Atherosclerosis is a progressive chronic inflammatory disease whereby plaques of lipids, cholesterol, and other substances build up within the wall of blood vessels [7]. These plaques can obstruct blood flow which can lead to several conditions including CAD, MI, heart failure, stroke and in some cases death. The severity and reversibility of these diseases depend on the size of the plaque, location, occlusion size, duration of complete occlusion and whether the plaque has ruptured [7]. Several steps are involved in the development of an atherosclerotic plaque (**Figure 1.1**) [8, 9]. If it ruptures, it releases all parts of the pro-thrombogenic plaque into the bloodstream [7, 8]. Although atherosclerosis is the main cause of IHD, coronary artery spasms, coronary artery dissection or trauma can also be responsible. Additionally, triggers such as drugs, tobacco and stress can also cause a sudden constriction of coronary arteries, which can reduce blood flow and in turn, prompt the formation of a thrombus [10].

## 1.2. Myocardial Infarction

The primary cause of a MI is an atherosclerotic build-up and subsequent blockage in one or more of the major coronary arteries that supply the heart (**Figure 1.1**) [9]. It can also occur when the atherosclerotic plaque inside the coronary artery ruptures and subsequently blocks downstream vessels. Plaque rupture accounts for approximately 70% of MI fatalities [11]. A blockage of the coronary artery results in myocardial tissue not receiving the O<sub>2</sub> and nutrients required for normal physiological activity. This initiates a period of ischaemia, which can ultimately lead to cardiac tissue death and the development of a necrotic lesion called an infarct. If not treated, MI can lead to heart failure, cardiogenic shock, cardiac arrest, and death [12]. There are three main coronary arteries: (i) left anterior descending (LAD) artery, which supplies the interventricular septum, anterolateral wall and ventricular apex (ii) left circumflex artery feeding the inferolateral and inferior walls and the (iii) right coronary artery feeding the right ventricle (RV) and inferior wall [11, 13].

Tissue ischaemia leads to the initiation of an inflammatory response and platelet aggregation and thrombus formation, which in turn further augments the blockage and flow of oxygenated blood to the myocardium [12]. A patient with MI would typically present with chest pain (known as angina) which may radiate to the back, neck, jaw, upper abdomen, arms or shoulders, as well as exhibit shortness of breath, nausea, fatigue, and sweating [14]. There are two forms of angina. Stable angina is more common and occurs when the plaque causes a partial obstruction of the lumen, with pain triggered by activity (increased O<sub>2</sub> demand) but stopping within a few minutes of resting. In contrast, unstable

angina is continuous chest pain that can occur even at rest due to critical narrowing and would be considered a medical emergency [12].

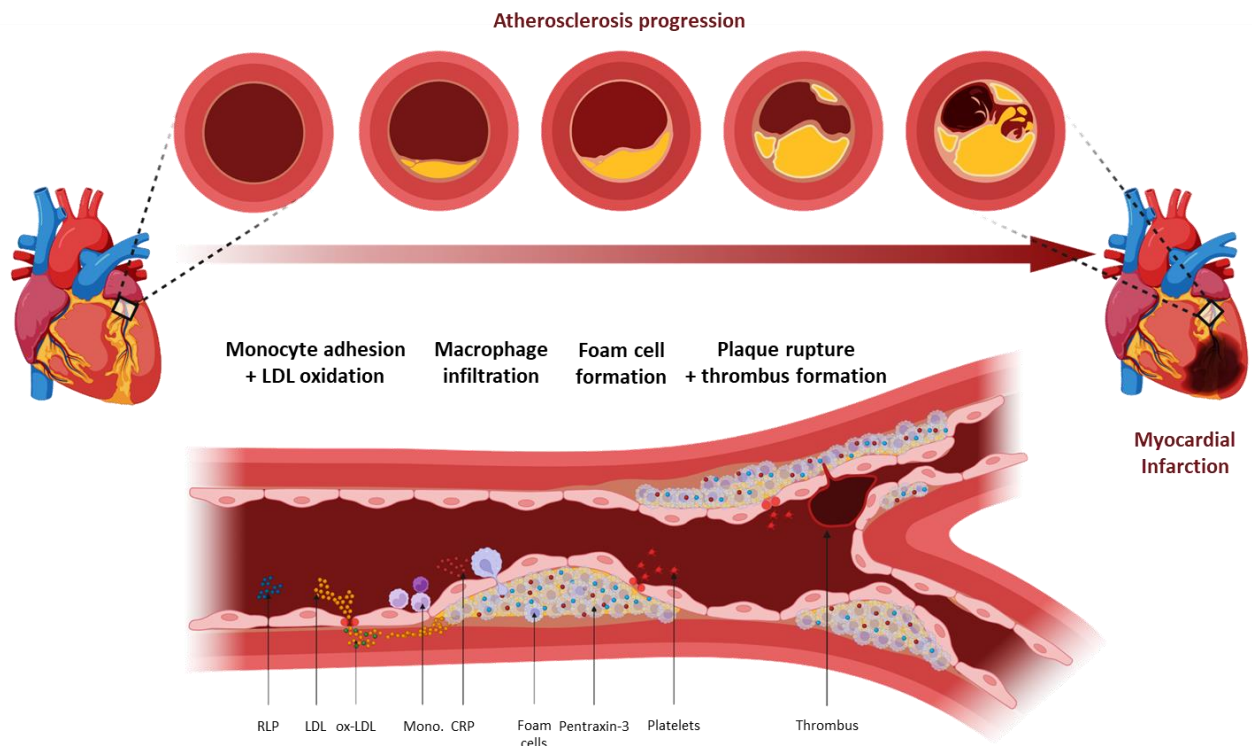
A patient suspected of having acute coronary syndrome (ACS) would typically undergo an electrocardiogram (ECG), a blood test for cardiac troponin (cTnT) and a coronary angiography [13]. These tests are performed to confirm a MI, determine what type of MI the patient is suffering from, locate the blocked area and determine the best treatment plan [11]. There are three main types of ACS: unstable angina, non-ST segment elevation MI (NSTEMI) and ST segment elevation MI (STEMI) (**Figure 1.2**) [13]. Unstable angina is when the vessel is partially obstructed due to a plaque rupture and subsequent thrombus formation around it. Patients with unstable angina do not have tissue infarction and cTnT levels generally remain normal. During an NSTEMI, a partial occlusion resulted in subendocardial myocardial infarction and elevated cTnT levels. In both unstable angina and NSTEMI patients, an ECG trace would have an inverted T wave or an ST segment depression. In contrast, a STEMI is characterised by complete occlusion of the vessel resulting in a transmural infarction. Patients with a STEMI have elevated cTnT levels, and an ECG trace would show either an ST segment elevation or hyperacute T wave (**Figure 1.2**) [11].

As a consequence of myocardial ischaemia, dysfunction in cardiac contractility occurs rapidly [15]. Within approximately one minute of coronary ischaemia, creatine phosphate reserves, used for energy generation in cardiac myocytes, are depleted as it is broken down into inorganic phosphate. These inorganic phosphates inhibit contractile proteins and thus contractile force is reduced or lost [15, 16]. As a result of the anaerobic glycolysis and the lowered intracellular pH, calcium binding to contractile proteins is inhibited, thus further reducing contractility [10, 17]. Additionally, alterations that occur during MI can lead to

the development of arrhythmias through triggering factors such as ionic and osmolality disturbances in the form of calcium influx, potassium efflux, and acidosis [17, 18].

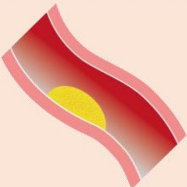
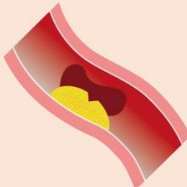
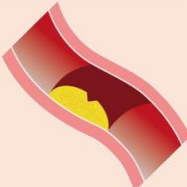
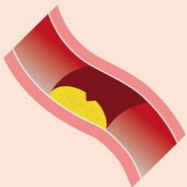








### 1.2.1. Current Treatment of Myocardial Infarction

During ischaemia, myocardial cells can start to die either through necrosis or apoptosis. Tissue death can be irreversible, but this is dependent on the duration for which the tissue remains ischaemic. Hence ischaemic time plays a vital role in the final infarct size [19]. Restoring blood flow before the development of cellular necrosis can reverse the cessation of aerobic metabolism, hypo-contractility, and mitochondrial and cellular swelling [20]. Therefore, it is crucial for reperfusion treatment to start as soon after the onset of ischaemia as possible in order to minimize the infarct size and improve prognosis. There are several therapeutic strategies for acute MI, but the backbone of all these therapies focuses on establishing reperfusion. Therapeutic strategies will also depend on the type of MI. Ultimately, all therapies aim to quickly establish reperfusion, reduce ischaemia and reduce the incidence of re-infarction [10].



**Figure 1.1. Atherosclerosis is a multistep process that can lead to a cardiovascular event.**

Presence of circulating irritants such as excess lipids, LDL cholesterol, toxins from cigarette smoking, or chronic exposure to high blood pressure damage the endothelium. This results in the endothelial barrier function being lost, which subsequently allows cholesterol to start settling at the surface and build up to form a fatty streak. When cholesterol enters the blood vessel wall, it oxidizes, resulting in the production of messengers which drive the immune system to direct monocytes to the damaged surface. Monocytes then convert into macrophages and start to engulf these fatty streaks. However, this process of engulfment is insufficient, and the macrophages die and form foam cells. During death, they release cytokines and other circulating messengers, which causes further monocyte-macrophage recruitment for reinforcements which starts this cycle again. During these cycles, the endothelium is continuously being damaged, cholesterol and platelets are accumulating with foam cells, and calcium and other substances found in the blood are being deposited, creating an increasingly more inflammatory and pro-coagulative milieu. Additionally, the smooth muscle layer starts to migrate along with collagen and elastin to form a fibrous cap around this plaque to stop it from being exposed to the blood. The growing plaque occludes the vessel, impeding circulation. In some instances, the plaque can rupture, releasing all parts of the pro-thrombogenic plaque into the bloodstream. CRP, C-reactive protein; LDL, low-density lipoprotein; ox-LDL, oxidized low-density lipoprotein; RLP, remnant-like particle; Mono., monocyte. Created using Biorender. Adapted from [9].

	<b>Stable Angina</b> Demand Ischaemia	<b>Unstable Angina</b> Supply Ischaemia	<b>NSTEMI</b>	<b>STEMI</b>
<b>Blood Vessel</b>				
<b>Description</b>	<ul style="list-style-type: none"> <li>Partial occlusion of the blood vessel lumen due to plaque</li> <li>Stable plaque</li> <li>Pain brought on by activity</li> </ul>	<ul style="list-style-type: none"> <li>Partial occlusion of the blood vessel lumen due to thrombus formation around the ruptured plaque</li> <li>Medical emergency</li> <li>Occurs at rest</li> </ul>	<ul style="list-style-type: none"> <li>Partial occlusion of the blood vessel lumen due to thrombus formation around the ruptured plaque</li> <li>Medical emergency</li> </ul>	<ul style="list-style-type: none"> <li>Complete occlusion of the blood vessel lumen due to thrombus formation around the ruptured plaque</li> <li>Medical emergency</li> </ul>
<b>ECG</b>	 Normal	 Normal, Inverted T-waves or ST depression	 Normal, Inverted T-waves or ST depression	 Hyperacute T waves or ST elevation
<b>Troponin</b>	Normal	Normal	Elevated	Elevated
<b>Infarct</b>	 No infarct	 No infarct	 Subendocardial infarct	 Transmural infarct

**Figure 1.2. Myocardial infarction classification.** The occlusion of a coronary blood vessel can lead to a myocardial infarction (MI). In order to differentiate the type of MI a patient may be suffering from, patients undergo an electrocardiogram (ECG), cardiac troponin blood test, and a coronary angiography. Patients with stable or unstable angina do not develop an infarction and have normal levels of troponin, while non-ST segment elevation MI (NSTEMI), and ST segment elevation MI (STEMI) patients develop a subendocardial and transmural infarct, respectively and have elevated troponin levels. Unstable angina and NSTEMI patients have a partial occlusion of the coronary vessel as a result of thrombus formation around the plaque and present with a normal, inverted T wave, or ST depression on their ECG, while STEMI patients have a complete occlusion, and their ECG presents either a hyperacute T wave or ST elevation. Created using Biorender. Adapted from [12, 13].

#### 1.2.1.1. Pharmacological Agents to Prevent another MI

There are several pharmacological interventions which are given to patients with an MI, which include anti-platelet and anti-coagulants drugs, statins, anti-hypertensives, and pain relievers [21]. Anti-platelet drugs such as aspirin, clopidogrel, and ticagrelor can be used to prevent further clotting and reduce the ultimate coronary artery thrombus size. This can reduce the mortality rate post-acute-MI by 50% [20]. Heparin can also be used to reduce thrombus progression and has also been shown to reduce mortality post-acute-MI [22]. Statins have been shown to have a protective effect, thought to be due to their ability to reduce lipids and cholesterol, exert angiogenic effects and inhibit cardiac myocyte hypertrophy [21]. Another key treatment,  $\beta$ -adrenergic blockers, have an array of benefits in MI which include modestly reducing infarct size, incidence of re-infarction, myocardial  $O_2$  demand and improving contractility. These benefits are a result of their protective effect on remodelling and protection of cardiac myocytes from ischaemic death, as well as additional anti-arrhythmic effects [23, 24]. Some survival benefits have also been seen with MI patients who take angiotensin converting enzyme (ACE) inhibitors early on [25]. ACE inhibitors produce their beneficial effect by preventing cardiac myocyte hypertrophy, reducing the dilation of the ventricle, and reducing the expansion of the infarct [25]. Glyceryl trinitrate (GTN), is a nitrate vasodilator which acts by increasing nitric oxide (NO) levels, which results in coronary vasodilation and in turn, improves the blood supply to the heart [26]. Lastly, painkillers such as morphine are used to manage the pain associated with unstable angina or MI and thereby reduce anxiety [26].

### 1.2.1.2. Thrombolytics and PCI to Reperfuse the Ischaemic Heart

Reperfusion is a restoration of blood flow to the vascular network following reopening of an obstructed coronary vessel and is the most important therapeutic step during a MI to reduce mortality [27]. It acts to prevent further necrosis, limit infarct size, and reduce myocardial dysfunction. However, its effectiveness is highly time dependent [27]. The physiological events that occur during reperfusion are distinct from those occurring during the ischaemic phase and involve an increased inflammatory reaction and the removal of apoptotic and necrotic cardiac myocytes [10, 28]. Clinically, myocardial reperfusion can be achieved either using pharmacological agents or by mechanical intervention [23]. Pharmacological agents include thrombolytics (also known as fibrinolytics), which act to dissolve or lyse thrombus in the coronary artery, prevent them from growing and ultimately improve blood flow to avoid further heart damage. They are used in patients with a STEMI, where mechanical interventions cannot be achieved within four hours. Thrombolytics primarily include tissue plasminogen activators (tPA) such as streptokinase, alteplase, reteplase, and urokinase. These drugs activate circulating plasminogen to form plasmin, the main proteolytic enzyme that degrades crosslinks between the fibrin molecules that hold a thrombus together, thus enabling its breakdown [29].

Mechanical interventions, which are the preferred acute therapy for MI, include primary percutaneous coronary intervention (PCI), also known as angioplasty, which removes the blockage by physical manipulation [27]. This is more effective than pharmacological options due to its superior safety, efficacy, and long-term outcomes. A primary PCI procedure involves the insertion of a small wire through one of the peripheral blood vessels

(femoral or radial artery) until it reaches the occluded coronary arteries, where the thrombus is cleared by suctioning, and a balloon or stent are used to open residual narrowing [27]. Patients are then usually placed on a dual anti-platelet anti-coagulant therapy for one year. Primary PCI is the method of choice for patients with a STEMI within the first four hours and is recommended for patients with a NSTEMI between one to three days [30].

### 1.2.2. Myocardial Ischaemia-Reperfusion Injury

Reperfusion achieved by thrombolysis or primary PCI, is vital to limit MI size, preserve myocardial tissue and avoid heart failure and left ventricular (LV) systolic dysfunction [31]. However, paradoxically, reperfusion is associated with an acute worsening of the ischaemic injury to heart tissue, a phenomenon known as ischaemia-reperfusion (IR) injury [31]. Indeed, it is estimated that reperfusion of the heart following an ischaemic episode is responsible for approximately 50% of the final necrotic infarct size, which limits the full benefit of reperfusion therapy. It is therefore an area of significant interest as interventions administered at the point of reperfusion have the potential to improve the prognosis of patients following an MI [32]. However, successful therapies that can prevent reperfusion-related myocardial injury have not been identified and thus remain one of the key unmet clinical needs in cardiology.

Once reperfusion starts, an enhancement in the inflammatory response begins. Reactive oxygen species (ROS) form through a variety of mechanisms in cardiac myocytes and endothelial cells (ECs), of which an electron transfer to  $O_2$  occurs by a damaged enzyme

from the ischaemic phase (**Figure 1.3**) [33, 34]. These, alongside activated neutrophils, platelets, ECs, and macrophages, release more ROS and in turn, the formation of mediators such as chemokines and cytokines. This inflammatory response disturbs coronary microvascular perfusion as a result of alterations in the production of NO and endothelin-1 (a potent vasoconstrictor), as well as enhanced coagulation. Collectively, these events produce cytotoxicity and in turn, induce further cell injury and death [35].

In addition to inflammation, reperfusion is associated with several additional factors that may cause tissue injury, including intracellular  $\text{Ca}^{2+}$  overload, oxidative stress, and consequences of pH restoration. Intracellular  $\text{Ca}^{2+}$  overload occurs during the ischaemic phase but is worsened following reperfusion as a result of mitochondrial re-energisation and the generation of oxidative stress. Entry of  $\text{Ca}^{2+}$  into the mitochondria occurs through the mitochondrial  $\text{Ca}^{2+}$  uniporter, which in turn induces the opening of the mitochondrial permeability transition pore (mPTP) and mitochondrial re-energisation occurs (**Figure 1.3**) [32]. Although pharmacological inhibition of the  $\text{Ca}^{2+}$  channel reduced infarct size by 50% in animal models, similar effects have not been seen in clinical studies [36, 37]. The recent discovery of a mitochondrial  $\text{Ca}^{2+}$  uniporter inhibitor may provide better clinical outcomes through its pharmacological inhibition. The mPTP channel is non-selective, and its opening results in a dissipation of the mitochondrial membrane ionic gradient, cessation of ATP generation through oxidative phosphorylation and subsequent cell death. The mPTP remains closed during ischaemia but may open following reperfusion in response to the  $\text{Ca}^{2+}$  overload, relative depletion of ATP, oxidative stress, and pH restoration (**Figure 1.3**). Pharmacological inhibition of this channel at the time of reperfusion was able to reduce MI

size by about 45% in animal models and could provide a potential therapeutic target for IR injury [38].

A rush of oxidative stress is also produced following reperfusion which can mediate cardiac myocyte death. Antioxidants have been shown to be beneficial in some studies but are generally not cell-permeable, and so their intracellular efficacy is hindered. Therefore, the use of specific mitochondrial antioxidants may provide better results experimentally and clinically [32, 39]. Lastly, intracellular pH is rapidly restored following reperfusion. The activation of the  $\text{Na}^+\text{H}^+$  exchanger and washing out of lactate following reperfusion rapidly returns the pH from 7 during ischaemia to its physiological condition within minutes. This process results in cardiac myocyte injury and death through the opening of the mPTP channels and hypercontractility of cardiac myocytes. Therefore, a slow restoration of the pH at the time of reperfusion could prevent IR injury. Consistent with this mechanism, pharmacological inhibition of the  $\text{Na}^+\text{H}^+$  exchanger has been shown to be cardioprotective [32, 40].

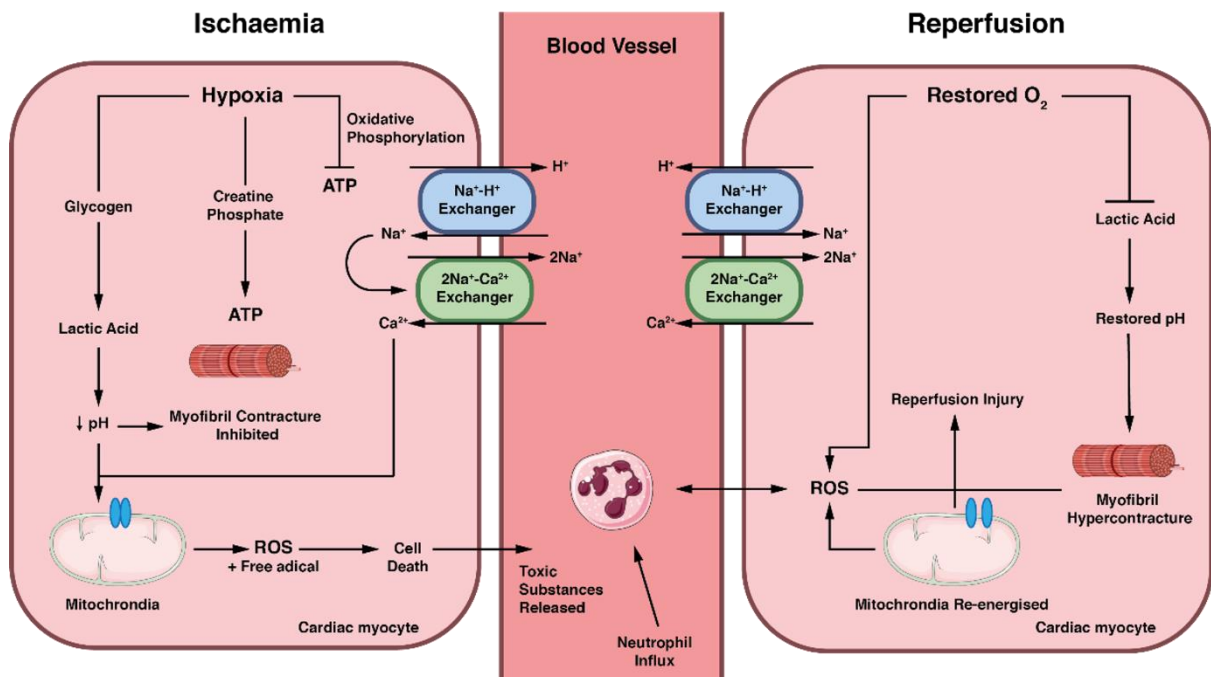


**Figure 1.3. Mechanism of energy supply during ischaemia and reperfusion.** Generation of energy in cardiac myocytes usually occurs in the presence of O<sub>2</sub>, via a mechanism relying on oxidative phosphorylation in the mitochondria to produce ATP. In the absence of O<sub>2</sub>, ATP generation through oxidative phosphorylation stops, and ADP levels increase, which results in a transient production of ATP from creatine phosphate until this is depleted (usually within about 1 minute). Simultaneously, anaerobic glycolysis starts to convert intracellular glycogen to lactic acid, which results in intracellular acidosis. As a result, ion transport pumps which rely on ATP will fail. Na<sup>+</sup>/K<sup>+</sup> pump failure will increase intracellular levels of Na<sup>+</sup>, which leads to a disturbance in cell osmolality and results in swelling, a loss of conductivity and membrane damage. To balance Na<sup>+</sup> overload, the Na<sup>+</sup>/Ca<sup>2+</sup> ion exchanger removes Na<sup>+</sup> and increases Ca<sup>2+</sup>. Within about 20 minutes, anaerobic glycolysis becomes insufficient to substitute ATP, and consequently Ca<sup>2+</sup> and Na<sup>+</sup> overload will result in the generation of reactive oxygen species (ROS), free radicals and other harmful substances, which will also damage the cell membrane. More harmful substances are then generated and cause the mitochondria to break down and release further toxic metabolites, which leads to cell death. Cellular death releases toxic substances into the surrounding environment, which causes additional cell death. Once reperfusion starts, anaerobic glycolysis is stopped, pH is restored, mitochondrial production of ATP is resumed, and an inflammatory response is activated. The inflammatory response can be triggered by the components of damaged or dead cells or the disordered tissue matrix. These cells, alongside activated neutrophils, platelets, endothelial cells, and macrophages, can then release ROS and free radicals. ROS and free radicals are formed via a number of pathways in cardiac myocytes, one of which involves an electron transfer to O<sub>2</sub> by xanthine oxidase (which is itself generated by cleavage of xanthine dehydrogenase due to high intracellular Ca<sup>2+</sup> levels in the ischaemic phase). Some of these then result in cytotoxicity and in turn, induce further cell injury and death. Created using Biorender. Adapted from [31].

### 1.3. Coronary Microcirculation

#### 1.3.1. Role of the Coronary Microcirculation in Ischaemia-Reperfusion Injury

The sinuses of Valsalva, at the origin of the aorta as it leaves the heart, gives rise to the two main epicardial arteries, the left (LCA) and right (RCA) coronary arteries, which then continue to branch out even further into smaller vessels to feed specific areas of the heart. The LCA supplies the left side of the heart, with the left main stem branching into two arteries, the left anterior descending (LAD) and the left circumflex (LCx) artery [41]. The LAD artery perfuses the anterior wall of the left ventricle, and the anterior interventricular septum, whilst the LCx perfuses the lateral left ventricular free wall. The RCA branches into right marginal arteries to perfuse the right ventricle and usually forms the posterior interventricular artery to supply the septum from behind. Initial branching starts on the epicardial surface of the heart and continues to branch into the myocardium to form a tree-like microcirculatory network ending as an extensive network of capillaries running between all muscle fibres providing almost every fibre with its own capillary (**Figure 1.4**) [41]. Indeed, coronary microcirculation accounts for around 75-80% of the total myocardial blood flow and hence plays an integral role in regulating the distribution of blood flow in the heart to ensure demand is met during metabolic, endothelial, neuronal, and myogenic changes through its control of coronary resistance [42]. However, it also plays an important role in permitting the thromboinflammatory response during ischaemia and the subsequent reperfusion phases that accompanies the flow restoring treatment of MI.

Clinically, restoration of normal epicardial coronary artery blood flow, but with sub-optimal myocardial perfusion, can be observed in as many as 50% of patients undergoing PCI, which leads to worse outcomes than in patients with full perfusion recovery [41, 43, 44]. This suggests myocardial tissue damage likely occurs subsequent to inadequate perfusion at the level of the coronary microcirculation [43, 45]. Indeed, a no 're-flow' phenomenon noted post-PCI is likely brought about by targeted damage of the smallest blood vessels of the heart as a result of both the ischaemic and reperfusion insults.

### 1.3.2. MINOCA and Microvascular Angina

The no-reflow phenomenon often observed post-PCI is not the only evidence that indicates an important pathophysiological role in coronary microcirculation [46]. As stated earlier, MI occurs when there is a blockage in one or more of the three main coronary arteries. This can be a partial or a complete blockage, described earlier as NSTEMI or STEMI, respectively. These large vessel obstructions can be easily detected in a clinical setting using x-ray angiography (**Figure 1.5**). However, at least 15% of patients presenting with typical symptoms of an acute MI show no angiographic evidence of obstructive coronary lesions, suggesting ischaemic problems may be likely occurring due to perturbations within the downstream microcirculation [47]. Therefore, despite changes indicative of a heart attack being evident on an ECG (ST-segment elevation) and biochemically (raised cardiac troponin levels that measure heart muscle damage), no stenosis of  $\geq 50\%$  in a major epicardial artery is demonstrated on coronary angiography (**Figure 1.5**). This condition, called MI with non-obstructive coronary arteries or MINOCA, results from various causes,

including microvascular diseases, thromboembolism, plaque disturbance or coronary artery dissection or spasm [48]. Interestingly, MINOCA is diagnosed more frequently in younger patients and in women. The importance of coronary microcirculation in CVDs is further exemplified in conditions such as microvascular angina (also called cardiac syndrome X). Patients with microvascular angina present with chest pain during physical exertion, but no ST-elevation is seen on an ECG, and basal circulating troponin levels are usually normal. Similar to MINOCA, there is an absence of obstructive angiographic visible coronary arteries. Coronary microvascular dysfunction has also been attributed to be the main cause of heart failure with preserved ejection fraction (HFpEF), which makes up around 50% of all patients diagnosed with heart failure [49, 50].

Increased clinical recognition of the importance of coronary microcirculation has resulted in the need to identify strategies to improve perturbations within it, and these have gained attention recently [51]. However, clinical research into the role of coronary microcirculation in cardiovascular disease has been limited. This has meant no efficient strategy to improve microvascular flow post-PCI; the time when reperfusion injury is initiated has yet been identified. This is due to several challenges which have made it difficult to investigate dynamic events within the coronary microcirculation clinically. The most significant is the fact that the microvessels of interest are small, less than 200 $\mu$ m in diameter, making imaging modalities such as cardiac magnetic resonance (CMR) and positron emission tomography (PET) unsuitable due to their limited spatial resolution [52]. This inability to directly image coronary microvessels in patients has led to cardiologists focusing their efforts on improving flow post-MI within the angiographically visible part of the coronary circulation. Hence, little is known about the full range of coronary

microcirculatory responses, particularly at a cellular level, to IR in the clinical setting [53, 54].

Most of our knowledge of what may be happening within the coronary microvessels post-IR injury has been obtained from experimental studies, in which heart tissue has been interrogated histologically and biochemically for morphological deterioration, thromboinflammatory cell infiltration and infarct size. Various microvascular perturbations noted in tissue sections include the presence of (i) swollen endothelial cells surrounded by cardiac myocytes that are themselves swollen, (ii) presence of endothelial gaps, (iii) red blood cell (RBC) congestion, (iv) platelet and fibrin microthrombi, and (v) a high number of intraluminal leucocytes or platelet-leucocyte aggregates [51]. However, these one-time static snapshots cannot indicate which of these events actually reduce or prevent myocardial flow post-reperfusion, nor can they provide real-time data on the trafficking kinetics of thromboinflammatory cells in the presence of pathophysiological flow. Therefore, it is not possible to know whether thromboinflammatory cells noted in coronary microvessels in histological sections are actually adherent, occlusive, and inhibiting the passage of blood or simply circulating cells or remote emboli that were freely passing through the heart at the time of tissue retrieval. Leucocyte recruitment follows a well-characterised adhesion cascade, including crawling, rolling, adhesion, spreading, and transendothelial migration (**Section 1.4.6**). However, histological analysis cannot really ascertain which of these dynamic events are critical in mediating their recruitment in the heart *in vivo*. Moreover, important microvascular functional information such as the ability of IR injury to modify flow, vessel diameters, functional capillary density, microvessel integrity, and leakage are impossible to determine from static sections.

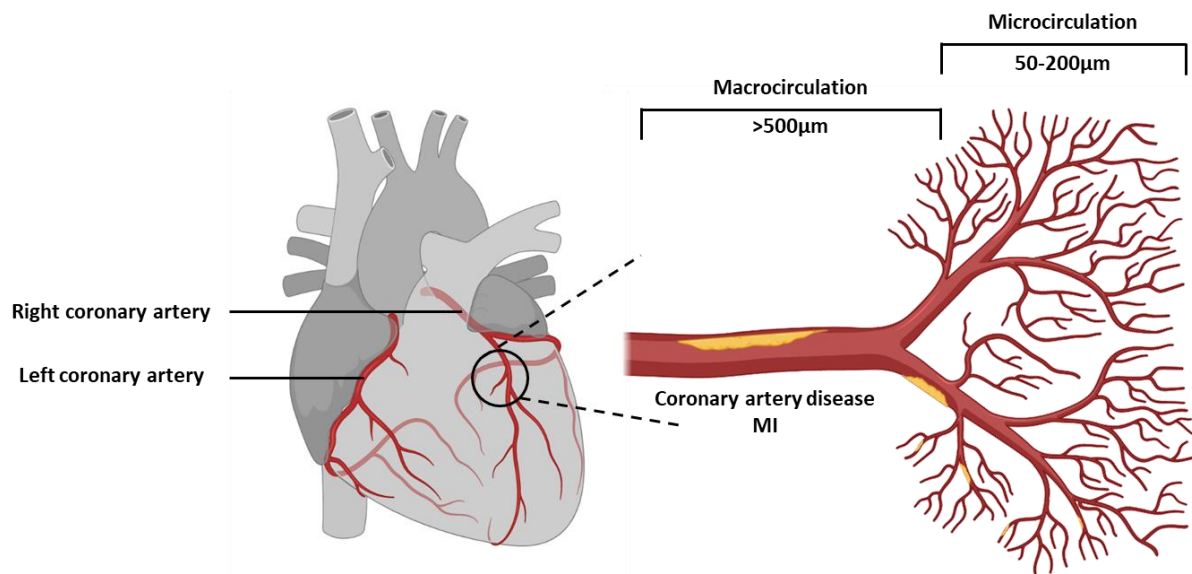


**Figure 1.4. Epicardial microcirculation and coronary microcirculation.** The left and right coronary arteries and their branches are epicardial coronary vessels that lie on the surface of the heart. Their distal branches penetrate the heart muscle to become the coronary microcirculation and are typically less than 500µm in diameter. The coronary microcirculation cannot be visualised during coronary angiography or other routine clinical imaging tools such as single-photon emission computed tomography (SPECT), positron emission tomography (PET), ultrasound and magnetic resonance imaging (MRI). Hence, only blockages in coronary arteries can be seen clinically and not those that they may present in the smaller microvessels. Created using Biorender.

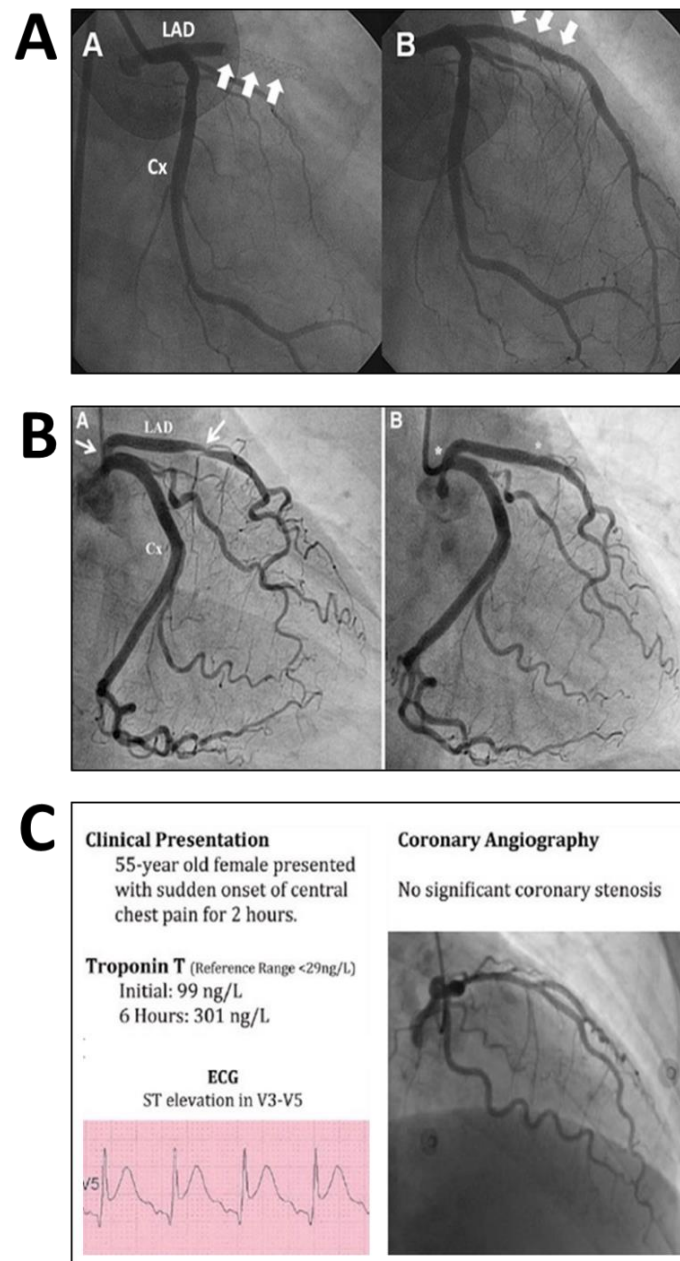


**Figure 1.5. X-ray angiography of patients with symptoms of myocardial infarction (MI) either in the presence or absence of occlusions within coronary arteries. (A) (Left)** Angiogram demonstrating a total occlusion in the proximal left anterior descending (LAD) coronary artery with no downstream blood flow (arrows). A normal left circumflex artery (Cx) is shown. **(Right)** The same vessel in which flow has been restored after insertion of a stent. Image: Hwang *et al.*, 2015 **(B) (Left)** Angiogram demonstrating a partial occlusion (arrow) in the LAD which has some downstream flow (arrow). **(Right)** The same vessel after the occlusion is relieved with a stent. Image: Playán-Escribano *et al.*, 2019 [55]. **(C)** 55-year-old female patient with MINOCA presenting with classical symptoms of an MI, raised troponin levels and an ST-elevation in her ECG, but with no stenosis in her coronary arteries. Image: Pasupathy *et al.*, 2016 [46].

#### 1.4. Inflammation during Myocardial Infarction

Inflammation is a localised biological response to infections or sterile tissue damage. Infectious factors include bacteria, viruses, and other microorganisms, while sterile inflammation occurs following exposure to chemical irritants, physical, and biological injuries, and psychological mediators [56]. The immune system is made up of two complementary sub-systems, namely the innate and adaptive immune systems [57]. The innate immune system is responsible for the first line of defence against any new pathogen or injury and does not need prior exposure to the pathogen [56]. Instead, immune cells such as resident macrophages, dendritic cells, and mast cells contain pattern recognition receptors (PRRs) which act to recognise pathogen-specific molecules, known as pathogen-associated molecular patterns (PAMPs), or components of the host damaged or dead cells, known as damage-associated molecular patterns (DAMPs). Toll-like receptors (TLRs) are a class of PRRs that have been widely studied. Following infection or injury, TLRs become activated through their recognition of PAMPs or DAMPs and, through a signalling cascade, induce the secretion of cytokines and chemokines, which recruit neutrophils and macrophages to the site of inflammation. These different categories of inflammatory triggers ultimately converge on the same downstream signalling effectors with neutrophils and macrophages then engulfing the pathogens or damaged/dead cells [56].

By contrast, the adaptive immune system is responsible for antigen-specific immune responses, whereby pathogens are identified through the recognition of unique antigens. The adaptive immune response is more focussed as each pathogen is targeted specifically by specialized immune cells known as lymphocytes (B- and T-cells). Some of the activated

B- and T-cells become memory B- and T-cells, respectively, which allows for the development of immunological memory, by which pathogens are identified and neutralised rapidly in subsequent exposures to the pathogen. Establishing a significant adaptive immune response to a new pathogen usually takes around six days [56].

Inflammation can be categorized as either acute or chronic. The initial response to infections, irritants, or injury is considered an acute response and is characterised by the movement and transmigration of immune cells such as neutrophils from the vasculature into the inflamed area. If the acute inflammatory response fails to eradicate the infection, irritant, or injury, then chronic inflammation follows. This persistent, prolonged inflammation is characterised by concurrent destruction and repair of the tissue. A change in the type of immune cells present at the site to a more specialized type of immune cells is also observed. Atherosclerosis is a chronic inflammatory disease, while the initial inflammatory response in a MI is an acute inflammation [56, 58].

### **1.4.1. Pro-inflammatory Response in a Myocardial Infarction**

The onset of an ischaemic event during MI, and reperfusion through primary PCI, can both induce inflammation because of cellular injury and death to cardiac myocytes, ECs, and fibroblasts. This acute inflammatory response is triggered through several initiation processes including, the release of the intracellular content of necrotic cells such as DAMPs, production of ROS, and activation of the complement cascade. This initiation then activates the nuclear factor kappa B (NF- $\kappa$ B) system and generates pro-inflammatory mediators such as chemokines, cytokines, and adhesion molecules at the infarct site. Recruitment and

extravasation of circulating neutrophils and other leucocytes to the infarction site then occurs, which serves to help wound healing and scar formation [59]. However, a prolonged and excessive inflammatory response can worsen the condition, leading to larger infarct size, LV remodelling and heart failure.

### 1.4.2. DAMPS, TLRs, and the Inflammasome

Cellular injury and death to myocardial tissue and cardiac myocytes result in the release of endogenous DAMPs (**Figure 1.6**) [60]. These can be nuclear in nature such as histones, DNA, mitochondrial DNA (mtDNA) the nuclear factor high mobility group box 1 (HMGB1) and interleukin-1 (IL-1 $\alpha$ ) or cytosolic such as ATP, uric acid, heat shock proteins (HSP) and F-actin. Specific TLRs become activated through their recognition of these DAMPS. Extracellular DNA, mtDNA, RNA, and HMGB1 have all either been shown to be elevated in patients following a MI or to be anti-inflammatory and cardioprotective. This has been demonstrated by the ability of DNAase, RNAase1 or HMGB1 inhibitors to reduce MI size [61, 62]. There are more than 10 known TLRs, located either on the surface of cardiac cells (TLR1, TLR2, TLR4) or intracellularly (TLR3, TLR7, TLR9). Surface TLRs sense extracellular damage or danger signals (such as HMGB1), whereas intracellular TLRs act to sense signals within cells (such as DNA or nucleic acid) [60]. Once a DAMP is recognised by a TLR, the cytoplasmic myeloid differentiation factor 88 (MyD88) is activated. This stimulates the NF- $\kappa$ B pathway and, through a signalling cascade and gene transcription, leads to the production and release of several inflammatory mediators such as pro-interleukin (IL)-1 $\beta$  (pro-IL-1 $\beta$ ) (**Figure 1.6**) [63]. TLR4, in particular, has been shown to be integral in inducing

inflammation during myocardial ischaemia and IR injury. Indeed, genetic depletion or pharmacological inhibition of TLR4 in mice results in reduced neutrophil/monocyte infiltration and decreased cytokine/chemokine production, which ultimately leads to reduced MI size and LV remodelling [64, 65], [66, 67].

Pro-inflammatory responses following an acute MI or post-reperfusion can also be triggered through inflammasomes. Inflammasomes are a complex of multiple cytoplasmic proteins which form in response to the release of DAMPs (such as ATP), and function to activate pro-inflammatory cytokines such as IL-1 $\beta$  [58]. The most described and studied inflammasome in relation to MI is nucleotide-binding oligomerization domain receptor family protein 3 (NLRP3). Release of extracellular ATP leads to Ca<sup>2+</sup> overload within the mitochondria, subsequent ROS generation, and mitochondrial cardiolipin release, which activates the NLRP3 inflammasome [60]. This inflammasome then promotes cleavage of pro-Caspase-1 into Caspase-1, which in turn converts pro-IL-1 $\beta$  (inactive form) into the active IL-1 $\beta$  form (**Figure 1.6**). In 2013, Sandanger *et al.* identified an up-regulation of NLRP3 in mouse myocardial fibroblasts following an acute MI [68]. Several research groups were also able to see a significant reduction in MI size in murine hearts following pharmacological inhibition or genetic depletion of NLRP3, thus suggesting this as a potential therapeutic target to limit myocardial cell death following an acute MI [68-70].

Therefore, release of IL-1 $\beta$  from cardiac cells involves two steps: (i) pro-IL-1 $\beta$  transcription through the DAMP-TLR-NF- $\kappa$ B signalling cascade and (ii) processing of pro-IL-1 $\beta$  into its active form (IL-1 $\beta$ ) through the NLRP3 inflammasome. IL-1 $\beta$  drives further pro-inflammatory mediator release, thereby exacerbating the acute inflammatory response (**Figure 1.6**).

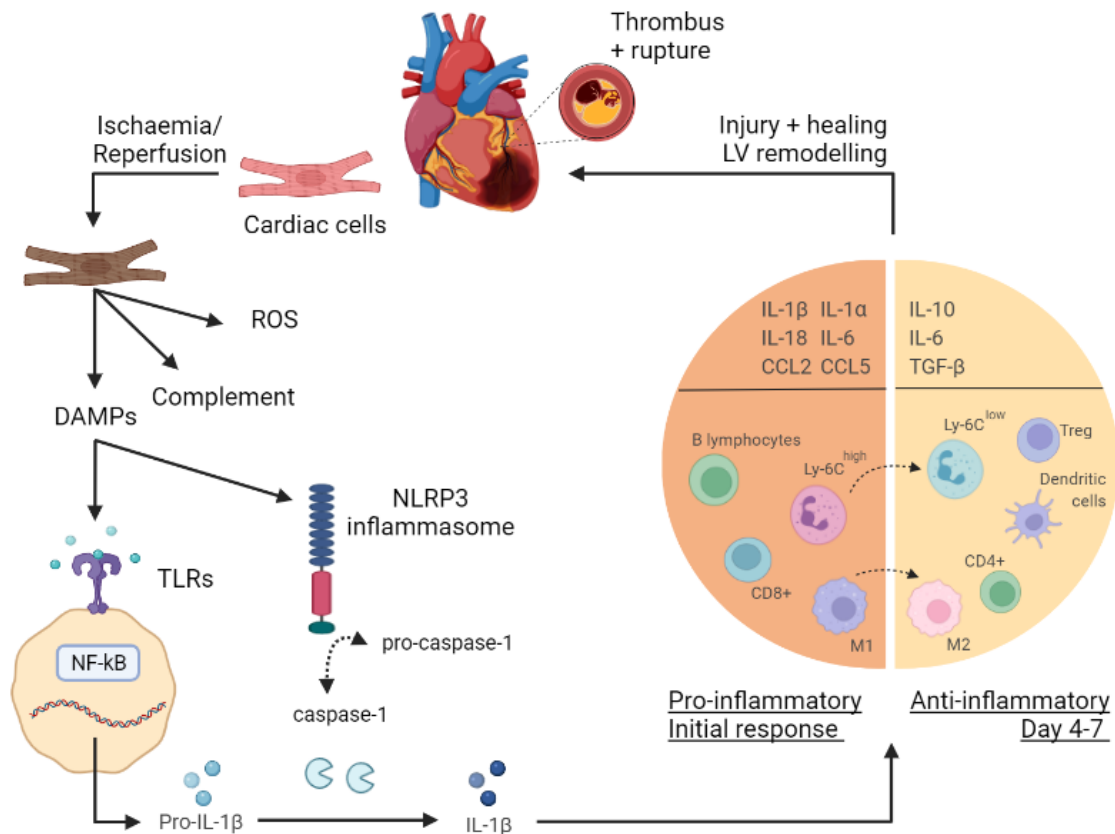


**Figure 1.6. Overview of the IL-1 $\beta$  inflammatory response in a myocardial infarction.** The onset of acute myocardial infarction (MI) leads to cellular injury and necrosis of cardiac cells (cardiac myocytes, endothelial cells, and fibroblasts), resulting in the release of intracellular content such as damage-associated molecular patterns (DAMPs), production of reactive oxygen species (ROS) and activation of the complement cascade. Once a DAMP (such as DNA, mitochondrial DNA (mtDNA), RNA, the nuclear factor - high mobility group box 1 (HMGB1), and ATP) is recognised by toll-like receptors (TLRs), cytoplasmic myeloid differentiation factor 88 (MyD88) is activated. This in turn, stimulates the NF- $\kappa$ B pathway and through a signalling cascade and transcription, leads to the release of several inflammatory mediators such as pro-interleukin (IL)-1 $\beta$ . Additionally, in response to the release of DAMPs, inflammasomes (such as nucleotide-binding oligomerization domain receptor family protein 3, NLRP3) are activated to promote the cleavage of pro-Caspase-1 into Caspase-1, which in turn processes the pro-IL-1 $\beta$  into the active IL-1 $\beta$  form. As a result, pro-inflammatory mediators such as cytokines (IL-1 $\beta$ , IL-1 $\alpha$ , IL-18, and IL-6), chemokines (CCL2, and CCL5), and cell adhesion molecules are increased at the infarct site. Extravasation and recruitment of neutrophils and other leucocytes (monocytes, macrophages, B lymphocytes, and CD8 $^{+}$  T cells) to the infarction site then occurs as a result of the interactions between endothelial cells and infiltrating leucocytes. The subsequent anti-inflammatory phase (day 4-7) facilitates the resolution and repair through anti-inflammatory cytokines (IL-10, IL-1, and TGF- $\beta$ ), changes in macrophages (M1 to M2) and monocytes (Ly6C $^{\text{high}}$  to Ly6C $^{\text{low}}$ ), and recruitment of cells (T-regs, dendritic cells, CD4 $^{+}$  T cells). This response serves to help wound healing and scar formation; however, a prolonged and excessive inflammatory response can worsen the condition, leading to larger infarct size, LV remodelling and heart failure. Created using Biorender. Adapted from [60]

### 1.4.3. Pro-inflammatory Cytokines and Chemokines

In response to ischaemia or reperfusion injury, pro-inflammatory cytokines, such as IL-1 $\beta$ , tumour necrosis factor- $\alpha$  (TNF $\alpha$ ) and IL-6 are produced, primarily by resident myocardial cells or circulating inflammatory cells, and function to recruit immune cells to the area. These agents promote leucocyte recruitment by activating leucocyte integrins and enhancing the expression of endothelial cell adhesion molecules (CAM) at the site of injury. Chemoattractant cytokines or chemokines are also secreted and regulate the locomotion and trafficking of leucocytes along concentration gradients, thus increasing leucocyte recruitment and infiltration to the infarcted area [58, 60].

### 1.4.4. Pro-inflammatory Cytokines

Cytokines are a broad class of proteins (~6-20kDa) produced by a wide variety of immune, endothelial, and other tissue-resident cells and are involved in cell signalling. They include chemokines, interleukins (ILs), interferons (IFNs), TNFs and lymphokines. These agents can act as either pro- or anti-inflammatory mediators for the immune system. Several pro-inflammatory cytokines are up-regulated in acute MI during the ischaemia and reperfusion phases. Predominant cytokines include IL-1 family members (IL-1 $\alpha$  and IL-1 $\beta$ ), IL-6, TNF- $\alpha$ , and C-reactive protein (CRP). IL-1 family members have a key role within most systemic and local inflammatory responses and are one of the early and leading cytokines to mediate an inflammatory response following an acute MI. In experimental mouse models of MI, IL-1 $\alpha$  has been shown to be released by damaged or dead cardiac myocytes, while

IL-1 $\beta$  is primarily released from immune cells and cardiac myocytes (**Figure 1.6**) [71, 72]. Following reperfusion, plasma levels of IL-1 $\beta$  have been strongly linked to decreased cardiac function and adverse LV remodelling [73]. Multiple research groups have shown a reduction in adverse LV remodelling and MI size following pharmacological inhibition of IL-1 $\beta$  or genetic depletion of the IL-1 receptor (IL-1R) in experimental mouse models of MI [74]. IL-6 is also released from both immune and myocardial cells following IR injury and has been shown to have both anti- and pro-inflammatory effects, including the secretion of CRP. Studies in mice with genetically depleted or pharmacologically inhibited IL-6, have returned varied results on MI size and LV remodelling, with some studies showing a worsened LV remodelling following inhibition [75-77]. Increased plasma levels of IL-6, TNF $\alpha$  and CRP have been shown to be associated with worse adverse outcomes and higher mortality in patients with MI [60]. A reduction in MI size was also seen following TNF $\alpha$  inhibition [74].

### 1.4.5. Pro-inflammatory Chemokines

Chemokines are a class of cytokines (~8-14KDa) which have a similar tertiary structure and are released in response to pro-inflammatory cytokines. They are classified into sub-families depending on their cysteine residues: CC, CXC, CX3C, and XC. They have a key role in neutrophil, monocyte and lymphocyte locomotion, trafficking, and adhesion. The most abundant chemokines are the CC chemokines, which include CCL2 (also known as monocyte chemoattractant protein 1 (MCP-1) and CCL5. CCL2 and CCL5 are both significantly and rapidly up regulated in a MI and function to attract immune cells. CCL2

attracts mononuclear cells such as monocytes, while CCL5 attracts neutrophils and macrophages (**Figure 1.6**). Genetic depletion of CCL2 or its receptor or inhibiting CCL5 using a monoclonal antibody resulted in a reduction of infiltrating immune cells to the infarcted area, reduced MI size, stopped LV remodelling, and reduced mortality [78, 79]. CXC chemokines include CXCL12, also known as stromal cell-derived factor 1 (SDF-1), which is also up regulated in MI. Pharmacological inhibition of CXCL12 also resulted in a reduced MI size and a reduction in infiltrating neutrophils, most likely through an indirect effect [60, 80].

### 1.4.6. Pro-inflammatory Cell Adhesion Molecules

Following the release of chemokines, leucocytes are captured from the circulation and aided to cross the vascular endothelium and enter the site of injury. The pathway of events that underlie this process form what is referred to as the leucocyte adhesion cascade. In response to a MI, this process involves leucocytes tethering and rolling within the blood vessel, followed by their subsequent arrest and firm adhesion to the endothelium and finally their migration through the endothelium into the subendothelial space (**Figure 1.7**) [81]. This process is mediated by selectins in the initial step followed by chemokines and CAMs in the remainder of the cascade [81]. CAMs are a class of receptors which are located on the surface of cells, aid in the binding or adhesion to other cells. They are often upregulated, activated, or clustered following the activation of leucocytes, ECs, and platelets. They are generally classified but not limited to four main groups: selectins, integrins, immunoglobulin super family (IgSF) and cadherins. Selectins are a class of

heterophilic CAMs (whereby a CAM must bind to a different CAM) and are made up of three members, E-selectin (expressed on ECs), L-selectin (expressed on most leucocytes and endothelial cells), and P-selectin (expressed on platelets and ECs) and are responsible for the initial leucocyte capture, rolling and tethering. Integrins are heterodimeric CAMs, which are made up of an  $\alpha$  (18 types) and  $\beta$  (8 types) subunit, and through their various combinations, make up 24 known integrins. These include the beta-1 integrin  $\alpha_4\beta_1$  (also called very late antigen 4 [VLA-4] or CD49d/CD29) and the beta-2 integrins  $\alpha_L\beta_2$  (also called lymphocyte function-associated antigen 1 [LFA-1] or CD11a/CD18) and  $\alpha_M\beta_2$  (also called macrophage-1 antigen [MAC-1] or CD11b/CD18). They are responsible for facilitating the subsequent arrest of leucocytes on the endothelium or extracellular matrix (ECM) by binding to other CAMs present on these surfaces.  $\alpha_4\beta_1$  integrin present on leucocytes and lymphocytes can interact with ECs by binding to vascular cell adhesion molecule 1 (VCAM-1). Similarly,  $\alpha_L\beta_2$  and  $\alpha_M\beta_2$  integrins can bind to intercellular adhesion molecule 1 (ICAM-1). Members of the IgSF are the most diverse class of CAMs, and include VCAM1, ICAM1 and PECAM1 (platelet endothelial CAM-1). The interactions between VCAM1 or ICAM1 with their respective integrin results in the firm adhesion of leucocytes on the endothelium. PECAM1 (CD31) is found most densely at endothelial intracellular junctions and can also be found on platelets, neutrophils, and monocytes to facilitate homophilic interactions [81, 82]. Cadherins are mainly found between cells at the intermediate cell junctions (adherence junctions). They are classified based on their location; these include E-cadherins (epithelium), P-cadherins (placenta) and N-cadherins (neuronal). Transmigration of adherent leucocytes through the endothelium requires several CAMs, including ICAM1, VCAM1, PECAM1, integrins, and cadherins [81, 82] (**Figure 1.7**). Following

a MI, studies have shown several circulating CAMs to be elevated and therefore may have a role in predicting adverse outcomes [83].

#### **1.4.7. Role of Inflammatory Cells in Myocardial Infarction**

The inflammatory response following myocardial IR injury is mediated through the coordinated activity of several types of cells, both within and distant to the infarcted area. A hallmark of patients with MI is leukocytosis, an increased number of white blood cells (WBCs) in the blood. This has been widely used as a predictor of mortality within this group of patients. Neutrophils are thought to be the first type of cells to be recruited during myocardial IR injury, followed by monocytes, mast cells, and lymphocytes (such as B- and T-cells, and natural killer [NK]-cells). Each of these cells has a distinct role within the inflammatory process during myocardial IR injury [58, 84].

##### **1.4.7.1. Role of Neutrophils in Myocardial Infarction**

Neutrophils are the most abundant type of WBC (50-75% of total WBCs) in the circulation and are a key player within the innate immune system. Their primary role as phagocytes is to internalise and kill foreign microbes and particles. In addition, they are able to release a variety of proteins and chemical mediators, which help combat infection and recruit other inflammatory cells to the site. Even in sterile injuries, such as myocardial IR injury, significant neutrophil recruitment occurs in which their phagocytic functions serve to contribute to the clearance of debris. However, the vast array of hydrolytic, oxidative, and

pore-forming molecules released by an overabundance of phagocytic neutrophils, alongside their delayed removal from the infarct site, end up causing significant collateral heart tissue destruction [60, 85, 86]. In an MI, neutrophil counts are found to be significantly raised as a result of mobilisation from the bone marrow, and this is used as a predictor of adverse outcomes and mortality [87]. Circulating neutrophil counts peak within 1-3 days and drop after day 4. Neutrophils are present within the infarcted area within hours following myocardial IR injury. In 2016, Ma *et al.* further showed that neutrophils harvested from the heart on day 1 post-MI were N1 neutrophils (pro-inflammatory), that express highly pro-inflammatory mediators, whereas those isolated between days 5-7 were N2 (anti-inflammatory) neutrophils [60, 88]. Pharmacological inhibition of neutrophil CD11/CD18 has been shown to reduce MI size in various animal models [89].

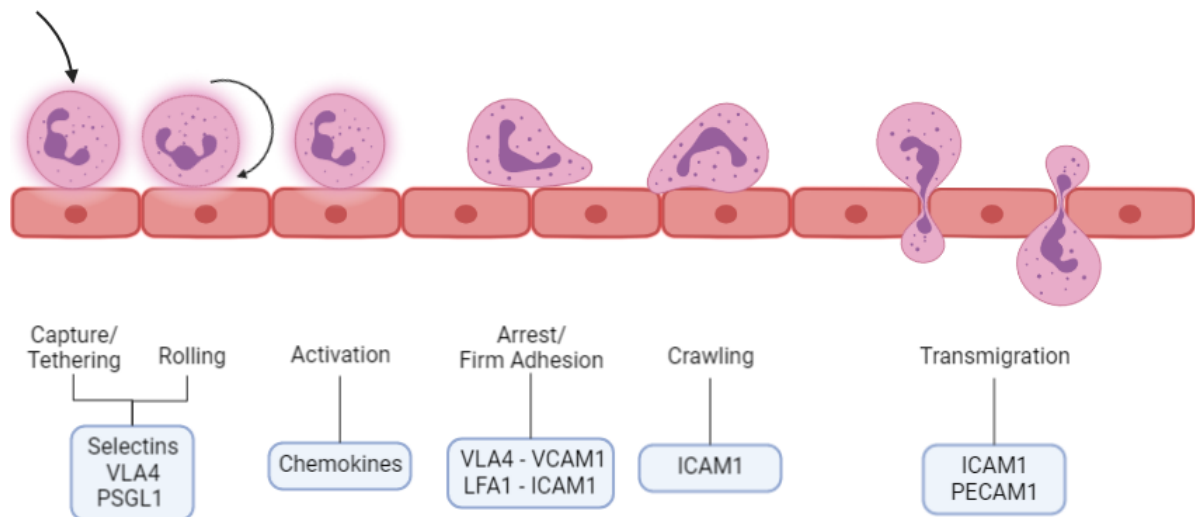


**Figure 1.7. Leucocyte adhesion cascade.** Following the release of chemokines and cytokines to attract various leucocytes, leucocytes then follow a course of events that facilitates their capture from the circulation and allows their subsequent travel across the vascular endothelium and to the site of injury. This process is referred to as the leucocyte adhesion cascade. To regulate the type and number of leucocytes infiltrating the area, this process is mediated by chemokines in the initial step and cell adhesion molecules in the remainder of the cascade. In response to a MI, this process firstly involves leucocytes tethering and rolling within the blood vessel using selectins, very late antigen 4 (VLA-4) and P-selectin glycoprotein ligand 1 (PSGL-1). This is followed by arrest and firm adhesion of the leucocyte to the endothelium using lymphocyte function-associated antigen 1 (LFA-1), vascular cell adhesion molecule 1 (VCAM-1) and intercellular adhesion molecule 1 (ICAM-1). Finally, the leucocyte transmigrates through the endothelium to the site of injury using ICAM-1 and PECAM-1 (platelet endothelial CAM-1). Created using Biorender. Adapted from [81].

#### 1.4.7.2. Role of Monocytes, Macrophages, and Lymphocytes in MI

Monocytes can differentiate into macrophages, dendritic cells, and mesenchymal progenitors, which can then further regulate the adaptive immune system's response to inflammation. There are three main subsets of monocytes in both human and mice (**Table 1.1**) [90]. In response to an MI, monocytes (from bone marrow and spleen) enter the circulation and are recruited to the site of injury via chemotaxis. Indeed, peripheral monocytosis can also be used as a predictor of adverse LV remodelling [91]. In murine studies, pro-inflammatory classical or Ly6C<sup>high</sup> monocytes arrive peaking between day 3 and 4, and are transformed into pro-inflammatory M1 macrophages, which produce proteases (MMPs), cytokines (IL-1, IL-6, TNF- $\alpha$ , IFN- $\gamma$ ), chemokines (CCL2), and growth factors to clear cell debris and initiate wound healing [92]. Thereafter, recruitment of anti-inflammatory non-classical or Ly6C<sup>low</sup> monocytes occurs, which peaks at day 7 [58, 60]. M1 macrophage numbers decline, and M2 anti-inflammatory macrophages coordinate wound healing in this reparative phase. The extended presence of M1 macrophages can exacerbate the pro-inflammatory phase, extend damage beyond the original infarcted area, and cause adverse LV remodelling. This may explain why their pharmacological inhibition has been shown to be cardioprotective [60, 93]. Additionally, monocytes can differentiate into antigen presenting dendritic cells and initiate the adaptive immune system through production of chemokines and cytokines (IFN- $\gamma$ , IL-6) that stimulate the activation of T cells [94, 95].

Lymphocytes can induce a cell-mediated cytotoxic innate immune response, and various subsets are involved. NK cells and their receptor expression were seen to be significantly

reduced following a MI, and recent studies showed these cells to have a protective role in atherosclerosis [96]. Both T and B lymphocyte sub-sets have been shown to infiltrate the site of injury in animal models of MI. Following an acute MI, patients display an increase in pro-inflammatory CD4<sup>+</sup> Th1 and cytotoxic CD8<sup>+</sup> T cells and a reduction in anti-inflammatory and protective CD4<sup>+</sup> Th2 cells. Prolonged presence of the harmful lymphocytes was associated with a worsened prognosis [97, 98]. An increase in peripheral B cells was also noted in MI with mature B cell infiltration peaking at around day 5. In 2013, Zouggari *et al.* showed that B cells secrete CCL7 that mobilizes bone marrow Ly6C<sup>high</sup> monocytes to the site of injury, which in turn induces further tissue damage. They also demonstrated a potential therapeutic role following B cell genetic depletion, as evidenced by reduced systemic inflammation, LV remodelling and MI size [99].

MONOCYTE SUBSETS	
HUMAN – based on their cell surface expression of CD14 and CD16	MICE – based on cell surface expression of lymphocyte antigen 6 complex (Ly6C)
<b>Classical – CD14<sup>++</sup>/CD16<sup>-</sup></b> 80-95% of circulating monocytes, highly phagocytic and scavenger cells, high expression of CCR2 (chemokine receptor)	<b>Ly6C<sup>high</sup></b> Pro-inflammatory and express high levels of CCR2 (homologue of classical monocytes in humans)
<b>Intermediate – CD14<sup>++</sup>/CD16<sup>+</sup></b> 2-8% of circulating monocytes, pro-inflammatory, generate ROS, key role in atherosclerosis	<b>Ly6C<sup>middle</sup></b> Pro-inflammatory and express high levels of CCR2 (homologue of classical monocytes in humans)
<b>Non-classical – CD14<sup>+</sup> CD16<sup>++</sup></b> 2-11% of circulating monocytes, patrol the endothelium in search of injury, low expression of CCR2	<b>Ly6C<sup>low</sup></b> Involved in tissue repair and patrolling and express low levels of CCR2 (homologues of non-classical monocytes in humans)

Table 1.1. Monocyte subsets in humans and mice.

#### **1.4.7.3. Role of Platelets in a Myocardial Infarction**

Platelets have been well characterised for their role in thrombosis. More recently, they have been recognised to play a role in inflammation as participants in the innate immune response by aggregating in the injured area, localising the inflammatory response, and contributing to the production of a provisional matrix. In an inflammatory response such as an acute MI or post-reperfusion, platelets secrete inflammatory mediators, including cytokines and chemokines, as well as platelet-derived growth factor (PDGF). In response to myocardial IR injury, platelet pro-inflammatory activity up-regulates ICAM-1, VCAM-1, and selectins on leucocytes, induces ROS production, activates macrophages and cytotoxic lymphocytes, and increases circulating microparticle production. They can also interact with and modulate the activity of leucocytes by forming platelet-leucocyte (P-L) aggregates mediated by P-selectin/PSGL-1 interactions. A peripheral blood increase in P-L aggregates has been observed in patients following acute MI, and it has been suggested that circulating P-L aggregates could be used as an early biomarker for patients with MI [100]. Inhibition of P-L aggregates using anti-platelet treatments was able to reduce inflammation and the risk of onward complications in patients with MI.

#### **1.5. Therapeutic Targets for Inflammation in a Myocardial Infarction**

A potential therapeutic target for limiting infarct size, reducing adverse ventricular remodelling, and enhancing prognosis could be to target the pro-inflammatory responses observed following myocardial IR injury [60, 101]. Several studies and clinical trials have

targeted individual elements in the inflammatory adhesion cascade and have shown some benefits in preclinical animal models. The effects of inflammatory cytokines on the immune system are pleiotropic, which makes them an ideal therapeutic target for reducing inflammation. Several clinical trials have been conducted that target inflammatory cytokines, mainly IL-1, IL-6 and TNF- $\alpha$ .

### 1.5.1.1. Targeting Interleukin-1 in Myocardial Infarction

There is significant evidence to suggest that IL-1 (and its extended family members – see **Section 1.5**) are canonical DAMPs of the immune system as they possess all of the characteristics expected of DAMPs and initiate inflammation in a manner strikingly similar to that utilized by the other major category of inflammatory triggers, namely PAMPs [102]. IL-1 also acts at the apex of the inflammatory cascade. For these various reasons, it has been considered an ideal target for inflammatory disorders, including CVD. Inhibition of IL-1 in experimental models of myocardial IR injury have been largely successful. Toldo and colleagues (2012) showed a significant reduction in infarct size and improvement in LV ejection fraction in mice undergoing myocardial IR injury following treatment with anakinra, a recombinant human IL-1 receptor antagonist (IL-1Ra) [103]. Similar results were seen in a study in rat hearts, where overexpression of IL-1Ra protected the myocardium against IR injury by attenuating cell death and reducing infarct size through its anti-inflammatory properties on neutrophils [104].

There have also been several clinical studies that have looked at the effects of using anakinra (currently used for the treatment of rheumatoid arthritis) or canakinumab, a

monoclonal antibody against IL-1 $\beta$ , in patients with either STEMI or NSTEMI. In 2010, Abbate and colleagues reported a double-blinded randomized pilot clinical trial for anakinra to assess LV remodelling in 10 patients with STEMI and showed improved LV end-systolic volume index (LVESVi) with treatment [105]. This was further expanded in 2013 to 25 patients, and while serum CRP levels were suppressed, LVESVi remained unchanged between the treatment and placebo groups [106]. In a follow-up meta-analysis, anakinra treated patients had a reduced risk of developing heart failure and death [107]. In 2014, a larger clinical study was initiated on 99 patients with STEMI, and while systemic inflammation decreased, LV end-systolic volume, LV end-diastolic volume and LVESVi were not different from the placebo-treated group [108]. In 2015, Morton and colleagues published a double-blinded randomized phase II clinical trial of anakinra in 182 patients with NSTEMI. They found that although CRP levels decreased, there was actually a significant increase in adverse outcomes (recurrent MI, stroke, and death) after one year [60, 109].

More recently in 2017, Ridker and colleagues reported a double-blinded randomized phase III clinical trial to test canakinumab, an IL-1 $\beta$  monoclonal antibody, in 10,061 high-risk patients with the established atherosclerotic disease who had already survived a MI. This canakinumab anti-inflammatory thrombosis outcome study, or CANTOS trial, demonstrated a significantly lowered inflammatory burden as evidenced by reduced CRP and importantly had no effect on LDL (low-density lipoprotein) cholesterol. Overall, the trial showed a significant reduction in the incidence of nonfatal MI, stroke, or cardiovascular death during the median 3.7-year follow-up. This was the first major clinical trial to show that targeting inflammation can confer modest cardiovascular benefits in very

high-risk patients and has been credited with providing an exciting glimpse at the potential for using anti-inflammatory therapies for treating CVD.

#### **1.5.1.2. Targeting Neutrophils in Myocardial Infarction**

Neutrophils, as previously described, have a key role in mediating IR injury following an acute MI. Inhibition of the  $\beta_2$  integrin receptor complexes has been shown to reduce neutrophil adhesion and reduce MI size in various animal models [89]. There have been two major clinical studies that have targeted neutrophils in patients with MI. In 2001, Baran and colleagues reported a double-blinded randomized clinical trial (LIMIT AMI trial) for a monoclonal anti-CD18 antibody (rhuMAb CD18) in 394 patients with MI, also receiving a plasminogen activator, aspirin, and heparin. However, they were unable to demonstrate any beneficial effect on multiple cardiac end points, including infarct size and coronary blood flow [110]. They suggested that one of the reasons for the failure of anti-CD18 therapy in humans was that the duration of ischemia was so long that endothelial cell barrier function had already failed. The following year, Faxon et al., reported a double-blind randomized clinical trial using a humanized monoclonal antibody that inhibits both CD11a/CD18 and CD11b/CD18 interactions (Hu23F2G – LeukoArrest) in 420 patients prior to primary PCI. Again, treatment with this antibody had no effect on MI size, although the authors accepted that their study was underpowered [111]. Moving forward, a potential therapeutic strategy may be the polarization and modulation of neutrophils from pro-inflammatory N1 to anti-inflammatory N2 neutrophils in the early stages of inflammation.

### 1.5.2. Need for a New Anti-inflammatory Target in Myocardial Infarction

Reperfusion injury post-PCI remains one of the key unmet clinical needs in cardiology. Despite experimental studies identifying a number of components of the thromboinflammatory process to be beneficial in reducing infarct size, these strategies have not translated well in clinical trials. This may be due to differences in the design of experimental studies, treatment potency, time-point of therapeutic intervention and dosing in animals and the involvement of different pathophysiological mechanisms in animal models, all of which can play a major role in affecting clinical outcomes. Furthermore, experimental models do not usually fully recapitulate the mechanisms of pathogenesis in humans. For instance, animal models do not account for the fact that the majority of patients with MI patients are elderly, have additional co-morbidities such as diabetes and hypertension and are often already on multiple medications. Many animal models also do not consider the differences in the outcomes for MI between male and female patients [60]. Therefore, in addition to identifying a new anti-inflammatory target, it is imperative that these are tested in animal models that better replicate the clinical situation.

Given that cytokines are major contributors to the pathogenesis of various inflammatory and immune diseases, they have received considerable interest in recent years as potential therapeutic targets [112]. To date, IL-1, TNF $\alpha$  and IL-6 have been the most researched targets for various inflammatory diseases and have been trialled in humans initially for treating sepsis and then later for rheumatoid arthritis, Crohn disease, and psoriasis. Infliximab and etanercept, monoclonal antibodies that neutralise the action of TNF $\alpha$ , are

used clinically for treating many inflammatory disorders. Furthermore, Canakinumab, an IL-1 $\beta$  monoclonal antibody, is used to treat inflammatory disorders such as gout and also reduce secondary events in patients with prior MI as described in the CANTOS trial. However, whether targeting cytokines can prevent thromboinflammatory events that take place within the coronary microcirculation during myocardial IR injury, and preserve blood perfusion in the heart, has not been determined *in vivo* either experimentally or clinically. Hence the search for a cytokine target that maintains perfusion within the coronary microcirculation, limits myocardial damage, reduces infarct size and improves patient prognosis after reperfusion is worthwhile.

### 1.6. Therapeutic Targets in the Interleukin-1 Super Family

IL-1 is actually part of an IL-1 superfamily (IL-1F) that is made up of 11 pro- and anti-inflammatory cytokines that modulate the innate immune response primarily through their manipulation of integrin expression on target cells and promotion of cytokine release from stromal cells). Pro-inflammatory members include IL-1 $\alpha$ , IL-1 $\beta$ , IL-18, IL-36 $\alpha$ , IL-36 $\beta$ , IL-36 $\gamma$  and IL-33, while anti-inflammatory members can be further divided into immunosuppressive cytokines (IL-37, and IL-38) and antagonist cytokines (IL-1Ra - antagonist for IL-1 $\alpha$  and IL-1 $\beta$ , and IL-36Ra - antagonist for IL-36 $\alpha$ , IL-36 $\beta$  and IL-36 $\gamma$ ). All the IL-1 family members, except for IL-1Ra, are initially synthesized as a precursor protein which needs to be proteolytically cleaved into a shorter form, termed a mature protein [113]. There is a significant body of literature on some of these cytokines, particularly the IL-1 cytokines (IL-1 $\alpha$  and IL-1 $\beta$ ), both of which are agonists found in the cytoplasm and have

been shown to be expressed in several cells, including neutrophils, monocytes, macrophages, and hepatocytes. However, some members have only recently been discovered, and the literature is relatively sparse on their function (IL-36 cytokines) [114]. Importantly, these are frequently the first and most upstream cytokines produced in response to injury, thus good targets for intervention for inflammatory disorders [115]. Since IL-1F members critically mediate inflammation, they may be key mechanistic contributors causing myocardial microcirculatory disturbances. In the last decade, genes encoding a novel cytokine cluster, namely IL-36, with structural and functional similarities to IL-1 were discovered [116, 117].

### 1.6.1. Interleukin-36: Characterization and Expression

IL-36, a relatively novel IL-1 family member, was identified approximately 20 years ago and is involved in pro-inflammatory mediator production, activation of immune cells, and antigen presentation [118]. This subfamily is composed of 5 members with different effects on the IL-36 receptor (IL-36R); IL-36 $\alpha$  (IL-1F6), IL-36 $\beta$  (IL-1F8), and IL-36 $\gamma$  (IL-1F9) cytokines have agonistic effects, while IL-36Ra (IL-1F5) and IL-38 (IL-1F10) have antagonistic effects. IL-36R, also known as the interleukin-1 receptor-like 2 (IL-1RL2), is a ligand-binding chain that is composed of TIR (Toll/IL-1 receptor) domain in the cytoplasm and an immunoglobulin domain in the extracellular space [119]. Like the IL-1 cytokines, the gene which encodes IL-36 cytokines and IL-36R is also found on human chromosome 2 and IL-36Ra is encoded by gene *IL-36RN* [120]. As well as amplifying IL-1 effects, IL-36 is also a mediator of inflammation in its own right. Indeed, its critical role in psoriasis, equalling if

not surpassing that of IL-1, is well established with emerging roles in Crohn disease, airway infections and rheumatoid arthritis recently identified [121-123].

IL-36R and its cytokines are predominantly expressed on the body's external barriers such as dermal, bronchial, oesophageal, and intestinal epithelium. They are constitutively expressed on keratinocytes, microglial cells, dendritic cells, T cells, and other immune cells, thus indicating their importance in homeostasis and inflammation. Furthermore, IL-36 cytokines and IL-36R are expressed on and released from a wide range of immune cells, including neutrophils, monocytes, macrophages, and lymphocytes, and their expression is inducible in response to inflammation, infection, or injury [118, 124-126]. IL-36 cytokines are also regulated through the actions of several other cytokines and inflammatory mediators. For example, cultured human keratinocytes exposed to IL-17, IL-22, TNF- $\alpha$  or IFN- $\gamma$  were able to induce the synthesis of one or more of the three IL-36 cytokines [127]. Stimulation of bronchial epithelial cells with cytokines, smoke, viruses, or bacteria-induced expression of IL-36, mainly IL-36 $\gamma$  [128].

### 1.6.2. Interleukin-36: Signalling Pathway

The signalling pathway of IL-36 members is similar to IL-1 $\alpha$  and IL-1 $\beta$ . Ligand engagement results in the activation of the adaptor protein MyD88, various kinases such as MAPK which then activate the transcription factor NF- $\kappa$ B. NF- $\kappa$ B will traffic to the nucleus and alter the transcription of numerous genes, including those that encode pro-inflammatory cytokines, ultimately leading to subsequent infiltration of immune cells (**Figure 1.8**) [118]. Activation of IL-36R requires heterodimer formation with the IL-1 receptor accessory protein (IL-

1RacP), the common accessory protein of the IL-1 family, which is recruited following agonist ligand binding. IL-36R is found in two forms: a precursor (~85kDa) and active form (~65kDa). The precursor needs to be glycosylated for the receptor to be able to signal [126]. Similarly, the N-terminus of IL-36 cytokines - made up of 9 amino acids - must be cleaved in order for the cytokine to bind to the receptor with high affinity. This cleavage enhances their bioactivity over 10,000-fold [129]. In 2016, Henry *et al.* showed that the bioactivity of IL-36 $\alpha$ , IL-36 $\beta$ , and IL-36 $\gamma$  was increased by ~500-fold due to the activity of neutrophil-derived proteases such as cathepsin G, proteinase-3, and elastase. The same study also showed that within psoriatic skin, these neutrophil proteases contributed to the N-terminus cleavage of the IL-36 cytokines [130]. Additionally, IL-36 cytokines were activated following their incubation with activated neutrophil supernatants, further suggesting that neutrophil proteases released in response to DAMPs or PAMPs activate IL-36 cytokines [130, 131].

### 1.6.3. Interleukin-36: Effect on the Immune System

Over the last decade, most of our knowledge on the activity of IL-36 cytokines has been obtained by understanding how they can drive responses in human keratinocytes. Keratinocytes from healthy patients were shown to be a potent source of neutrophil, macrophage, and T cell chemokines (such as CXCL8, CCL3, CCL4 and CCL20) following their activation with IL-36 $\alpha$ , IL-36 $\beta$ , and IL-36 $\gamma$  [132]. They were also able to upregulate MAPK signalling genes (such as IRAK2), IL-8 and MMP9 suggesting an amplified inflammatory response involving T helper cell signalling [133]. Expression of interferon encoding genes

are also increased in keratinocytes following activation with IL-36 cytokines. Additionally, IL-36 $\alpha$  and IL-36 $\gamma$  were able to be up-regulated in an autocrine manner [128, 134]. Furthermore, keratinocytes activated with IL-36 $\beta$  also upregulate the expression of IL-17 and TNF- $\alpha$  [135]. ECs activated with IL-36 $\gamma$  up-regulated IL-8, VCAM-1, and ICAM-1, thus suggesting that IL-36 cytokines have pro-inflammatory effects on both ECs and keratinocytes [118, 136-139].

The effect of these cytokines on immune cells has also been studied. Neutrophil recruitment was significantly decreased in IL-36 $\alpha^{-/-}$  mice which was associated with a downregulation in CXCL1 [127]. IL-1 $\alpha$ , IL-1 $\beta$  and IL-6 were all up-regulated following monocyte culture with IL-36 cytokines [132]. Murine dendritic cells and monocyte-derived dendritic cells both induced cytokine and chemokine production following their activation with IL-36 cytokines [140, 141]. In 2017, Harusato *et al.* showed that culturing CD4 $^{+}$  T cells from IL-36R $^{-/-}$  mice with IL-36 $\gamma$  resulted in the inhibition T<sub>reg</sub> cell differentiation when compared to wild-type mice [142]. Taken together, these results suggest that IL-36 cytokines and receptors play an important role in the immune system response.

### 1.6.4. Antagonism of the Interleukin-36 Receptor

Antagonism of the IL-36R can occur through either of the endogenous inhibitors, IL-36Ra or IL-38. They work by preventing agonist binding to the IL-36R and subsequently block the dimer formation, which is required to trigger downstream signalling (**Figure 1.8**) [119, 126]. Similar to the other cytokines, IL-36Ra and IL-38 must also be cleaved into a mature active form. Studies suggest that neutrophil-derived elastase is an important mediator of this

modification for IL-36Ra. The mechanism responsible for IL-38 cleavage remains unclear; there is no identified caspase-1 cleavage site for IL-38. Furthermore, IL-1Ra and IL-36Ra share a 52% homologous sequence of amino acids, whereas IL-38 shares a 43% and 39% homology with IL-36Ra and IL-1Ra, respectively. IL-38 has also been shown to bind to IL-1R1 with low affinity [119, 143]. IL-36Ra and IL-38 have been shown to have similar effects on immune responses. Healthy human PBMCs cultured with either recombinant IL-38 or IL-36Ra resulted in the inhibition of candida-induced T cell cytokines (IL-22 and IL-17) synthesis. Both were also able to decrease IL-8 synthesis induced by IL-36 $\gamma$ , but this decrease was greater with IL-36Ra [143].

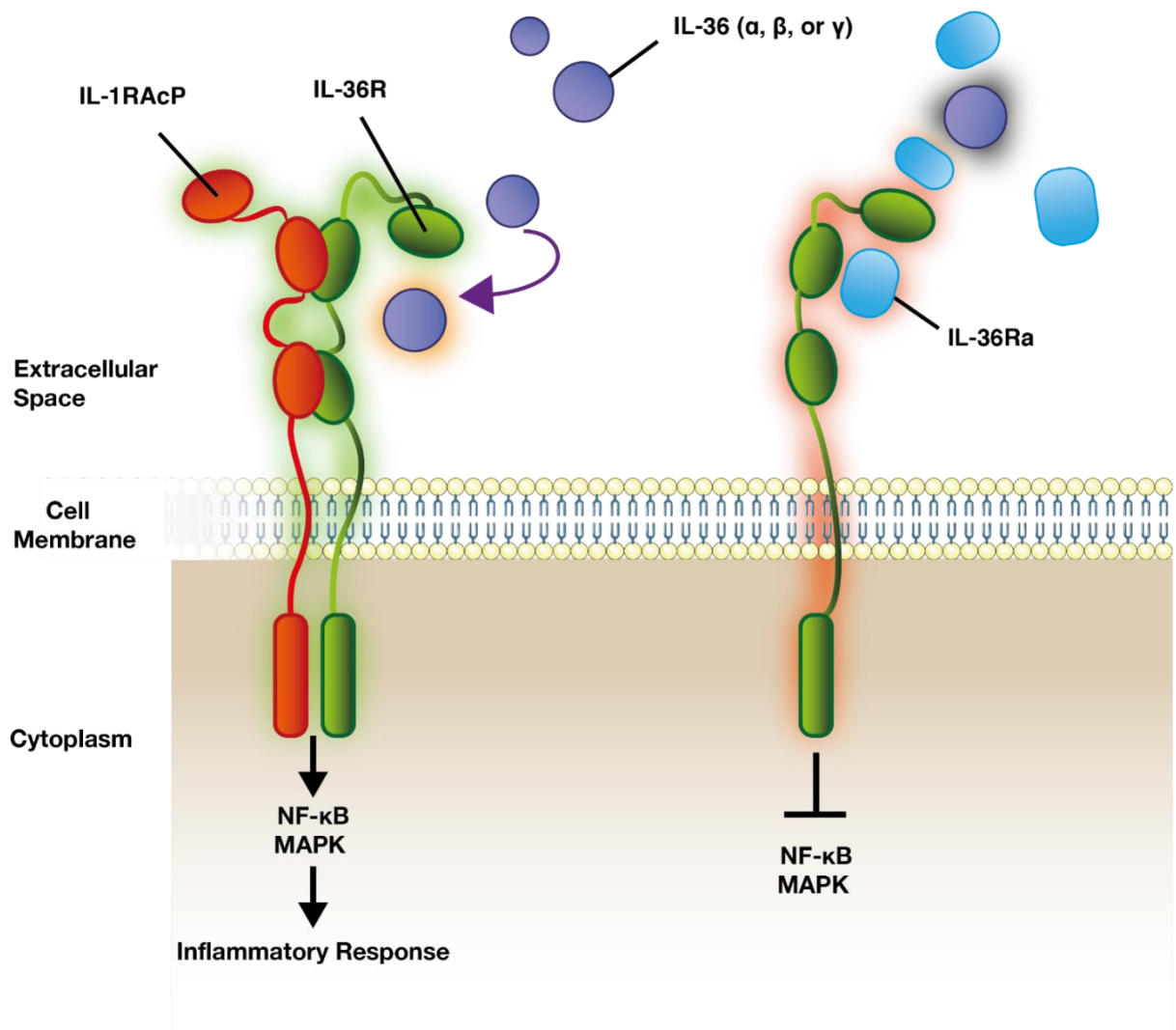


**Figure 1.8. IL-36/IL-36R pathway.** IL-36 cytokines (IL-36 $\alpha$ , IL-36 $\beta$  or IL-36 $\gamma$ ) bind to the same receptor (IL-36R) which then forms a heterodimer with IL-1 receptor accessory protein (IL-1RAcP). This formation triggers a downstream signalling cascade by activating the nuclear factor kappa-light-chain-enhancer of activated B cells (NF- $\kappa$ B) and mitogen-activated protein kinase (MAPK) to induce an inflammatory response through the release of pro-inflammatory cytokines. The receptor antagonist (IL-36Ra) acts by blocking heterodimer formation and preventing the formation of the signalling complex. Created using Biorender. Adapted from [119]

### 1.6.5. Interleukin-36: Role in Inflammatory Diseases

Members of the IL-36 family have been shown to play a key role in many inflammatory diseases, including psoriasis, rheumatoid arthritis, Crohn disease, psoriatic arthritis, and systemic lupus erythematosus (SLE). Indeed, expression levels of IL-36 cytokines and its receptor are significantly increased in these conditions. Boutet *et al.* (2016) found that human skin biopsies from patients with psoriasis had an increased expression of IL-36 $\alpha$ , IL-36 $\gamma$ , and IL-36Ra. This was also correlated with the enhanced presence of other cytokines and immune cells such as IL-1 $\beta$  and T helper cells [144]. Levels of IL-36 cytokines were also increased in the serum of patients with psoriasis, and these levels correlated with disease severity [145]. In 2019, a phase 1 clinical trial was conducted on 7 patients with generalized pustular psoriasis episodes using a single dose of a monoclonal antibody against IL-36R (BI 655130 – 10mg/kg). Levels of CRP in these patients significantly decreased, and pustules were entirely cleared in 6 patients within 2 weeks, thus suggesting that BI 655130 may reduce the severity of pustular psoriasis [146]. In 2011, Marrakchi *et al.* showed that mutations in IL-36Ra led to pustular psoriasis [147]. This was further subsequently supported in an induced-psoriasis model, whereby IL-36Ra<sup>-/-</sup> mice expressed IL-17, IL-22 and IL-23 and developed skin lesions, whereas wild-type mice did not [148]. Deficiency in IL-36Ra (DITRA), resulting from a mutation in the *IL36RN* gene, can be life-threatening to patients suffering from systemic inflammation and episodes of generalized pustular psoriasis [149].

Boutet *et al.* (2016) found that synovium obtained from patients with rheumatoid arthritis contained increased levels of IL-36 $\alpha$ , IL-36 $\beta$ , IL-36 $\gamma$ , IL-36Ra and IL-38, which were

correlated with increasing levels of IL-1 $\beta$ . The same study also identified increased levels of IL-36 $\alpha$  and IL-36 $\gamma$  in colonic biopsies specimens which were obtained from patients with Crohn disease, and the disease severity correlated with the magnitude of the increase [144]. Furthermore, biopsies of nephritic kidneys from patients with SLE showed increased levels of IL-36 $\alpha$  and IL-36 $\gamma$ , which correlated with the disease severity index [150]. In 2017, Chu *et al.* treated SLE mice with murine recombinant IL-38 and saw a significant decrease in circulating levels of IL-17 and IL-22, and a decrease in the manifestations of the disease when compared with untreated mice [151].

### 1.6.6. Interleukin-36: Role in IR Injury

Although there has been extensive research on IL-36 as a highly pro-inflammatory cytokine in several inflammatory diseases and tissues, as discussed above, there have been no investigative studies on IL-36 in CVD until recently. In 2020, Luo *et al.* studied the effect of IL-36R deficiency in a rat cardiopulmonary bypass model where IR injury also occurs. IL-36R knockouts had significantly decreased infiltration of inflammatory macrophages as determined immunohistochemically, reduced oxidative stress, reduced cardiac myocyte apoptosis, and improved systolic function [152]. Recent work has also examined the potential role of IL-38 in the heart following MI. Plasma IL-38 concentrations were shown to increase during an acute MI (peaking at 24 hours) and significantly decrease post-reperfusion [153]. In 2019, Wei *et al.* (2019) studied the effects of IL-38 on ventricular remodelling following an acute MI in mice. They showed that IL-38 was inducibly expressed post-MI in the infarcted myocardium, and when mice were injected with recombinant

mouse IL-38, decreases in inflammation, cardiac fibrosis, and myocardial injury were observed. Thus, IL-38 may improve cardiac remodelling following MI [154]. These recent studies suggest a potentially novel role for IL-36 in modulating cardiac IR injury. However, despite recent increases in our understanding of how the IL-36 / IL36R pathway is highly pro-inflammatory in skin and lungs, we are still at a very early stage in our current understanding of its *in vivo* biology, and only a handful of studies have recently investigated a role for this pathway in the heart.

### **1.7. Risk Factors Associated with Myocardial Infarction – Age and Sex**

#### **1.7.1. Ageing and Myocardial Infarction**

According to projections from the United Nations, the world's aged population (>60 years) will increase from 10% in 2000 to 21% by 2050 [155]. The ageing process is not only characterised by well-known ageing symptoms (such as wrinkles, decrease in fertility, grey/white hairs, frailty, and sensory losses) but include more biological characteristics such as cellular senescence, immunosenescence, inflammaging, altered intracellular communications, and metabolic changes. These result from a wide range of environmental, genetic, epigenetic and stochastic factors [156]. A major consequence of ageing is the fact that the prevalence of IHD increases in patients over 50, making age a major risk factor independent of other risk factors. Moreover, age is associated with increased myocardial damage and a worsened prognosis following an acute MI [157]. Experimental studies have demonstrated a significantly larger infarct size and increased susceptibility to IR injury in

aged mice with coronary blood flow restoration post-ischaemia much lower in senescent rats [158, 159]. Interestingly, increased infarct size is not seen in aged humans following an acute MI [160, 161], but they do lose their ability to respond to cardioprotective interventions such as ischaemic preconditioning and have an increased rate of “no reflow” [162].

### 1.7.1.1. Inflammaging

The recently coined term ‘*inflammaging*’ explains the phenomenon that ageing is accompanied by a chronic low-grade, systemic up-regulation of inflammation that persists in the absence of an overt inflammatory stimulus [163, 164]. It is thought to be driven by an increase in circulating neutrophils, production of pro-inflammatory cytokines (TNF- $\alpha$ , IL-6, and CRP), ROS, and changes in the functional structure of other cells, including platelets [165]. These changes lead to irregular responses to acute inflammation and long-term gradual tissue damage [166-169]. Inflammaging may also result from the accumulation of cell debris (such as DAMPs or macromolecules) with age as a result of an impaired removal pathway and/or increased production following infections or injuries.

The main mechanisms which are involved in the inflammaging process are thought to be the activation of the NF- $\kappa$ B and NLRP3 inflammasome pathways to induce the production of pro-inflammatory mediators. Mitochondrial dysfunction and DNA damage also play a role through the excess production of ROS. Neutrophil chemotaxis has also been suggested to be impaired with age, which would result in continuous damage to the tissue through the release of destructive mediators and ROS as they are unable to transmigrate away [170,

171]. The most common cytokine to be increased in age-related diseases is IL-6 and is currently used as an inflammatory marker and a hallmark for chronic disorders. IL-1 and TNF- $\alpha$  are also commonly increased in age-related diseases, and their addition to fibroblasts *in vitro* accelerates their senescence [164].

Inflammaging may contribute to the enhanced age-related cardiovascular risk and poorer outcomes following an MI. However, little is known about how age impacts coronary microcirculation in health or following myocardial IR injury.

### 1.7.2. Biological Sex and Myocardial Infarction

Sex differences in CVD outcomes have been widely studied. The general consensus suggests that males develop CVD 7-10 years earlier than females and have worse age-matched outcomes, including a higher risk of mortality. In a 2014 study, the age-adjusted death rate per 100,000 person-years for heart disease was 38% less in women than in men. However, key sex differences were observed in one manifestation of CVD, namely in acute MI [172]. Men have approximately twice the risk of suffering an MI compared with women. Not only is the incidence of MI lower in women, but they are also generally older than men when they experience their first MI. Indeed, in the global case-control INTERHEART study spanning 52 countries, women were seen to experience their first MI on average 9 years later than men [173].

This has often been misinterpreted as females being 'protected' against heart disease. It is well established that overall, women have a longer stay in the hospital, have a higher risk

of hospitalized death, and have a greater incidence of mortality at follow-up (1-year post-MI) [174, 175]. Moreover, younger women who suffered from acute MI are at a higher risk of mortality than age-matched men [176]. Interestingly, the symptoms of an MI are also generally different, with men tending to have a crushing chest pain sensation with women experiencing pain in the abdomen or under the breastbone resulting in potential misinterpretation of their condition [177]. These differences are summarised in **Table 1.2**.

Cardiac function is significantly impacted by sex hormones such as oestrogen and testosterone, produced in both men and women. Prior to the menopause, the risk of an MI is much lower in women than men of the same age. However, this risk is significantly increased after menopause when circulating levels of oestrogen are reduced. For this reason, oestrogen has been deemed to be cardioprotective. There are two types of oestrogen receptors (ER), ER $\alpha$  and ER $\beta$ , in which oestrogen binds to promote cell survival. The cardioprotective effect of oestrogen is phosphoinositol 3-kinase (PI3K) and protein kinase B (Akt) dependent. When Akt is activated and present in the nucleus, it promotes cardiac myocyte survival. Levels of activated Akt are seen to be higher in young women in comparison with age-matched men and post-menopausal women [178, 179]. ER $\beta$  is expressed in the heart at greater levels in men than in women, while ER $\alpha$  is equally expressed in both sexes [177]. In female mice, both ER $\alpha$ , and ER $\beta$  are required for the cardioprotective effects against myocardial IR injury [180].

<b>Myocardial Infarction – men vs women</b>
Women with MI generally older than men – 72 vs 62 years old
Women generally older than men when they have their first MI which is experienced on average approximately 9 years after men
Women generally have higher rates of hypertension, diabetes mellitus and hyperlipidaemia - less likely to be smokers
Women more likely to have non-specific symptoms such as non-chest pain (pain in jaw, throat, neck, shoulder, arm, hand, back), mild pain, nausea, shortness of breath – cold-sweats less likely
Delayed presentation to the hospital - women reported to be less likely than men to believe that they are having a heart attack when they experience symptoms of MI
Men have roughly twice the risk of MI compared with women
Lower incidence of MI in women but a higher mortality
Risk of mortality more pronounced in younger women than older women
MINOCA more common in women, especially younger women – less extensive obstructive and more diffuse coronary artery disease compared with men, who typically develop plaque build-up in the largest coronary arteries – the microvascular involvement in women may be related to endothelial reactivity, low endogenous oestrogen levels, coagulation disorders, abnormal inflammatory reactions
Longer stay in hospital for women
Higher risk of in-hospital mortality in women – could be linked to have more co-morbidities and generally being older than men
Greater incidence of mortality at a 1 year follow-up in women

**Table 1.2. Differences in the incidence, symptoms, and prognosis of acute myocardial infarction between men and women.**

### 1.7.2.1. Sex Hormones

The higher incidence of MI in men led to the earlier view that testosterone had detrimental effects on the heart. Although large observational and randomized studies supported this, more recent studies have suggested a cardioprotective role for testosterone. The effects of testosterone on the heart are less understood than those of oestrogen, although testosterone and oestrogen have been shown to have opposing effects on cardiac function and remodelling in mouse models of MI [181]. Production of testosterone increases in post-menopausal women, which further supports a link between testosterone and an increased risk for CVDs [182]. Similarly, studies on weightlifters who use anabolic steroids (altered by-products of testosterone) showed an increased risk of CVDs such as MI and sudden cardiac death through impaired diastolic function and cardiac hypertrophy [183].

### 1.7.2.2. Sex Differences in Immune Responses

Sex differences in the immune response is a well-established phenomenon and is seen in many diseases affecting both the innate and adaptive immune responses. For example, males have a larger number of NK cells in the circulation than females [184]. Neutrophils and macrophages from females have a greater phagocytic and activation activity than in males. Additionally, macrophage IL-10 production was higher in females, while macrophage pro-inflammatory cytokine production was greater in males [185]. Alterations in receptor expression may underlie some of the sex-dependent differences in immune responses. TLR4, which was found to be an integral receptor in inducing inflammation in

myocardial IR injury, has been shown to be expressed at higher levels on human male neutrophils than females, which also produced more TNF $\alpha$  when compared to females [186]. Moreover, peritoneal macrophages from male mice were seen to express higher levels of TLR4 and chemokines following LPS activation than their female counterparts [187]. This increased TLR4 expression on male immune cells more than in female cells, leading to greater inflammatory responses in males following LPS [188].

Similarly, adaptive immune cell counts, and their activity are also sex-dependent. Pre-puberty, the majority of adaptive immune cell populations and ratios are equal between males and females. However, a larger number of B cells and activated T cells as well as a higher count of CD4<sup>+</sup> T cells, have been observed in females (adulthood and persisting with age). Females also have an altered CD4/CD8 T cell ratio (increased towards CD4), greater T cell proliferation and an increased cytotoxic T cell activity, whereas males have a higher CD8<sup>+</sup> T cell and T<sub>reg</sub> cell number [188]. In general, the innate and adaptive immune responses within humans are stronger in adult females than in adult males. Pathogens are cleared faster in adult females, but this increases their susceptibility to autoimmune diseases and inflammation [188].

## 1.8. Summary

### 1.8.1. Imaging the Coronary Microcirculation in a Beating Heart *in vivo*

Treatment of MI focuses on rapidly re-establishing perfusion following a blockage in one or more of the coronary arteries. However, whilst necessary to end the period of ischaemia, reperfusion paradoxically worsens inflammation causing additional tissue damage beyond that caused by ischemia alone. Reperfusion, therefore, is responsible for approximately 50% of the final infarct size. Restoring blood flow in occluded coronary arteries can still be associated with sub-optimal myocardial perfusion, leading to worse outcomes than in patients with more extensive perfusion recovery. This indicates inadequate perfusion at the level of the coronary microcirculatory, which likely contributes to the additional tissue damage. Increased clinical recognition of the importance of coronary microcirculation has meant identifying strategies to improve potential perturbations within it have gained recent attention. However, current clinical imaging tools cannot resolve these microvessels, and so little is known about the full range of cardiac microcirculatory responses to IR injury *in vivo*.

As stated earlier, most of our understanding of microvascular dysfunction post-reperfusion injury has been obtained from heart tissue imaged histologically for morphological deterioration, inflammatory cell infiltration, and infarct size. However, these static snapshots provide no indication of the real-time kinetics of deleterious thromboinflammatory cell recruitment. Ultimately, restoration of blood flow and ventricular muscle perfusion is key to the survival of the myocardium, yet static assays cannot 'show' dynamic events such as blood flow. Hence critical information on

microvessel integrity, functional capillary density or whether flow is present in the heart or not needs to be acquired using *in vivo* imaging methods.

Intravital microscopy (IVM) is an experimental imaging modality used to experimentally image the microcirculation of solid organs (e.g. liver, kidney, gut) or transparent tissues (e.g. mesentery, cremaster muscle) in anaesthetised rodents in real-time. It has previously been used to investigate cellular events in areas such as immunology, tumour biology and neurology, and much of our existing knowledge of the impact of IR injury on microcirculation has been obtained using transparent preparations such as the cremaster muscle or gut mesentery [189-191]. The advantage of IVM is the ability to image a single cell and track its movement in real-time *in vivo* [192]. However, the application of this powerful technique to the beating heart in rodents has been challenging primarily due to the cardiac cycle and respiratory-related movement of the heart in all three dimensions, thus imposing a practical limitation on the imaging resolution of the coronary microvasculature as reviewed by Neena Kalia (2021) [51]. As such, other surrogate tissue beds, particularly the cremaster, have been used as models of the cardiac microcirculation [193]. However, coronary microcirculation is unique in both its anatomical and physical properties, particularly its contractile activity, which compresses coronary capillaries during systole, reducing their diameter up to 20% [194, 195]. As such, the impact of IR injury and the mechanisms by which therapeutic vasculoprotective strategies act, may vary in a site-specific manner. This research aims to utilise this method to image the mouse beating heart and ascertain the impact of IR injury specifically at the level of the coronary microcirculation *in vivo*.

### 1.8.2. Requirement for novel anti-inflammatory targets

Evidence suggests that a persistent and prolonged pro-inflammatory response, as observed during IR injury, severely impacts adverse LV remodelling and infarct size. Therefore, therapeutic targets that either modulate inflammation and/or prevent additional microvascular disturbances may hold promise for future treatments [60, 101, 196]. Several studies and clinical trials have already targeted individual contributors to the pro-inflammatory response, specifically IL-1 [103, 109, 197, 198], IL-6 [199], and TNF- $\alpha$  [200]. Although such treatments have been beneficial in preclinical animal models, clinically, they have really only reduced inflammatory markers and the risk of recurrence but not infarct size [103, 109, 197-200]. Moreover, these studies have not focussed on investigating whether these therapies are vasculoprotective at the level of the microcirculation post-reperfusion, with the final outcome measured predominantly being infarct size.

Therefore, studies that can identify other potential therapeutic agents may be clinically useful. IL-36, a relatively novel IL-1 superfamily member, is involved in the production of pro-inflammatory mediators and activation of immune/ECs [201]. The IL-36 / IL-36R pathway has been shown to play a key role in a number of inflammatory diseases, including psoriasis and rheumatoid arthritis [125, 201, 202]. However, only a couple of studies have provided limited data on its therapeutic potential in the heart [153, 203]. It is anticipated that investigating new IL-1F members will unravel novel mechanistic pathways that have the potential to become therapeutic targets in sterile inflammatory conditions of the heart. Certainly, members of the IL-1 family, including IL-36, are typically among the most upstream cytokines to be released upon injury and appear critical in triggering subsequent synthesis and release of a multitude of inflammatory mediators. Hence IL-36 holds

significant promise as a therapeutic target. It has been largely overlooked since its discovery in 2001, with fewer than 140 studies published investigating the role of IL-36 cytokines. However, important, and novel biologic roles are recently being described for IL-36, and it is anticipated that this will represent one of the most dynamic areas of research in immunology in coming years. It is worth speculating that since IL-36 levels are dramatically raised in patients with psoriasis, this could mechanistically explain the known link between psoriasis and increased cardiovascular disease.

### **1.8.3. Inclusion of co-morbidities and risk factors**

In the field of myocardial IR injury, there has been a recurrent failure of anti-inflammatory interventions that were promising in animal models to translate to the clinic. This may be because they do not accurately model the human scenario, particularly when it comes to the inclusion of comorbidities and/or risk factors such as age, sex, diabetes, and hypertension. By 2030, it is expected that 20% of the population will be over 65 years old, and cardiovascular disease is set to account for 40% of the deaths within this age group. Increasing age is a major contributor to worsened prognosis and increased myocardial damage following MI, independent of other risk factors. Therefore, detailed consideration of the effects of ageing on the post-ischemic heart is critical. However, almost all studies applied to the murine heart have involved young animals. In this thesis, we will provide original contributions on the architecture of the aged heart microcirculation and how its response to IR injury differs from young hearts.

Furthermore, biological sex differences in CVD outcomes have been widely studied and have been shown to be a key factor in determining outcomes following a MI. However, little is known *in vivo* about how age and sex impact coronary microcirculation in health and whether they increase the likelihood of microvascular disturbances post-reperfusion injury.

Although studies on both age-related and sex-related changes in the inflammatory and immune system have gathered pace, the work presented in this thesis is the first to explore *in vivo*, in an intravital imaging model of the IR injured mouse beating heart, the role of a novel inflammatory cytokine pathway in mediating microcirculatory disturbances in young/aged, male/female, hearts in both health and post-injury. Understanding these processes and identifying contributing mechanisms is essential if we are to devise and optimise therapies that will be effective, specifically in an age-related myocardial pathology.

### 1.9. Aims and Hypotheses

Although we know the IL-36/IL36R pathway is highly pro-inflammatory in the skin and lungs, we are still at an early stage in our current understanding of its *in vivo* biology in the heart. The major hypothesis of this thesis is that IL-36 is a key mechanistic contributor to myocardial microcirculatory disturbances post-reperfusion, and its inhibition will ameliorate myocardial IR injury. We will explore the hypothesis that the extent of thromboinflammation and microvascular perturbations mediated in aged IR injured mice exceeds that mediated in adult mice, which may be linked to an existing basal inflammatory

presence even in the absence of injury (*inflammaging*). We also hypothesise that the clinical differences in the outcome of males and females to MI, may be linked to differences in the susceptibility of their coronary microcirculation to IR injury. To address this, the aims of this thesis are as follows:

- Intravitaly image the healthy, uninjured, and IR injured adult and aged mouse beating hearts in order to characterise and compare the full extent of the microcirculatory response at a cellular level *in vivo*.
- Determine whether IL-36R and its cytokines are present in the healthy, uninjured mouse heart and whether IR injury, age, or sex impacts their local expression.
- Investigate intravitaly whether IL-36 agonists are functional in the heart by determining whether they can elicit an inflammatory response within the mouse beating coronary microcirculation *in vivo*.
- Investigate intravitaly whether therapeutic intervention with IL-36Ra is vasculoprotective at the level of the coronary microcirculation in the IR injured adult and aged mouse beating hearts *in vivo*.
- Intravitaly image the IR injured male and female mouse beating hearts in order to characterise and compare the full extent of the microcirculatory response at a cellular level *in vivo* and determine the effectiveness of IL-36Ra in both sexes.
- Investigate whether IL-36 and IL-36R are present in neonatal, infant/toddler, older children and elderly human myocardium and determine whether there are any correlations between expression levels and age.

# **Chapter 2:**

## **Materials & Methods**

## 2.0. Materials and Methods

### 2.0. Reagents and Materials

**Staining buffer** was composed of Dulbecco's phosphate buffered saline (DPBS) containing 5% FBS and 1% penicillin-streptomycin. **Endothelial cell expansion media** was made up of 1% minimum essential medium (MEM) D-valine powder (DMEM), 0.1% sodium bicarbonate, 8.9% FBS, 1% penicillin-streptomycin, 1% MEM non-essential amino acids, 1% vitamin mix, 10 units/ml IFN- $\gamma$  and subsequently adjusted to pH 7.4. **Endothelial cell experimental media** consisted of DMEM-high glucose, 10% foetal bovine serum (FBS), and 1% penicillin-streptomycin. **Tris-buffered saline (TBS)** was composed of 12% tris-base, distilled water and subsequently adjusted to pH 7.4. **Radioimmunoprecipitation assay (RIPA)** buffer containing 50 mM Tris, 150 mM sodium chloride, 1.0% triton X-100, 0.5% sodium deoxycholate, and 0.1% sodium dodecyl sulfate (SDS), supplemented with a protease inhibitor tablet and subsequently adjusted to pH 8.0. **Ammonium persulphate solution (APS)** was made up of 10% ammonium persulphate in distilled water. **Running buffer** was composed of 10% Tris-glycine-SDS in distilled water, while **transfer buffer** was composed of 10% Tris-glycine in distilled water. **Magnetic activated cell sorting (MACS) buffer** was composed of PBS containing 0.5% BSA and 2 mM EDTA. **Triphenyl tetrazolium chloride (TTC) solution** was composed of 1% 2,3,5-triphenyltetrazolium chloride, 76%  $\text{Na}_2\text{HPO}_4$  (0.1M), 23%  $\text{NaH}_2\text{PO}_4$  (0.1M) and subsequently adjusted to pH 7.4, and before use was pre-heated to 37°C.

A list of all other reagents and materials used can be in the tables 2.1, 2.2, and 2.3.

Table 2.1: List of reagents

Product Name	Abbreviation	Company	Location
Accutase	-	Sigma Aldrich	Poole, UK
Acetone	-	Sigma Aldrich	Poole, UK
Acrylamide	-	National Diagnostics	Nottingham, UK
Ammonium-Chloride-Potassium Lysing Buffer	ACK	Thermo Fisher Scientific	Paisley, UK
Ammonium Persulphate	-	Sigma Aldrich	Poole, UK
Bicinchoninic Acid	BCA	Sigma Aldrich	Poole, UK
Bovine Serum Albumin	BSA	Sigma Aldrich	Poole, UK
Corkboard	-	Thermo Fisher Scientific	Paisley, UK
Collagenase Type 1	Collagenase	Wako chemicals	Osaka, Japan
Complete Ultra-Tablets Easy Pack	Protease inhibitor	Roche	Switzerland
DMEM-High Glucose	-	Sigma Aldrich	Poole, UK
Dulbecco's Phosphate-Buffered Saline	DPBS	Gibco	Paisley, UK
Dulbecco's Modified Eagle's Medium	DMEM	Sigma Aldrich	Poole, UK
Ethylenediaminetetraacetic Acid	EDTA	Sigma Aldrich	Poole, UK
Evans Blue	-	Sigma Aldrich	Poole, UK
FcR blocking reagent	-	Miltenyi Biotec	Germany
Foetal Bovine Serum	FBS	Gibco	Paisley, UK
Formalin	-	Sigma Aldrich	Poole, UK
HibiScrub	-	Regent Medical Ltd	Manchester, UK
ImmEdge Pen	Wax pen	Vector Laboratories	Burlingame, USA
Immunomount	-	National Diagnostics	Nottingham, UK
Interferon-Gamma	IFN- $\gamma$	Sigma Aldrich	Poole, UK
Ketamine Hydrochloride	-	Pfizer	New York, USA
Liquid-Skin	-	Liquid-Skin	Middlesex, UK
Medetomidine Hydrochloride	-	Pfizer	New York, USA
MEM D-Valine Powder	-	Sigma Aldrich	Poole, UK
MEM Non-Essential Amino Acids	-	Sigma Aldrich	Poole, UK
Nitrocellulose Membrane	-	Thermo Fisher Scientific	Paisley, UK
Non-Fat Milk Powder	-	Marvel	Manchester, UK
Optical Cutting Temperature	OCT	Sakura Finetek	Netherlands
Penicillin-Streptomycin	-	Gibco	Paisley, UK
Phosphate-Buffered Saline	PBS	Sigma Aldrich	Poole, UK
Prolene 9.3mm Suture	-	Ethicon	New Jersey, USA
Resolving Buffer	-	National Diagnostics	Nottingham, UK
Sodium Bicarbonate	NaHCO <sub>3</sub>	Sigma Aldrich	Poole, UK

Sodium Chloride	NaCl	Sigma Aldrich	Poole, UK
Sodium Chloride 0.9%	Saline	MacroPharma	Twickenham, UK
Sodium Deoxycholate	-	Sigma Aldrich	Poole, UK
Sodium Dodecyl Sulphate	SDS	Sigma Aldrich	Poole, UK
Sodium Phosphate Dibasic	Na <sub>2</sub> HPO <sub>4</sub>	Sigma Aldrich	Poole, UK
Sodium Phosphate Monobasic	NaH <sub>2</sub> PO <sub>4</sub>	Sigma Aldrich	Poole, UK
Stacking Buffer	-	National Diagnostics	Nottingham, UK
SuperFrost Glass Slides, Ground 90°	Glass slides	Thermo Fisher Scientific	Paisley, UK
Tetramethylethylenediamine	TEMED	National Diagnostics	Nottingham, UK
Tris-Base	-	Sigma Aldrich	Poole, UK
Tris-glycine	-	Geneflow	Lichfield, UK
Tris-glycine-SDS	-	Geneflow	Lichfield, UK
Triton-X	-	Sigma Aldrich	Poole, UK
Tween	-	Sigma Aldrich	Poole, UK
Veet	-	Reckitt Benckiser	Norwich, UK
Vitamin Mix	-	Sigma Aldrich	Poole, UK
2,3,5-Triphenyltetrazolium Chloride	-	Serva	Germany
3-Aminopropyltriethoxysilane	APES	Sigma Aldrich	Poole, UK
5-0 Suture	-	Ethicon	New Jersey, USA
70µm Strainer	-	Thermo Fisher Scientific	Paisley, UK

Table 2.2: List of antibodies

Experiment	Antibody	Label	Clone	Source	Target	Company	Conc.
<b><i>In vitro</i> Mouse Experiments</b>	Anti-IL-1 Rrp2 / IL-36R	UC	Polyclonal IgG	Goat	Mouse	R&D Systems	0.2mg/mL
	Anti-IL-36 $\alpha$ / IL-1F6	UC	Polyclonal IgG	Goat	Mouse	R&D Systems	0.2mg/mL
	Anti-IL-36 $\beta$ / IL-1F8	UC	Polyclonal IgG	Goat	Mouse	R&D Systems	0.2mg/mL
	Anti-IgG control	UC	Polyclonal IgG	Goat	Mouse	R&D Systems	0.2mg/mL
	anti-goat IgG	AF488	Polyclonal IgG	Donkey	Goat	Abcam	2mg/mL
	anti-CD31	PE	Monoclonal: 390	Rat	Mouse	Biolegend	0.2mg/mL
	Anti-IgG2a control	PE	Monoclonal: RTK2758	Rat	Mouse	Biolegend	0.2mg/mL
	Anti-CD31	BV421	Monoclonal: 390	Rat	Mouse	Biolegend	0.2mg/mL
	Anti-IgG2a control	BV421	Monoclonal: RTK2758	Rat	Mouse	Biolegend	0.2mg/mL
	Anti-cardiac TnT	PE	Monoclonal: REA400	Cell Line	Mouse + Human	Miltenyi Biotec	NS
	REA Control	PE	Monoclonal: REA293	Cell Line	Mouse + Human	Miltenyi Biotec	NS
	Anti-VCAM-1 / CD106	AF647	Monoclonal: 429	Rat	Mouse	Biolegend	0.5mg/mL
	Anti-IgG2a control	AF647	Monoclonal: RTK2758	Rat	Mouse	Biolegend	0.5mg/mL
	Anti-DNA/RNA damage	FITC	Monoclonal: 15A3	Mouse	SI	Abcam	1mg/mL
	Anti-IgG2b control	FITC	Monoclonal: PLPV219	Mouse	SI	Abcam	1mg/mL
	Zombie Aqua	Violet 405	NS	NS	NS	Biolegend	NS
	Anti-Ly-6G/Ly-6C (Gr-1)	PE	Monoclonal: RB6-8C5	Rat	Mouse	Biolegend	0.2mg/mL

<b><i>In vivo</i> Mouse Experiments</b>	Anti-CD41	APC	Monoclonal: MWReg30	Rat	Mouse	Biolegend	0.2mg/mL
	Anti-BSA	FITC	NS	NS	NS	NS	NS
<b><i>In vitro</i> Human Experiments</b>	Anti-IL-1 Rrp2 / IL- 36R	UC	Monoclonal IgG <sub>1</sub> : 116004	Mouse	Human	R&D Systems	0.2mg/mL
	Anti-IL- 36 $\alpha$ / IL- 1F6	UC	Polyclonal IgG	Goat	Human	R&D Systems	0.2mg/mL
	Anti-IL- 36 $\beta$ / IL- 1F8	UC	Polyclonal IgG	Goat	Human	R&D Systems	0.2mg/mL
	Anti-IL- 36 $\gamma$ / IL- 1F9	UC	Polyclonal IgG	Goat	Human	R&D Systems	0.2mg/mL
	Anti-IgG Control	UC	Polyclonal IgG	Goat	Human	R&D Systems	0.2mg/mL
<b><i>In vitro</i> Human Experiments</b>	Anti-mouse IgG	AF647	Monoclonal: RMG1-1	Rat	Mouse	Biolegend	0.5mg/mL
	Anti-goat IgG	AF647	Polyclonal IgG	Donkey	Goat	Abcam	2mg/mL
	Anti-CD31	PE	Monoclonal: WM59	Mouse	Human	Biolegend	0.2mg/mL
	Anti-IgG1 control	PE	Monoclonal: MOPC-21	Mouse	Human	Biolegend	0.2mg/mL
	Anti- cardiac TnT	PE	Monoclonal: REA400	Cell Line	Mouse + Human	Miltenyi Biotec	NS
	REA Control	PE	Monoclonal: REA293	Cell Line	Mouse + Human	Miltenyi Biotec	NS
	Anti- DNA/RNA damage	FITC	Monoclonal: 15A3	Mouse	SI	Abcam	1mg/mL
	Anti- IgG2b control	FITC	Monoclonal: PLPV219	Mouse	SI	Abcam	1mg/mL

NS – Not specified; SI – species independent; UC – unconjugated; TnT – Troponin

**Table 2.3: List of recombinant proteins**

Protein	Source	Target	Company	Concentration
IL-36 $\alpha$ / IL-1F6	E. coli	Mouse	R&D Systems	100 $\mu$ g/ml
IL-36 $\beta$ / IL-1F8	E. coli	Mouse	R&D Systems	100 $\mu$ g/ml
IL-36 $\gamma$ / IL-1F9	E. coli	Mouse	R&D Systems	100 $\mu$ g/ml
IL-1 $\beta$	E. coli	Mouse	PeproTech	100 $\mu$ g/ml
TNF- $\alpha$	E. coli	Mouse	Boster Biological	100 $\mu$ g/ml
IL-36Ra/IL-1F5	E. coli	Mouse	Novus	1 $\mu$ g/mouse

## 2.1. Animals

All animal experiments were conducted in accordance with a UK Home Office license (Licenses: P5552D447 and P95F39B96) and in accordance with the Animals Scientific Procedures Act of 1986 (ASPA). For studies investigating the impact of ageing on the coronary microcirculation, experiments were carried out using female C57BL/6 mice and classified as either adult mice (9-15 weeks) or aged (78-82 weeks) mice. For studies investigating the impact of sex on the coronary microcirculation, experiments were carried out using adult male C57BL/6 mice (9-15 weeks). All mice were purchased at least 7 days prior to experiments to allow them to acclimatize and were housed in a pathogen-free environment at the Biomedical Services Unit (BMSU), University of Birmingham, UK. Mice were given ad libitum access to food and water.

### 2.1.1. Myocardial IR Injury

#### 2.1.1.1. Surgical Preparation

All surgical instruments and tools were heat sterilised, and the workbench and associated hardware were sterilised using HibiScrub. Mice were anaesthetised by an intraperitoneal (IP) injection of ketamine hydrochloride (100mg/kg) and medetomidine hydrochloride (10mg/kg) in a 0.9% saline solution. Anaesthetic depth was monitored by checking the pedal reflex every 15 minutes, with anaesthesia maintained as required through IP administration. The skin over the left thoracic region and neck were shaved using an electric shaver and then a depilatory cream (Veet) was used to remove the remaining hair.

These areas were then disinfected with HibiScrub, and the mouse was placed on a customised surgical board in a supine position (**Figure 2.1A**). A heating pad connected to a rectal probe was used throughout the surgery to maintain the body temperature at 37°C.

### 2.1.1.2. Surgical Procedure

The surgical procedure was performed as previously described [42]. A tracheostomy was initially performed to ventilate the anaesthetised mouse artificially. To expose the trachea, an initial incision was made in the neck area, and the connective tissue and muscle surrounding the trachea were bluntly dissected. A small incision was then made between two rings of cartilage. An endotracheal tube, connected to a mechanical ventilator (MiniVent rodent ventilator, Biochrom Ltd/Harvard Apparatus, UK), was then placed into the trachea and held in place using a 5-0 suture (Ethicon, USA). This provided medical oxygen to the anaesthetised mouse at a respiratory rate of 130 breaths / minute with a tidal volume of 220µL / breath (**Figure 2.1A**). Medical oxygen was provided by an oxygen concentrator (VetTech, UK).

In order to facilitate the delivery of antibodies and saline, the left carotid artery was cannulated. The artery was initially exposed using blunt dissection and freed from the vagus nerve and connective tissue. A 5-0 suture was used to permanently tie off the superior end, and the inferior end was clamped using a non-traumatic mini arterial clamp. A small incision was then made between the suture and clamp, and a carotid cannula, connected to a 1ml saline syringe, was inserted, and secured in place using a 5-0 suture.

The clamp was then removed, and a single bolus dose of saline was given to maintain hydration during the experiment (5ml/kg) (**Figure 2.1A**).

To access the heart, the mouse was placed in a right lateral decubitus position, and an incision was made in the left thoracic region to uncover the pectoral muscles. Muscle and connective tissue were carefully cauterised to expose the left rib cage. A thoracotomy between the third and fourth left ribs was performed, and the pericardium was bluntly opened. Surgical retractors were used to hold back the ribs so that the heart could be easily accessed.

Myocardial IR injury of the LV was performed using a well-established model involving reversible occlusion of the left anterior descending (LAD) coronary artery [42]. The LAD artery was identified, a silk suture (Prolene 9.3mm, W8703, Ethicon) was gently passed underneath it and tightened around a piece of plastic tubing (**Figure 2.1B & C**). The plastic tubing applied pressure to the LAD artery and occluded the vessel. A successful occlusion was apparent when the apical region of the LV appeared pale (**Figure 2.1C**). Following 45 minutes of ischaemia, the ligature was removed, and reperfusion of the myocardium was allowed to proceed for either 2 hours for tissue analysis experiments, 2.5 hours for intravital observations or 4 hours when measuring infarct size [42]. At the end of these various reperfusion durations, mice were culled by cervical dislocation and organs of interest were harvested for later use. Mice undergoing sham surgery underwent the same procedure as above, which included the passing of the silk suture under the LAD artery. However, in sham mice, this was not tightened. For pre-treatment studies, recombinant mouse IL-36Ra (15µg/mouse) was injected intra-arterially at both 10 minutes pre-reperfusion and 60 minutes post-reperfusion.

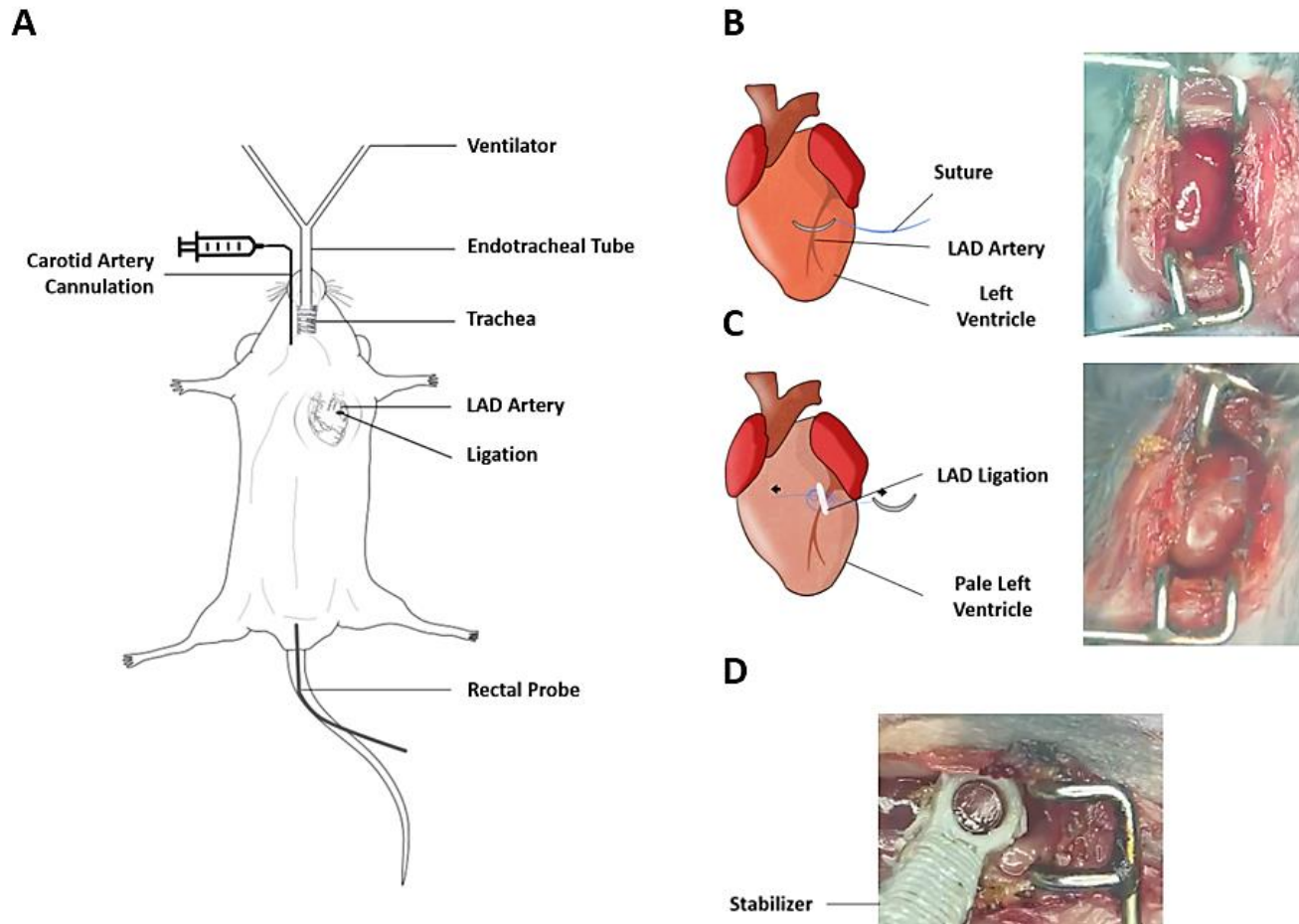


**Figure 2.1. Intravital microscopy of the mouse beating heart microcirculation in vivo.** (A) Adult and aged mice underwent sham or ischemia reperfusion injury (IRI) surgery. All surgeries involved endotracheal intubation to supply medical oxygen, carotid artery cannulation to deliver antibodies and saline, and a sham or left anterior descending (LAD) artery occlusion for 45 minutes prior to reperfusion. (B) Schematic and representative image of the heart prior to occlusion. (C) Schematic and representative image of the heart during LAD artery occlusion. (D) Representative image of the stabilised heart.

## 2.2. *In Vivo* Experiments

### 2.2.1. Intravital Imaging of the Coronary Microcirculation in the Mouse

#### Beating Heart *in vivo*

Intravital imaging of the anaesthetised mouse beating heart following myocardial IR injury was performed as previously described by the Kalia group [42]. Following the initiation of reperfusion, an in-house designed 3D printed stabiliser (internal diameter: 2.25mm and external diameter: 4mm) was gently lowered onto the LV using a micromanipulator downstream of the occlusion site for the LAD artery and fixed permanently using clinical-grade surgical glue (Liquid-Skin). Stabilisation of this area reduced motion sufficiently to allow high-quality videos to be captured through the central window, whilst the remainder of the heart was able to beat normally. The stabilizer was made of polylactic acid printed on a MakerBot 3D printer (Stratasys, USA) and designed using Tinkercard software (Autodesk, USA) (**Figure 2.1D**). This stabilisation process took place within 5-10 minutes of untying the LAD artery suture, meaning the first intravital imaging could only take place at 15 minutes post-reperfusion. To prevent moisture loss in the stabilised region, a small piece of saran wrap (3cm<sup>2</sup>) was used to keep the area covered, and 0.9% saline was applied every 15 minutes to the central region of the stabiliser.

A region of the LV within the stabiliser centre was randomly identified, and a first intravital recording, lasting for 2 minutes, was captured at 15 minutes post-reperfusion. Thereafter, 2-minute recordings were captured every 15 minutes for a duration of 2.5 hours from the same pre-selected area. All recordings were captured and stored digitally using Slidebook 6 software for later offline analysis (Intelligent Imaging Innovations, USA).

### 2.2.1.1. Monitoring Thromboinflammatory Cells and Microvascular Perfusion in the Coronary Microcirculation

In order to intravitaly image the kinetics of endogenous thromboinflammatory cells, 20µl of phycoerythrin (PE)-conjugated anti-mouse Gr-1 and 20µl of allophycocyanin (APC)-conjugated anti-mouse CD41 antibodies (100µl with 60µl saline) were injected via the carotid artery cannula at 5 minutes pre-reperfusion to label neutrophils (Gr-1 binds to both neutrophils and monocytes) and platelets respectively. PE and APC fluorochromes are excited at 566nm and 651nm and have emissions at 574nm and 660nm respectively, thus allowing neutrophils and platelets to be visualised near-simultaneously in the same mouse. Imaging of the beating heart was performed using an upright Olympus microscope (BX61WI, Olympus, USA) equipped with a Nipkow spinning disk confocal head (Yokogawa, Japan), an Evolve EMCCD camera (Photometrics, USA), and a x10 objective (Olympus, USA) (**Figure 2.2A**).

Experiments to investigate microvascular perfusion involved the infusion of 30µl of FITC conjugated BSA (in 100µl of saline) via the carotid artery cannula at 120 minutes of reperfusion (i.e. at the end of intravital experimentation). This fluorescein labelled albumin was retained within the blood vessels allowing them to be identified against a relatively darker, non-fluorescent background. However, under conditions where the vascular integrity was disturbed, FITC-BSA leaked out of the vasculature. To qualitatively determine vascular leakage, a piece of tissue paper was placed between captures in the centre of the stabiliser in order to absorb any leaked fluorescent albumin. This was later imaged to detect the transfer of FITC-BSA to the tissue paper. FITC-BSA also allowed the qualitative analysis of functional capillary density as the dye was only able to perfuse patent, non-occluded vessels.

### 2.2.1.2. Imaging the Coronary Microcirculation Immediately after Ischaemia

Due to the time it took to untie the LAD artery suture, subsequently, attach the stabiliser, and move the mouse to the microscope stage, the first time point after which intravital imaging could technically take place was at 15 minutes post-reperfusion. However, previous experiments conducted in the Kalia lab demonstrated that inflammatory events had already occurred by this time point [42]. In order to view the thromboinflammatory events taking place during the 15 minutes immediately after reperfusion, the existing stabilisation protocol described in **Section 2.3.1** was optimised. For hyper-acute imaging, the stabiliser was not permanently glue-fixed to the LV, a process that was time-consuming, but was applied to the same area of interest with very little pressure, but sufficient enough to form a seal. This process was performed at 35 minutes of ischaemia rather than after reperfusion. The mouse was then transferred to the microscope stage. This modified stabilisation protocol permitted a 2-minute intravital recording to be captured during the removal of the LAD ligature. Subsequent images were captured at 5-, 10-, and 15-minutes post-reperfusion in addition to the routine recordings that were captured every 15 minutes for a duration of 2.5 hours. Intravital analysis was then performed as described in **Section 2.2.3.1**.

### 2.2.1.3. Topical application of IL-36 Cytokines on the Beating Heart

The ability of topically applied IL-36 cytokines to directly mediate an inflammatory response *in vivo* in the beating heart was investigated in a separate set of mice. The heart was prepared for imaging as described in **Section 2.2.1.2**, but no sham or IR injury procedure was

performed. PE-conjugated anti-mouse Gr-1 and APC-conjugated anti-mouse CD41 antibodies were again injected via the carotid artery 5 minutes before the stabilizer was placed on the healthy LV. Using a fine-needle (31G) syringe, 2 drops of the cytokine (approximately 20 $\mu$ l at a concentration of 200ng/ml - IL-36 $\alpha$ , IL-36 $\beta$ , IL-36 $\gamma$ , TNF- $\alpha$ , or IL-1 $\beta$ ) or PBS (vehicle control) were topically applied to the epicardial surface of the heart within the centre of the stabiliser. The stabiliser was capable of containing this liquid due to its ring link structure and depth. After 15 minutes, the solution within the stabiliser was removed using tissue paper, and a 2-minute recording was captured. Following capture, the solution was replaced, and this cycle of topical applications and recordings were repeated every 15 minutes for a total duration of 150 minutes. Intravital analysis was then performed as described in **Section 2.2.3.1**.

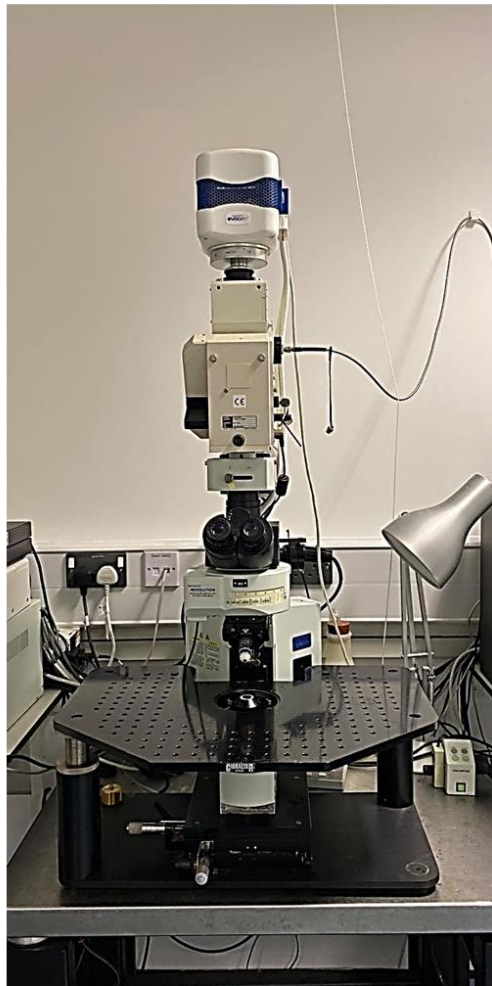
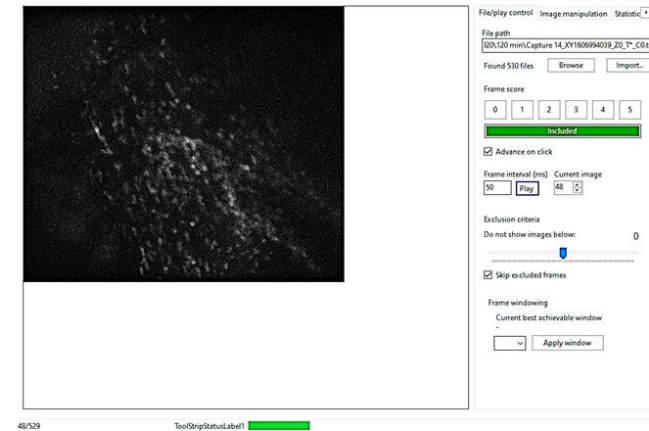
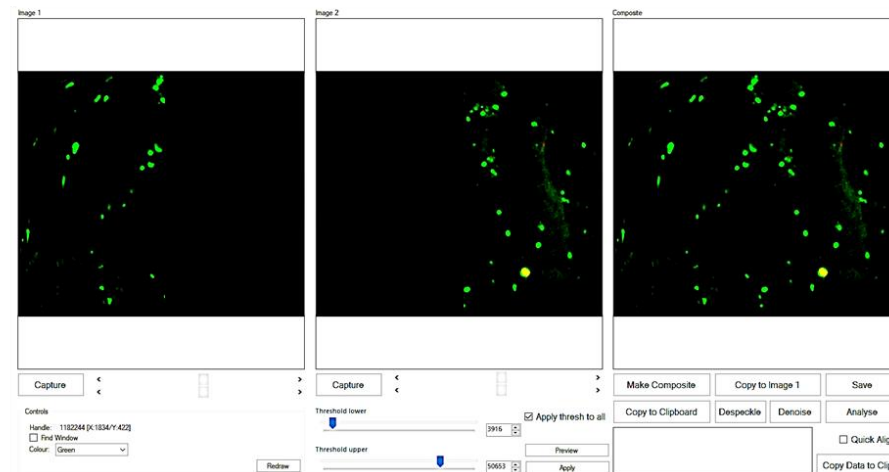
### **2.2.2. Laser Speckle Contrast Imaging**

Laser speckle contrast imaging (LSCI) is a large field-of-view or full-field, non-contact and non-scanning optical technique used for quantitating blood flow in real-time. It has been widely used in both pre-clinical and clinical studies to visualise perfusion in many organs. The setup is made up of a near-infrared laser diode, which emits a low powered laser after passing through a diffuser to illuminate an object. When the laser light hits the object, it is backscattered to form an interference pattern on the detector called a speckle pattern. If the illuminated object is static, the speckle pattern is stationary. When there is movement in the object, such as RBCs in a tissue, the speckle pattern will change.

The use of LSCI in the beating heart has been very limited due to the fact that the non-static physical nature of the heart and the dynamics of microvascular blood flow during systole and

diastole present challenges for interpretation of LSCI of ventricular muscle blood flow. However, the Kalia group have previously validated this technique in order to quantitate blood flow in the anaesthetised mouse beating LV [42]. They demonstrated that although some proportion of the flux value was derived from the movement of the beating heart itself, the remainder was attributable to the blood flow events taking place in the myocardium.

LSCI was therefore performed in adult and aged mice undergoing IR injury  $\pm$  IL-36Ra treatment. Mice underwent surgery as previously described in **Section 2.2.1**. Once the heart was exposed, and prior to inducing ischaemia, a 1-minute capture was recorded (around 1400 frames) using a moorFLPI-2 laser speckle contact imager (Moor Instruments, UK) and was noted as the baseline (**Figure 2.3A**). Sixty-second video captures were then obtained during ischaemia at 1, 5, 10, 15, 30, and 44 minutes and similarly during reperfusion at 1, 5, 10, 15, 30, 60, 90, 120, and 150 minutes. For treatment studies, recombinant mouse IL-36Ra was injected intra-arterially at both 10 minutes pre-reperfusion and 60 minutes post-reperfusion. LSCI analysis was then performed as described in **Section 2.2.3.2**.

**A****B****C**

**Figure 2.2. Intravital microscopy of the beating heart microcirculation in vivo.** Mice underwent sham or ischaemia reperfusion injury surgery. To image the kinetics of endogenous neutrophils and platelets, anti-mouse Gr-1 and anti-mouse CD41 antibodies were injected via the carotid artery cannula 5 minutes pre-reperfusion. **(A)** Representative image of the intravital set up. **(B)** Representative image of the in-house designed software Tify, in which out-of-focus frames are removed. **(C)** Representative image of Focus Repair, which is used to quantify neutrophils and platelet aggregates/microthrombi by first creating a still image and then calculating the integrated fluorescence density.

## 2.2.3. Analysis of *In Vivo* Experiments

### 2.2.3.1. Analysis of Intravital Imaging of the Coronary Microcirculation

Intravital images captured using Slidebook software were exported and opened using ImageJ for off-line analysis. Free-flowing neutrophils were counted manually over the 2-minute capture. To analyse adherent neutrophil and platelet presence, captured videos were subjected to post-acquisition image repair using machine learning via an in-house designed software (Tify; open source, available online: <https://github.com/kavanagh21/TifyVBNET>) in which out-of-focus and blurred frames were removed (**Figure 2.2B**) [204]. Neutrophils and platelet aggregates/microthrombi were then quantitated by first creating a still image using a software tool designed to repair partially focused images (Focus Repair; open source, available online: <https://github.com/kavanagh21/flatZ>; **Figure 2.2C**). A mask was then placed around PE-Ly6G<sup>+</sup> and APC-CD41<sup>+</sup> areas respectively, and the integrated fluorescence density was calculated using ImageJ.

To analyse microvascular perfusion following sham, IR injury, and IL-36Ra treatment in adult and aged mice, captured videos were subjected to post-acquisition image repair using Tify. FITC-BSA<sup>+</sup> vasculature was then quantitated by creating a still image using Focus Repair, and a score was given to each blinded image by a blinded external observer (**Table 2.4**).

### 2.2.3.2. Analysis of Laser Speckle Imaging of the Beating Heart

Analysis of LSCI was performed using mFLPI-2 software (V5, Moor Instruments, UK) on captured videos. Using the freehand selection feature within the software, an area of the heart tissue downstream of the LAD artery was drawn to extract flux data using spatial processing with a time constant of 0.1s and at a frame rate of 25Hz (**Figure 2.3B**). This flux data were exported into an in-house designed software, Speckle Analyser (SpAn; open source, available online at <https://github.com/kavanagh21/SpAN>) (**Figure 2.3C**).

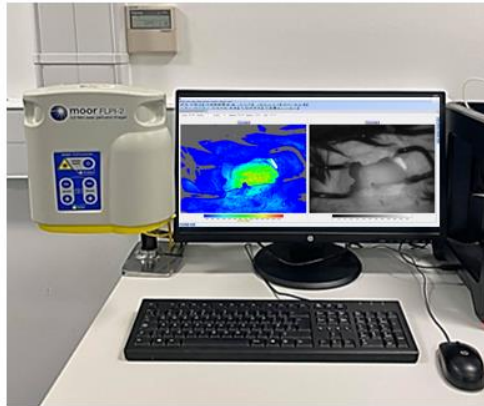
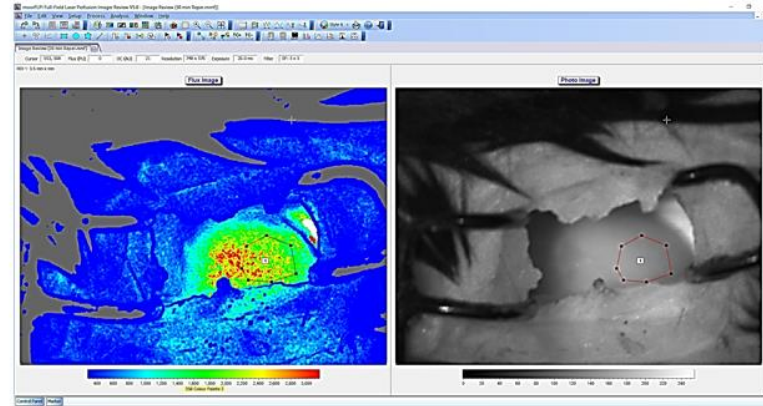
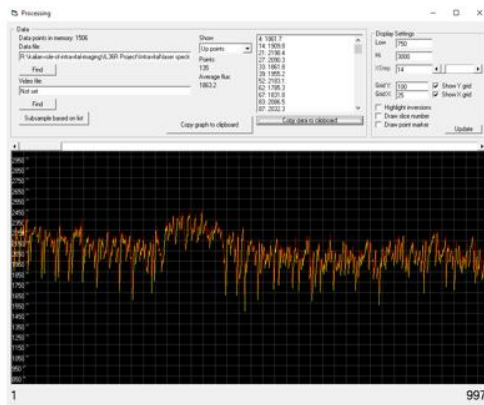
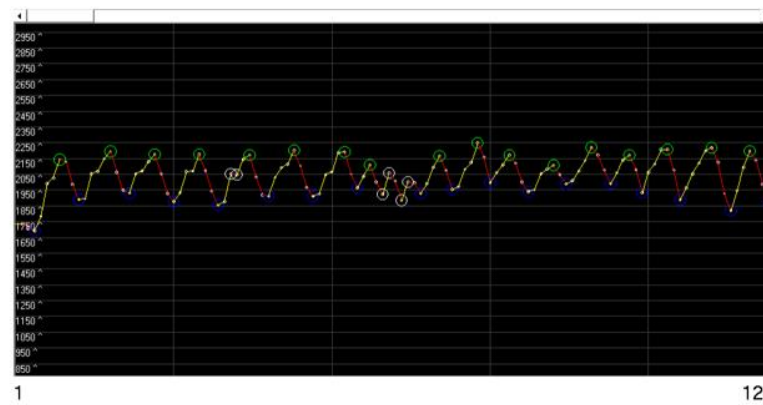
In each cardiac cycle, there are two points at which the heart is still; peak systole and peak diastole. At these points, the flux reading from LSCI is likely to be much less dependent on the movement of the heart and more clearly driven by blood flow. The blood flow during these phases of the cardiac cycle is clearly identified by LSCI as the peaks and troughs on flux readouts. SpAn was used to identify and collate these high and low points from flux images. In order for the SpAn software to achieve a complete cycle and consider a peak as a high point and a trough as a low point, the software must detect at least two concurrent movements within the appropriate trajectory (either upward or downward steps), i.e., a low point must be preceded by two decreasing points and followed by at least two increasing points. If this is achieved, SpAn will mark these high and low points for further analysis (labelling them in green and blue circles on outputs). On the other hand, if this is not achieved, the software will omit these points from analysis and mark them in white circles (**Figure 2.3D**).

Both systolic and diastolic data were then exported into Excel, and various readings were extrapolated for each time point: (i) average flux values from diastole were used to represent overall perfusion within the left ventricular myocardial coronary circulation; (ii) the distance

between each systolic cycle (between one systolic point and the next) was calculated and then averaged for each time point - standard deviation was then calculated to identify any arrhythmic pattern between beats; (iii) beats per minute were calculated and represented the heart rate; (iv) average flux values from diastole were then compared to the average flux values from systole to illustrate the function of the LV during systole and diastole.

Score	Description
<b>5</b>	Well perfused, no areas of poor perfusion at all. Uniform vessel structure across the image, which is easy to identify.
<b>4</b>	Well generally perfused, some patchy areas. Almost all small vessels can be identified easily.
<b>3</b>	Some small areas of poor perfusion, generally good flow. Most small vessels can be identified easily. Could be evidence of dye accumulation in vessels. Possibly some evidence of leakage.
<b>2</b>	More significant areas of no perfusion, large areas (>10% of each image) may be without flow. Some small vessels can be identified. If leakage is present, it is significant despite what appears to be good perfusion.
<b>1</b>	Large areas without perfusion, regional loss of perfusion, >50% without flow. Large vessels may be the only ones visible, difficult to identify others. If leakage is present, it is substantial.
<b>0</b>	Very large areas without perfusion, almost without flow, only big vessels with perfusion.

Table 2.4: Vascular perfusion point-scoring

**A****B****C****D**

**Figure 2.3. Laser speckle contrast imaging of the beating heart. (A)** Representative image of the laser speckle contrast imaging set up using a moorFLPI-2 laser speckle contact imager (Moor Instruments, UK). **(B)** Representative image of the mFLPI-2 imager (V5, Moor Instruments, UK) analysis software. **(C)** Representative image of the in-house designed software, Speckle Analyser (SpAn) used to correlate the peaks and troughs extracted from the flux data with the myocardial perfusion during left ventricular systolic and diastolic events. **(D)** In order for the SpAn software to achieve a complete cycle and consider a peak as a high point (green) and a trough as a low point (blue), the following two points must be within the appropriate trajectory. If this is not achieved, the software will omit these points from analysis and mark them in white circles.

## **2.3. In Vitro Experiments**

### **2.3.1. Immunofluorescence Assay**

#### **2.3.1.1. Mouse Immunofluorescence Assay**

In order to characterise the expression of IL-36R, IL-36 $\alpha$ , IL-36 $\beta$ , CD31, and VCAM-1 on sham and IR injured adult and aged hearts, immunofluorescence was performed. Harvested hearts were embedded on corkboard using OCT compound and then snap-frozen in liquid nitrogen and stored at -80°C until required. These frozen tissues were then sectioned on a cryostat (Bright instruments, UK). In order to avoid freeze-thaw cycles, which could lead to structural changes, all transportation was performed in liquid nitrogen. The corkboard was fixed onto the cryostat chuck using OCT, and the tissue was sectioned at 10 $\mu$ m thickness. The initial 50 $\mu$ m section of the hearts were removed prior to acquiring the first section. Sections were then transferred onto glass slides which were treated with APES. The slides were then allowed to air dry for 10 minutes before being fixed with acetone for a further 10 minutes. Slides were then covered with aluminium foil and stored at -20°C until required. Prior to staining, slides were thawed to room temperature and were then washed with DPBS. A water repellent circle was drawn around each section on the slides using a wax pen to keep reagents localised on the tissue specimen. To prevent non-specific binding, each section was incubated with 100 $\mu$ l staining buffer for 30 minutes at room temperature. Sections were then washed with DPBS three times.

Staining of the sections was performed using a two-step method. Firstly, sections were incubated with primary antibody solution for IL-36R, IL-36 $\alpha$ , IL-36 $\beta$  or IgG control (100 $\mu$ l, 1:100 dilution in DPBS). Subsequently, sections were washed with DPBS and then incubated

with 100µl of secondary antibody solution conjugated to Alexa Fluor 488 (1:100 dilution in DPBS). Each of the primary and secondary incubations were performed in a light-protected humidified tray at room temperature and for a duration of 1.5 hours. Additional antibodies were added into the second step to determine whether the IL-36/IL-36R staining was vascular in nature (CD31; 1:100 dilution in DPBS) and the impact of age and IR injury on inflammatory adhesion molecules (VCAM-1; 1:100 dilution in DPBS). The sections were then washed again with DPBS and left to air dry. A drop of Immunomount was added in order to help preserve the fluorescent signal and help fix the coverslip over the section. Imaging and analysis of slides was performed as described in **Section 2.3.1.5**.

### 2.3.1.2. Human Immunofluorescence Assay

#### 2.3.1.2.1. Patient Samples

All immunofluorescence experiments using human tissue were conducted within the scope of the ethical approval obtained by the Human Biomaterial Resource Centre (HBRC) at the University of Birmingham (15/NW/0079) and approved by the internal Access Review Panel (19-352). From February 2017 to December 2021, heart tissue samples were obtained from 24 patients undergoing cardiac surgery. These included 19 patients at Birmingham Children's Hospital (BCH) and 5 patients at the Queen Elizabeth Hospital Birmingham (QEH) (**Table 2.5**). At BCH, tissue samples were collected from neonates (0-4 weeks old), infant/toddlers (1-24 months old), and older children (2-19 years old) undergoing repair of congenital heart defects with routine resection of overtly healthy right ventricular myocardium. The resected

specimens were either a transmural disc of the myocardium from the RV free wall or hypertrophic muscle bundles from the right ventricular outflow tract (RVOT). At QEHB, samples were collected from adults with an age range of 29-65 years old. The resected specimens were of LV apex myocardium obtained from patients during LV assist device (LVAD) implantation for heart failure.

#### **2.3.1.2.1.1. Obtaining Right Ventricular Samples from Children**

Parental consent to retain resected RV samples from children was obtained by Mr Nigel Drury, Consultant in Paediatric Cardiac Surgery at BCH. All surgical procedures were performed by Mr Tim Jones, Ms Natasha Khan, or Mr Phil Botha, Consultant Paediatric Cardiac Surgeons. Surgery involved a median sternotomy with cardiopulmonary bypass and cardioplegic arrest.

#### **2.3.1.2.1.2. Neonate Group**

Tissue was collected between August 2017 to December 2020 from neonates undergoing the Norwood operation for hypoplastic left heart syndrome (HLHS; N=3) or for complete repair of truncus arteriosus (N=3). Ages at operation ranged from 4 to 16 days ( $7.8 \pm 5.3$  days). The Norwood operation aims at 're-plumbing' the congenital defects of the heart in order to help it become a more efficient pump [205]. During this procedure, a disc of RV myocardial free wall is routinely removed, which was washed in ice-cold saline, placed in a Nunc cryotube (Thermo Fisher Scientific, USA) and promptly snap-frozen in liquid nitrogen.

<i>Age &amp; Sex</i>	<i>Group</i>	<i>Height (cm)</i>	<i>Weight (kg)</i>	<i>Heart Disease</i>	<i>Operation</i>	<i>Resting O<sub>2</sub> Saturation</i>	<i>Genetic Syndrome</i>	<i>Drugs</i>	<i>Ischaemia time (mins)</i>
<i>4 days F</i>	Neonate	48	2.9	HLHS	Norwood	95	None	Prostin	40
<i>4 days F</i>	Neonate	44	2	TA	TR	100	None	None	36
<i>5 days M</i>	Neonate	51	3.9	HLHS	Norwood	95	None	None	24
<i>5 days M</i>	Neonate	61	4	TA	TR	88	DiGeorge	None	50
<i>13 days F</i>	Neonate	49	3.1	TA	TR	93	DiGeorge	None	19
<i>16 days F</i>	Neonate	52	3.3	HLHS	Norwood	88	None	Prostin	7
<i>3 months M</i>	Inf/Tod	60	5.4	ToF	ToF repair	86	None	Propranolol	12
<i>3 months M</i>	Inf/Tod	63	7.1	ToF	ToF repair	97	Xq28 duplication	Propranolol	32
<i>8 months M</i>	Inf/Tod	66	7	ToF	ToF repair	85	Trisomy 21	None	47
<i>11 months M</i>	Inf/Tod	71	7.2	PA/IVS	ToF repair	96	None	Propranolol	11
<i>14 months M</i>	Inf/Tod	77	8.2	ToF	ToF repair	83	None	Aspirin, omeprazole	23
<i>21 months M</i>	Inf/Tod	83	83	ToF	ToF repair	78	None	Aspirin, propranolol	24
<i>23 months F</i>	Inf/Tod	72	72	ToF	ToF repair	90	None	Propranolol	35
<i>7 years M</i>	Children	109	26.3	VSD/DCRV	RVOT resection	97	MIDAS syndrome	Growth hormone, hydrocortisone	11
<i>8 years F</i>	Children	116	22.9	TA	RV-PA conduit	98	DiGeorge	Aspirin, furosemide, spironolactone	83
<i>10 years F</i>	Children	138	46	TA	RV-PA conduit	95	None	Lisinopril	3
<i>12 years F</i>	Children	150	73	TA	RV-PA conduit	99	None	None	13
<i>16 years M</i>	Children	151	46.4	TA	RV-PA conduit	98	Trisomy 21	Aspirin, ranitidine, iron	10
<i>16 years F</i>	Children	159	53.4	TA	RV-PA conduit	95	None	Furosemide, spironolactone	0
<i>29 years M</i>	OA	177	105	HF	LVAD	60	None	Mozaminol	78
<i>42 years F</i>	OA	159	78.4	HF	LVAD	60	None	Metaraminol	102
<i>50 years M</i>	OA	185	103.85	HF	LVAD	55	None	Mozaminol	92
<i>54 years F</i>	OA	158	76.9	HF	LVAD	55	None	Mozaminol	90
<i>65 years F</i>	OA	185	83.45	HF	LVAD	60	None	Metaraminol + Heparin	85

**Table 2.5: List of patient details** - HLHS - Hypoplastic left heart syndrome; TA – Truncus arteriosus; HF – Heart failure; TR – Truncus repair; Inf/Tod – Infant/Toddler; OA – Older adult; ToF – Tetralogy of Fallot; PA/IVS – Pulmonary atresia with intact ventricular septum; IUGR – Intrauterine growth restriction; VSD/DCRV - Ventricular septal defect with double-chambered RV; RVOT – Right ventricular outflow tract; LVAD – LV assist device. Ischemia time - ischaemic time to obtaining RV sample; in one patient, the sample was obtained prior to ischaemic arrest

#### **2.3.1.2.1.3. Infant/Toddler Group**

Tissue was collected between January 2018 to February 2020 from infant/toddlers undergoing either tetralogy of Fallot repair (ToF; N=6) or isolated RV outflow tract muscle resection (RVOT; N=1). Ages at operation ranged from 3 to 23 months ( $11.9 \pm 8$  months). Briefly, closure of the ventricular septal defect in ToF patients was performed using a prosthetic patch graft, while relief of RVOT obstruction was performed by resection of hypertrophied septoparietal muscle bundles from the RVOT [206]. Again, the resected heart sample was washed in cold saline and promptly snap-frozen in liquid nitrogen.

#### **2.3.1.2.1.4. Older Children Group**

Tissue was collected between August 2018 to April 2021 from older children undergoing either right ventricular-pulmonary artery (RV-PA) conduit replacement (N=5) or RVOT muscle resection with ventricular septal defect closure (N=1). Ages at operation ranged from 7 to 16 years ( $11.5 \pm 3.9$  years). In the RV-PA conduit replacement group, the old conduit was excised, and the defect in the RV free wall was enlarged by further resection of muscle to accommodate the larger proximal anastomosis [207]. Relief of RVOT obstruction was performed by resection of hypertrophied septoparietal muscle bundles from the RVOT [206]. Resected samples were washed in cold saline and promptly snap-frozen in liquid nitrogen.

### 2.3.1.2.1.5. Obtaining Older Left Ventricular Patient Samples – Left Ventricular Assist Device Implantation

All surgical procedures to obtain LV samples from older adult patients were performed by Mr Aaron Ranasinghe, Consultant Cardiac Surgeon at QEHB. Tissue was collected between February 2021 to December 2021 from older patients (N=5) with heart failure who were undergoing implantation of a LVAD, a type of artificial heart pump [208]. Ages at operation ranged from 29 to 65 years ( $48 \pm 12$  years). Briefly, patients underwent a sternotomy and were placed on cardiopulmonary bypass, during which time the LVAD was connected between the apex of the heart and the aorta. This involved removing a section from the LV apex which was washed in cold saline and promptly snap-frozen in liquid nitrogen.

### 2.3.1.2.2. Human Immunofluorescence Assay

To confirm whether IL-36R, IL-36 $\alpha$ , IL-36 $\beta$  and IL-36 $\gamma$  was present in the human heart, and whether expression differed between young and elderly patients, immunofluorescence was also performed on human samples. In a similar manner to the mouse protocol, human heart tissue samples were fixed on to corkboard and sectioned. Sections were then incubated with 100 $\mu$ l of FcR blocker (CD16/32) for 30 minutes at room temperature to block unspecific binding. Staining of the human sections was performed as previously described in **Section 2.4.1.1**. Briefly, sections were incubated with primary antibody solution for IL-36R, IL-36 $\alpha$ , IL-36 $\beta$ , IL-36 $\gamma$ , or IgG control (100 $\mu$ l, 1:100 dilution in DPBS), washed, and then incubated with 100 $\mu$ l of secondary antibody solution conjugated to Alexa Fluor 647 (1:100 dilution in DPBS).

Additional antibodies were added into the second step to determine whether the staining was vascular in nature (CD31; 1:100 dilution in DPBS), or co-localised with CMs (cTnT; 1:100 dilution in DPBS). An additional antibody was also added into the second step to assess oxidative damage (DNA/RNA damage; 1:100 dilution in DPBS). Each of the incubations was performed in a light-protected humidified tray at room temperature for a duration of 1.5 hours. The sections were then washed again and a drop of Immunomount was added.

### 2.3.1.3. Frozen Tissue Section Analysis of Immunofluorescence

Using a x20 objective (Olympus, UK), eight fields of view per section were imaged in a pre-defined arrangement using a fluorescent microscope (EVOS, ThermoFisher Scientific, USA) (**Figure 2.4**). Fields that contained cracks in the tissue were dismissed and additional fields were captured (following the same pre-defined pattern of field-to-field movement). In addition, two random fields of view per section were captured using a multiphoton microscope (Olympus FVMPE-RS, Olympus, UK) and a x25 objective to capture images with a better signal-to-noise ratio and improved resolution.

Image analysis was performed using Image J (NIH, USA) to quantify the intensity of each image using mean fluorescence intensity (MFI). An analysis region of a pre-defined size and location was applied to each image (width: 900, height: 900, X coordinate: 250, Y coordinate: 50) before the MFI was measured. This was used to analyse the intensity for IL-36R, IL-36 $\alpha$ , IL-36 $\beta$ , IL-36 $\gamma$ , CD31, cTnT, VCAM-1, and DNA/RNA damage separately.

In order to further detail whether localisation of IL-36R, IL-36 $\alpha$ , or IL-36 $\beta$  occurred alongside CD31+ vasculature, areas on the section containing only microvasculature were imaged separately from regions of macrovasculature (mouse experiments only). MFI of the microvasculature was measured using a measurement field of pre-defined size and location applied to each image (width: 400, height: 400, X coordinate: 500, Y coordinate: 250). Areas that contained tears in the tissue or overlapped a large blood vessel, were dismissed and the coordinates were moved along to the next clear area. MFI on the macrovasculature was measured after large blood vessels were segmented from the field of view using the freehand selection feature within ImageJ.

### 2.3.2. Western Blotting Analysis

Western blotting was used to qualify and quantify the expression of IL-36R in the sham, and IR injured adult and aged mouse hearts as previously described [126]. Hearts were harvested as previously described from sham, and IR injured mice in **Section 2.5.1.1** and kept on ice throughout the experiment. Hearts were placed in a tube containing the cell lysis RIPA buffer and homogenized for 30 seconds at a speed of 5.65Hz (Bead Ruptor 12, Omni International, UK). Lysates were then clarified through centrifugation at 10,000G for 60 seconds. This process was repeated 2 times at 4°C. The remaining lysate was then sonicated (Q Sonica, USA) for a further 20 seconds. The protein concentrations of the lysates were determined against a BSA protein standard using a BCA assay as a loading control could not be used, whereby various concentrations of the sample and protein standard were placed in a 96 well plate. Bicinchoninic acid and copper sulphate were then added to the wells to start the chemical

reaction. The plate was then placed on a shaker for 5 minutes before being left to warm up for 30 minutes. The plate was then taken to a plate reader, and lysates were normalized to 2mg/ml and stored at -20°C until required.

SDS-PAGE gel, used to run the samples, was prepared, and consisted of a 10% resolving gel (4.1ml distilled water, 3.3ml acrylamide, 2.5ml buffer, 30µl 10% APS, and 5µl TEMED) and 6% stacking gel (5.4ml distilled water, 2ml acrylamide, 2.5ml buffer, 30µl 10% APS, and 5µl TEMED). Each of the gels were left to set for 30 minutes. During this time, samples were placed in a heat block (Grant QBT2 digital block heater, Akribis scientific limited, UK) for 2 minutes and were then centrifuged alongside the protein ladder at 16,000G for 1 minute at 23°C. 25µl of each sample was then placed in a well and run at 200V for 35 minutes in a container with running buffer. Upon completion, gels were allowed to transfer onto a nitrocellulose membrane (sandwiched between sponge and filter paper either side) for 65 mins at 100V as previously described in a container with transfer buffer [209]. The nitrocellulose membrane was then washed twice with TBS buffer and then blocked with 5% non-fat milk powder in TBS for an hour while being rotated. The membrane was then incubated with the appropriate primary antibody solution for IL-36R (1:200 dilution) overnight at 4°C. After three 10-minute washes with 0.1% TBS-tween, the membrane was incubated with the secondary antibody solution conjugated to Alexa Fluor 488 (1:1000 dilution) for an hour. The washing step with 0.1% TBS-tween was repeated, and the protein bands were visualized using a fluorescence detection system (ChemiDoc, Bio-Rad, UK). Image analysis was performed by measuring the MFI of each band using ImageJ.

### 2.3.3. Expression of IL-36R, IL-36 $\alpha$ , and IL-36 $\beta$ on VCECs

#### 2.3.3.1. Murine VCEC Culture

In order to characterise the expression of IL-36R, IL-36 $\alpha$ , and IL-36 $\beta$  on ECs, conditionally immortalised murine vena cava endothelial cells (VCECs) were used (provided by Dr J Stephen Alexander, Louisiana State University, Health Science Centre, USA) [210]. To set up cultures for experiments, VCECs were firstly expanded after being thawed and subsequently cultured in 10ml of expansion media. Cells were expanded in 25cm<sup>3</sup> tissue culture flasks in an incubator at 37°C, and 5% CO<sub>2</sub> with a change of media and a DPBS wash every 48 hours. Once cells reached 95-100% confluency, they were detached from the flask using 1ml Accutase enzyme. Further enzyme activity was stopped by the addition of 6ml experimental media. The flask was then split into 3 new flasks with 10ml experimental media in each of the new flasks and incubated as previously described.

When VCECs were ready for experiments, they were detached as previously described and then centrifuged at 8,000 G for 5 minutes. The pellet was mixed with 1ml of experimental media, and cells were counted using a haemocytometer. The pellet was then suspended in a volume of experimental media which was determined by the number of cells counted. The cell solution was seeded into 24 well plates at a seeding density of 50,000 cells per well, incubated and allowed to reach confluency for 48 hours.

### 2.3.3.2. Assessing IL-36R, IL-36 $\alpha$ and IL-36 $\beta$ Expression in Stimulated VCECs

The expression of IL-36R after stimulation with either the experimental media (vehicle control) or an IL-36 cytokine ( $\alpha$ ,  $\beta$  and  $\gamma$ ) was determined and compared with the well characterized inflammatory cytokine TNF $\alpha$ . When VCECs reached confluency in 24 well plates, cells were washed with DPBS twice and then incubated for 4 hours with 500 $\mu$ l of either: experimental media (vehicle), an IL-36 cytokine (3, 30, or 300 ng/ml), or TNF $\alpha$  (3, 30, or 300 ng/ml). Subsequently, VCECs were fixed with 2% formalin at room temperature for 10 minutes, washed with DPBS, and then incubated for an hour with staining buffer at room temperature. VCECs were then washed with DPBS before an overnight incubation with 500 $\mu$ l of primary antibody solution for IL-36R (1:100 dilution). Next, the VCECs were washed with DPBS, and a secondary antibody solution conjugated to Alexa Fluor 488 (1:100 dilution) was added before they were washed again. Imaging and analysis of stained cells was performed as described in **Section 2.3.3.3**.

In a similar manner, the ability of the IL-36 cytokines to stimulate the production of IL-36 $\alpha$  and IL-36 $\beta$  was determined and compared to the ability of TNF $\alpha$  to do so. This was performed in a similar manner to IL-36R expression on VCECs, using the same secondary antibody; however, the primary antibodies used were targeted against IL-36 $\alpha$  and IL-36 $\beta$  respectively.

### 2.3.3.3. Analysis of VCEC Culture Assay

Using an x25 objective, eight fields of view per well were imaged in a pre-defined arrangement using a multiphoton microscope (Olympus FV1000-MPE, Olympus). Areas that were not confluent were dismissed and additional fields were captured (following the same pattern of field-to-field movement). Image analysis was performed using ImageJ to quantify the MFI for the entire field of view for IL-36R, IL-36 $\alpha$ , and IL-36 $\beta$  separately.

### 2.3.4. Flow Cytometry Based Experiments

Flow cytometry studies were performed to determine IL-36R expression and DNA/RNA damage on CMs and myocardial ECs in various experimental groups. Hearts from sham, IR injury and IR with IL-36Ra treatment surgeries were obtained from adult and aged mice as previously described in **Section 2.1.1**. In addition, mice were culled at 0 minutes of reperfusion (ischaemia only), 30 minutes of reperfusion, and 150 minutes of reperfusion for further comparisons of how DNA/RNA damage and IL-36R expression develop in response to ischaemia alone and IR injury.

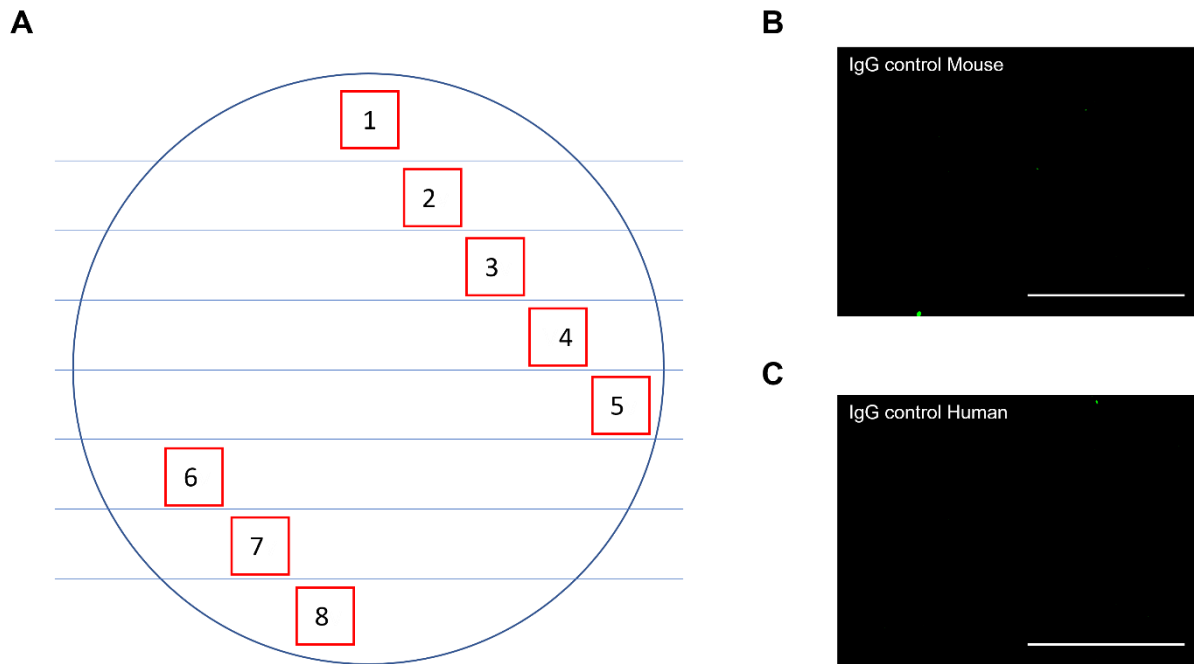


**Figure 2.4. Predefined arrangement for frozen tissue section analysis.** Murine or clinical heart samples were harvested and snap frozen following surgery. The ventricular sample was sectioned using a cryostat into 10 $\mu$ m sections and then immunostained with antibodies or IgG controls. Sections were imaged using an EVOS microscope. **(A)** Schematic of the predefined arrangement for imaging the frozen tissue sections, starting from 1 and ending at 8. Representative image of the IgG control for IL-36 in **(B)** mouse and **(C)** clinical sample.

### 2.3.4.1. Digestion of the Mouse Heart

Following surgeries, hearts were harvested and immediately placed in 3ml of cold PBS in an ice box. In a petri dish, excess blood was flushed out by squeezing the fresh hearts using surgical forceps. The hearts were then manually minced into very small fragments using a scalpel for 5 minutes until they were approximately 1mm<sup>3</sup>. A few drops of 0.1% collagenase solution were added if the tissue became dry. All tissue was then collected into a 15ml tube, and 2ml of 0.1% collagenase solution (diluted in PBS) was added to start the enzymatic digestion. The tube was placed on a rotator in a 37°C incubator for 15 minutes. After the initial incubation, the suspension was allowed to settle, and the supernatant was removed and placed into a 50ml falcon tube containing 10ml MACS buffer on ice, while the remaining tissue was re suspended in 2ml of 0.1% collagenase solution and re-incubated. This process was repeated twice for a total digestion period of 45 minutes, and then the 50ml falcon tube was centrifuged at 20,000 G for 10 minutes. In order to lyse red blood cells, the supernatant was discarded, and 2ml of ACK lysis buffer was added to the pellet for 3 minutes. MACS buffer (5ml) was then added to stop ACK activity, and the remaining cells were centrifuged at 20,000 G for 10 minutes into a pellet.

To achieve a single cell suspension, the supernatant was discarded, the pellet was suspended in 20ml of experimental media and run several times through a 70µm strainer. The suspension was then centrifuged, supernatant discarded, and the pellet was washed with 20ml PBS; this process was repeated 2 times. To prevent non-specific binding, the pellet was incubated with 5ml staining buffer for 30 minutes in an ice box, and the suspension was then centrifuged.

### 2.3.4.2. Assessing Oxidative Damage and IL-36R Expression in the Mouse Heart

To assess oxidative damage and IL-36R expression levels on myocardial ECs and CMs in the experimental groups, fluorescently labelled antibodies against these markers were used. Following centrifugation, the supernatant was discarded, and cells were incubated with a primary antibody solution for IL-36R (100µl, 1:100 dilution in DPBS). Subsequently, cells were washed with DPBS, centrifuged at 20,000 G for 10 minutes, and then incubated with 100µl of secondary antibody solution conjugated to Alexa Fluor-647. Additional antibodies were added into the second step to assess damage (anti-DNA/RNA damage; 1:100 dilution in DPBS), to label ECs (CD31; 1:100 dilution in DPBS), CMs (cTnT; 1:100 dilution in DPBS), and dead cells (Zombie; 1:500 dilution in DPBS).

Single colour controls were also performed for each of the fluorescently labelled antibodies to be able to compensate for potential fluorescence spillover during analysis. In addition, cells were incubated with the appropriate IgG controls for the fluorescently labelled antibodies as above. Each of the primary and secondary antibody incubations were performed in a light-protected icebox placed under slight agitation for a duration of 30 minutes. Following the second incubation, cells were fixed using 4% formalin for 10 minutes and were then washed with DPBS. The supernatant was discarded, and cells were resuspended in 400µl of DPBS in the appropriate flow cytometry tubes ready for acquisition.

### 2.3.4.3. Acquisition and Analysis of Flow Cytometry Studies

Acquisition of cells was performed using a CyAn™ ADP (Beckman Coulter, USA) and data analysis was performed using Summit 4.3 software (Beckman Coulter, USA). Channels used to assess the markers described above were FITC (voltage – 575), PE (voltage – 600), APC (voltage – 650), Violet 1 (voltage – 725), and Violet 2 (voltage – 650). Forward scatter (FS) was set at a gain of 8.0 and side scatter (SS) was set a voltage of 500. For each sample, 250,000 events were captured and used in the analysis.

An initial gate was drawn on the SS Lin Vs FS Lin density plot to exclude any debris. A second gate was then created to exclude doublets on the FS Lin Vs pulse width plot. The appropriate IgG controls for each of the fluorescently labelled antibodies were run and used to determine gating for each of these channels (**Figure 2.5**). These gates were used for all experimental groups and repeats. Using the single colour control samples, post-acquisition compensation was performed for each sample to minimise any potential fluorescence spillover. This was performed by compensating each fluorescently labelled antibody with the other antibodies.

To determine the cell population counts in each sample, the percentage of CMs, ECs, and dead cells were measured. To analyse the oxidative damage levels on each of CMs and ECs, previous gating of DNA/RNA damage fluorescence channels was applied on the individual cell type channels, and the MFI calculated. Similarly, IL-36R expressions levels were determined on each of the cell types.

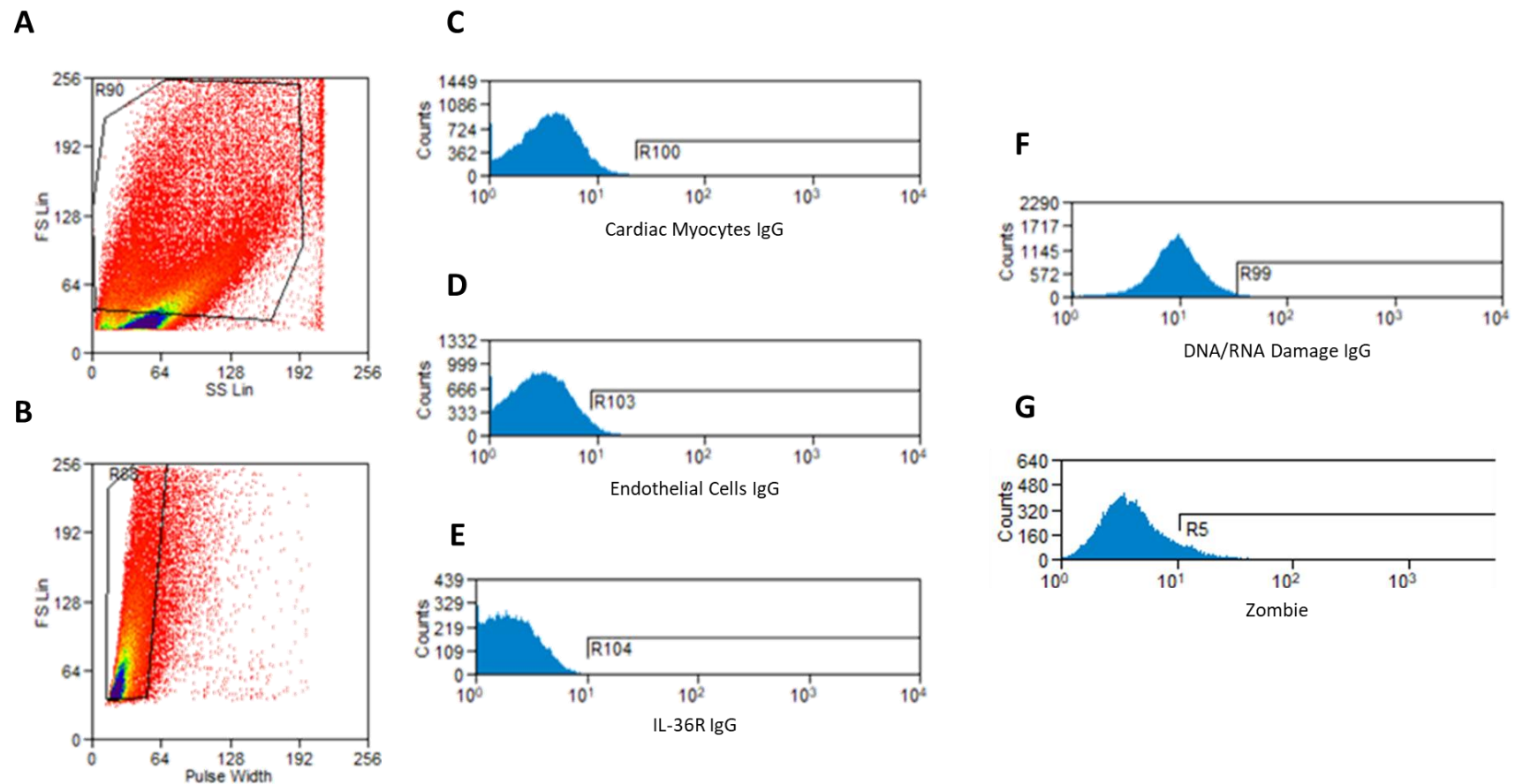


**Figure 2.5. Gating strategy for flow cytometry-based experiments.** Sham or IRI inducing surgery was performed on adult and aged mice. Mice were culled following reperfusion, and hearts were harvested and digested. The cell suspension was stained with an anti-cTnT, anti-CD31, anti-IL-36R, anti-DNA/RNA damage, zombie dye and IgG control antibodies and acquisition were performed using a CyAn™ ADP cytometer. Representative density plots showing the **(A)** initial gate drawn to capture the greatest number of cells whilst ensuring any debris were excluded, and **(B)** the second gate drawn to exclude potential duplicates. Representative histogram of IgG controls for **(C)** cardiac myocytes, **(D)** endothelial cells, **(E)** IL-36R, **(F)** DNA/RNA damage, and **(G)** Zombie. Abbreviations – FS: forward scatter, SS: side scatter.

## 2.3.5. Myocardial Infarct Size Analysis

### 2.3.5.1. Preparation of Mouse Heart Samples

Infarct size analysis was used to determine the impact of myocardial IR injury and the potential benefit of IL-36Ra as a therapeutic treatment in the mouse heart [211]. Surgeries were performed as previously described in **Section 2.1.1** in adult and aged mice with a reperfusion period of 4 hours. The LAD artery was then re-ligated to occlude blood flow in the LV, and 500µl of 0.5% Evans blue dye was retrograde infused via the carotid cannula. Ligation of the LAD prevents the dye from entering and staining regions of the heart downstream of the LAD artery while staining other vasculature. The area that does not stain is known as the area at risk (AAR). The mouse was then immediately culled by cervical dislocation; the heart was harvested, wrapped in saran film, and placed in a -20°C freezer for 60 minutes. Sequential transverse cuts were then made into the heart using a scalpel to achieve 4 equal sections of around 2mm in depth. For treatment studies, recombinant mouse IL-36Ra was injected intra-arterially at both 10 minutes pre-reperfusion and 60 minutes post-reperfusion.

### 2.3.5.2. Triphenyl Tetrazolium Chloride (TTC) Staining

TTC staining solution was used to stain heart sections to determine the extent of infarction post-IR injury and treatment. Tissue that is rich in dehydrogenase enzyme/co-factors (i.e., likely viable tissue) responds to TTC solution by turning a deep red colour, whilst dead or damaged tissue is identified as pale regions. These pale regions are defined as the infarct region. Heart slices were incubated at 37°C in TTC solution for a duration of 20 minutes with

continuous agitation. These slices were then removed and fixed in 10% formalin for a further 20 minutes at room temperature. Slices were washed in PBS and lightly dried and then placed on a slide for imaging using a stereomicroscope (Nikon, UK). In order to ensure reliable thickness while imaging, a 250g weight was placed at both ends of the slide.

### 2.3.5.3. Analysis of Infarct Assay

Images were captured from a stereomicroscope using a standard mobile camera (iPhone X, Apple, USA) and were analysed using ImageJ. Prior to analysis, the background was subtracted. The area of 3 regions was determined on ImageJ: area not at risk (TTC negative, Evans blue positive), AAR (TTC positive red regions, Evans blue negative), and infarcted area (TTC negative white regions, Evans blue negative) (**Figure 2.6**). ImageJ was used to quantitate the infarcted area as a percentage of the AAR.

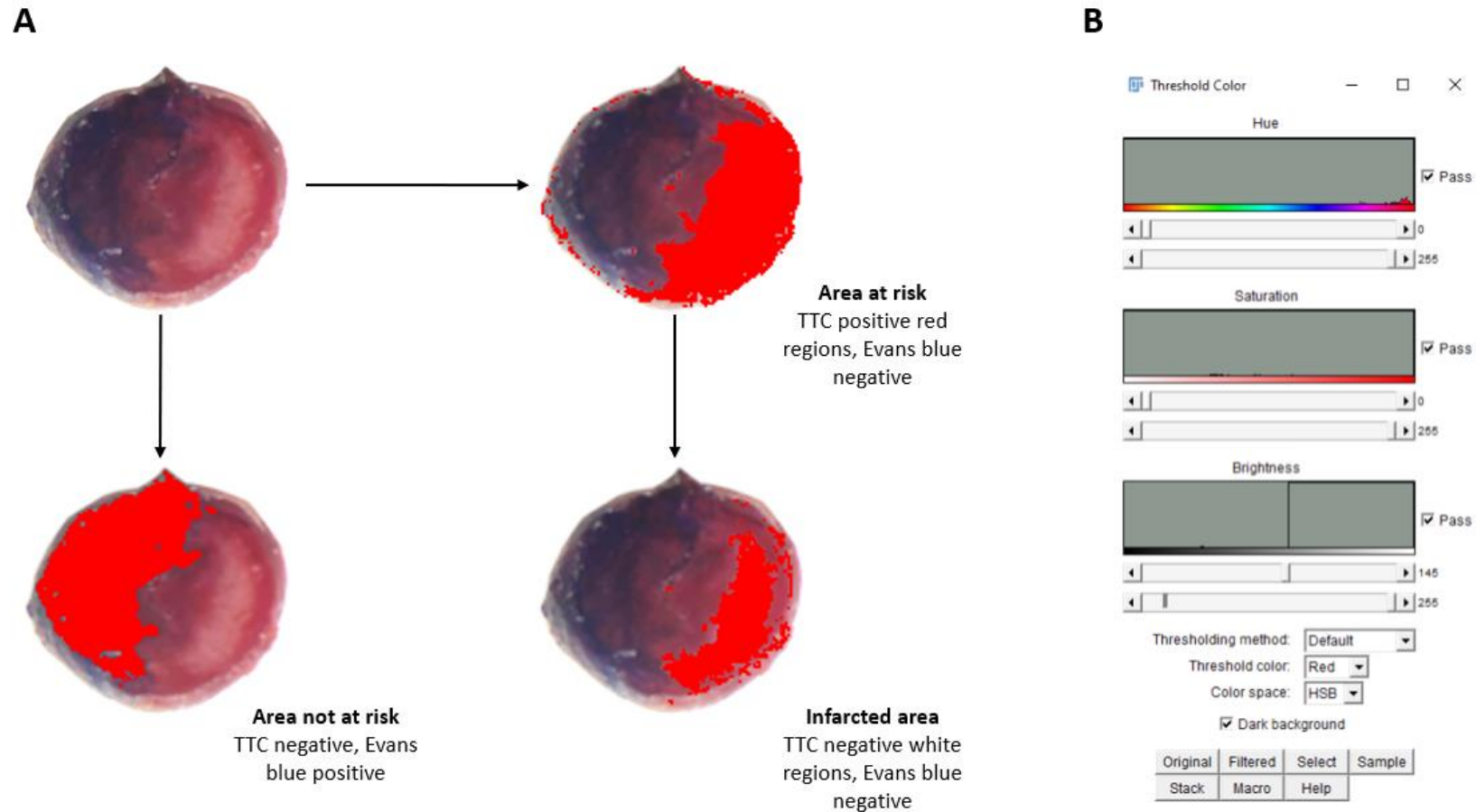


**Figure 2.6. Myocardial infarct size analysis.** Surgery was performed on adult and aged mice. Following 4-hours of reperfusion, the left anterior descending (LAD) artery was re-ligated, and Evans Blue was injected. Mice were culled, and the heart was harvested, sectioned, stained with TTC and imaged. **(A)** Representative image of the TTC stained IR injured hearts. The area of 3 regions was determined on ImageJ: area not at risk (TTC negative, Evans blue positive), AAR (TTC positive red regions, Evans blue negative), and infarcted area (TTC negative white regions, Evans blue negative). **(B)** Representative image of the threshold colour panel on ImageJ, which was used for the infarct analysis.

### 2.3.6. Multiphoton Imaging of Heart Sections

Intravital imaging captured microvascular thromboinflammatory events from the surface of the beating heart with a depth of approximately 50-60 $\mu$ m. To determine whether these events were mirrored throughout the thickness of the ventricular wall, multiphoton microscopy was performed on hearts harvested at the end of intravital experiments detailed in **Section 2.1.1**. Following intravital imaging, hearts were harvested, immediately placed in 3ml of cold PBS in an icebox and were dried. To section the hearts using a tissue vibratome (Campden Instruments Limited, UK), hearts were glued using Liquid-Skin to the metal disc with the LV facing upwards. The LV was then sectioned into four 300 $\mu$ m sections and imaged from the outer epicardial end through to the inner endocardial end using a multiphoton microscope (FVMPE-RS Olympus). Z-stacks from the four layers were rendered to form 3D stack images, which were processed and displayed using ImageJ (**Figure 2.7**). In order to ensure the tissue was visible for imaging during Z-stack capture, a pre-defined setting was used for neutrophils in each of the 4 layers of the heart; Z position 0 – laser 9% and 550V, Z position 50 – laser 9% and 550V, Z position 100 – laser 10% and 550V, Z position 150 – laser 11% and 590V, Z position 200 – laser 12% and 636V, and Z position 250 – laser 12.5% and 650V. The presence of neutrophils was analysed as the sum fluorescence intensity for each section (ImageJ).

## 2.4. Statistical Analysis

All statistical analysis was performed using GraphPad 7.0 software (GraphPad Software Inc., USA). Direct comparisons between two groups were performed using a Student's unpaired t-test. Multiple comparisons between three or more groups were performed by a one-way ANOVA, followed by a Tukey's post-hoc test. For experiments that followed a time course, the area under the curve (AUC) was also calculated, plotted into a bar graph, and used for subsequent analysis as a summation of the entire period. The *n* values in the animal experiments represent the number of animals used, while in cellular experiments (such as the VCECs culturing) it represents the experimental repeat number. All data are presented as mean  $\pm$  standard error of the mean (SEM). Statistical significance was defined when  $p < 0.05$ .

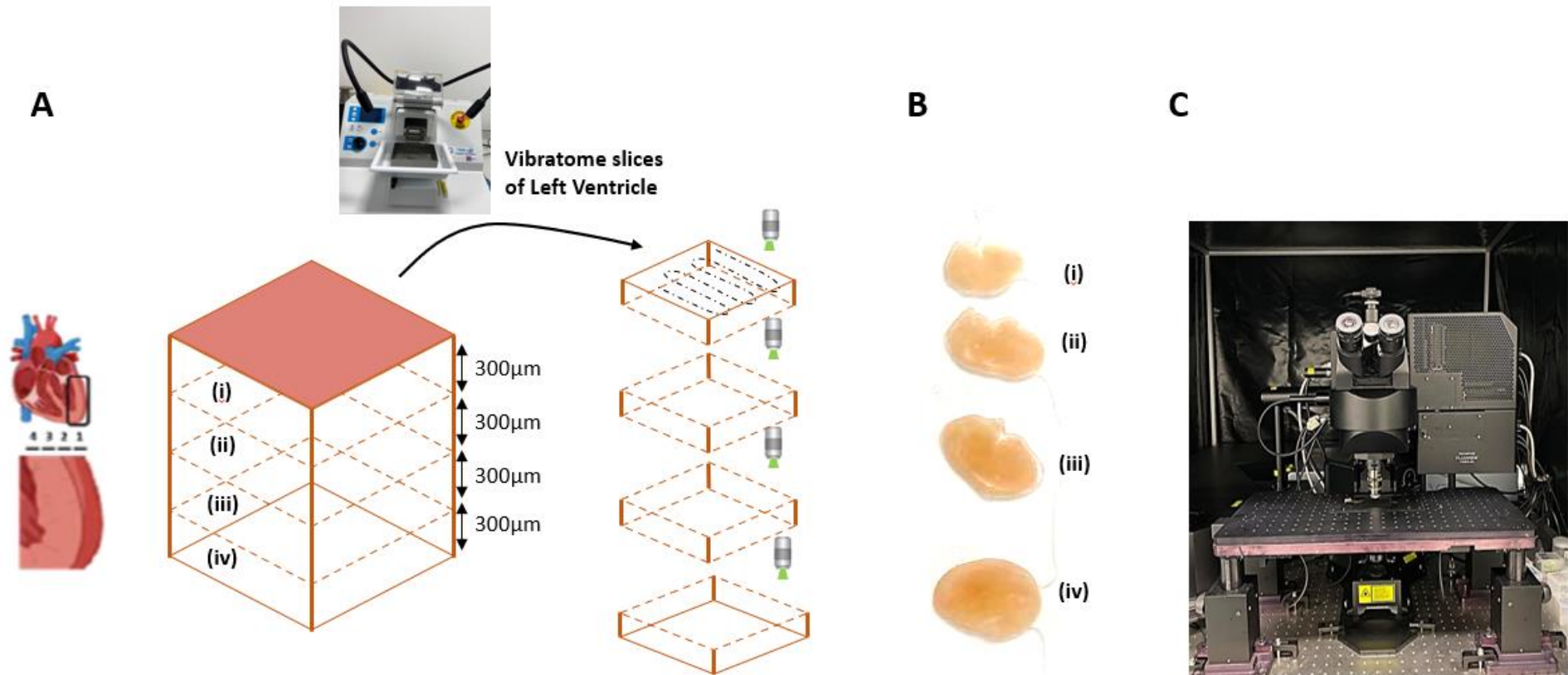


**Figure 2.7. Preparing the mouse LV for multiphoton imaging ex vivo.** (A) To ascertain whether any thromboinflammatory events imaged using intravital microscopy on the surface of the heart were also occurring in the deeper layers of the myocardium, multiphoton microscopy was used. The heart was cut in half longitudinally from the base to apex to expose the inner endocardial layer lining the LV chamber. It was then placed on a specimen holder and attached to a tissue vibratome to precisely section the LV wall into 4 sections from the outermost layer closest to the epicardium through to the inner layer closest to the endocardium. Sections of 300µm thickness were cut. (B) Representative images of the tissue sections. Multiphoton z-stacks were taken from all 4 layers, namely the (i) outermost layer closest to the epicardium – epi-to-mid (ii) outer myocardial layer – mid-to-mid (iii) inner myocardial layer – mid-to-mid and the (iv) innermost layer closest to the endocardium – mid-to-endo, avoiding the last section if it had ‘missing’ myocardium due to sectioning through the actual ventricle chamber. Images from each layer were then rendered to form 3D stack images. (C) Representative image of the multiphoton set-up. Imaging was performed using a multiphoton microscope (FVMPE-RS Olympus).

# **Chapter 3:**

## **Microcirculatory**

### **Disturbances in Adult and**

### **Aged Ischaemia -**

## **Reperfusion Injured Hearts**

\* Part of this chapter makes up the published paper in the appendix

### 3.1. Introduction

Treatment of MI focuses on rapidly re-establishing perfusion following a blockage in one or more of the coronary arteries. This can be achieved by a primary PCI using a coronary stent to open the culprit artery. Despite these interventions, a significant proportion of patients still incur extensive muscle damage and develop heart failure post-MI [212]. This is partly due to reperfusion paradoxically leading to additional tissue damage. Indeed, restoration of normal epicardial blood vessel flow, but with sub-optimal myocardial perfusion, can be observed in up to 50% of patients following PCI, leading to worse outcomes than in patients with full perfusion recovery [32]. This suggests tissue damage likely occurs subsequent to inadequate coronary microcirculatory perfusion [41, 213].

Growing evidence suggests that dysfunction in the coronary microcirculation through thromboinflammatory responses and MVO may ultimately be responsible for most of the damage attributable to myocardial IR injury [53, 214]. Increased clinical recognition of the importance of the coronary microcirculation has meant identifying strategies to improve potential perturbations within it has gained recent attention [41, 213]. However, current clinical tools cannot resolve coronary microvessels  $<200\mu\text{m}$ , and so little is known about the full range of cardiac microcirculatory responses to IR injury. This has led researchers to refer to the coronary microcirculation as a research 'black box', with cardiologists having focussed on treating the angiographically visible circulation [53, 54].

Age is a major risk factor for MI, increasing the cardiac damage caused by IR injury independent of 'traditional' risk factors [215-217]. The term '*inflammaging*' describes the phenomenon of ageing accompanied by a chronic low-grade sterile inflammation, that

persists in the absence of an overt inflammatory stimulus [163]. Inflammaging may contribute to enhanced age-related cardiovascular risk and poorer outcomes through actions on myocardial microcirculation. However, little is known about how age impacts the coronary microcirculation in health and whether it increases the likelihood of microvascular disturbances post-IR injury. This chapter therefore focuses on investigating microcirculatory disturbances with age and IR injury using *in vivo* and *in vitro* methods.

#### 3.1.1. Hypotheses and Aims

In this chapter, we aim to assess the microcirculatory responses of the healthy uninjured, and IR injured aged hearts and compare them with adult hearts *in vivo* using laser speckle and intravital imaging of the beating heart and *in vitro* using multiphoton microscopy. Secondly, in this chapter, we investigate the mechanisms underlying the microcirculatory perturbations in adult and aged, sham and injured harvested hearts *in vitro* using immunofluorescence and flow cytometry-based studies. Lastly, in this chapter, we assess the impact of IR injury and age on infarct size. We hypothesize:

1. Overall coronary perfusion is significantly reduced with ageing and IR injury.
2. Microcirculatory neutrophil and platelet recruitment are increased in healthy aged, and IR injured aged hearts when compared to adult hearts.
3. Microcirculatory perfusion and capillary leakage will be worse in aged IR injured hearts compared to adult IR injured hearts.
4. VCAM-1 expression and oxidative stress will be increased in aged IR injured hearts when compared to adult IR injured hearts.

## 3.2. Results

### 3.2.1. General Observations

Aged mice had a few distinct features which were not present in adult mice. During animal handling and surgery, the fur of aged mice fell out easily. They also required more maintenance anaesthetic during *in vivo* imaging procedures. Other typical senescent phenotypes in aged mice such as balding, loss of colour (white/grey) and kyphosis (curvature of the spine) were also observed. Hearts harvested and sectioned from aged mice were structurally more fragile and so sometimes had larger gaps between CMs.

### 3.2.2. Laser Speckle Contrast Imaging (LSCI) Demonstrated a Decreased Overall Perfusion of the Aged Heart Post-Reperfusion *in vivo*

LSCI was used to firstly investigate the overall perfusion of the left ventricular myocardium in response to IR injury in adult and aged female mice. High and low flux points were calculated from flux recordings and were attributed to diastolic and systolic events respectively (**Figure 3.1a-b**). Systolic events were used for comparative purposes between different experimental groups. As expected, in both adult and aged hearts, ischaemia decreased perfusion following LAD artery ligation (**Figure 3.2a**). This was rapidly reversed as soon as the artery was untied. In adult mice, reperfusion resulted in ventricular perfusion returning to the basal levels seen prior to ischaemia (**Figure 3.2a**). In some individual mice, reperfusion was accompanied by an immediate but transient, reactive

hyperaemic response. However, in aged injured mice, perfusion failed to reach basal levels (**Figure 3.2a**) and remained significantly lower than in adult injured hearts (**Figure 3.2b**).

To determine whether IR injury impacted perfusion differently during systole and diastole, the average flux during these two phases of the cardiac cycle in adult mice was compared to the average flux during these phases in aged mice. As expected, ischaemia decreased ventricular perfusion during both systole and diastole in both adult and aged mice (**Figure 3.4a-b**). However, there was no significant difference in the ischaemic perfusion during systole and diastole between adult and aged mice (**Figure 3.4c**). Again, reperfusion resulted in a resumption of ventricular perfusion in systole and diastole in both adult and aged mice. However, perfusion was decreased in both systolic and diastolic phases in aged mice when compared to adult mice, although this only reached statistical significance in the diastolic phase (**Figure 3.4c**).

LSCI also allowed ventricular arrhythmia to be investigated from the flux recordings using the standard deviation of the inter-beat distance as a means to identify irregularity in the rhythm of the heartbeat (**Figure 3.3**). Both ischaemia and reperfusion resulted in an arrhythmic response in adult and aged injured mice. However, there were no significant differences between the two groups (**Figure 3.2c-d**). Similarly, both ischaemia and reperfusion resulted in changes in the heart rate in adult and aged injured mice, but again there was no significant difference between the two groups. (**Figure 3.2e-f**). Additional differences were observed in some aged injured hearts that were not seen in adult injured hearts, which included unusual heart rhythm patterns noted in some aged hearts (**Figure 3.4d**). Also, flux/perfusion data showed that prior to induction of ischaemia, adult hearts were significantly better perfused basally than aged hearts (**Figure 3.4e**).

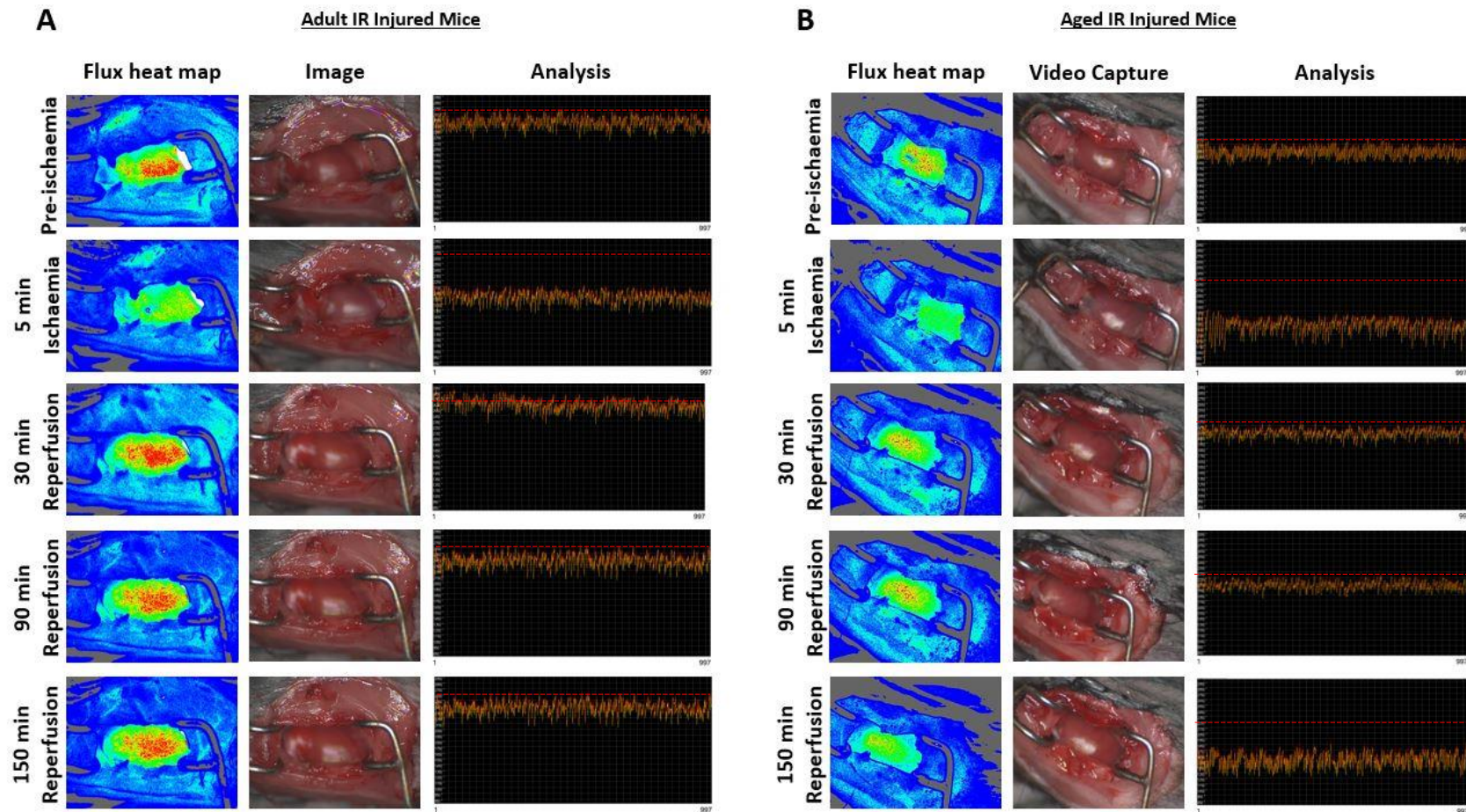


**Figure 3.1.** Laser speckle contrast imaging (LSCI) allows changes in the overall perfusion of the left ventricle to be quantitated during ischaemia and reperfusion in the (A) adult and (B) aged female beating heart coronary circulation *in vivo*. Flux heat maps show warm colours under basal conditions, cooler colours during ischaemia and warmer colours again as reperfusion is initiated. Note how in this particular aged female mouse heart, the flux heat map colour is not as warm at 150 minutes post-reperfusion as its own basal levels, nor as warm as 150 minutes post-reperfusion in adult mice. Note how in this particular adult mouse heart, there is a temporary hyperaemic response noted at 30 minutes post-reperfusion.  $n \leq 6/\text{group}$ .

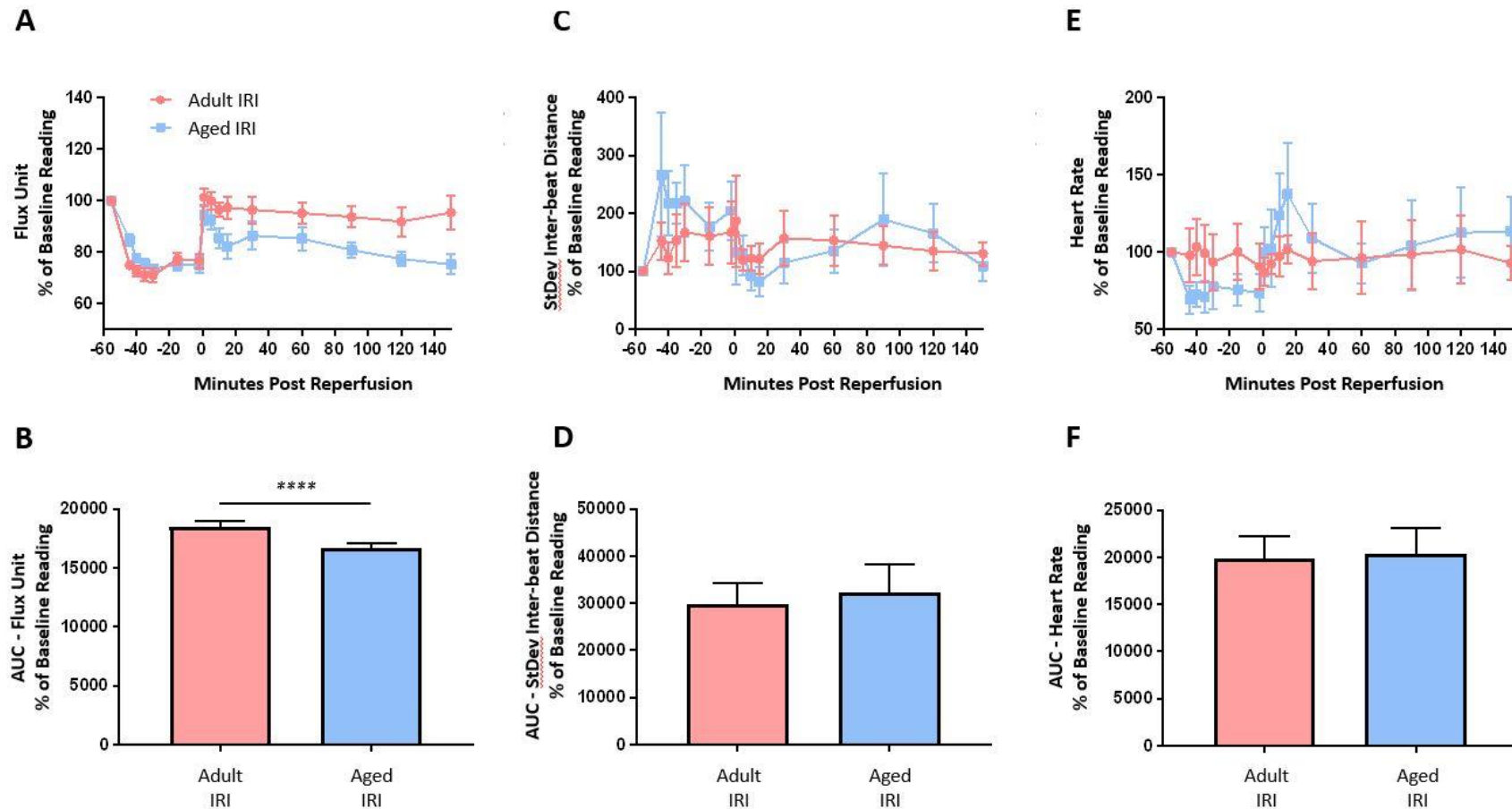


**Figure 3.2. Laser speckle contrast imaging (LSCI) demonstrated a decreased overall perfusion of the aged female heart left ventricle post-reperfusion *in vivo*.** Quantitative time-course analysis of LSCI data during systole for (A) flux unit (perfusion) (C) standard deviation of the inter-beat distance (arrhythmia), and (E) heart rate. Baseline capture prior to ischaemia was used as the baseline reading. Area under the curve (AUC) analysis for (B) flux unit, (D) standard deviation of the inter-beat distance and (F) heart rate over a time course of 150 minutes post-reperfusion. Aged mice had significantly less perfusion in the ventricle than adult mice post-reperfusion. Although the standard deviation of the inter-beat distance and heart rate changed in both adult and aged mice throughout the duration of the experiment, there were no significant differences between the two groups. Statistical analysis was performed using a Student's unpaired t-test. Abbreviations - IRI: ischaemia reperfusion injury, StDev: standard deviation.  $n \leq 6/\text{group}$ . Mean  $\pm$  SEM. \*\*\*\* $p < 0.0001$ .

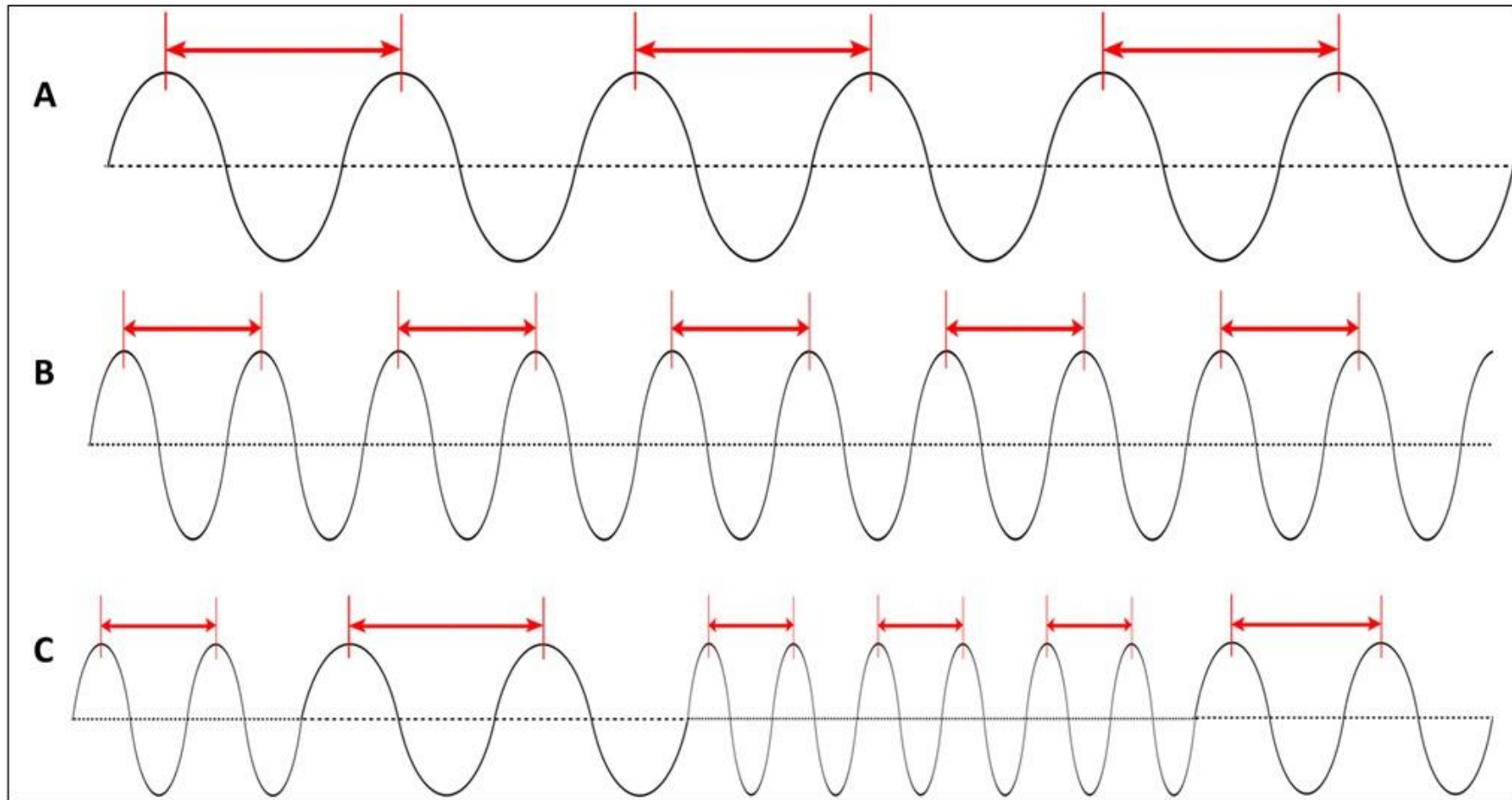


**Figure 3.3. Laser speckle data can be analysed to determine the inter-beat distance and subsequently the standard deviation (SD) of the inter-beat distance. The SD of the inter-beat distance can provide an indication of whether there is an irregularity in the heartbeat rhythm. (A-B)** Although the inter-beat distance (arrows), and thus heart rate, varies between these two examples, the SD of the inter-beat distance would not change as the inter-beat distance remains constant for both. Hence, although the heart may be beating faster or slower, the beating pattern is regular. This is indicative of there being no irregularity or arrhythmia in the heart's rhythm. **(C)** The inter-beat distance (arrows) is different in this example, and so the SD of the inter-beat distance would change. Hence, the heart may be beating faster but, importantly, it is also not beating regularly. This is indicative of an irregularity or arrhythmia in the heart's rhythm.

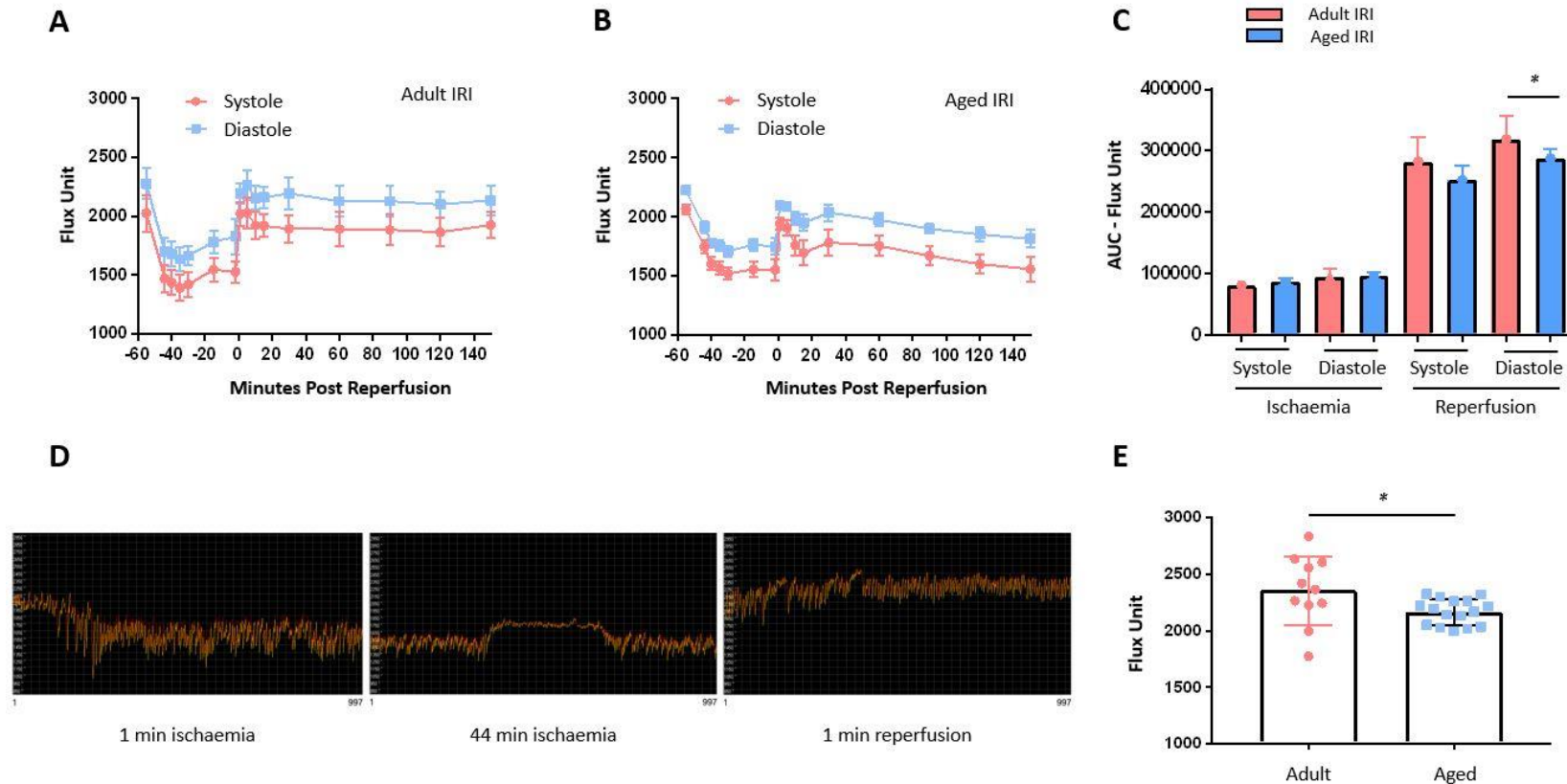


**Figure 3.4. Laser speckle contrast imaging (LSCI) demonstrated a decreased overall perfusion of the aged female heart left ventricle post-reperfusion during both systolic and diastolic phases of the cardiac cycle *in vivo*. A decreased basal perfusion in the aged hearts was also demonstrated.** Quantitative time-course analysis of LSCI data during systole and diastole for flux unit (perfusion) in **(A)** adult and **(B)** aged mice. Baseline capture prior to ischaemia was used as the baseline reading. **(C)** Area under the curve (AUC) analysis for systole and diastole flux unit in the ischaemia and reperfusion phases in adult and aged mice. Statistical analysis was performed using a one-way ANOVA, followed by a Tukey's post-hoc test between the following groups: systole adult versus systole aged for each of ischaemia and reperfusion, and diastole adult versus diastole aged for each of ischaemia and reperfusion. **(D)** Representative images of LSCI analysis graph at various time points showing anomalies in the aged IR injured beating heart, including a prolonged time to reach ischaemia and reperfusion and irregularities in rhythm. **(E)** Quantitative analysis of LSCI baseline capture prior to ischaemia during systole. Statistical analysis was performed using a Student's unpaired t-test. Abbreviations - IRI: ischaemia reperfusion injury. \* $p < 0.05$ . Mean  $\pm$  SEM.

### 3.2.3. Age Increased Thromboinflammatory Disturbances within the Healthy and IR Injured Coronary Microcirculation *in vivo*

Intravital studies were conducted to assess the impact of ageing and IR injury at a more cellular level on thromboinflammatory events in the beating mouse heart. Images were taken between 15 and 150 minutes-post reperfusion. Although some adherent neutrophils were observed in adult sham hearts, their presence did not increase with time. However, neutrophil recruitment significantly increased with injury in adult mice. Interestingly, basal neutrophil adhesion was significantly higher at all time points in aged sham hearts when compared with adult sham hearts (**Figure 3.6a-b**). However, the greatest level of neutrophil recruitment was observed in injured aged mice, reaching almost double that seen in adult IR injured mice. This increase was noted at all time points post-reperfusion and continued to rise. This was significantly greater than neutrophils numbers in both aged sham and adult injured hearts (**Figures 3.5 and 3.6a-b**). In both adult sham, adult injured, and aged sham mice, adherent neutrophils were present primarily within the coronary capillaries (**Figure 3.5**). However, in aged injured hearts, adherent neutrophils were also observed within medium-sized blood vessels as well as in the coronary capillaries. Individual neutrophils within this group were often difficult to demarcate and appeared as clusters (**Figure 3.5**).

The number of free-flowing neutrophils observed circulating through the field of view decreased in all groups when compared to adult sham hearts (**Figure 3.6e-f**). However, this was only statistically significant in the adult injured and aged sham groups when compared to adult sham hearts (**Figures 3.6c-d**). In all mice, free-flowing neutrophils were observed circulating through coronary capillaries as well as in medium-sized blood vessels. However,

in the medium-sized vessels, neutrophils were also observed to tether and roll along the vessel wall (**Figure 3.7a**). Interestingly, in one adult injured mouse heart, a large diameter epicardial coronary artery was captured serendipitously within the field of view. In this large blood vessel, free-flowing neutrophils were observed circulating at very rapid speeds but, unlike in medium-sized vessels, no tethering or rolling was observed. Furthermore, very large aggregates of platelet-rich and mixed platelet-neutrophil aggregates were observed circulating through this blood vessel, presumably having detached from the ligation site (**Figure 3.7b**).

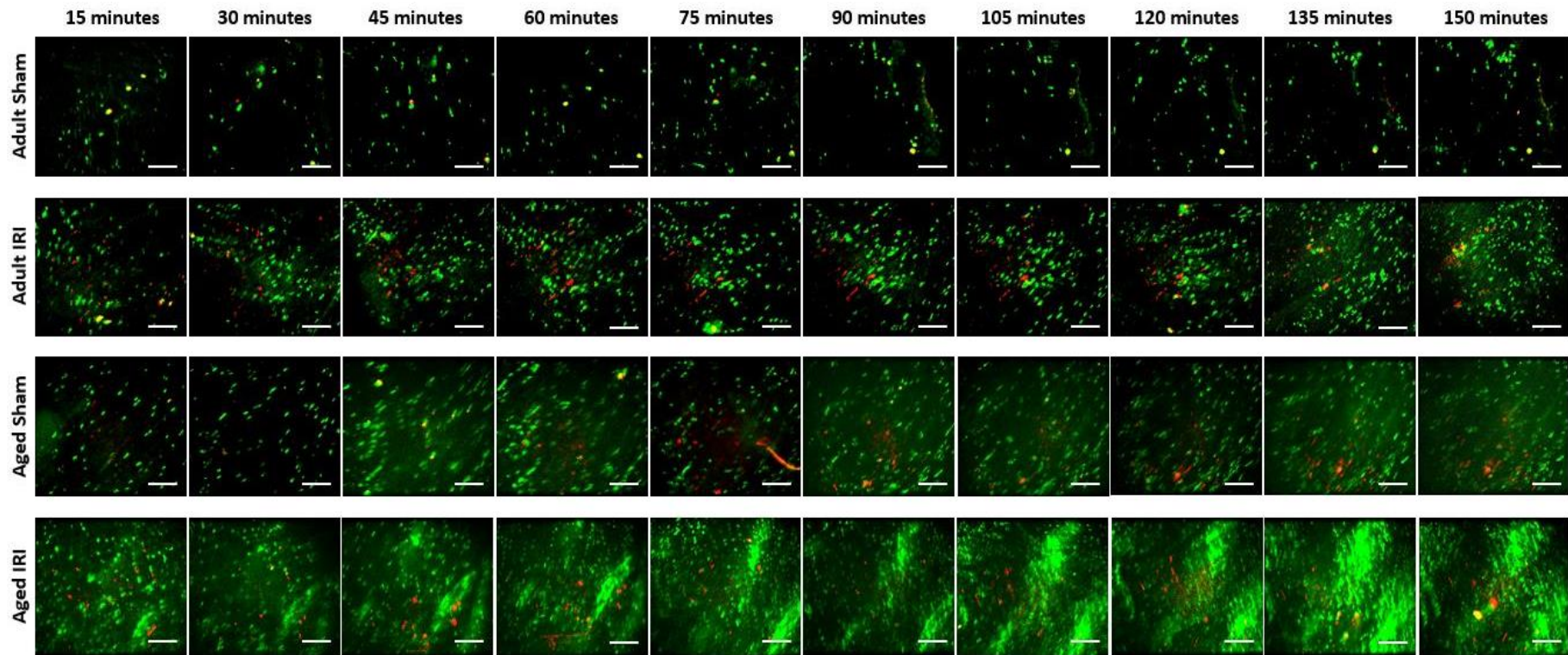
The presence of adherent platelet aggregates was also significantly increased with injury in adult mice when compared to sham adults (**Figure 3.6c-d**). Interestingly, basal platelet presence was also significantly higher in aged sham hearts when compared with adult sham hearts and increased further with injury. Indeed, adherent platelet aggregates were identified most consistently across all-time points in the injured aged mice (**Figures 3.6e-f**). Platelet-platelet as well as platelet-neutrophil aggregates were observed in both coronary capillaries and medium-sized blood vessels (**Figure 3.5**).

The surgical and stabilisation protocol was optimised to allow the impact of IR injury on thromboinflammatory events in the immediate aftermath of reperfusion to be assessed rather than after just 15 minutes of reperfusion. Studies were only conducted on adult female mice, and intravital images were captured before, during and immediately after reperfusion. Prior to reperfusion, only a limited number of neutrophils (and very occasional platelet microthrombi) were observed within the coronary microcirculation (**Figures 3.8 and 3.9**). However, within minutes of the suture around the LAD artery being untied, neutrophil presence increased and continued to increase over the remainder of the imaged

150 minutes of reperfusion (**Figure 3.9a and 3.9c**). In contrast, platelet microthrombi presence increased sharply within the first 30 minutes of reperfusion, before decreasing and reaching a plateau (**Figures 3.9b & 3.9d**).

#### **3.2.4. Age Increased Neutrophil Presence within the Deeper Layers of the Healthy and IR Injured Myocardium**

Intravital imaging captured microvascular thromboinflammatory events from the surface of the beating heart with a depth of approximately 50-60 $\mu$ m. To determine whether these events were mirrored throughout the thickness of the ventricular wall, multiphoton microscopy was performed on hearts harvested at the end of intravital experiments. Minimal neutrophil presence was identified in adult sham hearts throughout the depth of the left ventricular wall when imaged *ex vivo* using multiphoton microscopy. However, in adult injured hearts, a significantly increased presence of neutrophils was observed in the first three layers of the heart, from the outermost epicardial side inwards, when compared to adult sham hearts, with the least neutrophil number present in the layer closest to the endocardium (chamber side). However, the largest neutrophil presence in response to injury occurred within the outermost 300 $\mu$ m layer. Basal neutrophil presence was also significantly increased throughout all four layers of the ventricle in aged sham hearts when compared with adult sham hearts. This was further significantly increased in aged injured hearts when compared to adult injured hearts, with the greatest presence again noted within the outermost layer of the ventricle wall (**Figures 3.10 and 3.11**).



Green : Neutrophils  
Red : Platelets

**Figure 3.5. Intravital imaging demonstrated that age increased thromboinflammatory disturbances within sham and IR injured beating heart coronary microcirculation *in vivo*.** Sham surgery or IR injury was performed in adult and aged female mice. Representative intravital images are shown over a time course of 150 minutes post-reperfusion. Fluorescently labelled antibodies against neutrophils (green) and platelets (red) were injected via the carotid cannula 5 minutes before reperfusion. Adherent neutrophils and platelet microthrombi are observed primarily within coronary capillaries in injured hearts. However, in aged IR injured hearts. Abbreviations - IRI: ischaemia reperfusion injury. Scale bar indicates 100µm. n ≤ 5/group.

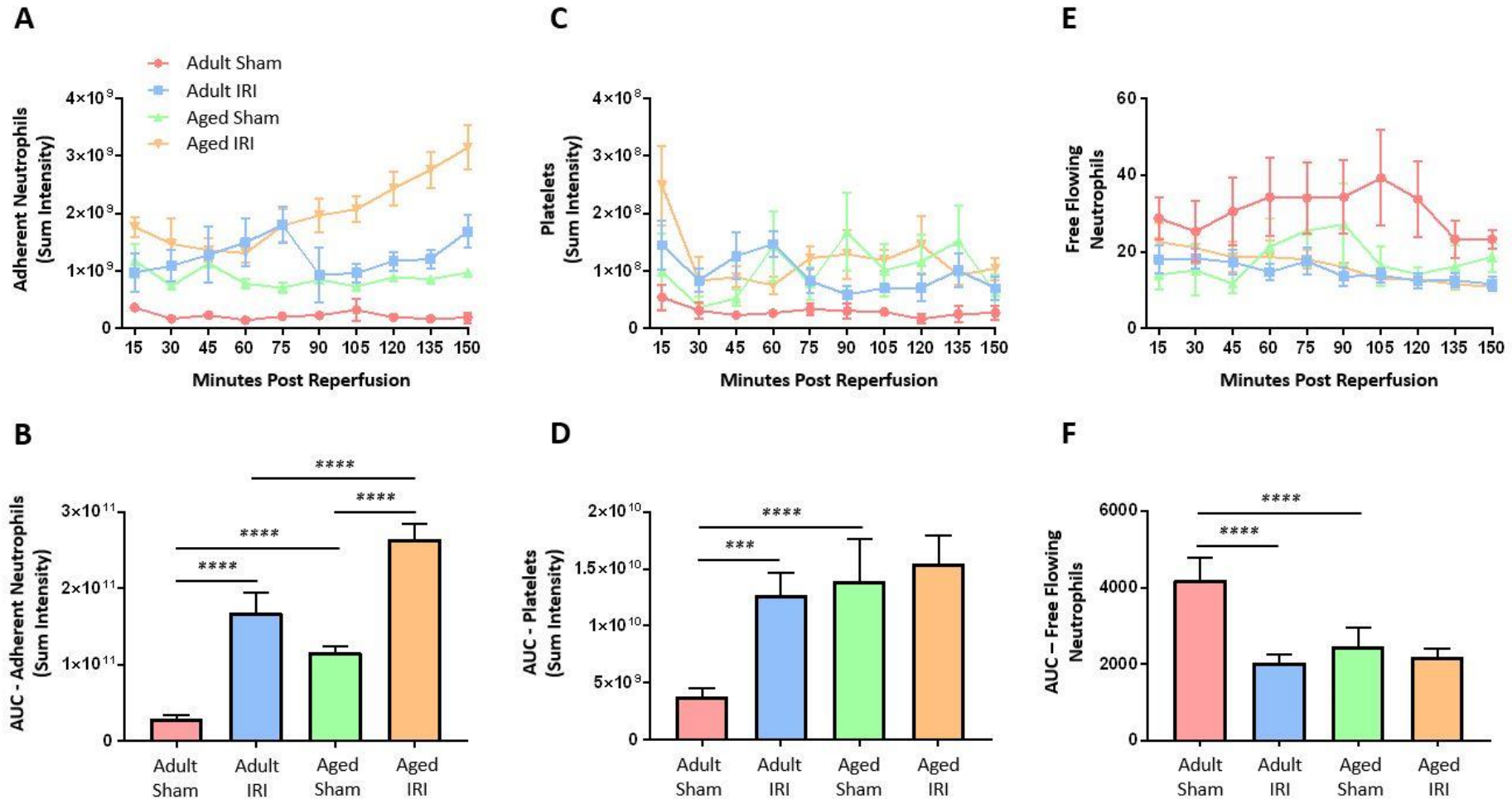


**Figure 3.6. Intravital imaging demonstrated that age increased thromboinflammatory disturbances within sham and IR injured beating heart coronary microcirculation *in vivo*.** Sham surgery or IR injury was performed in adult and aged female mice. Quantitative time-course analysis of intravital data for (A) adherent neutrophils (C) platelets and (E) free-flowing neutrophils. Area under the curve (AUC) analysis for (B) adherent neutrophils (D) platelets and (F) free-flowing neutrophils over a time course of 150 minutes post-reperfusion. Statistical analysis was performed using a one-way ANOVA, followed by a Tukey's post-hoc test between the following groups: adult sham versus adult IR injury, adult sham versus aged sham, aged sham versus aged IR injury, and adult IR injury versus aged IR injury. Abbreviations - IRI: ischaemia reperfusion injury.  $n \leq 5/\text{group}$ . Mean  $\pm$  SEM. \*\*\* $p < 0.001$ , \*\*\*\* $p < 0.0001$ .

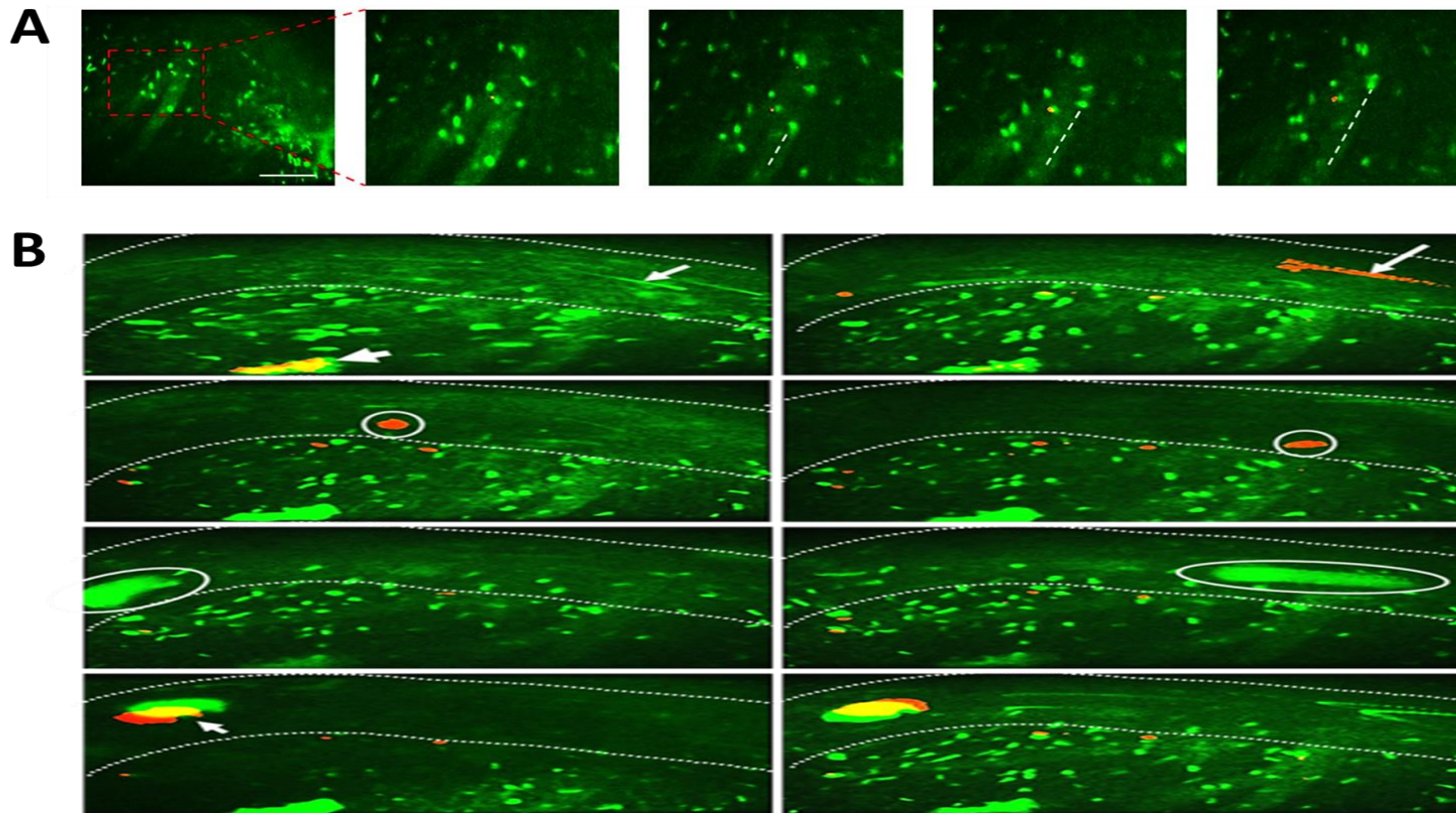


**Figure 3.7. Intravital images showing neutrophil rolling within medium-sized blood vessels and thromboinflammatory emboli within a large coronary blood vessel *in vivo*.** These intravital images are taken from two different adult female mice after IR injury. Fluorescently labelled antibodies against neutrophils (green) and platelets (red) were injected via the carotid cannula 5 minutes before reperfusion. Adherent neutrophils are observed primarily within coronary capillaries. **(A)** In this mouse, a medium-sized blood vessel can be seen in which a neutrophil (tracked by the dotted line) can be observed rolling and then adhering to the vessel wall. **(B)** In this mouse, a large diameter epicardial artery, that was downstream of the LAD artery ligature site is demarcated by dotted lines. Neutrophils and platelets circulated through it at very high velocities - note the fluorescent streaks they leave behind (arrows in upper panel). Large neutrophil-rich (green), platelet-rich (red) and mixed (yellow) aggregates passed through this vessel immediately after the LAD artery was untied, presumably embolising downstream from the ligature site. The same circulating aggregate is shown in the left and right panels. Scale bar indicates 100 $\mu$ m.  $n \leq 5$ /group.

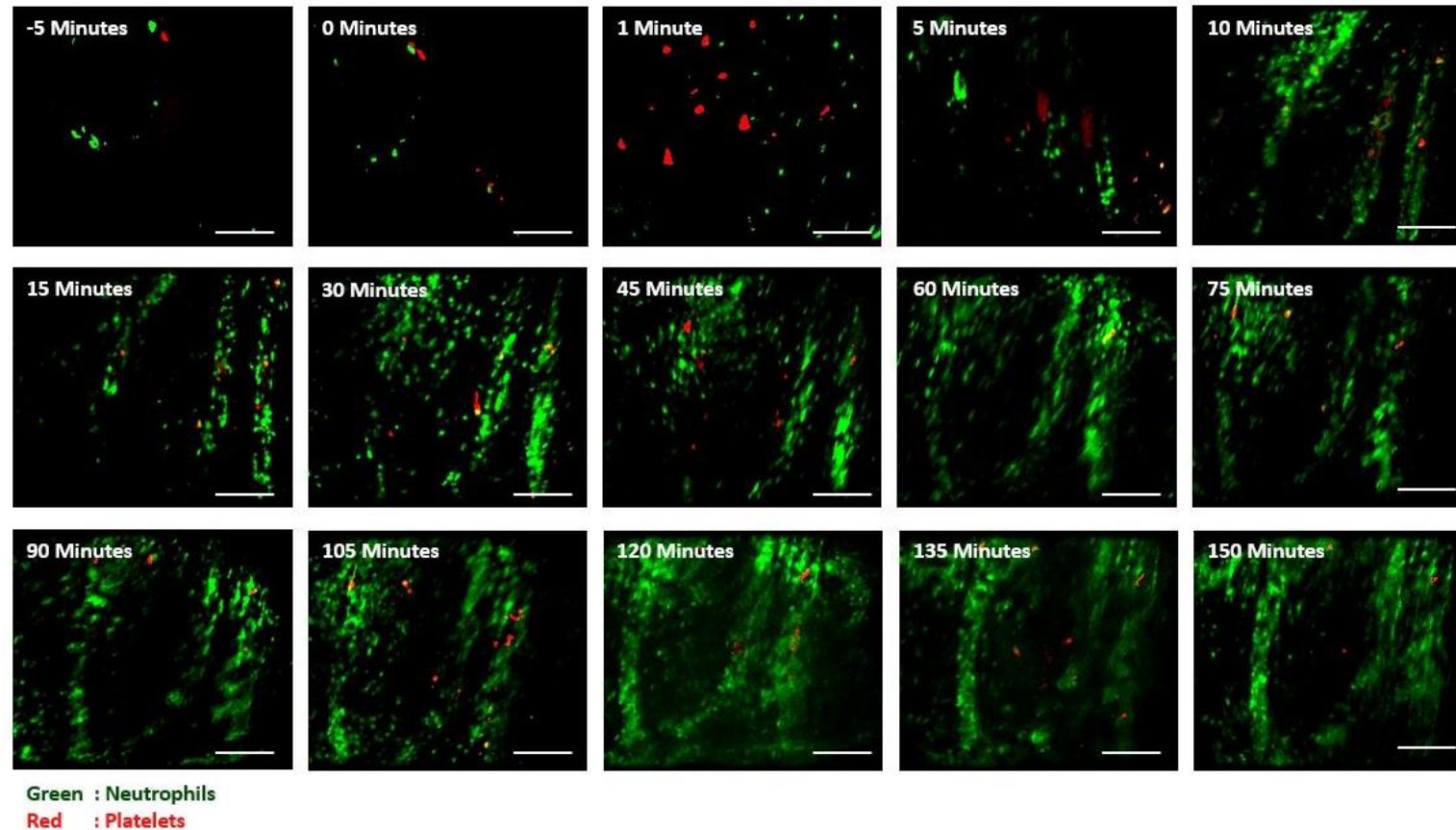


**Figure 3.8. Intravital imaging demonstrated that a thromboinflammatory response was mediated as soon as reperfusion was initiated.** The surgical and stabilisation protocol was optimised to allow the impact of IR injury on thromboinflammatory events in the immediate aftermath of reperfusion to be assessed rather than after just 15 minutes of reperfusion. Representative intravital images are shown following IR surgery in adult female mice over a time course of 150 minutes post-reperfusion. Fluorescently labelled antibodies against neutrophils (green) and platelets (red) were injected via the carotid cannula 10 minutes before reperfusion and imaged intravitaly. Prior to reperfusion, only a limited number of neutrophils (and very occasional platelet microthrombi) were observed within the coronary microcirculation. However, within minutes of the suture around the LAD artery being untied, neutrophil presence increased within the first 30 minutes post-reperfusion and continued to increase over the remainder of the imaged 150 minutes of reperfusion. In contrast, platelet microthrombi presence increased sharply within the first 30 minutes of reperfusion before decreasing to a plateau. Scale bar indicates 100 $\mu$ m. n= 6.

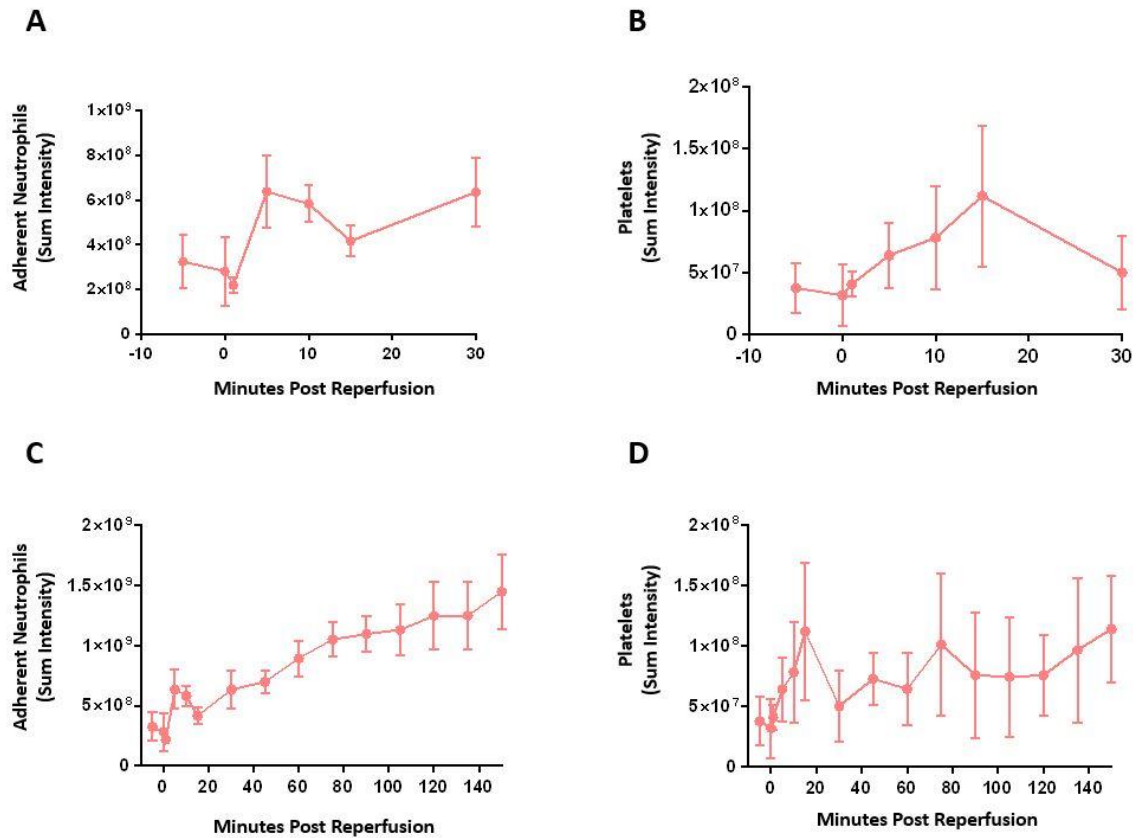


**Figure 3.9. Intravital imaging demonstrated that a thromboinflammatory response was mediated as soon as reperfusion was initiated.** The surgical and stabilisation protocol was optimised to allow the impact of IR injury on thromboinflammatory events in the immediate aftermath of reperfusion to be assessed rather than after just 15 minutes of reperfusion. IR surgery was performed on adult female mice. Quantitative time-course analysis of intravital data in the first 30 minutes of reperfusion for **(A)** adherent neutrophils and **(B)** platelets. The same data are then provided again for the same mice but over a period of 150 minutes post-reperfusion for **(C)** adherent neutrophils and **(D)** platelets. Prior to reperfusion, only a limited number of neutrophils were adherent. In contrast, platelet microthrombi presence increased sharply within the first 30 minutes of reperfusion before decreasing to a plateau.  $n = 6$ . Mean  $\pm$  SEM.

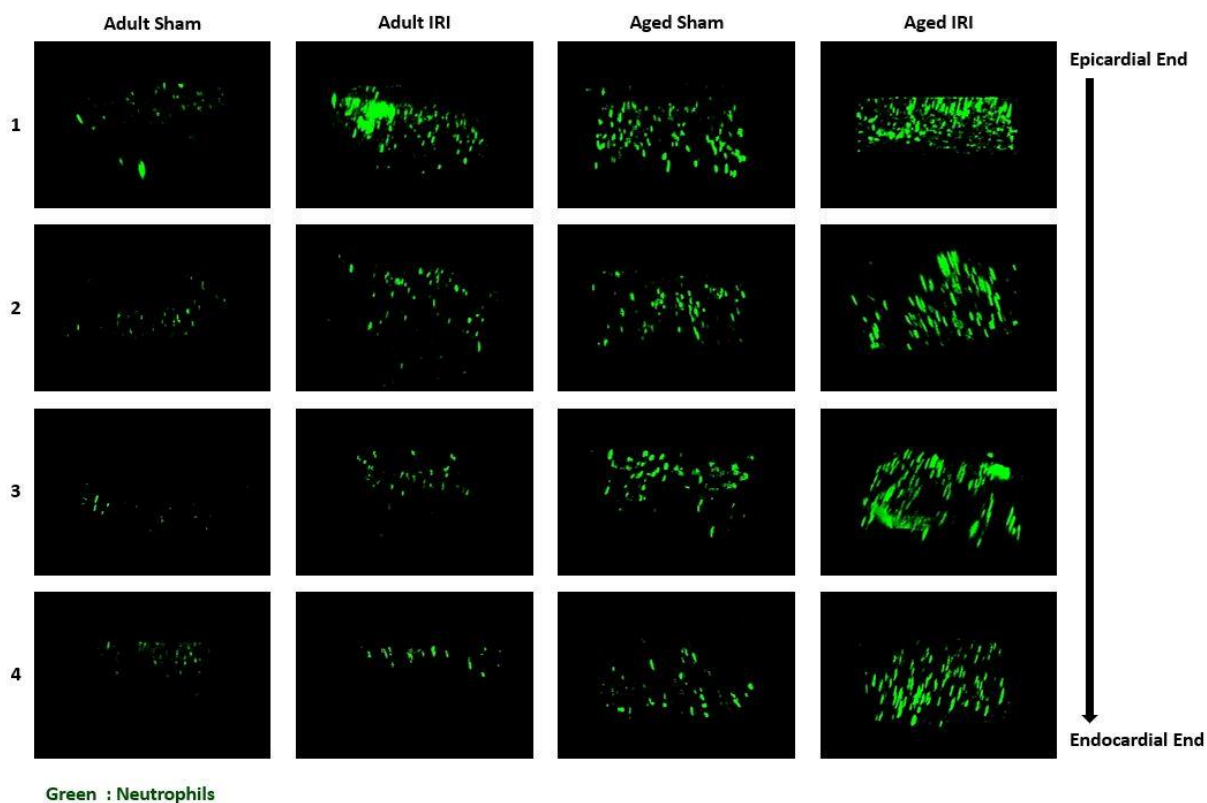


**Figure 3.10. Multiphoton *ex vivo* imaging demonstrated that age increased inflammatory disturbances within sham and IR injured beating hearts even within the deeper layers of the myocardium.** Sham or IR surgery was performed on adult and aged female mice. Fluorescently labelled antibodies against neutrophils were injected via the carotid cannula 5 minutes before reperfusion. Mice were culled following 150 minutes of reperfusion, and hearts were harvested. The LV was vibratome sectioned into four 300µm sections and imaged using a multiphoton microscope. Representative z-stack multiphoton images of neutrophils (green) in the 4 layers of the LV taken from the outermost layer closest to the epicardium (1), outer myocardial layer (2), inner myocardial layer (3) and the innermost layer closest to the endocardium (4). Abbreviations - IRI: ischaemia reperfusion injury.  $n \leq 5/\text{group}$ . Mean  $\pm$  SEM.

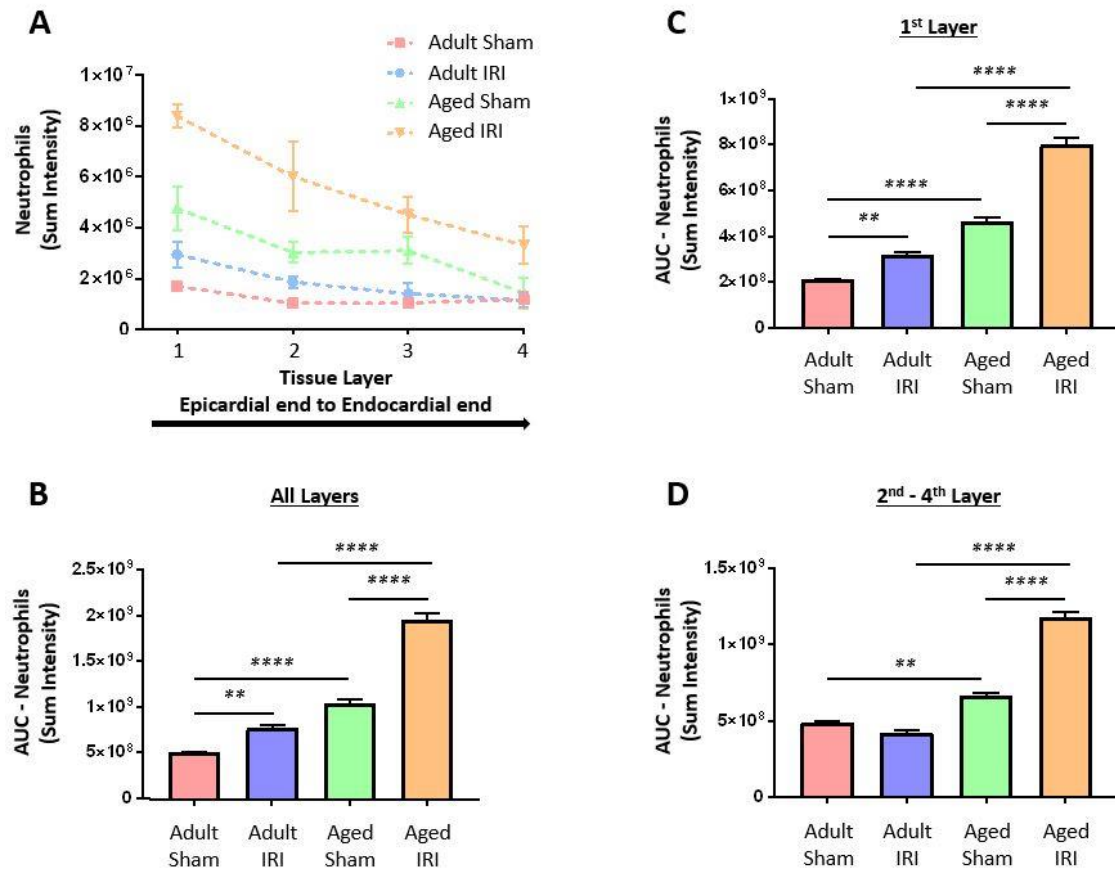


**Figure 3.11. Multiphoton *ex vivo* imaging demonstrated that age increased inflammatory disturbances within sham and IR injured beating hearts even within the deeper layers of the myocardium.** Sham or IR surgery was performed on adult and aged female mice. The LV was vibratome sectioned into four 300 $\mu$ m sections and imaged using a multiphoton microscope. Quantitative analysis of the multiphoton data at various depths for **(A)** adherent neutrophils and the corresponding **(B)** area under the curve (AUC) for adherent neutrophils for all four layers. **(C)** AUC for adherent neutrophils in the outermost first layer. **(D)** AUC for adherent neutrophils in layers 2-4. Statistical analysis was performed using a one-way ANOVA, followed by a Tukey's post-hoc test between the following groups: adult sham versus adult IR injury, adult sham versus aged sham, aged sham versus aged IR injury, and adult IR injury versus aged IR injury. Abbreviations - IRI: ischaemia reperfusion injury. (1) Outermost layer closest to the epicardium, (2) outer myocardial layer, (3) inner myocardial layer and (4) the innermost layer closest to the endocardium.  $n \leq 5/\text{group}$ . Mean  $\pm$  SEM. \*\* $p < 0.01$ , \*\*\*\* $p < 0.0001$ .

### 3.2.5. IR Injury Decreased Functional Capillary Density within the Adult and Aged Beating Heart Coronary Microcirculation *in vivo*

Intravital studies were also conducted to assess coronary microcirculatory perfusion with greater resolution than LSCI. An extensive network of FITC-BSA perfused capillaries was observed in both adult and aged sham mice. Focussing up and down the field of view revealed no evidence of areas devoid of perfusion. Well perfused medium-sized vessels were also visible in some fields of view (**Figure 3.12a**). In contrast, IR injury of adult hearts was associated with a significant reduction in perfusion with multiple areas observed where FITC-BSA did not perfuse the microvessels when compared to the adult sham (**Figure 3.12c**). This resulted in patchy areas devoid of any microvasculature, indicating reduced functional capillary density (FCD). This was significantly reduced in aged injured hearts when compared with aged sham hearts. Indeed, in some fields of view, up to half of the imaged area appeared to lack FITC-BSA perfusion. Interestingly, medium-sized vessels were still readily visible and well perfused in both adult and aged injured hearts (**Figure 3.12a**).

To determine whether vascular integrity was disturbed, a qualitative assessment of vascular leakage was made by using a piece of tissue paper to collect liquid from within the centre of the stabilizer between video captures. This was later imaged to detect FITC-BSA fluorescence. Both adult and aged sham hearts had little or no leakage throughout the duration of the surgery, as determined by no fluorescent dye on the tissue paper. Moreover, only one tissue paper section was required every 15 minutes to 'mop up' any fluid on the heart. In contrast, injury of adult hearts was associated with extensive leakage of FITC-BSA, which was further

exacerbated in aged injured hearts. Indeed, multiple (around 3-6) tissue paper sections had to be used every 15 minutes to absorb the leaked fluid (**Figure 3.12b**).

#### 3.2.6. Age and IR Injury Increased Expression of VCAM-1 and Oxidative Damage

Expression of VCAM-1 was investigated by immunofluorescence on frozen heart sections to understand better the inflammatory mechanisms occurring during ageing and IR injury. VCAM-1 was expressed on the larger vasculature rather than on coronary capillaries in all four experimental groups. However, some capillary staining was observed in the aged injured hearts. Expression was seen to increase in a stepwise manner with injury and age (**Figures 3.13a**). Indeed, expression of VCAM-1 significantly increased in the aged sham group when compared to the adult sham group, as well as in the aged injured group in comparison with the adult injured group (**Figure 3.13b**).

To further understand the detrimental effects of ageing and IR injury on the coronary vasculature, oxidative damage was also investigated by immunofluorescence on frozen heart sections using an anti-DNA/RNA damage antibody. This antibody binds with high specificity and affinity to various products of oxidative damage induced by ROS including 8-hydroxy-2'-deoxyguanosine, one of the most widely recognized biomarkers of oxidative damage of DNA. Oxidative damage was found to be constitutively present, albeit at very low levels, in adult sham hearts, as evidenced by a positive stain on frozen tissue sections, which was not seen in the IgG controls (**Figure 3.14a**). Oxidative damage was significantly increased following injury

in adult hearts. IR injury in aged hearts also significantly increased oxidative damage further when compared to aged sham hearts (**Figure 3.14b**).

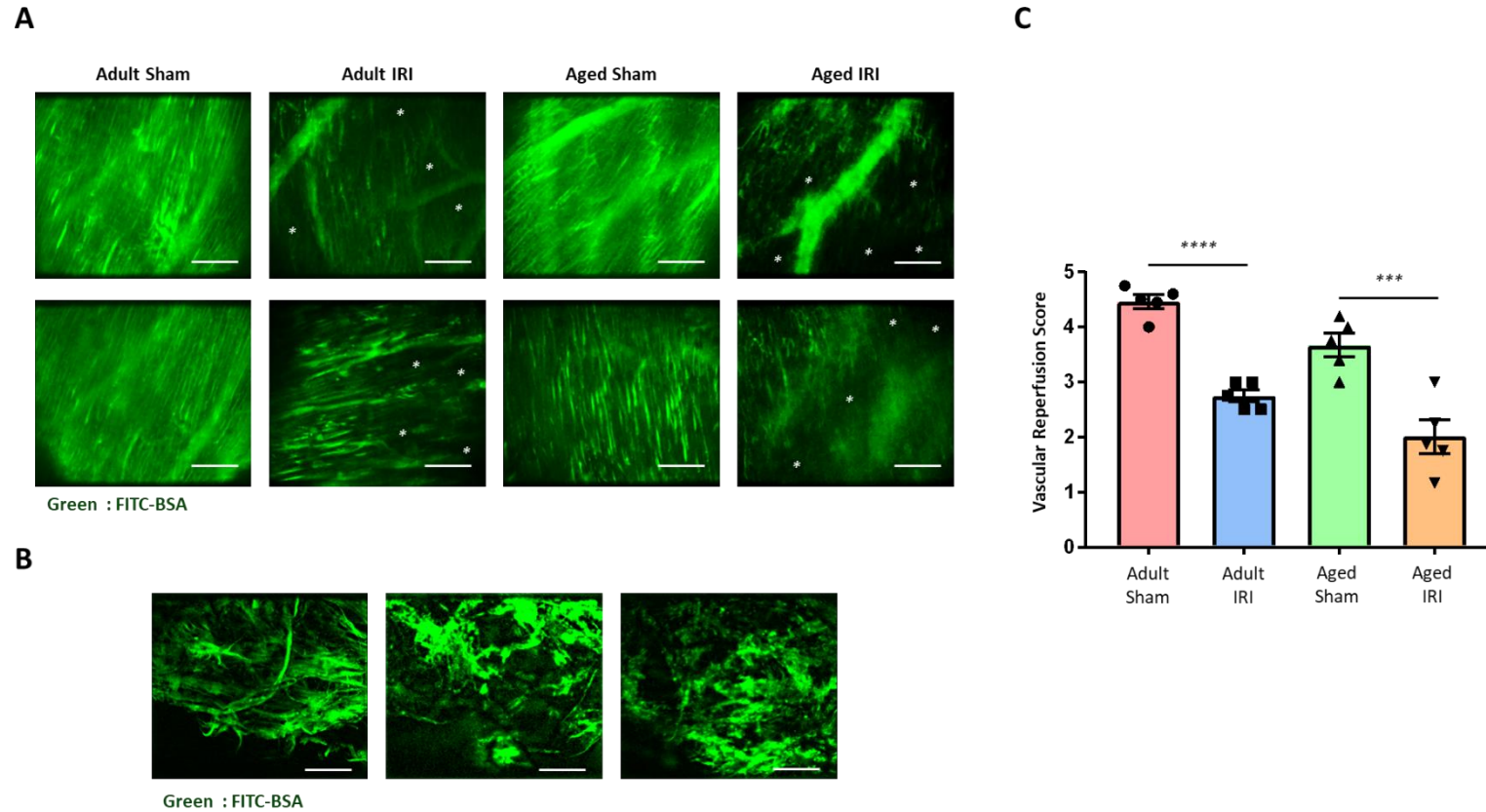
Vascular density was also investigated in these same sections by quantifying CD31 expression levels. There were no significant differences between the four experimental groups in terms of vascular density except for a significant increase in CD31 expression in the aged injured group when compared with the adult injured group (**Figures 3.14c**). Moreover, the merged images (anti-CD31 antibody labelling with anti-DNA/RNA antibody labelling) demonstrated that oxidative damage was not limited to vascular structures but also to CMs.

Flow cytometry on collagenase digested hearts, harvested at 150 minutes post-reperfusion, was also performed to better quantitate the degree of oxidative damage on CMs and ECs. CMs made up around 65% of the total cell population, with ECs making up around 7% in adult hearts (**Figures 3.15a-f**). However, in aged hearts, CMs made up 55% of the total cell population which was significantly reduced compared to adult hearts. ECs made up 10% of the aged heart population which was not significantly different to the EC population in adult hearts. Flow cytometry analysis confirmed the immunofluorescence findings of increased oxidative damage with IR injury and ageing, as evidenced by a distinct shift to the right at the peak of the histogram plots (**Figures 3.16a**). Adult sham CMs demonstrated oxidative damage, albeit at very low levels. This significantly increased in adult injured CMs when compared to adult sham CMs. Aged sham CMs also had significantly greater oxidative damage when compared to adult sham CMs. However, the greatest degree of oxidative CM damage was noted on aged injured CMs, which was significantly greater than both adult IR injured CMs and aged sham CMs (**Figure 3.16b**). A similar pattern of oxidative damage was demonstrated on coronary ECs (**Figure 3.16c**).

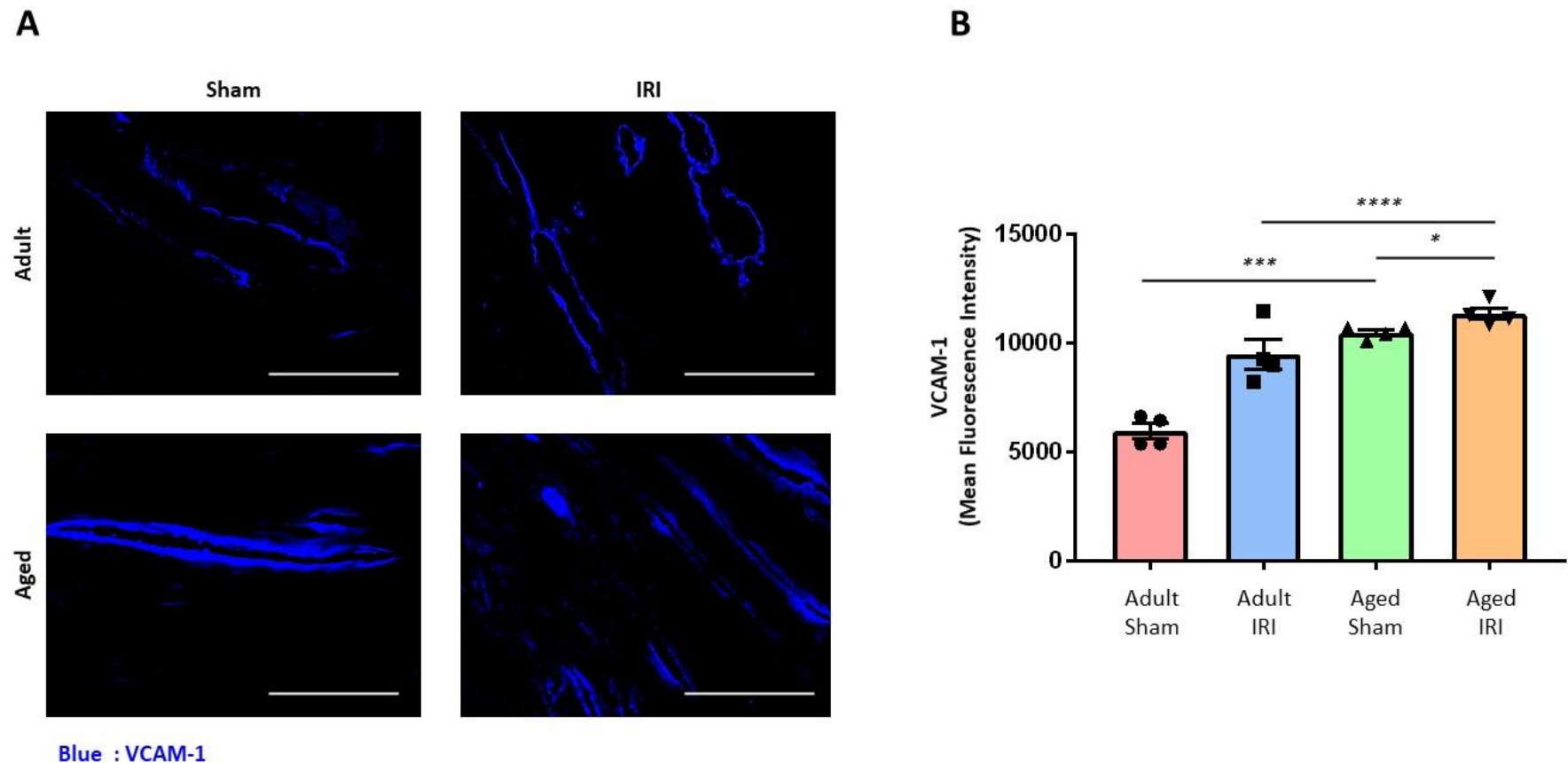
The above flow cytometry data were collected after mice were culled at 150 minutes post-reperfusion. To better understand when the oxidative damage took place, flow cytometry experiments were also conducted on adult and aged injured hearts harvested at 0 (ischaemia only), 30 and 150 minutes of reperfusion. Ischaemia alone induced oxidative damage in adult CMs, albeit at very low levels. However, ischaemia significantly increased oxidative CM damage in aged hearts when compared to adult CMs. Increased oxidative CM damage was noted as early as 30 minutes post-reperfusion in both adult and aged hearts which was significantly increased in aged CMs at both 30 and 150 minutes post-reperfusion when compared to oxidative damage in adult CMs at similar time points (**Figures 3.17a-c**). A similar pattern of oxidative damage was demonstrated on coronary ECs, which only reached statistical significance between the adult and aged hearts at 150 minutes post-reperfusion (**Figures 3.17d-f**).

#### 3.2.7. Myocardial Infarct Size does not Significantly Increase with Age

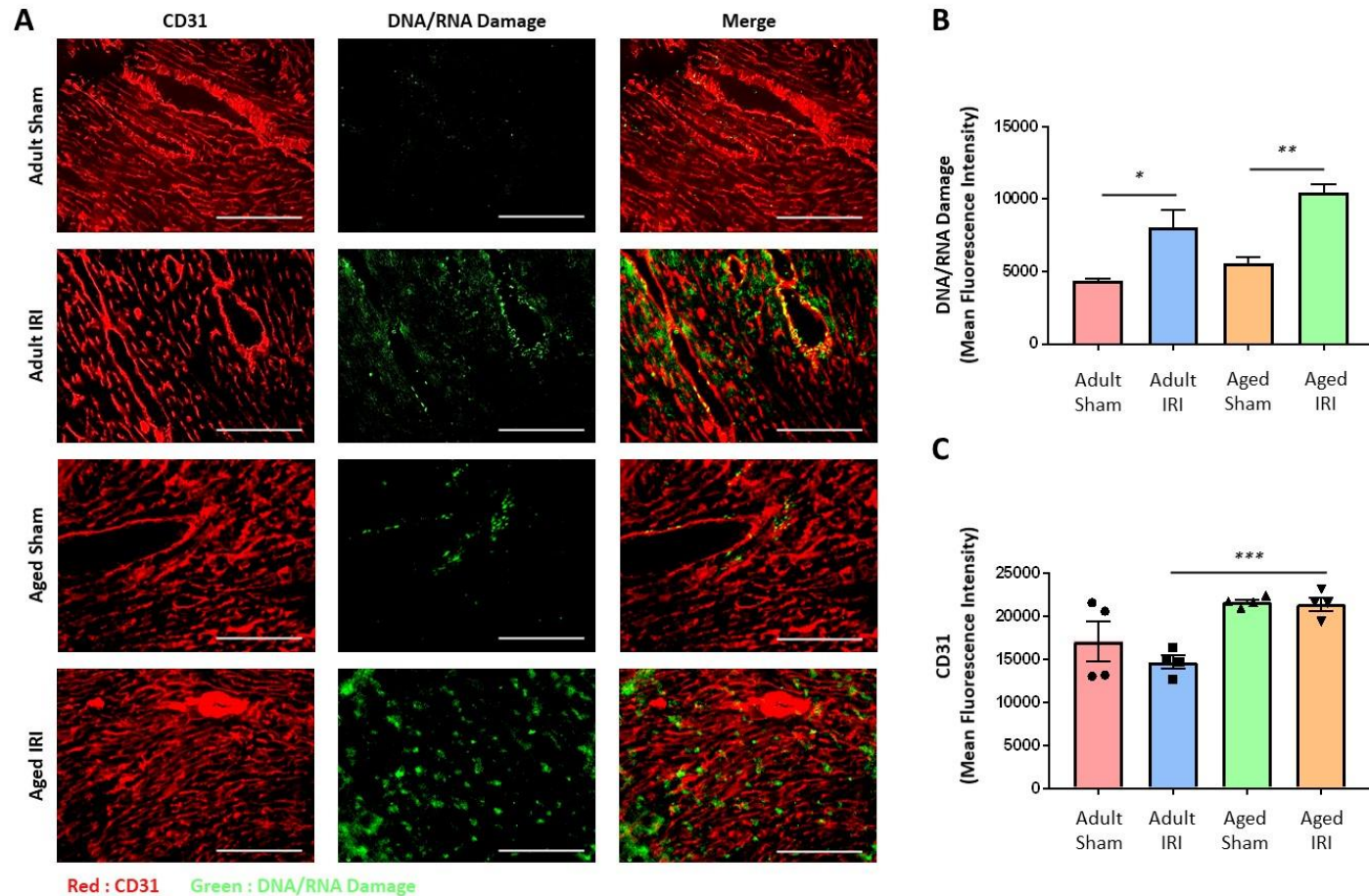
Dual Evans blue and TTC staining were used to determine the impact of IR injury on infarct size in three layers of the adult and aged hearts (**Figure 3.18a**). Infarct size appeared slightly larger in aged mice in all three layers of the heart when compared to adult mice, but this did not attain statistical significance. There was a significant increase in infarct size between layer 1 and layer 3 in the aged IR injured heart (**Figures 3.18b and 3.18c**). Area at risk (AAR) and area not at risk were not significantly different in the various layers within the same age group nor between adult and aged injured hearts (**Figure 3.18d and e**).



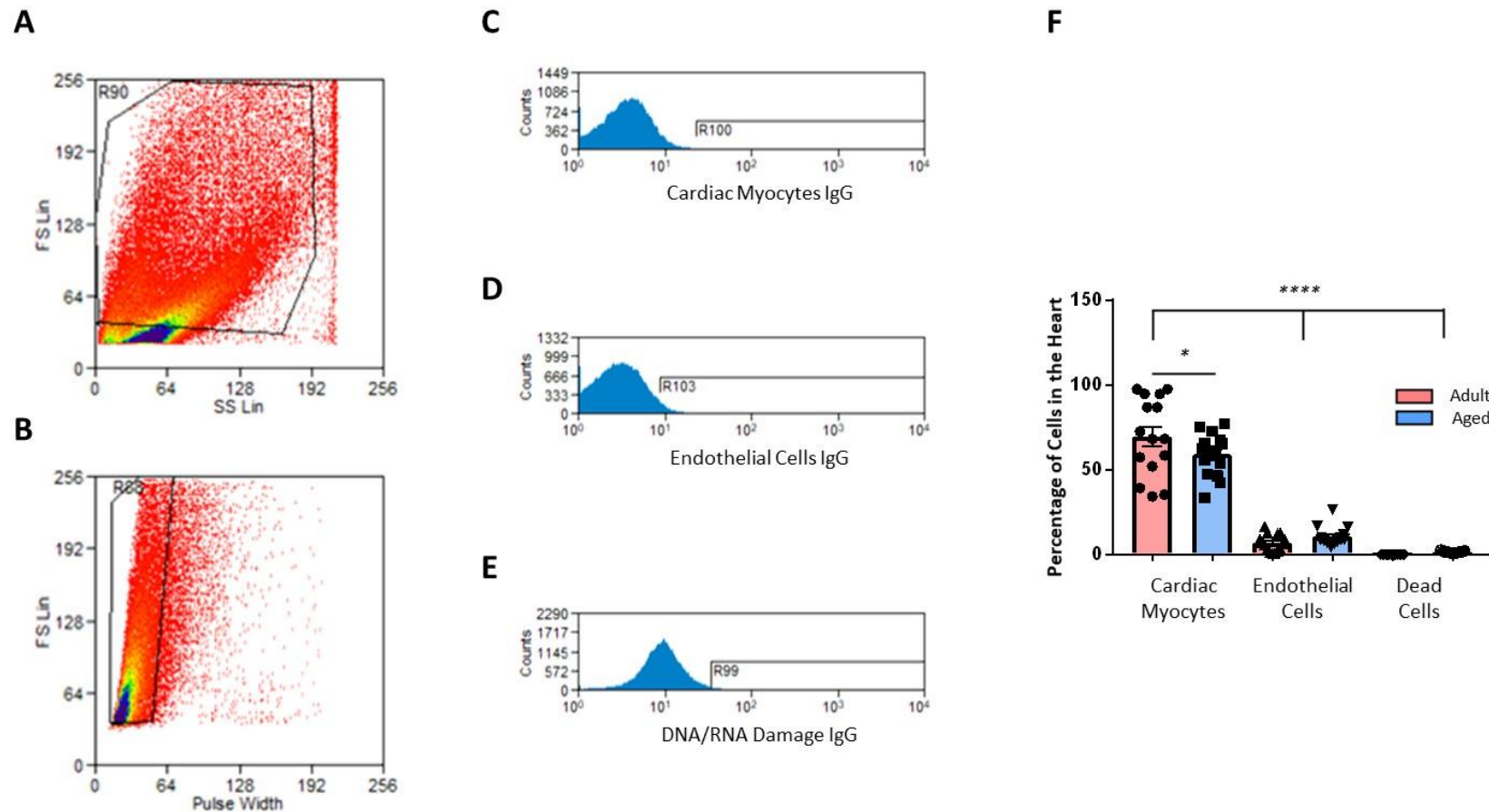
**Figure 3.12. Intravital imaging demonstrated that IR injury decreased functional capillary density within the beating heart coronary microcirculation *in vivo*.** Sham or IR surgery was performed on adult and aged female mice. Fluorescently labelled antibody conjugated to bovine serum albumin (FITC-BSA; green) was injected via the carotid cannula at 120 minutes post-reperfusion and imaged intravitaly. Tissue paper was used to remove any liquid from the stabilised region, which was imaged to detect leaked FITC-BSA. **(A)** Representative intravital images of FITC-BSA perfused coronary microvessels at 150 mins in sham hearts or 150 mins post-reperfusion in Injured hearts. **(B)** Representative fluorescent images of FITC-BSA stained tissue paper (IRI). **(C)** Quantitative analysis of intravital vascular perfusion data. Statistical analysis was performed using a one-way ANOVA, followed by a Tukey's post-hoc test between the following groups: adult sham versus adult IR injury, adult sham versus aged sham, aged sham versus aged IR injury, and adult IR injury versus aged IR injury. Abbreviations - IRI: ischaemia reperfusion injury. \*Areas not perfused with FITC-BSA. Scale bar indicates 100µm.  $n \leq 5$ /group. Mean  $\pm$  SEM. \*\*\* $p < 0.001$ , \*\*\*\* $p < 0.0001$ .



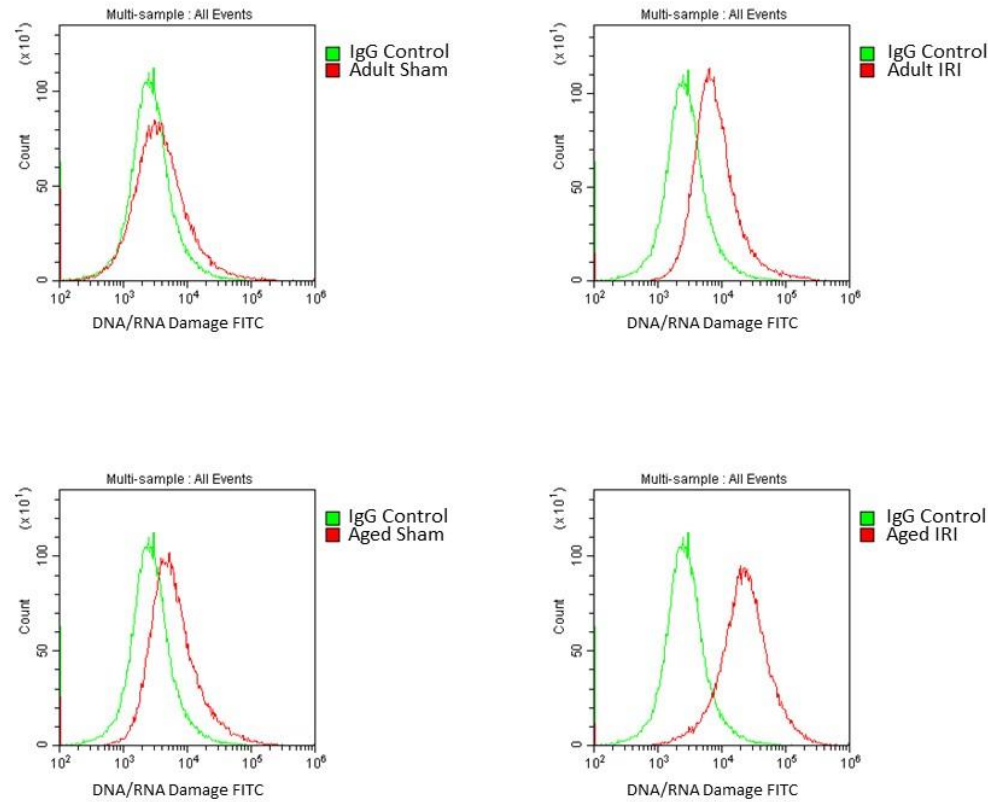
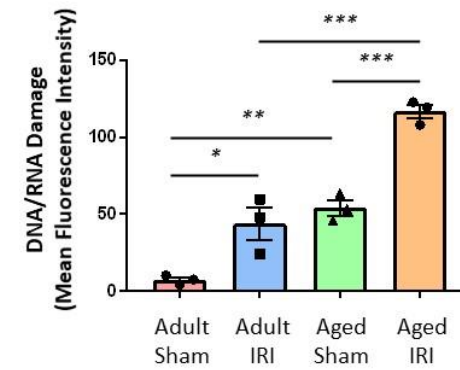
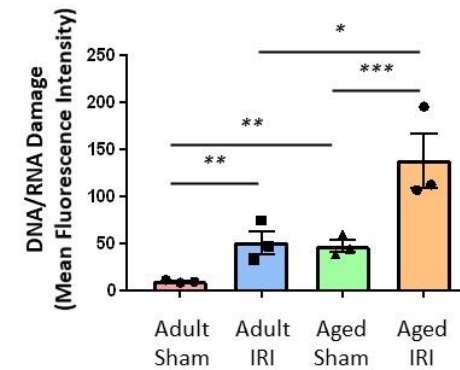
**Figure 3.13. Age and IR injury increases expression of VCAM-1 as determined by immunofluorescence studies on frozen heart sections.** Sham or IR surgery was performed on adult and aged female mice. Mice were culled following 120 minutes of reperfusion, and hearts were harvested and snap frozen. The LV was transversely sectioned using a cryostat into 10µm sections and then immunostained with an anti-VCAM-1 antibody. Sections were imaged using a EVOS microscope. **(A)** Representative images of VCAM-1 (blue) staining of frozen heart sections. Scale bar indicates 200µm. **(B)** Quantitative analysis of the immunofluorescent images of VCAM-1 expression. Statistical analysis was performed using a one-way ANOVA, followed by a Tukey's post-hoc test between the following groups: adult sham versus adult IR injury, adult sham versus aged sham, aged sham versus aged IR injury, and adult IR injury versus aged IR injury. Abbreviations - IRI: ischaemia reperfusion injury. n=4/group. Mean ±SEM. \*p<0.05, \*\*\*p<0.001, \*\*\*\*p<0.0001.



**Figure 3.14. Age and IR injury increases oxidative damage as determined by immunofluorescence studies on frozen heart sections.** Sham or IR surgery was performed on adult and aged female mice. Mice were culled following 120 minutes of reperfusion, and hearts were harvested and snap frozen. The LV was transversely sectioned using a cryostat into 10 $\mu$ m sections and then immunostained with an anti-DNA/RNA damage antibody and an anti-CD31 antibody. Sections were imaged using a EVOS microscope. **(A)** Representative images of DNA/RNA damage (green) and CD31 (red) staining on frozen heart sections. Scale bar indicates 200 $\mu$ m. Quantitative analysis of the immunofluorescent images of **(B)** DNA/RNA damage and **(C)** CD31 expression. Statistical analysis was performed using a one-way ANOVA, followed by a Tukey's post-hoc test between the following groups: adult sham versus adult IR injury, adult sham versus aged sham, aged sham versus aged IR injury, and adult IR injury versus aged IR injury. Abbreviations - IRI: ischaemia reperfusion injury. n=4/group. Mean  $\pm$  SEM. \* $p$ <0.05, \*\* $p$ <0.01, \*\*\* $p$ <0.001.



**Figure 3.15. Gating strategy for flow cytometry-based experiments on adult and aged collagenase digested hearts.** Sham or IR surgery was performed on adult and aged mice, and hearts were harvested and digested. The cell suspension was stained with anti-CD31, anti-cTnT, anti-DNA/RNA damage, and zombie antibodies and acquisition was performed using a CyAn™ ADP cytometer (100,000 events captured). Representative density plots showing the **(A)** initial gate drawn to capture the greatest number of cells whilst ensuring any debris was excluded, and **(B)** the second gate drawn to exclude potential duplicates. Representative histogram of IgG controls for **(C)** cardiac myocytes, **(D)** endothelial cells, and **(E)** DNA/RNA damage. **(F)** Quantitative analysis of the CM and EC population within the adult and aged samples. Statistical analysis was performed using a one-way ANOVA, followed by a Tukey's post-hoc test between the following groups: cardiac myocytes versus endothelial cells, cardiac myocytes versus dead cells, and endothelial cells versus dead cells between the adult and aged groups; as well as between adult versus aged cardiac myocytes, adult versus aged endothelial cells, and adult versus aged dead cells. Abbreviations – FS: forward scatter, SS: side scatter. Mean  $\pm$  SEM. \* $p < 0.05$ , \*\*\*\* $p < 0.0001$ .

**A****B****Cardiac Myocytes****C****Endothelial Cells**

**Figure 3.16. Age and IR injury increases oxidative damage on cardiac myocytes and endothelial cells as determined by flow cytometry of digested heart tissue.** Sham or IR surgery was performed on adult and aged female mice. Mice were culled following 150 minutes of reperfusion, and hearts were harvested and digested. The cell suspension was stained with anti-CD31, anti-cTnT, and anti-DNA/RNA damage antibodies and acquisition was performed using a CyAn™ ADP flow cytometer. **(A)** Representative histogram of DNA/RNA damage marker showing a shift in expression in response to IR injury and age. Quantitative analysis of DNA/RNA damage expression on **(B)** cardiac myocytes, and **(C)** endothelial cells. Statistical analysis was performed using a one-way ANOVA, followed by a Tukey's post-hoc test between the following groups: adult sham versus adult IR injury, adult sham versus aged sham, aged sham versus aged IR injury, and adult IR injury versus aged IR injury. Abbreviations - IRI: ischaemia reperfusion injury. n=3/group. Mean  $\pm$  SEM. \*p<0.05, \*\*p<0.01, \*\*\*p<0.001.

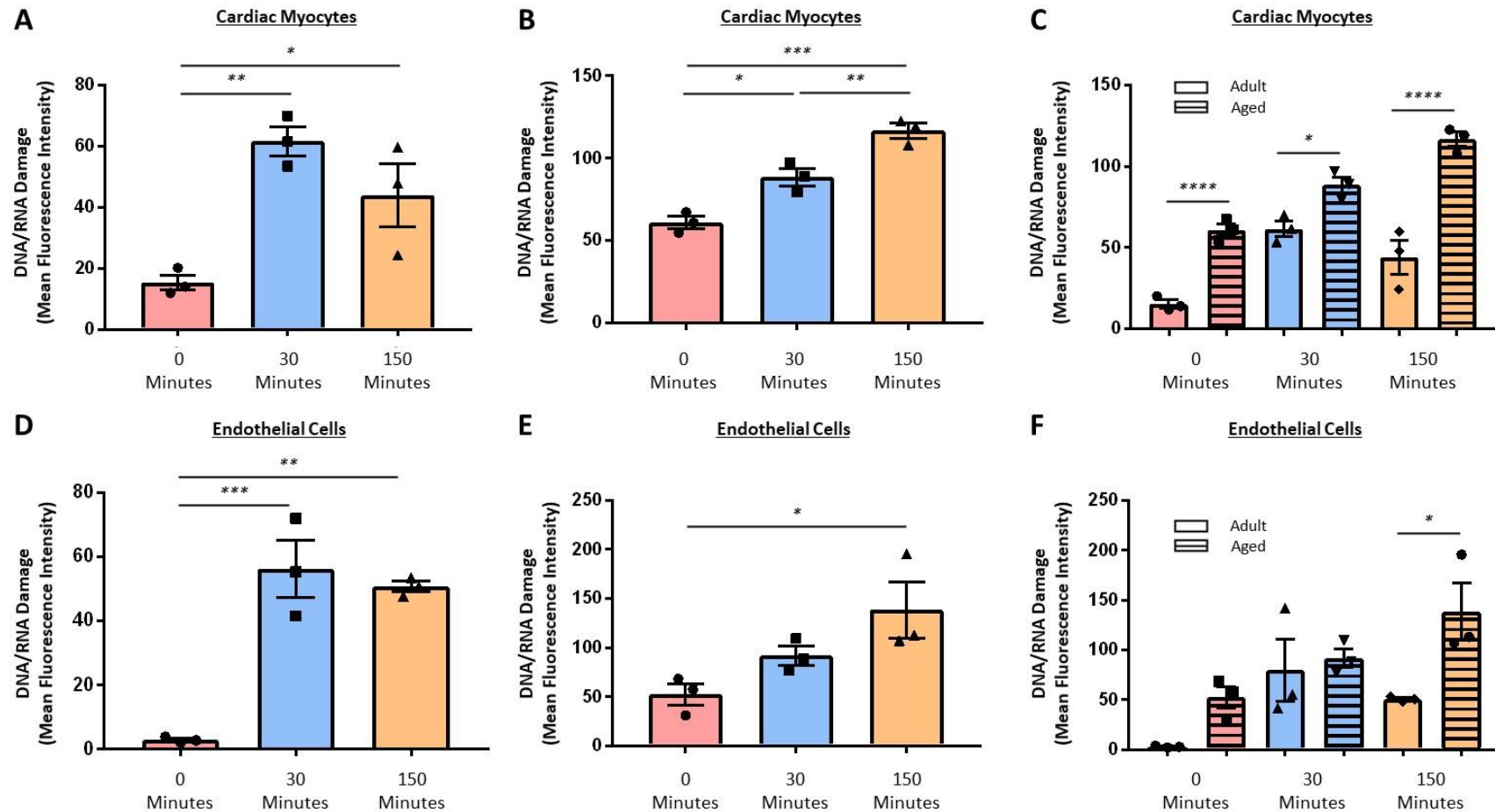


**Figure 3.17. IR injury induces oxidative damage to cardiac myocytes and endothelial cells within the first 30 minutes of reperfusion in adult and aged mice as determined by flow cytometry of digested heart tissue.** IR surgery was performed on adult and aged female mice. Mice were culled following 0, 30, or 150 minutes of reperfusion and hearts were harvested and digested. The cell suspension was stained with anti-CD31, anti-cTnT, and anti-DNA/RNA damage antibodies and acquisition was performed using a CyAn™ ADP cytometer. Quantitative analysis of DNA/RNA damage on cardiac myocytes in (A) adult mice, (B) aged mice, and (C) adult and aged mice. Quantitative analysis of DNA/RNA damage on endothelial cells in (D) adult mice, (E) aged mice, and (F) adult and aged mice. Statistical analysis was performed using a one-way ANOVA, followed by a Tukey's post-hoc test between the following groups (A, B, C, D): 0 minutes versus 30 minutes, 0 minutes versus 150 minutes, and 30 minutes versus 150 minutes - (E, F): 0 minutes adult versus aged, 30 minutes adult versus aged, and 150 minutes adult versus aged. n=3/group. Mean  $\pm$  SEM. \* $p$ <0.05, \*\* $p$ <0.01, \*\*\* $p$ <0.001, \*\*\*\* $p$ <0.0001.

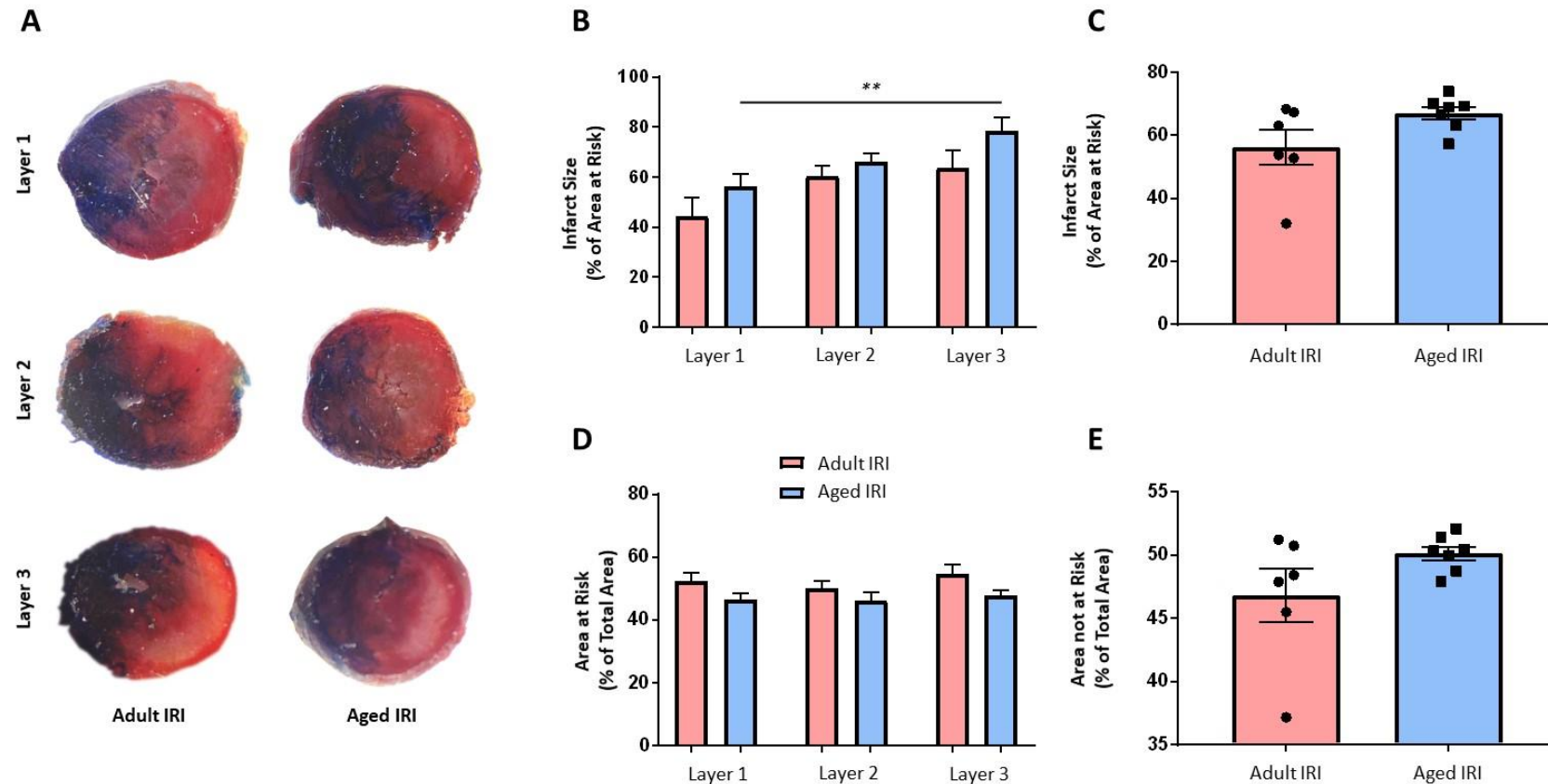


**Figure 3.18. Infarct size following IR injured is not worsened with age.** IR surgery was performed on adult and aged female mice. Following 4-hours of reperfusion, the left anterior descending artery was re-ligated, and Evans Blue was retrograde injected via the carotid artery. Mice were culled, and the heart was harvested, sectioned, stained with TTC and imaged. **(A)** Representative images of the TTC stained adult and aged IR injured hearts within each layer. Layer 1 represents the first layer below the ligature, and layer 3 represents the apex of the heart. Quantitative analysis of infarct size in **(B)** the individual layers of the heart and **(C)** in all three layers of the heart. Statistical analysis was performed using a one-way ANOVA followed by a Tukey's post-hoc test between the following groups: layer 1 versus layer 2, layer 1 versus layer 3, and layer 2 versus layer 3 for each of the adult and aged IRI groups, as well as adult IRI versus aged IRI for each of the three layers. Quantitative analysis of the area at risk in **(D)** the individual layers of the heart and **(E)** in all three layers of the heart. Statistical analysis was performed using a Student's unpaired t-test. Abbreviations - IRI: ischaemia reperfusion injury.  $n \leq 6/\text{group}$ . Mean  $\pm$  SEM. \*\* $p < 0.01$ .

### 3.2.8. Age Increases Oxidative Damage in Human Ventricular Samples

Oxidative damage was also investigated in the young and old human samples using a human anti-DNA/RNA antibody. Oxidative damage was found to be constitutively present, albeit at low levels, in newborn, infant/toddler and child hearts, as evidenced by a positive stain on frozen tissue sections, which was not seen in the IgG controls (**Figure 3.19a**). Oxidative damage was significantly increased in the adult hearts when compared with younger hearts (**Figure 3.19b**).

CM density was also determined by quantifying cTnT expression levels. There were no statistically significant differences between the groups, except for an increase in cTnT expression in the child and older adult group when compared with the infant/toddler group (**Figures 3.19c**).

Vascular density was also investigated by quantifying CD31 expression levels. There were no statistically significant differences between the groups, other than a decrease in CD31 expression in the infant/toddler and older adult group when compared with the newborn group (**Figures 3.19d**).

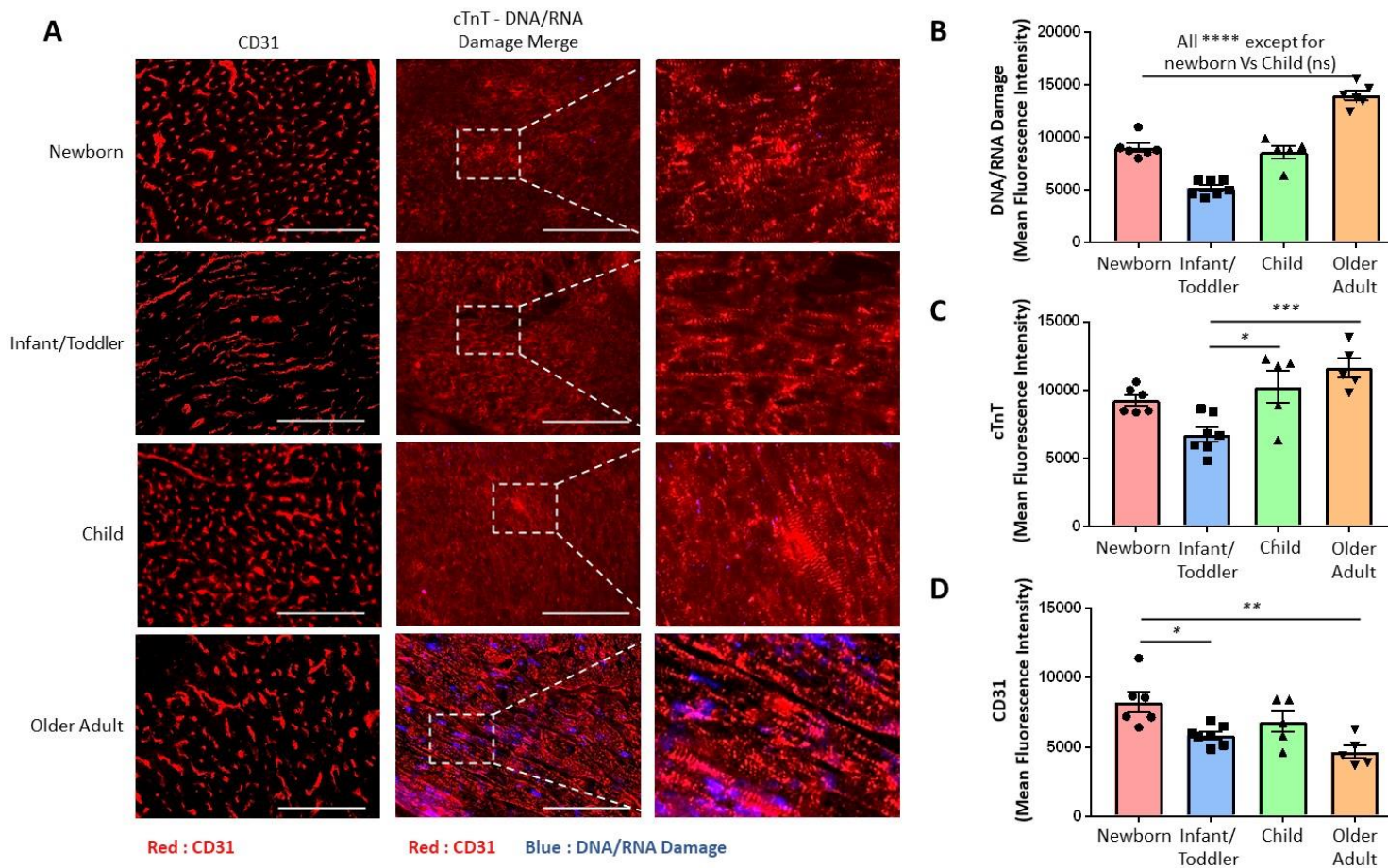


**Figure 3.19. Age increases oxidative damage in human tissue as determined by immunofluorescence studies on frozen heart sections.** Clinical samples were harvested and snap frozen from young and old patients following surgery. The ventricular sample was sectioned using a cryostat into 10μm sections and then immunostained with; the first column: anti-CD31 antibody, second, and third column: anti-cTnT antibody and anti-DNA/RNA damage. Sections were imaged using a EVOS microscope. **(A)** Representative images of CD31 (red: first column), cTnT (red: second and third column), and DNA/RNA damage (blue: second and third column) staining on frozen heart sections. Scale bar indicates 200μm. Quantitative analysis of the immunofluorescent images of **(C)** DNA/RNA damage, **(D)** cTnT, and **(E)** CD31 expression. Statistical analysis was performed using a one-way ANOVA, followed by a Tukey's post-hoc test between the following groups: newborn versus infant/toddler, newborn versus child, newborn versus older adult, infant/toddler versus child, infant/toddler versus older adult, and child versus older adult.  $n \leq 5$ /group. Mean  $\pm$  SEM. \* $p < 0.05$ , \*\* $p < 0.01$ , \*\*\* $p < 0.001$ , \*\*\*\* $p < 0.0001$ .

### 3.3. Discussion

By 2030, it is expected that 20% of the population will be over 65 years old, and CVD is set to account for 40% of the deaths within this age group [27]. Increased age is associated with a worse prognosis post-MI and may be explained by biological characteristics such as cellular senescence, immunosenescence, changes to many cell types and tissues, altered intracellular communications, and metabolic changes [156]. Since the inflammaging phenomenon can also explain the poor prognosis in the elderly, consideration of the effects of ageing on the post-ischaemic coronary microcirculation, where inflammatory events take place, is critical. In this chapter, we provide original contributions on the architecture of the aged beating heart coronary microcirculation and how its response to myocardial IR injury differs from younger hearts *in vivo*. The main results are summarised in **Table 3.1**.

#### 3.3.1. Overall Ventricular Blood Perfusion – a false indicator of all being well?

Age-related differences in regional ventricular perfusion following myocardial IR injury have not been studied directly *in vivo*. Therefore, we firstly sought to investigate the effects of IR injury, as well as age, on overall blood perfusion of the LV. For this, large field LSCI was applied to the beating mouse heart *in vivo*. LSCI has been widely used in both pre-clinical and clinical studies to visualise perfusion in many organs. However, its use within the beating heart has been limited so far to the Kalia group [32]. In both age groups, flow resumed immediately upon reperfusion and was maintained throughout the duration

of imaging. Indeed, in some individual adult mice, a transient reactive hyperaemic response was also observed. However, although this returned to basal levels in adult mice, it remained significantly below basal levels in aged mice.

On its own, this overall resumption of flow within a large region of the LV, be it to normal or slightly below normal levels in adult and aged mice respectively, could have been interpreted as blood flow being adequately re-established to repay the debt acquired during ischaemia. Yet, despite this, we observed significant infarction in both adult and aged mice. It was not until subsequent cellular level intravital studies were performed that it became clear that this overall ventricular perfusion was poorly transmitted to the coronary capillaries and thus did not correspond to adequate perfusion at a microvascular level. Indeed, patchy areas with little or no perfused capillaries was observed intravitaly. Hence, there exists a mismatch between what looks like a global resumption of blood flow during reperfusion and microcirculatory flow heterogeneity.

The poorer resumption of overall ventricular blood flow in injured adult and aged hearts was most likely linked to the observed thromboinflammatory response, which was markedly higher in aged hearts – this is discussed later. However, it well established that ageing is also associated with a reduction in the ability of various resistance arterioles (coronary, cerebral, femoral, carotid etc.) to respond to vasodilatory agonists both experimentally and in humans [218]. Therefore, the ability of vasodilators and vasodilatory metabolites, known to be released and accumulate during the ischaemic phase, may not be as effective in dilating coronary arterioles and decreasing vascular resistance in the aged heart compared to the adult heart. In addition to exacerbated thromboinflammatory responses, this may also explain the poorer blood flow in reperfused aged hearts.

Reduction in the synthesis and release of dilatory NO, increased activity of vasoconstrictive prostanoids, poor diffusion of NO to smooth muscle because of increased intimal thickness, and degradation of NO by ROS are all potential mechanisms that could also explain the poorer resumption of blood flow in the aged hearts [218, 219]. One of the principal coronary vasodilators is adenosine which plays an important role in maintaining coronary blood flow post-ischaemic events. Its production is stimulated by low oxygen levels. However, it is well established that the functional responses to adenosine are decreased with age due to loss of adenosine receptors in the heart [220]. Collectively, these perturbations may all contribute to the decreased ventricular perfusion in the aged heart, as observed by LSCI.

#### Chapter 4: Targeting IL-36 in Myocardial IR Injury – A New Therapeutic Target

	Adult sham	Aged sham	Adult IR injured	Aged IR Injured
Laser speckle studies on the beating heart <i>in vivo</i>				
Overall ventricular perfusion	Good baseline ventricular perfusion prior to ischaemia	Baseline perfusion is significantly lower than that in adult sham mice	Perfusion returns to pre-ischaemic levels after initiation of reperfusion	Perfusion significantly lower than pre-ischaemic levels (particularly during diastole) and decreases with time
St.Dev. of the inter-beat distance			Not significantly different	
Heart rate			Not significantly different	
Intravital studies on the beating heart <i>in vivo</i>				
Adherent neutrophils	Low levels	↑	↑↑	↑↑↑ and rising
Free-flowing neutrophils	~30-40 circulating through the FOV at each time point	↓↓	↓↓	↓↓
Adherent platelet microthrombi	Low levels	↑	↑	↑
FITC-BSA perfusion to assess functional capillary density	Good microvessel perfusion observed at the end of 2 hours of reperfusion	↓	↓↓	↓↓↓
Multiphoton studies on the excised heart <i>ex vivo</i>				
Adherent neutrophils	Low levels	↑	↑↑	↑↑↑
Immunostaining of frozen heart sections <i>in vitro</i>				
VCAM-1	Low levels	↑	↑↑	↑↑↑
DNA/RNA oxidative damage	Low levels	↑	↑↑	↑↑↑
Flow cytometry studies on digested heart cells <i>in vitro</i>				
Number of cardiomyocytes	Significantly reduced in aged hearts			
Number of endothelial cells	Not significantly different			
DNA/RNA oxidative damage of cardiomyocytes	Low levels	↑	↑↑	↑↑↑
DNA/RNA oxidative damage of endothelial cells	Low levels	↑	↑	↑↑↑
TTC / Evans Blue staining of heart sections <i>in vitro</i>				
Infarct size			Higher in aged hearts than adult hearts but not statistically significant	

**Table 3.1. Summary of the major observations between adult and aged sham and IR injured female mouse hearts.** Studies conducted were laser speckle and intravital microscopy *in vivo* studies on the beating heart and multiphoton, flow cytometry, and immunostaining *in vitro* studies. Abbreviation: FOV – field of view

### 3.3.2. Enhanced Thromboinflammatory Response with Age Alone

This study provides the first direct intravital evidence that ageing increases the thromboinflammatory response of the coronary microcirculation to IR injury. However, it is also the first to show that even ageing alone, in the absence of any injury, is associated with a chronic low-grade inflammatory cell presence in otherwise healthy hearts. Indeed, the impact of age alone on cellular recruitment to the coronary microcirculation was not negligible. Our data showed an almost 5-fold enhanced basal neutrophil recruitment in the microvasculature in aged but otherwise healthy coronary capillaries. This may be linked to our observed age-related up-regulation of endothelial VCAM-1 and oxidative damage in the heart or due to increased structural and functional changes in the neutrophils themselves that have been observed by others [31, 32]. Indeed, neutrophils in aged individuals have been shown to adopt a pre-activated state whereby they constitutively secrete more neutrophil elastase and ROS in close proximity to the endothelium, which can lead to vascular damage and promote their subsequent adhesion [221, 222]. Importantly, our multiphoton data not only confirmed this increased basal neutrophil presence in aged hearts but also showed that this was uniformly increased throughout all layers of the LV from the outermost epicardial side to the innermost endocardial side.

This data are consistent with previous studies, which have shown that neutrophil counts in tissues without injury are significantly increased in otherwise healthy aged patients, further supporting the inflammaging phenomenon [223]. This was also identified recently intravitaly in the mouse cremaster muscle by Barkaway *et al.* (2021) who found a significant increase in firmly adherent neutrophils in otherwise healthy mice as a result of

age increasing from approximately 3 to 18 months [224]. Despite the increased basal adhesion of neutrophils in adult and aged healthy hearts, they did not appear to obstruct microvessels, as evidenced by the presence of free-flowing neutrophils circulating within those same capillaries. This was also previously described intravitaly by the Kalia group in healthy sham adult hearts [42]. We speculate that adhesion in healthy hearts might also be due to some trafficking neutrophils becoming trapped as blood vessels become compressed during systole. Indeed, extravascular compression during isovolumetric contraction markedly reduces coronary flow, something supported by our LSCI data which clearly identified decreased myocardial blood flow during systole [225-227].

Interestingly, a marked reduction (almost 2-fold) in freely circulating neutrophils was also observed in the aged hearts. This may be linked to the decreased tissue perfusion in the aged heart that was noted during laser speckle imaging. Indeed, the decreased coronary flow has also been observed in humans assessed using laser doppler [228].

In addition to inflammatory changes, platelet changes in sham aged hearts were also observed. Rounded or elongated platelet aggregates were observed in the microvasculature, something not observed in sham adult hearts. However, although there was an approximate 7-fold increase between adult sham and aged sham hearts, overall, the number of microthrombi was quite small. Unlike adherent neutrophils, these were sometimes occlusive, as evidenced by the lack of circulating neutrophils passing through affected microvessels. Interestingly, Culmer *et al.* (2013) and Dayal *et al.* (2013) both showed an increase in platelet count in mice aged from 4 to 18 months. However, in the absence of significant endothelial activation or endothelial denudation, this would not be a likely explanation for why there was an increased microthrombus formation with age

alone [229, 230]. Having said that, a dramatic increase in thrombogenicity in the elderly population is well described. This has been thought to be due to increased thickness of vessel walls, fragmentation of the internal elastic lamina, and vascular smooth muscle cells hypertrophy within the vessel walls, all of which results in an endothelial injury that can promote thrombosis. Ageing also alters the ratio of pro-coagulants to anti-coagulants in favour of pro-coagulants, particularly von Willebrand factor, which can initiate platelet adhesion to both endothelium and sub-endothelial surfaces [231]. Any one of these events may explain the slightly increased presence of platelets within the aged, but otherwise healthy coronary microcirculation. Elucidating the exact mechanisms involved would, however, require further investigation.

Collectively, our intravital studies directly imaged the presence of a chronic low-grade inflammation in the aged but otherwise healthy heart and also alluded to a mildly pro-thrombotic state as well. Although an age-related capillary loss or rarefaction has been described [232], no visible reduction in FCD or increased vascular leakage was noted in non-injured aged hearts in the current study. The presence of a pre-existing, age-related chronic thromboinflammatory presence likely increases the susceptibility of the coronary microcirculation to an additional acute injurious insult such as an MI / IR injury.

### **3.3.3. Additional Characteristics Noted in the Healthy Aged Heart**

Flow cytometric analysis of digested mouse hearts demonstrated a decrease in CM number in aged hearts. This may be linked to an age-related apoptosis and a decrease in left ventricular mass [233, 234]. Indeed, a greater number of apoptotic myocytes in older

hearts in both animal and human studies has previously been described [233, 234]. Although Anversa *et al.* (1986) showed a decrease in the number of rat CMs with age, which was associated with CM hypertrophy [235], no age-related difference CM number in human heart sections has been observed [236]. In contrast to CM number, the current study showed no change in murine EC number when analysed flow cytometrically using digested mouse hearts or when immunostaining murine heart sections. However, immunostaining of human heart sections with an anti-CD31 antibody demonstrated a significant decrease in EC number with increasing age. This is most likely the result of the CM's being larger in size in adults compared to neonates/infants, and so when using the same imaging magnification, this would result in less vasculature being observed. Having said that, studies in the brain have shown age-related decreases in capillary count (capillary rarefaction) [237], but this has not been described so far in the heart. Whether our results are actually indicative of an age-related capillary rarefaction also occurring in the ageing human heart would require further investigation.

### 3.3.3.1. Mechanisms for Neutrophil Recruitment in the Aged Heart

Cellular senescence is a fundamental phenomenon of ageing, and ROS are implicated in its development, alongside other SASPs, to clear away senescent cells from the tissue [238]. ROS, particularly generated by the high numbers of mitochondria in cardiomyocytes, can enhance the expression of endothelial adhesion molecules, such as VCAM-1 and ICAM-1, both of which are critical for leucocyte recruitment [239]. The anti-DNA/RNA antibody used in the study binds with high specificity and affinity to 8-hydroxy-2'-deoxyguanosine, 8-oxo-

7,8-dihydroguanine and 8-oxo-7,8-dihydroguanosine. These oxidative lesions serve as excellent markers for DNA and RNA damage produced specifically by ROS. Flow cytometric and immunofluorescence studies demonstrated a significant increase in the basal levels of CM oxidative damage as a result of mouse ageing. Enhanced levels of CM oxidative damage levels were also seen in clinical samples from aged patients when compared to younger patients. Our data supports the recent observations of Rizvi *et al.* (2021), where they showed a build-up of ROS in cardiomyocytes with age in both rat (6 vs 24 months old) and human tissue (18-65 vs >65years old) [240]. Furthermore, the current study also showed age-related increases in oxidative damage on ECs in mouse hearts, but with no difference between ROS mediated damage to CMs and ECs. This may be linked to emerging evidence suggesting that direct and indirect functional redox crosstalk between cardiomyocytes and coronary ECs occurs during normal functioning of the heart as well as during pathophysiological situations. For example, ROS generated by CMs during cardiac hypertrophy communicate with ECs in order to promote angiogenesis [43]. The opposite has also been observed whereby EC ROS increased CM fibrosis [43]. Hence, it is plausible that increased CM ROS and EC ROS generation leads to pro-inflammatory phenotypic changes in ECs through paracrine and autocrine cross-communication respectively.

Our results identified low levels of VCAM-1 expression in adult sham mice, which may result from the surgical technique [241]. This basal VCAM-1 was significantly up-regulated with age, which further supports the idea of a chronic low-grade inflammatory state in ageing. These results also support the findings of Miller *et al.* (2007), who identified an up-regulation in VCAM-1 on thoracic arteries from aged rats, as well as other groups who noted similar changes in the aorta [242, 243]. Furthermore, Yousef and colleagues showed

over 1,000 differentially expressed genes in aged brain ECs including those involved in cell adhesion, immune cell activation, stress response and vascular remodelling. However, among the proteins expressed in or related to the vasculature, soluble VCAM-1 correlated most strongly with age, an observation they confirmed by immunostaining of brain sections [244]. In the current study, while VCAM-1 expression was predominantly on macrovessels in adult and aged sham hearts, some microvessels staining was noted on aged sham hearts. The emergence of microvascular VCAM-1 staining could be a result of prolonged low-grade inflammation in ageing. Bowden *et al.* (2002) suggested that VCAM-1 staining is time-dependent when they showed increasing VCAM-1 expression from 3 – 24 hours on macrovessels from injured adult mice [245].

Overall, our flow cytometric and immunofluorescence mechanistic studies further demonstrate the presence of chronic low-grade inflammation in the aged heart. These basal disturbances in oxidative damage and adhesion molecule expression may explain the heightened levels of inflammatory neutrophils within the aged coronary microcirculation.

### **3.3.4. Exacerbated Inflammatory and Perfusion Responses in Aged IR Injured Mice**

Reperfusion is often associated with inflammatory injury to cardiac tissue, which can lead to heart failure and death through an uncontrolled inflammatory response [35, 246]. Moreover, MVO can cause no reflow, which can also induce excessive inflammatory responses [52, 247]. However, current clinical imaging methods are unable to visualise

these microcirculatory disturbances in the reperfusing heart. Our intravital data and multiphoton data show an increase in neutrophil recruitment in the microvessels of adult IR injured hearts, confirming previously published data by the Kalia group [32]. An enhanced neutrophil presence is certainly involved in mediating lethal injury following reperfusion [248]. However, for the first time we directly showed a remarkable inflammatory cell presence in the coronary microvessels of aged IR injured beating hearts *in vivo*. This was so striking that individual neutrophils were often difficult to demarcate, with clusters observed occupying the full width of medium-sized vessels (which we assume to be post-capillary venules) and capillaries. Larger coronary blood vessels were also lined with individual adherent neutrophils, something not noted in adult injured hearts. Activated neutrophils are well known to become stiff which contributes to their retention specifically within capillaries that have a smaller diameter than their own [249].

Although neutrophil recruitment plateaued in the adult hearts, this was not the case in injured aged hearts, where neutrophils continued to be recruited. Furthermore, our multiphoton data showed that this increase was not limited to just the surface of the heart but was consistent throughout all layers of the LV. There have been no previous intravital or multiphoton microscopy studies on aged myocardial IR injured mice. However, a recent study by Barkaway *et al.* (2021) using IVM on the mouse cremaster has shown similar increases in neutrophil recruitment following IL-1 $\beta$  intrascrotal injury in aged mice when compared to adult injury [224].

This significant presence of neutrophils in the aged injured heart has serious implications with regards tissue damage, not simply because of the sheer numbers present. Spontaneous ROS production from neutrophils has been shown to increase with age in

elderly patients [250]. Furthermore, peripheral blood neutrophils from older 20–27-month-old mice have been shown to have a greater tendency to release NETs either with or without stimulation [251]. Such phenotypic changes, combined with the increased local presence of these cells in the heart, can lead to increased microvascular and surrounding tissue damage.

Increased platelet presence was also noted in the aged injured heart, but this was not greater than that observed in adult injured hearts. Nor was the effect of age and injury on platelets as remarkable as the effect on neutrophils. This was a surprising observation as a greater presence of platelet microthrombi was expected in the aged injured hearts. Indeed, their presence was not as remarkable as that previously described by the Kalia group when male adult IR injured hearts were imaged intravitaly [32]. Increased hypercoagulability of the blood and an impaired fibrinolytic system in the elderly has been described [252]. Moreover, one of the most documented changes in platelet function during ageing is platelet hyperactivity, decreased bleeding time and a greater sensitivity to aggregation induced by classical agonists [253]. Therefore, the intravital observation in the current study was somewhat surprising. This may be linked to the already heightened number of adherent platelet aggregates present in the aged sham hearts, or it may be that a longer reperfusion time is required to identify significant changes.

Ultimately, in both adult and aged hearts, these thromboinflammatory events resulted in occlusion of flow, with the poorest coronary microcirculatory perfusion and microvascular leakage (of FITC-BSA) noted in aged injured hearts where significantly more areas devoid of flow were observed. Although overall ventricular perfusion plateaued in the reperfused adult hearts, of concern for the aged heart was the LSCI observation that myocardial

perfusion continued to decrease in the reperfusion phase. This age-related impairment may result from the exacerbated number of thromboinflammatory cells within the microvasculature and the capability of a high number of activated neutrophils to obstruct capillaries [249, 254]. Our data supports the findings of Willems *et al.* (2005) who found coronary flow post-reperfusion injury was much lower in the isolated hearts of aged (18-28 month old) mice when compared to younger (2-4 month old) mice [255]. The current study provides the first real-time demonstration of the rapid and debilitating impact of reperfusion on the smallest blood vessels of the aged heart *in vivo*. This likely contributes to the worsened outcomes in aged MI patients and also the reduced myocardial tolerance to IR injury previously demonstrated to occur as early as 12 months (middle-age) in mice [255].

To identify potential underlying mechanisms behind explain these age-related inflammatory exacerbations and perfusion perturbations, studies were performed to again identify oxidative damage on CM/ECs and EC VCAM-1 expression following IR injury. Flow cytometric and immunofluorescence studies demonstrated the greatest levels of VCAM-1 expression and oxidative damage occurred in aged IR injured hearts, which significantly surpassed that noted in adult injured hearts. Although it is well documented that IR injury increases levels of ROS and VCAM-1, as far as we are aware, this is the first demonstration of this in the aged coronary microcirculation and heart tissue. As stated earlier, this could be explained by the compromised antioxidant ability and chronic low grade inflammation within aged hearts [165, 256]. Indeed, in a rat model, increased levels of oxygen free radicals were detected under both normal and prolonged intense exercise conditions when the age of the rat increased from 8 to 25 months [257].

Interestingly, although previous studies have demonstrated significantly larger infarct size in aged mice hearts compared to adult mice [2, 4], this was not the case in the current study. Whilst infarct size was larger in aged injured hearts; this was not significantly different. However, even a statistically non-significant small increase in infarct size or scarring can have a significantly adverse effect on heart function and on the patient's prognosis [258].

### 3.3.5. Immediate Aftermath of Reperfusion – Early Intervention is Critical

A number of anti-inflammatories, shown to be successful in experimental studies, have met with translational failure when used clinically in patients with MI [259]. The major outcome measured in such clinical trials is usually a long-term one, namely the ability to prevent infarction, post-MI remodelling, a secondary non-fatal MI, or death. We show multiple microcirculatory perturbations take place in the reperfused heart, are enhanced with age, and likely contribute to the reduced perfusion at the level of the microvessels. Therefore, it is important to consider whether anti-inflammatories can actually protect and keep patent the coronary microcirculation post-reperfusion. Furthermore, it is important to know exactly when to intervene in order for therapies to be vasculoprotective.

The investigation of the immediate effects of reperfusion on thromboinflammatory responses *in vivo*, tissue perfusion *in vivo*, and build-up of ROS is limited. If these detrimental events occur early i.e., within minutes of reperfusion, it is possible that the observed translational failure of tested therapeutics is linked to a lack of early benefit at the level of the coronary microcirculation and is therefore dependent on the time of

intervention. In order to study the immediate responses that occur during the onset of reperfusion, the intravital imaging and stabilisation protocol was optimised to allow imaging during the first 30 minutes of the reperfusion phase. We were successfully able to image during this time period and noted a very rapid neutrophil and platelet infiltration as soon as reperfusion commenced (only investigated in adult mice). It is possible that this immediate recruitment is linked to the release of thromboinflammatory debris embolising into the downstream coronary microcirculation from the occlusion site, where they have been shown to accumulate [260]. Our data showed that platelet recruitment peaked within 15 minutes and then plateaued during the remaining 150 minutes of reperfusion. However, neutrophil infiltration experienced a much earlier peak, within 5 minutes of reperfusion. This may be linked to the reactive hyperaemic response, noted in some mice within minutes of reperfusion, which would have delivered more blood cells to the heart.

This very rapid neutrophil infiltration has serious implications – they can damage the local microvascular environment, transmigrate into the myocardium and damage CMs, but also their activation may predispose to subsequent thrombogenesis. Indeed, Darbousset *et al.* (2012) demonstrated that neutrophils reached the site of injury before platelets in a mouse study of laser-induced damage [261]. They further demonstrated that these neutrophils were a key source of tissue factor (TF), a major *in vivo* initiator of coagulation, which enhanced subsequent thrombotic processes. Moreover, in patients with MI, the accumulation of neutrophils in the culprit artery led to the release of NETs decorated with TF that was subsequently delivered to downstream microvessels [262]. Whether the intense neutrophil presence in the reperfused aged mouse coronary microcirculation

employs NETs and TF to mediate subsequent thrombosis in the coronary capillaries will require further investigation.

As described earlier, this rapid thromboinflammatory recruitment could also be linked to increased myocardial oxidative damage. Indeed, flow cytometric studies demonstrated a significant early increase in the levels of DNA/RNA oxidative damage within 30 minutes of reperfusion in both CMs and ECs of adult mice, which was heightened in aged cells. This damage persisted even at 150 minutes of reperfusion and, in aged mice only, a gradual increase was observed as the duration of reperfusion increased. This very rapid oxidative damage may therefore explain the immediate thromboinflammatory and perfusion perturbations which occur within the same time frame. These disturbances within the first 30 minutes of reperfusion highlight the importance of therapeutically targeting the period immediately after re-opening of the occluded vasculature and suggest clinical studies appropriately factor in the importance of this period.

### 3.3.6. Conclusion

In conclusion, we have shown that ageing is associated with a chronic low-grade inflammatory environment in otherwise healthy hearts and that age has an additive detrimental impact on the microvasculature in the presence of an acute IR injury [247]. We show that age alone is associated with heightened levels of oxidative damage on both CMs and ECs in otherwise healthy hearts, as well as supporting an aggravated oxidative damage response during reperfusion [165]. This chapter has demonstrated that exacerbated age-related microvascular perturbations lead to areas devoid of perfusion

within the injured LV and likely contribute to the infarction of the myocardium. This is in part due to the very rapid thromboinflammatory cell accumulation within the coronary microvasculature following injury. Importantly, we show that resumption of regional blood flow in the ventricle is not a sure sign that all is well in the smallest blood vessels of the heart. Collectively, our findings of enhanced coronary microcirculatory perturbations associated with age may explain the poorer outcomes in elderly MI patients.

# **Chapter 4:**

## **Targeting Interleukin-36 in Myocardial Ischaemia Reperfusion Injury – A New Therapeutic Target**

\* Part of this chapter makes up the published paper in the appendix

### 4.1. Introduction

Studies have shown that approximately 50% of the final infarct size is a result of IR injury [35, 246]. We have shown in the previous chapter this could be partly explained by the multiple disturbances taking place in the coronary microcirculation post-reperfusion. Moreover, these were remarkably increased in the reperfused aged heart resulting in a number of areas in the LV myocardium that were devoid of perfusion. Therefore, a potential therapeutic target for limiting infarct size (and subsequent ventricular remodelling) could be to target these microvascular perturbations; specifically, the significant pro-inflammatory response observed [60, 101]. Several experimental studies and clinical trials have targeted the individual elements in the inflammatory leukocyte adhesion cascade following myocardial IR. These have included targeting potent inflammatory cytokines, such as IL-1 and IL-6 with humanized anti-IL-1 or anti-IL-6 receptor antibodies or preventing neutrophil adhesion with a humanized P-selectin inhibitor antibody (adhesion molecule between ECs and leukocytes or platelets) [109, 197, 263-265]. Although such treatments have been shown to be beneficial in preclinical animal models, many of these studies failed to improve measurable outcomes or reduce infarct size when used in humans.

Having said that, targeting inflammatory cytokines (e.g., IL-1 and IL-6) have produced the most promising studies in enhancing long-term outcomes. Indeed, the large scale canakinumab anti-inflammatory thrombosis outcomes study (CANTOS) trial provided exciting evidence that targeting IL-1 was beneficial in preventing major adverse cardiac events (death, another MI, stroke etc) in the absence of lipid-lowering, although no effect

on impact size was noted [12, 18-23]. Hence, cytokines are exciting targets due to their potent effects on initiating inflammation, something the previous chapter has described to be one of the prominent disturbances in the adult and aged heart post-reperfusion.

The interleukin-1 family (IL-1F) consists of 11 known pro- and/or anti-inflammatory cytokines, some of which have been studied extensively, whilst others have received less attention [266]. These are frequently the first upstream cytokines produced in response to injury and so are considered good targets for intervention [267]. Since IL-1F members critically mediate sterile inflammation, they may be key mechanistic contributors causing myocardial microcirculatory disturbances post-reperfusion [266]. In the last decade, genes encoding a novel cytokine cluster, namely interleukin-36 (IL-36), with structural and functional similarities to IL-1, was discovered [116, 117]. Although we know the IL-36/IL36R pathway is highly pro-inflammatory in the skin and lungs, we are still at a very early stage in our current understanding of its *in vivo* biology in the heart. We do know that IL-38 (an IL-1F member that shares 43% homology with IL-36Ra) can improve cardiac remodelling [27] and IL-36R deficiency in rats improves cardiac function and protection of CMs following cardiopulmonary bypass injury [28]. The downstream transcription factor NF- $\kappa$ B is already a known mediator of coronary microvascular injury, as inhibition of NF- $\kappa$ B in two independent rabbit models of myocardial IR injury reduced inflammation and the no-reflow area [268, 269]. These studies suggest a potential novel role for IL-36 in mediating myocardial injury. Therefore, in this chapter we focus on investigating whether IL-36 and its receptor are present and functional within the IR injured adult and aged heart, and whether targeting this novel pathway improves perturbations in the coronary microcirculation.

#### 4.1.1. Hypotheses and Aims

In this chapter, we firstly investigate whether IL-36R and its cytokines are present in the healthy uninjured heart and whether age, or IR injury impacts their expression. This was assessed *in vitro* using immunofluorescence, Western blotting, multiphoton microscopy, cell culture and flow cytometry-based studies. Secondly, in this chapter, we intravitaly investigate the functional capacity of the IL-36R within the heart *in vivo* following topical application of IL-36 cytokines. Lastly, in this chapter, we aim to assess the vasculoprotective ability of IL-36Ra therapy, specifically its effects on thromboinflammatory events, vascular perfusion, and infarct size in both adult and aged hearts *in vivo*. This was assessed using intravital and laser speckle imaging of the beating heart and *in vitro* using multiphoton microscopy and TTC staining. We hypothesized:

5. Expression of IL-36 and IL-36R in the murine and human heart increases with age
6. Expression of IL-36 and IL-36R in the murine heart will increase as a result of IRI
7. Topical application of IL-36 ( $\alpha$ ,  $\beta$  and  $\gamma$ ) on a healthy heart will induce a thromboinflammatory response
8. Microcirculatory perturbations and infarct size will be reduced following IL-36Ra treatment leading to enhanced capillary perfusion
9. The above benefits will be mechanistically explained by the extent of VCAM-1 expression and oxidative damage on CMs, and ECs being decreased following IL-36Ra treatment.

## 4.2. Results

### 4.2.1. IL-36R is Expressed in the Murine Heart, and Expression Increased with Age and IR injury

To determine the expression and localisation of IL-36R in the murine heart, frozen sections from adult and aged mice were stained for IL-36R using immunofluorescence. IL-36R was found to be expressed, albeit at very low levels, in sham adult hearts as evidenced by a positive stain (**Figure 4.1a**), which was not seen in the IgG controls (**Figure 2.4b**). Expression of IL-36R was significantly increased as a result of IR injury in adult hearts. Basal expression was further significantly increased in aged sham hearts when compared to adult sham hearts. Indeed, this increase was higher than that observed in adult IR injured hearts (**Figure 4.1b**). Moreover, IL-36R expression was significantly higher in aged IR injured hearts when compared to adult IR injured hearts (**Figure 4.1b**).

Staining of frozen heart sections for IL-36R demonstrated that this receptor was expressed on all macrovessels regardless of IR injury and age (**Figure 4.1a, 4.2**). Microvascular co-localisation was also identified. To confirm this vascular expression, sections were co-stained with an anti-CD31 antibody. Multiphoton imaging of dual stained sections identified that this expression was intense within the wall of larger blood vessels, particularly in the tunica adventitial layer (**Figures 4.2a-b**). Coronary microvessels also stained positive for the IL-36R (**Figure 4.2c**). IL-36R was also detected in CMs, particularly in the aged groups (**Figure 4.1a**).

Staining of frozen heart sections for IL-36R was performed using an Alexa Fluor 488 (AF488) secondary antibody. However, despite localisation with vascular structures, the staining

did appear to be somewhat amorphous (**Figures 4.1a and 4.2a-c**). Therefore, immunofluorescence staining was repeated, but in adult mice only, using a different secondary antibody, namely an Alexa Fluor 647 (AF648) secondary antibody. Using IL-36R/AF647, expression appeared to follow a similar pattern to IL-36R/AF488. However, the background staining was markedly reduced, allowing better confirmation of the localisation of IL-36R with microvessels (**Figure 4.3a**), macrovessels (**Figure 4.3b**) and CMs (**Figure 4.3a**).

Western blotting was also performed to confirm and quantitate the presence of IL-36R in tissue lysates from all four experimental groups. Again, a stepwise increase in IL-36R with injury and ageing was observed as evidenced by changes in the density of the bands. The molecular weight of IL-36R is approximately 65kDa, but it migrates to the position of approximately 85kDa in denaturing protein gels [270]. Thus, the two bands observed correspond to the 65kDa active protein due to cleavage of its signalling peptide and a less potent 85kDa glycosylated form (**Figure 4.4a**). Again, adult sham hearts expressed very low levels of IL-36R. This increased in adult IR injured hearts where the highest levels of the glycosylated 85kDa protein was observed. However, significant increases in IL-36R protein were identified in aged sham hearts when compared to adult sham hearts, particularly of the more potent 65kDa protein (**Figures 4.4b**). This expression significantly increased further in aged IR injured hearts when compared to adult IR hearts, which exhibited the highest levels of the active 65kDa IL-36R protein (**Figure 4.4b**).  $\beta$ -actin bands appeared to also increase with age and IR injury, and thus, normalisation of lysates using a BCA protein assay kit to 2mg/ml was used instead of the housekeeping gene (**Figure 4.4a**).

Flow cytometry was performed to better analyse IL-36R expression, specifically on CMs and ECs in collagenase digested hearts from all four experimental groups. Flow cytometry also showed IL-36R expression increasing with IR injury and ageing on CMs and ECs (**Figures 4.4c-d**). Both CMs and ECs expressed IL-36R, albeit at very low levels, in adult sham hearts. On CMs, IL-36R expression significantly increased in adult IR injured tissue, and aged sham tissue when compared to adult sham tissue, and in aged IR injured tissue when compared with aged sham (**Figure 4.4c**). Similarly, ECs IL-36R expression significantly increased in adult IR injured tissue when compared to adult sham tissue and in aged IR injured tissue when compared with aged sham (**Figure 4.4d**).

The above flow cytometry data were obtained from mice culled after 150 minutes post-reperfusion. Additional experiments were conducted to see if ischaemia alone, and an earlier time point post-reperfusion, could increase IL-36R expression. Therefore, IL-36R expression levels on adult and aged CMs and ECs following 0-, 30- and 150-minutes post-reperfusion was investigated. Both adult and aged CMs and ECs expressed IL-36R, albeit at very low levels in the adult heart, as a consequence of ischaemia alone (**Figures 4.5a-f**). However, this was significantly higher on aged CMs and EC's when compared to adult CMs and ECs. Expression of IL-36R on adult and aged CMs and ECs was significantly increased as early as 30 minutes post-reperfusion compared to cells investigated after ischaemia alone, and further still by 150 minutes post-reperfusion. However, the expression of IL-36R was always higher on aged CMs and ECs at all time points investigated (**Figures 4.5a-f**).

#### 4.2.2. IL-36R Expressed on Murine VCECs

Since IL-36R was highly expressed in the vasculature of the heart, we then sought to determine whether IL-36R was expressed specifically on ECs. Immortalised murine VCECs were cultured and stained for IL-36R in the absence of any pre-stimulation. However, IL-36R expression was minimal on unstimulated VCECs (**Figure 4.6a**). In order to identify if IL-36R expression was inducible using cytokine stimulation, VCECs were stimulated with either TNF $\alpha$  (3, 30, or 300ng/ml) or individual IL-36 cytokine agonists (3, 30, or 300ng/ml) for 4 hours. IL-36R was significantly up-regulated after stimulation with either TNF $\alpha$ , IL-36 $\alpha$ , IL-36 $\beta$ , or IL-36 $\gamma$  but only at the highest dose for each cytokine (300ng/ml). Expression levels with the high-dose cytokine treatments were not significantly different between TNF $\alpha$  and IL-36 cytokines. Expression of IL-36R was on the surface of the VCECs as these cells were not permeabilized (**Figures 4.6a-b**).

#### 4.2.3. IL-36 Cytokines Expressed in the Murine Heart

Having seen that the receptor for IL-36 was expressed in the murine heart and murine ECs, we then sought to identify whether the IL-36 cytokines (IL-36 $\alpha$  and IL-36 $\beta$ ) were also present in the heart. Immunofluorescence staining was performed on adult and aged, sham, and IR injured frozen heart sections using relevant antibodies. Generally, IL-36 $\alpha$  and IL-36 $\beta$  had a similar pattern of expression to IL-36R, such that staining was identified on macrovessels and microvessels. CM expression was also noted, particularly within the aged groups (**Figures 4.7a and 4.8a**). Similar to IL-36R, expression of IL-36 $\alpha$  increased in a

stepwise manner in adult IR injured tissue and aged sham tissue when compared to adult sham tissue. Moreover, a significant increase in IL-36 $\alpha$  expression was also seen between the adult and aged IR injured groups (**Figure 4.7b**). Similarly, IL-36 $\beta$  expression increased in a stepwise manner in adult IR injured tissue (NS) and aged sham tissue when compared with adult sham tissue and in aged IR injured tissue when compared with aged sham. A significant increase in IL-36 $\beta$  expression was also seen between the adult and aged IR injured groups (**Figure 4.8b**).

#### **4.2.4. IL-36 Cytokines Expressed on Murine VCECs**

In order to investigate whether IL-36 cytokines were expressed specifically by ECs, VCECs were again stained with the respective antibodies. In a similar manner to IL-36R, staining for either IL-36 $\alpha$  and IL-36 $\beta$  was not identified on unstimulated cells (**Figure 4.7c and 4.8c**). To determine whether the generation of IL-36 cytokines was inducible, VCECs were again pre-treated with either TNF $\alpha$  (3, 30, or 300ng/ml) or an IL-36 cytokine agonist (3, 30, or 300ng/ml). The only treatments that significantly increased expression of IL-36 $\alpha$  on VCECs were 300ng/ml TNF $\alpha$ , 300ng/ml IL-36 $\beta$  and 30ng/ml IL-36 $\gamma$  (**Figure 4.7d**). IL-36 $\beta$  staining was significantly enhanced when VCECs were stimulated with either 30 and 300ng/ml of TNF $\alpha$ , 30ng/ml IL-36 $\alpha$ , 30 or 300ng/ml IL-36 $\beta$  and 300ng/ml IL-36 $\gamma$  (**Figure 4.8d**). Hence, IL-36 $\beta$  expression could be stimulated by a larger range of cytokines and at lower concentrations than IL-36 $\alpha$ . However, the expression of the cytokines was not as prominent as the expression of the receptor on these cells.

#### 4.2.5. Increased Expression of IL-36R/ $\alpha$ / $\beta$ with IR Injury and Age was Observed Specifically on the Murine Coronary Microvessels

Having identified on frozen heart sections that vascular expression of IL-36R and its ligands increased with IR injury and age, we sought to identify at which specific level of the vasculature this increase was occurring on. To achieve this, the mean fluorescent intensity of IL-36R, IL-36 $\alpha$ , and IL-36 $\beta$  on the microvessels and macrovessels was analysed separately. Analysis of the macrovasculature revealed no significant differences between the expression of IL-36R, IL-36 $\alpha$ , or IL-36 $\beta$  between any of the four experimental groups (**Figure 4.9a**). In contrast, IL-36 $\alpha$  expression significantly increased in adult IR injured hearts when compared to adult sham hearts. Moreover, there was a significant increase in the basal expression levels of IL-36R, IL-36 $\alpha$  and IL-36 $\beta$  as a result of age alone on the microvasculature in sham hearts. IL-36R and IL-36 $\beta$  expression was also significantly increased on aged IR injured microvessels when compared to microvessels in aged sham mice. In the case of all three markers, staining in the microcirculation was significantly higher in aged IR mice than in the respective adult IR mice (**Figure 4.9b**).

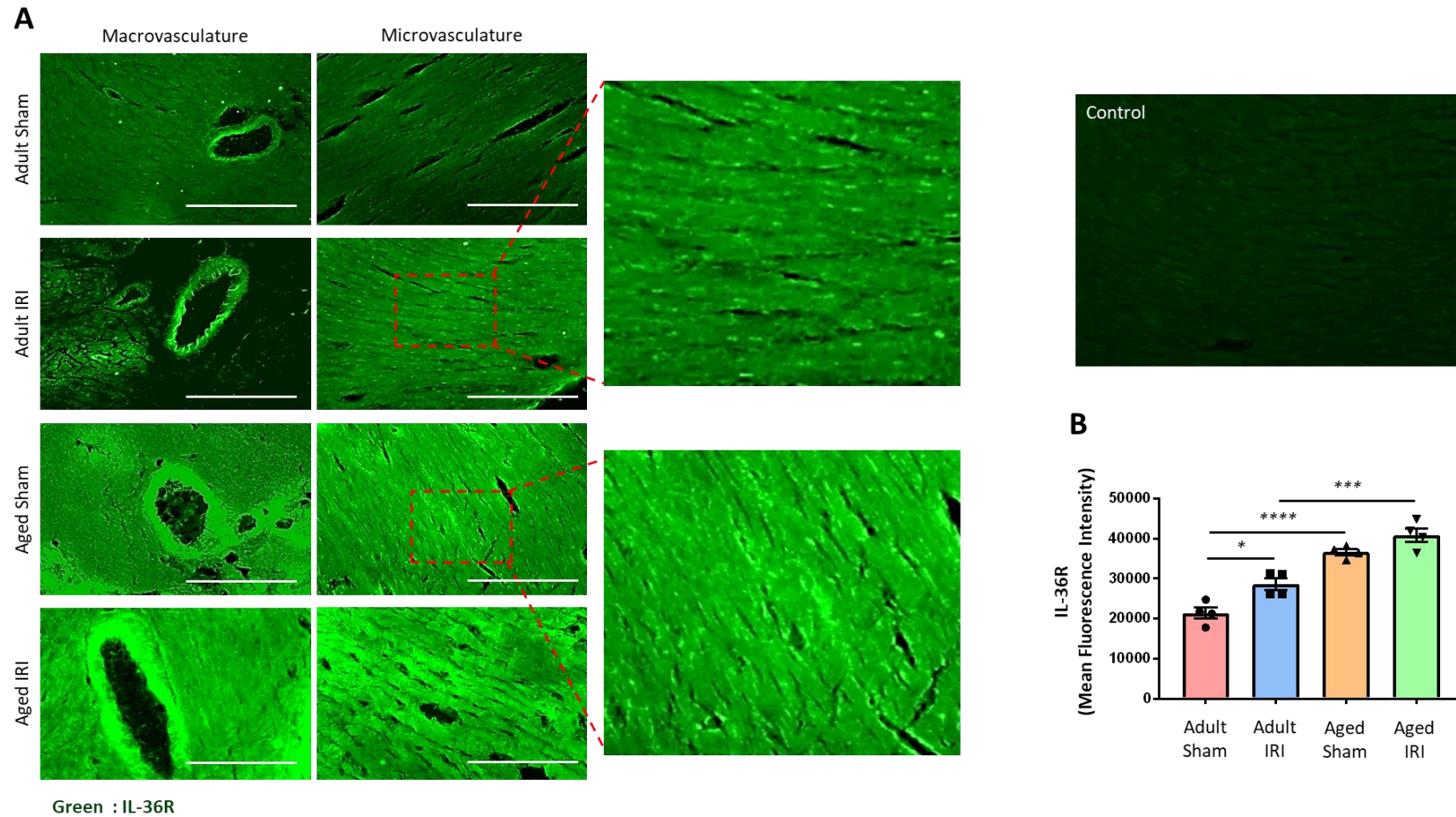


**Figure 4.1. Age increases the expression of IL-36R within healthy, and IR injured heart.** Sham or IRI inducing surgery was performed on adult and aged female mice. Mice were culled following 120 minutes of reperfusion and hearts were harvested and snap frozen. The LV was transversely sectioned using a cryostat into 10µm sections and then immunostained with an antibody against IL-36R (AF488). Sections were imaged using a EVOS microscope. **(A)** Representative images of IL-36R (green) staining of frozen heart sections, alongside the IgG control. Scale bar indicates 200µm. **(B)** Quantitative analysis of the immunofluorescent images of IL-36R expression. Statistical analysis was performed using a one-way ANOVA, followed by a Tukey's post-hoc test between the following groups: adult sham versus adult IR injury, adult sham versus aged sham, aged sham versus aged IR injury, and adult IR injury versus aged IR injury. Abbreviations - IRI: ischaemia reperfusion injury. n=4/group. Mean ±SEM. \*p<0.05, \*\*\*p<0.001, \*\*\*\*p<0.0001.

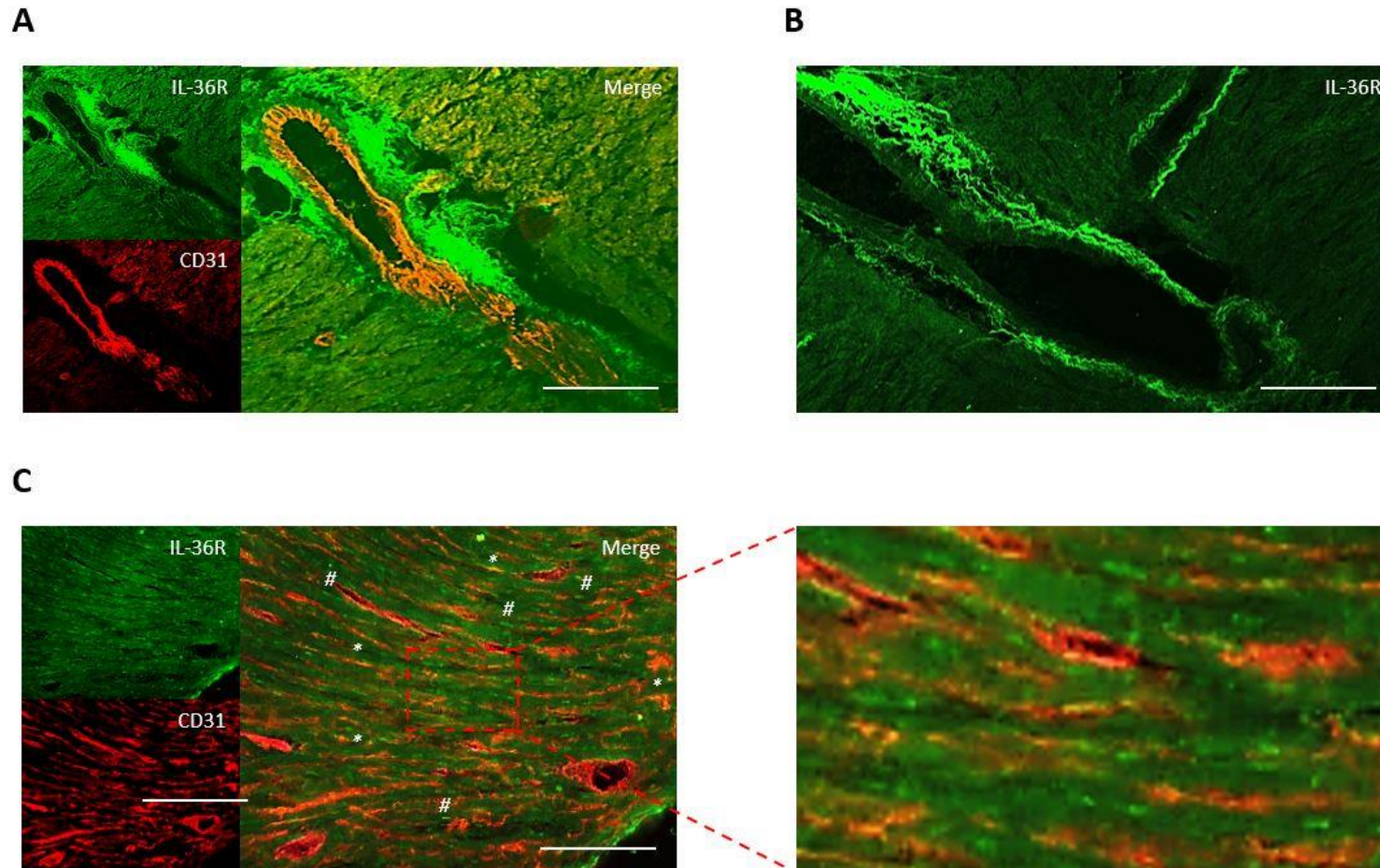


**Figure 4.2. Expression of IL-36R is on both coronary macrovasculature and microvasculature.** IRI inducing surgery was performed on adult female mice. Mice were culled following 120 minutes of reperfusion and hearts were harvested and snap frozen. The LV was transversely sectioned using a cryostat into 10 $\mu$ m sections and then immunostained with an antibody against IL-36R (AF488). To determine whether IL-36R (green) expression was vascular in nature, heart sections were co-stained with an anti-CD31 antibody (red) and imaged using a multiphoton microscope. Representative image of **(A-B)** coronary macrovasculature and **(C)** microvasculature for an adult IR injured mouse. Scale bar indicates 200 $\mu$ m. n = 4.

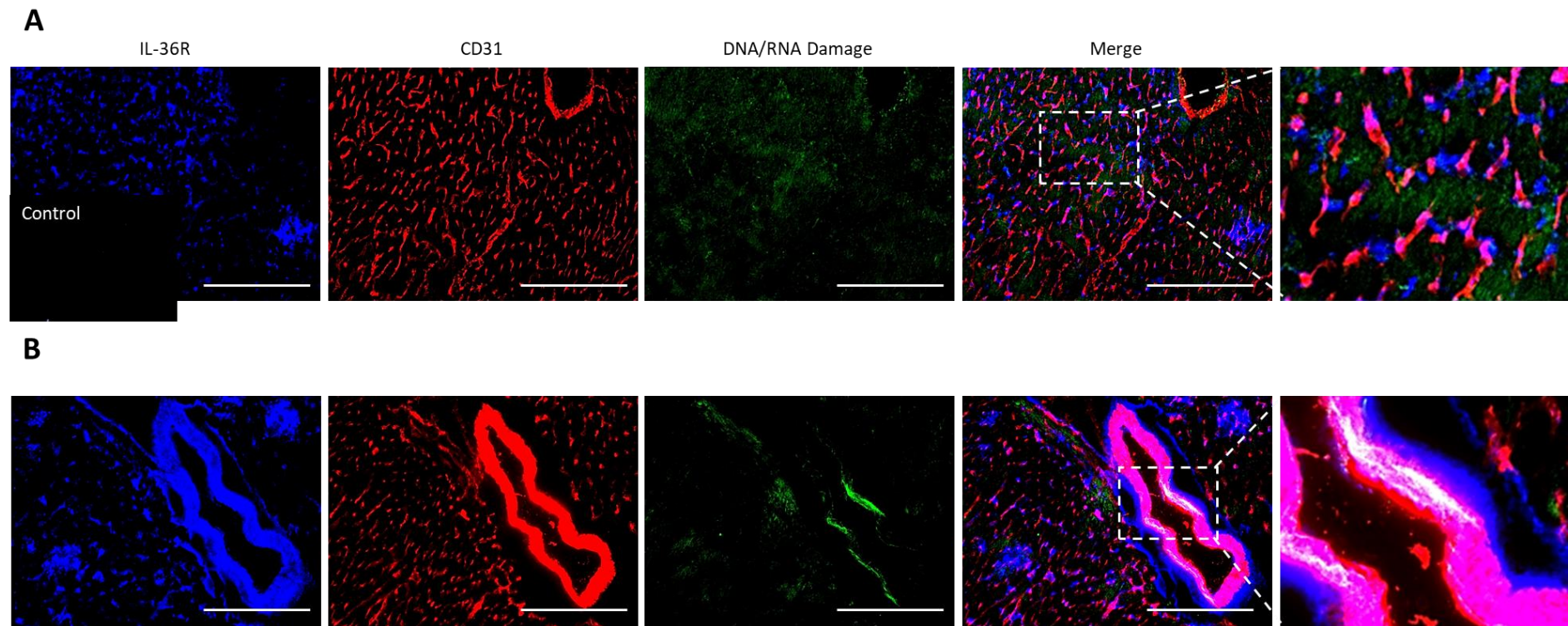


**Figure 4.3. Cardiac expression of IL-36R confirmed using a different secondary antibody.** IRI inducing surgery was performed on adult female mice. Mice were culled following 120 minutes of reperfusion and hearts were harvested and snap frozen. The LV was transversely sectioned using a cryostat into 10µm sections and then immunostained with an antibody against IL-36R, namely Alex Fluor 647 (AF647). To determine whether IL-36R (blue) expression was vascular in nature, heart sections were co-stained with an anti-CD31 antibody (red). A DNA/RNA oxidative damage (green) detecting antibody was used to assess oxidative damage and imaged using a EVOS microscope. Representative image of **(A)** coronary microvasculature, alongside the IgG control and **(B)** macrovasculature for an adult IR injured mouse. Scale bar indicates 200µm. n = 4.

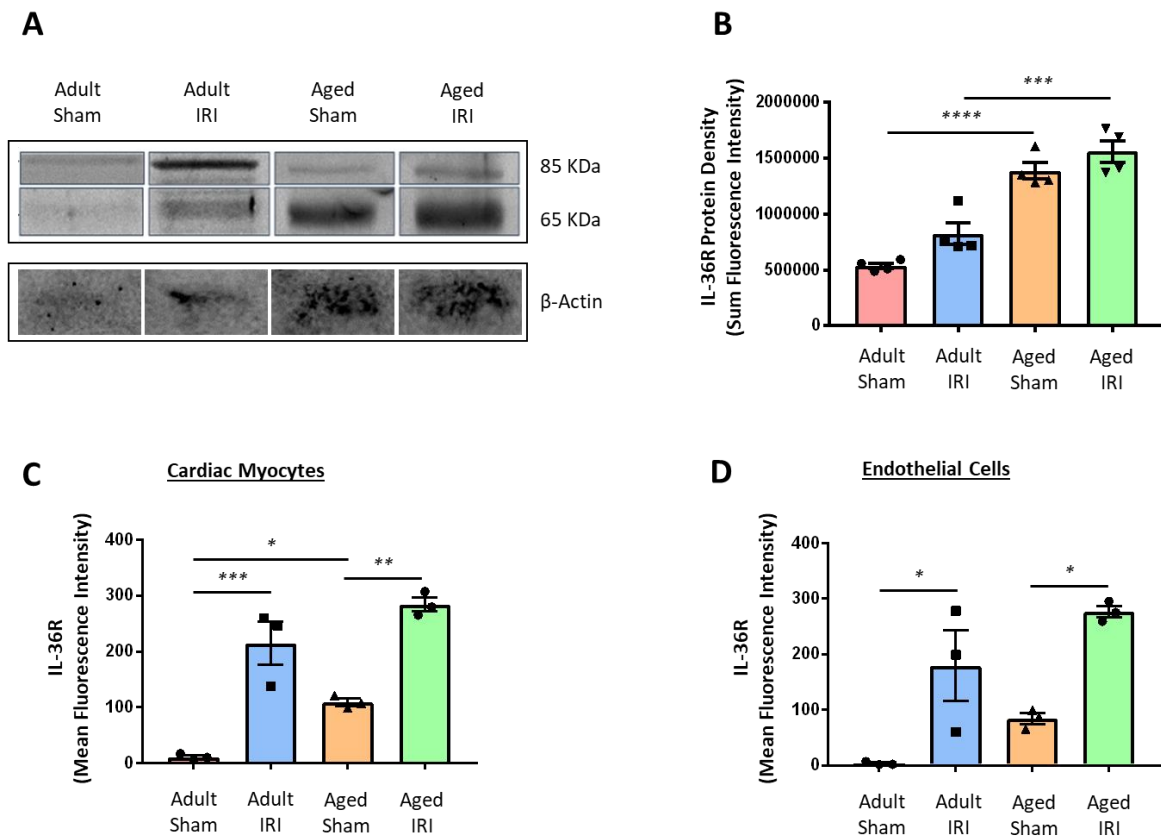


**Figure 4.4. Age increases expression of IL-36R within the healthy and IR injured heart.** Sham or IRI inducing surgery was performed on adult and aged female mice. **(A-B)** Mice were culled following 120-minutes of reperfusion, and harvested hearts were lysed and normalised to 2mg/ml. Blot membranes were stained with an antibody against IL-36R (AF488) and protein bands were visualized using ChemiDoc fluorescence detection system. **(A)** Representative images of the western blots. The molecular weight of IL-36R is about 65kDa, but it migrates to the position of about 85kDa in denaturing protein gels. Hence, two bands were observed corresponding to 65kDa, the more active protein due to cleavage of its signalling peptide, and 85kDa, the less potent glycosylated form. **(B)** Quantitative analysis of the western blot of IL-36R expression (both 65 and 85KDa). **(C-D)** Mice were culled following 150-minutes of reperfusion and hearts were harvested and digested. Cell suspension was stained with an anti-CD31, anti-cTnT, and anti-IL-36R (AF488) antibodies and acquisition was performed using a CyAn™ ADP cytometer. Quantitative analysis of IL-36R expression on **(C)** cardiac myocytes and **(D)** endothelial cells. Statistical analysis was performed using a one-way ANOVA, followed by a Tukey's post-hoc test between the following groups: adult sham versus adult IR injury, adult sham versus aged sham, aged sham versus aged IR injury, and adult IR injury versus aged IR injury. Abbreviations - IRI: ischaemia reperfusion injury. n=4/group. Mean  $\pm$ SEM. \*p<0.05, \*\*p<0.01, \*\*\*p<0.001, \*\*\*\*p<0.0001.

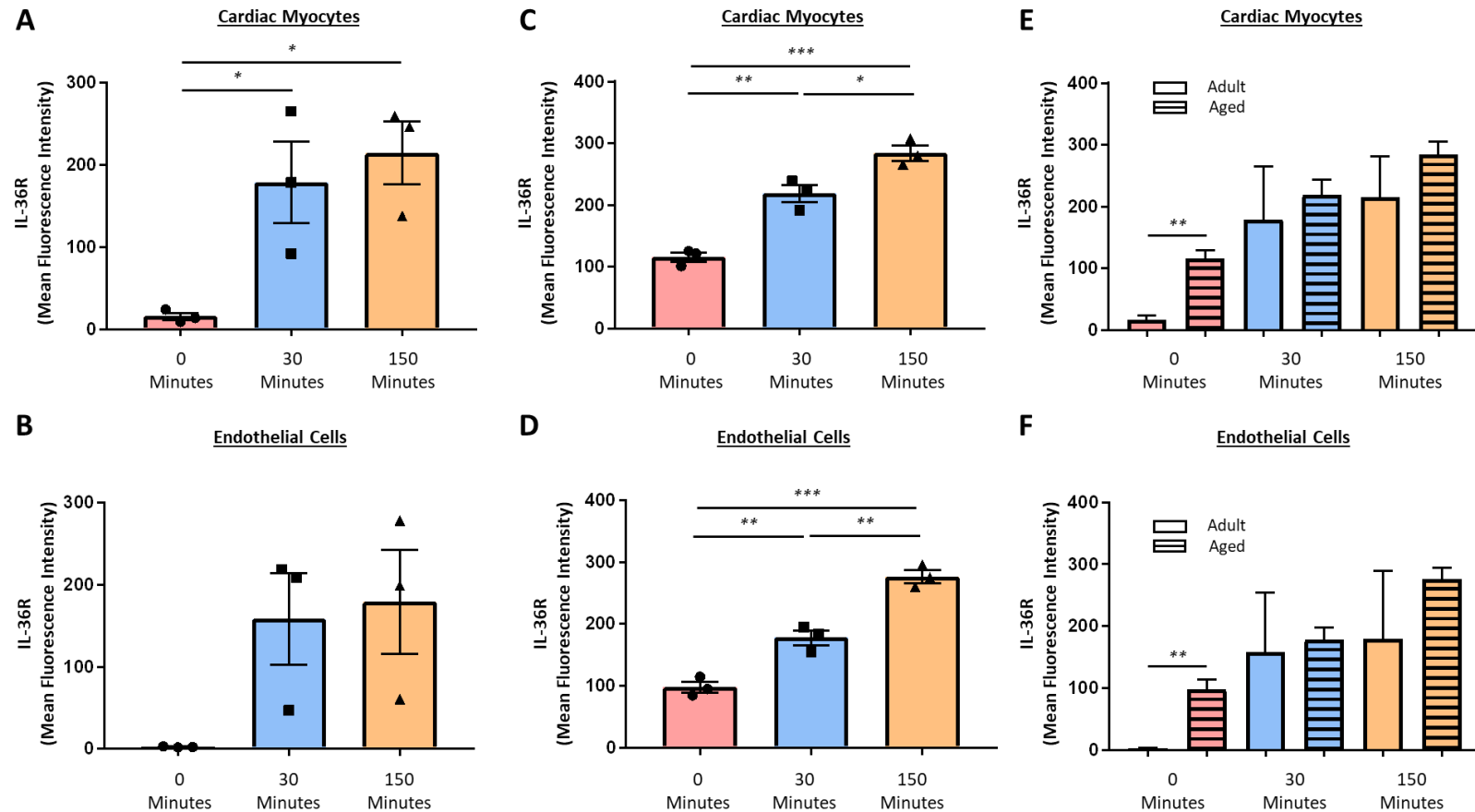


**Figure 4.5. Age and IR injury increase IL-36R expression on cardiac myocytes and endothelial cells within the first 30 minutes of reperfusion.** IRI inducing surgery was performed on adult and aged female mice. Mice were culled following 0, 30 or 150-minutes of reperfusion and hearts were harvested and digested. Cell suspension was stained with an anti-CD31, anti-cTnT, and anti-IL-36R (AF488) antibodies and acquisition was performed using a CyAn™ ADP cytometer. Quantitative analysis of IL-36R expression on cardiac myocytes in (A) adult mice, (C) aged mice, and (E) adult and aged mice. Quantitative analysis of IL-36R expression on endothelial cells in (B) adult mice, (D) aged mice, and (F) adult and aged mice. Statistical analysis was performed using a one-way ANOVA, followed by a Tukey's post-hoc test between the following groups (A-D): 0 minutes versus 30 minutes, 0 minutes versus 150 minutes, and 30 minutes versus 150 minutes; (E-F): 0 minutes adult versus aged, 30 minutes adult versus aged, and 150 minutes adult versus aged. n=3/group. Mean ±SEM. \*p<0.05, \*\*p<0.01, \*\*\*p<0.001

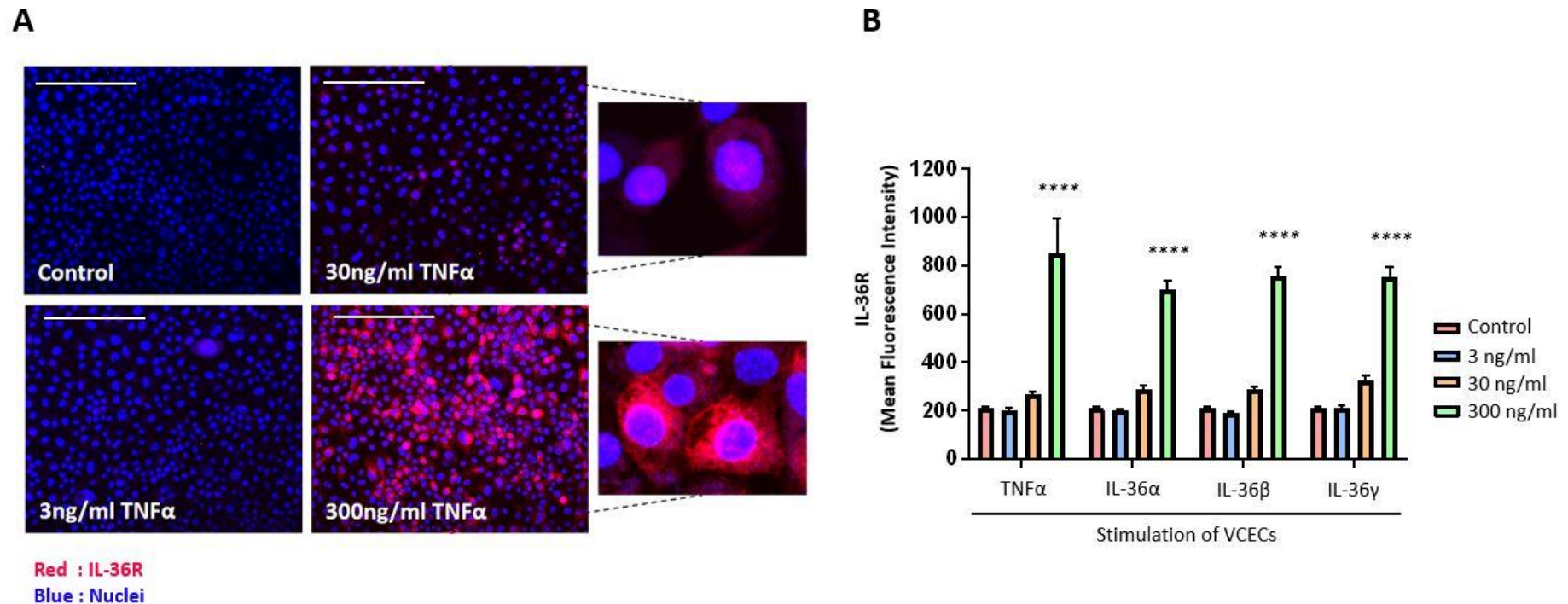


**Figure 4.6. Expression of IL-36R on endothelial cells increases with TNF $\alpha$  or IL-36 cytokine stimulation.** Murine vena cava endothelial cells (VCECs) were cultured and stimulated for 4 hours with experimental media (vehicle control), an IL-36 cytokine ( $\alpha$ ,  $\beta$  or  $\gamma$ ) or TNF $\alpha$ . Cells were stained with an antibody against IL-36R (AF488) and imaged using a multiphoton microscope. **(A)** Representative images of IL-36R (red) expression on stimulated non-permeabilised cells (Hoechst 33342 stained nuclei in blue). Scale bar indicates 200 $\mu$ m. **(B)** Quantitative analysis of IL-36R expression on VCECs following stimulation. Statistical analysis was performed using a one-way ANOVA, followed by a Tukey's post-hoc test: control versus 3ng/ml, control versus 30ng/ml, control versus 300ng/ml, 3ng/ml versus 30ng/ml, 3ng/ml versus 300ng/ml, and 30ng/ml versus 300ng/ml for each of the IL-36 cytokine ( $\alpha$ ,  $\beta$  or  $\gamma$ ) and TNF $\alpha$  as well as 300ng/ml between the various cytokines. n=3/group. Mean  $\pm$  SEM. \*\*\*\*p<0.0001.

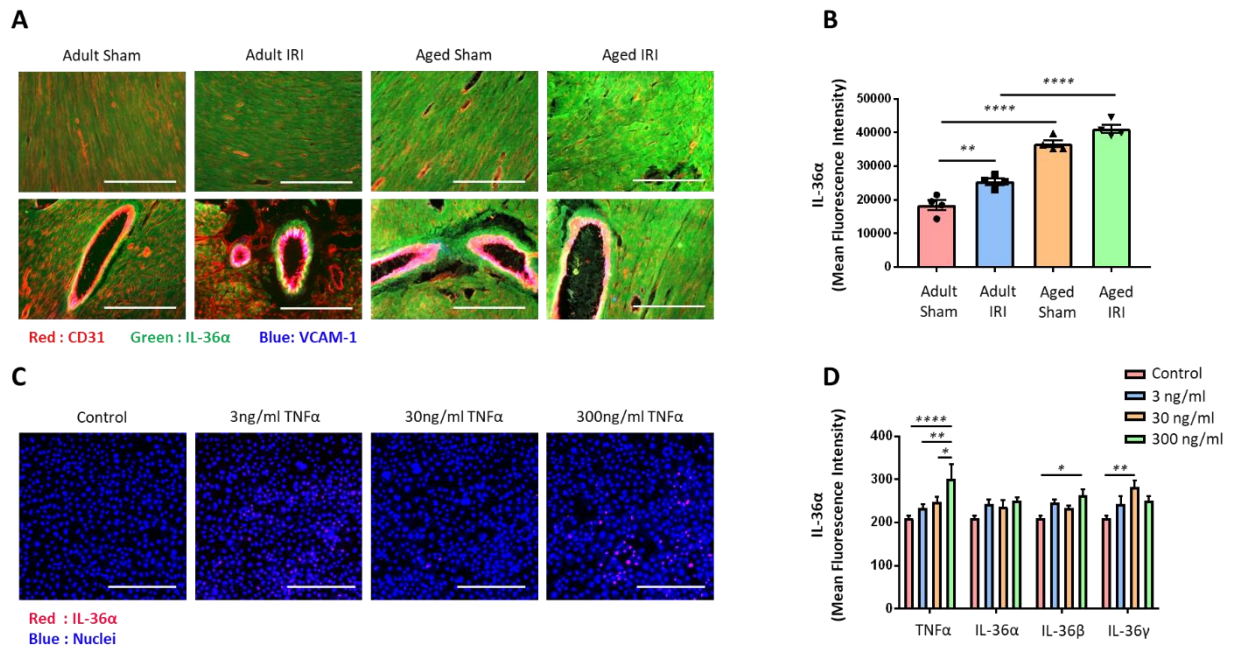


**Figure 4.7. Age increases expression of IL-36α within the healthy and IR injured heart, which can also be released from endothelial cells with TNFα, IL-36β, or IL-36γ cytokine stimulation. (A-B)** Sham or IRI inducing surgery was performed on adult and aged female mice. Mice were culled following 120 minutes of reperfusion and hearts were harvested and snap frozen. The LV was transversely sectioned using a cryostat into 10μm sections and then immunostained with an antibody against IL-36α (AF488). Additional antibodies were also used to determine whether the staining was vascular in nature (CD31) and co-localised with adhesion molecules (VCAM-1). Sections were imaged using a EVOS microscope. **(A)** Representative images of IL-36α (green), CD31 (red), and VCAM-1 (blue) staining of frozen heart sections. Scale bar indicates 200μm. **(B)** Quantitative analysis of the immunofluorescent images of IL-36α expression. Statistical analysis was performed using a one-way ANOVA, followed by a Tukey's post-hoc test between the following groups: adult sham versus adult IR injury, adult sham versus aged sham, aged sham versus aged IR injury, and adult IR injury versus aged IR injury. n=4/group. **(C-D)** Murine vena cava endothelial cells (VCECs) were cultured and stimulated for 4 hours with experimental media (control), an IL-36 cytokine (α, β or γ) or TNFα. Cells were stained with an antibody against IL-36α (AF488) and imaged using a multiphoton microscope. **(A)** Representative images of IL-36α (red) expression on stimulated non-permeabilised cells (Hoechst 33342 stained nuclei in blue). Scale bar indicates 200μm. **(B)** Quantitative analysis of IL-36α expression on VCECs following stimulation. Statistical analysis was performed using a one-way ANOVA, followed by a Tukey's post-hoc test: control versus 3ng/ml, control versus 30ng/ml, control versus 300ng/ml, 3ng/ml versus 30ng/ml, 3ng/ml versus 300ng/ml, and 30ng/ml versus 300ng/ml for each of the IL-36 cytokine (α, β or γ) and TNFα as well as 300ng/ml between the various cytokines. n=3/group. Abbreviations - IRI: ischaemia reperfusion injury. Mean ±SEM. \*p<0.05, \*\*p<0.01, \*\*\*\*p<0.0001.

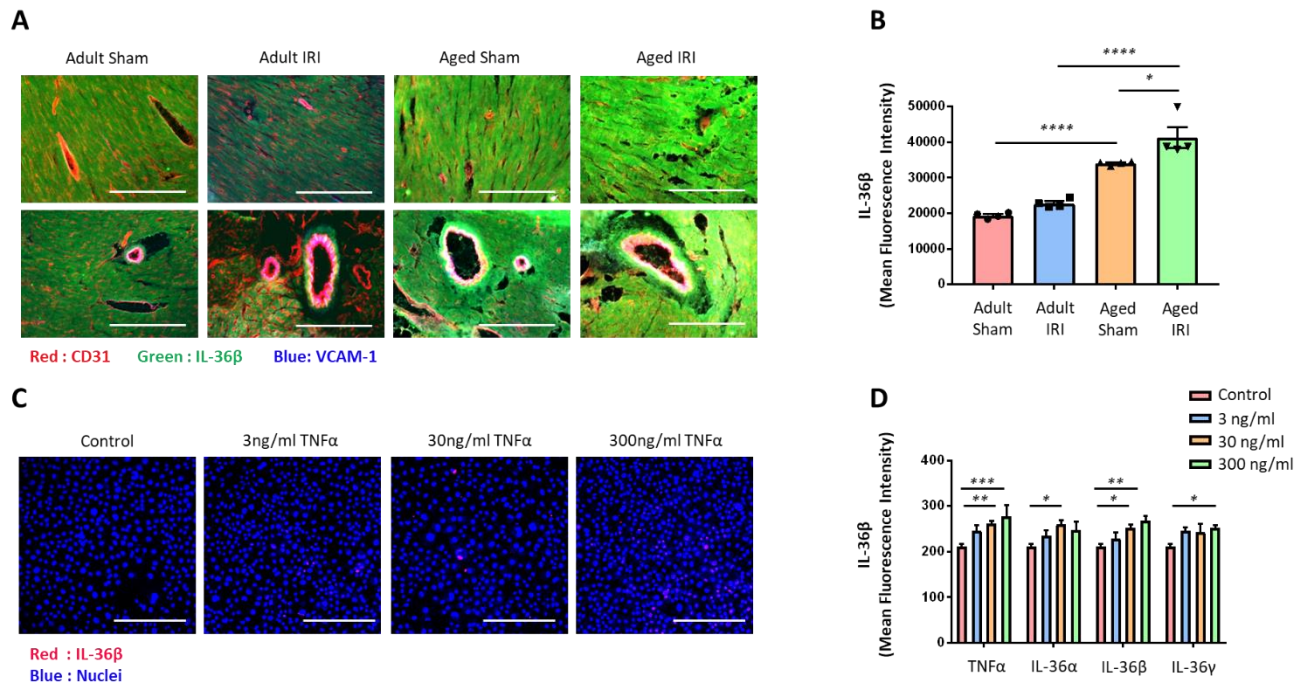
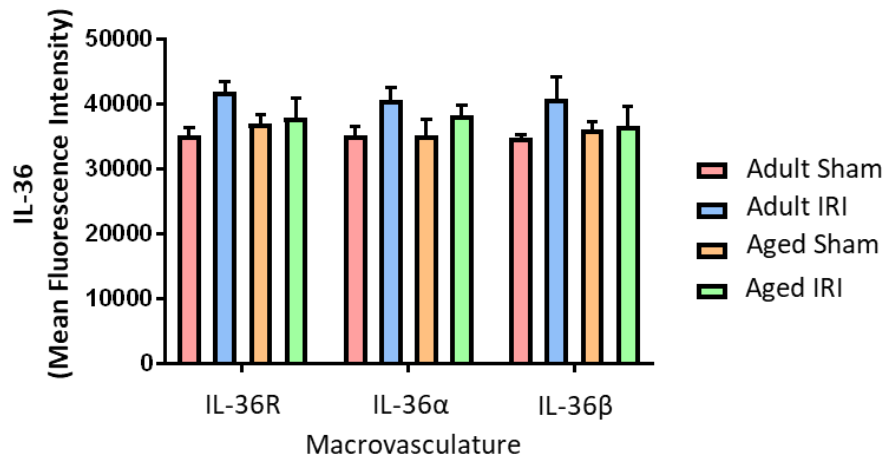


**Figure 4.8. Age increases expression of IL-36β within the healthy and IR injured heart, which can also be induced released from endothelial cells with TNFα, or IL-36 cytokine stimulation. (A-B)** Sham or IRI inducing surgery was performed on adult and aged female mice. Mice were culled following 120 minutes of reperfusion and hearts were harvested and snap frozen. The LV was transversely sectioned using a cryostat into 10μm sections and then immunostained with an antibody against IL-36β (AF488). Additional antibodies were also used to determine whether the staining was vascular in nature (CD31) and co-localised with adhesion molecules (VCAM-1). Sections were imaged using a EVOS microscope. **(A)** Representative images of IL-36β (green), CD31 (red), and VCAM-1 (blue) staining of frozen heart sections. Scale bar indicates 200μm. **(B)** Quantitative analysis of the immunofluorescent images of IL-36β expression. Statistical analysis was performed using a one-way ANOVA, followed by a Tukey's post-hoc test between the following groups: adult sham versus adult IR injury, adult sham versus aged sham, aged sham versus aged IR injury, and adult IR injury versus aged IR injury. n=4/group. **(C-D)** Murine vena cava endothelial cells (VCECs) were cultured and stimulated for 4 hours with experimental media (control), an IL-36 cytokine (α, β or γ) or TNFα. Cells were stained with an antibody against IL-36β (AF488) and imaged using a multiphoton microscope. **(A)** Representative images of IL-36β (red) expression on stimulated non-permeabilised cells (Hoechst 33342 stained nuclei in blue). Scale bar indicates 200μm. **(B)** Quantitative analysis of IL-36β expression on VCECs following stimulation. Statistical analysis was performed using a one-way ANOVA, followed by a Tukey's post-hoc test: control versus 3ng/ml, control versus 30ng/ml, control versus 300ng/ml, 3ng/ml versus 30ng/ml, 3ng/ml versus 300ng/ml, and 30ng/ml versus 300ng/ml for each of the IL-36 cytokine (α, β or γ) and TNFα as well as 300ng/ml between the various cytokines. n=3/group. Abbreviations - IRI: ischaemia reperfusion injury. Mean ±SEM. \*p<0.05, \*\*p<0.01, \*\*\*\*p<0.0001.

**A**



**B**

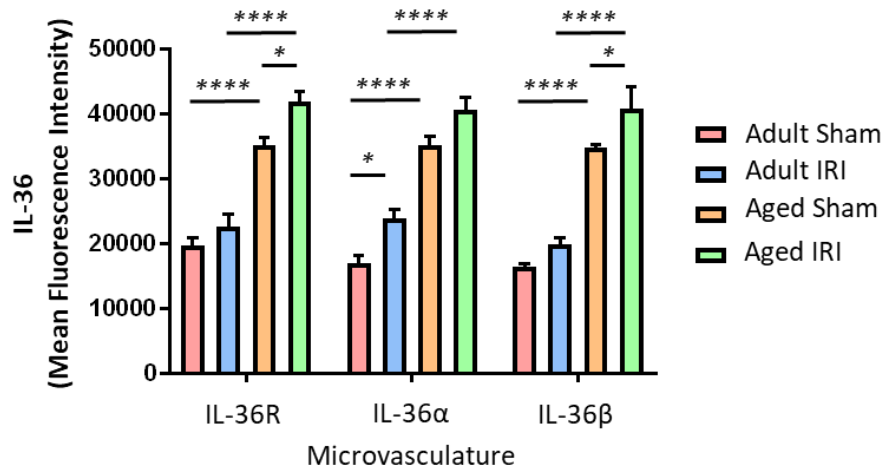


**Figure 4.9. Changes in the expression of IL-36 cytokines and its receptor occurs on the coronary microvasculature and not on the large blood vessels.** Sham or IRI surgery was performed on adult and aged female mice. Mice were culled following 120-minutes of reperfusion and hearts were harvested and snap frozen. The LV was transversely sectioned using a cryostat into 10μm sections and then immunostained with an antibody against IL-36R, IL-36α, or IL-36β (AF488). Sections were imaged using a EVOS microscope, and analysis of the macrovasculature versus microvasculature was performed. Quantitative analysis of IL-36R, IL-36α, and IL-36β expression is shown for the **(A)** macrovasculature and **(B)** microvasculature of the adult and aged, sham and IR injured heart. Statistical analysis was performed using a one-way ANOVA, followed by a Tukey's post-hoc test: adult sham versus adult IR injury, adult sham versus aged sham, aged sham versus aged IR injury, and adult IR injury versus aged IR injury for each of the IL-36 (R, α or β). n=4/group. Abbreviations - IRI: ischaemia reperfusion injury. Mean ±SEM. \*p<0.05, \*\*\*\*p<0.0001.

#### 4.2.6. Age Increase Expression of IL-36R/ $\alpha$ / $\beta$ / $\gamma$ in Human Ventricular Samples.

All of the above studies were conducted on mouse tissue and cells. However, for the IL-36/IL-36R pathway to be considered a potential therapeutic target, its presence in human tissue needs to be considered. Therefore, the impact of age on IL-36R/IL-36 $\alpha$ / $\beta$ / $\gamma$  expression was also investigated in samples of human heart from both young and adult / elderly patients (see **Table 2.5** for patient demographics). IL-36R/ $\alpha$ / $\beta$ / $\gamma$  was found expressed in newborn, infant/toddler, child, and older adult hearts as evidenced by a positive stain on frozen tissue sections (**Figures 4.10a-4.13a**) which was not seen in the IgG controls (**Figure 2.4c**). Expression of IL-36R and IL-36 $\alpha$ / $\beta$ / $\gamma$  significantly increased in stepwise pattern with age, with the highest expression noted in older adults (**Figures 4.10b-4.13b**). Staining for IL-36R on frozen heart sections clearly demonstrated that this receptor co-localised with vessels in the coronary vasculature regardless of age. Moreover, IL-36R was also detected within CMs and co-localised with oxidative damage, particularly in the older groups (**Figure 4.10a**).

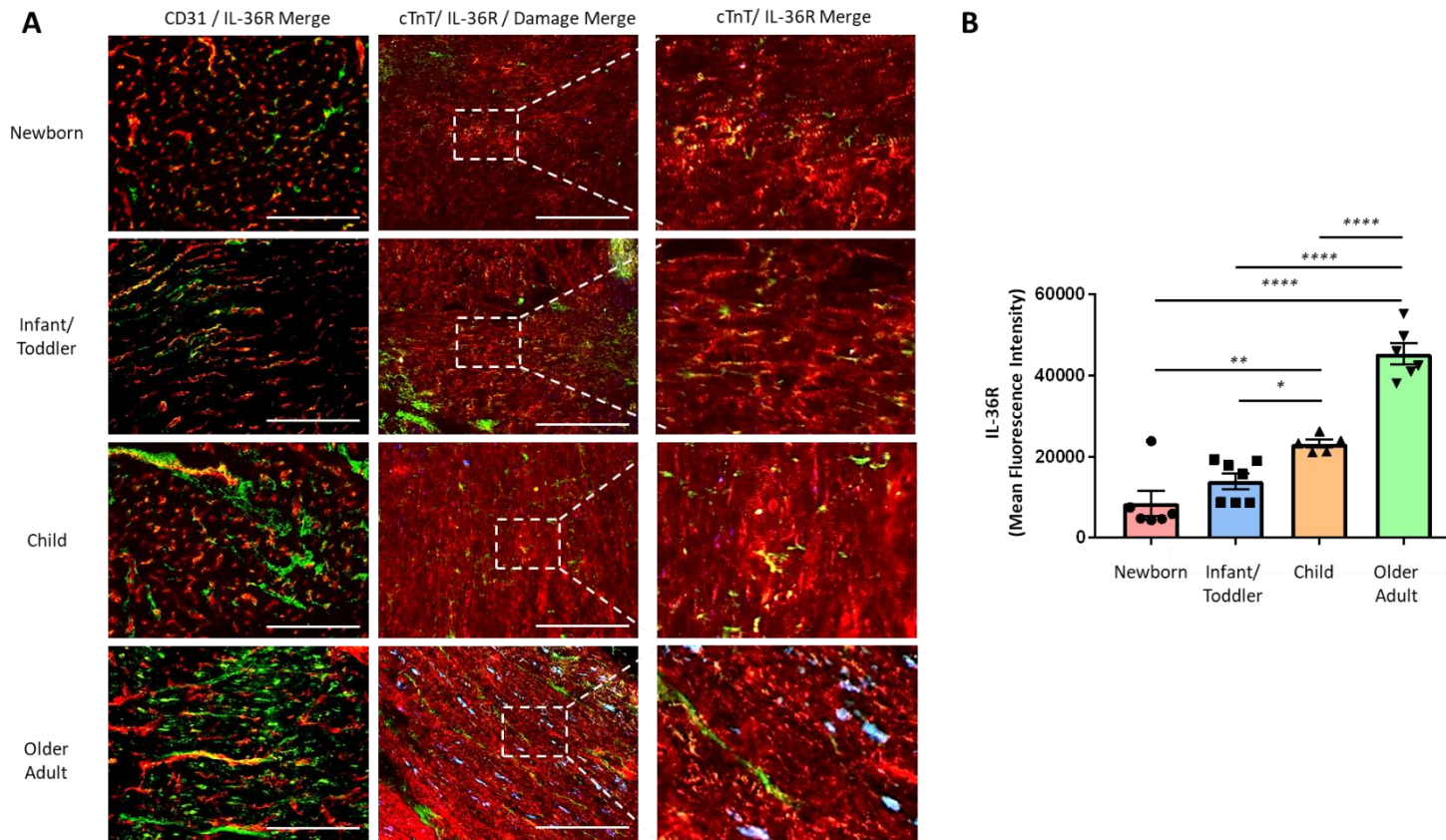


**Figure 4.10. Age increases expression of IL-36R in human tissue.** Clinical samples were harvested and snap frozen from young and old patients following surgery. The ventricular sample was sectioned using a cryostat into 10 $\mu$ m sections and then immunostained with an antibody against IL-36R (AF488). Additional antibodies were also used; first column: anti-CD31 antibody, second, and third column: anti-cTnT antibody and anti-DNA/RNA damage. Sections were imaged using a EVOS microscope. **(A)** Representative images of IL-36R (green), CD31 (red: first column), cTnT (red: second and third column), and DNA/RNA damage (blue: second and third column) staining on frozen heart sections. Scale bar indicates 200 $\mu$ m. **(B)** Quantitative analysis of the immunofluorescent images of IL-36R expression. Statistical analysis was performed using a one-way ANOVA, followed by a Tukey's post-hoc test between the following groups: newborn versus infant/toddler, newborn versus child, newborn versus older adult, infant/toddler versus child, infant/toddler versus older adult, and child versus older adult.  $n \leq 5$ /group. Mean  $\pm$  SEM. \* $p < 0.05$ ,  $p < 0.01$ , \*\*\* $p < 0.001$ , \*\*\*\* $p < 0.0001$ .

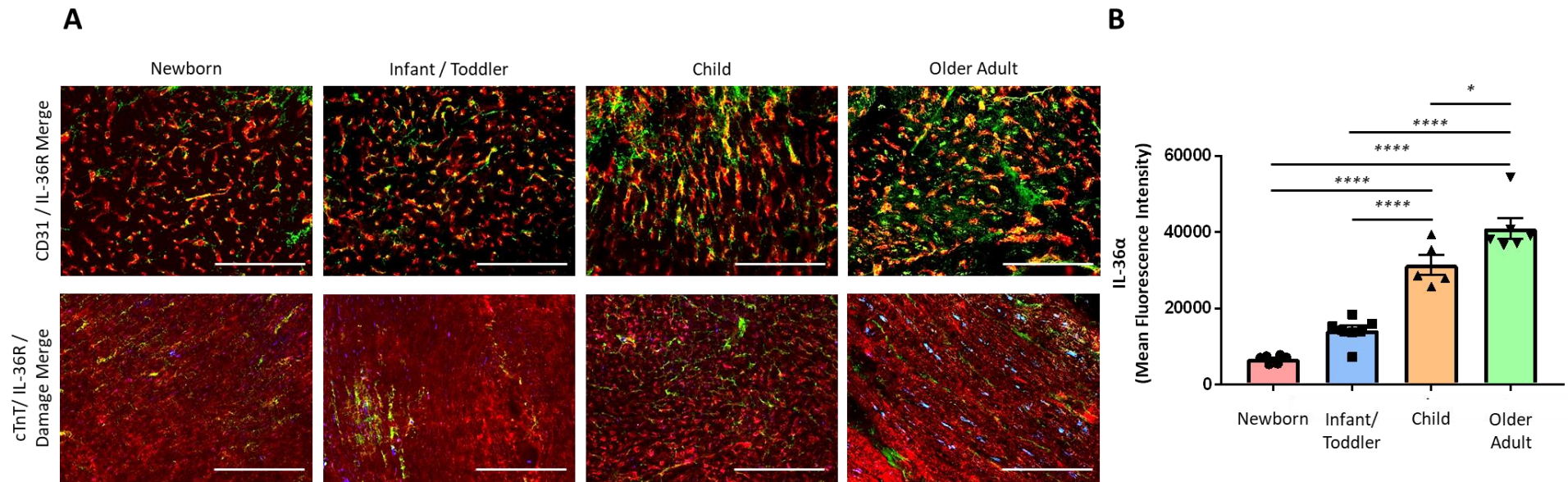


**Figure 4.11. Age increases expression of IL-36 $\alpha$  in human tissue.** Clinical samples were harvested and snap frozen from young and old patients following surgery. The ventricular sample was sectioned using a cryostat into 10 $\mu$ m sections and then immunostained with an antibody against IL-36 $\alpha$  (AF488). Additional antibodies were also used; first row: anti-CD31 antibody, second row: anti-cTnT antibody and anti-DNA/RNA damage. Sections were imaged using a EVOS microscope. **(A)** Representative images of IL-36 $\alpha$  (green), CD31 (red: first row), cTnT (red: second and third row), and DNA/RNA damage (blue: second and third row) staining on frozen heart sections. Scale bar indicates 200 $\mu$ m. **(B)** Quantitative analysis of the immunofluorescent images of IL-36 $\alpha$  expression. Statistical analysis was performed using a one-way ANOVA, followed by a Tukey's post-hoc test between the following groups: newborn versus infant/toddler, newborn versus child, newborn versus older adult, infant/toddler versus child, infant/toddler versus older adult, and child versus older adult.  $n \leq 5$ /group. Mean  $\pm$  SEM. \* $p < 0.05$ , \*\*\*\* $p < 0.0001$ .

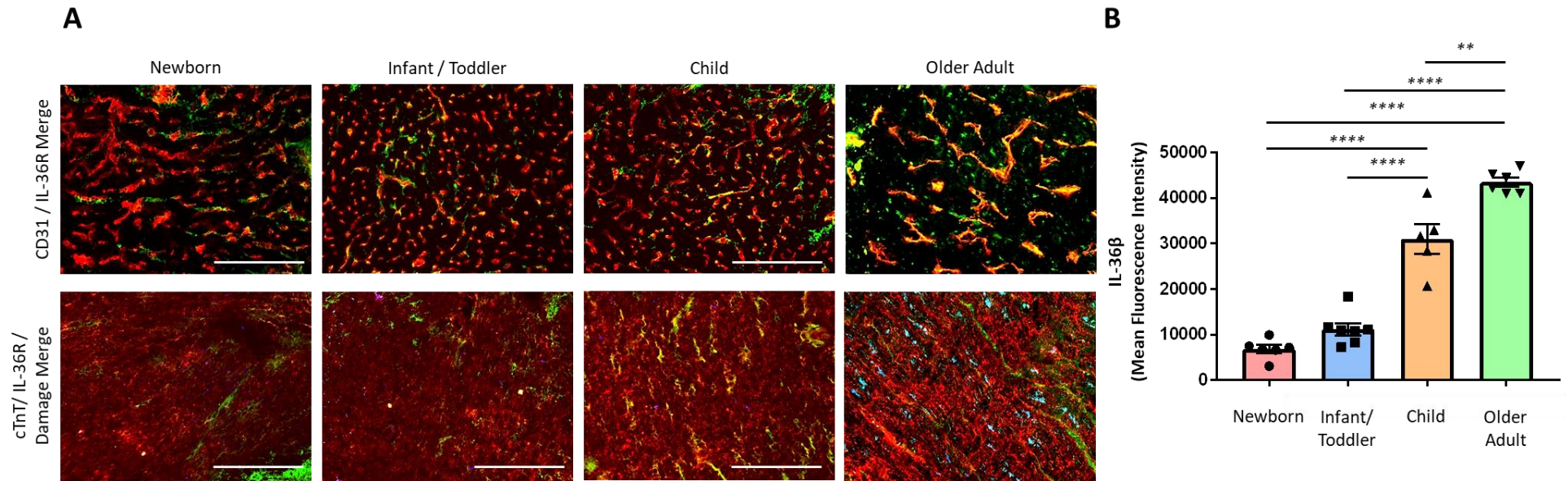


**Figure 4.12. Age increases expression of IL-36 $\beta$  in human tissue.** Clinical samples were harvested and snap frozen from young and old patients following surgery. The ventricular sample was sectioned using a cryostat into 10 $\mu$ m sections and then immunostained with an antibody against IL-36 $\beta$  (AF488). Additional antibodies were also used; first row: anti-CD31 antibody, second row: anti-cTnT antibody and anti-DNA/RNA damage. Sections were imaged using a EVOS microscope. **(A)** Representative images of IL-36 $\beta$  (green), CD31 (red: first row), cTnT (red: second and third row), and DNA/RNA damage (blue: second and third row) staining on frozen heart sections. Scale bar indicates 200 $\mu$ m. **(B)** Quantitative analysis of the immunofluorescent images of IL-36 $\beta$  expression. Statistical analysis was performed using a one-way ANOVA, followed by a Tukey's post-hoc test between the following groups: newborn versus infant/toddler, newborn versus child, newborn versus older adult, infant/toddler versus child, infant/toddler versus older adult, and child versus older adult.  $n \leq 5$ /group. Mean  $\pm$  SEM. \* $p < 0.01$ , \*\*\*\* $p < 0.0001$ .

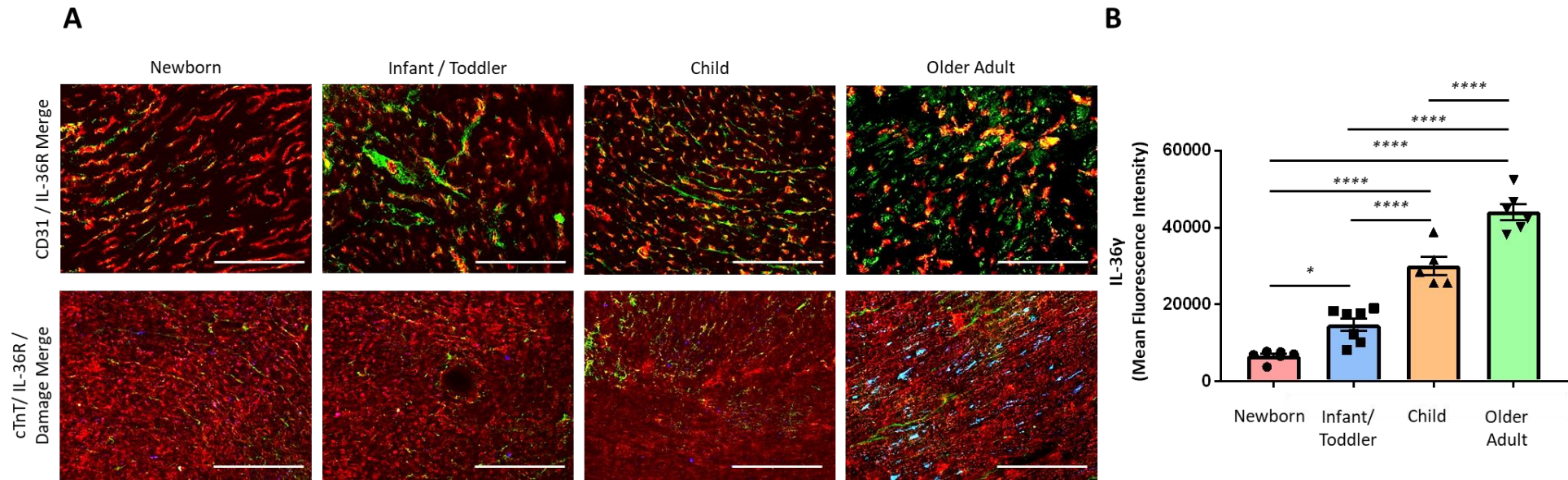


**Figure 4.13. Age increases expression of IL-36 $\gamma$  in human tissue.** Clinical samples were harvested and snap frozen from young and old patients following surgery. The ventricular sample was sectioned using a cryostat into 10 $\mu$ m sections and then immunostained with an antibody against IL-36 $\gamma$  (AF488). Additional antibodies were also used; first row: anti-CD31 antibody, second row: anti-cTnT antibody and anti-DNA/RNA damage. Sections were imaged using a EVOS microscope. **(A)** Representative images of IL-36 $\gamma$  (green), CD31 (red: first row), cTnT (red: second and third row), and DNA/RNA damage (blue: second and third row) staining on frozen heart sections. Scale bar indicates 200 $\mu$ m. **(B)** Quantitative analysis of the immunofluorescent images of IL-36 $\gamma$  expression. Statistical analysis was performed using a one-way ANOVA, followed by a Tukey's post-hoc test between the following groups: newborn versus infant/toddler, newborn versus child, newborn versus older adult, infant/toddler versus child, infant/toddler versus older adult, and child versus older adult.  $n \leq 5$ /group. Mean  $\pm$ SEM. \* $p < 0.05$ , \*\*\*\* $p < 0.0001$ .

#### 4.2.7. IL-36 Cytokine Application Induces an Inflammatory Response *in vivo*

##### 4.2.7.1. Topical Application of IL-36 Cytokines Increases Neutrophil Presence on the Surface of the Healthy Myocardium

We next sought to determine whether the IL-36R expressed in the heart was functional *in vivo*. IVM was used to directly visualise the ability of topical IL-36 to elicit an inflammatory response within the healthy adult and aged beating heart. This was initially investigated intravitaly following the topical application of a single dose of IL-36 $\gamma$  (200ng/ml) on the healthy, uninjured adult and aged heart. Neutrophil recruitment was enhanced at all time points in the adult heart when compared to topical application of the vehicle control. The increase in neutrophil adhesion was rapid, within 15 minutes of exposure, but plateaued thereafter (**Figures 4.14a-c**). Both the number of free-flowing neutrophils and platelet aggregation / microthrombi formation decreased in the adult heart in response to a single IL-36 $\gamma$  application (**Figures 4.14d-g**). Interestingly, in aged hearts exposed to a single application of topical IL-36 $\gamma$  (200ng/ml), neutrophil recruitment remained relatively unchanged when compared to a vehicle control (**Figures 4.15a-c**). However, the number of free-flowing neutrophils and platelet aggregation and microthrombi formation were again decreased (**Figures 4.15d-g**).

During IR injury, inflammatory cytokine release is likely to be relatively continual, and so a single application of IL-36 is not truly representative of the pathophysiological environment. Therefore, the above experiments were repeated in separate adult and aged mice, but this time IL-36 was topically applied and refreshed every 15 minutes throughout the 150 of minutes of imaging. These experiments were performed with 200ng/ml of either IL-36 $\alpha$ , IL-

36 $\beta$  or IL-36 $\gamma$ . In healthy adult hearts, all three IL-36 agonists were able to significantly increase neutrophil recruitment at all time points imaged and to a similar degree, although IL-36 $\gamma$  was slightly more potent. This pro-inflammatory response was rapid and increased gradually with time until a plateau was reached at approximately 60 minutes of topical exposure (**Figures 4.16a-b and 14.18a**). Interestingly, in addition to neutrophil adhesion within coronary capillaries, the involvement of more medium-sized blood vessels was also observed. In the absence of a specific tag to label the vasculature, these medium sized vessels were not usually visible. However, they were clearly identified when they became delineated with adherent neutrophils (**Figure 4.16a**). The number of free-flowing neutrophils significantly decreased in response to all three IL-36 cytokine treatments in adult hearts (**Figures 4.16c and 14.18b**). Platelet aggregates were occasionally observed in some of the medium-sized vessels and significantly increased, particularly in response to IL-36 $\beta$  and IL-36 $\gamma$ , in adult hearts. These were mostly present in vessels where extensive clusters of adherent neutrophils were observed (**Figures 4.16a, d and 4.18c**).

A similar response was also observed when cytokines were repeatedly topically applied to the aged beating heart. However, the speed of neutrophil recruitment was slower than that seen in adult mice. In addition, in aged hearts exposed to IL-36 $\alpha$  and IL-36 $\beta$ , neutrophil recruitment continued to rise rather than reaching a plateau at the end of imaging period. Although increases in neutrophil adhesion in response to all three IL-36 cytokines were significant in aged hearts when compared to vehicle controls, the extent of recruitment was slightly less than those noted in adult mice (**Figures 4.17a-b and 4.18a**). The number of free-flowing neutrophils generally significantly decreased in response to all three IL-36 cytokine treatments in aged hearts (**Figure 4.17c and 4.18b**). In aged hearts, the frequency of platelet

aggregates/accumulation was significantly decreased after IL-36 $\beta$  and IL-36 $\gamma$  application (**Figures 4.17d and 4.18c**).

We next compared the neutrophil dynamics between a single topical application of IL-36 $\gamma$  with the multiple/continuous topical application of IL-36 $\gamma$ . In adult hearts, neutrophil recruitment was enhanced at all time points following a continuous topical application of IL-36 $\gamma$  when compared to the single dose (**Figures 4.19a-b**). There was no difference in the number of free-flowing neutrophils between single and multiple application (**Figures 4.19c-d**), although platelet aggregation and microthrombi formation was enhanced in response to continuous topical application of IL-36 $\gamma$  when compared to the single dose (**Figures 4.19e-f**).

In aged hearts, neutrophil recruitment was again enhanced at most of the time points imaged in response to continuous topical application of IL-36 $\gamma$  when compared with the single-dose in aged hearts (**Figures 4.20a-b**). There were no significant differences in the number of free-flowing neutrophils (**Figures 4.20c-d**) or platelet aggregation and microthrombi formation (**Figure 4.20e-4.20f**) in response to continuous topical application of IL-36 $\gamma$  when compared to the single dose.

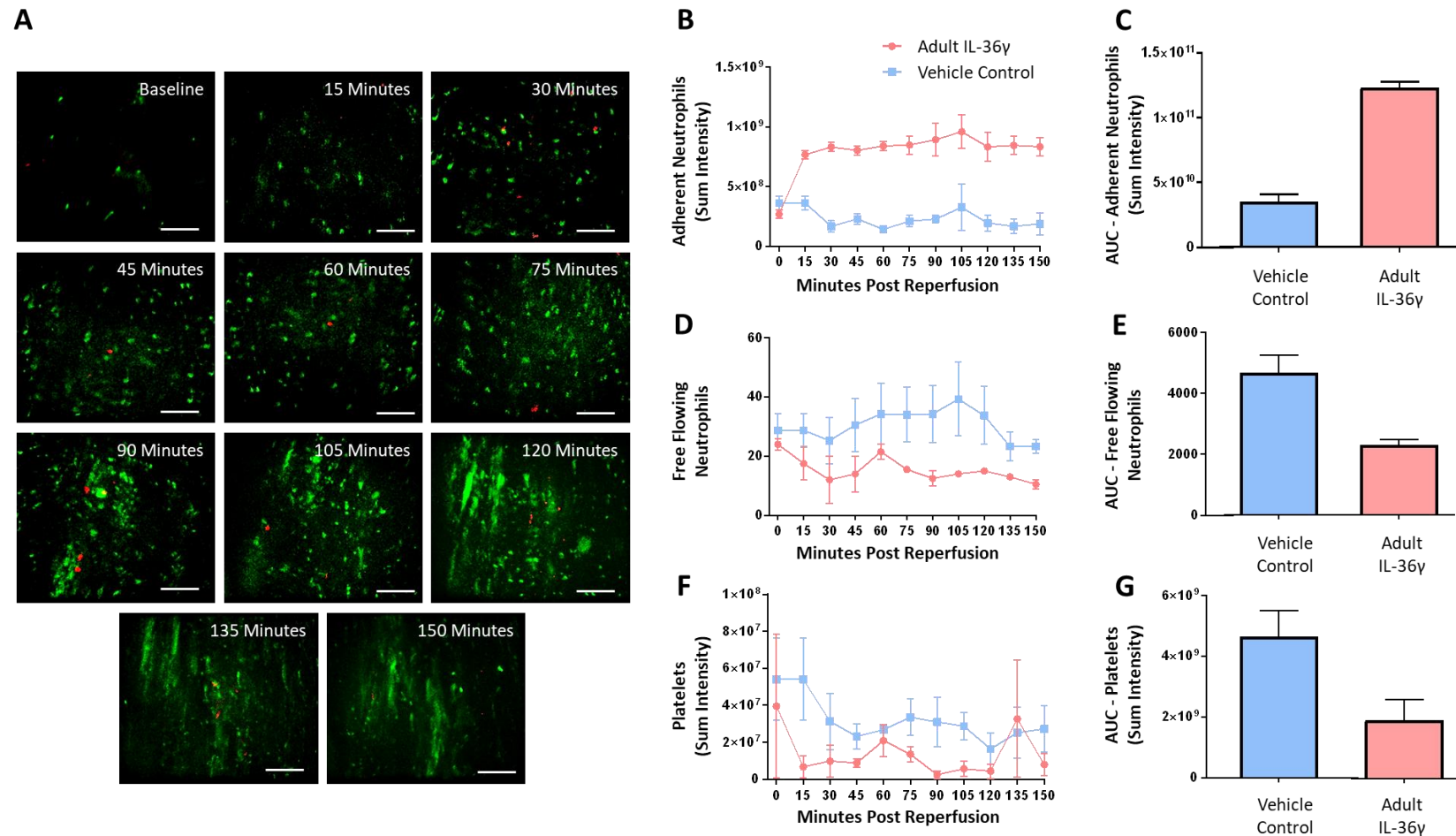


**Figure 4.14. Topically applied single dose of IL-36 $\gamma$  is pro-inflammatory in the adult beating heart *in vivo*.** A single dose of IL-36 $\gamma$  (200ng/ml) or PBS was topically applied to the healthy adult beating heart LV following opening of the chest. **(A)** Representative intravital images of the beating heart showing adherent neutrophils (green) and platelets (red) in the coronary microcirculation over a time course of 150 minutes post-application. Scale bar indicates 100 $\mu$ m. Quantitative time-course analysis of intravital data for **(B)** adherent neutrophils, **(D)** free-flowing neutrophils, and **(F)** platelets. Area under the curve (AUC) analysis for **(C)** adherent neutrophils, **(E)** free-flowing neutrophils, and **(G)** platelets, over a time course of 150 minutes post-application. Abbreviations - PBS: phosphate-buffered saline.  $n \leq 2$ /group. Mean  $\pm$ SEM.

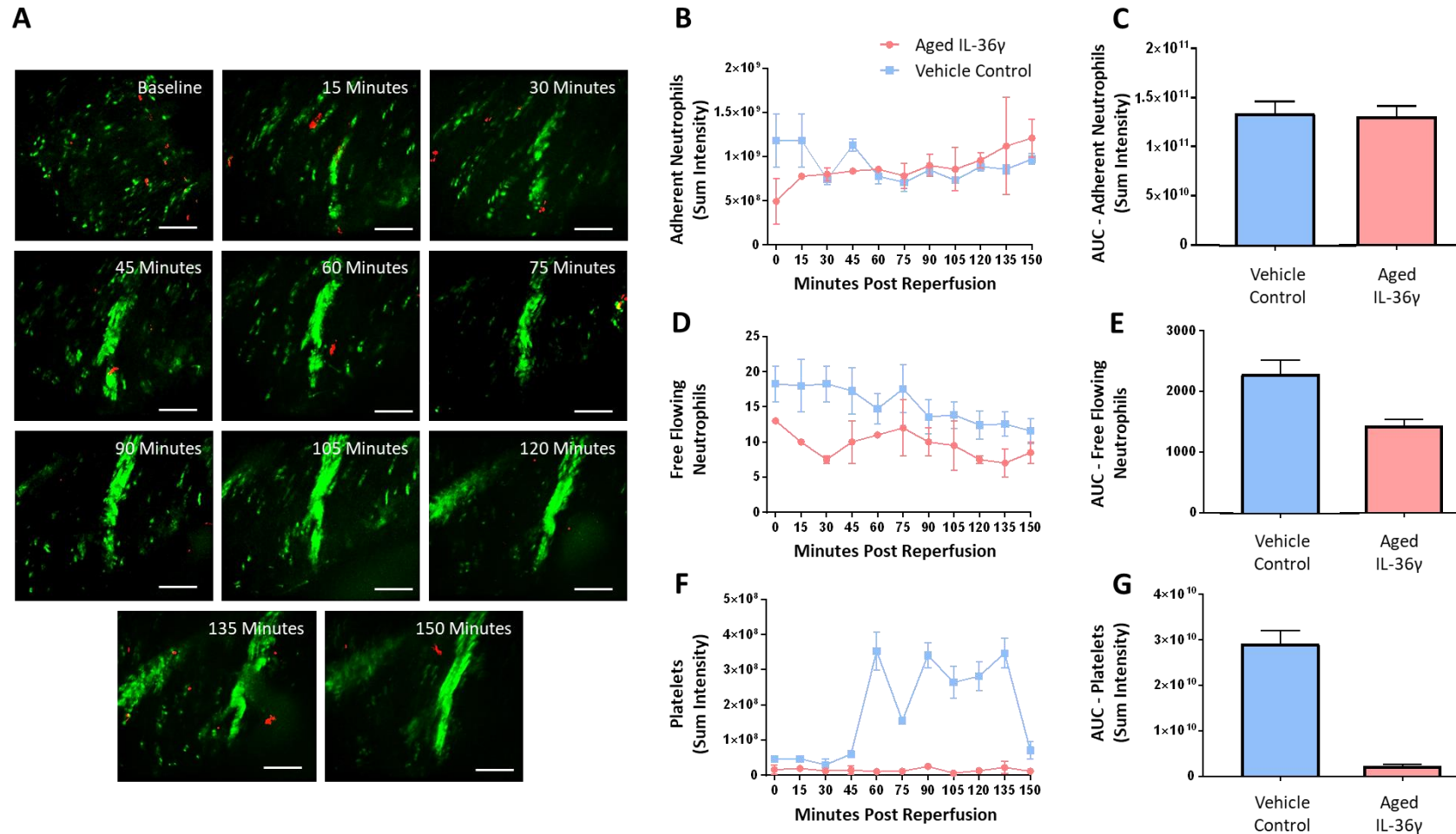


**Figure 4.15. Topically applied single dose of IL-36γ is pro-inflammatory in the aged beating heart *in vivo*.** A single dose of IL-36γ (200ng/ml) or PBS was topically applied to the healthy aged beating heart LV following the opening of the chest. **(A)** Representative intravital images of the beating heart showing adherent neutrophils (green) and platelets (red) in the coronary microcirculation over a time course of 150 minutes post-application. Scale bar indicates 100µm. Quantitative time-course analysis of intravital data for **(B)** adherent neutrophils, **(D)** free-flowing neutrophils, and **(F)** platelets. Area under the curve (AUC) analysis for **(C)** adherent neutrophils, **(E)** free-flowing neutrophils, and **(G)** platelets, over a time course of 150 minutes post-application. Abbreviations - PBS: phosphate-buffered saline.  $n \leq 2/\text{group}$ . Mean  $\pm$  SEM.

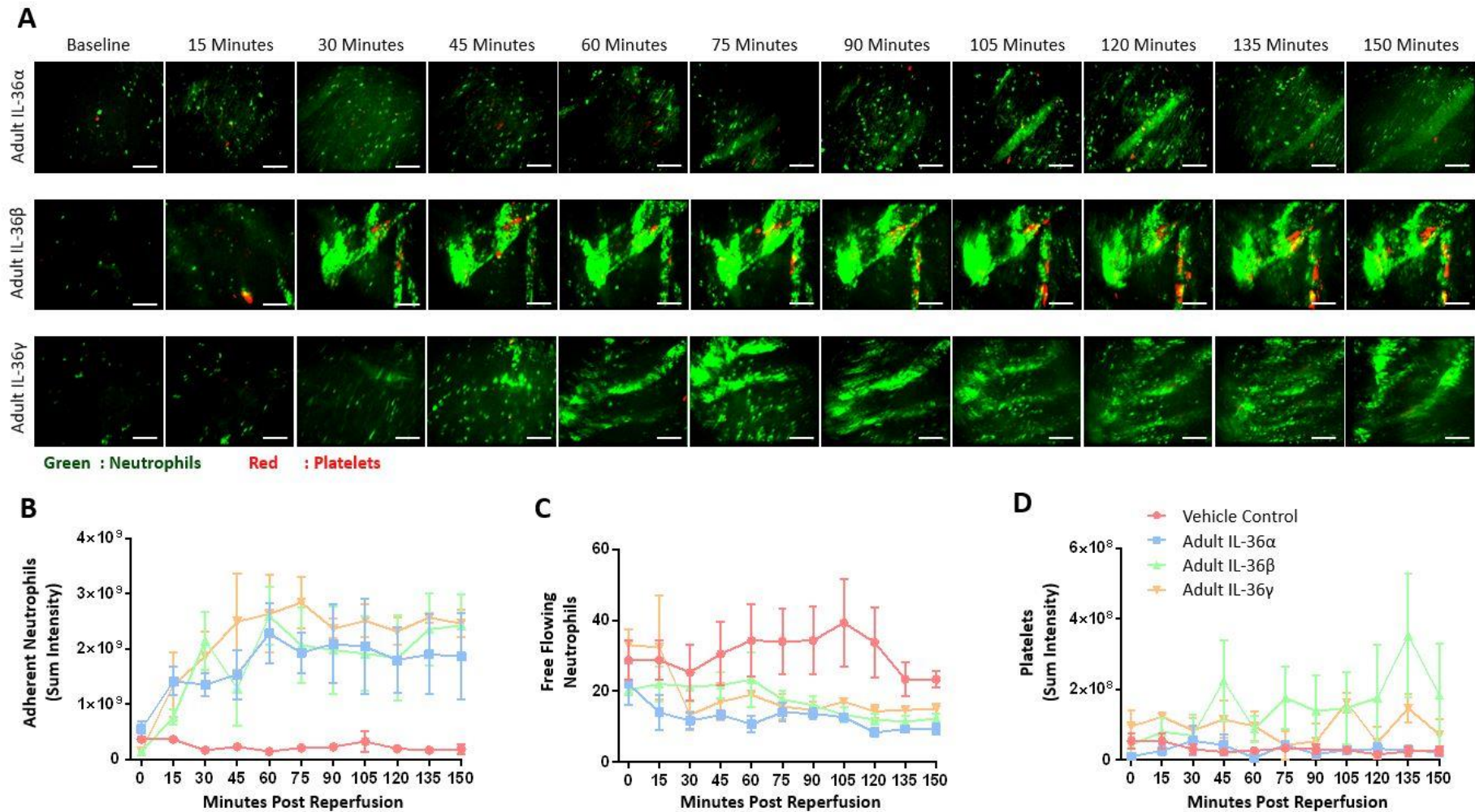


**Figure 4.16. Topically applied IL-36 is pro-inflammatory in the adult beating heart *in vivo*.** IL-36 $\alpha$ , IL-36 $\beta$  or IL-36 $\gamma$  (200ng/ml) or PBS was topically applied every 15 minutes to the healthy adult beating heart LV following opening of the chest. **(A)** Representative intravital images of the beating heart showing adherent neutrophils (green) and platelets (red) in the coronary microcirculation over a time course of 150 minutes post-application in the 3 adult IL-36 groups. Scale bar indicates 100 $\mu$ m. Quantitative time-course analysis of intravital data for **(B)** adherent neutrophils, **(C)** free-flowing neutrophils, and **(D)** platelets. Abbreviations - PBS: phosphate-buffered saline.  $n = 3$ /group. Mean  $\pm$  SEM.

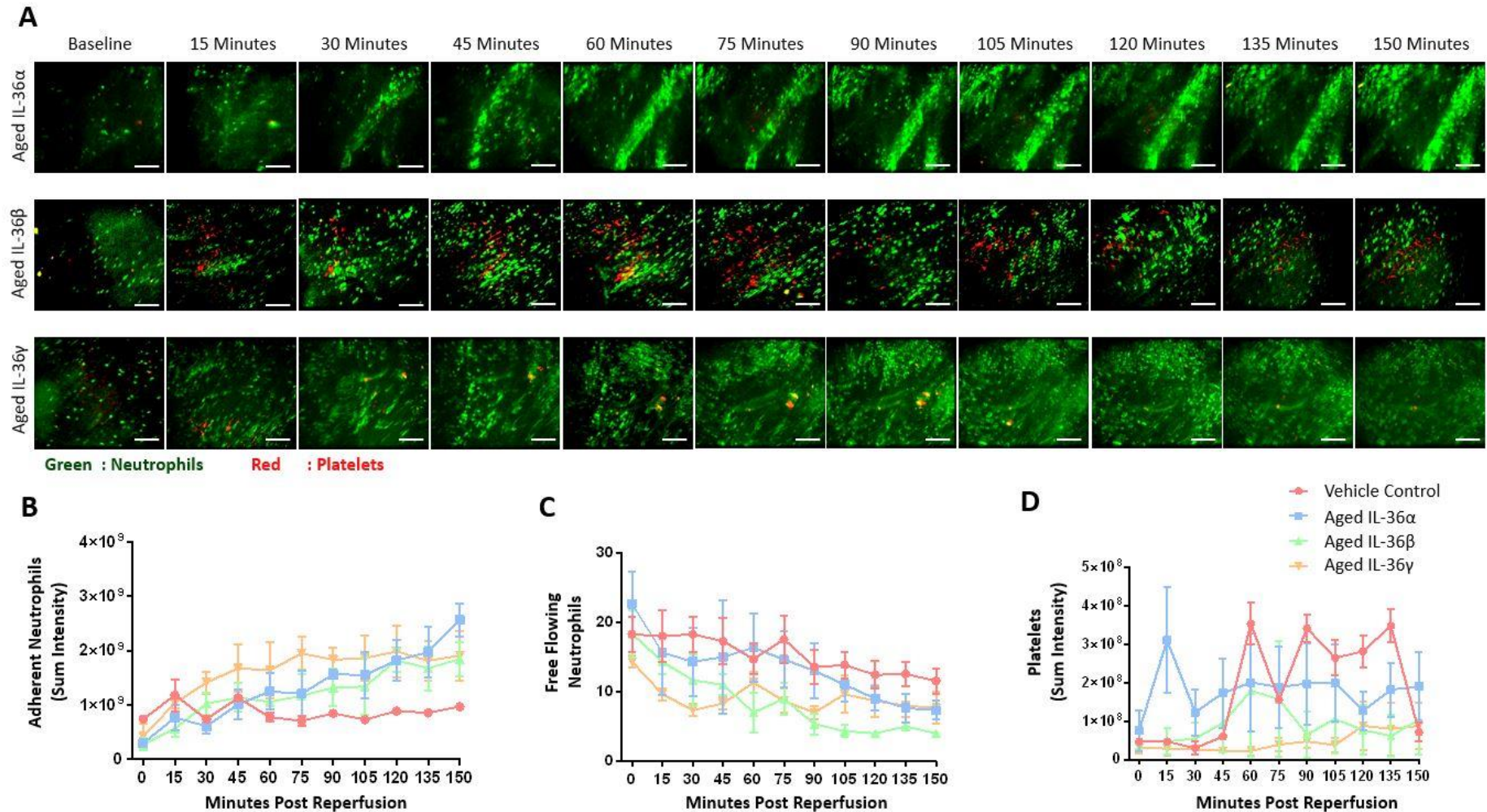


**Figure 4.17. Topically applied IL-36 is pro-inflammatory in the aged beating heart *in vivo*.** IL-36 $\alpha$ , IL-36 $\beta$  or IL-36 $\gamma$  (200ng/ml) or PBS was topically applied every 15 minutes to the healthy aged beating heart LV following opening of the chest. **(A)** Representative intravital images of the beating heart showing adherent neutrophils (green) and platelets (red) in the coronary microcirculation over a time course of 150 minutes post-application in the 3 adult IL-36 groups. Scale bar indicates 100 $\mu$ m. Quantitative time-course analysis of intravital data for **(B)** adherent neutrophils, **(C)** free-flowing neutrophils, and **(D)** platelets. Abbreviations - PBS: phosphate-buffered saline.  $n = 3$ /group. Mean  $\pm$  SEM.

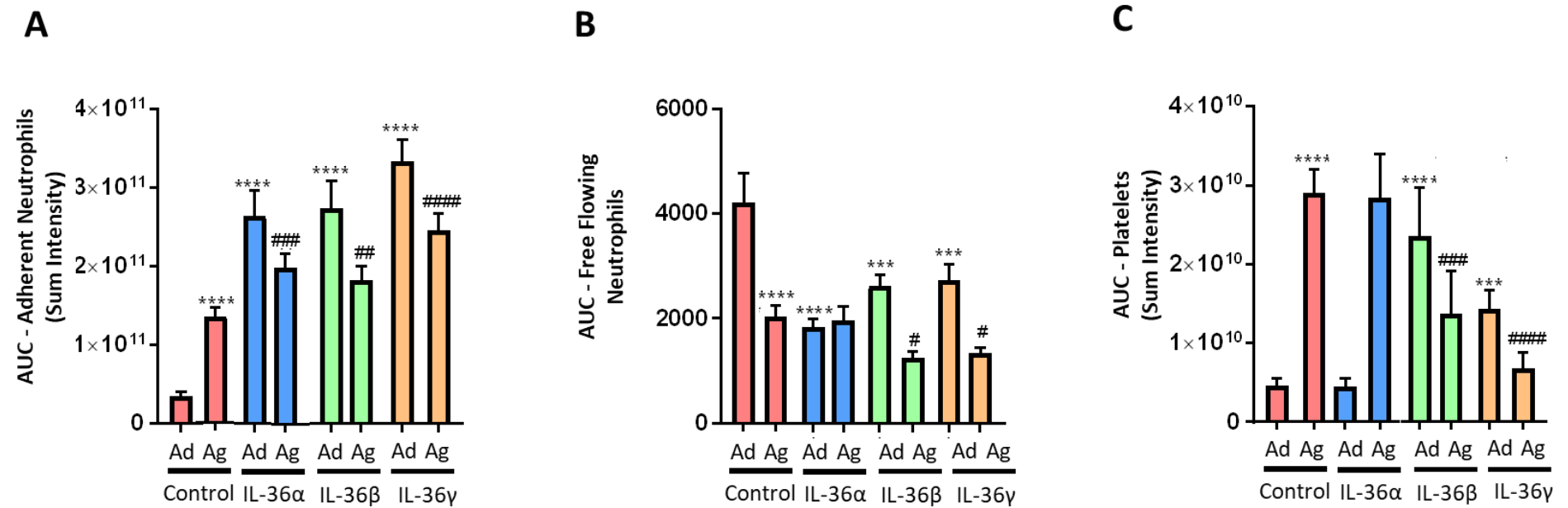


**Figure 4.18. Topically applied IL-36 is pro-inflammatory in the adult and aged beating heart *in vivo*.** IL-36α, IL-36β or IL-36γ (200ng/ml) or PBS was topically applied every 15 minutes to the healthy adult and aged beating heart LV following opening of the chest. Area under the curve (AUC) analysis for **(A)** adherent neutrophils, **(B)** free-flowing neutrophils, and **(C)** platelets, over a time course of 150 minutes post-application. Statistical analysis was performed using a one-way ANOVA, followed by a Tukey's post-hoc test. \* compared to adult control; # compared to aged control. Abbreviations - Ad: Adult; Ag: Aged. *n* = 3/group. Mean ± SEM. \*/+/#p<0.05, \*\*/+/#p<0.01, \*\*\*/+/#p<0.001, \*\*\*\*/+/#p<0.0001 with \*vs adult control, +vs adult treated and #vs aged control.

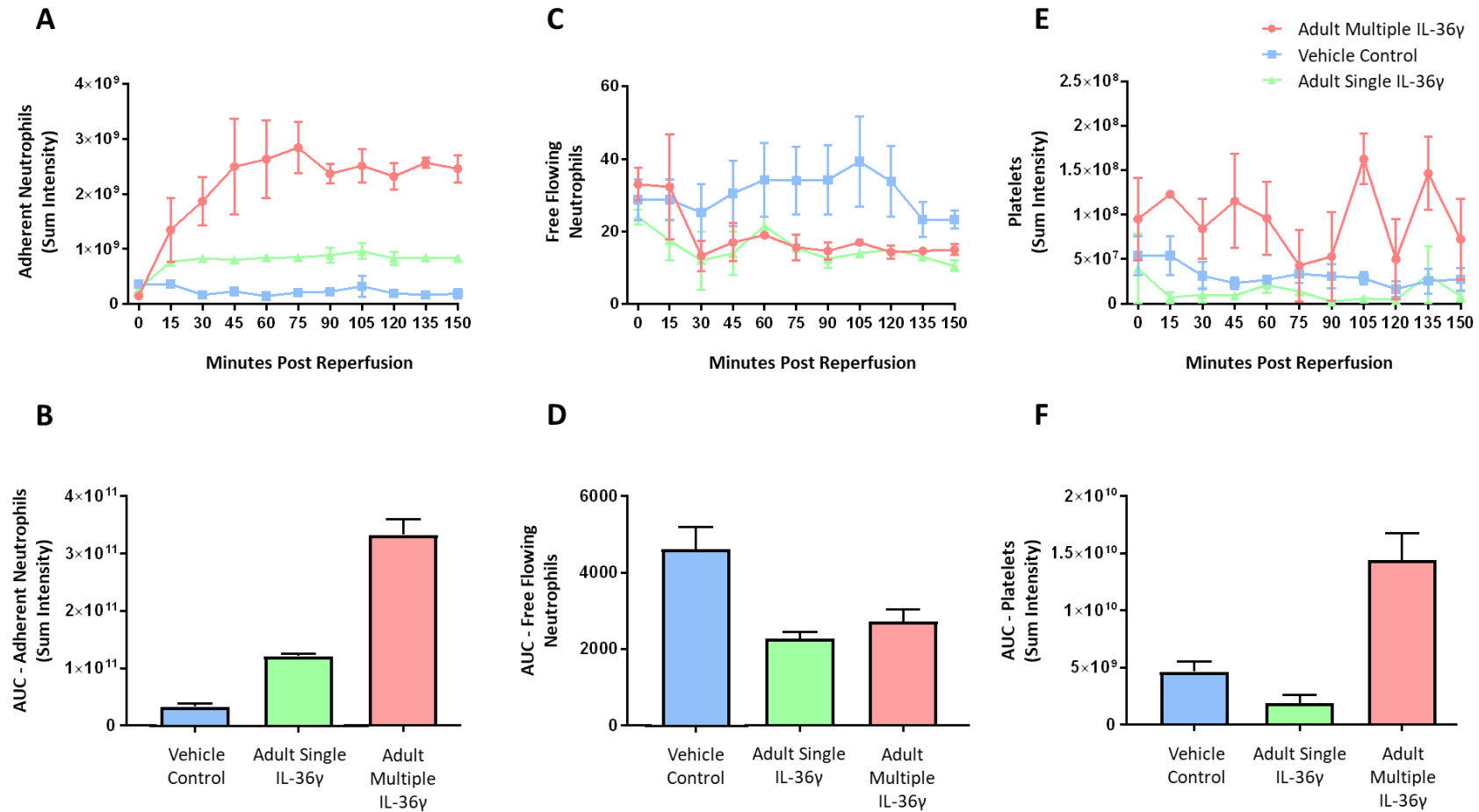


**Figure 4.19. Topical application of a single dose of IL-36γ does not reach maximum pro-inflammatory response in the adult beating heart *in vivo*.** IL-36γ (200ng/ml) was topically applied either as a single dose or every 15 minutes to the healthy adult beating heart LV following opening of the chest. Quantitative time-course analysis of intravital data for **(A)** adherent neutrophils, **(C)** free-flowing neutrophils, and **(E)** platelets. Area under the curve (AUC) analysis for **(B)** adherent neutrophils, **(D)** free-flowing neutrophils, and **(F)** platelets, over a time course of 150 minutes post-application.  $n \leq 2/\text{group}$ . Mean  $\pm$  SEM.

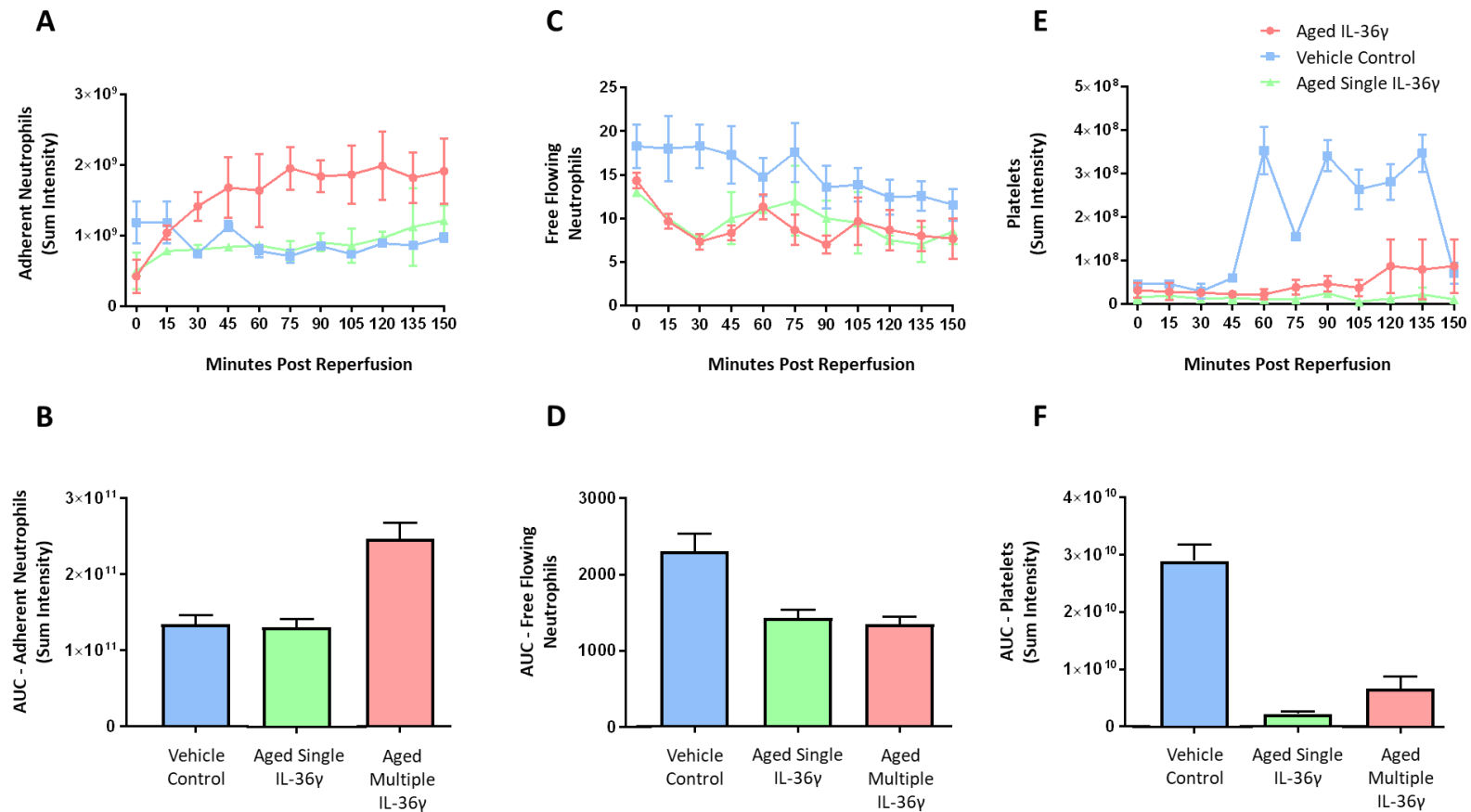


**Figure 4.20. Topical application of a single dose of IL-36γ does not reach maximum pro-inflammatory response in the aged beating heart *in vivo*.** IL-36γ (200ng/ml) was topically applied either as a single dose or every 15 minutes to the healthy aged beating heart LV following opening of the chest. Quantitative time-course analysis of intravital data for **(A)** adherent neutrophils, **(C)** free-flowing neutrophils, and **(E)** platelets. Area under the curve (AUC) analysis for **(B)** adherent neutrophils, **(D)** free-flowing neutrophils, and **(F)** platelets, over a time course of 150 minutes post-application.  $n \leq 2/\text{group}$ . Mean  $\pm$  SEM.

#### 4.2.7.2. Topical Application of IL-36 Cytokines Increases Neutrophil Presence within the Deeper Layers of the Healthy Myocardium

Using *ex vivo* multiphoton imaging of the depth of the ventricular wall, we sought to identify if topical treatment of the murine heart with IL-36 cytokines was able to elicit a pro-inflammatory response throughout the depth of the heart. The heart was vibratome sectioned into four 300 $\mu$ m sections and imaged from the outermost layer (site of topical application) through to the innermost layer closest to the endocardium. Generally, neutrophil presence decreased in both adult and aged mice from the outermost to the innermost layers of the heart. However, neutrophil presence was increased in all four layers of the heart in aged mice in response to all IL-36 isoforms when compared to adult mice (**Figures 4.21 and 4.22a-c**). Indeed, the AUC analysis showed significant increases in response to all IL-36 cytokine treatments in aged hearts when compared with the respective adult hearts (**Figure 4.22d**). Also, topical application of IL-36 $\beta$  and IL-36 $\gamma$  were more potent in aged hearts, while IL-36 $\alpha$  and IL-36 $\gamma$  were more potent in adult hearts (**Figure 4.22d**). In adult mice, this increased neutrophil presence was restricted to the more superficial or outermost 300 $\mu$ m layer of the heart, whereas in aged mice, an increased presence of neutrophils was observed in both the outermost and more deeper layers of the heart (**Figure 4.22e**). This increase was also seen on the surface layer for aged IL-36 $\beta$  and IL-36 $\gamma$ , but not for IL-36 $\alpha$  when compared to their respective adult hearts (**Figure 4.22e**).

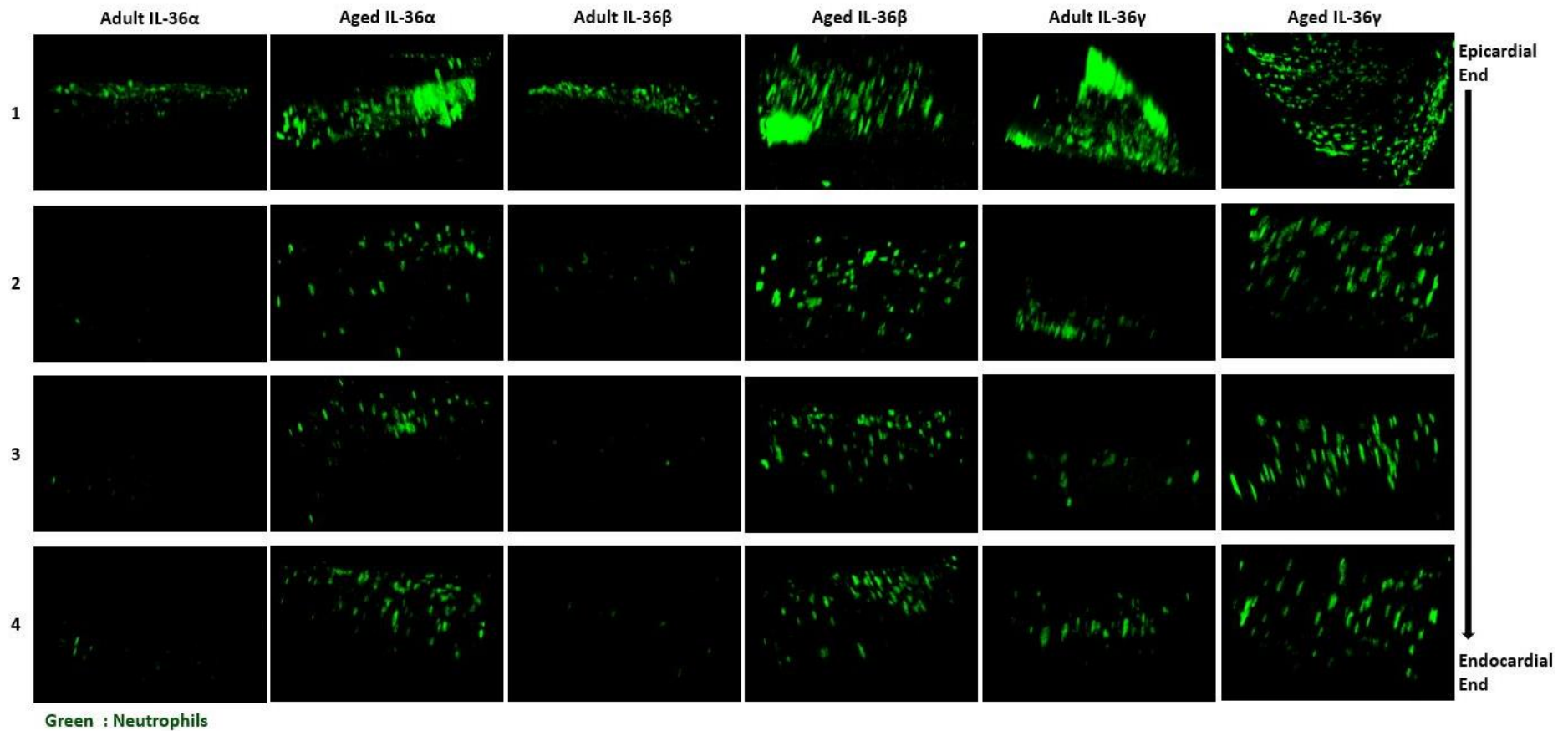


**Figure 4.21. Topical application of IL-36 cytokines increases neutrophil presence within the deeper layers of the healthy myocardium.** IL-36 $\alpha$ , IL-36 $\beta$ , IL-36 $\gamma$  (all 200ng/ml) or PBS was topically applied every 15 minutes to the healthy adult and aged beating heart LV following opening of the chest. Mice were culled following 150 minutes of application and hearts were harvested. The LV was vibratome sectioned into four 300 $\mu$ m sections and imaged using a multiphoton microscope. Representative z-stack multiphoton images of neutrophils (green) in the 4 layers of the LV taken from the outermost layer closest to the epicardium (1), outer myocardial layer (2), inner myocardial layer (3) and the innermost layer closest to the endocardium (4).  $n = 3/\text{group}$ . Mean  $\pm$  SEM.



#### 4.2.7.3. Topical TNF $\alpha$ and not IL-1 $\beta$ Application Induces an Inflammatory Response

Having shown that IL-36 agonists could elicit an inflammatory response in the adult and aged mouse heart, we next sought to determine whether other well established pro-inflammatory cytokines (IL-1 $\beta$  and TNF $\alpha$ ) were able to induce a similar inflammatory response when topically applied to the uninjured heart, and how this compared with IL-36 cytokines. Surprisingly, in response to topical application of IL-1 $\beta$ , neutrophil recruitment, free-flowing neutrophils, and platelet aggregates were not significantly different from the vehicle-treated controls in both adult and aged mice, except for a significant decrease in platelet aggregation and microthrombi formation in the aged IL-1 $\beta$  treated heart (**Figures 4.23a-d, 4.24a-d and 4.25a-c**).

In contrast, TNF $\alpha$  was able to significantly increase neutrophil recruitment at all time points imaged in the adult heart. This pro-inflammatory response was rapid but plateaued after 30 minutes of topical exposure (**Figure 4.23a-b and 4.25a**). A similar response was also observed when it was topically applied to the aged beating heart. However, the speed of the response was not as fast as that seen in adult mice, although in the aged heart, neutrophil recruitment continued to rise (**Figure 4.24a-b and 4.255a**). The number of free-flowing neutrophils was not significantly different from the controls in both adult and aged mice exposed to TNF $\alpha$  (**Figure 4.23c, 4.24c and 4.25b**). Moreover, platelet aggregates were significantly increased in adult exposed TNF $\alpha$  hearts, while a significant reduction was seen in aged hearts (**Figures 4.23d, 4.24d and 4.25c**).

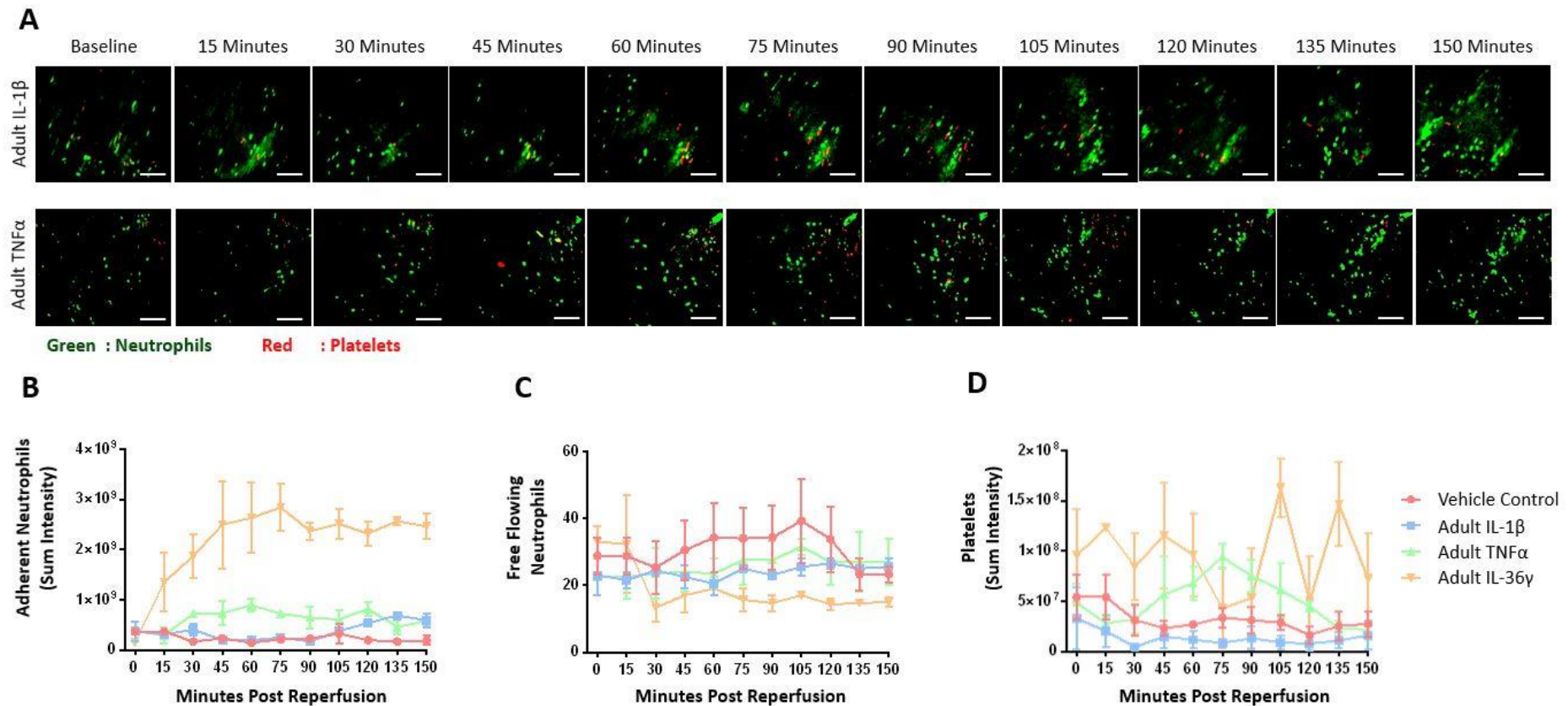


**Figure 4.23. Topically applied TNF $\alpha$  is pro-inflammatory in the adult beating heart *in vivo*.** TNF $\alpha$ , IL-1 $\beta$  or IL-36 $\gamma$  (200ng/ml) or PBS was topically applied every 15 minutes to the healthy adult beating heart LV following opening of the chest. **(A)** Representative intravital images of the beating heart showing adherent neutrophils (green) and platelets (red) in the coronary microcirculation over a time course of 150 minutes post-application. Scale bar indicates 100 $\mu$ m. Quantitative time-course analysis of intravital data for **(B)** adherent neutrophils, **(C)** free-flowing neutrophils, and **(D)** platelets. Abbreviations - PBS: phosphate-buffered saline.  $n = 3$ /group. Mean  $\pm$  SEM.

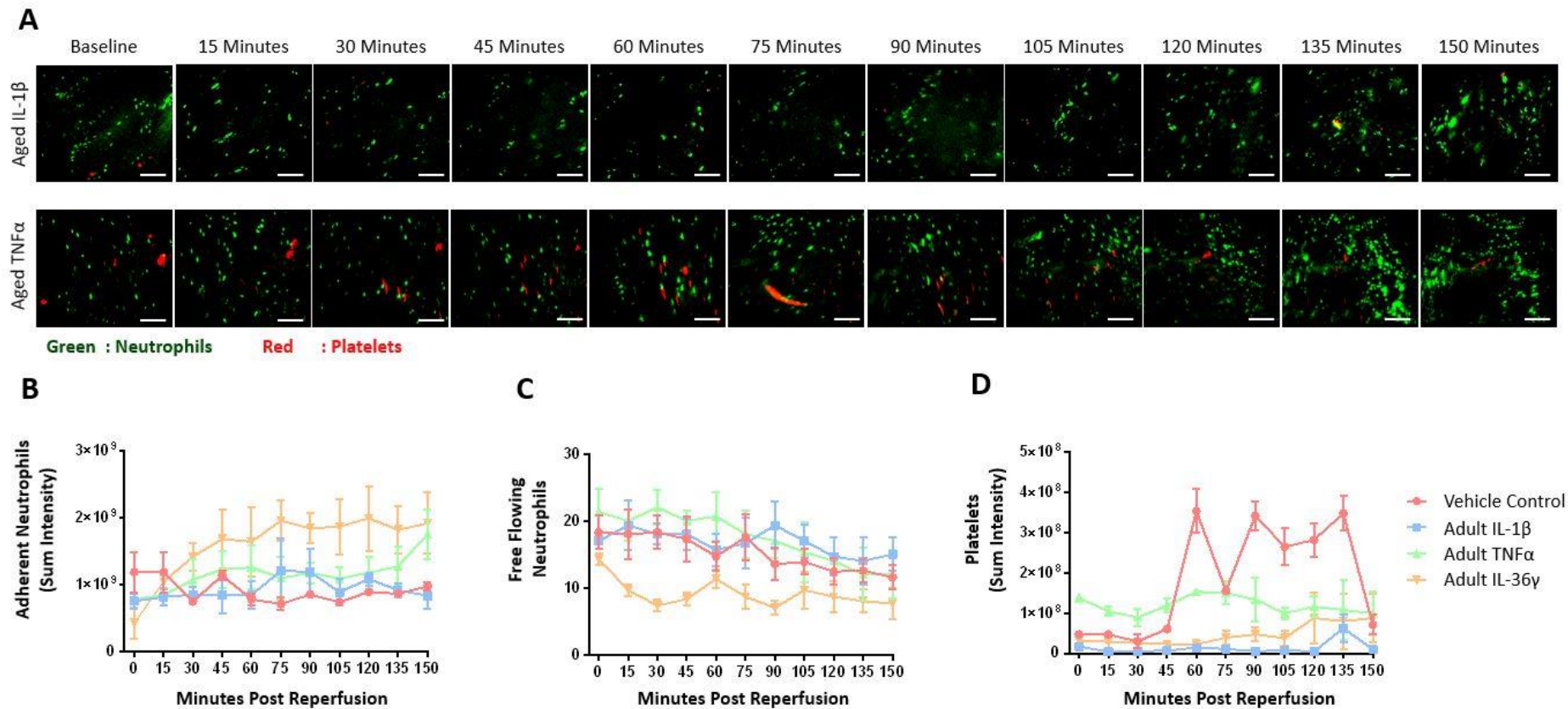


**Figure 4.24. Topically applied TNF $\alpha$  is pro-inflammatory in the aged beating heart *in vivo*.** TNF $\alpha$ , IL-1 $\beta$  or IL-36 $\gamma$  (200ng/ml) or PBS was topically applied every 15 minutes to the healthy aged beating heart LV following opening of the chest. **(A)** Representative intravital images of the beating heart showing adherent neutrophils (green) and platelets (red) in the coronary microcirculation over a time course of 150 minutes post-application. Scale bar indicates 100 $\mu$ m. Quantitative time-course analysis of intravital data for **(B)** adherent neutrophils, **(C)** free-flowing neutrophils, and **(D)** platelets. Abbreviations - PBS: phosphate-buffered saline.  $n = 3$ /group. Mean  $\pm$ SEM.

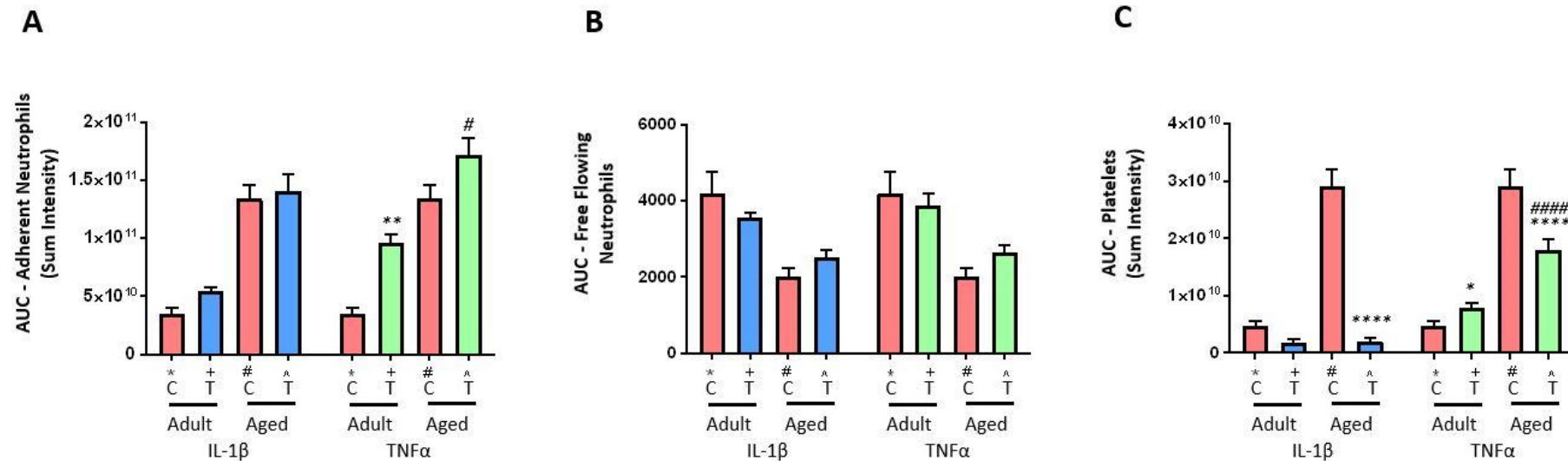


**Figure 4.25. Topically applied TNFα is pro-inflammatory in the adult and aged beating heart *in vivo*.** TNFα, or IL-1β (200ng/ml) or PBS was topically applied every 15 minutes to the healthy adult and aged beating heart LV following opening of the chest. Area under the curve (AUC) analysis for **(A)** adherent neutrophils, **(B)** free-flowing neutrophils, and **(C)** platelets, over a time course of 150 minutes post-application. Statistical analysis was performed using a one-way ANOVA, followed by a Tukey's post-hoc test between the following groups: adult control versus adult treatment, adult control versus aged control, aged control versus aged treatment, and adult treatment versus aged treatment for each of TNFα, and IL-1β. Abbreviations - C: control (PBS); T: treatment; PBS: phosphate-buffered saline. *n* = 3/group. Mean ± SEM. \*/+/#*p*<0.05, \*\*/++/##*p*<0.01, \*\*\*/+++/###*p*<0.001, \*\*\*\*/++++/####*p*<0.0001 with \*vs adult control, +vs adult treated and #vs aged control.

#### 4.2.8. IL-36R Inhibition Reduced Myocardial Inflammation *in vivo* in Adult and Aged IR Injured Hearts

We next sought to investigate whether inhibiting the IL-36R *in vivo* using an IL-36 receptor antagonist (IL-36Ra) could prevent microcirculatory perturbations in the IR injured adult and aged heart. A significant reduction in adherent neutrophils was observed in both adult IR injured and aged IR injured mice who received IL-36Ra when compared with their respective untreated IR injured groups. These reductions did not reach sham levels and remained significantly elevated in both adult IR + IL-36Ra and aged IR + IL-36Ra mice when compared to healthy sham hearts. Although capillary neutrophil presence was mostly inhibited, in some adult and aged mice, neutrophil adhesion could still be observed within the medium-sized coronary vessels, but this was much lower compared to non-treated groups (**Figures 4.26a-b, 4.27a-b and 4.28a**). The number of free-flowing neutrophils significantly increased with IL-36Ra treatment in adult IR injured hearts when compared with untreated IR injured hearts but still remained significantly lower than adult healthy sham mice (**Figures 4.26c and 4.28b**). No change was observed in free-flowing neutrophils in the aged IR + IL-36Ra treated group (**Figures 4.27c and 4.28b**). No significant impact of IL-36Ra treatment on the presence of platelet microthrombi within adult or aged IR injured hearts was observed (**Figures 4.26d, 4.27d and 4.28c**).

The ability of IL-36Ra to modify thromboinflammatory events immediately post-reperfusion in the adult mouse beating heart was also determined. Prior to reperfusion, little, or no neutrophil and platelet microthrombi presence was observed within the coronary microcirculation. However, within the first 30 minutes of reperfusion, neutrophil presence was significantly increased and continued to rise over the remainder of the reperfusion phase

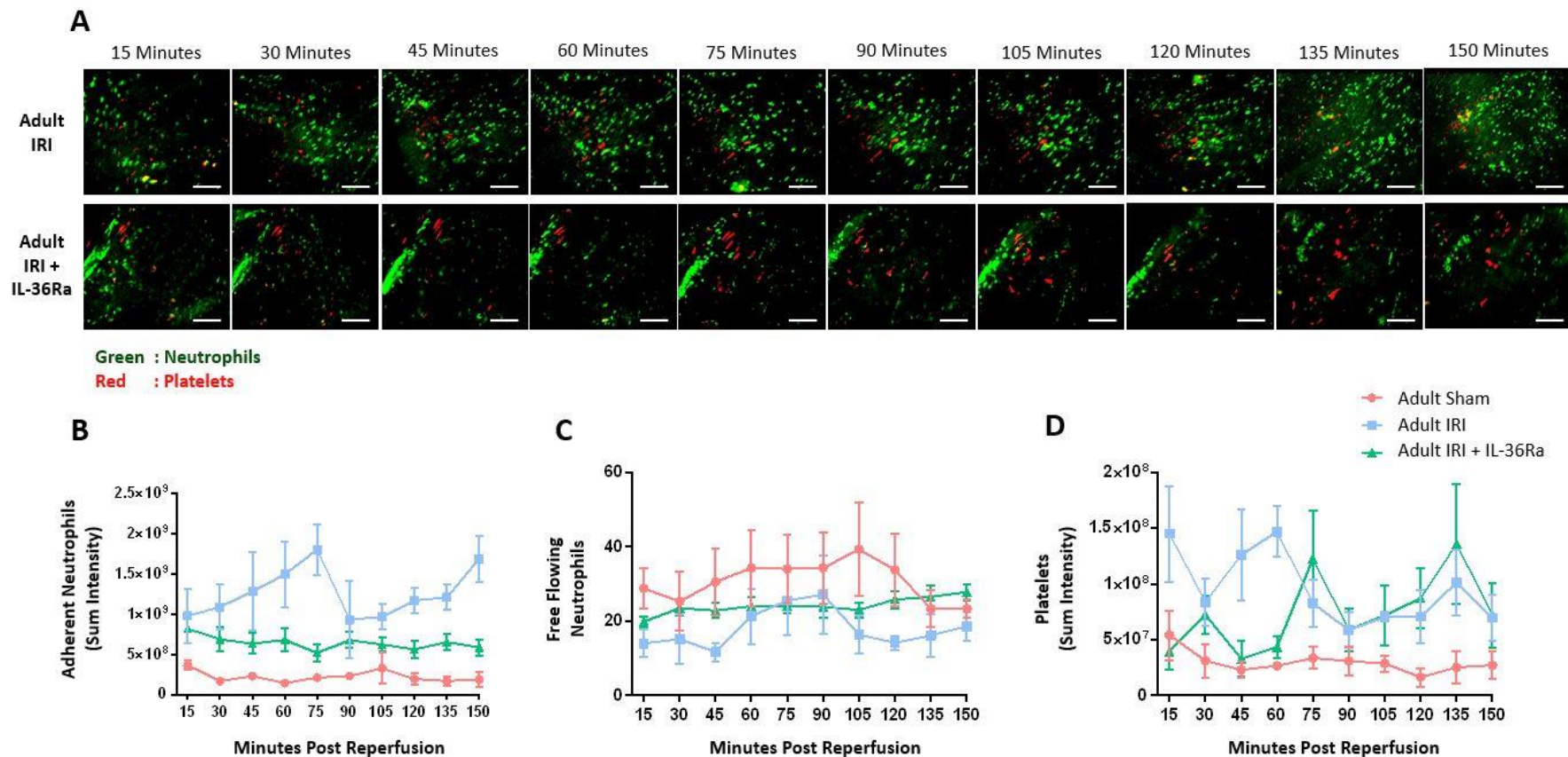
(Figures 4.29, 4.30a-b). Platelet presence increased rapidly upon reperfusion but did not increase further during the rest of the imaging period (Figures 4.29, 4.30c-d).

These data were then compared to the data obtained from adult IR injured untreated mice. During the first 30 minutes of reperfusion, intravital imaging of thromboinflammatory events in the beating heart identified a significant reduction in adherent neutrophils in adult IR mice who received IL-36Ra when compared with the non-treated IR injured group. Over the entire reperfusion period, this reduction was maintained as a significant reduction in adherent neutrophils was observed in adult IR mice who received IL-36Ra when compared with the non-treated IR injured group (Figures 4.31a-c). There was no significant change in platelet microthrombi during the first 30 minutes of reperfusion in adult IR mice who received IL-36Ra when compared with non-treated mice. However, over the entire reperfusion period, a significant increase in platelet microthrombi was observed in adult IR mice who received IL-36Ra when compared with the non-treated IR injured group (Figures 4.31d-f).

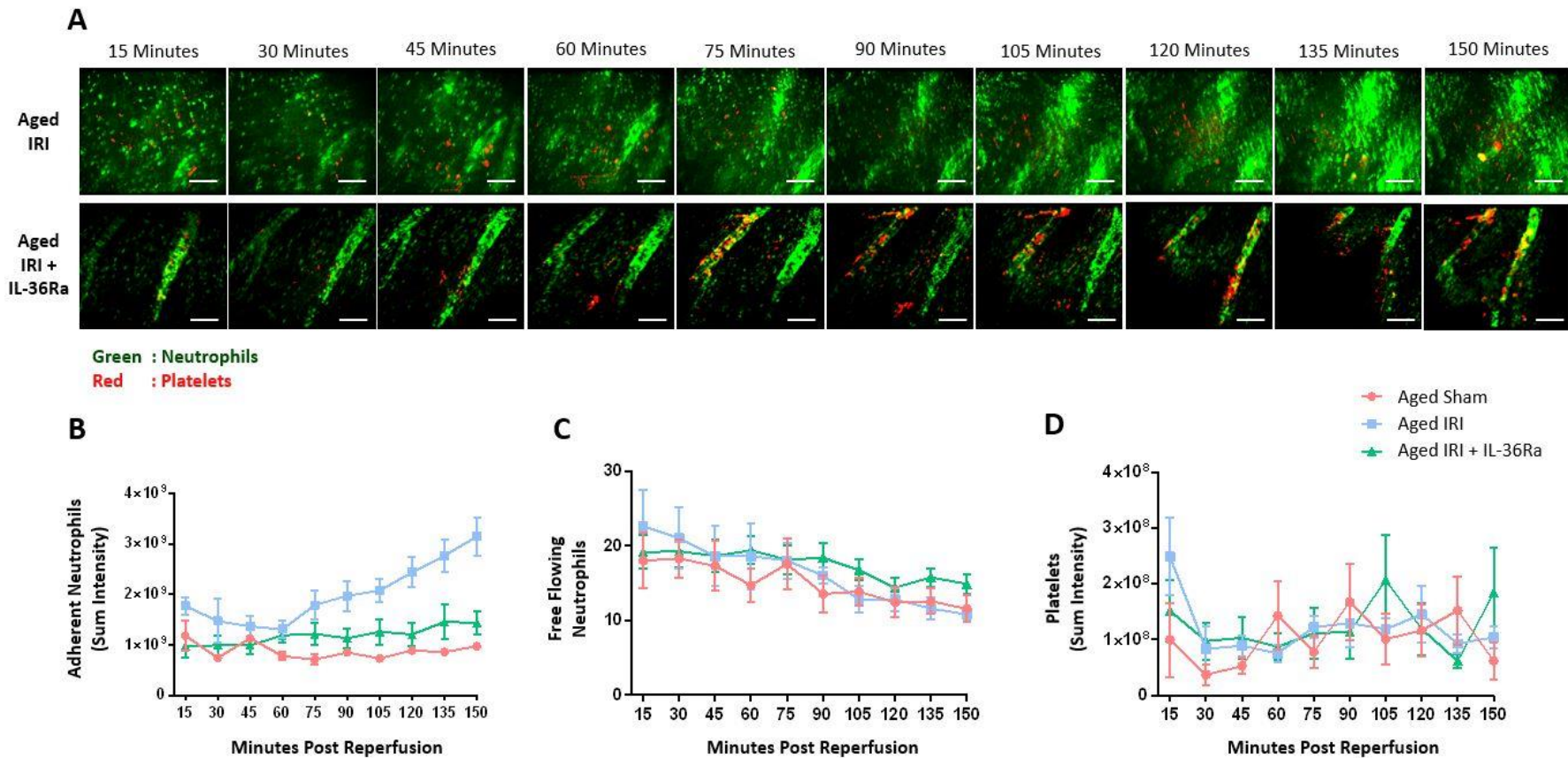
Intravital imaging captures microvascular thromboinflammatory events from first 50-60 $\mu$ m of the beating heart. To determine whether changes in recruitment were mirrored throughout the thickness of the ventricular wall, multiphoton microscopy was performed on hearts harvested at the end of intravital experiments. *Ex vivo* multiphoton imaging of the depth of the ventricular wall confirmed the ability of IL-36Ra to mediate an anti-inflammatory response throughout the depth of the tissue. Indeed, a significant reduction in neutrophil presence was observed in both adult IR injured and aged IR injured mice who received IL-36Ra treatment when compared with their respective non-treated IR injured group (Figures 4.32a-c).

#### 4.2.9. IL-36R Inhibition Increases Functional Capillary Density within the Beating Heart Coronary Microcirculation *in vivo*

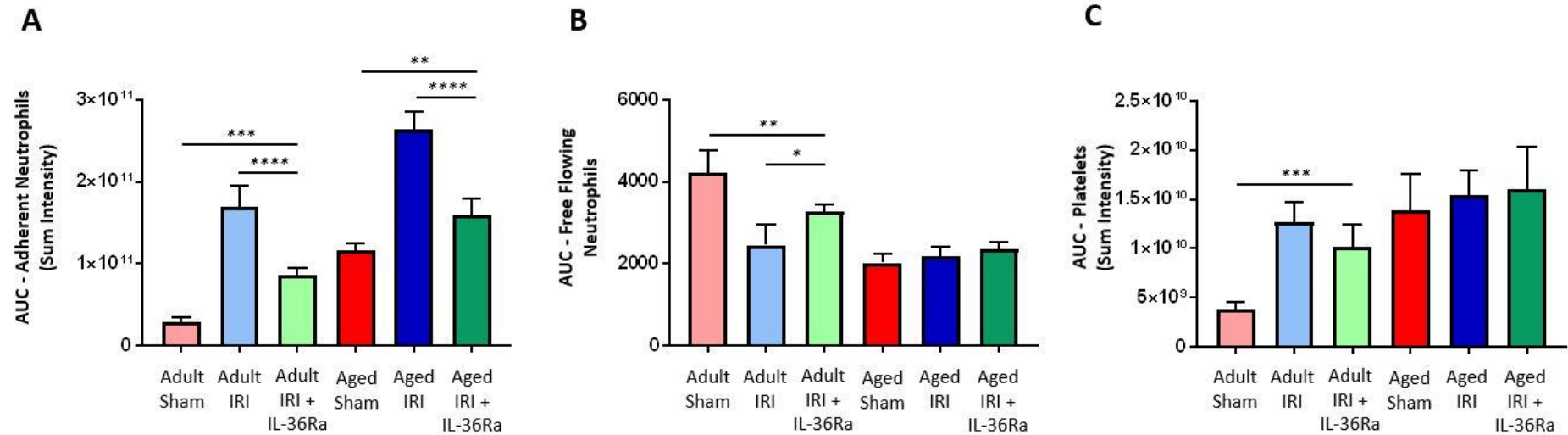
In order to assess microvascular perfusion following IL-36Ra treatment of adult and aged IR injured mice, FITC-BSA was administered via the carotid artery at the end of the imaging period. In adult IR injured mice, IL-36Ra resulted in an improvement in the presence of FITC-BSA perfused capillaries, although this was slightly less than that seen in healthy, uninjured hearts. Similar improvements were noted in aged mice, although there was also less perfusion than in healthy aged mice. Indeed, a few areas devoid of perfusion were still noted in both treated adult and aged IR injured hearts. Of note, medium-sized vessels were still readily visible and well perfused in both adult and aged IL-36Ra treated hearts (**Figures 4.33a-b**).



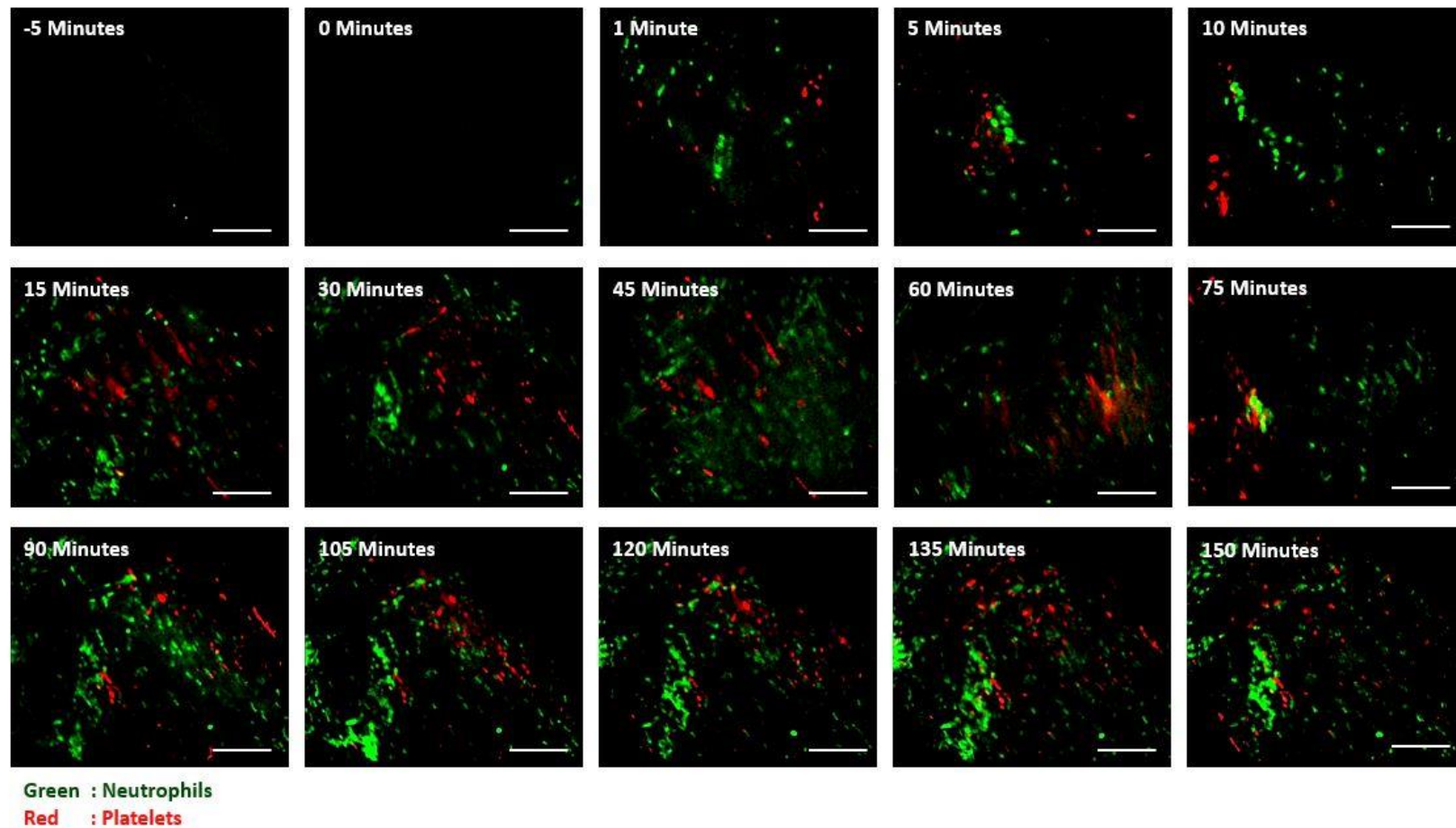
**Figure 4.26. IL-36R inhibition reduces myocardial inflammation *in vivo* in the IR injured adult heart.** IRI inducing surgery was performed on adult female mice. Fluorescently labelled antibodies against neutrophils and platelets were injected via the carotid cannula 5 minutes before reperfusion and imaged intravitaly. Additionally, an IL-36 receptor antagonist (IL-36Ra; 15µg/mouse) was injected intra-arterially at 10 mins pre-reperfusion and 60 mins post-reperfusion in adult mice. **(A)** Representative intravital images of the beating heart showing adherent neutrophils (green) and platelets (red) in the coronary microcirculation over a time course of 150 minutes post-reperfusion. Scale bar indicates 100µm. Quantitative time-course analysis of intravital data for **(B)** adherent neutrophils, **(C)** free-flowing neutrophils, and **(D)** platelets.  $n \leq 5$ /group. Mean  $\pm$  SEM.



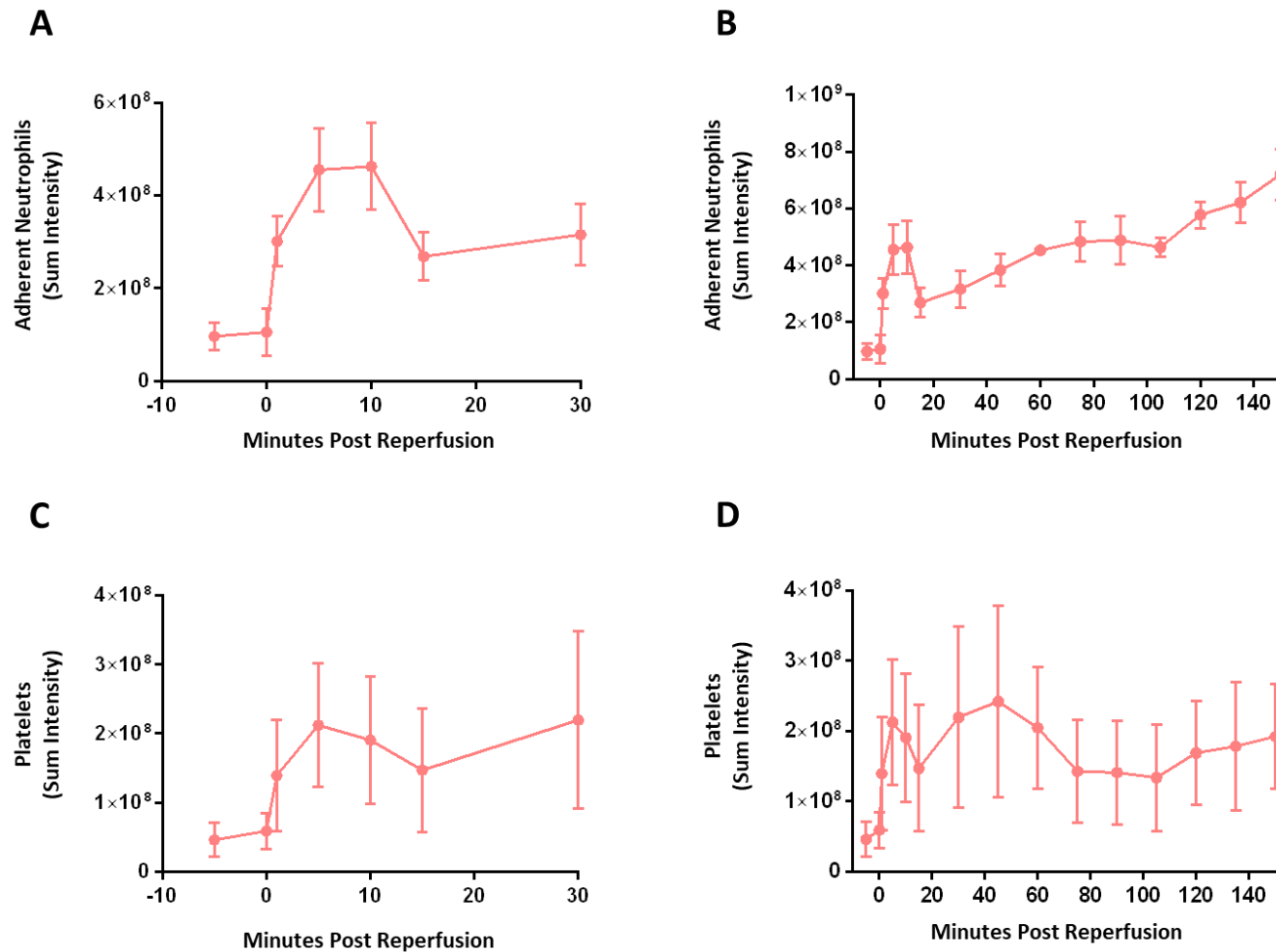
**Figure 4.27. IL-36R inhibition reduces myocardial inflammation *in vivo* in the IR injured aged heart.** IRI inducing surgery was performed on aged female mice. Fluorescently labelled antibodies against neutrophils and platelets were injected via the carotid cannula 5 minutes before reperfusion and imaged intravitaly. Additionally, an IL-36 receptor antagonist (IL-36Ra; 15μg/mouse) was injected intra-arterially at 10 mins pre-reperfusion and 60 mins post-reperfusion in aged mice. **(A)** Representative intravital images of the beating heart showing adherent neutrophils (green) and platelets (red) in the coronary microcirculation over a time course of 150 minutes post-reperfusion. Scale bar indicates 100μm. Quantitative time-course analysis of intravital data for **(B)** adherent neutrophils, **(C)** free-flowing neutrophils, and **(D)** platelets.  $n \leq 5$ /group. Mean  $\pm$  SEM.



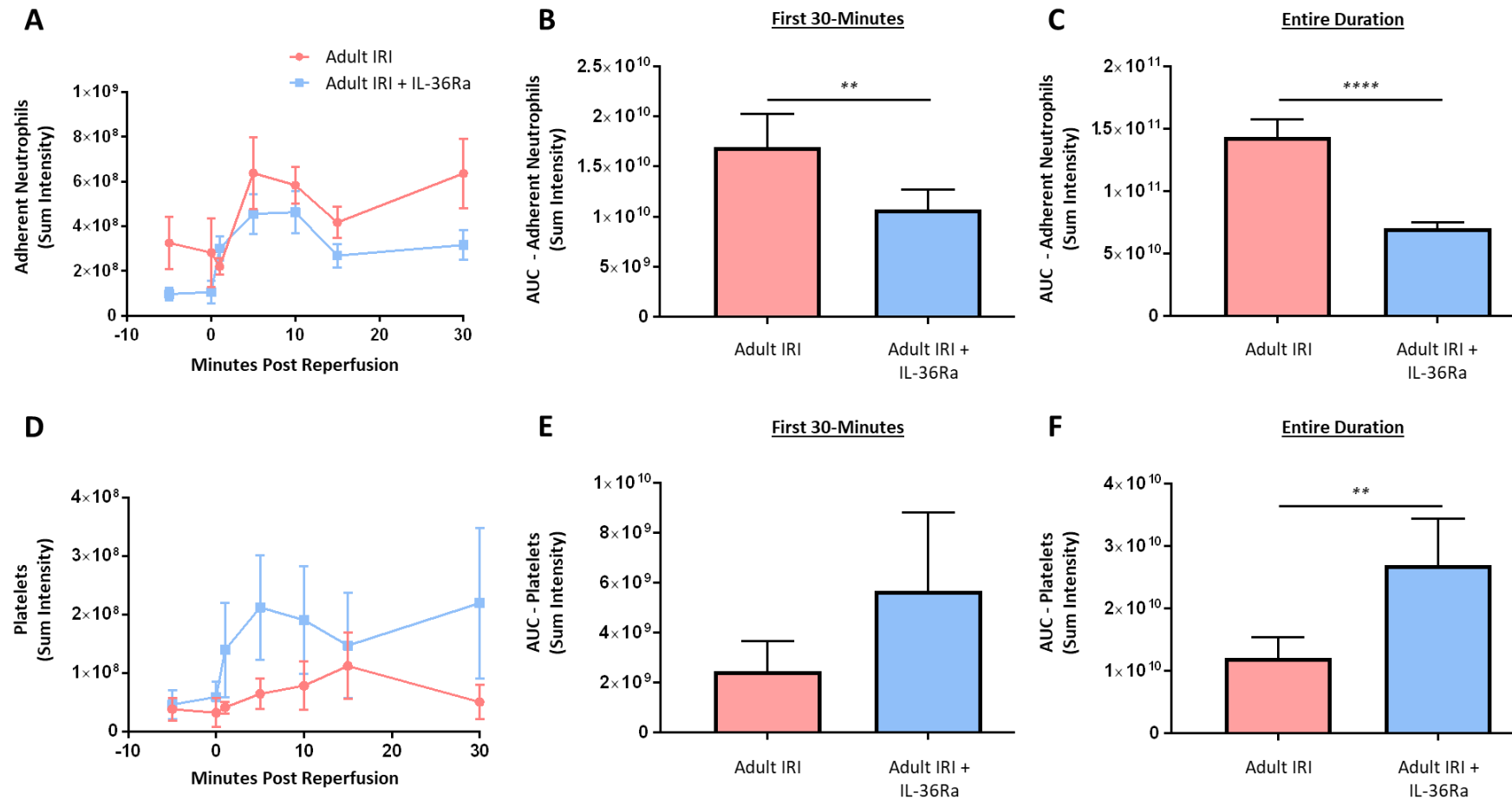
**Figure 4.28. IL-36R inhibition reduces neutrophil recruitment, and platelet accumulation *in vivo* in the IR injured adult and aged heart.** IRI inducing surgery was performed on adult and aged female mice. Fluorescently labelled antibodies against neutrophils and platelets were injected via the carotid cannula 5 minutes before reperfusion and imaged intravitaly. Additionally, an IL-36 receptor antagonist (IL-36Ra; 15µg/mouse) was injected intra-arterially at 10 mins pre-reperfusion and 60 mins post-reperfusion in adults and aged mice. Area under the curve (AUC) analysis for **(A)** adherent neutrophils, **(B)** free-flowing neutrophils, and **(C)** platelets, over a time course of 150 minutes post-reperfusion. Statistical analysis was performed using a one-way ANOVA, followed by a Tukey's post-hoc test between the following groups: sham versus IRI, sham versus IRI + IL-36Ra, and IRI versus IRI + IL-36Ra for both adult and aged groups. Abbreviations - IRI: ischaemia reperfusion injury. n≤5/group. Mean ±SEM. \*p<0.05, \*\*p<0.01, \*\*\*p<0.001, \*\*\*\*p<0.0001.



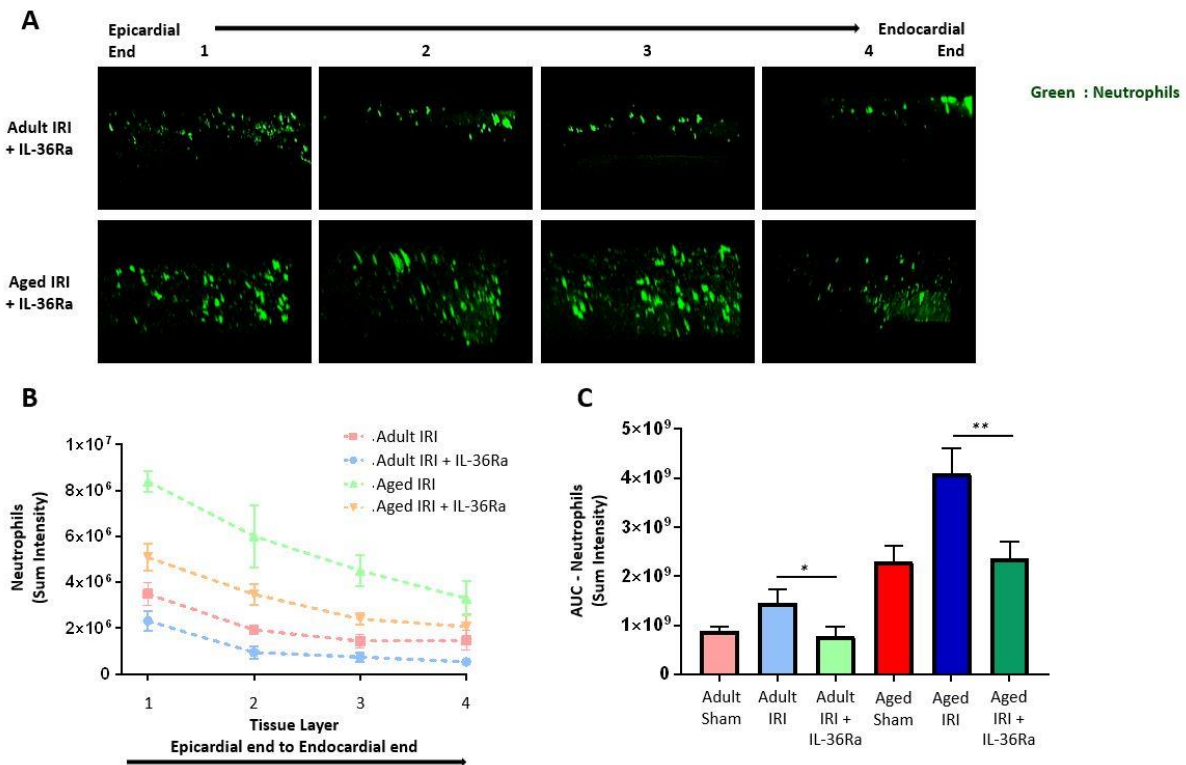
**Figure 4.29. IL-36R inhibition reduces neutrophil recruitment *in vivo* in the IR injured adult heart.** Representative intravital images following IR injury on adult female mice in the coronary microcirculation over a time course of 150 minutes post-reperfusion. An IL-36 receptor antagonist (IL-36Ra; 15µg/mouse) was injected intra-arterially at 10 mins pre-reperfusion and 60 mins post-reperfusion in adult mice. Fluorescently labelled antibodies against neutrophils (green) and platelets (red) were injected via the carotid cannula 10 minutes before reperfusion and imaged intravitaly. Scale bar indicates 100µm. n=6.



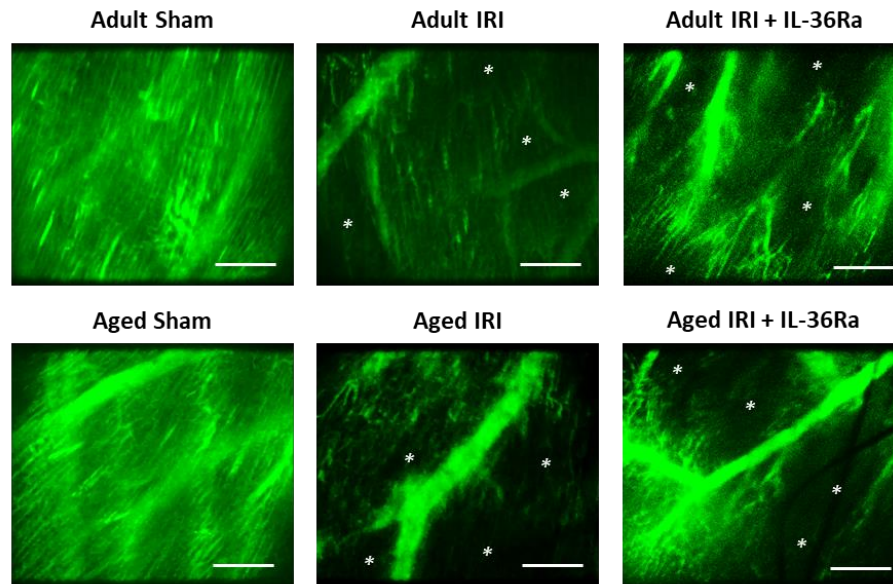
**Figure 4.30. IL-36R inhibition reduces neutrophil recruitment *in vivo* in the IR injured adult heart.** IRI inducing surgery was performed on adult female mice. Fluorescently labelled antibodies against neutrophils and platelets were injected via the carotid cannula 10 minutes before reperfusion and imaged intravitaly. Additionally, IL-36Ra (15µg/mouse) was injected intra-arterially at 10 mins pre-reperfusion and 60 mins post-reperfusion in adult mice. Quantitative time-course analysis of intravital data in the first 30 minutes for **(A)** adherent neutrophils, and **(C)** platelets and over the 150 minutes post-reperfusion for **(B)** adherent neutrophils, and **(D)** platelets. n=6/group. Mean ± SEM.



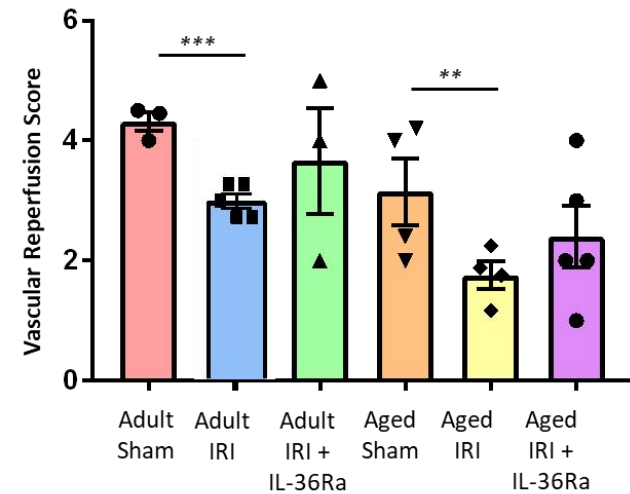
**Figure 4.31. IL-36R inhibition reduces myocardial inflammation *in vivo* in the IR injured adult heart.** IR injury was induced on adult female mice. Fluorescently labelled antibodies against neutrophils and platelets were injected via the carotid cannula 10 minutes before reperfusion and imaged intravitaly. Additionally, an IL-36 receptor antagonist (IL-36Ra; 15µg/mouse) was injected intra-arterially at 10 mins pre-reperfusion and 60 mins post-reperfusion in adults and aged mice. Quantitative time-course analysis of intravital data for **(A)** adherent neutrophils, and **(D)** platelets in the first 30 minutes. Area under the curve (AUC) analysis in the first 30 minutes for **(B)** adherent neutrophils, and **(E)** platelets and over the 150 minutes post-reperfusion for **(C)** adherent neutrophils, and **(F)** platelets. Statistical analysis was performed using a Student's unpaired t-test. Abbreviations—s - IRI: ischaemia reperfusion injury.  $n=6/\text{group}$ . Mean  $\pm$  SEM. \*\* $p<0.01$ , \*\*\*\* $p<0.0001$ .



**Figure 4.32. IL-36R inhibition reduces neutrophil presence within the deeper layers of the IR injured myocardium.** IR injury was induced in adult and aged female mice. Fluorescently labelled antibodies against neutrophils and platelets were injected via the carotid cannula 5 minutes before reperfusion and imaged intravitaly. Additionally, IL-36Ra (15 $\mu$ g/mouse) was injected intra-arterially at 10 mins pre-reperfusion and 60 mins post-reperfusion in adult and aged mice. Mice were culled following 150-minutes of reperfusion and hearts were harvested. The LV was vibratome sectioned into four 300 $\mu$ m sections and imaged using a multiphoton microscope. **(A)** Representative z-stack multiphoton images of neutrophils (green) in the 4 layers of the LV taken from the outermost layer closest to the epicardium (1), outer myocardial layer (2), inner myocardial layer (3) and the innermost layer closest to the endocardium (4). Quantitative analysis of the multiphoton data at various depths for **(B)** adherent neutrophils and corresponding **(C)** area under the curve (AUC) for adherent neutrophils for all layers. Statistical analysis was performed using a one-way ANOVA, followed by a Tukey's post-hoc test between the following groups: sham versus IRI, sham versus IRI + IL-36Ra, and IRI versus IRI + IL-36Ra for both adult and aged groups. Abbreviations - IRI: ischaemia reperfusion injury.  $n \leq 5$ /group. Mean  $\pm$  SEM. \* $p < 0.05$ , \*\* $p < 0.01$ .

**A**

Green : FITC-BSA

**B**

**Figure 4.33. IL-36R inhibition non significantly increases capillary density within the beating heart coronary microcirculation *in vivo*.** IRI inducing surgery was performed on adult and aged female mice. Fluorescently labelled antibody against bovine serum albumin (green) was injected via the carotid cannula at 120-minutes post reperfusion and imaged intravitaly. Additionally, an IL-36 receptor antagonist (IL-36Ra; 15µg/mouse) was injected intra-arterially at 10 mins pre-reperfusion and 60 mins post-reperfusion in adults and aged mice. **(A)** Representative intravital images of FITC-BSA perfused coronary microvessels at 150 mins in IRI and IRI + IL-36Ra hearts. **(B)** Quantitative analysis of intravital vascular perfusion data. Statistical analysis was performed using a one-way ANOVA, followed by a Tukey's post-hoc test between the following groups: adult sham versus adult IRI, adult sham versus adult IRI + IL-36Ra, adult IRI versus adult IRI + IL-36Ra, aged sham versus aged IRI, aged sham versus aged IRI + IL-36Ra, and aged IRI versus aged IRI + IL-36Ra. Abbreviations - IRI: ischaemia reperfusion injury. \*Areas not perfused with FITC-BSA. Scale bar indicates 100µm.  $n \leq 5/\text{group}$ . Mean  $\pm$  SEM. \*\* $p < 0.01$ , \*\*\* $p < 0.001$ .

#### 4.2.10. IL-36R Inhibition Increases Perfusion in Adult and Aged Beating Heart Coronary Circulation *in vivo*

LSCI was used to investigate the overall perfusion of the left ventricular myocardium in response to IL-36Ra treatment in IR injured adult and aged mice. High and low points were calculated from flux recordings and were attributed to diastolic and systolic events respectively (**Figures 4.34a-b**). Systolic events were used for comparative purposes between different experimental groups. As expected, in both adult and aged IL-36Ra treated hearts, ischaemia decreased tissue perfusion following LAD artery ligation. This was rapidly reversed as soon as the artery was untied. In adult untreated injured mice, reperfusion resulted in ventricular perfusion returning to the basal levels seen prior to ischaemia. However, in adult IL-36Ra treated injured mice, perfusion was significantly higher than in the non-treated adult injured mice. Indeed, this hyperaemic response preceded a slow but gradual return to a normal baseline flow (**Figures 4.34a and 4.35a-b**). In aged untreated injured mice, reperfusion also resulted in ventricular perfusion, but this failed to reach the basal levels seen prior to ischaemia. However, in aged IL-36Ra treated injured mice, perfusion was significantly higher than in the non-treated aged injured mice (**Figure 4.34b and 4.36a-b**).

LSCI also allowed ventricular arrhythmia to be investigated from the flux recordings using the standard deviation of the inter-beat distance as a means to identify irregularity in the rhythm of the heartbeat. Both ischaemia and reperfusion resulted in an arrhythmic response in adult and aged injured mice. Although this was significantly reduced in adult IL-36Ra treated injured mice when compared to untreated adult injured mice, there was no difference in treated aged mice when compared to untreated aged injured mice (**Figures 4.35c-d and 4.36c-d**). Heart rate was not significantly altered in response to either ischaemia or reperfusion between

adult or aged IL-36Ra treated injured mice and the respective untreated injured mice (**Figures 4.35e-f and 4.36e-f**).

To determine whether IL-36Ra treatment impacted perfusion differently during systole and diastole, the average flux during these two phases of the cardiac cycle in IL-36Ra treated and untreated adult and aged injured mice was compared. As expected, ischaemia decreased ventricular perfusion during systole and diastole in both adult and aged mice treated and untreated injured mice. However, there was no significant difference in the ischaemic ventricular perfusion during systole and diastole between treated and untreated adult and aged injured mice. Again, reperfusion resulted in a resumption of ventricular perfusion in systole and diastole in both treated and untreated adult and aged injured mice. However, perfusion was improved in both systolic and diastolic phases in adult and systolic and diastolic phases in aged IL-36Ra treated injured mice when compared to untreated injured mice (**Figures 4.37a-f**).

#### **4.2.11. IL-36R Inhibition Decreases Infarct Size in Adult Hearts**

Evans blue and TTC staining was used to determine the impact of IL-36Ra on infarct size in adult and aged IR injured mice. There were no statistically significant differences in infarct size in the various layers of the adult and aged IL-36Ra treated injured hearts. However, infarct size was significantly reduced in all three layers (layer 1 –  $p < 0.001$ ; layer 2 –  $p < 0.0001$ ; layer 3 –  $p < 0.0001$ ) of the adult IL-36Ra treated injured heart when compared to the untreated injured group (**Figures 4.38a-c**). A similar significant decrease in infarct size in all three layers (layer 1 –  $p < 0.001$ ; layer 2 –  $p < 0.0001$ ; layer 3 –  $p < 0.0001$ ) was observed in aged

IL-36Ra treated hearts (**Figures 4.39a-c**). Area at risk (AAR) and area not at risk were not significantly different in treated and untreated adult and aged hearts (**Figures 4.38d-f and 4.39d-f**).

### 4.2.12. IL-36R Inhibition Reduced Endothelial and Cardiac Myocyte Oxidative Damage and VCAM-1 Expression in the IR Injured Heart

To determine whether IL-36Ra treatment conferred vasculoprotection via mechanisms involving attenuation of oxidative stress, we performed flow cytometry on collagenase digested adult and aged hearts, and immunofluorescence on frozen heart sections. IL-36Ra treatment reduced ROS mediated oxidative damage on CMs in both adult and aged hearts when compared with untreated injured hearts as determined by flow cytometry (**Figure 4.40a**). A similar reduction was also seen on coronary ECs in both adult and aged hearts, although this did not attain statistical significance (**Figure 4.40b**). Reductions in oxidative damage were also confirmed using immunofluorescence on both adult and aged IL-36Ra treated hearts (**Figures 4.40c-d**). This was noted as punctate staining on both CD31<sup>+</sup> vascular and non-vascular structures (**Figure 4.40c**). Expression of VCAM-1 was also investigated using immunofluorescence on frozen heart sections. Expression of this endothelial adhesion molecule was also decreased in adult and aged IL-36Ra treated mice (**Figures 4.41a-b**).

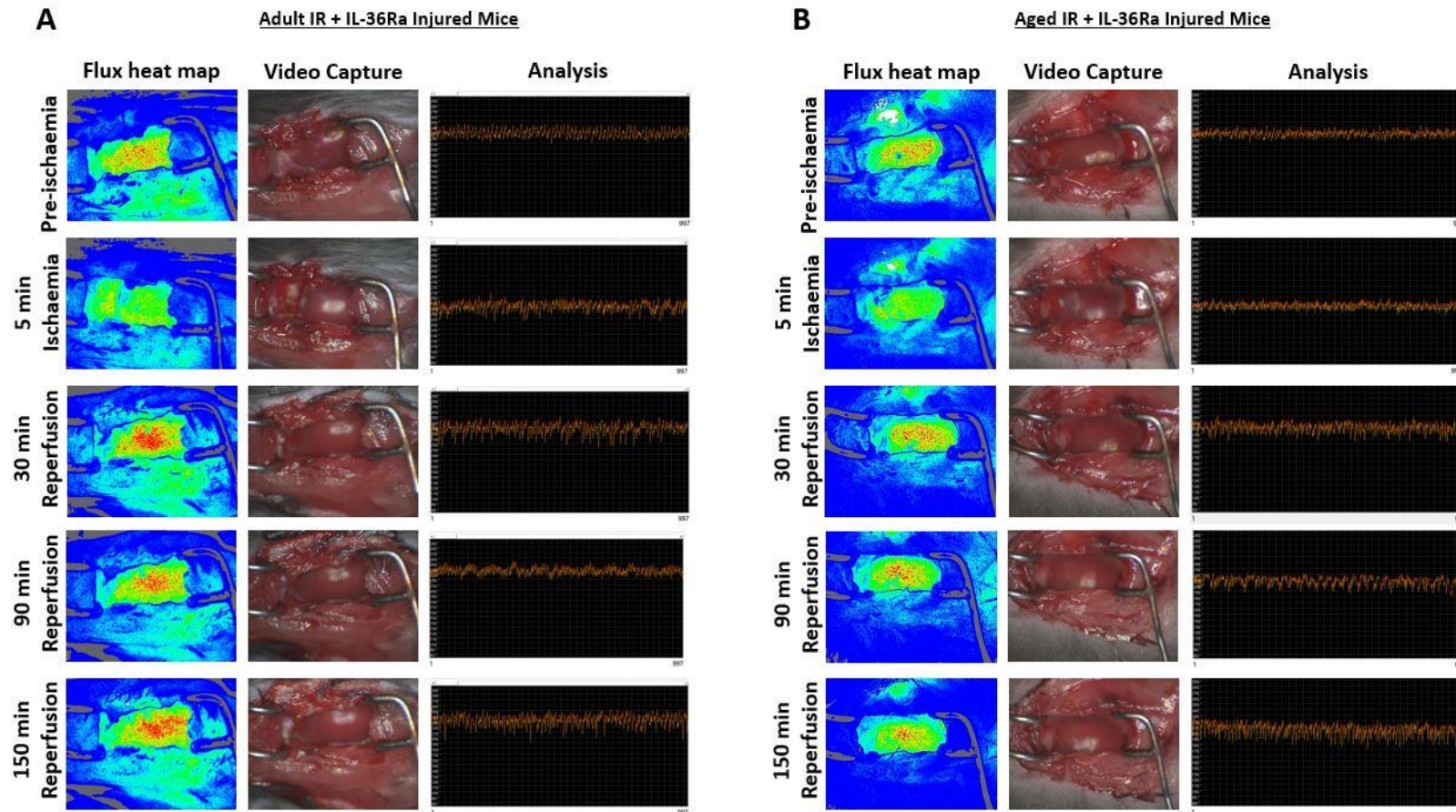


**Figure 4.34. IL-36R inhibition increases perfusion in adult and aged beating heart coronary circulation *in vivo*.** IRI inducing surgery was performed on adult and aged female mice. An IL-36 receptor antagonist (IL-36Ra; 15µg/mouse) was injected intra-arterially at 10 mins pre-reperfusion and 60 mins post-reperfusion. Video captures were obtained throughout the surgery using laser speckle contrast imaging (LSCI). Representative images of LSCI at various time points showing the flux heat map, still image of the beating heart, and analysis graph in **(A)** adult female and **(B)** aged female mice. Baseline capture prior to ischaemia was used as the baseline reading; indicating good perfusion.  $n = 6/\text{group}$ . Mean  $\pm$  SEM.

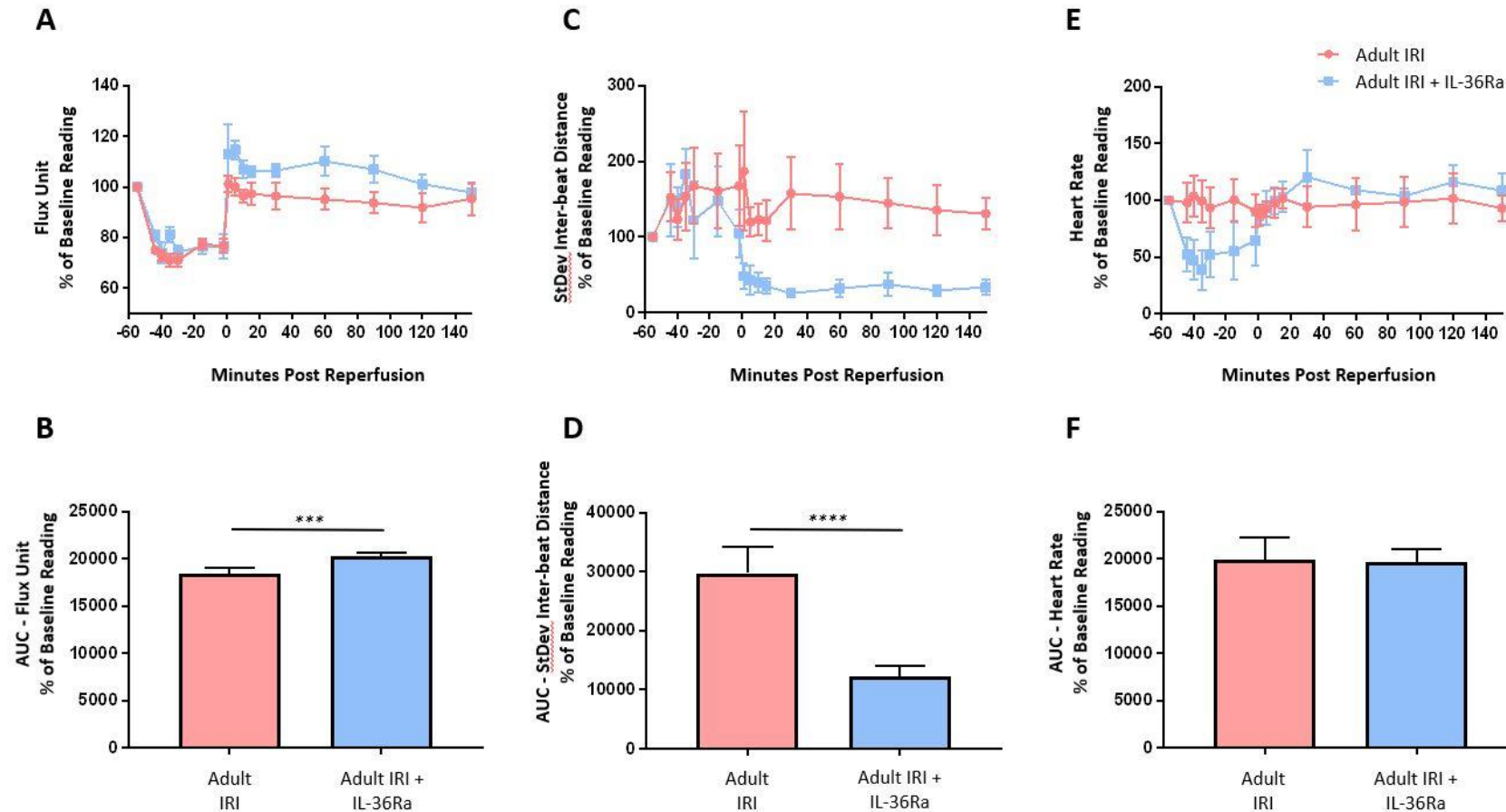


**Figure 4.35. IL-36R inhibition increases perfusion in adult beating heart coronary circulation *in vivo*.** IRI inducing surgery was performed on adult female mice. An IL-36 receptor antagonist (IL-36Ra; 15µg/mouse) was injected intra-arterially at 10 mins pre-reperfusion and 60 mins post-reperfusion. Video captures were obtained throughout the surgery using laser speckle contrast imaging (LSCI). Quantitative time-course analysis of LSCI data for **(A)** flux unit (perfusion), **(C)** standard deviation of the inter-beat distance (arrhythmia), and **(E)** heart rate. Area under the curve (AUC) analysis for **(B)** flux unit, **(D)** standard deviation of the inter-beat distance, and **(F)** heart rate over a time course of 150 minutes post-reperfusion. Statistical analysis was performed using a Student's unpaired t-test. Abbreviations - IRI: ischaemia reperfusion injury.  $n = 6/\text{group}$ . Mean  $\pm$  SEM. \*\*\* $p < 0.001$ , \*\*\*\* $p < 0.0001$ .

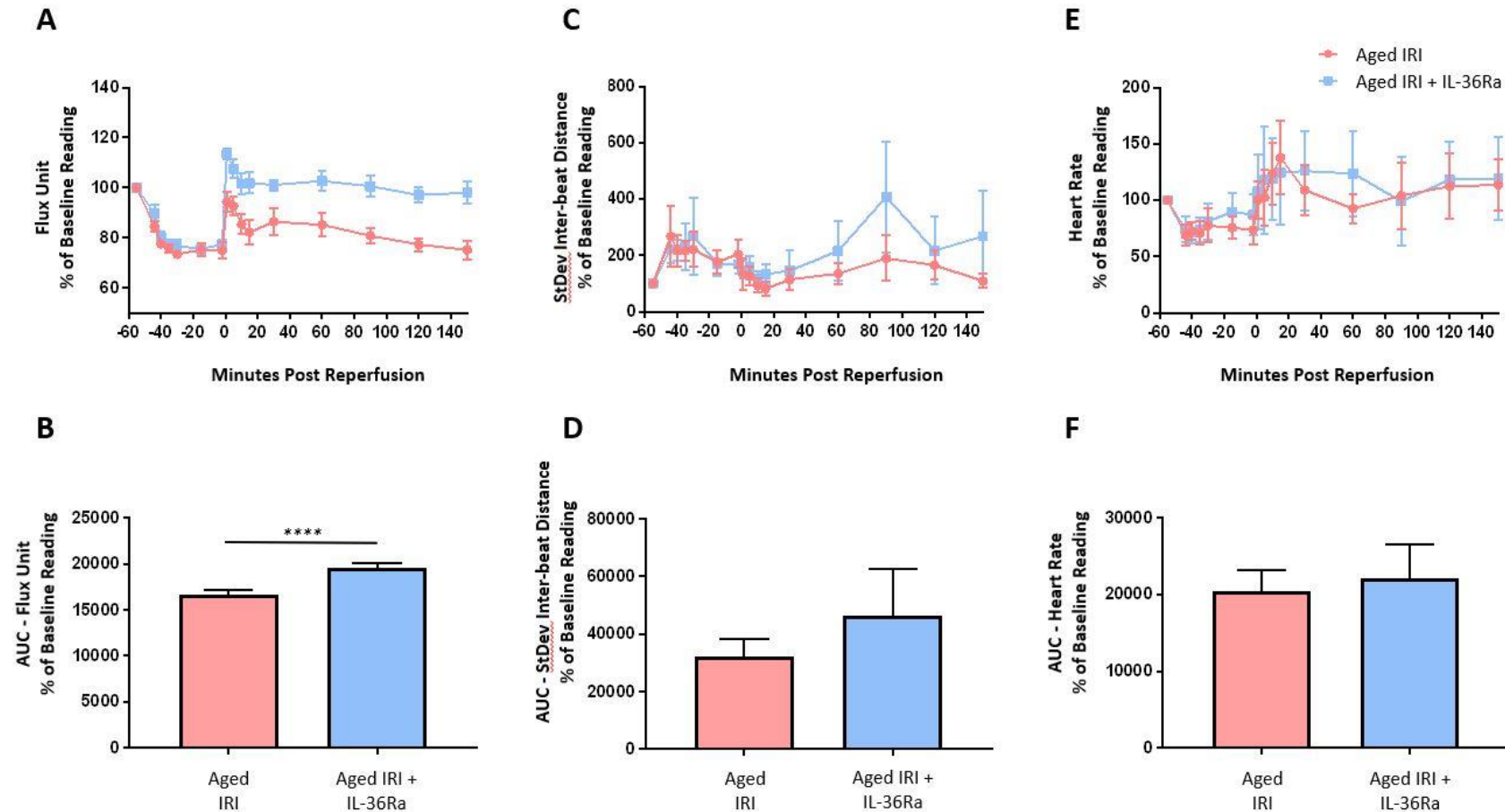


**Figure 4.36. IL-36R inhibition increases perfusion in aged beating heart coronary circulation *in vivo*.** IRI inducing surgery was performed on aged female mice. An IL-36 receptor antagonist (IL-36Ra; 15µg/mouse) was injected intra-arterially at 10 mins pre-reperfusion and 60 mins post-reperfusion. Video captures were obtained throughout the surgery using laser speckle contrast imaging (LSCI). Quantitative time-course analysis of LSCI data for **(A)** flux unit (perfusion), **(C)** standard deviation of the inter-beat distance (arrhythmia), and **(E)** heart rate. Area under the curve (AUC) analysis for **(B)** flux unit, **(D)** standard deviation of the inter-beat distance, and **(F)** heart rate over a time course of 150 minutes post-reperfusion. Statistical analysis was performed using a Student's unpaired t-test. Abbreviations - IRI: ischaemia reperfusion injury.  $n = 6/\text{group}$ . Mean  $\pm$  SEM. \*\*\*\* $p < 0.0001$ .

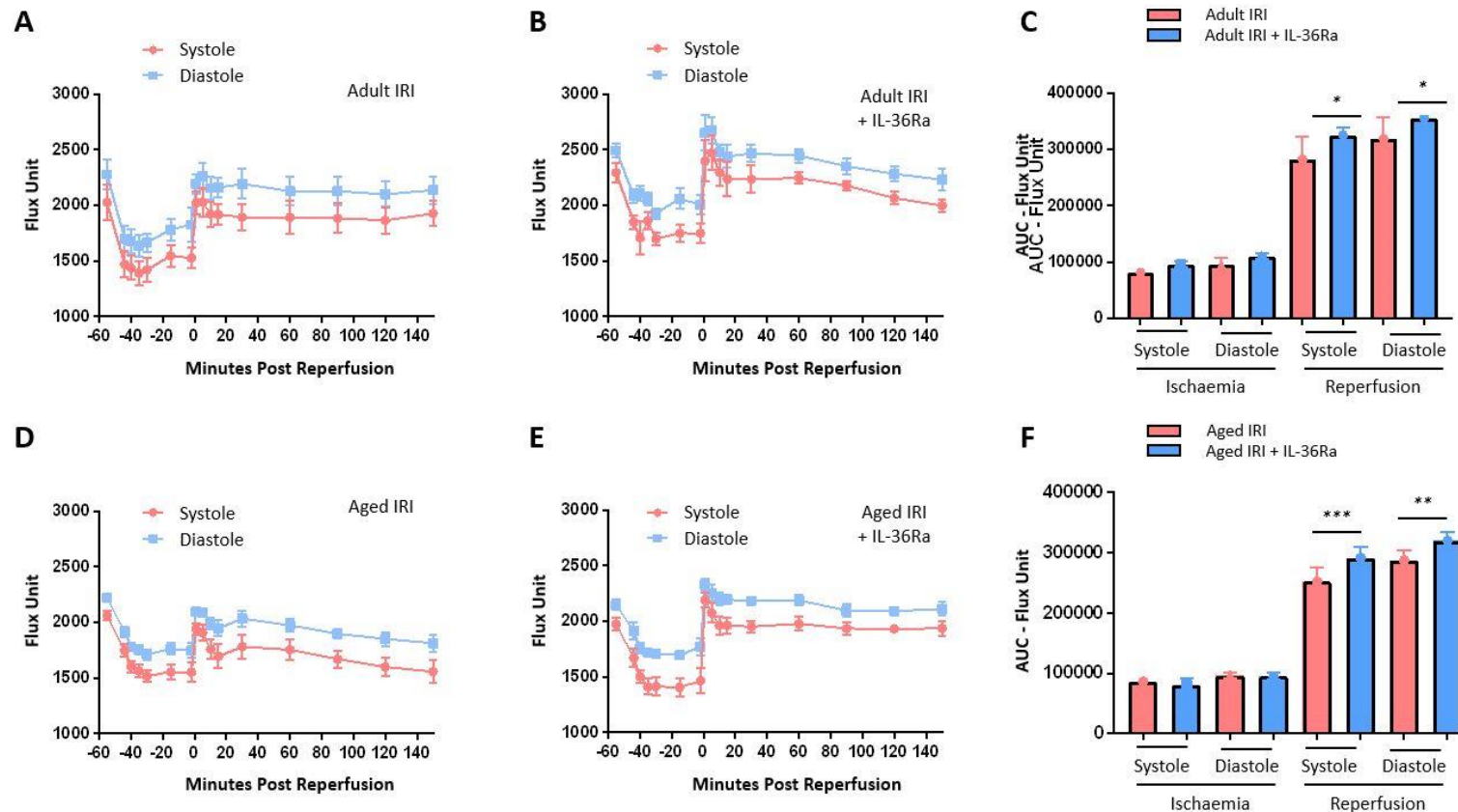


**Figure 4.37. IL-36R inhibition reduces systole and diastole anomalies following IR injury *in vivo*.** IRI inducing surgery was performed on adult and aged female mice. An IL-36 receptor antagonist (IL-36Ra; 15µg/mouse) was injected intra-arterially at 10 mins pre-reperfusion and 60 mins post-reperfusion. Video captures were obtained throughout the surgery using laser speckle contrast imaging (LSCI). Baseline capture prior to ischaemia was used as the baseline reading; indicating good perfusion. Quantitative systole and diastole time-course analysis of LSCI data for flux unit (perfusion) in (A) adult IRI, (B) adult IRI + IL-36Ra, (D) aged IRI, and (E) aged IRI + IL-36Ra mice. Area under the curve (AUC) analysis for systole and diastole flux unit in the ischaemia and reperfusion phases for (C) adult and (F) aged mice. Statistical analysis was performed using a one-way ANOVA, followed by a Tukey's post-hoc test between the following groups: systole IRI versus systole IRI + IL-36Ra for each of ischaemia and reperfusion, and diastole IRI versus diastole IRI + IL-36Ra for each of ischaemia and reperfusion in both adult and aged mice. Abbreviations - IRI: ischaemia reperfusion injury.  $n = 6/\text{group}$ . Mean  $\pm$  SEM. \*\*\*\* $p < 0.0001$ .

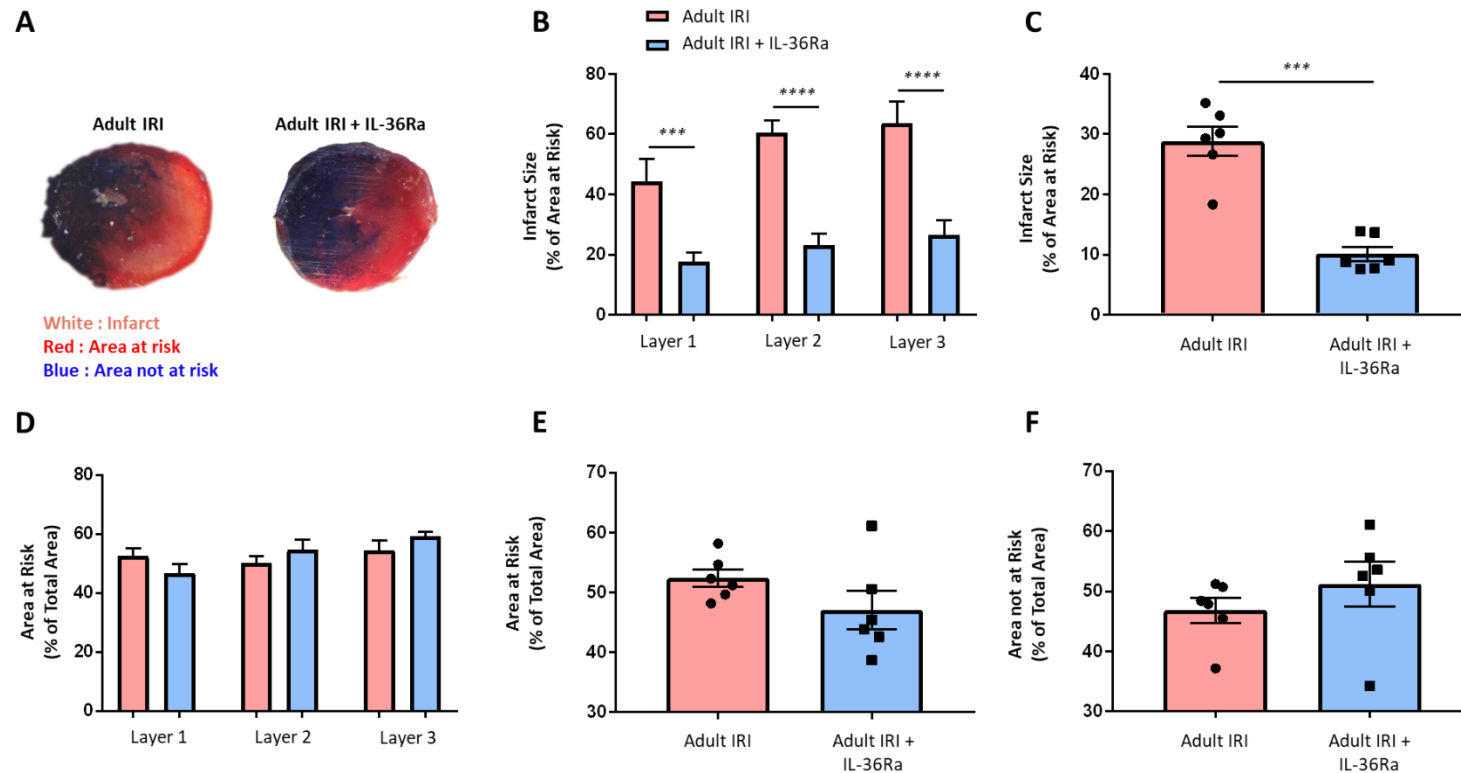


**Figure 4.38. IL-36R inhibition decreases infarct size in adult hearts.** IRI inducing surgery was performed on adult female mice. An IL-36 receptor antagonist (IL-36Ra; 15µg/mouse) was injected intra-arterially at 10 mins pre-reperfusion and 60 mins post-reperfusion. Following 4-hours of reperfusion, the left anterior descending artery was re-ligated, and Evans Blue was injected. Mice were culled, and the heart was harvested, sectioned, stained with TTC and imaged. **(A)** Representative images of the TTC stained adult hearts. Quantitative analysis of **(B)** infarct size and **(C)** area at risk in the various layers of the heart. Layer 1 represents the first layer below the ligature, and layer 3 represents the apex of the heart. Statistical analysis was performed using a one-way ANOVA, followed by a Tukey's post-hoc test between the following groups: adult IRI versus adult IRI + IL-36Ra in each of the 3 layers, as well as layer 1 versus layer 2, layer 1 versus layer 3, and layer 2 versus layer 3 for each of adult IRI and adult IRI + IL-36Ra groups. Quantitative analysis of the overall **(D)** infarct size, **(E)** area at risk, and **(F)** area not at risk throughout all the layers. Statistical analysis was performed using a Student's unpaired t-test. Abbreviations - IRI: ischaemia reperfusion injury.  $n \leq 6$ /group. Mean  $\pm$  SEM. \*\*\* $p < 0.001$ , \*\*\*\* $p < 0.0001$ .

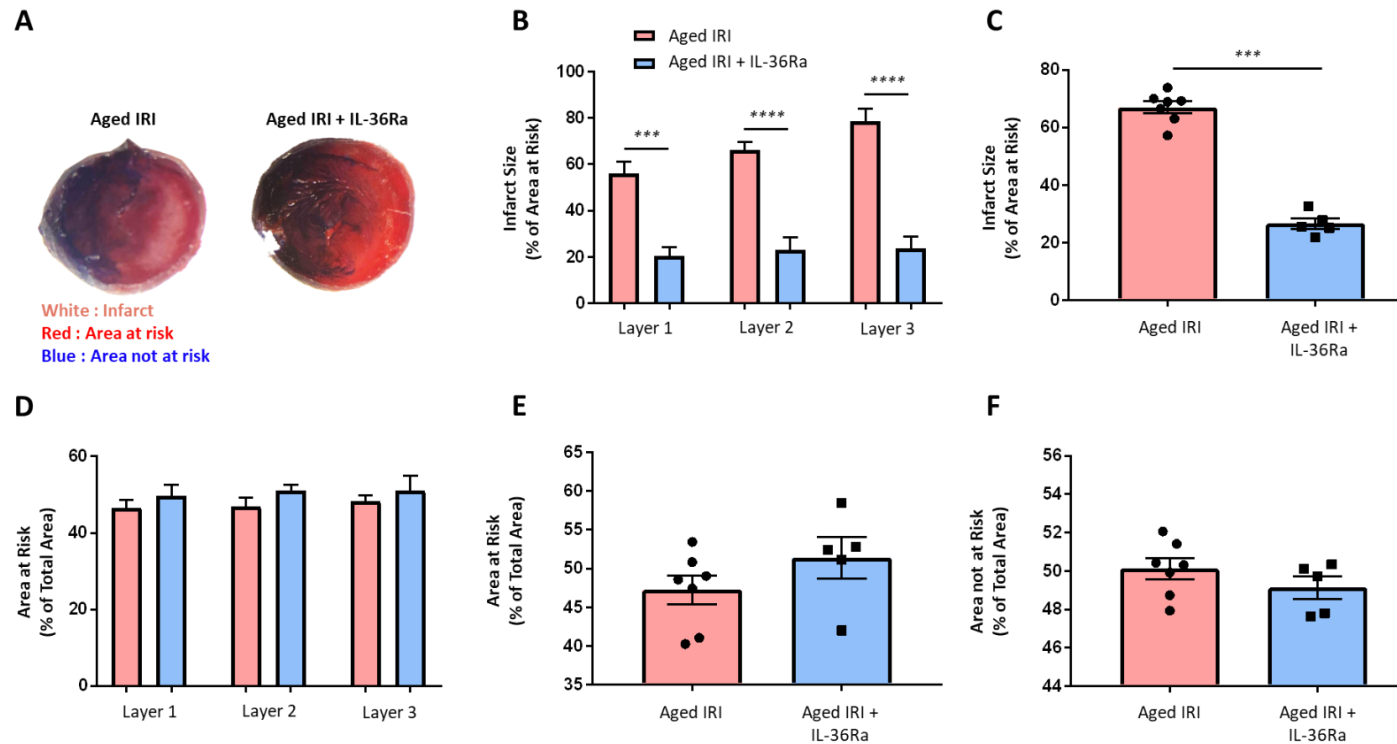


**Figure 4.39. IL-36R inhibition decreases infarct size in aged hearts.** IRI inducing surgery was performed on aged female mice. An IL-36 receptor antagonist (IL-36Ra; 15µg/mouse) was injected intra-arterially at 10 mins pre-reperfusion and 60 mins post-reperfusion. Following 4-hours of reperfusion, the left anterior descending artery was re-ligated, and Evans Blue was injected. Mice were culled, and the heart was harvested, sectioned, stained with TTC and imaged. **(A)** Representative images of the TTC stained adult hearts. Quantitative analysis of **(B)** infarct size and **(C)** area at risk in the various layers of the heart. Layer 1 represents the first layer below the ligature, and layer 3 represents the apex of the heart. Statistical analysis was performed using a one-way ANOVA, followed by a Tukey's post-hoc test between the following groups: aged IRI versus aged IRI + IL-36Ra in each of the 3 layers, as well as layer 1 versus layer 2, layer 1 versus layer 3, and layer 2 versus layer 3 for each of aged IRI and aged IRI + IL-36Ra groups. Quantitative analysis of the overall **(D)** infarct size, **(E)** area at risk, and **(F)** area not at risk throughout all the layers. Statistical analysis was performed using a Student's unpaired t-test. Abbreviations - IRI: ischaemia reperfusion injury.  $n \leq 6$ /group. Mean  $\pm$  SEM. \*\*\* $p < 0.001$ , \*\*\*\* $p < 0.0001$ .

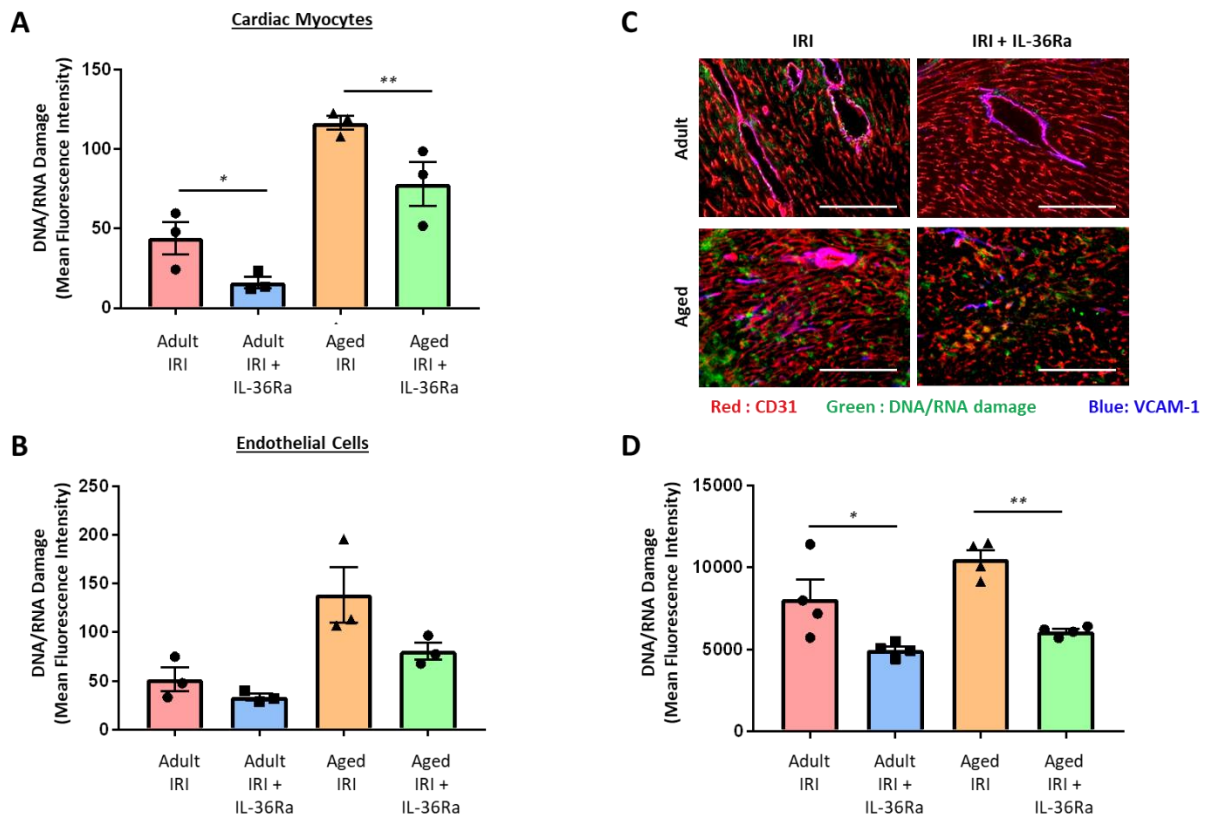


**Figure 4.40. IL-36R inhibition decreases expression of DNA/RNA damage on cardiac myocytes and endothelial cells.** IRI inducing surgery was performed on adult and aged female mice. An IL-36 receptor antagonist (IL-36Ra; 15µg/mouse) was injected intra-arterially at 10 mins pre-reperfusion and 60 mins post-reperfusion. **(A-B)** Mice were culled following 150-minutes of reperfusion and hearts were harvested and digested. Cell suspension was stained with an anti-CD31, anti-cTnT, and anti-DNA/RNA damage antibodies and acquisition was performed using a CyAn™ ADP cytometer. Quantitative analysis of DNA/RNA damage expression on **(A)** cardiac myocytes, and **(B)** endothelial cells. n=3/group. **(C-D)** Mice were culled following 120-minutes of reperfusion and hearts were harvested and snap frozen. The LV was transversely sectioned using a cryostat into 10µm sections and then immunostained with an anti-DNA/RNA damage, anti-CD31, and anti-VCAM-1 antibodies. Sections were imaged using a EVOS microscope. **(C)** Representative images of DNA/RNA damage (green), VCAM-1 (blue), and CD31 (red) staining of frozen heart sections. Scale bar indicates 200µm. **(D)** Quantitative analysis of the immunofluorescent images of DNA/RNA damage expression. n=4/group. Statistical analysis was performed using a one-way ANOVA, followed by a Tukey's post-hoc test between four groups: adult IRI versus adult IRI + IL-36Ra, aged IRI versus aged IRI + IL-36Ra, and adult IRI + IL36Ra versus aged IRI + IL-36Ra. Abbreviations - IRI: ischaemia reperfusion injury. Mean ±SEM. \*p<0.05, \*\*p<0.01.

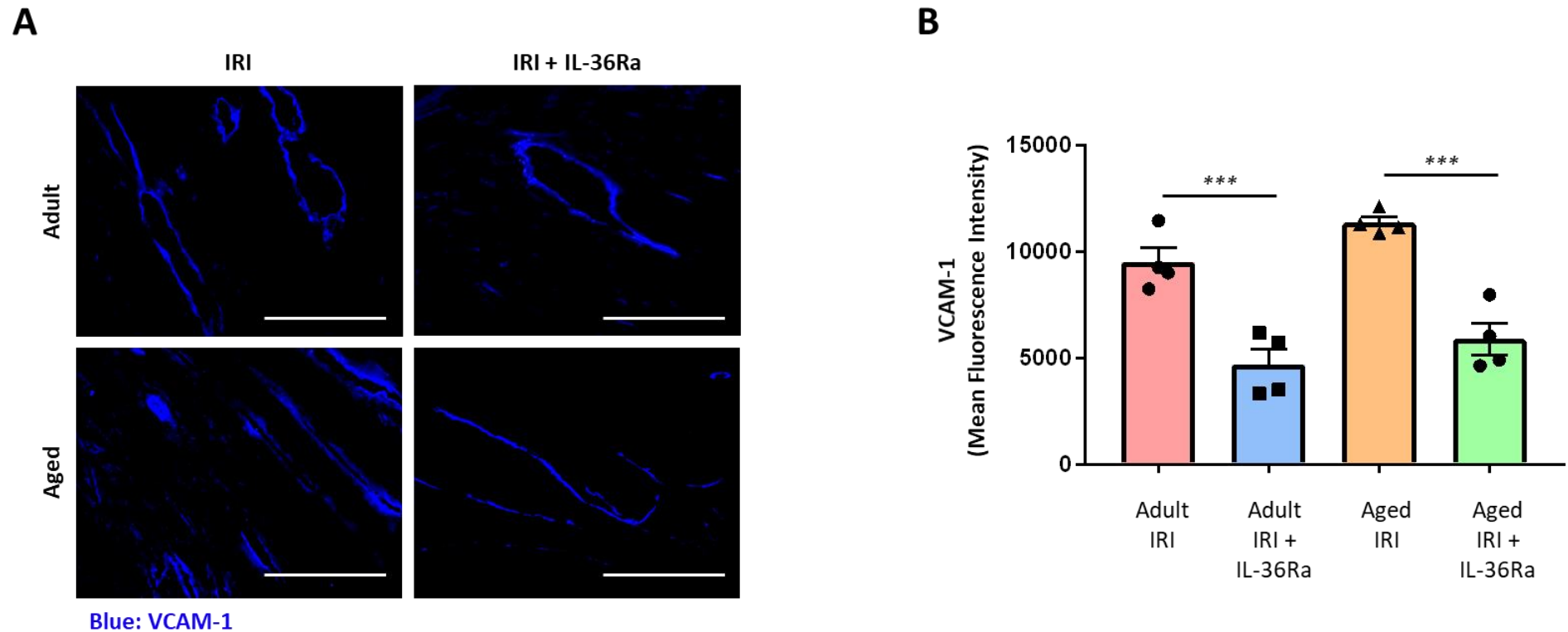


**Figure 4.41. IL-36R inhibition decreases expression of VCAM-1.** IRI inducing surgery was performed on adult and aged female mice. An IL-36 receptor antagonist (IL-36Ra; 15μg/mouse) was injected intra-arterially at 10 mins pre-reperfusion and 60 mins post-reperfusion. Mice were culled following 120-minutes of reperfusion and hearts were harvested and snap frozen. The LV was transversely sectioned using a cryostat into 10μm sections and then immunostained with an anti-VCAM-1 antibody. Sections were imaged using a EVOS microscope. **(A)** Representative images of VCAM-1 (blue) staining of frozen heart sections. Scale bar indicates 200μm. **(B)** Quantitative analysis of the immunofluorescent images of VCAM-1 expression. n=4/group. Statistical analysis was performed using a one-way ANOVA, followed by a Tukey's post-hoc test between four groups: adult IRI versus adult IRI + IL-36Ra, aged IRI versus aged IRI + IL-36Ra, and adult IRI + IL36Ra versus aged IRI + IL-36Ra. Abbreviations - IRI: ischaemia reperfusion injury. Mean ±SEM. \*\*\*p<0.001.

	Adult sham	Adult IR injured	Aged sham	Aged IR Injured
IL-36R and IL-36 cytokine expression				
IL-36 receptor by immunofluorescence	↑	↑	↑↑	↑↑↑
IL-36 receptor by Western blotting	↑	↑ Mostly 85kDa	↑↑ Mostly 65kDa	↑↑↑ Mostly 65kDa
	Receptor noted on both cardiomyocytes and endothelial cells and as early as during ischaemia. IL-36R also noted increasing in an age dependent manner on human heart sections			
IL-36α / IL-36β by immunofluorescence	↑	↑	↑↑	↑↑↑
	IL-36 noted increasing in an age dependent manner on human heart sections			
Intravital studies on the beating heart <i>in vivo</i> in mice treated with topical IL-36				
Adherent neutrophils	↑↑↑	---	↑↑	----
Free-flowing neutrophils	↓↓	---	↓↓	---
Adherent platelet microthrombi	↑↑ IL-36β / IL-36γ	---	↓↓ IL-36β / IL-36γ	---
Intravital studies on the beating heart <i>in vivo</i> in mice treated with IL-36Ra				
Adherent neutrophils	---	↓↓ compared to untreated	---	↓↓ compared to untreated
Free-flowing neutrophils	---	↑↑ compared to untreated	---	No effect
Adherent platelet microthrombi	---	No effect	---	No effect
FITC-BSA perfusion to assess FCD	---	Improved	---	Improved
Laser speckle studies on the beating heart <i>in vivo</i> in mice treated with IL-36Ra				
Overall ventricular perfusion	---	Perfusion exceeds pre-ischaemic levels after reperfusion	---	Perfusion exceeds pre-ischaemic levels after reperfusion
St.Dev. of the inter-beat distance	Improved in IL-36Ra treated adult injured mice when compared to adult untreated mice but not in IL-36Ra treated aged injured mice when compared to aged untreated mice			
Heart rate	Not significantly different in adult or aged IL-36Ra treated mice when compared to untreated mice			
Immunostaining of frozen heart sections <i>in vitro</i> in mice treated with IL-36Ra				
VCAM-1	---	↓↓ compared to untreated	---	↓↓ compared to untreated
DNA/RNA oxidative damage	---	↓↓ compared to untreated	---	↓↓ compared to untreated
Flow cytometry studies on digested heart cells <i>in vitro</i> in mice treated with IL-36Ra				
DNA/RNA oxidative damage of CMs	---	↓↓ compared to untreated	---	↓↓ compared to untreated
DNA/RNA oxidative damage of ECs	---	↓↓ compared to untreated	---	↓↓ compared to untreated
TTC / Evans Blue staining of heart sections <i>in vitro</i> in mice treated with IL-36Ra				
Infarct size	---	↓↓↓ compared to untreated	---	↓↓↓ compared to untreated

**Table 4.1. Summary of the major observations on IL-36R/IL-36 expression and between IL-36Ra treated and untreated adult and aged IR injured female mouse hearts.** Studies conducted were intravital microscopy and laser speckle *in vivo* studies on the beating heart and multiphoton, flow cytometry, and immunostaining *in vitro* studies.

### 4.3. Discussion

In the last decade, IL-36, a newly discovered pro-inflammatory member of the IL-1 superfamily, has been shown to be highly pro-inflammatory in a range of conditions. However, its role in diseases of the heart, particularly MI, has yet to be studied [118, 137-139]. In light of the significant inflammatory response observed intravitaly in the reperfused beating heart coronary microcirculation, an understanding of the potential role of IL-36 in the post-ischaemic heart is essential. In this chapter, we provide original contributions on the pathophysiological roles the IL-36/IL-36R pathway play following myocardial IR injury in both an adult and aged environment. It also provides the first evidence that IL-36Ra may be a novel therapeutic target that remains effective in an aged heart where the microcirculatory perturbations are worse than in the adult heart. The main results are summarised in **Table 4.1**.

#### 4.3.1. Expression of IL-36R Increases with Age and IR Injury

IL-36 has recently been identified as being one of the most upstream and up-regulated cytokines released upon tissue injury and cellular necrosis and is thus critical in driving subsequent inflammatory processes through the synthesis and release of a multitude of inflammatory mediators [269]. Whether the receptor is expressed in the heart, where and whether it is functional has not previously been investigated in detail. Moreover, whether the heightened inflammatory response in aged hearts is linked to greater expression of the IL-36R is not known. Indeed, currently, there is a paucity of literature on whether cytokine receptor number and their cell surface distribution changes with ageing, except for that of

IL-2 receptor [271]. Our novel data suggest that IL-36R is present on vascular and non-vascular cells of the healthy adult murine heart, albeit at very low levels. A basal expression of IL-36R was also supported by Towne *et al.* (2004) who showed IL-36R expression in human hearts using quantitative polymerase chain reaction (qPCR) [272]. Our Western blot results identified 2 distinct bands for IL-36R at approximately 65kDa and 85kDa, with the smaller but biologically active, version identified predominantly in aged healthy and aged injured hearts. The observation of two bands is consistent with previous findings by other groups on non-cardiac tissues and cells. Indeed, Yi *et al.* (2016) showed two bands in HEK 293T cells transfected with the IL-36R using western blotting [126].

Importantly, we show that IL-36R expression levels increased simply as a result of the advancing mouse age (from approximately 3 to 18 months) in the absence of any injury. Similarly, an increase in IL-36R expression was also observed in clinical samples (increasing from newborn to 65 years) in which the young heart samples were from relatively healthy and not diseased hearts. This increased expression with age could be due to a potential increase in vascular density in larger older hearts. However, when healthy sham adults and aged tissues were stained with CD31, no significant change in CD31 expression was noted with age (previously discussed in chapter 3). This suggests that the increases in IL-36R observed with ageing are not a result of an increase in vascular density. Although there are no studies identifying a reduction in capillary density in the heart with ageing, similar studies in the brain have shown an age-related decrease in capillary count (capillary rarefaction) [237]. However, our data does not suggest that age-related capillary rarefaction occurs in the ageing heart.

Further increases in IL-36R expression were observed on adult and aged IR injured hearts when compared to adult and aged healthy sham hearts. This could be due to the persistent low-grade inflammation associated with ageing (inflammaging) increasing the susceptibility of the aged heart to an acute injury [165]. Indeed, our flow cytometric data confirmed that both age and IR injury increased IL-36R expression on adult CMs and ECs, and that this happened within 30 minutes of reperfusion on both cell types. These results indicate that increases in IL-36R expression can occur fairly immediately after myocardial reperfusion, and this can, therefore, likely explain the rapid thromboinflammatory and microvascular perfusion perturbations which occur within this time frame. Having said this, it has been suggested that the receptor number on cell surface is not that critical but rather their capability for transducing the signal from the receptor to the nucleus, and that this ability is actually reduced with ageing [273].

### 4.3.2. Expression of IL-36 also Increases with Age and IR Injury

Although cytokine receptor changes have not been studied extensively with age, there are several studies to show enhanced age-related production of cytokines such as IL-6 [271, 274]. In the current study, both IL-36 $\alpha$  and IL-36 $\beta$  were identified in healthy sham adult hearts and their levels also significantly increased with age in the absence of any injury. Interestingly, we also identified increases in IL-36 $\alpha$ , IL-36 $\beta$ , and IL-36 $\gamma$  expression in clinical samples (increasing from approximately newborn to 65 years). These results suggest a link between ageing and the production of pro-inflammatory members of the IL-36 subfamily. An increase in basal levels of pro-inflammatory cytokines in response to age (independent

of injury) is a well-established phenomenon. An age-related increase in IL-6 concentration has been found in serum, plasma, and mononuclear cell supernatants from elderly patients free of any age-related diseases [271]. Yang *et al.* showed that ageing could significantly enhance basal production of IL-6 in mouse aorta [165, 275]. It is the persistence of this chronic inflammatory stimulus over time that favours a heightened inflammatory response when an acute injurious stimulus, such as an MI, occurs.

Our results also show an increase in IL-36 $\alpha$  staining as a result of IR injury in adult hearts and an increase of IL-36 $\beta$  as a result of IR injury in aged hearts. These results indicate that IL-36 $\alpha$  may play a more predominant role in adults, while IL-36 $\beta$  may be the most important IL-36 cytokine in aged organisms. However, this would require further investigation. Expression levels of IL-36R, IL-36 $\alpha$ , and IL-36 $\beta$  were all significantly increased in aged IR injured hearts when compared to their respective adult hearts. Expression of IL-36 agonists have been shown to increase at both the mRNA and protein level in murine kidney tissue following renal IR injury [276]. Additionally, IL-36 $\beta$  mRNA expression increased in lung homogenates 24 hours after allergic lung inflammation [277]. Our study examined IL-36 after a much shorter duration of injury, so the full extent of IL-36 upregulation may not have been observed. Enhanced expression of these cytokines suggests a more pro-inflammatory environment in aged IR injury, which could contribute to the age-related increases in myocardial damage and worsened prognosis following MI [160, 161].

### 4.3.3. Vascular Localisation of IL-36R and IL-36

IL-36 and IL-36R expression was observed on the majority of coronary capillaries as evidenced by co-localisation with CD31<sup>+</sup> endothelial cells. Moreover, it was only on microvessels that an age- and injury-related increase in cytokine and receptor expression was observed. This elevated age-related expression, specifically on microvessels, increases the likelihood of this signalling pathway exacerbating IR injury through specific actions at the level of the coronary microcirculation in elderly patients with MI. Thus MVO, which is largely driven by the inflammatory cascade, could potentially be targeted through IL-36 antagonism in the microvasculature [28, 52]. While other studies have shown an increase in inflammatory cytokines in the microvessels following inflammation or obstruction, there have been no studies reporting cytokine differences between the coronary micro and macro-vasculature [278].

Having seen all three IL-36 members co-localise on microvessels, specific expression on endothelial cells was confirmed using VCECs. We show that IL-36R, IL-36 $\alpha$ , or IL-36 $\beta$  had a little constitutive expression on VCECs. EC expression of IL-36 was also recently shown by Bridgewood *et al.* (2016) on human umbilical vein and dermal lymphatic ECs where it was functionally important in mediating up-regulation of ICAM-1/VCAM-1 and chemokine production in response to IL-36 stimulation [136]. We further demonstrated that all three IL-36 agonists, as well as TNF $\alpha$ , could up-regulate endothelial surface expression of their receptor. Levels of upregulation observed between different treatments were not significantly different from each another. This suggests that at similar doses, IL-36 cytokines are as potent at driving IL-36R expression on VCEC as the well characterised inflammatory cytokine TNF $\alpha$ . These data provide what we believe to be new insights into

the fundamental biology of this cytokine. The ability of some cytokines to increase the expression of their receptor is not new. Indeed, Takii and colleagues showed that IL-1 $\beta$  could enhance gene and surface expression of its own receptor in pulmonary fibroblast cells within 2 hours (45). Autoregulation forms a positive feedback loop, which drives a strengthened activation of the signalling pathway of a given cytokine. Here we show that IL-36 cytokines may also utilise this autoregulatory phenomenon to enhance their own activity.

Interestingly, expression of IL-36 cytokines on VCECs was not as prominent as the IL-36 receptor. This may be linked to the fact that these cells were not permeabilised, and so the labelling antibody was likely not able to enter the cell where the cytokine was located. It is possible that there was some cytokine 'secreted' onto the surface of the cells when the cells were stimulated with TNF $\alpha$  or IL-36, but this was at low concentrations as evident from the immunofluorescence images. Unlike other cytokines, IL-36 cytokines are not released by viable cells via the classical ER-Golgi export pathway and is, instead liberated by triggers that promote cell necrosis [112]. Indeed, early studies demonstrated that IL-36 could only be secreted by stimulating macrophages with LPS/ATP, or keratinocytes with the poly(I:C), a viral mimic. In lung macrophages, IL-36 was observed to be secreted in a Golgi-independent manner within vesicles and exosomes [112]. In this respect and others, IL-36 acts very much like a classical DAMP.

Interestingly, intense IL-36/IL-36R staining was noted on the outer tunica adventitial layer of larger blood vessels. Inflammatory responses are generally considered to be initiated in an 'inside-out' manner through the capture of circulating leukocytes by the endothelial surface. However, growing evidence supports a 'outside-in' model in which the adventitia,

previously considered an inert layer that simply provides structural support, acts as an injury ‘sensor’ within the vessel wall and subsequently directs responses to a wide array of stimuli, including ischaemia. In this model, it is proposed that resident adventitial cells such as fibroblasts become activated and secrete inflammatory cytokines and chemokines, which leads to expression of endothelial surface adhesion markers such as VCAM-1 and subsequent neutrophil recruitment to the intimal layer [279]. Although recent studies have extended IL-36 and IL-36R expression to include stromal cells such as fibroblasts, further studies will be required to determine whether their presence in the adventitial vascular layer is of significance in mediating inflammatory responses in the heart post-reperfusion injury.

### 4.3.4. Topical IL-36 Cytokine can induce an Inflammatory Response in the Beating Murine Heart *in vivo*

A common finding in diseases where IL-36 cytokines contribute to pathology is the significant presence of neutrophils. Indirect evidence supporting the ability of IL-36 to recruit neutrophils has been obtained primarily from histological or flow cytometric studies in which inhibiting IL-36R signalling reduced recruitment in diseases such as psoriasis and colitis. Recent findings by Koss and colleagues also identified IL-36 as an early and upstream driver of acute and chronic pulmonary inflammation by promoting neutrophil recruitment and production of pro-inflammatory IL-1 family cytokines and IL-6 [280]. However, the ability of IL-36 cytokines to directly promote the recruitment of inflammatory cells *in vivo* in any vascular bed, let alone the heart, has not previously been shown by real-time

imaging. To directly demonstrate that IL-36 could be pro-inflammatory in the heart, we topically applied agonists within the centre of the attached water-tight stabiliser ring. Our novel results showed that all IL-36 isoforms significantly and quickly enhanced neutrophil recruitment in the stimulated region of the beating LV in both adult and aged mice when applied topically. Neutrophil recruitment was observed in both coronary capillaries and PCVs.

Unexpectedly, aged mice appeared to have a slower 'reaction' and a reduced degree of neutrophil recruitment when compared to adult mice. For instance, the inflammatory response was rapid and appeared to plateau beyond 60 minutes in adult hearts. Although it was slower and less potent in aged hearts, neutrophil recruitment did continue to rise beyond 150 minutes. This could be due to reduced neutrophil responsiveness with age or as a consequence of inflammaging, where the already heightened basal inflammatory state seen in ageing requires a more substantial cytokine application before it is able to promote additional recruitment [165, 168, 281]. It is possible that with a more prolonged imaging period, these inflammatory responses may have reached similar, or exceeded, the maximal levels observed in adult mice. It is also possible that increases in the expression of IL-36R in aged mice may be associated with concomitant increases in circulating levels of the endogenous inhibitor IL-36Ra. This would act to protect the balance of IL-36 signalling in aged mice by inhibiting the engagement of IL-36 cytokines with their receptor. This could also explain why the same dose of topical IL-36 was unable to elicit similar or greater inflammatory responses in aged compared to adult hearts. Indeed, this has been shown to be true for IL-1Ra where higher circulating levels of this endogenous inhibitor are detected

in elderly patients and have been suggested to play a role in the decline in the inflammatory response with age [239].

Interestingly, we also showed that topical application of IL-36 was more potent than similar concentrations of topical IL-1 $\beta$  and TNF $\alpha$  at stimulating neutrophil recruitment in both adult and aged hearts. However, making simple comparisons between different cytokines is complex due to differing pharmacokinetics. Indeed, Dangerfield *et al.* (2004) showed that 30ng of IL-1 $\beta$  or 300ng of TNF- $\alpha$  is needed to induce neutrophil recruitment and transmigration in the cremaster intravital mouse model [282].

Free-flowing neutrophils decreased in response to all three IL-36 cytokine treatments in adult hearts and in response to IL-36 $\beta$  and IL-36 $\gamma$  in aged hearts. The number of free-flowing neutrophils circulating through the coronary microcirculation acts as an indirect marker of blood flow or hypoperfusion and can be attributed to events such as vasoconstriction or loss of vascular density. Whether IL-36 can change vascular tone is not known and would require further investigation. However, it is plausible that reduced blood flow, and thus free-flowing leukocytes, was due to the enhanced neutrophil (and in some cases, platelet) recruitment, reducing the ability of blood to flow in the imaged area. Previous studies have shown a reduction in blood flow as a result of neutrophil recruitment [283]. Indeed, in mouse models of Alzheimer's disease, increased neutrophil adhesion was demonstrated to slow and / or transiently inhibit flow in capillary segments. Interestingly, this study also showed that inhibition of blood flow in just 2% of capillaries due to neutrophil adhesion could dramatically reduce cerebral blood flow. This was explained by the fact that each occluded capillary decreased blood flow in both up and downstream vessels, and so a small number of occluded capillaries had an 'outsized' impact on cerebral

blood flow [284]. It is likely that a similar phenomenon also occurs in the inflamed heart in response to neutrophil adhesion within coronary capillaries.

Platelet aggregation / microthrombi formation were also enhanced following topical treatment with IL-36 $\beta$  and IL-36 $\gamma$  in adult hearts but were reduced in aged hearts. This opposing effect with ageing may be a result of structural and functional age-related changes in platelets and neutrophils [221, 222, 285]. It is not known whether the pro-thrombotic effect on platelets is driven through a direct response of IL-36 on platelets which would need to be investigated further. Indeed, IL-1 has been shown to directly activate platelets [286]. It is also possible that circulating platelets simply became trapped in vessels downstream of regions where significant occlusive neutrophil adhesion occurred. Collectively, these studies provided a rationale for exploring the therapeutic potential of IL-36 signalling blockade to attenuate microcirculatory disturbances associated with injury.

### 4.3.5. Vasculoprotective Effect of IL-36R Inhibition

The existence of three endogenous agonists but also two naturally occurring receptor antagonists, namely IL-36Ra and IL-38, underpins the importance of careful management of IL-36 pathway. Both of the endogenous inhibitors competitively bind the IL-1Rrp2 component of the heterodimer receptor, preventing recruitment of the accessory co-receptor IL-1RAcP and thus inhibiting subsequent intracellular signalling [116]. Given the potential role of IL-36 cytokines in cardiac inflammation, we sought to identify potential vasculoprotective effects of systemically injected IL-36Ra. We identified a significant

reduction (~50%) in neutrophil recruitment in IL36Ra treated adult and aged IR injured hearts. Multiphoton data showed this decrease was not limited to the surface of the heart but was reduced throughout the depth of the myocardial tissue. While there have been no previous studies which have looked at the effect of IL-36Ra on neutrophil recruitment within the heart, there have been several studies in other organs. A recent study by Contreras *at al.* (2016) showed reduced neutrophil recruitment in the gut following intestinal damage in IL-36R knockout mice [287]. IL-36Ra has also been shown to have anti-inflammatory effects in psoriasis [288]. Although in the heart, we observed no anti-platelet effect, IL-36Ra treatment still led to a significant decrease in infarct size in both adult and aged mice (around a two-fold and three-fold decrease, respectively). Since one dose of IL-36Ra was administered during the ischaemic period, it is plausible that IL-36 administration could be implemented during PCI procedures and be therapeutically efficacious in a clinical setting.

We and others have shown myocardial reperfusion is associated with an inability to return perfusion to pre-ischaemia levels particularly in the aged heart, which can lead to coronary vascular and non-vascular dysfunction [255]. Therefore, we sought to investigate the effects of IL-36Ra on overall ventricular perfusion using LSCI. The impact of IL-36Ra treatment on coronary perfusion was not negligible. Indeed, our data showed that in treated adult and aged mice, perfusion temporarily exceeded pre-ischaemic levels as soon as the LAD artery was unclamped, something not noted in untreated mice. Even after this hyperaemic response, blood flow throughout the duration of reperfusion remained elevated, during both systole and diastole, in treated adult and aged hearts compared to untreated hearts. Imaging of FITC-BSA also demonstrated an improvement in FCD at the

level of the coronary microcirculation. Improved overall perfusion and FCD may be linked to the fact that IL36Ra treatment decreased neutrophil recruitment as early as in the first 10 minutes of reperfusion, thus attenuating the build-up of activated and potentially occlusive inflammatory cells [249, 254]. These findings further highlight the importance of early anti-inflammatory interventions.

ROS are implicated in the pathogenesis of various cardiac disorders, including MI and heart failure and can promote the expression of endothelial adhesion molecules, such as ICAM-1 and VCAM-1, that are critical for neutrophil recruitment [289]. Therefore, whether IL-36Ra mechanistically conferred vasculoprotection by limiting endothelial ROS damage and VCAM-1 expression was considered in both adult and aged hearts. The anti-DNA/RNA antibody used in the study binds with high specificity and affinity to 8-hydroxy-2'-deoxyguanosine, 8-oxo-7,8-dihydroguanine and 8-oxo-7,8-dihydroguanosine. These oxidated nucleotides serve as excellent markers for DNA and RNA damage produced specifically by ROS. Flow cytometric and immunofluorescence studies demonstrated a significant decrease in IR injury mediated oxidative damage in the presence of IL-36Ra. Importantly, this decrease was evident in both adult and the more damaged aged hearts. Our data support the recent observation of reduced oxidative stress (measured using spectrophotometry of superoxide dismutase and malondialdehyde activity) in IL-36R knockout rats undergoing cardiopulmonary bypass [152]. However, we further detail that the anti-oxidative effects of IL-36Ra occur specifically on both coronary ECs and CM. It has recently been shown that IL-36 can up-regulate VCAM-1 and ICAM-1 on dermal ECs *in vitro* and that this can be reversed by the presence of an IL-36Ra [136]. Similarly, we were able to demonstrate the ability of IL-36Ra to decrease VCAM-1 expression in the IR injured

coronary microcirculation. Again, more importantly, this benefit was also observed in aged hearts where basal VCAM-1 expression was high. Collectively, our data provide novel mechanistic insights into how inhibition of IL-36/IL-36R signalling attenuates oxidative stress and VCAM-1 expression in adult and aged hearts, potentially preventing subsequent excessive neutrophil recruitment in the coronary microcirculation, which ultimately leads to decreased infarct size post-reperfusion.

### 4.3.6. Conclusion

New therapies need to be designed and optimised that are effective in improving the current poor prognosis of the ageing population post-MI. We and others have recommended that this must involve specific protection of the delicate coronary microcirculation from IR injury. Although studies on age-related changes in the inflammatory and immune systems have gathered pace, this study is the first, as far as we know, to explore the impact of age on the coronary microcirculation *in vivo* in both health and post-reperfusion injury. It is likely that the increased thromboinflammatory activation and microcirculatory perturbations that we have observed intravitaly in the aged injured heart may inhibit the therapeutic efficacy of existing and future cardiovascular drugs in the elderly. However, our finding that IL-36Ra was not only vasculoprotective but importantly remained beneficial in the setting of an age-related heightened inflammation in the coronary microvessels makes it a candidate worth pursuing clinically in elderly patients undergoing PCI for MI. In support of this is the recent work by Luo and colleagues, who

demonstrated experimentally that deficiency of IL-36 receptor protected cardiomyocytes in the setting of cardiopulmonary bypass [67].

A number of anti-inflammatories, shown to be successful in experimental studies, have met with translational failure when tested in patients with MI [5]. The major outcome measured in such clinical trials (and indeed experimental studies) is usually a long-term one – namely, the ability to prevent post-MI remodelling, a secondary non-fatal MI or death. Whether these anti-inflammatories can also protect and keep patent the coronary microcirculation in the immediate aftermath of PCI/reperfusion has received much less interest. However, this is imperative in order to improve long-term patient outcomes. It is, therefore, possible that translational failure is linked to a lack of early benefit at the level of the coronary microcirculation. In Chapter 3, we showed multiple microcirculatory perturbations, ultimately resulting in poor myocardial perfusion within minutes of reperfusion. Therefore, it is also important that the design of an anti-inflammatory therapy involves administration immediately before interventions designed to mediate reperfusion commence (e.g., PCI). However, not all clinical trials have delivered anti-inflammatories prior to reperfusion, with some administered days later [290]. Again, this may explain the lack of success of such compounds in clinical trials. Our data highlights a notable benefit to the coronary microcirculation and infarct size with early administration of IL-36Ra, which importantly is maintained in the presence of an aged co-morbidity. This indicates that early intervention with an IL-36R inhibitor is worth considering for future clinical investigations.

# **Chapter 5: Intravital Investigations of the Role of IL-36 in Mediating Sex- Specific Changes in the Injured Coronary Microcirculation**

## 5.1. Introduction

Previous research on intravital imaging of the beating heart by the Kalia group has always been conducted on male mice. However, the studies presented in this thesis so far were conducted on female mice because of the ease with which this sex of aged mice could be purchased. Interestingly, it was noted that platelet aggregation and microthrombus formation was not observed in the coronary microcirculation of adult female IR injured mice to the same extent as that previously noted by the Kalia Group in adult male IR injured mice. For this purpose, in this chapter, additional studies were conducted on adult male mice to determine whether there was a sex-dependent difference in the response of the coronary microcirculation to myocardial IR injury *in vivo*.

Clinically with regards to MI, it is well documented that women have a higher risk of hospitalized death and adverse events during an MI, and a greater incidence of mortality at 1 year follow up [174, 175]. Matetic and colleagues recently presented the results of the largest study of >7 million MI admissions in the USA and reported sex-based differences in the management and adverse outcomes over 12 years [175]. Although they noted that women were less likely to be offered a PCI, when they were, their outcome remained worse than men. They suggested that this could be linked to women consistently being older and having a higher risk profile and greater comorbidity burden (diabetes, hypertriglyceridemia, and metabolic syndrome) than men on presentation [291].

Sex differences could also be explained by the fact that cardiac function is significantly impacted by sex steroidal hormones, such as oestrogen and testosterone. While oestrogen is considered to be cardioprotective, which explains the low incidence of MI in pre-

menopausal women, excessive testosterone is seen to have detrimental effects on the heart [177]. Circulating levels of oestrogen are much lower in males and post-menopausal females than in pre-menopausal women, while levels of testosterone are found to be 10-fold higher in males than in females [177]. Moreover, and in terms of functional sex differences, the average adult heart rate in males is around 70-72 beats per minute (bpm), whereas females average around 78-82 bpm [292]. This is broadly linked to heart size, with females having a smaller heart, thus pumping less blood with each beat, and in turn, requiring a higher bpm than males. Females also have a different intrinsic rhythm to their heart which can underlie differences in bpm [292].

Sex differences in both the innate and adaptive immune response in various diseases is also a well-established phenomenon and have been seen to change with age. In general, innate, and adaptive immune responses are stronger in adult females than in males. As a result, pathogens are cleared faster in adult females, but this increases their susceptibility to autoimmune diseases and inflammation [188]. However, little is known about how biological sex impacts the thromboinflammatory responses in the coronary microcirculation *in vivo* in health and whether it increases the likelihood of microvascular disturbances post-reperfusion injury. This chapter will therefore focus on investigating whether there are any differences in the microcirculatory disturbances in adult males and adult females in response to myocardial IR injury.

### 5.1.1. Hypotheses and Aims

This chapter firstly aimed to compare the coronary microcirculatory responses to myocardial IR injured between adult male and female hearts using intravital and multiphoton microscopy. Furthermore, we sought to assess the impact of sex on overall ventricular perfusion, infarct size, IL-36/IL-36R/VCAM-1 expression and oxidative stress using LSCI, dual TTC/Evans blue staining, immunofluorescence, and flow cytometry studies. Lastly, we investigated whether the therapeutic benefits of IL-36Ra pre-treatment, demonstrated in the previous chapter, were similar in male and female mice. For the work included in this chapter, we hypothesised:

10. Coronary microcirculatory perturbations *in vivo* will differ following myocardial IR injury between adult male and female IR injured hearts
11. Expression of IL-36R, IL-36 $\alpha$ , IL-36 $\beta$  and VCAM-1, and the degree of oxidative damage will differ between adult males and females within healthy, and IR injured hearts
12. Therapeutic efficacy and mechanisms of action of IL-36Ra treatment will differ between adult male and female IR injured hearts

## 5.2. Results

### 5.2.1. General Observations

Some general differences were present between adult male mice and adult female mice. During animal handling, male mice tended to be more aggressive, and they required more

anaesthetic in the form of frequent top-ups. The average weight of male mice was also greater than females when controlled for age.

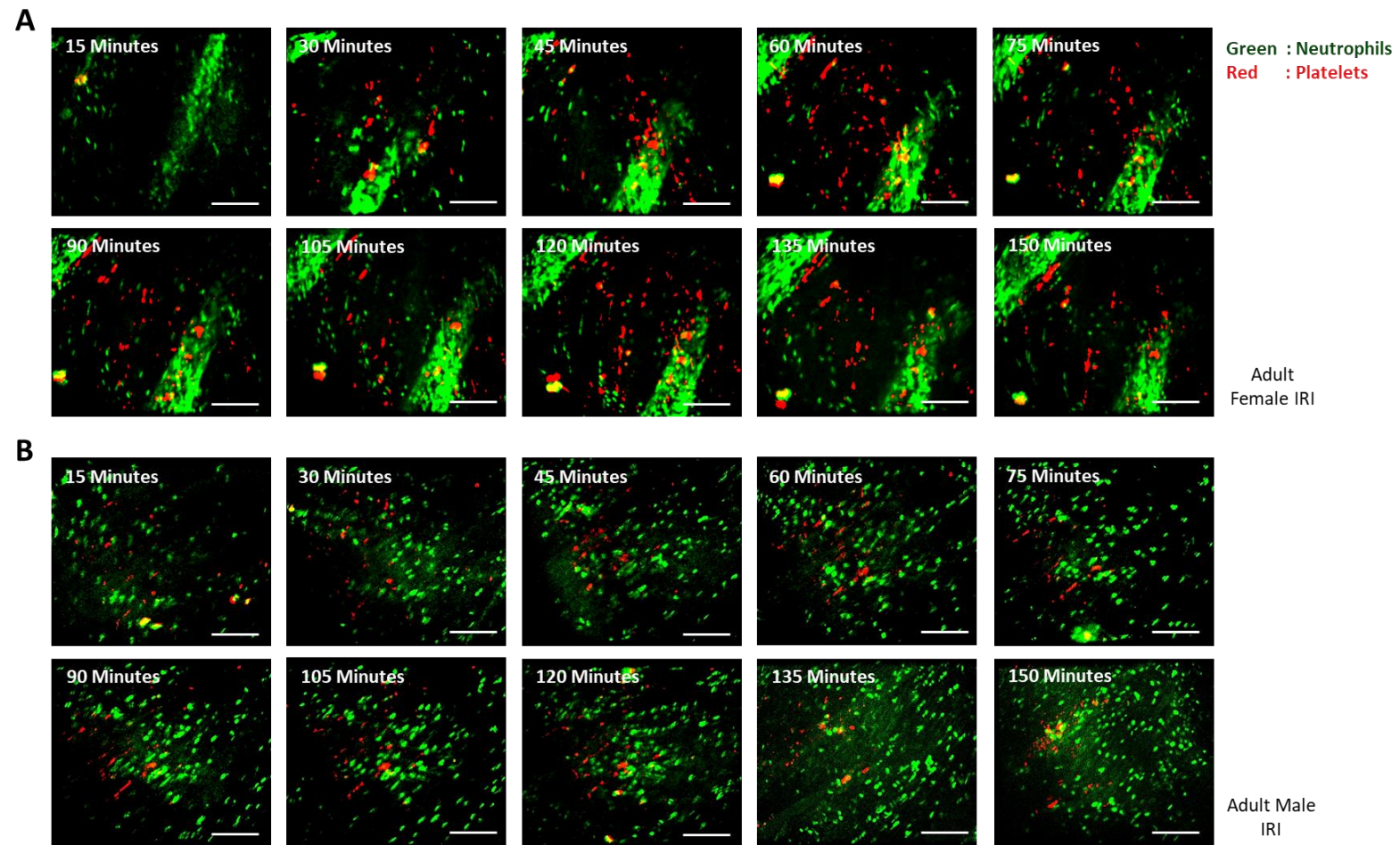
### **5.2.2. Sex-Related Differences in Thromboinflammatory Disturbances within the IR Injured Coronary Microcirculation *in vivo***

IVM studies were conducted to assess the impact of sex on thromboinflammatory events post-reperfusion in the beating mouse heart. Generally, more platelet microthrombi were observed adherent within the coronary capillaries of adult male injured hearts, and more adherent neutrophils were observed in adult female injured hearts. In some adult male injured mice, adherent neutrophils were also observed within the larger blood vessels appearing as clusters, as well as within the coronary capillaries, something not noted in adult female injured hearts (**Figure 5.1**). When analysed, a significant increase in adherent neutrophils was observed in female injured hearts when compared with their male counterparts (**Figures 5.2a-b**). However, the number of free-flowing neutrophils significantly decreased in injured male hearts when compared to their female counterparts (**Figures 5.2c-d**). A significant increase in the presence of small aggregates of platelets within capillaries was also observed in adult male injured hearts when compared to adult female injured hearts (**Figures 5.2e-f**).

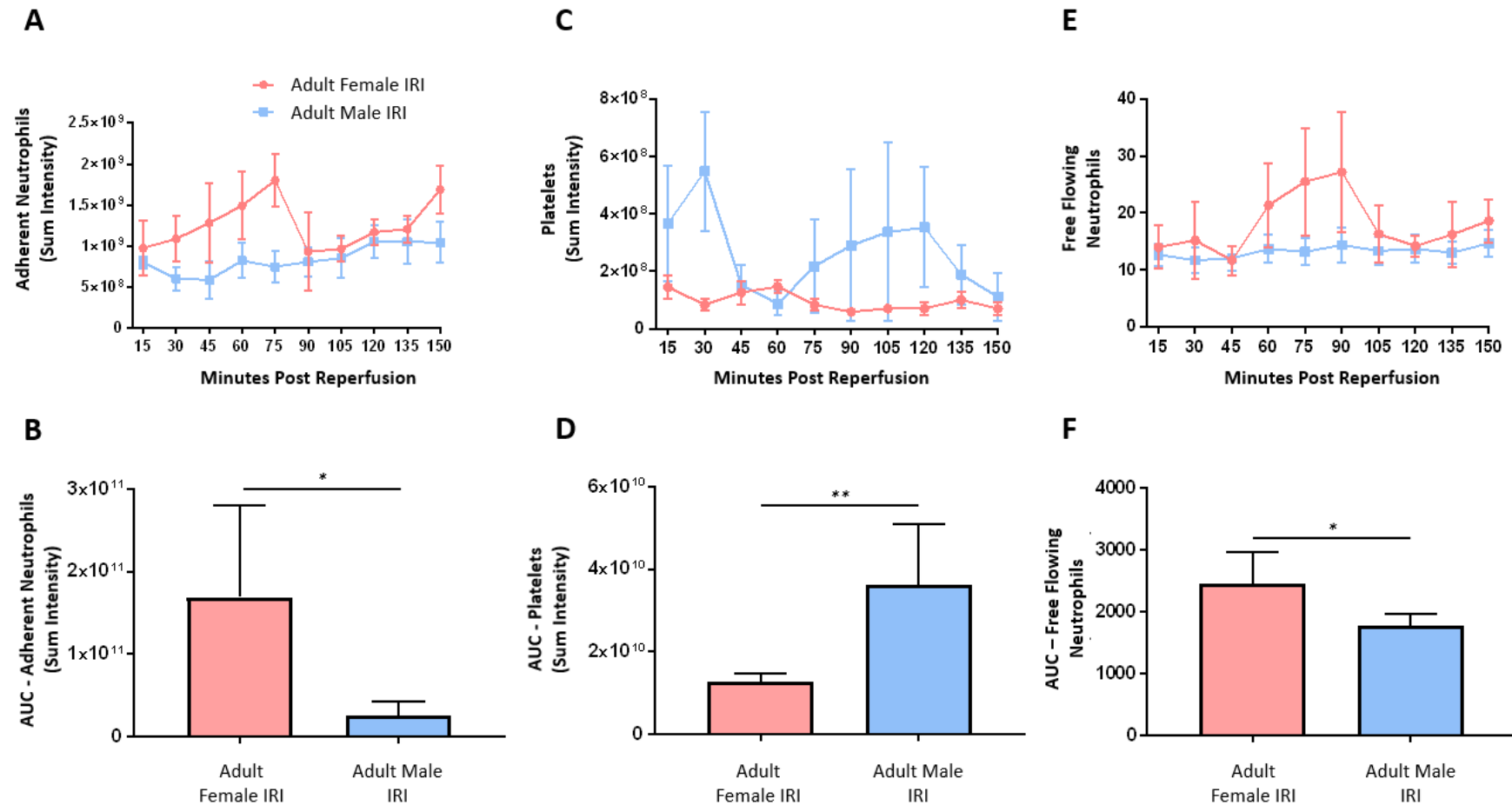
The surgical and stabilisation protocol was optimised to allow the impact of IR injury on thromboinflammatory events in the immediate aftermath of reperfusion to be assessed rather than after just 15 minutes of reperfusion. In adult male injured hearts, prior to reperfusion, a few neutrophils and platelet microthrombi were observed within the

coronary microcirculation, with neutrophil adhesion increasing with the duration of reperfusion (**Figure 5.3**). In both sexes, neutrophil presence increased within the first 30 minutes of reperfusion and continued to gradually increase over the remainder of the reperfusion phase. However, whilst no significant sex-related differences were observed within the first 30 minutes, adult female injured hearts showed significantly greater neutrophil presence as the duration of reperfusion progressed (**Figures 5.4a,c,e**). Similarly, platelet microthrombi presence also increased within the first 30 minutes of reperfusion, but more so in adult male injured hearts, although this failed to reach statistical significance. However, as the reperfusion period progressed, a significantly higher number of platelets aggregates were noted in the adult male injured coronary microcirculation (**Figures 5.4b,d,f**).

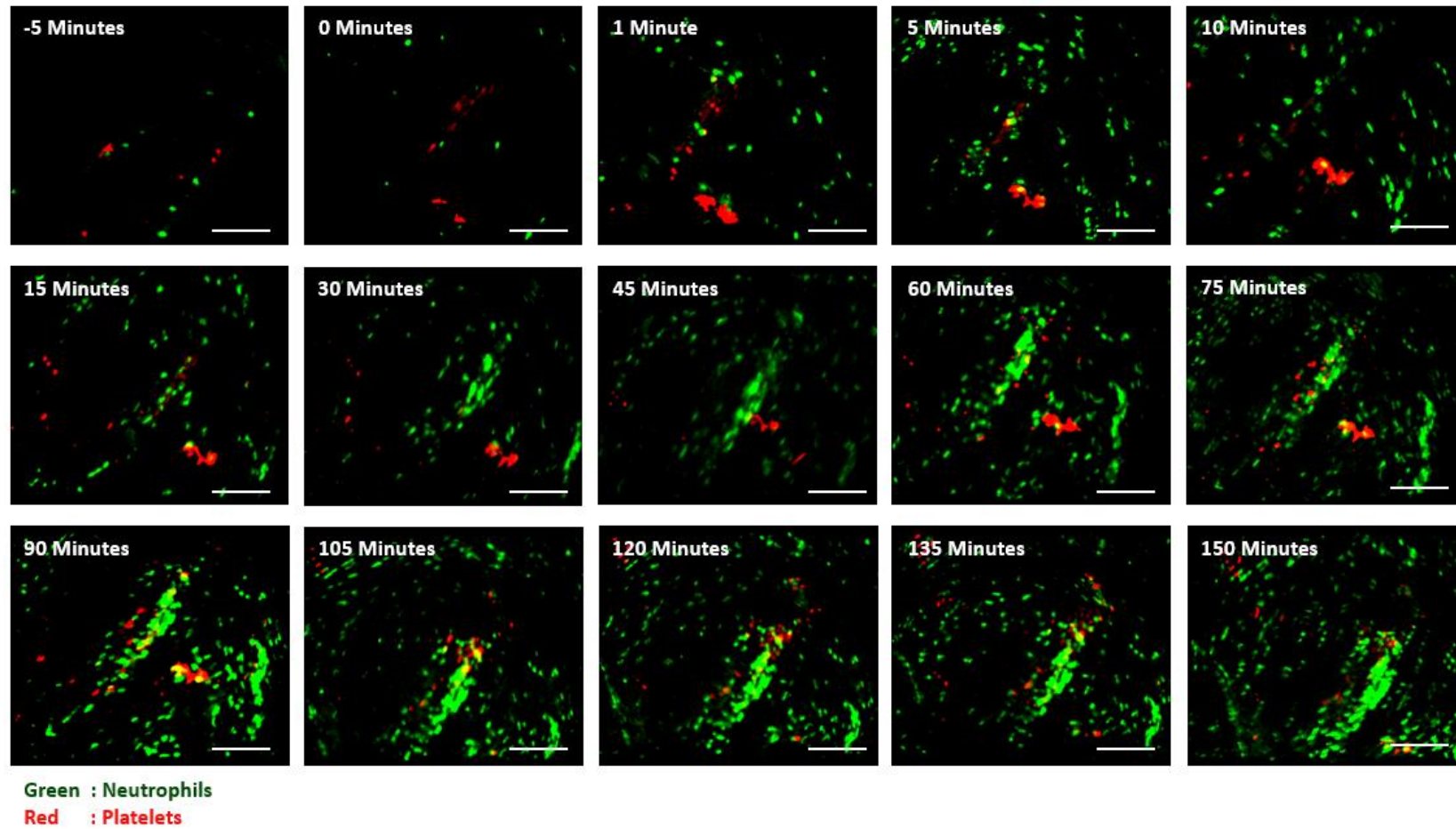
To determine whether these neutrophil events were mirrored throughout the thickness of the ventricular wall, multiphoton microscopy was performed on hearts harvested at the end of intravital experiments. Neutrophil presence was identified in both adult male and female injured hearts throughout the depth of the left ventricular wall when imaged *ex vivo* using multiphoton microscopy. In both sexes, the greatest presence of neutrophils was noted in the outermost layers of the heart closest to the epicardium and decreased with depth. However, in adult female injured hearts, a significantly greater presence of neutrophils was observed in all the layers of the heart when compared to adult male injured hearts (**Figures 5a-e**).



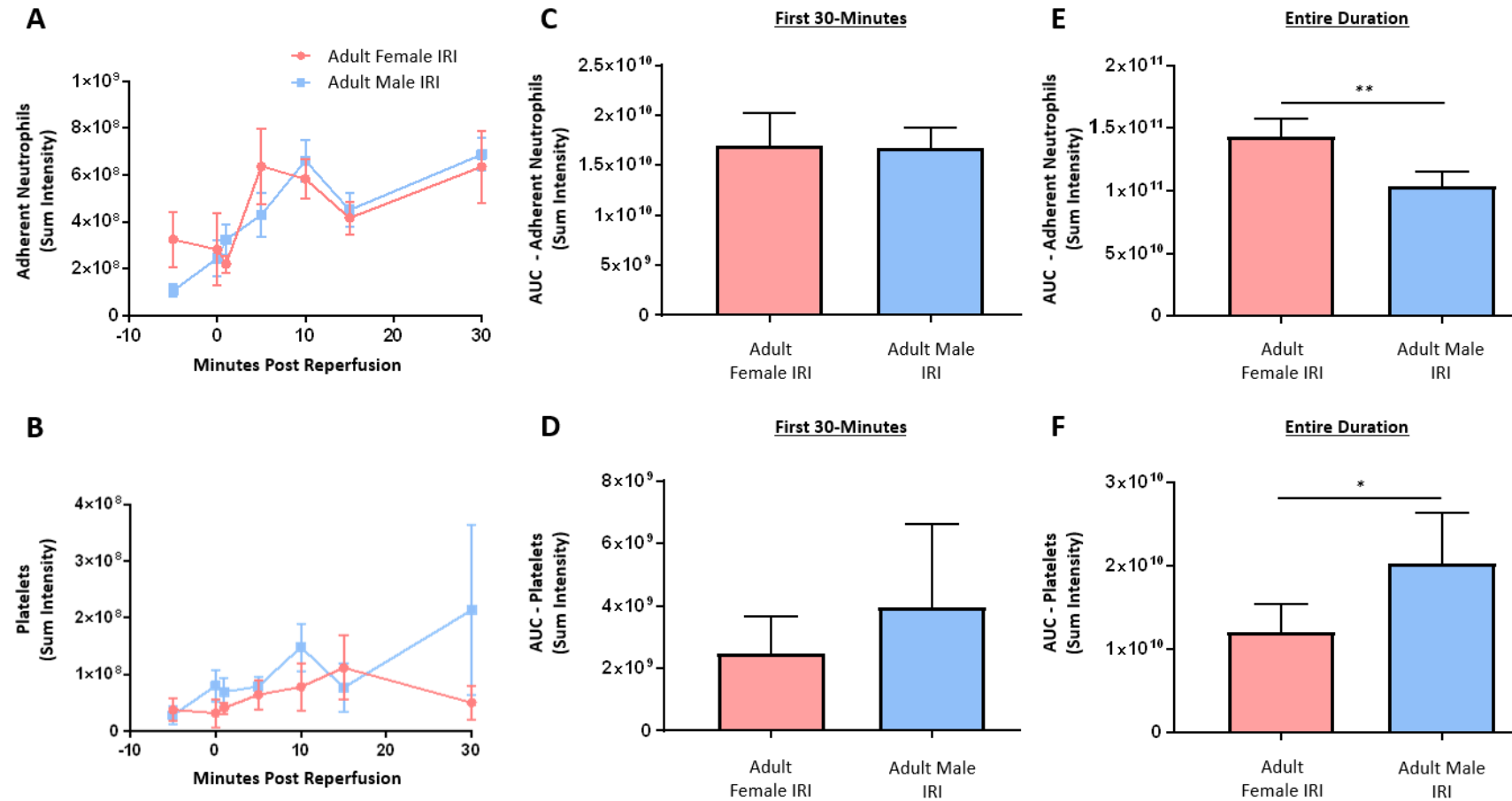
**Figure 5.1. Sex-related differences in thromboinflammation within the IR injured coronary microcirculation *in vivo*.** Representative intravital images following myocardial IR surgery in adult **(A)** male and **(B)** female mice over a time course of 150 minutes post-reperfusion. Fluorescently labelled antibodies against neutrophils (green) and platelets (red) were injected via the carotid cannula 5 minutes before reperfusion and imaged intravitaly. Scale bar indicates 100 $\mu$ m.  $n \leq 5$ /group.



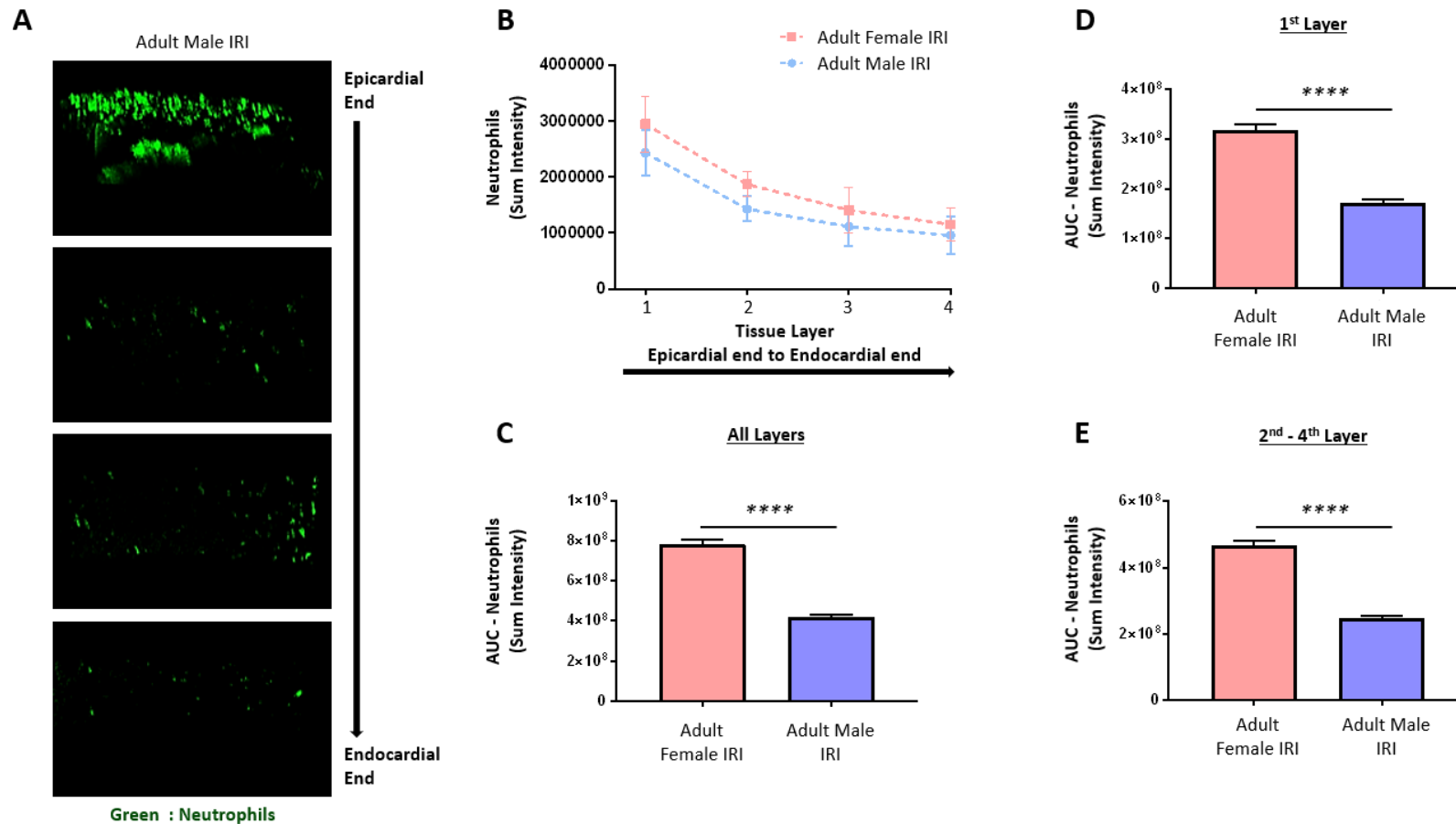
**Figure 5.2. Sex-related differences in thromboinflammation within the IR injured coronary microcirculation *in vivo*.** Myocardial IR surgery was performed on adult male and adult female mice. Fluorescently labelled antibodies against neutrophils and platelets were injected via the carotid cannula 5 minutes before reperfusion and imaged intravitaly. Quantitative time-course analysis of intravital data for **(A)** adherent neutrophils, **(C)** free-flowing neutrophils, and **(E)** platelets. Area under the curve (AUC) analysis for **(B)** adherent neutrophils, **(D)** free-flowing neutrophils, and **(F)** platelets over a time course of 150 minutes post-reperfusion. Statistical analysis was performed using a Student's unpaired t-test. Abbreviations - IRI: ischaemia reperfusion injury. n≤5/group. Mean ±SEM. \*p<0.05, \*\*p<0.01.



**Figure 5.3. IR injury induces a thromboinflammatory response immediately after reperfusion in the adult male mouse beating heart coronary microcirculation *in vivo*.** Representative intravital images following IR surgery in adult male mice over a time course of 150 minutes post-reperfusion. Fluorescently labelled antibodies against neutrophils (green) and platelets (red) were injected via the carotid cannula 10 minutes before reperfusion and imaged intravitaly. Scale bar indicates 100 $\mu$ m.  $n \leq 5$ /group.



**Figure 5.4. Sex-related differences in thromboinflammation within the IR injured coronary microcirculation only become apparent after the first 30 minutes of reperfusion *in vivo*.** IR surgery was performed on adult male and female mice. Fluorescently labelled antibodies against neutrophils and platelets were injected via the carotid cannula 10 minutes before reperfusion and imaged intravitaly. Quantitative time-course analysis of intravital data in the first 30 minutes of reperfusion for **(A)** adherent neutrophils, and **(B)** platelets. Area under the curve (AUC) analysis in the first 30 minutes for **(C)** adherent neutrophils, and **(D)** platelets and over the 150 minutes post-reperfusion for **(E)** adherent neutrophils, and **(F)** platelets. Statistical analysis was performed using a Student's unpaired t-test. Abbreviations - IRI: ischaemia reperfusion injury. n≤5/group. Mean ±SEM. \*p<0.05, \*\*p<0.01.

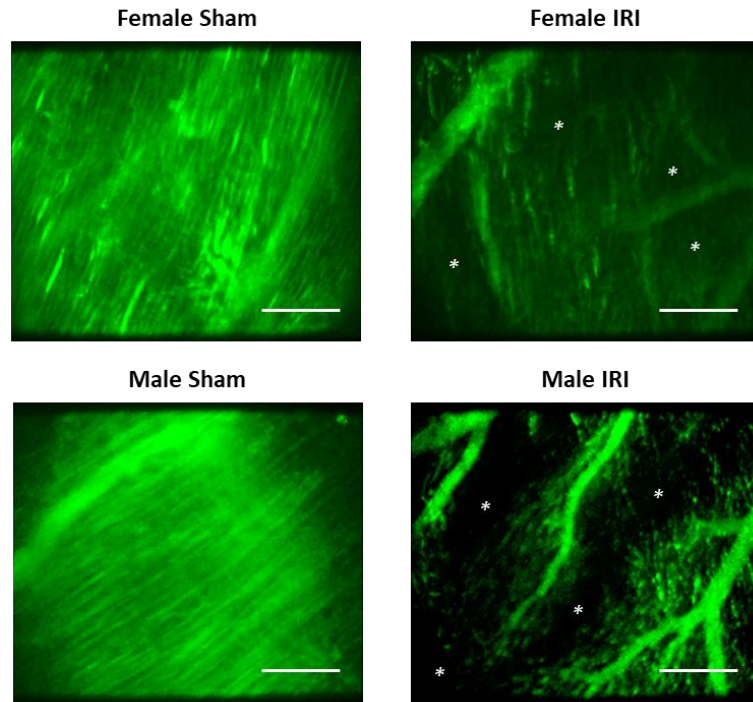


**Figure 5.5. Adult female IR injured mice have an increased neutrophil presence within the deeper layers of the myocardium when compared to male mice.** IR surgery was performed on male and female adult mice. Fluorescently labelled antibodies against neutrophils and platelets were injected via the carotid cannula 5 minutes before reperfusion and subsequently imaged intravitaly. Mice were culled following 150-minutes of reperfusion, and hearts were harvested. The LV was vibratome sectioned into four 300 $\mu$ m sections and imaged using a multiphoton microscope. **(A)** Representative Z-stack multiphoton images of neutrophils (green) in the 4 layers of the LV in the adult male IR injured mouse taken from the outermost layer closest to the epicardium (1), outer myocardial layer (2), inner myocardial layer (3) and the innermost layer closest to the endocardium (4). **(B)** Quantitative analysis of the multiphoton data at various depths for adherent neutrophils and **(C)** corresponding area under the curve (AUC) for all layers. **(D)** AUC for adherent neutrophils for the first layer, and **(E)** AUC for adherent neutrophils from layer 2-4. Statistical analysis was performed using a Student's unpaired t-test.  $n \leq 5/\text{group}$ . Mean  $\pm$  SEM. \*\*\*\* $p < 0.0001$ .

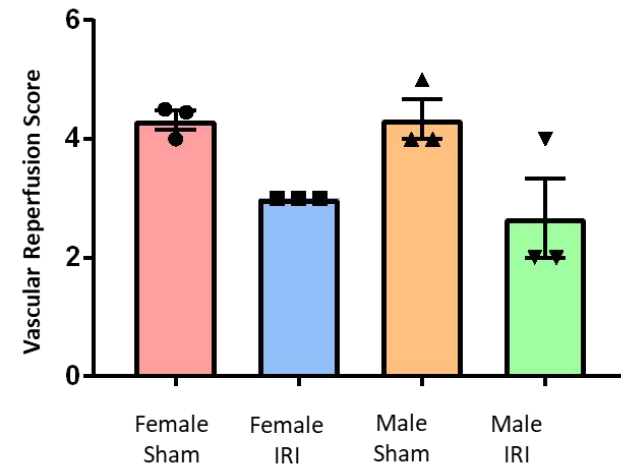
### 5.2.3. No Sex-Related Differences in Functional Capillary Density within the IR Injured Coronary Microcirculation *in vivo*

FITC-BSA was injected systemically and intravitaly imaged to assess microvascular perfusion at the level of the coronary capillaries following IR surgery in adult male and female mice. An extensive network of FITC-BSA perfused capillaries was observed in both male and female sham mice, paralleling the arrangement of muscle fibres with cross-connections along their length. Focussing up and down on the field of view showed no areas devoid of perfused capillaries. Well perfused medium-sized vessels were also visible in some fields of view (**Figure 5.6a**). In contrast, IR injury was associated with an increase in the number of areas with no perfusion, evidenced by a lack of FITC-BSA fluorescence, resulting in a poorer vascular reperfusion score in both female and male injured hearts when compared to the appropriate sex sham hearts. This patchy FITC-BSA appearance suggests reduced FCD in both sexes. However, there were no significant differences in microvascular perfusion scores between adult male and female IR injured hearts (**Figure 5.6b**).

To determine vascular leakage, a piece of tissue paper was used to collect liquid within the centre of the stabilizer between captures and was later imaged to detect FITC-BSA fluorescence. Both male and female sham hearts had little or no leakage throughout the duration of the surgery, which was evident by the use of only one tissue paper section being required to collect fluid every 15 minutes (data not presented). In contrast, IR injury of male and female hearts were associated with a similar degree of extensive leakage, whereby multiple (around 3-6) tissue paper sections had to be used every 15 minutes to collect leaked fluid.

**A**

Green : FITC-BSA

**B**

**Figure 5.6. No sex-related differences in functional capillary density within the IR injured coronary microcirculation *in vivo*.** IR surgery was performed on male and female adult mice. Fluorescently labelled antibody against bovine serum albumin (green) was injected via the carotid cannula at 120-minutes post-reperfusion and imaged intravitaly. **(A)** Representative intravital images of FITC-BSA perfused coronary microvessels in the injured hearts. Scale bar indicates 100µm. **(B)** Quantitative analysis of intravital vascular perfusion data. Statistical analysis was performed using a one-way ANOVA, followed by a Tukey's post-hoc test between four groups: adult male sham versus adult male IR injury, adult male sham versus adult female sham, adult female sham versus adult female IR injury, and adult male IR injury versus adult female IR injury. Abbreviations - IRI: ischaemia reperfusion injury. \*Areas not perfused with FITC-BSA.  $n \leq 3$ /group. Mean  $\pm$ SEM. \* $p < 0.05$ , \*\*\* $p < 0.001$ .

#### 5.2.4. Sex-Related Differences in Overall Ventricular Perfusion within the IR Injured Beating Heart *in vivo*

LSCI was used to investigate the overall myocardial perfusion of the LV in response to IR injury in adult male and female mice. As expected, ischaemia immediately decreased flow following ligation of the LAD artery in both male and female hearts. This decrease in flow was reversed as soon as reperfusion commenced in both male and female hearts. However, unlike in female hearts, perfusion failed to return to baseline pre-ischaemic levels in male hearts. Indeed, blood flow was significantly lower in IR injured male hearts when compared to IR injured female hearts (**Figures 5.7a,b and 5.8a-b**).

LSCI also allowed ventricular arrhythmia to be investigated from the flux recordings using the standard deviation of the inter-beat distance as a means to identify irregularity in the rhythm of the heartbeat. Both ischaemia and reperfusion resulted in an arrhythmic response in adult male and female IR injured mice; however, there was no significant difference between the two sexes (**Figures 5.7c and 5.8c-d**). Heart rate was not significantly changed in response to either ischaemia or reperfusion in female IR injured mice. However, a significant decrease in heart rate was seen in the male IR injured mice during reperfusion when compared to female IR injured hearts (**Figures 5.7d and 5.8e-f**).

To determine whether sex was associated with differences in overall ventricular perfusion, specifically during systole and diastole, the average flux during these two phases of the cardiac cycle in adult male and adult female injured mice was compared. As expected, ischaemia decreased ventricular perfusion during systole and diastole in both sexes. However, there was no significant difference in the ischaemic ventricular perfusion during

systole and diastole between the sexes. Again, reperfusion resulted in resumption of ventricular perfusion in systole and diastole in both adult male and female injured mice. However, perfusion was significantly decreased in both systolic and diastolic phases in adult male hearts when compared to adult females (**Figures 5.9a-d**).

#### **5.2.5. Sex-Related Differences in Myocardial Infarct Size with Females having Larger Infarcts**

Dual Evans blue and TTC staining was used to determine the impact of myocardial IR injury on the infarct size in adult male and female hearts. Overall infarct size in adult female IR injured mice were significantly larger when compared with adult male IR injured mice, particularly in layer 2 and layer 3 of the heart (**Figures 5.10a-c**). The overall AAR and area not at risk was not significantly different between male and female IR injured hearts (**Figures 10d-f**).

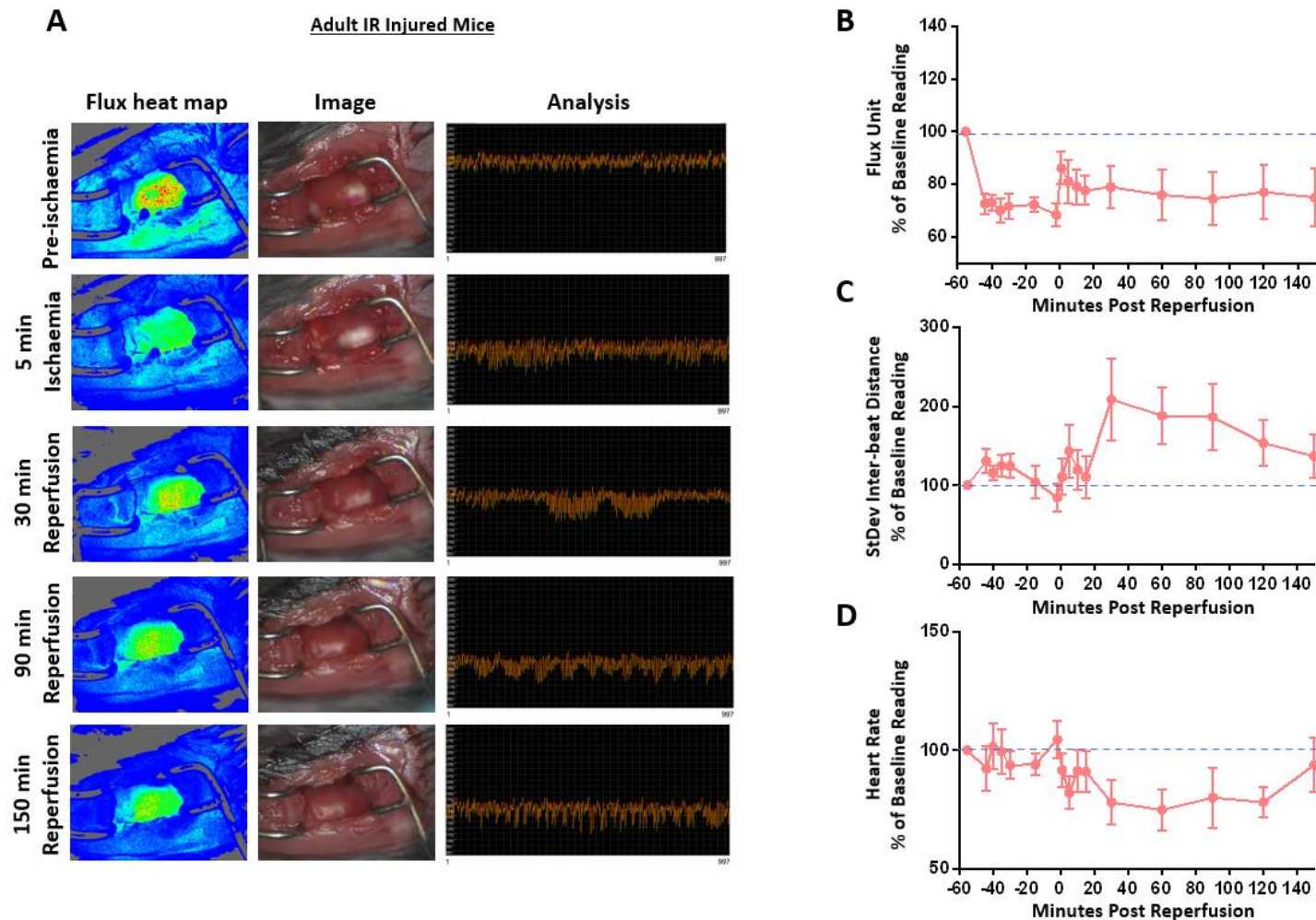


**Figure 5.7. Typical LSCI readings from an adult male mouse undergoing myocardial IR injury showing perfusion not returning to baseline values after reperfusion is commenced.** IR surgery was performed on adult male mice. Video captures were obtained throughout the surgery using laser speckle contrast imaging (LSCI). **(A)** Representative images of LSCI at various time points showing the flux heat map, still image of the beating heart, and analysis graph in adult male mice. Baseline capture prior to ischaemia was used as the baseline reading; indicating good perfusion. Quantitative time-course analysis of LSCI data for **(B)** flux unit (perfusion), **(C)** standard deviation of the inter-beat distance (arrhythmia), and **(D)** heart rate. Mean  $\pm$ SEM.  $n = 6$ /group.

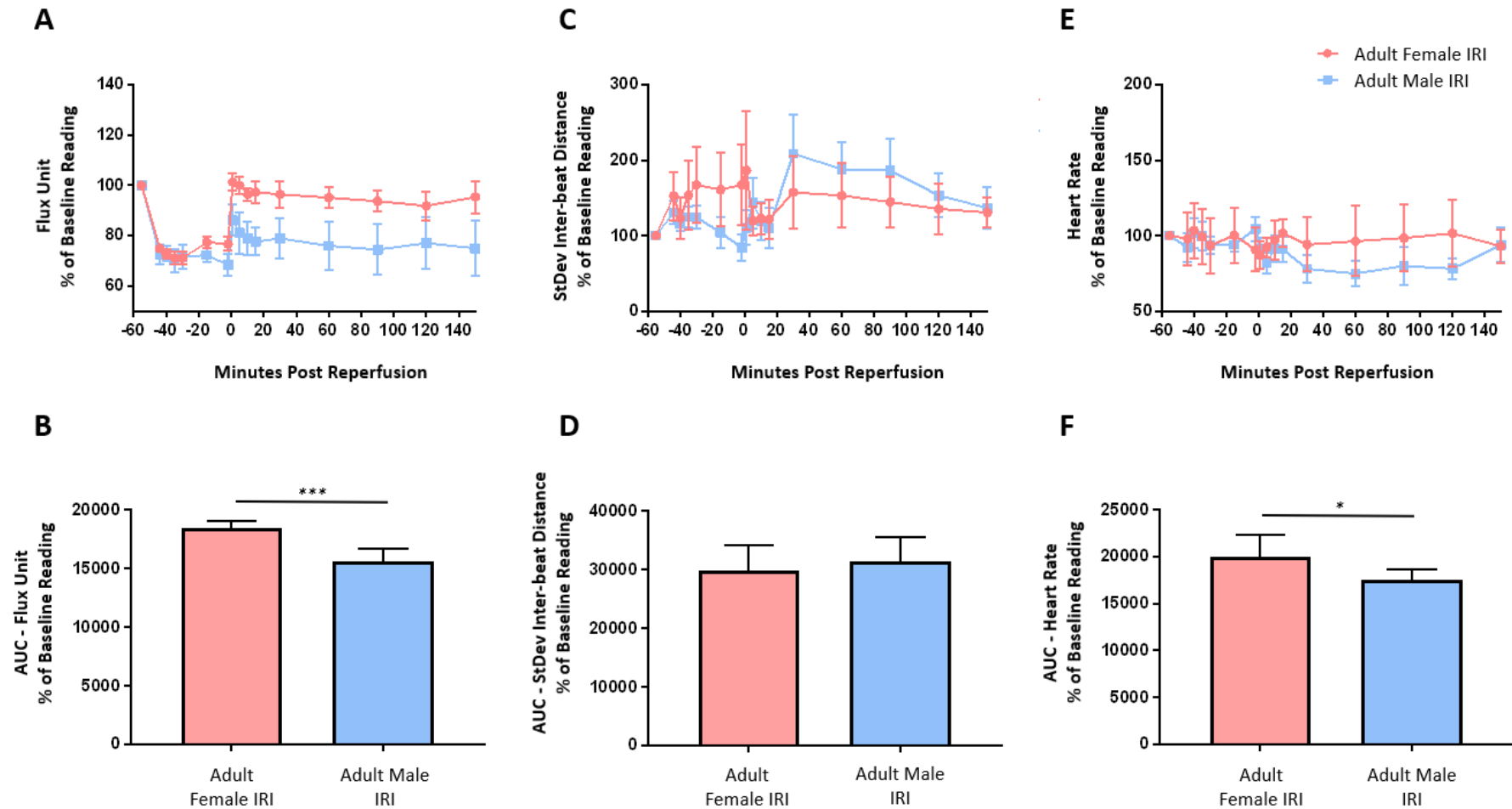


**Figure 5.8. Sex-related differences in overall ventricular perfusion within the IR injured beating heart *in vivo* with adult mice having decreased overall perfusion than females.** IR surgery was performed on adult male and female mice. Video captures were obtained throughout the surgery using laser speckle contrast imaging (LSCI). Quantitative time-course analysis of LSCI data for **(A)** flux unit (perfusion), **(C)** standard deviation of the inter-beat distance (arrhythmia), and **(E)** heart rate. Area under the curve (AUC) analysis for **(B)** flux unit, **(D)** standard deviation of the inter-beat distance, and **(F)** heart rate over a time course of 150 minutes post-reperfusion. Statistical analysis was performed using a Student's unpaired t-test. Abbreviations - IRI: ischaemia reperfusion injury.  $n = 6/\text{group}$ . Mean  $\pm$  SEM. \* $p < 0.05$ , \*\*\* $p < 0.001$ .

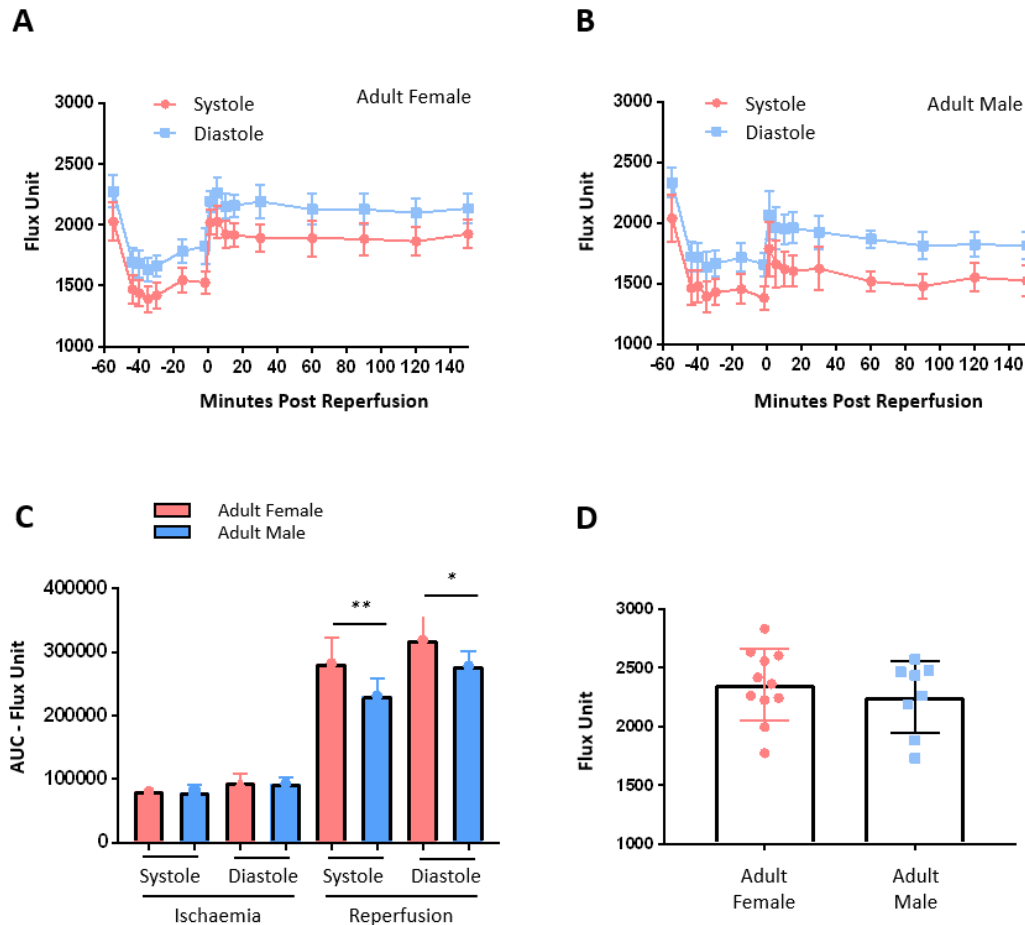


**Figure 5.9. Sex-related differences in overall ventricular perfusion within the IR injured beating heart *in vivo* with adult mice having decreased overall perfusion than females.** IR surgery was performed on adult male and female mice. Video captures were obtained throughout the surgery using laser speckle contrast imaging (LSCI). Baseline capture prior to ischaemia was used as the baseline reading; indicating good perfusion. Quantitative systole and diastole time-course analysis of LSCI data for flux unit (perfusion) in **(A)** female and **(B)** male adult mice. **(C)** Area under the curve (AUC) analysis for systole and diastole flux unit in the ischaemia and reperfusion phases. Statistical analysis was performed using a one-way ANOVA, followed by a Tukey's post-hoc test between the following groups: systole female versus systole male for each of ischaemia and reperfusion, and diastole female versus diastole aged for male of ischaemia and reperfusion. **(D)** Quantitative analysis of LSCI baseline capture prior to ischaemia. Statistical analysis was performed using a Student's unpaired t-test. Abbreviations - IRI: ischaemia reperfusion injury.  $n = 6/\text{group}$ . Mean  $\pm$ SEM. \* $p < 0.05$ , \*\* $p < 0.01$ .

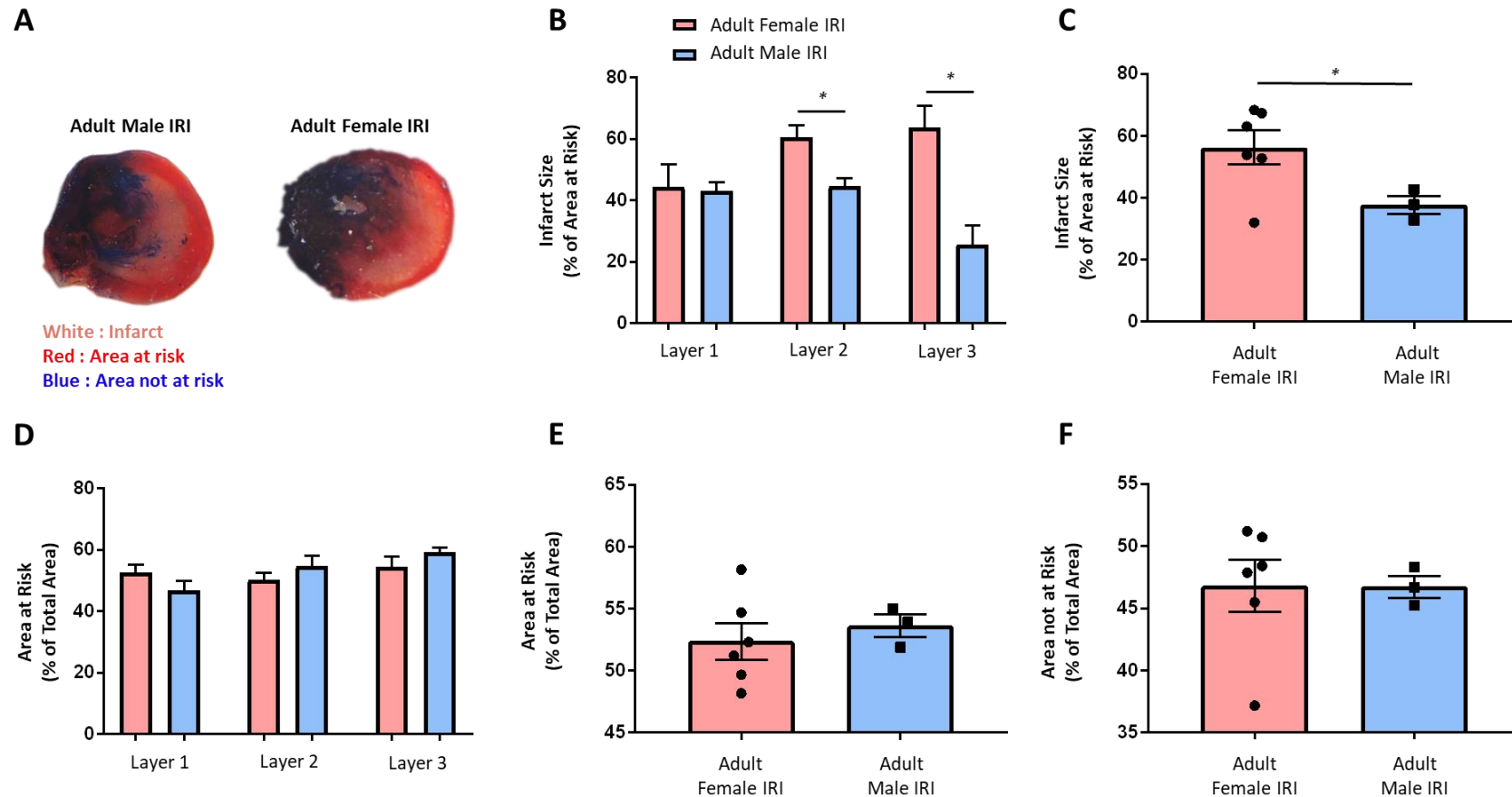


**Figure 5.10. Sex-related differences in myocardial infarct size with adult injured female mice having larger infarcts.** IR surgery was performed on male and female adult mice. Following 4-hours of reperfusion, the left anterior descending artery was re-ligated, and Evans Blue was injected. Mice were culled, and the heart was harvested, sectioned, stained with TTC and imaged. **(A)** Representative images of the TTC stained adult male and female IR injured hearts. Quantitative analysis of **(B)** infarct size in the various layers and **(C)** in the overall of the heart. Layer 1 represents the first layer below the ligature and layer 3 represents the apex of the heart. Quantitative analysis of **(D)** area at risk in the various layers, **(E)** area at risk, and **(F)** area not at risk throughout all the layers. **(B, D)** Statistical analysis was performed using a one-way ANOVA, followed by a Tukey's post-hoc test between the following groups: adult male IRI versus adult female IRI in each of the 3 layers, as well as layer 1 versus layer 2, layer 1 versus layer 3, and layer 2 versus layer 3 for each of the sexes. **(C, E, F)** Statistical analysis was performed using a Student's unpaired t-test. Abbreviations - IRI: ischaemia reperfusion injury.  $n \leq 6/\text{group}$ . Mean  $\pm$  SEM. \* $p < 0.05$ .

### 5.2.6. Sex-Related Differences in IL-36R Expression, but not VCAM-1, with Females Having a Higher Expression both Basally and after IR injury

To determine the expression and localisation of IL-36R in adult male and female mouse hearts, frozen sections were stained for IL-36R using immunofluorescence. IL-36R was found to be expressed in adult male sham hearts, albeit at very low levels, as evidenced by a positive stain on frozen tissue sections, which was not seen in the IgG controls (**Figure 5.11a**). Basal expression of IL-36R was significantly higher in adult female sham hearts when compared to adult male sham hearts. Expression of IL-36R was further significantly increased due to IR injury in both adult male and adult female hearts. However, IR injury on adult female hearts increased IL-36R expression to levels significantly higher than those seen in adult male injured hearts (**Figure 5.11b**).

Expression of VCAM-1 was also assessed in male and female hearts. VCAM-1 was expressed on the larger vasculature rather than on coronary capillaries in all 4 groups in the murine heart. Basal VCAM-1 expression was not significantly different between the sexes. Expression was seen to significantly increase in response to IR injury in both male and female mice when compared to their respective sham groups. However, there was no significant differences in VCAM-1 expression between the sexes (**Figure 5.11a and 5.11c**).

Flow cytometry was also performed to determine IL-36R expression specifically on CMs and ECs in collagenase digested hearts. CMs made up the largest portion of the cell population (around 70%), followed by ECs which made up around 15%. Dead cells made up around 0.05% of the total cell population in adult hearts. Interestingly, in male hearts, the percentage of cells that were CMs was significantly higher than in female hearts, but there were no

differences between EC percentages in males and females (**Figure 5.12a**). Flow cytometry analysis firstly confirmed the immunofluorescence results of an overall increased expression of IL-36R on CMs and ECs in response to IR injury on adult male hearts. However, it further showed that this increased expression took place on both CMs and ECs as early as 30 minutes post-reperfusion and this increase was maintained at 150 minutes (**Figures 5.12b-c**). When compared to IL-36R expression on female hearts, female CM expression was higher at both time points post-reperfusion, although this failed to attain statistical significance. However, IL-36R expression on female ECs was significantly higher at both 30 and 150 minutes post-reperfusion when compared to the expression on male ECs (**Figures 5.12d-e**).

### 5.2.7. Sex-Related Differences in IL-36 $\alpha$ and IL-36 $\beta$ Expression, with Females

#### Having a Higher Expression Basally and after IR Injury

Immunofluorescence staining for IL-36 $\alpha$  and IL-36 $\beta$  was also performed on heart sections, and expression was compared between the two sexes. Generally, IL-36 $\alpha$  and IL-36 $\beta$  had a similar pattern of receptor expression. Both cytokines were expressed on large blood vessels and a substantial number of microvessels, and also on CMs (**Figure 5.13a**). IL-36 $\alpha$  was present in male and female sham hearts albeit at very low levels. However, this basal expression of IL-36 $\alpha$  was significantly higher in female sham hearts when compared to male sham hearts. Expression of IL-36 $\alpha$  was significantly increased due to IR injury in both male and female hearts. However, IR injury on female hearts increased IL-36R expression to levels significantly higher than those seen in male IR injured hearts (**Figure 5.13b**). A similar pattern of events was observed for IL-36 $\beta$  (**Figure 5.13c**).

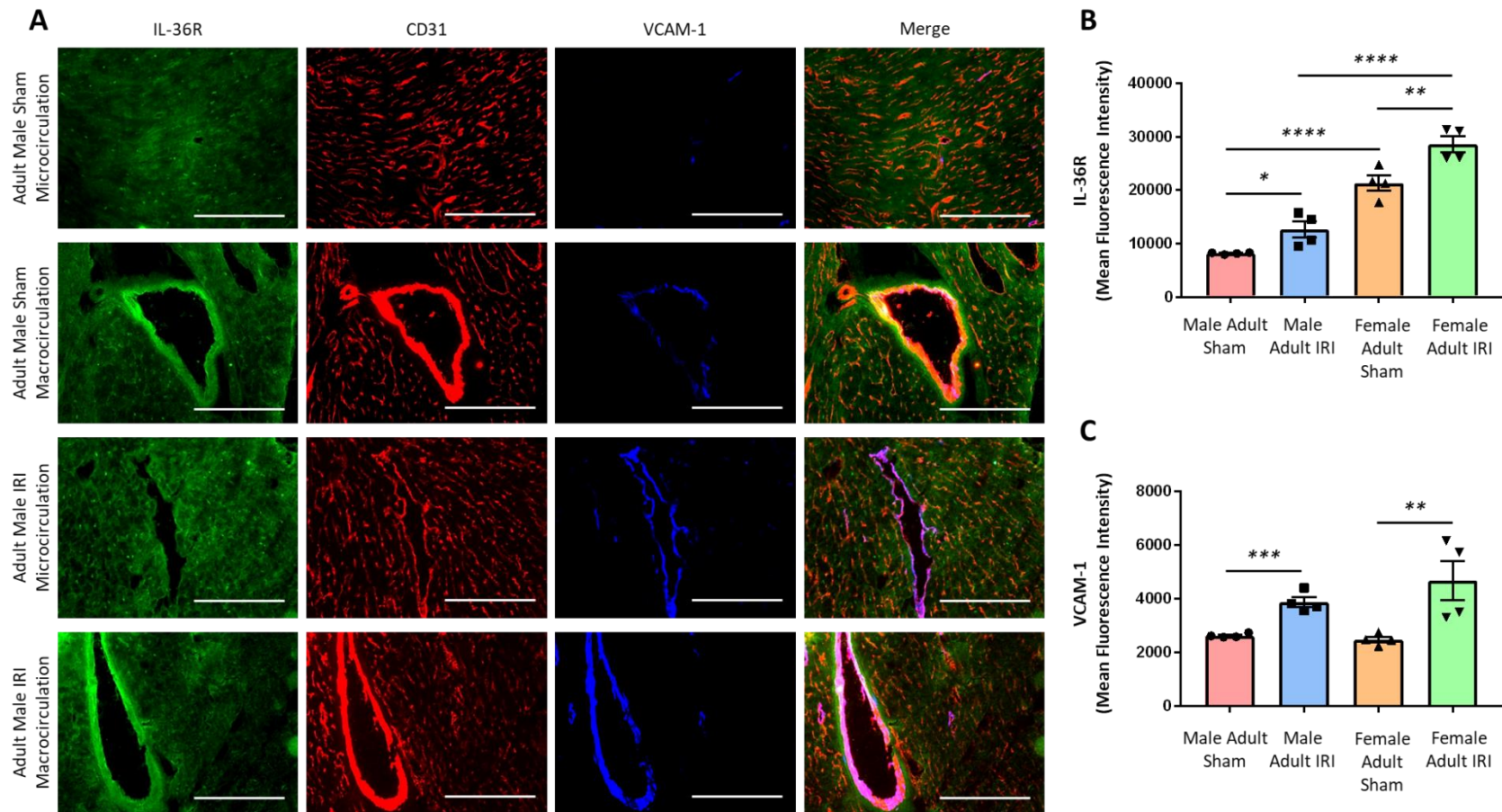


**Figure 5.11. Sex-related differences in IL-36R expression, but not VCAM-1, with adult females having a higher expression basally and after IR injury compared to adult male hearts.** Sham or IR surgery was performed on adult male and female mice. Mice were culled following 120-minutes of reperfusion, and hearts were harvested and snap frozen. The LV was transversely sectioned using a cryostat into 10µm sections and then immunostained with an antibody against IL-36R (AF488). To determine whether IL-36R (green) expression was vascular in nature and co-localised with adhesion molecules, heart sections were co-stained with an anti-CD31 antibody (red) and anti-VCAM-1 (blue) respectively. Sections were imaged using a EVOS microscope. **(A)** Representative images of IL-36R staining of frozen adult male heart sections. Scale bar indicates 200µm. Quantitative analysis of the immunofluorescent images of **(B)** IL-36R, and **(C)** VCAM-1 expression. Statistical analysis was performed using a one-way ANOVA, followed by a Tukey's post-hoc test between four groups: adult male sham versus adult male IR injury, adult male sham versus adult female sham, adult female sham versus adult female IR injury, and adult male IR injury versus adult female IR injury. Abbreviations - IRI: ischaemia reperfusion injury. n=4/group. Mean ±SEM. \*p<0.05, \*\*p<0.01, \*\*\*p<0.001, \*\*\*\*p<0.0001.

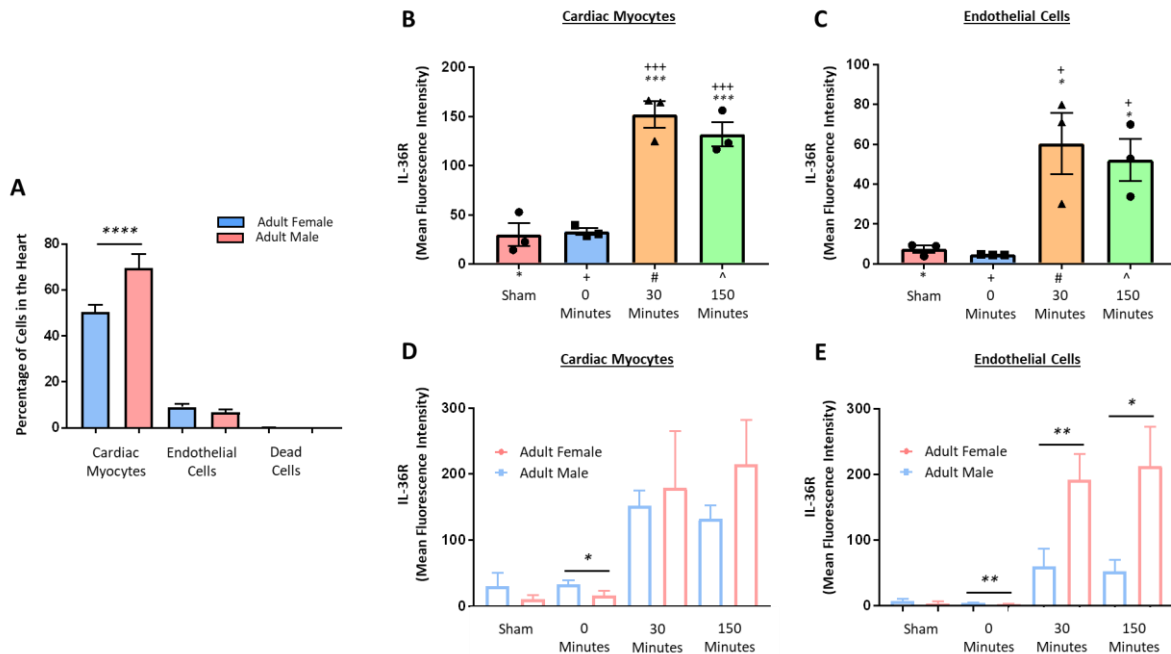


**Figure 5.12. Sex-related differences in IL-36R expression, with females having a higher expression particularly on ECs.** IR surgery was performed on adult male and female mice. Mice were culled following 0, 30 or 150-minutes of reperfusion and hearts were harvested and digested. Cell suspension was stained with an anti-CD31, anti-cTnT, and anti-IL-36R (AF488) antibodies and acquisition was performed using a CyAn™ ADP cytometer. **(A)** Quantitative analysis of the cell population within the male and female samples. Quantitative analysis of IL-36R expression in adult male mice on **(B)** cardiac myocytes, and **(C)** endothelial cells. Quantitative analysis of IL-36R expression between male and female mice on **(D)** cardiac myocytes, and **(E)** endothelial cells. Statistical analysis was performed using a one-way ANOVA, followed by a Tukey's post-hoc test between the following groups **(A)**: cardiac myocytes versus endothelial cells, cardiac myocytes versus dead cells, and endothelial cells versus dead cells between the male and female groups; as well as between male versus female cardiac myocytes, male versus female endothelial cells, and male versus female dead cells - **(B-C)**: sham versus 0 minutes, sham versus 30 minutes, sham versus 150 minutes, 0 minutes versus 30 minutes, 0 minutes versus 150 minutes, and 30 minutes versus 150 minutes - **(D-E)**: adult male sham versus adult female sham, adult male 0 minute versus adult female 0 minute, adult male 30 minutes versus adult female 30 minutes, and adult male 150 minutes versus adult female 150 minutes.  $n=3/\text{group}$ . Mean  $\pm$ SEM.  $*/+/\#p<0.05$ ,  $*/++/\##p<0.01$ ,  $*/++/\###p<0.001$  with  $*$ vs adult male sham,  $+$ vs adult male 0 minutes,  $\#$ vs adult male 30 minutes,  $\wedge$ vs adult male 150 minutes.

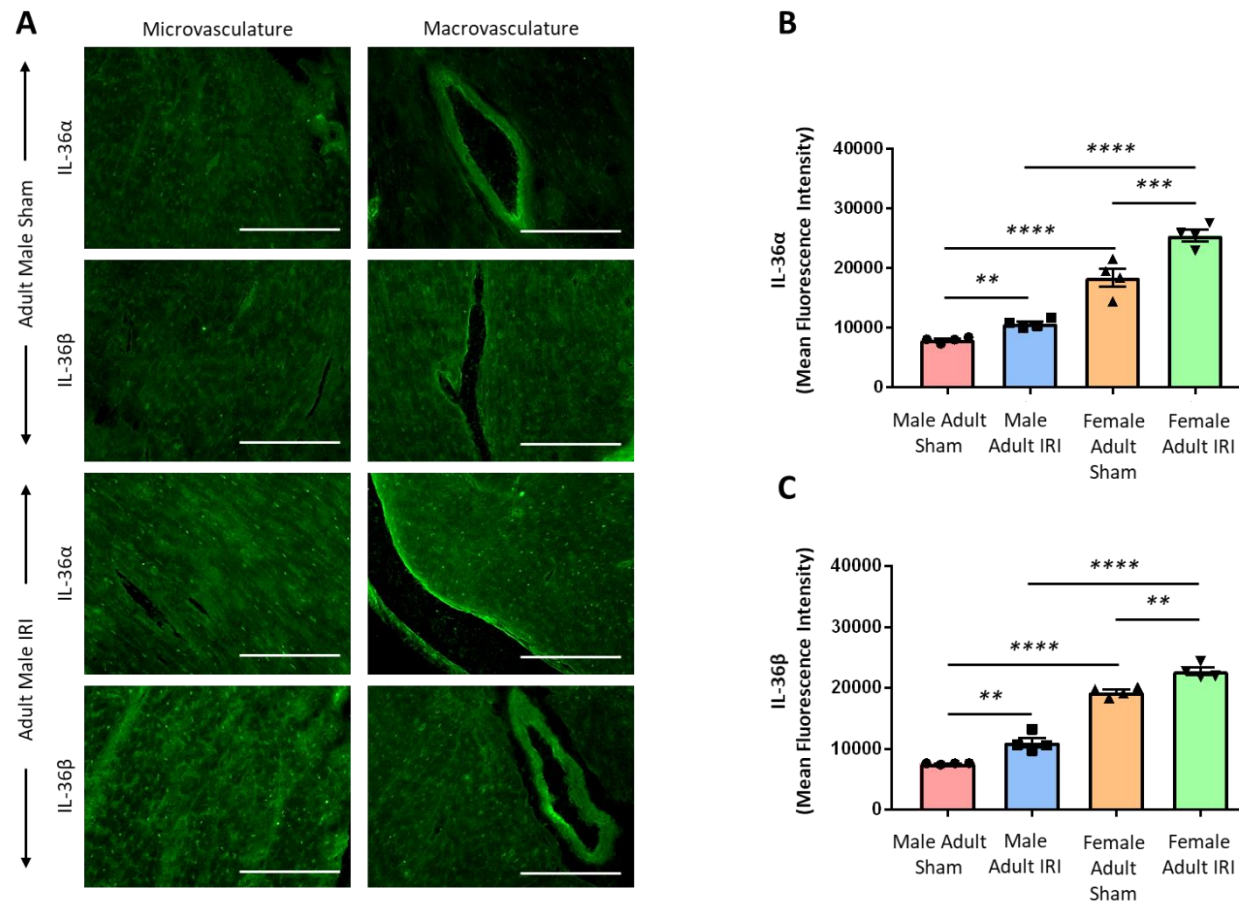


**Figure 5.13. Sex-related differences in IL-36 $\alpha$  and IL-36 $\beta$  expression with females having a higher expression basally and after IR injury compared to adult male hearts.** Sham or IR surgery was performed on adult male and female mice. Mice were culled following 120-minutes of reperfusion, and hearts were harvested and snap frozen. The LV was transversely sectioned using a cryostat into 10 $\mu$ m sections and then immunostained with an antibody against either IL-36 $\alpha$  or IL-36 $\beta$  (AF488). Sections were imaged using a EVOS microscope. **(A)** Representative images of IL-36 $\alpha$  and IL-36 $\beta$  staining of frozen adult male heart sections. Scale bar indicates 200 $\mu$ m. Quantitative analysis of the immunofluorescent images of **(B)** IL-36 $\alpha$ , and **(C)** IL-36 $\beta$  expression. Statistical analysis was performed using a one-way ANOVA, followed by a Tukey's post-hoc test between the following groups: adult male sham versus adult male IR injury, adult male sham versus adult female sham, adult female sham versus adult female IR injury, and adult male IR injury versus adult female IR injury. Abbreviations - IRI: ischaemia reperfusion injury. n=4/group. Mean  $\pm$  SEM. \*p<0.01, \*\*\*p<0.001, \*\*\*\*p<0.0001.

### 5.2.8. Sex-Related Differences in DNA/RNA Oxidative Damage, with Males having Greater Oxidative Damage, Particularly on Cardiomyocytes

Oxidative damage was determined on both CMs and ECs by using flow cytometry of collagenase digested hearts from all four groups. Significant oxidative damage took place on both CMs and ECs as early as 30 minutes post-reperfusion in adult male injured hearts when compared to adult male sham hearts. This oxidative damage remained significantly elevated on CMs and ECs even at 150 minutes post-reperfusion when compared to adult male sham hearts, but was no different to that seen at 30 minutes post-reperfusion (**Figures 5.14a-b**). This was then compared to oxidative damage on adult female hearts. Oxidative damage on adult male CMs was significantly higher in healthy sham hearts, at 0 minutes post-reperfusion, 30 minutes post-reperfusion and 150 minutes post-reperfusion when compared to adult female CMs (**Figure 5.14c**). Even on ECs, oxidative damage on male ECs was significantly higher in healthy sham hearts and at 0 minutes post-reperfusion, but not at 30- or 150-minutes post-reperfusion when compared to adult female CMs (**Figure 5.14d**).

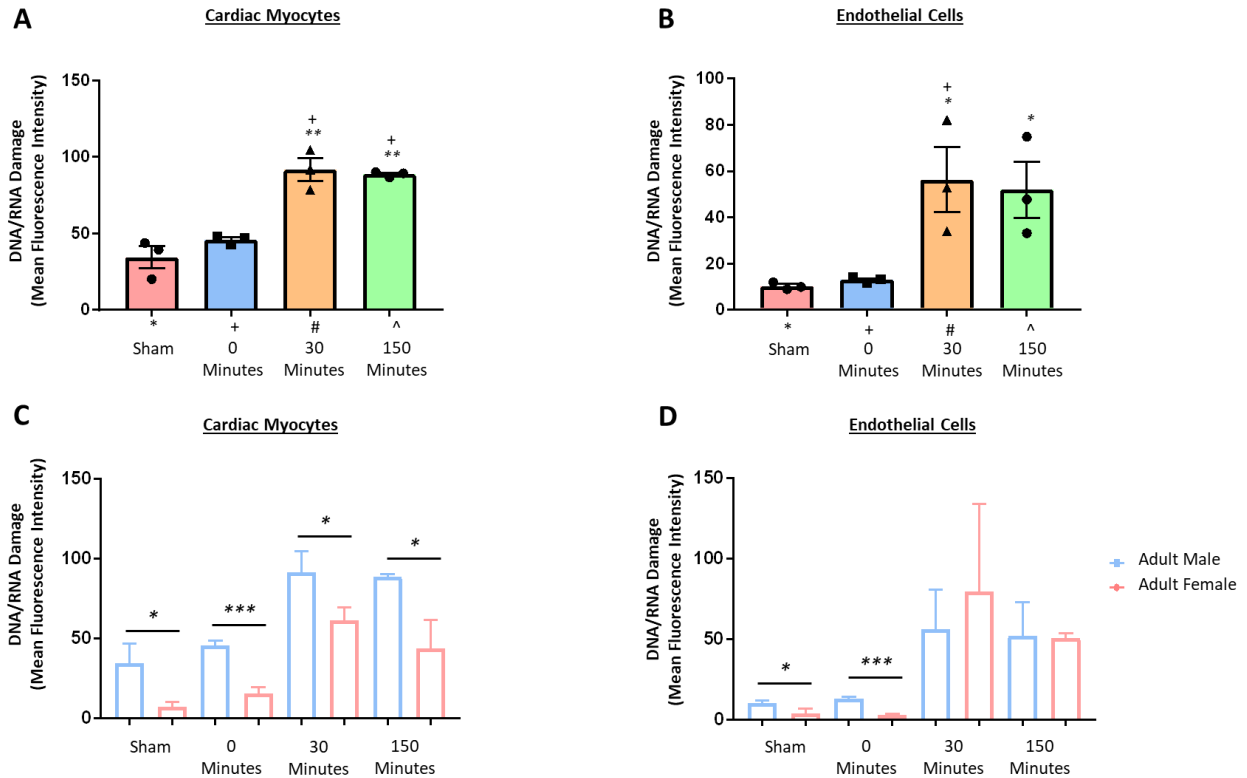


**Figure 5.14. Sex-related differences in DNA/RNA Damage, with males having greater damage, particularly on cardiomyocytes.** IR surgery was performed on adult male and female mice. Mice were culled following 0, 30 or 150-minutes of reperfusion and hearts were harvested and digested. Cell suspension was stained with an anti-CD31, anti-cTnT, and anti-DNA/RNA damage antibodies and acquisition was performed using a CyAn™ ADP cytometer. Quantitative analysis of DNA/RNA damage in adult male mice on (A) cardiac myocytes, and (B) endothelial cells. Quantitative analysis of DNA/RNA damage between male and female mice on (C) cardiac myocytes, and (D) endothelial cells. Statistical analysis was performed using a one-way ANOVA, followed by a Tukey's post-hoc test between the following groups (A-B): sham versus 0 minutes, sham versus 30 minutes, sham versus 150 minutes, 0 minutes versus 30 minutes, 0 minutes versus 150 minutes, and 30 minutes versus 150 minutes – (C-D): adult male sham versus adult female sham, adult male 0 minute versus adult female 0 minute, adult male 30 minutes versus adult female 30 minutes, and adult male 150 minutes versus adult female 150 minutes.  $n=3/\text{group}$ . Mean  $\pm$  SEM. \*/+/# $p<0.05$ , \*\*/+/# $p<0.01$ , \*\*\*/++/### $p<0.001$  with \*vs adult male sham, +vs adult male 0 minutes, #vs adult male 30 minutes, ^vs adult male 150 minutes.

### 5.2.9. No Sex-Related Differences in the Ability of IL-36R Inhibition to Reduce Myocardial Inflammation *in vivo*

In the previous chapter, we showed that the IL-36Ra could reduce inflammatory events in the adult (and aged) female injured heart. In this chapter, we looked to see if this inhibitor could also prevent thromboinflammatory perturbations in the adult male injured heart. This was assessed using the modified stabilisation protocol that allowed the coronary microcirculation to be imaged immediately after reperfusion was initiated. IL-36Ra significantly reduced neutrophil adhesion within the first 30 minutes of reperfusion as well as during the remaining 150 minutes of reperfusion when compared to untreated adult injured mice (**Figures 5.15 and 5.16a-c**). This anti-neutrophil effect was no different to that noted in adult female injured mice pre-treated with IL-36Ra (**Figures 5.17a-c**).

In adult male injured mice treated with the IL-36Ra, there were no significant changes in platelet microthrombi formation during the first 30 minutes of reperfusion. However, over the entire 150 minutes reperfusion period, a significant increase in platelet microthrombi presence was when compared with non-treated adult injured mice (**Figures 5.15 and 5.16d-f**). This lack of ability to prevent platelet presence in the first 30 minutes was also noted in adult female injured mice pre-treated with IL-36Ra. Also, the increased presence of platelet microthrombi over the remainder of the reperfusion phase was also noted in adult female injured mice pre-treated with IL-36Ra, although this increase was significantly higher in IL-36Ra treated adult male injured mice when compared to female injured mice (**Figures 5.17d-f**).

To determine whether these anti-neutrophil events were mirrored throughout the thickness of the ventricular wall, multiphoton microscopy was performed on hearts harvested at the end of intravital experiments. *Ex vivo* multiphoton imaging of the depth of the ventricular wall confirmed the ability of IL-36Ra to mediate a significant anti-inflammatory response throughout the depth of the tissue (**Figures 5.18a-e**). Although this was also noted in female mice, the ability of IL-36Ra to reduce neutrophil presence was better in adult male injured mice, as significantly lower neutrophils were observed in the adult male injured heart when compared to the adult female injured heart (**Figures 19a-d**).

### 5.2.10. IL-36R Inhibition Increases Functional Capillary Density, with Improvements More Notable in Female Mice *in vivo*

In order to assess microvascular perfusion following IL-36Ra treatment of adult male and female IR injured mice, FITC-BSA was administered via the carotid artery at the end of imaging. In adult male injured mice, IL-36Ra resulted in some improvement in the presence of FITC-BSA perfused capillaries when compared to untreated adult male injured mice. However, this still remained lower than that seen in healthy uninjured male sham hearts. Indeed, areas devoid of perfusion were still noted in IL-36Ra treated adult male injured hearts. In adult female injured mice, the improvements observed were more notable. Medium-sized vessels were still readily visible and well perfused in both adult male and female IL-36Ra treated hearts (**Figures 5.20a-b**).

To determine vascular leakage, a piece of tissue paper was used to collect liquid within the centre of the stabilizer between captures and was later imaged to detect FITC-BSA

fluorescence. Both male and female IL-36Ra treated hearts had reduced leakage throughout the duration of the surgery when compared with their respective non-treated IR injured group. This was evident by the use of only two to four tissue paper sections every 15 minutes in contrast to around three to six in the IR injured groups.

#### **5.2.11. IL-36R Inhibition Increases Overall Left Ventricular Perfusion in the Adult Male Beating Heart Coronary Circulation *in vivo***

LSCI was used to investigate the overall perfusion of the left ventricular myocardium in response to IL-36Ra pre-treatment in adult male and female mice. High and low points were extrapolated from flux analysis recordings and were attributed to diastolic and systolic left ventricular events, respectively (**Figure 5.21a-b**). Analysis was performed on systolic events for comparative purposes. As expected, in adult male IL-36Ra treated mice, ischaemia decreased tissue perfusion following LAD artery ligation. This was rapidly reversed as soon as the artery was untied. In adult male untreated injured mice, although flow returned, it remained below pre-ischaemic baseline values throughout reperfusion. However, in IL-36Ra treated mice, reperfusion was accompanied by a transient reactive hyperaemic response, which plateaued but remained above pre-ischaemic baseline values at all-time point post-reperfusion (**Figures 5.21b and 5.22a**). Indeed, AUC analysis showed that perfusion was significantly better in male IL-36Ra treated injured hearts when compared to non-treated adult IR hearts (**Figures 5.22b**).

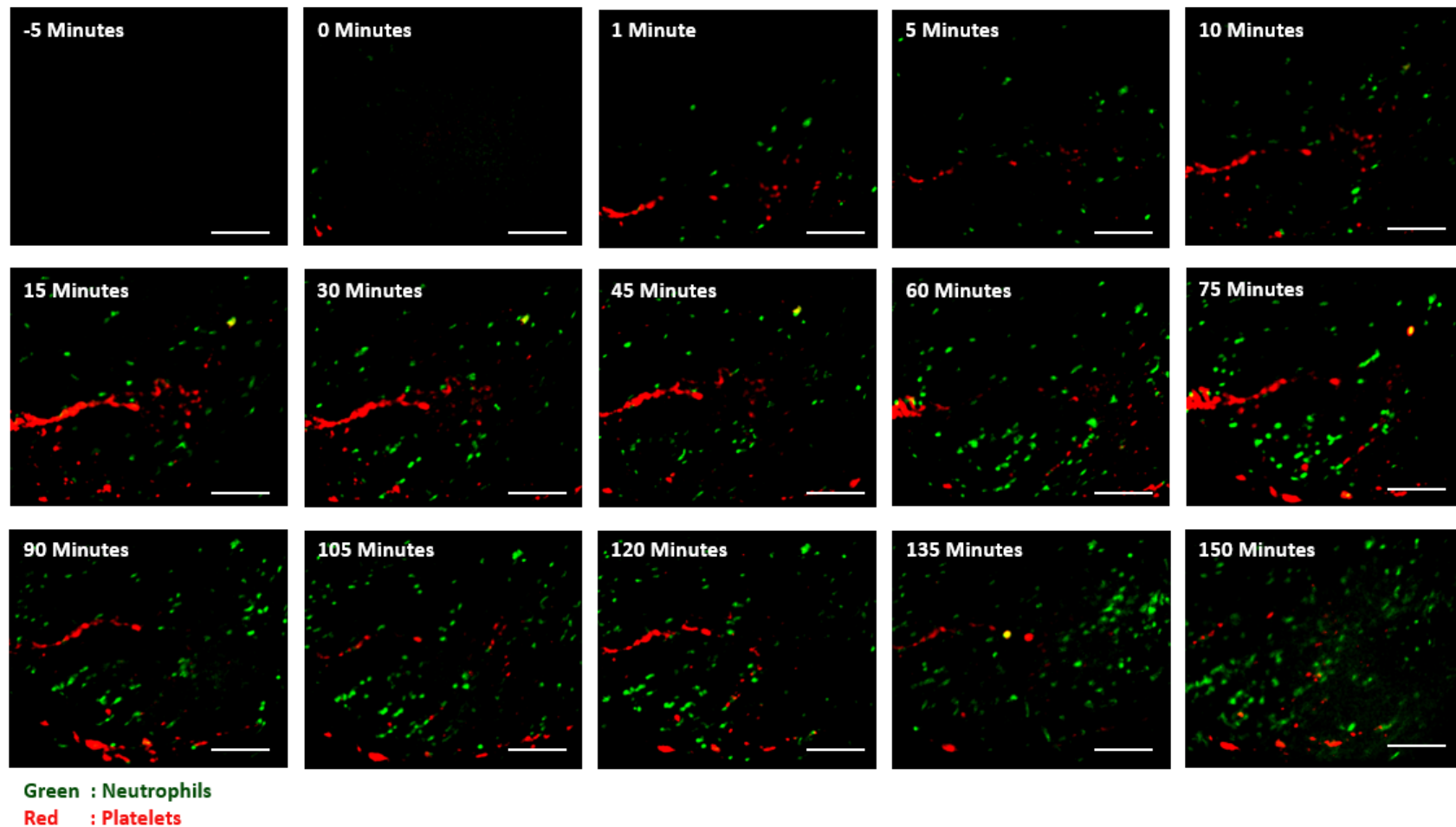
LSCI also allowed ventricular arrhythmia to be investigated from the flux recordings using the standard deviation of the inter-beat distance as a means to identify irregularity in the rhythm of the heartbeat. Both ischaemia and reperfusion resulted in arrhythmic responses in untreated male injured mice which was significantly reduced in treated adult male mice (**Figures 5.22c-d**). Interestingly, heart rate was significantly increased in response to reperfusion in adult IL-36Ra treated injured mice when compared to non-treated mice (**Figures 5.22e-f**).

To determine whether IL-36Ra treatment impacted perfusion differently during systole and diastole, the average flux during these two phases of the cardiac cycle in IL-36Ra treated and untreated adult male mice was compared. As expected, ischaemia decreased ventricular perfusion during systole and diastole in treated and untreated adult male injured mice. However, there was no significant difference in the ischaemic ventricular perfusion during systole and diastole. Again, reperfusion resulted in resumption of ventricular perfusion in systole and diastole in both treated and untreated adult male injured mice. However, perfusion was improved in both systolic and diastolic phases in adult male IL-36Ra treated injured mice when compared to untreated injured mice (**Figures 5.23a-c**).

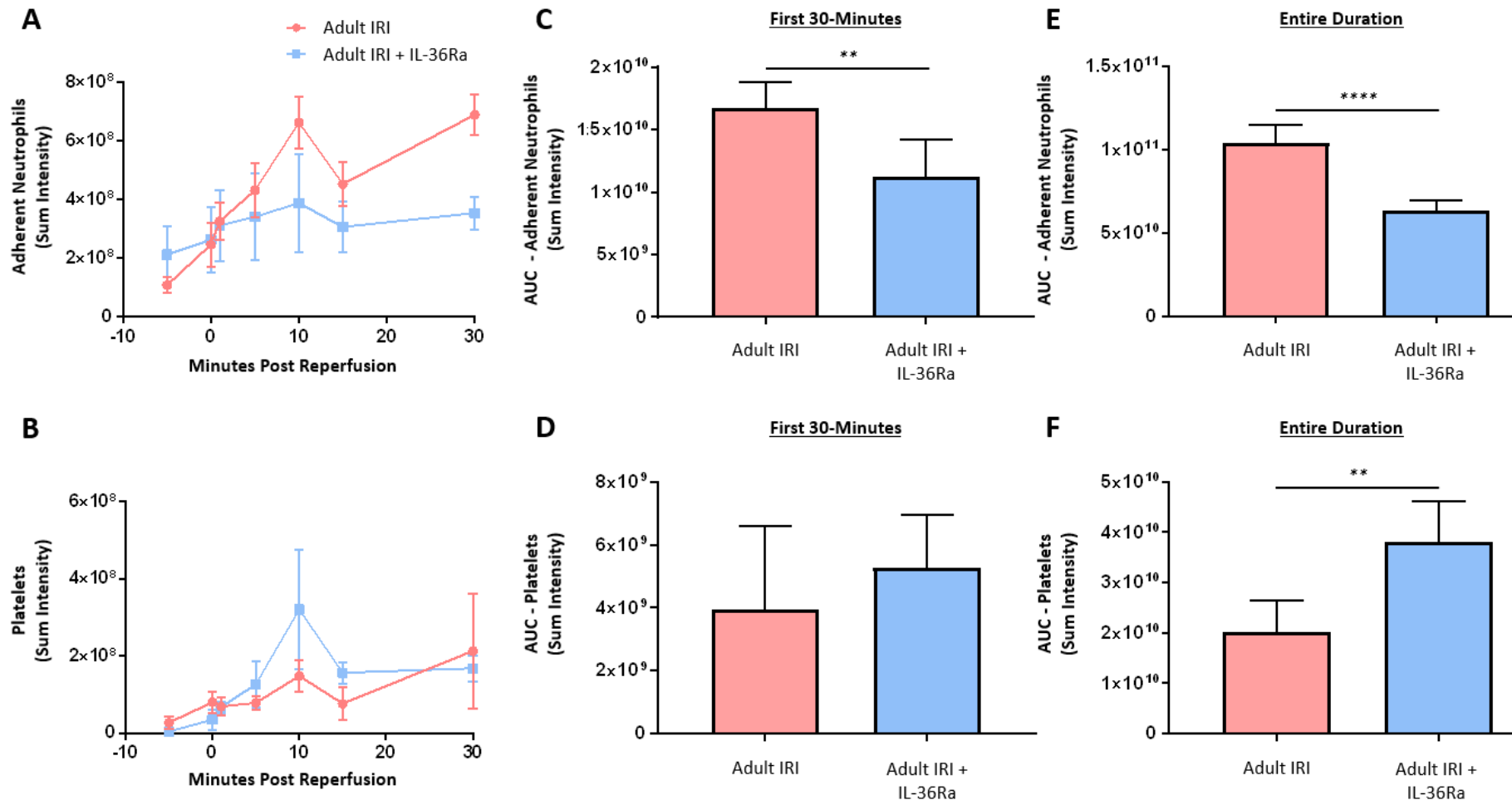
### 5.2.12. IL-36R Inhibition Decreases Infarct Size in Adult Hearts

Dual Evans blue and TTC staining was used to determine the impact of IL-36Ra on infarct size in male and female IR injured mice. There were no statistically significant differences in infarct size in the various layers of the adult male IL-36Ra treated injured hearts. However, infarct size was significantly decreased in all three layers (layer 1 –  $p < 0.05$ ; layer 2 –  $p < 0.05$ ; layer 3

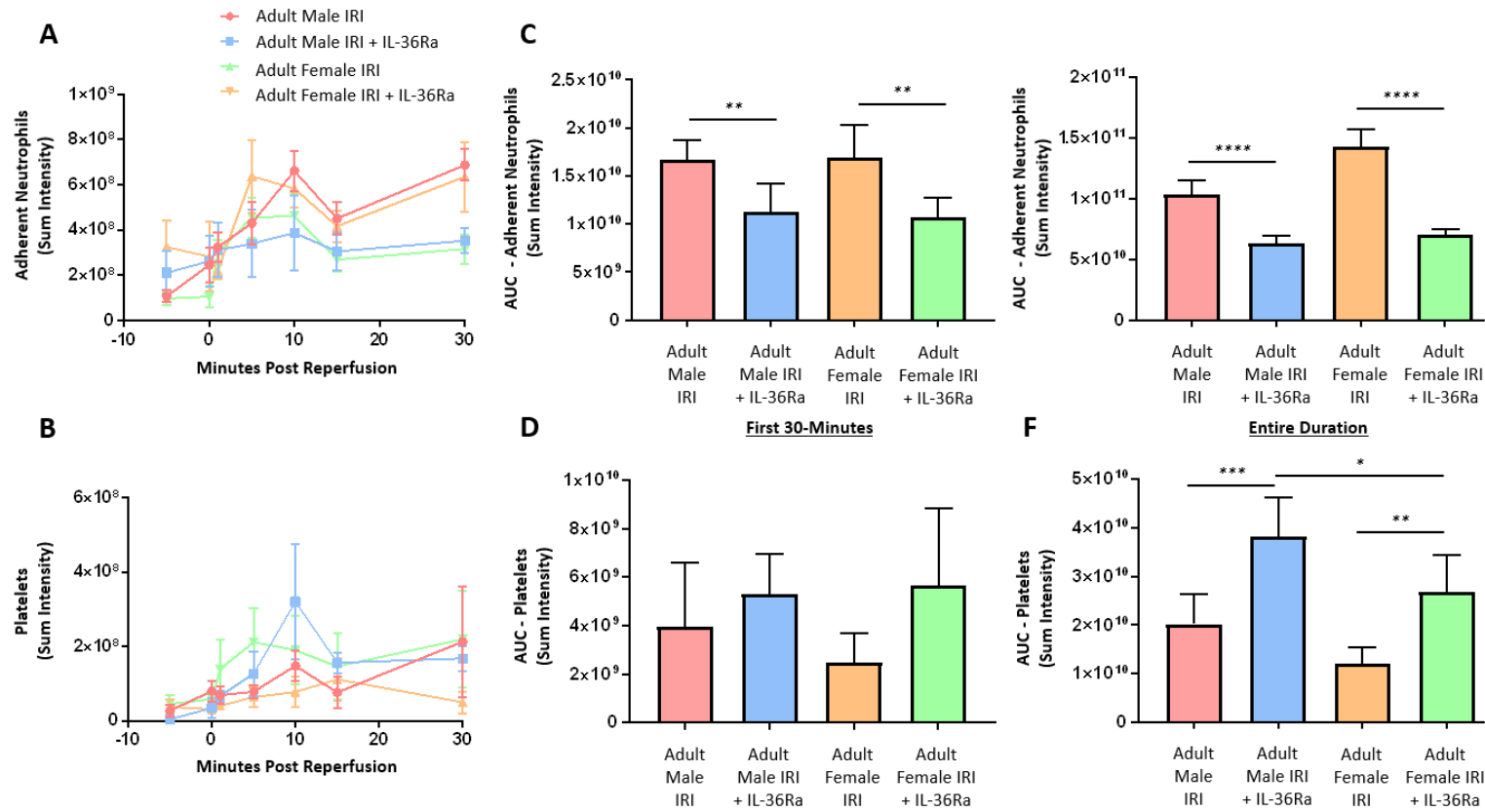
–  $p < 0.05$ ) of the male IL-36Ra when compared with the non-treated male IR injured hearts. Overall infarct size in all layers was also significantly reduced in male hearts when compared to non-treated male IR injured hearts, something which was also seen in female hearts (**Figures 5.24a-d**). AAR were not significantly different either in the various layers of the male heart or overall in all layers (**Figures 5.24e-f**).



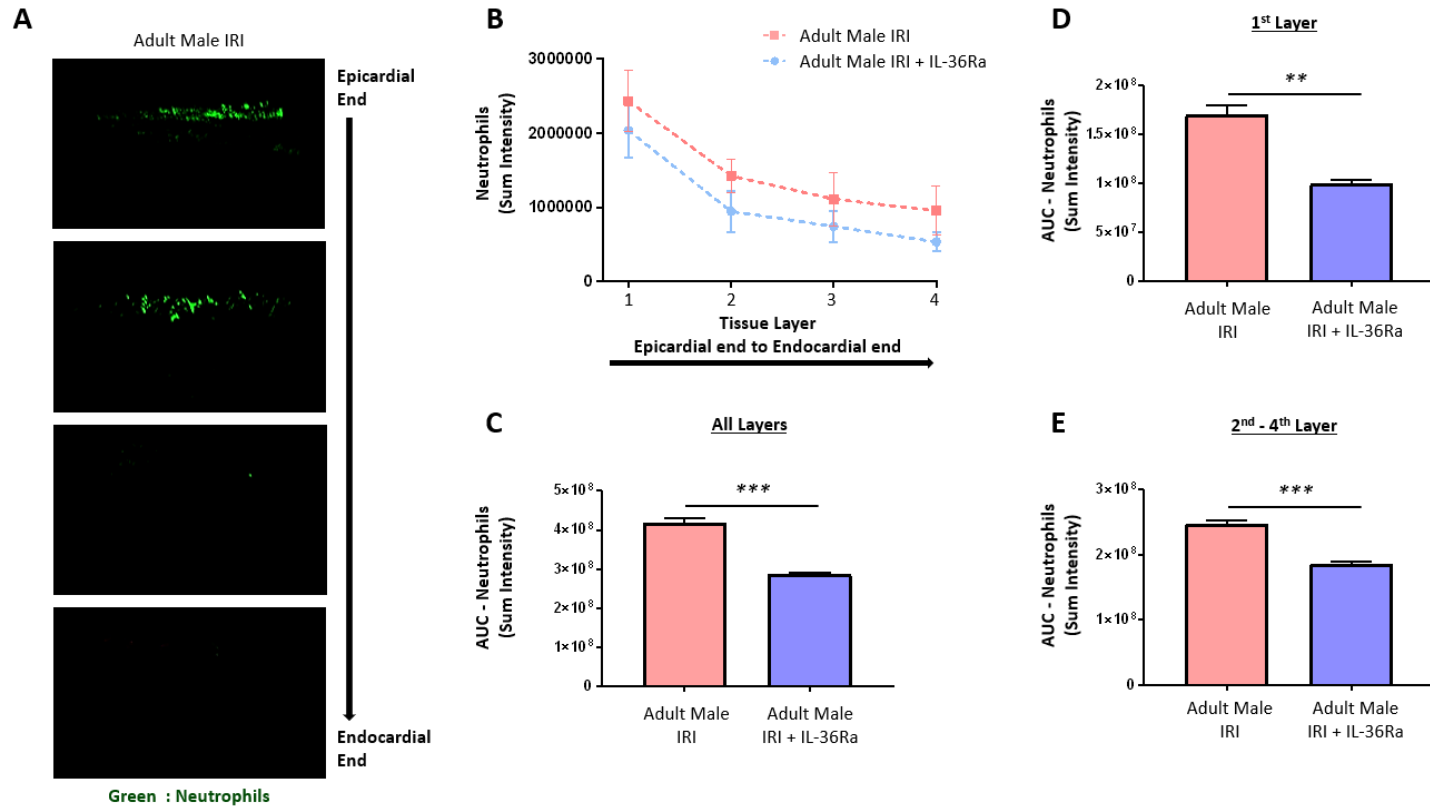
**Figure 5.15. IL-36R inhibition reduces myocardial inflammation *in vivo* in the IR injured adult male heart.** Representative intravital images following IR surgery on adult male mice in the coronary microcirculation over a time course of 150 minutes post-reperfusion. An IL-36 receptor antagonist (IL-36Ra; 15µg/mouse) was injected intra-arterially at 10 mins pre-reperfusion and 60 mins post-reperfusion in adult male mice. Fluorescently labelled antibodies against neutrophils (green) and platelets (red) were injected via the carotid cannula 10 minutes before reperfusion and imaged intravitaly. Scale bar indicates 100µm. n≤5.



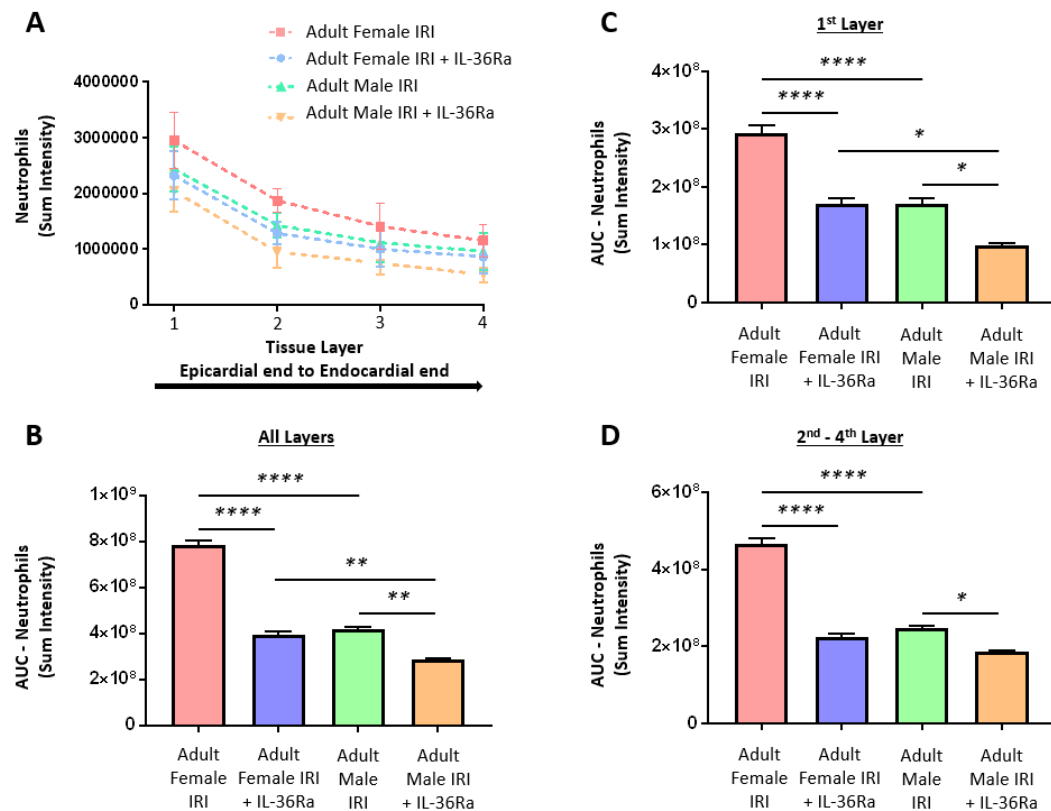
**Figure 5.16. IL-36R inhibition reduces myocardial inflammation *in vivo* in the IR injured adult male heart.** IR surgery was performed on adult male mice. Fluorescently labelled antibodies against neutrophils and platelets were injected via the carotid cannula 10 minutes before reperfusion and imaged intravitaly. Additionally, an IL-36 receptor antagonist (IL-36Ra; 15 $\mu$ g/mouse) was injected intra-arterially at 10 mins pre-reperfusion and 60 mins post-reperfusion in adult male mice. Quantitative time-course analysis of intravital data for **(A)** adherent neutrophils, and **(D)** platelets in the first 30 minutes. Area under the curve (AUC) analysis in the first 30 minutes for **(B)** adherent neutrophils, and **(E)** platelets and over the 150 minutes post-reperfusion for **(C)** adherent neutrophils, and **(F)** platelets. Statistical analysis was performed using a Student's unpaired t-test. Abbreviations - IRI: ischaemia reperfusion injury. n $\leq$ 5/group. Mean  $\pm$ SEM. \*\*p<0.01, \*\*\*\*p<0.0001.



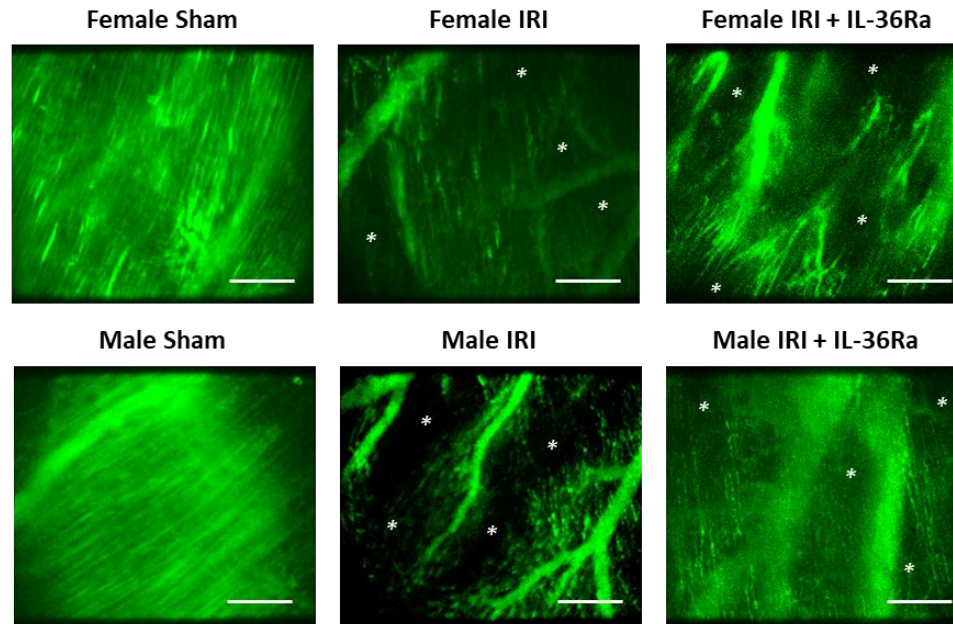
**Figure 5.17. No Sex-related differences in the ability of IL-36R inhibition to reduce myocardial inflammation *in vivo*.** IR surgery was performed on adult male and female mice. Fluorescently labelled antibodies against neutrophils and platelets were injected via the carotid cannula 10 minutes before reperfusion and imaged intravitaly. Additionally, an IL-36 receptor antagonist (IL-36Ra; 15µg/mouse) was injected intra-arterially at 10 mins pre-reperfusion and 60 mins post-reperfusion in adult male and female mice. Quantitative time-course analysis of intravital data for **(A)** adherent neutrophils, and **(D)** platelets in the first 30 minutes. Area under the curve (AUC) analysis in the first 30 minutes for **(B)** adherent neutrophils, and **(E)** platelets and over the 150 minutes post-reperfusion for **(C)** adherent neutrophils, and **(F)** platelets. Statistical analysis was performed using a one-way ANOVA, followed by a Tukey's post-hoc test between the following groups: adult male IRI versus adult male IRI + IL-36Ra, adult female IRI versus adult female IRI + IL-36Ra, adult male IRI + IL-36Ra versus adult female IRI + IL-36Ra. Abbreviations - IRI: ischaemia reperfusion injury. n≤5/group. Mean ±SEM. \*\*p<0.01, \*\*\*\*p<0.0001.



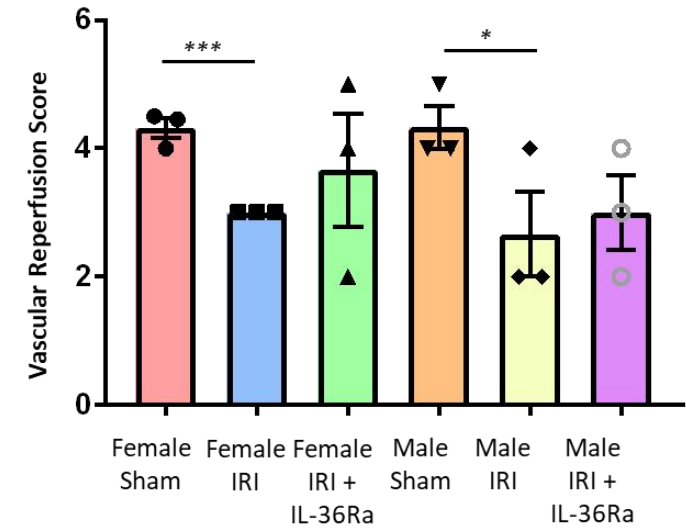
**Figure 5.18. IL-36R inhibition reduces neutrophil presence within the deeper layers of the IR injured male myocardium.** IR surgery was performed on adult male mice. Fluorescently labelled antibodies against neutrophils and platelets were injected via the carotid cannula 5 minutes before reperfusion and imaged intravitaly. Additionally, an IL-36 receptor antagonist (IL-36Ra; 15µg/mouse) was injected intra-arterially at 10 mins pre-reperfusion and 60 mins post-reperfusion in adult male mice. Mice were culled following 150-minutes of reperfusion, and hearts were harvested. The LV was vibratome sectioned into four 300µm sections and imaged using a multiphoton microscope. **(A)** Representative z-stack multiphoton images of neutrophils (green) in the 4 layers of the LV taken from the outermost layer closest to the epicardium (1), outer myocardial layer (2), inner myocardial layer (3) and the innermost layer closest to the endocardium (4). Quantitative analysis of the multiphoton data at various depths for **(B)** adherent neutrophils and corresponding **(C)** area under the curve (AUC) for adherent neutrophils for all layers. **(D)** AUC for adherent neutrophils for the first layer, and **(E)** AUC for adherent neutrophils from layer 2-4. Statistical analysis was performed using a Student's unpaired t-test. Abbreviations - IRI: ischaemia reperfusion injury.  $n \leq 5$ /group. Mean  $\pm$  SEM. \*\* $p < 0.01$ , \*\*\* $p < 0.001$ .



**Figure 5.19. IL-36R inhibition reduces neutrophil presence within the deeper layers of the IR injured male and female myocardium.** IR surgery was performed on adult male and female mice. Fluorescently labelled antibodies against neutrophils and platelets were injected via the carotid cannula 5 minutes before reperfusion and imaged intravitaly. Additionally, an IL-36 receptor antagonist (IL-36Ra; 15µg/mouse) was injected intra-arterially at 10 mins pre-reperfusion and 60 mins post-reperfusion in adult male and female mice. Mice were culled following 150-minutes of reperfusion, and hearts were harvested. The LV was vibratome sectioned into four 300µm sections and imaged using a multiphoton microscope. Quantitative analysis of the multiphoton data at various depths for **(A)** adherent neutrophils and corresponding **(B)** area under the curve (AUC) for adherent neutrophils for all layers. **(C)** AUC for adherent neutrophils for the first layer, and **(D)** AUC for adherent neutrophils from layer 2-4. Statistical analysis was performed using a one-way ANOVA, followed by a Tukey's post-hoc test between the following groups: adult male IRI versus adult male IRI + IL-36Ra, adult female IRI versus adult female IRI + IL-36Ra, adult male IRI + IL-36Ra versus adult female IRI + IL-36Ra. Abbreviations - IRI: ischaemia reperfusion injury. n≤5/group. Mean ±SEM. \*p<0.05, \*\*p<0.01, \*\*\*\*p<0.0001.

**A**

Green : FITC-BSA

**B**

**Figure 5.20. IL-36R inhibition increases functional capillary density within the beating heart coronary microcirculation *in vivo*, with improvements more notable in adult injured female mice than adult injured male mice.** IR surgery was performed on adult male and female mice. Fluorescently labelled antibody against bovine serum albumin (green) was injected via the carotid cannula at 120-minutes post reperfusion and imaged intravitaly. Additionally, an IL-36 receptor antagonist (IL-36Ra; 15µg/mouse) was injected intra-arterially at 10 mins pre-reperfusion and 60 mins post-reperfusion in adult male and female mice. **(A)** Representative intravital images of FITC-BSA perfused coronary microvessels at 150 mins in IRI and IRI + IL-36Ra adult male and female hearts. **(B)** Quantitative analysis of intravital vascular perfusion data. Statistical analysis was performed using a one-way ANOVA, followed by a Tukey's post-hoc test between the following groups: adult male sham versus adult male IRI, adult male sham versus adult male IRI + IL-36Ra, adult male IRI versus adult male IRI + IL-36Ra, adult female sham versus adult female IRI, adult female sham versus adult female IRI + IL-36Ra, and adult female IRI versus adult female IRI + IL-36Ra. (1) outermost layer closest to the epicardium, (2) outer myocardial layer, (3) inner myocardial layer, and (4) the innermost layer closest to the endocardium. n = 3/group. Mean ± SEM. \*p<0.05, \*\*\*p<0.001.

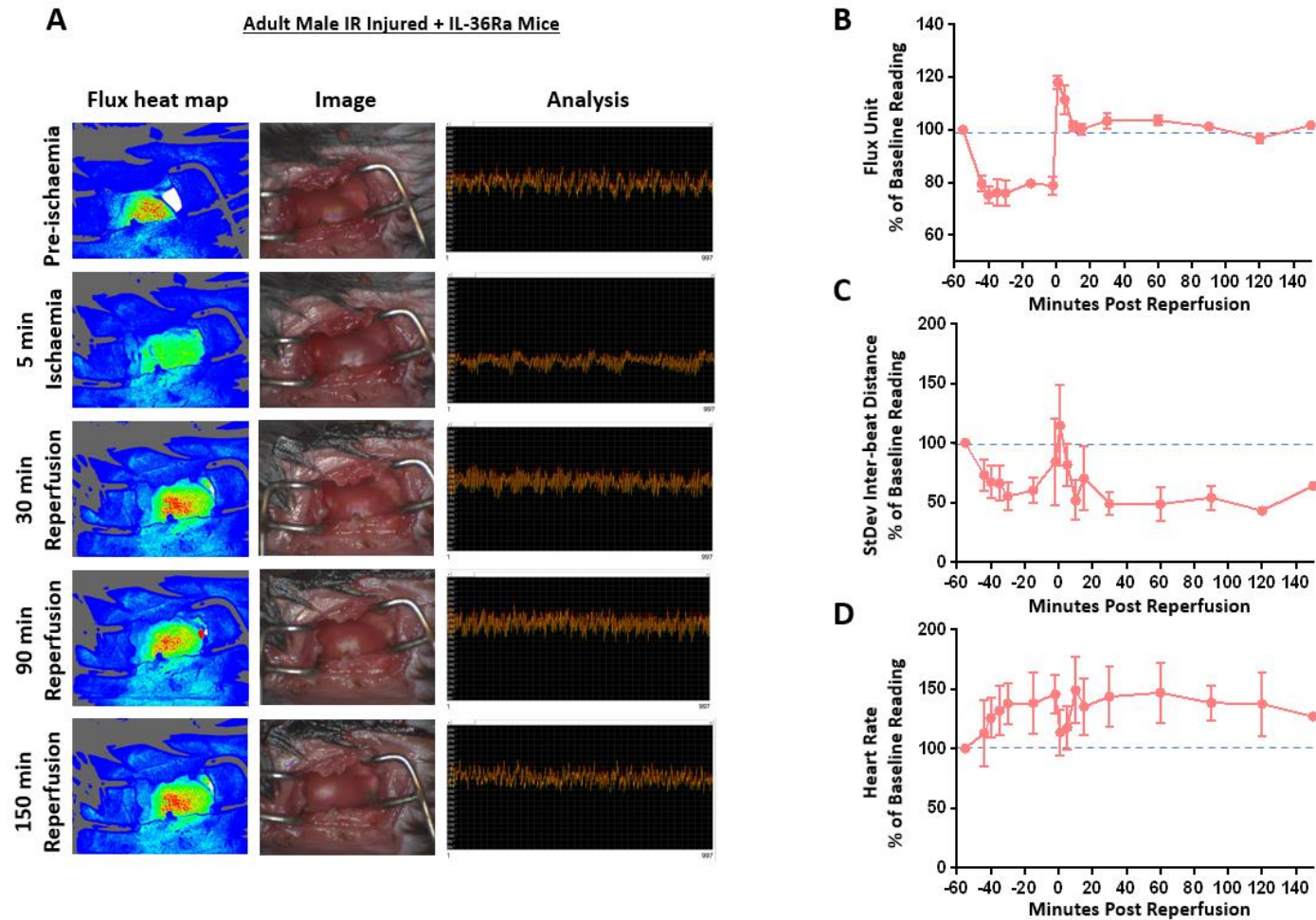


**Figure 5.21. IL-36R inhibition increases perfusion in adult male beating heart coronary circulation *in vivo*.** IR surgery was performed on adult male mice. An IL-36 receptor antagonist (IL-36Ra; 15 $\mu$ g/mouse) was injected intra-arterially at 10 mins pre-reperfusion and 60 mins post-reperfusion. Video captures were obtained throughout the surgery using laser speckle contrast imaging (LSCI). **(A)** Representative images of LSCI at various time points showing the flux heat map, still image of the beating heart, and analysis graph in adult male mice. Baseline capture prior to ischaemia was used as the baseline reading; indicating good perfusion. Quantitative time-course analysis of LSCI data for **(B)** flux unit (perfusion), **(C)** standard deviation of the inter-beat distance (arrhythmia), and **(D)** heart rate.  $n = 6/\text{group}$ . Mean  $\pm$  SEM.

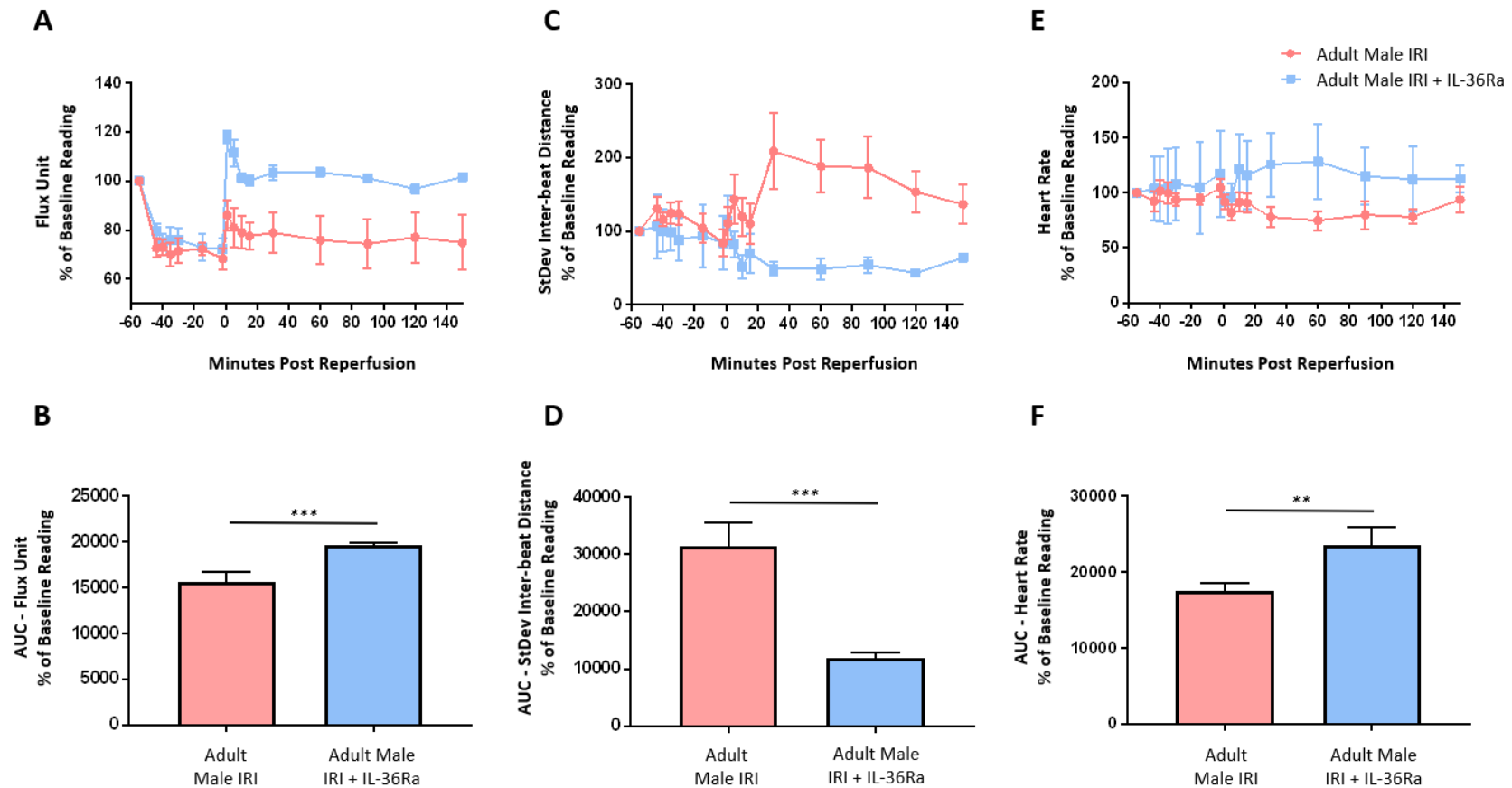


**Figure 5.22. IL-36R inhibition increases perfusion in adult male beating heart coronary circulation *in vivo*.** IR surgery was performed on adult male. An IL-36 receptor antagonist (IL-36Ra; 15µg/mouse) was injected intra-arterially at 10 mins pre-reperfusion and 60 mins post-reperfusion. Video captures were obtained throughout the surgery using laser speckle contrast imaging (LSCI). Quantitative time-course analysis of LSCI data for **(A)** flux unit (perfusion), **(C)** standard deviation of the inter-beat distance (arrhythmia), and **(E)** heart rate. Area under the curve (AUC) analysis for **(B)** flux unit, **(D)** standard deviation of the inter-beat distance, and **(F)** heart rate over a time course of 150 minutes post-reperfusion. Statistical analysis was performed using a Student's unpaired t-test. Abbreviations - IRI: ischaemia reperfusion injury.  $n = 6/\text{group}$ . Mean  $\pm$  SEM. \* $p < 0.05$ , \*\*\* $p < 0.001$ .

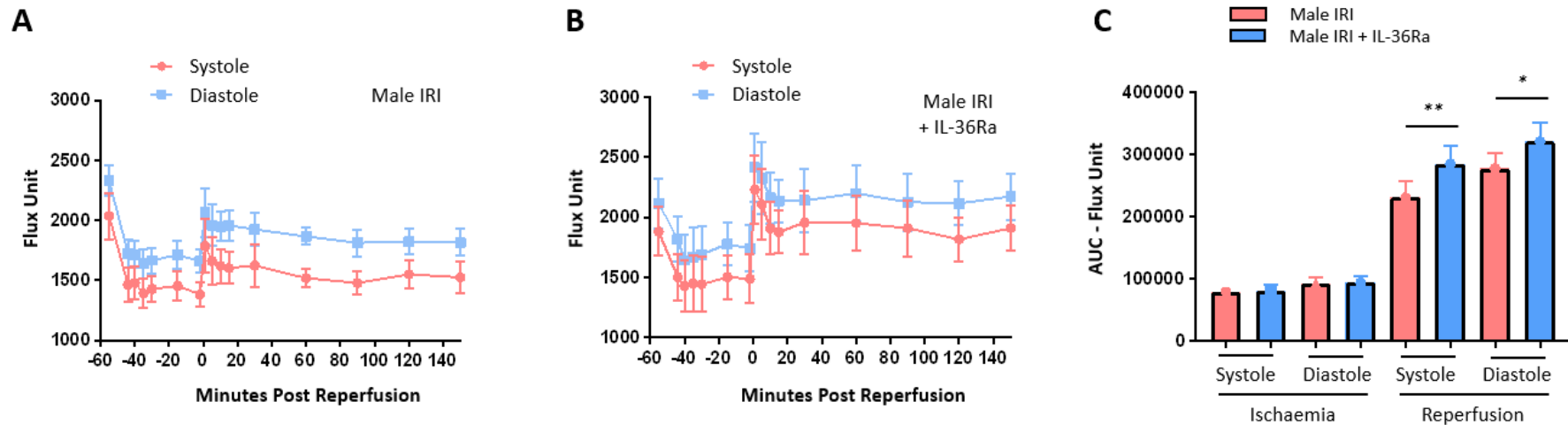


**Figure 5.23. IL-36R inhibition reduces systole and diastole anomalies following IR injury *in vivo*.** IR surgery was performed on adult male. An IL-36 receptor antagonist (IL-36Ra; 15µg/mouse) was injected intra-arterially at 10 mins pre-reperfusion and 60 mins post-reperfusion. Video captures were obtained throughout the surgery using laser speckle contrast imaging (LSCI). Baseline capture prior to ischaemia was used as the baseline reading; indicating good perfusion. Quantitative systole and diastole time-course analysis of LSCI data for flux unit (perfusion) in **(A)** male IRI and **(B)** male IRI + IL-36Ra mice. **(C)** Area under the curve (AUC) analysis for systole and diastole flux unit in the ischaemia and reperfusion phases. Statistical analysis was performed using a one-way ANOVA, followed by a Tukey's post-hoc test between the following groups: systole male IRI versus systole male IRI + IL-36Ra for each of ischaemia and reperfusion, and diastole male IRI versus diastole male IRI + IL-36Ra for both ischaemia and reperfusion. **(D)** Quantitative analysis of LSCI baseline capture prior to ischaemia. Statistical analysis was performed using a Student's unpaired t-test. Abbreviations - IRI: ischaemia reperfusion injury.  $n = 6/\text{group}$ . Mean  $\pm$  SEM. \* $p < 0.05$ , \*\* $p < 0.01$ .

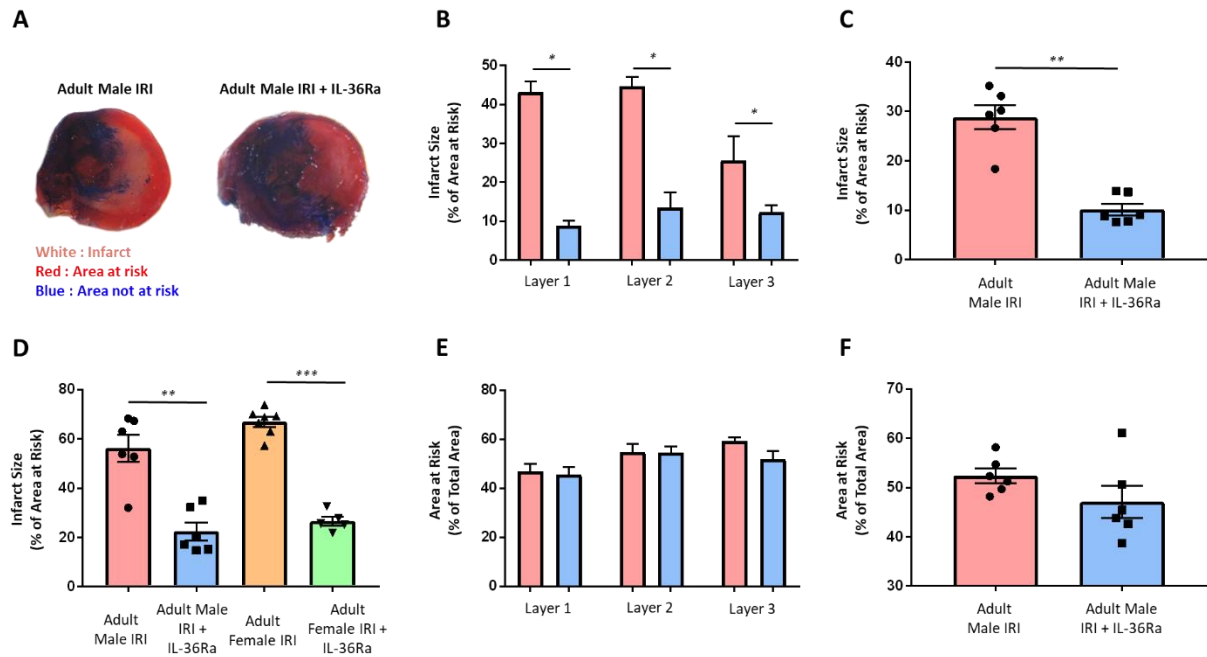


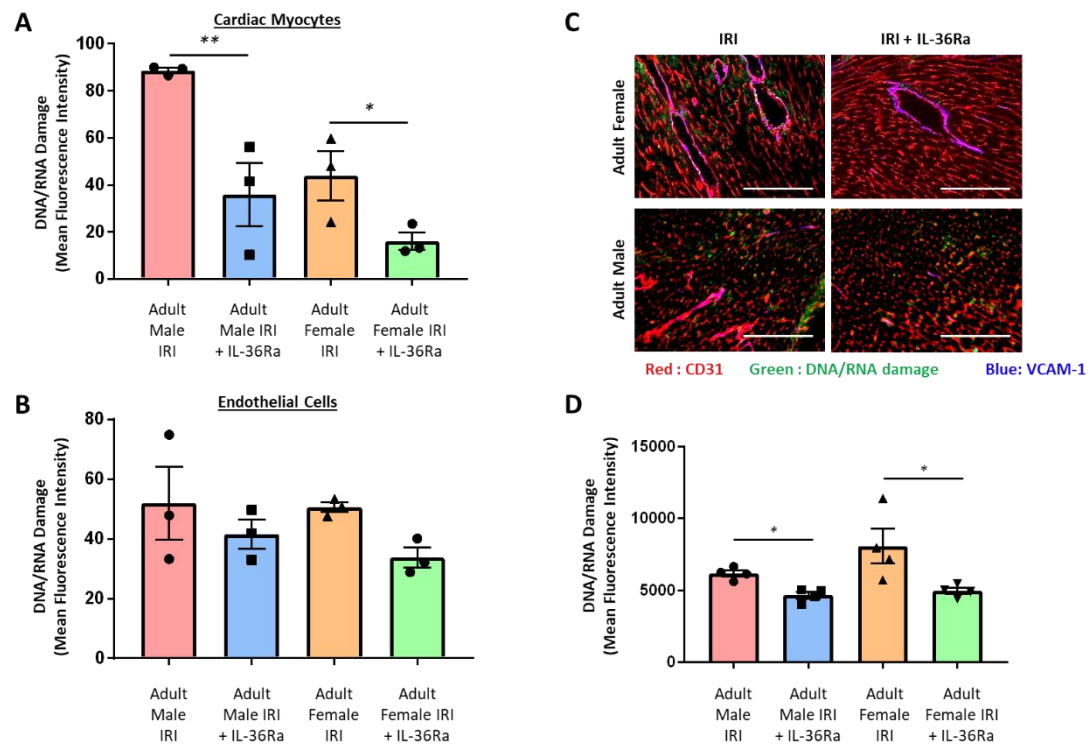
**Figure 5.24. IL-36R inhibition decreases infarct size in adult male and female hearts.** IR surgery was performed on male and female adult mice. Following 4-hours of reperfusion, the left anterior descending artery was re-ligated, and Evans Blue was injected. An IL-36 receptor antagonist (IL-36Ra; 15µg/mouse) was injected intra-arterially at 10 mins pre-reperfusion and 60 mins post-reperfusion. Mice were culled, and the heart was harvested, sectioned, stained with TTC and imaged. **(A)** Representative images of the TTC stained adult male IR injured + IL-36Ra hearts. Quantitative analysis of infarct size **(B)** in the various layers and **(C)** in the overall of the heart, and **(D)** between males and females throughout all the layers. Layer 1 represents the first layer below the ligature and layer 3 represents the apex of the heart. Quantitative analysis of the area at risk **(E)** in the various layers, and **(F)** in the overall of the heart. Statistical analysis was performed using **(B, E)** a one-way ANOVA, followed by a Tukey's post-hoc test between the following groups: adult male IRI versus adult male IRI + IL-36Ra in each of the 3 layers, as well as layer 1 versus layer 2, layer 1 versus layer 3, and layer 2 versus layer 3 for adult IRI + IL-36Ra, **(C, F)** Student's unpaired t-test, **(D)** one-way ANOVA, followed by a Tukey's post-hoc test between the following groups: adult male IRI versus adult male IRI + IL-36Ra, adult female IRI versus adult female IRI + IL-36Ra, adult male IRI + IL-36Ra versus adult female IRI + IL-36Ra. Abbreviations - IRI: ischaemia reperfusion injury.  $n \leq 6/\text{group}$ . Mean  $\pm$  SEM. \* $p < 0.05$ , \*\* $p < 0.01$ , \*\*\* $p < 0.001$ .

### 5.2.13. IL-36R Inhibition Reduced Endothelial and Cardiac Myocyte Oxidative Damage and VCAM-1 Expression in the Male IR Injured Heart

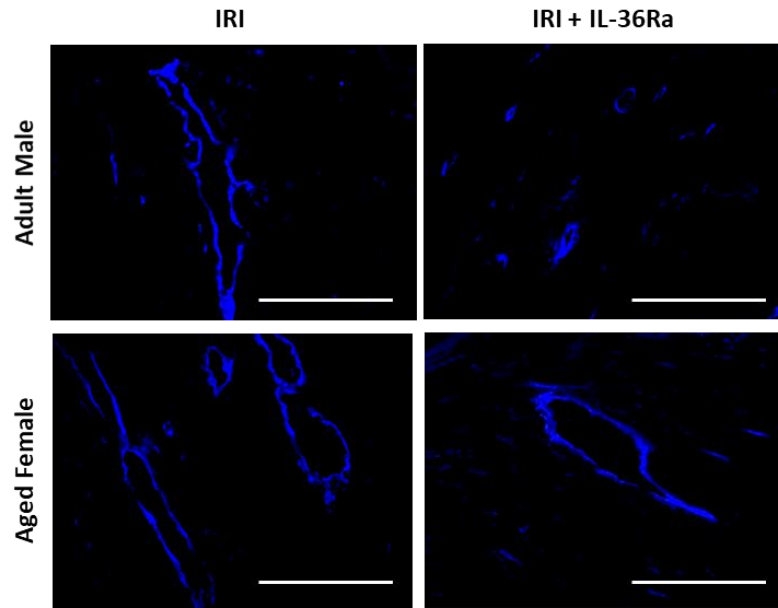
To determine whether IL-36Ra treatment conferred vasculoprotection via similar mechanisms in male and female hearts, flow cytometry of collagenase digested hearts, as well as immunofluorescent staining on frozen heart sections was performed. IL-36Ra treatment significantly decreased ROS mediated oxidative damage on CMs from both adult male and adult female injured hearts when compared with non-treated injured hearts as determined by flow cytometry (**Figure 5.25a**). A reduction in oxidative damage was also seen on coronary ECs in both treated adult male and female injured hearts but did not reach statistical significance (**Figure 5.25b**).

Significant reductions in oxidative damage were also confirmed by immunofluorescent staining for oxidized DNA/RNA on both adult male and adult female IL-36Ra treated. This was noted as punctate staining on both CD31<sup>+</sup> vascular and non-vascular structures (**Figures 5.25c-d**).

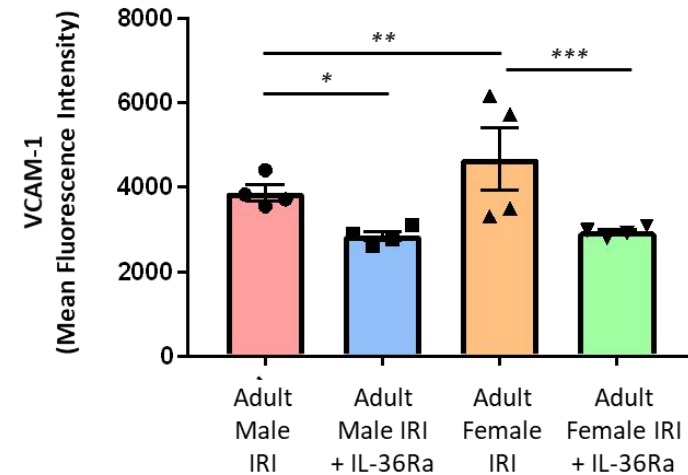
Expression of VCAM-1 was also investigated by immunofluorescence on frozen heart sections. Expression of this endothelial adhesion molecule was significantly decreased in adult male and adult female IL-36Ra treated injured mice (**Figures 5.26a-b**).



**Figure 5.25. IL-36R inhibition decreases expression of DNA/RNA damage on cardiac myocytes and endothelial cells.** IR surgery was performed on adult male and female mice. An IL-36 receptor antagonist (IL-36Ra; 15µg/mouse) was injected intra-arterially at 10 mins pre-reperfusion and 60 mins post-reperfusion. **(A-B)** Mice were culled following 150-minutes of reperfusion, and hearts were harvested and digested. Cell suspension was stained with an anti-CD31, anti-cTnT, and anti-DNA/RNA damage antibodies and acquisition was performed using a CyAn™ ADP cytometer. Quantitative analysis of DNA/RNA damage expression on **(A)** cardiac myocytes, and **(B)** endothelial cells. n=3/group. **(C-D)** Mice were culled following 120-minutes of reperfusion, and hearts were harvested and snap frozen. The LV was transversely sectioned using a cryostat into 10µm sections and then immunostained with an anti-DNA/RNA damage, anti-CD31, and anti-VCAM-1 antibodies. Sections were imaged using a EVOS microscope. **(C)** Representative images of DNA/RNA damage (green), VCAM-1 (blue), and CD31 (red) staining of frozen heart sections. Scale bar indicates 200µm. **(D)** Quantitative analysis of the immunofluorescent images of DNA/RNA damage expression. n=4/group. Statistical analysis was performed using a one-way ANOVA, followed by a Tukey's post-hoc test between four groups: adult male IRI versus adult male IRI + IL-36Ra, adult female IRI versus adult female IRI + IL-36Ra, and adult male IRI + IL36Ra versus adult female IRI + IL-36Ra. Abbreviations - IRI: ischaemia reperfusion injury. Mean ±SEM. \*p<0.05, \*\*p<0.01.

**A**

Blue: VCAM-1

**C**

**Figure 5.26. IL-36R inhibition decreases expression of VCAM-1.** IR surgery was performed on adult male and female mice. An IL-36 receptor antagonist (IL-36Ra; 15µg/mouse) was injected intra-arterially at 10 mins pre-reperfusion and 60 mins post-reperfusion. Mice were culled following 120-minutes of reperfusion, and hearts were harvested and snap frozen. The LV was transversely sectioned using a cryostat into 10µm sections and then immunostained with an anti-VCAM-1 antibody. Sections were imaged using a EVOS microscope. **(A)** Representative images of VCAM-1 (blue) staining of frozen heart sections. Scale bar indicates 200µm. **(B)** Quantitative analysis of the immunofluorescent images of VCAM-1 expression. n=4/group. Statistical analysis was performed using a one-way ANOVA, followed by a Tukey's post-hoc test between four groups: adult male IRI versus adult male IRI + IL-36Ra, adult female IRI versus adult female IRI + IL-36Ra, and adult male IRI + IL36Ra versus adult female IRI + IL-36Ra. Abbreviations - IRI: ischaemia reperfusion injury. Mean ±SEM. \*p<0.05, \*\*p<0.01, \*\*\*p<0.001.

	Adult Male IR injured	Adult Female IR injured
<b>Intravital studies on the beating heart <i>in vivo</i></b>		
Adherent and free-flowing neutrophils	↑	↑↑↑
Adherent platelet microthrombi	↑↑↑	↑
FITC-BSA perfusion to assess FCD	↓↓↓	↓↓
<b>Laser speckle studies on the beating heart <i>in vivo</i></b>		
Overall ventricular perfusion	Does not return to baseline values	Returns to baseline values
St.Dev. of the inter-beat distance	Same	Same
Heart rate	Lower	Higher
<b>TTC / Evans Blue staining of heart sections <i>in vitro</i></b>		
Infarct size	Smaller	Larger
<b>VCAM-1, oxidative damage, IL-36R and IL-36 cytokine <i>in vitro</i></b>		
VCAM-1	↑	↑↑
DNA/RNA oxidative damage of CMs and ECs	↑↑↑	↑
IL-36 receptor	↑	↑↑↑ More so on cardiac ECs than CMs
IL-36 $\alpha$ / IL-36 $\beta$	↑	↑↑↑
<b>Intravital studies on the beating heart <i>in vivo</i> in mice treated with IL-36Ra</b>		
Adherent neutrophils	↓↓↓	↓↓
Adherent platelet microthrombi	↑↑ Higher than untreated male injured mice	↑ Higher than untreated female injured mice
FITC-BSA perfusion to assess FCD	↑	↑↑
<b>Laser speckle studies on the beating heart <i>in vivo</i> in mice treated with IL-36Ra</b>		
Overall perfusion	Perfusion exceeds baseline levels	Perfusion exceeds baseline levels
St.Dev. of the inter-beat distance	Improved	Improved
Heart rate	Increased	No different
<b>VCAM-1 and oxidative damage <i>in vitro</i> in mice treated with IL-36Ra</b>		
VCAM-1	↓↓	↓↓
DNA/RNA oxidative damage of CMs and ECs	↓↓	↓↓
<b>TTC / Evans Blue staining of heart sections <i>in vitro</i> in mice treated with IL-36Ra</b>		
Infarct size	↓↓↓	↓↓↓

**Table 5.1. Summary of the major sex-related differences between adult male and female IR injured mouse hearts.** Studies conducted were intravital microscopy and laser speckle *in vivo* studies on the beating heart and multiphoton, flow cytometry and immunostaining *in vitro* studies.

### 5.3. Discussion

Sex differences in the onset of CVD and outcomes have been widely studied and have been associated with differences in cardiac structure and function, sex hormones, innate and adaptive immune responses, risk factors, and age [172]. Therefore, consideration of the effects of sex on the post-ischaemic heart, particularly on the cardiac microcirculation, is critical. This chapter provides original contributions on sex-related differences in the response of the coronary microcirculation to myocardial IR injury and IL-36 targeted therapy *in vivo*. The main results are summarised in **Table 5.1**.

Briefly, although thromboinflammatory disturbances were noted in both sexes, a greater burden of thrombotic disease was noted in adult male injured coronary microvessels whilst a greater inflammatory or neutrophil presence was identified in adult female injured hearts. FCD was reduced in the coronary microcirculation of both sexes but slightly more so in male hearts. LSCI also detected sex specific differences in overall left ventricular perfusion. Unlike female injured mice, male injured mice were unable to restore ventricular perfusion to pre-ischaemic baseline values as soon as the LAD artery was untied. Interestingly, IL-36R and IL-36 cytokine expression was higher in female hearts, particularly on coronary ECs. These various differences were directly or indirectly associated with infarct size being larger in female hearts than in male hearts. Despite these various differences, the use of the IL-36Ra resulted in similar beneficial effects with regards to decreasing oxidative CM/EC damage, decreasing VCAM-1 expression, and improving thromboinflammation in both male and female injured mice. Ultimately, this resulted in a reduction in the infarct size to a relatively similar degree in both sexes. Interestingly, this

was despite the fact that IL-36Ra resulted in increased platelet adhesion within male and female hearts, but significantly more so in male hearts.

### **5.3.1. Sex-Related Thromboinflammatory and Perfusion Perturbations**

#### **Following Myocardial IR Injury *in vivo***

##### **5.3.1.1. Increased Neutrophils in IR Injured Female Hearts**

The innate and adaptive immune responses are stronger in adult females than in males. As a result, pathogens are cleared faster in adult females, but this increases their susceptibility to inflammatory and autoimmune diseases [188]. In the current study, the innate immune response was certainly stronger in female hearts, and so the impact of sex on the coronary microcirculation was notable. Our novel *in vivo* data showed an approximately 4-fold increased neutrophil recruitment following IR injury in the female microvasculature compared to their male counterparts. These differences were also confirmed in our multiphoton studies, which showed neutrophil presence was not only uniformly increased throughout all layers of the LV in female IR injured hearts but was also significantly higher than in male hearts. It is well recognised that neutrophils are critically involved in tissue injury following reperfusion. Moreover, activated neutrophils are well known to become stiffer, which contributes to their retention, specifically within capillaries that have a smaller diameter than their own [249]. Therefore, our demonstrated enhanced neutrophil recruitment observed in females may drive worsened IR injury, and thus the larger infarct size noted in female mice [248].

The sex differences in neutrophil presence in the injured heart may be due to inherent differences in the neutrophils themselves. Indeed, a recent study by Gupta *et al.* (2020) performed mRNA-sequencing on isolated human neutrophils and demonstrated significant differences in gene expression between female and male neutrophils, with 106 genes up-regulated and 128 genes down-regulated in females compared to male neutrophils. They also showed neutrophils in females existed in a basally activated state leading to greater proinflammatory responses, including greater ability to form NETs [293]. Such neutrophil differences have also been shown in mice where male mouse neutrophils appeared to have more degranulation activity, as evidenced by higher levels of the neutrophil protein elastase and females exhibited more NETosis [294].

Sex-related differences in neutrophil recruitment have also been demonstrated in other types of injuries and tissues/organs. Madalli *et al.* (2015) showed a greater number of adherent neutrophils in the male mesenteric microcirculation in a model of intestinal IR injury in rats at early (30 minutes) and late (120 minutes) time points post-reperfusion [295]. Gwak *et al.* (2007) showed that the number of neutrophils identified following gastrectomy surgical intervention was significantly higher in females than in males [296]. These contrasting results may be explained by differences in the species used, injury model and the vascular bed studied.

### 5.3.1.2. Increased Platelets in IR Injured Male Hearts

An approximately 3-fold increase in platelet presence was noted in the male injured coronary microcirculation compared to their female counterparts. These appeared as rounded and elongated aggregates or microthrombi, which seemed to occlude the affected microvessels, which was evidenced by the lack of circulating neutrophils passing through affected microvessels. Although this increased platelet presence may be explained by sex differences in platelet function, our results do not conform to the current general consensus that females have a more hypercoagulable profile. For example, females have been shown to have a higher platelet count than in males [297]. Leng and colleagues conducted the first study using mouse platelets and showed that platelets of female mice were more sensitive to agonists such as ADP and CRP than platelets of males [298]. However, Coleman *et al.* later found that although human female platelets had an increased activation (and aggregation) response to ADP stimulation, male platelets had a greater response to PAF stimulation, suggesting sex-dependent activation and receptor responses. [299]. Whether the involvement or presence of platelet agonists and their receptors differs in male and female mice in response to myocardial IR injury is not known and would require further investigation.

A recent study by Kim and colleagues showed that during health, human female platelets were more reactive to three different agonists, namely ADP (activates P2Y<sub>12</sub> receptor), TRAP-4 (activates PAR-1 receptor) and U46619 (activates thromboxane receptor). However, contrary to these observations in health, when platelets from patients with MI were tested, male platelets were 2.7-fold more reactive to TRAP-4 and 1.6-fold more reactive to ADP, with no difference to U46619. They confirmed their human data in

platelets from healthy and MI mice [300]. This increased responsiveness of male platelets to agonists in disease situations like MI compared to health may explain our findings of increased microthrombus presence within the coronary microcirculation of male IR injured mice.

Intravitaly, we noted that in the actual coronary microvessels occupied by platelet aggregates, no free-flowing neutrophils could be observed passing through them. This suggests these microthrombotic events were likely occlusive. This may explain why overall ventricular perfusion was not able to return to pre-ischaemic levels once the LAD was untied and also why there was a greater lack of FITC-BSA perfusion (and thus decreased FCD) in male injured hearts. In contrast, in female IR injured hearts, where there was a much higher inflammatory presence, ventricular blood flow was able to return to baseline levels upon reperfusion, suggesting that neutrophils, even though present in high numbers, may not have necessarily been occlusive. Although decreased FITC-BSA perfusion was observed in female mice intravitaly, perfusion at a microscopic level was mildly better than in male hearts. As far as we are aware, there have been no studies that have investigated sex-related myocardial perfusion disturbances post-MI. However, a recent study by Nickander *et al.* (2020) identified a significant decrease in myocardial perfusion following adenosine-induced stress in male participants compared to their female counterparts [301].

### 5.3.2. Sex-Related Changes in VCAM-1 and Oxidative Damage

Since VCAM-1 is critical for recruiting leukocytes to the vascular endothelium during an inflammatory response; we investigated whether differences in the expression of this adhesion molecule could explain the increased recruitment of neutrophils in females hearts. Basal expression was low in male and female sham mice, and there were no significant sex-related differences. This low-level basal expression may be the result of the surgical technique [241]. Levels of VCAM-1 increased in both males and females following IR injury. Although females had higher levels VCAM-1, this did not attain statistical significance. Whether this mild difference was biologically sufficient enough to contribute to the enhanced number of recruited neutrophils within the coronary microcirculation would need further investigation. Although there were no clear basal or injury-induced differences in VCAM-1 in the current study, others have shown oestrogen to be cardioprotective in pre-menopausal women due to its ability to suppress TNF $\alpha$  induced VCAM-1 (and ICAM-1) expression on human aortic ECs and thus subsequent monocyte recruitment. Hence, it is capable of exerting an anti-inflammatory response [302]. In contrast, testosterone has been shown to increase VCAM-1 mRNA in a dose- and time-dependent manner in HUVECS [303]. Such sex-related differences, however, were not apparent in the current study in either the healthy or IR injured coronary vasculature and so may not mechanistically explain the differences in the neutrophil recruitment.

It is possible that differences in thrombotic and inflammatory events could be due to sex-related differences in CM/EC oxidative damage. Indeed, flow cytometric and immunofluorescence studies demonstrated a significant increase in CM/EC oxidative damage, both basally and during the ischaemic period, in male mice when compared to

female mice. This oxidative damage continued to be significantly higher throughout reperfusion on male CM's but was similar on ECs between the two sexes. Several studies have shown a similar enhanced response in males. Barp *et al.* showed an increase in myocardial oxidative stress, as assessed by lipid peroxidation, and a decrease in critical antioxidants such as superoxide dismutase, in male rats versus females and suggested this to be related to the anti-oxidant role of oestrogen in the heart, while the same was not true for testosterone [304]. The pro-oxidant / anti-oxidant balance being in favour of anti-oxidants in female hearts was also noted in human tissue, where male individuals had evidence of higher basal levels of *in vivo* markers of oxidative stress than females of the same age [305]. Vascular oxidative stress is well known to be associated with elevated thrombosis due to suppressed bioavailability of anti-thrombotic NO [306]. Therefore, the higher presence of platelet microthrombi in male hearts that had higher EC oxidative damage is understandable. However, why this is also not associated with greater neutrophil recruitment (or why there was increased neutrophil presence in female hearts when they demonstrated significantly less CM/EC oxidative damage) is not clear and would require further investigation.

### 5.3.3. Sex-Related Changes in IL-36R and IL-36

Following MI, cytokine production drives the initial inflammatory response after the ischaemic phase. IL-36 is typically one of the most upstream and up-regulated cytokines released upon tissue injury and cellular necrosis, and is critical in triggering the subsequent synthesis and release of a multitude of inflammatory mediators [269]. We investigated

basal IL-36R, IL-36 $\alpha$ , and IL-36 $\beta$  expression was low in both sexes, supporting the observation of Towne *et al.* (2004) who also showed minimal IL-36 expression in human and murine hearts using qPCR [272]. Interestingly, immunofluorescence studies showed basal expression of all three to be significantly higher in female hearts whereas flow cytometry showed no differences between sexes or less expression on male CMs/ECs. Differences in basal expression does not seem to be unique to this particular cytokine. In the GTEX study, RNA-sequencing data were obtained from the left ventricle of 46 non-diseased deceased donors and showed 178 differentially expressed genes, of which 124 were up-regulated in females and 54 in males [307]. Importantly, this study showed that under basal conditions, the female heart over expressed genes involved in inflammatory pathways. For example, females over expressed TNFAIP3, a gene involved in immune and inflammatory responses signalled by TNF $\alpha$  and IL-1 $\beta$ , as well as chemokines CX3CL1 and CCL4, adhesion molecule VCAM1 and the transcription factor NF $\kappa$ B.

We further showed, both by tissue staining and flow cytometry, that although IL-36 and IL-36R expression was increased in both sexes after IR injury, this was more pronounced in injured female hearts. As far as we are aware, this is the first demonstration that members of this novel cytokine pathway are expressed differentially in injured male and female hearts. There is a plethora of data on inflammatory cytokines (not so much on their receptors) and how their synthesis / release varies between sexes during different diseases. Some of these studies show increased release in males, but most confirm our results of increased production in females. For example, IL-1 $\alpha$  and IL-1 $\beta$  have both previously been shown to be secreted at higher levels from female peripheral blood mononuclear cells than in males, both basally and in response to LPS stimulation [308].

Increased expression of inflammatory IL-36 / IL-36R in injured female hearts may explain the increased levels of neutrophils within the coronary microcirculation of female rather than male hearts and warrants further investigation.

### 5.3.4. Vasculoprotective Effect of IL-36R Inhibition

To date, several clinical trials have been conducted which target inflammatory cytokines post-MI - mainly IL-1, IL-6, and TNF- $\alpha$  [103, 109, 197-200]. In the case of IL-36, there have been no studies on the use of the endogenous antagonist IL-36Ra in myocardial IR injury, and thus we sought to identify if systemic administration of IL-36Ra was protective against the deleterious effects of IR. In addition, there have been no previous studies which have looked at potential sex-related differences in the response to myocardial anti-inflammatory therapies post-MI. This is clearly important in light of our demonstrated differences in the microvascular perturbations exhibited by male and female mice post-reperfusion. However, it is also important given that many studies have shown sex-related differences in the efficacy of drugs with anti-inflammatory properties [309]. Our novel data shows administration of IL-36Ra is associated with a 30% and 50% reduction in neutrophil recruitment in both adult male and female IR injured hearts respectively, but the number of adherent neutrophils at the end of imaging was similar in both sexes. This suggests the IL-36Ra, at the dose used, can only inhibit neutrophil adhesion to a certain level. While there have been no previous studies that have looked at the effect of IL-36Ra on neutrophil recruitment within the heart, there have been several studies on other organs. A recent study by Contreras *et al.* (2016) showed neutrophil recruitment to be reduced following intestinal damage in IL-36R knockout mice, further suggesting its benefit in promoting

resolution [287]. Indeed, IL-36Ra has been demonstrated to have anti-inflammatory effects in many inflammatory conditions, such as psoriasis and rheumatoid arthritis [288].

Somewhat worrying was the observed increase in the presence of platelet microthrombi following IL-36Ra treatment in both sexes, with a greater increase in male mice. It was anticipated that thrombosis would have decreased in the coronary microvessels once neutrophil recruitment was inhibited, especially since NETs, the web-like structures released by neutrophils, can act as a scaffold for entrapping platelets and contributing to their adhesion, activation, and aggregation. We speculate that this increased platelet presence may be linked to the significant intravascular neutrophil accumulation being reduced, which may have enabled enhanced microvascular entry of platelets, facilitating microthrombi formation on any damaged microvascular surfaces. Indeed, previous studies have shown activated inflammatory cells can obstruct the microvasculature [249, 254] and so we propose that their removal would have increased the surface area available for platelet adhesion. Whilst there have been no previous studies that have shown similar results, unpublished data by Kobkaew Bumroongthai from the Kalia Group has also shown an increase in myocardial platelet presence following stem cell treatments which reduce neutrophil presence post-myocardial IR injury (UoB, PhD thesis).

We and others have shown myocardial reperfusion to be associated with a worsening of coronary flow to the heart [255]. In the current study, LSCI showed this to be worse in adult male injured mice compared to adult female injured mice. However, our novel data demonstrated that IL-36Ra treatment not only improved blood to reperfused LV, but actually transiently enhanced it above baseline values in both male and female mice. This hyperaemic response was accompanied by a sustained increase in perfusion than in the

non-treated mice, highlighting the importance of timely anti-neutrophil interventions. Our data supports the observations of Kerckhoven *et al.* (2004) who also showed that the use of an anti-inflammatory, namely methylprednisolone, could improve FCD following myocardial IR injury in rats [310]. However, this was quantitated by staining ECs with lectin in paraffin sections in recovery mice at 21 days MI. LSCI provides a functional readout of dynamic blood flow in the beating heart *in vivo*. Although IL-36Ra treatment was associated with improvements in overall ventricular perfusion in both sexes, at a microvascular level, areas of no-reflow were still present, albeit at lower levels than in non-treated injured hearts. As neutrophil reduction was accompanied by an increase in platelet accumulation, this may potentially explain the lack of FITC-BSA presence in some microvessels following IR injury in IL-36Ra treated animals.

Mechanistically, our study demonstrated reduced neutrophil recruitment could be due to the associated significant decrease in CM/EC oxidative damage and VCAM-1 expression following IR injury in the presence of the IL-36Ra. Our data support recent observations of reduced oxidative stress in IL-36R knockout rats undergoing cardiopulmonary bypass [152]. Importantly we show that similar mechanisms are targeted by IL-36Ra in both sexes post-IR injury.

### 5.3.5. Infarct Size Reduction with IL-36R Inhibition

Despite the increased platelet microthrombi presence in treated mice, and the varying level of neutrophil presence within male and female hearts, IL-36Ra treatment still led to a significant decrease in infarct size in both sexes. Since infarct size is strongly associated

with prognosis [311], the ability of IL-36Ra to reduce this to equal levels in both sexes suggests targeting the IL-36 pathway may be beneficial to both sexes. This benefit is likely linked to the anti-neutrophil effect of IL-36R antagonism, but whether there are other additional cardioprotective effects of IL-36Ra is not yet known. Having said that, we noted significantly reduced oxidative damage of CMs and ECs in IL-36Ra treated mice.

Myocardial IR injury appears within minutes of reperfusion, and so it is essential that any novel cardioprotective therapy is administered prior to myocardial reperfusion in order for it to be effective. The design of a number of clinical trials involved administering a therapy *after* reperfusion had already taken place. Since one dose of IL-36Ra was administered during the ischaemic period, it permitted an immediate anti-neutrophil effect as evidenced by decreased neutrophil adhesion in both sexes within 30 minutes of reperfusion. This opens up the possibility of targeting IL-36 during PCI procedures and it thus being therapeutically efficacious in a clinical setting. IL-36 is a relatively newly discovered member of the IL-1 superfamily, and even targeting IL-1 with an IL-1Ra has been associated with a reduction in infarct size [104].

### 5.3.6. Conclusion

There remains an unmet need to discover novel therapeutic strategies, particularly vasculoprotective therapies, which are capable of preventing myocardial IR injury and reducing infarct size. This is critical in order to preserve LV systolic function and prevent the onset of heart failure in patients with MI undergoing reperfusion following PCI. Importantly, these strategies need to be effective in both males and female patients. We

have shown for the first time that notable sex-related differences exist with regards to the microcirculatory perturbations that take place in the IR injured beating coronary microcirculation *in vivo*. The higher neutrophil presence in IR injured female hearts may be linked to the raised levels of IL-36, IL-36R and VCAM-1 in the female myocardium and coronary microcirculation compared to males. Our study does not really shed light on why the male injured coronary microcirculation had a greater presence of microthrombi compared to females, and this warrants further investigation.

Sex differences in the coronary microcirculatory response to IR injury may explain why younger women who suffer from an acute MI are at a higher risk of mortality than age-matched men [176]. Our study highlights an important pathophysiological role for neutrophils. We further provide novel mechanistic insights into how inhibition of IL-36/IL-36R signalling ultimately decreases infarct size post-reperfusion, most likely mediated by reducing ROS damage, decreasing VCAM-1, and decreasing neutrophil recruitment. Importantly, we show that similar vasculoprotective mechanisms are at play in both sexes and emphasise the importance of targeting the thromboinflammatory cellular events that occur immediately upon reperfusion.

# **Chapter 6:**

## **General Discussion**

## 6.0. General Discussion

### 6.1. Summary of Main Findings

CVDs still remain the leading cause of global mortality, with IHD accounting for 49% of the total global burden [4, 6]. Age is a major risk factor for IHD, with patients exhibiting worsened cardiac damage and resulting in poorer outcomes, independent of ‘traditional’ risk factors [215-217]. Biological sex also plays a major role in determining patient prognosis [172]. Treatment of MI focuses on rapidly re-establishing perfusion following a blockage in one or more of the coronary arteries. Restoring perfusion is primarily achieved by patients undergoing a primary PCI using a coronary stent to open the culprit artery [10]. Despite these interventions, which do largely re-establish perfusion within the heart, a significant proportion of patients still incur extensive muscle damage and develop heart failure post-MI [212]. This is partly due to reperfusion paradoxically leading to additional inflammation and tissue damage, a condition termed IR injury.

The IL-1 family are the first and most upstream inflammatory cytokines produced in response to injury and so are considered good targets for intervention in models of IR [115]. While targeting these and other elements in the inflammatory cascade has shown some benefits in pre-clinical animal models, they have not demonstrated significant improvements in the clinical setting [109, 197, 263-265]. These discrepancies have largely been attributed to poor/sub-optimal choices of animal models, varying efficacies of anti-inflammatories used, differing involvement of MVO, and clinical applicability of the time of intervention used in experimental models [60]. Interestingly, the ability of the heart to respond to cardioprotective interventions is also diminished with ageing [158, 312].

Therefore, timely therapeutic strategies which target myocardial IR injury, particularly the microvasculature, and retain therapeutic efficacy in aged organisms are needed. In the last decade, genes encoding a novel cytokine cluster, namely IL-36, were discovered [116, 128]. These cytokines appear to act as regulators of the innate and adaptive immune response in several disorders. Their importance in some inflammatory disorders is thought to surpass that of IL-1, a classic IL-1F inflammatory mediator [121]. Therefore, this thesis explored the potential role of IL-36 as a therapeutic agent, with a focus on coronary microvascular cardioprotection and efficacy in IR models incorporating comorbidities / risk factors and early intervention.

One of the main aims of this thesis was to identify any age- and sex-related differences in microcirculatory responses to myocardial IR injury. Of particular interest was the immediate aftermath of reperfusion. A number of studies suggest that IR injury is self-exacerbating, and early intervention may be critical in ensuring treatments are efficacious. Therefore, we optimised IVM and LSCI protocols in order to be able to visualise the coronary microcirculation *in vivo* before reperfusion commences. In turn, we were able to understand the immediate kinetics of endogenous thromboinflammatory cells and perfusion perturbations that follow myocardial IR injury. Our novel data provides not only new insight into how age and sex impact the IR injured coronary microcirculation but also identifies subtle changes in healthy hearts too. We show that the most significant perturbation in aged (female) IR injured mice was the remarkable recruitment of neutrophils, which was associated with a (non-significant) increase in infarct size. In adult female mice, we again noted that neutrophil recruitment was the more obvious perturbation when compared to male mice, in part due to the raised levels of IL-36 and

VCAM-1 in the female coronary microcirculation, and this was again associated with the greater infarct size in females. This suggests that this particular microcirculatory perturbation is critical and one that needs to be successfully targeted. It is therefore unfortunate that contemporary treatment of MI in patients undergoing PCI only involves an anti-platelet strategy.

To this effect, we identified the recently discovered IL-36/IL-36R pathway as a novel target capable of effectively alleviating the neutrophil disturbances in both adult and aged, male, and female hearts post-IR injury. We supplement this data by providing mechanistic insights into how targeting this signalling pathway may confer cardio- and vasculoprotection. Critical to this was the age- and IR injury-related increase in IL-36R expression, as well as increased pro-inflammatory IL-36 $\alpha$  and IL-36 $\beta$  cytokine expression within the coronary microvasculature. We also demonstrated that all three IL-36 cytokines can drive an inflammatory response in the adult and aged heart, with IL-36 $\gamma$  appearing to drive the most potent response in aged hearts. We showed cardioprotective effects of IL-36Ra through decreases in neutrophil recruitment, enhancement of FCD/perfusion, and reduced infarction via attenuation of ROS mediated endothelial and CM oxidative damage and vascular adhesion molecule expression. Importantly, the ability of the heart to respond to IL-36Ra was not lost with ageing or when tested in different sexes. This makes it an ideal candidate for consideration in future clinical trials.

In this thesis, the major work was conducted using IVM of the healthy and IR injured beating hearts. This has allowed, for the first time, the microcirculation of the adult and aged heart to be imaged and has shown the potential impact of inflammaging on the coronary microcirculation *in vivo*. Previous studies have shown neutrophils found in aged

animals to exist in a pre-activated state and constitutively secrete ROS and neutrophil elastase in close proximity to endothelium [221, 222], which can subsequently contribute to enhanced endothelial VCAM-1 expression [31, 32]. However, we have complemented these existing studies by showing that these events are associated with increased active neutrophil recruitment and/or non-active physical retention primarily within the coronary capillaries, as well as a concomitant decrease in the number of free-flowing neutrophils circulating through the heart. These dynamic events have not been previously seen experimentally and certainly not in human studies due to clinical tools not being able to resolve coronary microvessels  $<200\mu\text{m}$ . Understanding the kinetics of neutrophil recruitment in real-time *in vivo*, specifically in the heart, is important as it allows the interaction of neutrophils with other cells of the immune system to be imaged and generates quantitative data with respect to neutrophil numbers, velocity, recruitment and migratory behaviour. All of these different aspects of neutrophil behaviour can potentially be targeted in future novel anti-inflammatory or anti-neutrophils therapies.

Intravital microscopy of the cremaster muscle blood vessels was one of the first models to be established and extensively used to study neutrophil interactions with blood vessels. This was mainly due to the ease of accessing and preparing this muscle for imaging and its transparency. Data using this model has taught us a lot about the molecular mechanisms involved in the sequential phases of the leukocyte adhesion cascade [313]. However, since we now know the site and disease-specific mechanisms govern the leukocyte adhesion cascade, it is important to define the pathophysiological mechanisms governing thromboinflammation in the heart. Our studies certainly highlight an important mechanistic role for IL-36 in mediating inflammation in the IR injured heart, both in ageing

and both sexes, but we have yet to define the mechanisms contributing to thrombotic events. This latter point is worthwhile pursuing in future studies as we noted adherent thromboinflammatory cells, particularly platelets, primarily occupied the smallest diameter capillaries leading to their occlusion. This restricted the flow of blood within them during reperfusion, thereby generating multiple areas devoid of perfusion. This worsened microvasculature function may be a significant contributor to the generation of larger infarcts and so also needs addressing from a therapeutic perspective.

For the various groups tested in this thesis, our flow cytometric results showed CMs and ECs both undergo oxidative stress following IR injury. There is contradictory evidence in the literature on which cell group is more susceptible. For example, when compared to ECs, CMs are considered more sensitive to ischaemic injury and it is for this reason they have received the most attention when designing strategies to combat myocardial IR injury [314]. CM susceptibility to oxidative damage can be explained by their reliance on high energy usage, while EC susceptibility may be explained by them being the first cells to be exposed to oxidative stress [315]. Our novel data suggests no differences between the susceptibility of these cell groups, and this is perhaps due to the acute reperfusion period studied within this thesis. Nevertheless, oxidative stress can activate surrounding thromboinflammatory cells and in turn, upregulate adhesion molecules [239].

Another major part of this thesis was to investigate the potential role of IL-36 in myocardial IR injury. Our immunostaining and flow cytometry data showed for the first-time age- and sex-related differences in IL-36R, IL-36 $\alpha$ , and IL-36 $\beta$  expression in the coronary microvasculature. Adult male basal levels were seen to be the lowest of all the groups investigated, followed by adult female, and aged females with a concurrent increase in

response to IR injury within these groups on both CMs and ECs. Increases in baseline IL-36 cytokine expression not only correlate with levels of neutrophil recruitment seen following IR, but also with infarction and outcomes. This suggests that IL-36 may be directly involved in myocardial IRI through its pro-inflammatory activity on cardiac cells to enhance adhesion molecule expression, and attract neutrophils, which may secrete ROS, ultimately driving an exacerbated inflammatory response (**Figure 6.1**). Cheng *et al.* (2020) showed IL-36R rat knockouts had a significantly decreased infiltration of inflammatory cells, reduced oxidative stress, and CM apoptosis was reduced following cardiopulmonary bypass induced IR injury [152]. An increase in expression of IL-36 following IR injury and inflammation is not unique to the heart and has been described by other groups in various organs [276, 277]. However, this is the first study to investigate age- and sex-related differences in IL-36 expression. Importantly, we have shown these differences are mediated at the level of the microcirculation, and thus, the inflammatory cascade, which plays a critical role in MVO, could potentially be targeted through an IL-36 antagonistic effect at the level of the microvasculature [28, 52].

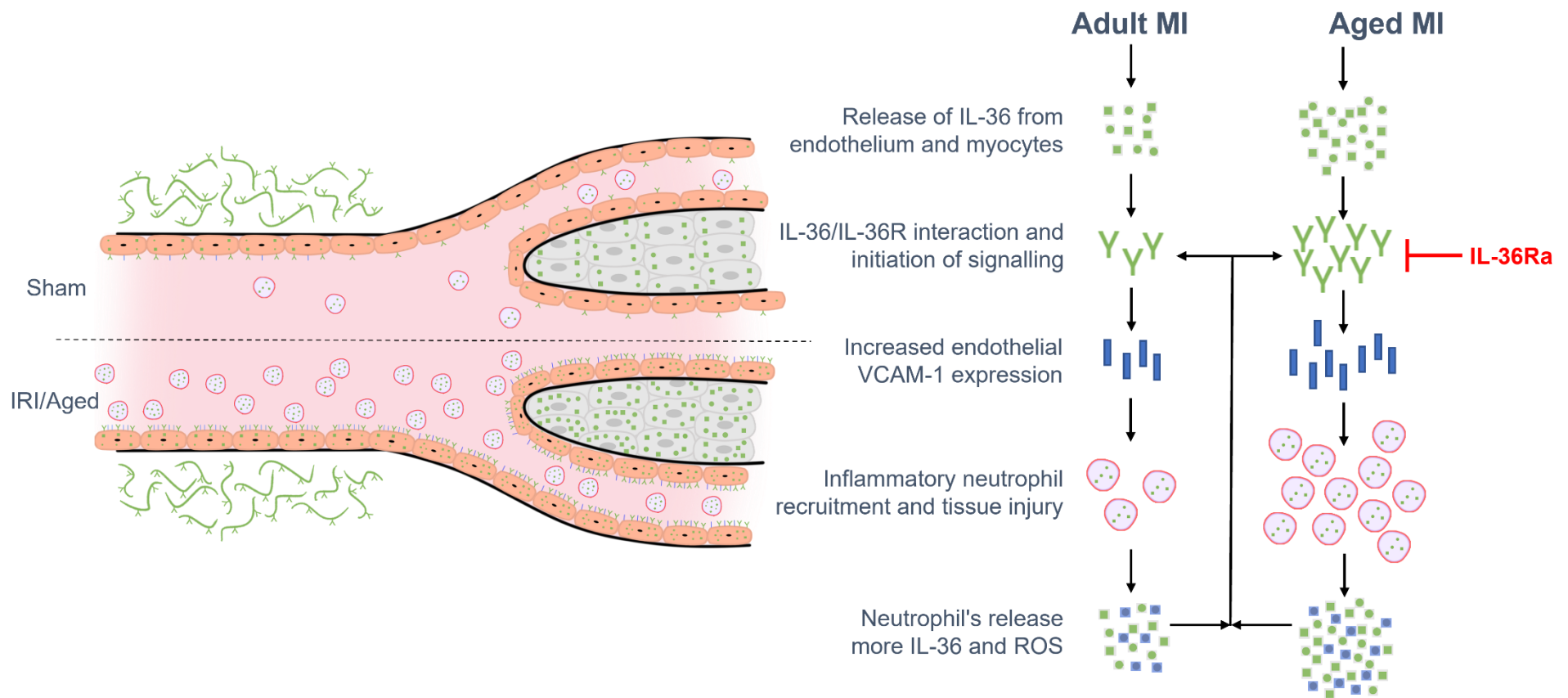


**Figure 6.1 – Schematic of a potential novel IL-36/IL-36R pathway in age and IR injury.** Based on the findings of this study, a potential novel mechanism of action for IL-36/IL-36R is proposed. Following reperfusion after a myocardial IR injury (MI) or in response to ageing, IL-36 cytokines are released from damaged, dead, or senescent cardiac cells (vascular, muscle, etc.). These interact with their receptor (IL-36R) and initiate a signalling cascade that increases the expression of vascular cell adhesion molecule-1 (VCAM-1), which in turn recruits neutrophils and other innate immune cells to the site of injury. Neutrophils then release IL-36 cytokines and ROS, and the cycle is repeated. This cycle may lead to the enhanced damage seen in ischaemia reperfusion (IR) injury and ageing and is inhibited using the IL-36R antagonist (IL-36Ra).

Activation of VCECs highlights that the various isoforms of the IL-36 cytokine could up-regulate the expression of their own receptor as well as themselves, suggesting a potential autocrine feedback loop. This positive feedback loop may serve to drive a potentiation of IL-36 signalling [316]. This may also be impacted by age; it is possible that the autoregulation of IL-36 becomes dysfunctional or desensitized as a result of inflammaging or cellular senescence. In the latter case, aged cardiac cells might not respond as efficiently to IL-36 when compared to adult cells. There are extensive studies in downstream pathways (including NF- $\kappa$ B, a signalling pathway downstream of IL-36) that provide evidence for the physiological presence of receptor desensitisation [317].

Topical application of cytokines on the heart has never been performed simultaneously alongside IVM studies, and thus we optimised the intravital set-up to facilitate this and allow us to directly activate inflammatory cells *in vivo* using IL-36 cytokines. Our findings showed that all IL-36 isoforms significantly enhanced neutrophil recruitment to the stabilized region of the beating LV in mice, suggesting that the IL-36/IL-36R pathway is functional within the heart and therefore IL-36 cytokines may be involved in the inflammatory responses within the heart. However, aged mice appeared to have a slower response to IL-36 cytokines and a reduced degree of neutrophil recruitment. Taken together with our previous findings of enhanced IL-36R and cytokine expression in aged mice, these findings appear contradictory. This seemingly contradictory finding could be explained in a number of ways. Firstly, increases in the expression of IL-36R in aged mice may correlate with concomitant increases in circulating endogenous antagonists. This would act to protect the balance of IL-36 pathway signalling in aged mice by inhibiting engagement of IL-36 cytokines with their receptor. However, it would also mean that the

same dose of IL-36 would be unlikely to deliver the same inflammatory response when comparing aged and adult mice. Indeed, this has been shown to be true for IL-1Ra where higher circulating levels of the endogenous antagonist are detected in elderly patients, and this has been suggested to play a role in the decline in the inflammatory response with age [239]. Secondly, in adult hearts, we saw that the inflammatory response was rapid and appeared to plateau beyond 60 minutes of topical application; in the aged heart, the inflammatory response continued to increase up to 150 minutes of topical cytokine application. This much slower response suggests that the response in the aged mice may not have reached its maxima by the end of the 150 minutes, possibly as a result of reduced neutrophil responsiveness with age [165, 168, 281]. It may be that with more prolonged imaging, this response would reach similar maximal levels to those observed in the adult mice.

Furthermore, IL-1 has been shown to also have direct activatory effects on platelets [286]. We have been able to show that platelet aggregation and microthrombi formation were enhanced with IL-36 $\beta$  and IL-36 $\gamma$  in adult hearts but were significantly reduced when topically applied in aged hearts. As such, it remains possible that some IL-36 isoforms may have an age-related direct thrombotic effect. However, further studies are required to elucidate the potential for IL-36 cytokines to directly activate platelets.

The final and most clinically translatable part of this thesis involved the use of IL-36Ra as a potential therapeutic for use following IR injury. New therapies and strategies need to be designed and optimised that are effective in improving the prognosis for aged patients post-MI. We and others have recommended therapies must involve specific and early protection of the delicate coronary microcirculation from IR injury [53, 54]. We have shown

IL-36Ra treatment to be anti-inflammatory at a functional, molecular, and cellular level within adult male and female IR injured hearts; these hearts had reductions in infarct size. This anti-inflammatory response was observed following IL-36Ra administration as a reduction in neutrophil recruitment. This may potentially be a result of decreased adhesion molecule expression in the coronary microcirculation (we observed reductions in VCAM-1 following IL-36Ra administration). Consequently, as less neutrophils are recruited, a decrease in ROS secretion by the ECs and CM was observed. This in turn, reduces the number of damaged cardiac cells, reduces MVO, and leads to reduced infarction (**Figure 6.1**). Moreover, a reduction in neutrophil recruitment may also be associated with less vessel occlusion as once neutrophils (in large numbers) become activated, they become stiffer and, in turn, result in MVO and enhance infarction [249]. Therefore, improvements in FCD, enhanced perfusion and maintenance of the initial hyperaemic response may be associated with this reduction. These effects were seen to be immediate and were sustained throughout reperfusion. In support of this is, recent work by Luo and colleagues demonstrated experimentally that deficiency of the IL-36 receptor protected CMs in the setting of a cardiopulmonary bypass [152]. It is likely that the increased thromboinflammatory activation and microcirculatory disturbances that we have observed intravitaly in the aged IR injured heart may inhibit the therapeutic efficacy of existing and future cardiovascular drugs in the elderly. However, our novel finding that IL-36Ra was not only vasculoprotective, but importantly remained beneficial in the setting of heightened age-related inflammation in the coronary microvessels, makes it a candidate worth pursuing clinically in the elderly patients undergoing PCI for MI.

A number of anti-inflammatories, shown to be successful in experimental studies, have met with translational failure when tested in patients with MI [259]. The major outcome measured in such clinical trials (and indeed experimental studies) are usually long-term ones – namely, the ability to prevent post-MI remodelling, a secondary non-fatal MI or death. Whether these anti-inflammatories can also protect and keep patent the coronary microcirculation in the immediate aftermath of PCI/reperfusion has received much less interest. However, this is imperative in order to improve long-term patient outcomes. It is therefore possible that translational failures are linked to a lack of early intervention at the level of the coronary microcirculation. Given the rapid development of microvascular no-reflow, the first hours, if not minutes, following reperfusion are likely to be a critical determinant of long-term outcomes. Since we have shown multiple microcirculatory disturbances resulting in poor myocardial perfusion within minutes of reperfusion, we posit that it is crucial that the design of anti-inflammatory therapies involve a timely administration. Our treatment strategy focused on introducing the antagonist at the end of the ischaemic phase, modelling the period immediately before interventions designed to mediate reperfusion commence (e.g., PCI). This is to establish an effective circulating concentration of antagonist in order to dampen the initial reperfusion-associated inflammatory response and maintain microvascular patency. However, not all clinical trials have delivered anti-inflammatories prior to reperfusion, with some administered days later [290]. Again, this may explain the lack of success of such compounds in clinical trials. Our novel data highlights a significant benefit to the coronary microcirculation in the immediate aftermath of reperfusion and infarct size with early administration of IL-36Ra, which importantly is maintained in the presence of an aging as a co-morbidity. This indicates that

early intervention with an IL-36R inhibitor is worth considering for future clinical investigations.

## **6.2. Future Work and Limitations to the Study**

Evidence obtained for this thesis has contributed significantly to our understanding of the role of IL-36 in the heart and has further expanded on age- and sex-related differences in myocardial IR injury. However, the data presented here only represents the first step towards a new therapeutic target, and many questions remain unanswered. A consistent finding throughout this thesis indicates a rapid thromboinflammatory response that initially peaks within the first 15 minutes of reperfusion. However, as all the IVM studies only lasted for 2.5 hours, we do not know what these responses might be like in the longer term in the presence or absence of the IL-36Ra. Indeed, this is not only relevant to thromboinflammatory responses but also to infarct size, perfusion, FCD, and at both a molecular and cellular level. Therefore, optimisation of our animal model to allow for recovery from surgery would be essential. This would then allow us to intravitaly image the heart days rather than minutes after reperfusion. Indeed, other groups have performed recovery experiments following myocardial IR injury and so optimisation of our current method should be achievable and would allow us to determine the long-term impact of IR injury and IL-36Ra therapy on the heart [318].

In the last decade, there has been a significant body of literature from experimental studies which have shown that targeting various elements in the inflammatory cascade is beneficial in the context of myocardial infarction. However, they were not able to

demonstrate a significant improvement in a clinical setting [109, 197, 263-265]. This has been associated with the animal model used, anti-inflammatory efficacy, involvement of MVO, and the time of intervention [60]. In this study, we have addressed questions round the time of intervention by administering the IL-36Ra prior to reperfusion commencing and the involvement of MVO through IVM and other studies. We have also sought to address concerns around the selection of the animal model by including a co-morbidity, namely ageing, in the study design. With that, we have shown evidence that IL-36Ra administration is efficacious in both adult and aged mice. Going forward, as diabetes and obesity are major risk factors and associated co-morbidities of MI, further studies could look to investigate whether IL-36Ra remains efficacious in hyperglycaemic and high-fat diet mice respectively. It would also be imperative to understand how IL-36 therapy differs from other anti-inflammatory therapies within the heart, especially therapies which have undergone clinical trials. These studies should be carried out using the same methods described within this thesis and would provide an insight into whether IL-36Ra provides the same level of anti-inflammatory benefit as other well-studied therapies – this would be a critical indicator as to whether pursuing IL-36 as a therapeutic target is worthwhile or not.

The broad inflammatory status of the heart and the circulation following myocardial IR injury would also be helpful in order to understand the mechanisms by which age- and sex-related differences are induced. The future use of gene and protein assays will allow researchers to determine elements that are either up or downregulated and provide a cellular and molecular mechanism to explain these differences. Moreover, these studies can also be used to identify mechanistic insights into how IL-36Ra confers protection. Such

studies have been performed in other organs, such as the skin; however, this has not been performed within the heart [112]. Cell polarization studies should also be conducted to determine whether IL-36Ra is anti-inflammatory through its actions on converting pro-inflammatory cells into a more anti-inflammatory phenotype (e.g., M1 to M2 or Ly6C<sup>lo</sup> to Ly6C<sup>high</sup>).

Although the current study suggests IL-36Ra is vasculoprotective through leukocyte-dependent mechanisms, it may also be protective through other unknown mechanisms. Indeed, IL-36R is also expressed on non-haematopoietic cells such as fibroblasts, and as we have shown, on ECs and CM [112]. Hence anti-IL-36 therapy may be protective through actions on these non-haematopoietic cells. However, the relative contributions of each cell type are not known as yet. The future use of IL-36R-floxed mice and cell culture experiments will allow researchers to determine the specific contributions of each cell type. Interestingly, IL-1 has been shown to have direct activatory effects on platelets, and as such, it remains possible that some IL-36 isoforms may have similar direct thrombotic effects [286]. We have also shown that IL-36Ra protects CM from oxidative damage, and this may be the result of a direct cardioprotective effect rather than an indirect effect of inhibiting inflammation. Therefore, these studies would be essential in identifying the mechanism of action. IL-36 research is steadily gaining pace, and future studies will unravel more about the beneficial mechanisms of action of this exciting cytokine.

### 6.3. Concluding Remarks

In the last decade, anti-inflammatory therapy for myocardial IR injury has been widely studied both experimentally and clinically. While these have been relatively successful in reducing infarction in experimental models, they have not translated into improved clinical outcomes. In this study, we have shown cardio- and vasculo-protective effects of IL-36Ra in adult and aged hearts. We have also demonstrated the thromboinflammatory events that occur in the immediate aftermath of reperfusion in the coronary microcirculation and how IL-36Ra can act immediately on this. In conclusion, we can no longer focus novel therapies solely on angiographically visible targets in the heart but need to carefully consider targets that maintain function in the coronary microcirculation during the earliest timepoints of reperfusion.

# **Chapter 7:**

# **References**

1. Feher, J., *Overview of the Cardiovascular System and the Blood*. 2012. p. 419-427.
2. Valensi, P., L. Lorgis, and Y. Cottin, *Prevalence, incidence, predictive factors and prognosis of silent myocardial infarction: A review of the literature*. Archives of Cardiovascular Diseases, 2011. **104**(3): p. 178-188.
3. Padsalgikar, A.D., *Cardiovascular System: Structure, Assessment, and Diseases*, in *Plastics in Medical Devices for Cardiovascular Applications*, A.D. Padsalgikar, Editor. 2017, William Andrew Publishing. p. 103-132.
4. Thomas, H., et al., *Global Atlas of Cardiovascular Disease 2000-2016: The Path to Prevention and Control*. Global Heart, 2018. **13**(3): p. 143-163.
5. Thomas, H., et al., *Global Atlas of Cardiovascular Disease 2000-2016: The Path to Prevention and Control*. Glob Heart, 2018. **13**(3): p. 143-163.
6. Roth, G.A., et al., *Global, Regional, and National Burden of Cardiovascular Diseases for 10 Causes, 1990 to 2015*. Journal of the American College of Cardiology, 2017. **70**(1): p. 1-25.
7. Lusis, A.J., *Atherosclerosis*. Nature, 2000. **407**(6801): p. 233-241.
8. Tedgui, A. and Z. Mallat, *[Atherosclerotic plaque formation]*. Rev Prat, 1999. **49**(19): p. 2081-6.
9. Berghuan, S.C., M.C. Bodde, and J.W. Jukema, *Pathophysiology and treatment of atherosclerosis : Current view and future perspective on lipoprotein modification treatment*. Neth Heart J, 2017. **25**(4): p. 231-242.
10. Steenbergen, C. and N.G. Frangogiannis, *Chapter 36 - Ischemic Heart Disease*, in *Muscle*, J.A. Hill and E.N. Olson, Editors. 2012, Academic Press: Boston/Waltham. p. 495-521.
11. Mechanic, O.J., M. Gavin, and S.A. Grossman, *Acute Myocardial Infarction*, in *StatPearls*. 2021: Treasure Island (FL).
12. Hombach, V., et al., *Pathophysiology of unstable angina pectoris--correlations with coronary angiographic imaging*. European heart journal, 1988. **9 Suppl N**: p. 40-5.
13. Haig, C., et al., *Current Smoking and Prognosis After Acute ST-Segment Elevation Myocardial Infarction: New Pathophysiological Insights*. JACC Cardiovasc Imaging, 2019. **12**(6): p. 993-1003.
14. Schmidt, A., et al., *Pathophysiology of unstable angina pectoris—correlations with coronary angiographic imaging*. European Heart Journal, 1988. **9**(suppl\_N): p. 40-45.
15. Allen, D.G. and H. Westerblad, *Role of phosphate and calcium stores in muscle fatigue*. The Journal of physiology, 2001. **536**(Pt 3): p. 657-665.
16. Kentish, J.C., *The effects of inorganic phosphate and creatine phosphate on force production in skinned muscles from rat ventricle*. The Journal of physiology, 1986. **370**: p. 585-604.
17. Elliott, A.C., et al., *Metabolic changes during ischaemia and their role in contractile failure in isolated ferret hearts*. The Journal of physiology, 1992. **454**: p. 467-490.
18. Carmeliet, E., *Cardiac Ionic Currents and Acute Ischemia: From Channels to Arrhythmias*. Physiological Reviews, 1999. **79**(3): p. 917-1017.
19. Konstantinidis, K., R.S. Whelan, and R.N. Kitsis, *Mechanisms of cell death in heart disease*. Arteriosclerosis, thrombosis, and vascular biology, 2012. **32**(7): p. 1552-1562.
20. Bhatt, D.L., et al., *Antiplatelet and Anticoagulation Therapy for Acute Coronary Syndromes*. Circulation Research, 2014. **114**(12): p. 1929-1943.
21. Lim, S.Y., *Role of statins in coronary artery disease*. Chonnam medical journal, 2013. **49**(1): p. 1-6.
22. Yedinak, K.C. and T.T. Sproat, *Heparin and warfarin therapy after acute myocardial infarction*. Clin Pharm, 1993. **12**(3): p. 197-215.
23. Zhang, Y. and Y. Huo, *Early reperfusion strategy for acute myocardial infarction: a need for clinical implementation*. Journal of Zhejiang University. Science. B, 2011. **12**(8): p. 629-632.

24. Hellawell, J.L. and K.B. Margulies, *Myocardial reverse remodeling*. Cardiovasc Ther, 2012. **30**(3): p. 172-81.
25. Landmesser, U., K.C. Wollert, and H. Drexler, *Potential novel pharmacological therapies for myocardial remodelling*. Cardiovasc Res, 2009. **81**(3): p. 519-27.
26. Ferreira, J.C.B. and D. Mochly-Rosen, *Nitroglycerin use in myocardial infarction patients*. Circulation journal : official journal of the Japanese Circulation Society, 2012. **76**(1): p. 15-21.
27. Antman, E.M., et al., *ACC/AHA guidelines for the management of patients with ST-elevation myocardial infarction--executive summary: a report of the American College of Cardiology/American Heart Association Task Force on Practice Guidelines (Writing Committee to Revise the 1999 Guidelines for the Management of Patients With Acute Myocardial Infarction)*. Circulation, 2004. **110**(5): p. 588-636.
28. Eltzschig, H.K. and T. Eckle, *Ischemia and reperfusion—from mechanism to translation*. Nature Medicine, 2011. **17**: p. 1391.
29. Hilleman, D.E., et al., *Fibrinolytic agents for the management of ST-segment elevation myocardial infarction*. Pharmacotherapy, 2007. **27**(11): p. 1558-70.
30. Antman, E.M., et al., *ACC/AHA Guidelines for the Management of Patients With ST-Elevation Myocardial Infarction&#x2014;Executive Summary*. Circulation, 2004. **110**(5): p. 588-636.
31. de Groot, H. and U. Rauen, *Ischemia-reperfusion injury: processes in pathogenetic networks: a review*. Transplant Proc, 2007. **39**(2): p. 481-4.
32. Hausenloy, D.J. and D.M. Yellon, *Myocardial ischemia-reperfusion injury: a neglected therapeutic target*. The Journal of clinical investigation, 2013. **123**(1): p. 92-100.
33. Li, C. and R.M. Jackson, *Reactive species mechanisms of cellular hypoxia-reoxygenation injury*. American Journal of Physiology-Cell Physiology, 2002. **282**(2): p. C227-C241.
34. Talukder, M.A.H. and J.L. Zweier, *The role of oxidants and free radicals in reperfusion injury*. Cardiovascular Research, 2006. **70**(2): p. 181-190.
35. de Groot, H. and U. Rauen, *Ischemia-Reperfusion Injury: Processes in Pathogenetic Networks: A Review*. Transplantation Proceedings, 2007. **39**(2): p. 481-484.
36. Miyamae, M., et al., *Attenuation of postischemic reperfusion injury is related to prevention of [Ca<sup>2+</sup>]<sub>m</sub> overload in rat hearts*. Am J Physiol, 1996. **271**(5 Pt 2): p. H2145-53.
37. Bär, F.W., et al., *Results of the first clinical study of adjunctive CALdaret (MCC-135) in patients undergoing primary percutaneous coronary intervention for ST-Elevation Myocardial Infarction: the randomized multicentre CASTEMI study*. Eur Heart J, 2006. **27**(21): p. 2516-23.
38. Hausenloy, D.J., M.R. Duchon, and D.M. Yellon, *Inhibiting mitochondrial permeability transition pore opening at reperfusion protects against ischaemia-reperfusion injury*. Cardiovasc Res, 2003. **60**(3): p. 617-25.
39. Smith, R.A., R.C. Hartley, and M.P. Murphy, *Mitochondria-targeted small molecule therapeutics and probes*. Antioxid Redox Signal, 2011. **15**(12): p. 3021-38.
40. Avkiran, M. and M.S. Marber, *Na(+)/H(+) exchange inhibitors for cardioprotective therapy: progress, problems and prospects*. J Am Coll Cardiol, 2002. **39**(5): p. 747-53.
41. Camici, P.G. and F. Crea, *Coronary microvascular dysfunction*. N Engl J Med, 2007. **356**(8): p. 830-40.
42. Kavanagh, D.P.J., et al., *Imaging the injured beating heart intravitaly and the vasculoprotection afforded by haematopoietic stem cells*. Cardiovascular Research, 2019. **115**(13): p. 1918-1932.
43. Bolognese, L., et al., *Impact of microvascular dysfunction on left ventricular remodeling and long-term clinical outcome after primary coronary angioplasty for acute myocardial infarction*. Circulation, 2004. **109**(9): p. 1121-6.

44. De Maria, G.L., et al., *How does coronary stent implantation impact on the status of the microcirculation during primary percutaneous coronary intervention in patients with ST-elevation myocardial infarction?* Eur Heart J, 2015. **36**(45): p. 3165-77.
45. McAlindon, E., et al., *Microvascular dysfunction determines infarct characteristics in patients with reperfused ST-segment elevation myocardial infarction: The MICROcirculation in Acute Myocardial Infarction (MICRO-AMI) study.* PLoS One, 2018. **13**(11): p. e0203750.
46. Pasupathy, S., R. Tavella, and J.F. Beltrame, *The What, When, Who, Why, How and Where of Myocardial Infarction With Non-Obstructive Coronary Arteries (MINOCA).* Circ J, 2016. **80**(1): p. 11-6.
47. Agewall, S., et al., *Myocardial infarction with angiographically normal coronary arteries.* Atherosclerosis, 2011. **219**(1): p. 10-14.
48. Mukherjee, D., *Myocardial Infarction With Nonobstructive Coronary Arteries: A Call for Individualized Treatment.* Journal of the American Heart Association, 2019. **8**(14): p. e013361.
49. Paulus, W.J. and C. Tschöpe, *A novel paradigm for heart failure with preserved ejection fraction: comorbidities drive myocardial dysfunction and remodeling through coronary microvascular endothelial inflammation.* J Am Coll Cardiol, 2013. **62**(4): p. 263-71.
50. Tschöpe, C. and S. Van Linthout, *New insights in (inter)cellular mechanisms by heart failure with preserved ejection fraction.* Curr Heart Fail Rep, 2014. **11**(4): p. 436-44.
51. Kalia, N., *A historical review of experimental imaging of the beating heart coronary microcirculation in vivo.* Journal of Anatomy, 2021. **n/a**(n/a).
52. Pries, A.R. and B. Reglin, *Coronary microcirculatory pathophysiology: can we afford it to remain a black box?* European Heart Journal, 2016. **38**(7): p. 478-488.
53. Pries, A.R. and B. Reglin, *Coronary microcirculatory pathophysiology: can we afford it to remain a black box?* European heart journal, 2017. **38**(7): p. 478-488.
54. Kavanagh, D.P.J. and N. Kalia, *Live Intravital Imaging of Cellular Trafficking in the Cardiac Microvasculature-Beating the Odds.* Frontiers in immunology, 2019. **10**: p. 2782-2782.
55. Playán-Escribano, J., P. Martínez-Losas, and M. Cobos-Gil, *Electrocardiographic Changes After Angioplasty of the Left Anterior Descending Coronary Artery.* Circulation, 2019. **139**(12): p. 1550-1553.
56. Chen, L., et al., *Inflammatory responses and inflammation-associated diseases in organs.* Oncotarget, 2017. **9**(6): p. 7204-7218.
57. Iwasaki, A. and R. Medzhitov, *Control of adaptive immunity by the innate immune system.* Nature immunology, 2015. **16**(4): p. 343-353.
58. Fang, L., et al., *Systemic inflammatory response following acute myocardial infarction.* Journal of geriatric cardiology : JGC, 2015. **12**(3): p. 305-312.
59. Frangogiannis, N.G., *The immune system and cardiac repair.* Pharmacological Research, 2008. **58**(2): p. 88-111.
60. Ong, S.-B., et al., *Inflammation following acute myocardial infarction: Multiple players, dynamic roles, and novel therapeutic opportunities.* Pharmacology & therapeutics, 2018. **186**: p. 73-87.
61. Stieger, P., et al., *Targeting of Extracellular RNA Reduces Edema Formation and Infarct Size and Improves Survival After Myocardial Infarction in Mice.* Journal of the American Heart Association, 2017. **6**(6): p. e004541.
62. Hu, G., et al., *Exendin-4 attenuates myocardial ischemia and reperfusion injury by inhibiting high mobility group box 1 protein expression.* Cardiol J, 2013. **20**(6): p. 600-4.
63. van Hout, G.P., et al., *Targeting danger-associated molecular patterns after myocardial infarction.* Expert Opin Ther Targets, 2016. **20**(2): p. 223-39.
64. Kim, S.C., et al., *Toll-like receptor 4 deficiency: smaller infarcts, but no gain in function.* BMC Physiol, 2007. **7**: p. 5.

65. Timmers, L., et al., *Toll-like receptor 4 mediates maladaptive left ventricular remodeling and impairs cardiac function after myocardial infarction*. Circ Res, 2008. **102**(2): p. 257-64.
66. Shimamoto, A., et al., *Inhibition of Toll-like receptor 4 with eritoran attenuates myocardial ischemia-reperfusion injury*. Circulation, 2006. **114**(1 Suppl): p. I270-4.
67. Arslan, F., et al., *Myocardial ischemia/reperfusion injury is mediated by leukocytic toll-like receptor-2 and reduced by systemic administration of a novel anti-toll-like receptor-2 antibody*. Circulation, 2010. **121**(1): p. 80-90.
68. Sandanger, Ø., et al., *The NLRP3 inflammasome is up-regulated in cardiac fibroblasts and mediates myocardial ischaemia-reperfusion injury*. Cardiovasc Res, 2013. **99**(1): p. 164-74.
69. Mezzaroma, E., et al., *The inflammasome promotes adverse cardiac remodeling following acute myocardial infarction in the mouse*. Proc Natl Acad Sci U S A, 2011. **108**(49): p. 19725-30.
70. Coll, R.C., et al., *A small-molecule inhibitor of the NLRP3 inflammasome for the treatment of inflammatory diseases*. Nature medicine, 2015. **21**(3): p. 248-255.
71. Dewald, O., et al., *Of mice and dogs: species-specific differences in the inflammatory response following myocardial infarction*. Am J Pathol, 2004. **164**(2): p. 665-77.
72. Lugin, J., et al., *Cutting edge: IL-1 $\alpha$  is a crucial danger signal triggering acute myocardial inflammation during myocardial infarction*. J Immunol, 2015. **194**(2): p. 499-503.
73. Ørn, S., et al., *Increased interleukin-18 levels are associated with left ventricular hypertrophy and remodelling following acute ST segment elevation myocardial infarction treated by primary percutaneous coronary intervention*. J Intern Med, 2012. **272**(3): p. 267-76.
74. Hartman, M.H.T., et al., *Translational overview of cytokine inhibition in acute myocardial infarction and chronic heart failure*. Trends in Cardiovascular Medicine, 2018. **28**(6): p. 369-379.
75. Kobara, M., et al., *Antibody against interleukin-6 receptor attenuates left ventricular remodelling after myocardial infarction in mice*. Cardiovascular Research, 2010. **87**(3): p. 424-430.
76. Müller, J., et al., *Interleukin-6-dependent phenotypic modulation of cardiac fibroblasts after acute myocardial infarction*. Basic Research in Cardiology, 2014. **109**(6): p. 440.
77. Anstensrud, A.K., et al., *Rationale for the ASSAIL-MI-trial: a randomised controlled trial designed to assess the effect of tocilizumab on myocardial salvage in patients with acute ST-elevation myocardial infarction (STEMI)*. Open Heart, 2019. **6**(2): p. e001108.
78. Dewald, O., et al., *CCL2/Monocyte Chemoattractant Protein-1 regulates inflammatory responses critical to healing myocardial infarcts*. Circ Res, 2005. **96**(8): p. 881-9.
79. Montecucco, F., et al., *CC chemokine CCL5 plays a central role impacting infarct size and post-infarction heart failure in mice*. Eur Heart J, 2012. **33**(15): p. 1964-74.
80. Frangogiannis, N.G., *The role of the chemokines in myocardial ischemia and reperfusion*. Curr Vasc Pharmacol, 2004. **2**(2): p. 163-74.
81. Ley, K., et al., *Getting to the site of inflammation: the leukocyte adhesion cascade updated*. Nature Reviews Immunology, 2007. **7**(9): p. 678-689.
82. Patten, D.A. and S. Shetty, *More Than Just a Removal Service: Scavenger Receptors in Leukocyte Trafficking*. Frontiers in Immunology, 2018. **9**(2904).
83. Luc, G., et al., *Circulating soluble adhesion molecules ICAM-1 and VCAM-1 and incident coronary heart disease: the PRIME Study*. Atherosclerosis, 2003. **170**(1): p. 169-76.
84. Núñez, J., et al., *Usefulness of the neutrophil to lymphocyte ratio in predicting long-term mortality in ST segment elevation myocardial infarction*. Am J Cardiol, 2008. **101**(6): p. 747-52.
85. Prabhu, S.D. and N.G. Frangogiannis, *The Biological Basis for Cardiac Repair After Myocardial Infarction: From Inflammation to Fibrosis*. Circulation research, 2016. **119**(1): p. 91-112.

86. McDonald, B., et al., *Intravascular danger signals guide neutrophils to sites of sterile inflammation*. Science, 2010. **330**(6002): p. 362-6.
87. Guasti, L., et al., *Neutrophils and clinical outcomes in patients with acute coronary syndromes and/or cardiac revascularisation. A systematic review on more than 34,000 subjects*. Thromb Haemost, 2011. **106**(4): p. 591-9.
88. Ma, Y., et al., *Temporal neutrophil polarization following myocardial infarction*. Cardiovascular research, 2016. **110**(1): p. 51-61.
89. Arai, M., et al., *An anti-CD18 antibody limits infarct size and preserves left ventricular function in dogs with ischemia and 48-hour reperfusion*. J Am Coll Cardiol, 1996. **27**(5): p. 1278-85.
90. Yang, J., et al., *Monocyte and macrophage differentiation: circulation inflammatory monocyte as biomarker for inflammatory diseases*. Biomarker research, 2014. **2**(1): p. 1-1.
91. Mariani, M., et al., *Significance of total and differential leucocyte count in patients with acute myocardial infarction treated with primary coronary angioplasty*. Eur Heart J, 2006. **27**(21): p. 2511-5.
92. Frangogiannis, N.G., *The inflammatory response in myocardial injury, repair, and remodelling*. Nature reviews. Cardiology, 2014. **11**(5): p. 255-265.
93. Harel-Adar, T., et al., *Modulation of cardiac macrophages by phosphatidylserine-presenting liposomes improves infarct repair*. Proceedings of the National Academy of Sciences of the United States of America, 2011. **108**(5): p. 1827-1832.
94. Yilmaz, A., et al., *Decrease in circulating myeloid dendritic cell precursors in coronary artery disease*. J Am Coll Cardiol, 2006. **48**(1): p. 70-80.
95. Yan, X., et al., *Temporal dynamics of cardiac immune cell accumulation following acute myocardial infarction*. J Mol Cell Cardiol, 2013. **62**: p. 24-35.
96. Backteman, K., J. Ernerudh, and L. Jonasson, *Natural killer (NK) cell deficit in coronary artery disease: no aberrations in phenotype but sustained reduction of NK cells is associated with low-grade inflammation*. Clinical & Experimental Immunology, 2014. **175**(1): p. 104-112.
97. Blum, A. and S. Yeganeh, *The role of T-lymphocyte subpopulations in acute myocardial infarction*. Eur J Intern Med, 2003. **14**(7): p. 407-410.
98. Al-Ahmad, R.S., A.M. Mahafzah, and E.N. Al-Mousa, *Immunological changes in acute myocardial infarction*. Saudi Med J, 2004. **25**(7): p. 923-8.
99. Zouggar, Y., et al., *B lymphocytes trigger monocyte mobilization and impair heart function after acute myocardial infarction*. Nature medicine, 2013. **19**(10): p. 1273-1280.
100. Furman, M.I., et al., *Circulating monocyte-platelet aggregates are an early marker of acute myocardial infarction*. J Am Coll Cardiol, 2001. **38**(4): p. 1002-6.
101. Huang, S. and N.G. Frangogiannis, *Anti-inflammatory therapies in myocardial infarction: failures, hopes and challenges*. British Journal of Pharmacology, 2018. **175**(9): p. 1377-1400.
102. Martin, S.J., *Cell death and inflammation: the case for IL-1 family cytokines as the canonical DAMPs of the immune system*. Febs j, 2016. **283**(14): p. 2599-615.
103. Toldo, S., et al., *Recombinant Human Interleukin-1 Receptor Antagonist Provides Cardioprotection During Myocardial Ischemia Reperfusion in the Mouse*. Cardiovascular Drugs and Therapy, 2012. **26**(3): p. 273-276.
104. Suzuki, K., et al., *Overexpression of Interleukin-1 Receptor Antagonist Provides Cardioprotection Against Ischemia-Reperfusion Injury Associated With Reduction in Apoptosis*. Circulation, 2001. **104**(suppl\_1): p. I-308-I-313.
105. Abbate, A., et al., *Interleukin-1 blockade with anakinra to prevent adverse cardiac remodeling after acute myocardial infarction (Virginia Commonwealth University Anakinra Remodeling Trial [VCU-ART] Pilot study)*. Am J Cardiol, 2010. **105**(10): p. 1371-1377.e1.

106. Abbate, A., et al., *Effects of interleukin-1 blockade with anakinra on adverse cardiac remodeling and heart failure after acute myocardial infarction [from the Virginia Commonwealth University-Anakinra Remodeling Trial (2) (VCU-ART2) pilot study]*. The American journal of cardiology, 2013. **111**(10): p. 1394-1400.
107. Abbate, A., et al., *Comparative Safety of Interleukin-1 Blockade With Anakinra in Patients With ST-Segment Elevation Acute Myocardial Infarction (from the VCU-ART and VCU-ART2 Pilot Studies)*. The American Journal of Cardiology, 2015. **115**(3): p. 288-292.
108. Abbate, A., et al., *Interleukin-1 Blockade Inhibits the Acute Inflammatory Response in Patients With ST-Segment–Elevation Myocardial Infarction*. Journal of the American Heart Association, 2020. **9**(5): p. e014941.
109. Morton, A.C., et al., *The effect of interleukin-1 receptor antagonist therapy on markers of inflammation in non-ST elevation acute coronary syndromes: the MRC-ILA Heart Study*. European Heart Journal, 2015. **36**(6): p. 377-384.
110. Baran, K.W., et al., *Double-blind, randomized trial of an anti-CD18 antibody in conjunction with recombinant tissue plasminogen activator for acute myocardial infarction: limitation of myocardial infarction following thrombolysis in acute myocardial infarction (LIMIT AMI) study*. Circulation, 2001. **104**(23): p. 2778-83.
111. Faxon, D.P., et al., *The effect of blockade of the CD11/CD18 integrin receptor on infarct size in patients with acute myocardial infarction treated with direct angioplasty: the results of the HALT-MI study*. J Am Coll Cardiol, 2002. **40**(7): p. 1199-204.
112. Buhl, A.-L. and J. Wenzel, *Interleukin-36 in Infectious and Inflammatory Skin Diseases*. Frontiers in immunology, 2019. **10**: p. 1162-1162.
113. Weber, A., P. Wasiliew, and M. Kracht, *Interleukin-1 (IL-1) Pathway*. Science Signaling, 2010. **3**(105): p. cm1-cm1.
114. Krumm, B., Y. Xiang, and J. Deng, *Structural biology of the IL-1 superfamily: key cytokines in the regulation of immune and inflammatory responses*. Protein science : a publication of the Protein Society, 2014. **23**(5): p. 526-538.
115. Ridker, P.M., *From C-Reactive Protein to Interleukin-6 to Interleukin-1: Moving Upstream To Identify Novel Targets for Atheroprotection*. Circ Res, 2016. **118**(1): p. 145-56.
116. Gresnigt, M.S. and F.L. van de Veerdonk, *Biology of IL-36 cytokines and their role in disease*. Semin Immunol, 2013. **25**(6): p. 458-65.
117. Gabay, C. and J.E. Towne, *Regulation and function of interleukin-36 cytokines in homeostasis and pathological conditions*. J Leukoc Biol, 2015. **97**(4): p. 645-52.
118. Buhl, A.-L. and J. Wenzel, *Interleukin-36 in Infectious and Inflammatory Skin Diseases*. Frontiers in Immunology, 2019. **10**(1162).
119. Yuan, Z.-C., et al., *Biology of IL-36 Signaling and Its Role in Systemic Inflammatory Diseases*. Frontiers in Immunology, 2019. **10**(2532).
120. Busfield, S.J., et al., *Identification and gene organization of three novel members of the IL-1 family on human chromosome 2*. Genomics, 2000. **66**(2): p. 213-6.
121. Ainscough, J.S., et al., *Cathepsin S is the major activator of the psoriasis-associated proinflammatory cytokine IL-36 $\gamma$* . Proc Natl Acad Sci U S A, 2017. **114**(13): p. E2748-e2757.
122. Hahn, M., S. Frey, and A.J. Hueber, *The novel interleukin-1 cytokine family members in inflammatory diseases*. Curr Opin Rheumatol, 2017. **29**(2): p. 208-213.
123. Johnston, A., et al., *IL-1 and IL-36 are dominant cytokines in generalized pustular psoriasis*. J Allergy Clin Immunol, 2017. **140**(1): p. 109-120.
124. Bozoyan, L., et al., *Interleukin-36 $\gamma$  is expressed by neutrophils and can activate microglia, but has no role in experimental autoimmune encephalomyelitis*. Journal of neuroinflammation, 2015. **12**: p. 173-173.
125. Kovach, M.A., et al., *IL-36 $\gamma$  is secreted in microparticles and exosomes by lung macrophages in response to bacteria and bacterial components*. Journal of leukocyte biology, 2016. **100**(2): p. 413-421.

126. Yi, G., et al., *Structural and Functional Attributes of the Interleukin-36 Receptor*. Journal of Biological Chemistry, 2016. **291**: p. jbc.M116.723064.
127. Milora, K.A., et al., *Unprocessed Interleukin-36 $\beta$ 1; Regulates Psoriasis-Like Skin Inflammation in Cooperation With Interleukin-1*. Journal of Investigative Dermatology, 2015. **135**(12): p. 2992-3000.
128. Gabay, C. and J.E. Towne, *Regulation and function of interleukin-36 cytokines in homeostasis and pathological conditions*. Journal of Leukocyte Biology, 2015. **97**(4): p. 645-652.
129. Towne, J.E., et al., *Interleukin-36 (IL-36) ligands require processing for full agonist (IL-36 $\alpha$ , IL-36 $\beta$ , and IL-36 $\gamma$ ) or antagonist (IL-36Ra) activity*. The Journal of biological chemistry, 2011. **286**(49): p. 42594-42602.
130. Henry, C.M., et al., *Neutrophil-Derived Proteases Escalate Inflammation through Activation of IL-36 Family Cytokines*. Cell Rep, 2016. **14**(4): p. 708-722.
131. Sullivan, G.P., et al., *Suppressing IL-36-driven inflammation using peptide pseudosubstrates for neutrophil proteases*. Cell death & disease, 2018. **9**(3): p. 378-378.
132. Foster, A.M., et al., *IL-36 promotes myeloid cell infiltration, activation, and inflammatory activity in skin*. J Immunol, 2014. **192**(12): p. 6053-61.
133. Mahil, S.K., et al., *An analysis of IL-36 signature genes and individuals with *IL1RL2* knockout mutations validates IL-36 as a psoriasis therapeutic target*. Science Translational Medicine, 2017. **9**(411): p. eaan2514.
134. Swindell, W.R., et al., *RNA-Seq Analysis of IL-1B and IL-36 Responses in Epidermal Keratinocytes Identifies a Shared MyD88-Dependent Gene Signature*. Frontiers in Immunology, 2018. **9**(80).
135. Carriere, V., et al., *IL-33, the IL-1-like cytokine ligand for ST2 receptor, is a chromatin-associated nuclear factor *in vivo**. Proceedings of the National Academy of Sciences, 2007. **104**(1): p. 282-287.
136. Bridgewood, C., et al., *IL-36 $\gamma$  has proinflammatory effects on human endothelial cells*. Experimental Dermatology, 2017. **26**(5): p. 402-408.
137. Blumberg, H., et al., *Opposing activities of two novel members of the IL-1 ligand family regulate skin inflammation*. The Journal of experimental medicine, 2007. **204**(11): p. 2603-2614.
138. Frey, S., et al., *The novel cytokine interleukin-36 $\alpha$  is expressed in psoriatic and rheumatoid arthritis synovium*. Annals of the Rheumatic Diseases, 2013. **72**(9): p. 1569-1574.
139. Ding, L., et al., *IL-36 cytokines in autoimmunity and inflammatory disease*. Oncotarget, 2017. **9**(2): p. 2895-2901.
140. Vigne, S., et al., *IL-36R ligands are potent regulators of dendritic and T cells*. Blood, 2011. **118**(22): p. 5813-5823.
141. Dietrich, D., et al., *Interleukin-36 potently stimulates human M2 macrophages, Langerhans cells and keratinocytes to produce pro-inflammatory cytokines*. Cytokine, 2016. **84**: p. 88-98.
142. Harusato, A., et al., *IL-36 $\gamma$  signaling controls the induced regulatory T cell–Th9 cell balance via NF $\kappa$ B activation and STAT transcription factors*. Mucosal Immunology, 2017. **10**(6): p. 1455-1467.
143. van de Veerdonk, F.L., et al., *IL-38 binds to the IL-36 receptor and has biological effects on immune cells similar to IL-36 receptor antagonist*. Proceedings of the National Academy of Sciences, 2012. **109**(8): p. 3001-3005.
144. Boutet, M.A., et al., *Distinct expression of interleukin (IL)-36 $\alpha$ ,  $\beta$  and  $\gamma$ , their antagonist IL-36Ra and IL-38 in psoriasis, rheumatoid arthritis and Crohn's disease*. Clinical and experimental immunology, 2016. **184**(2): p. 159-173.

145. Sehat, M., et al., *Evaluating Serum Levels of IL-33, IL-36, IL-37 and Gene Expression of IL-37 in Patients with Psoriasis Vulgaris*. Iran J Allergy Asthma Immunol, 2018. **17**(2): p. 179-187.
146. Bachelez, H., et al., *Inhibition of the Interleukin-36 Pathway for the Treatment of Generalized Pustular Psoriasis*. New England Journal of Medicine, 2019. **380**(10): p. 981-983.
147. Marrakchi, S., et al., *Interleukin-36-receptor antagonist deficiency and generalized pustular psoriasis*. N Engl J Med, 2011. **365**(7): p. 620-8.
148. Tortola, L., et al., *Psoriasiform dermatitis is driven by IL-36-mediated DC-keratinocyte crosstalk*. The Journal of Clinical Investigation, 2012. **122**(11): p. 3965-3976.
149. Tauber, M., et al., *IL36RN Mutations Affect Protein Expression and Function: A Basis for Genotype-Phenotype Correlation in Pustular Diseases*. Journal of Investigative Dermatology, 2016. **136**(9): p. 1811-1819.
150. Mai, S.-z., et al., *Increased serum IL-36 $\alpha$  and IL-36 $\gamma$  levels in patients with systemic lupus erythematosus: Association with disease activity and arthritis*. International Immunopharmacology, 2018. **58**: p. 103-108.
151. Chu, M., et al., *In vivo anti-inflammatory activities of novel cytokine IL-38 in Murphy Roths Large (MRL)/lpr mice*. Immunobiology, 2017. **222**(3): p. 483-493.
152. Luo, C., et al., *Deficiency of Interleukin-36 Receptor Protected Cardiomyocytes from Ischemia-Reperfusion Injury in Cardiopulmonary Bypass*. Medical science monitor : international medical journal of experimental and clinical research, 2020. **26**: p. e918933-e918933.
153. Zhong, Y., et al., *Elevated Plasma IL-38 Concentrations in Patients with Acute ST-Segment Elevation Myocardial Infarction and Their Dynamics after Reperfusion Treatment*. Mediators of Inflammation, 2015. **2015**: p. 490120.
154. Wei, Y., et al., *Interleukin-38 alleviates cardiac remodelling after myocardial infarction*. Journal of cellular and molecular medicine, 2020. **24**(1): p. 371-384.
155. Izekenova, A.K., et al., *Trends in ageing of the population and the life expectancy after retirement: A comparative country-based analysis*. Journal of research in medical sciences : the official journal of Isfahan University of Medical Sciences, 2015. **20**(3): p. 250-252.
156. Shakeri, H., et al., *Cellular senescence links aging and diabetes in cardiovascular disease*. American Journal of Physiology-Heart and Circulatory Physiology, 2018. **315**(3): p. H448-H462.
157. Dhingra, R. and R.S. Vasan, *Age as a risk factor*. The Medical clinics of North America, 2012. **96**(1): p. 87-91.
158. Besse, S., et al., *Cardioprotection with cariporide, a sodium-proton exchanger inhibitor, after prolonged ischemia and reperfusion in senescent rats*. Exp Gerontol, 2004. **39**(9): p. 1307-14.
159. Boengler, K., R. Schulz, and G. Heusch, *Loss of cardioprotection with ageing*. Cardiovascular Research, 2009. **83**(2): p. 247-261.
160. Abete, P., et al., *Ischemic threshold and myocardial stunning in the aging heart*. Experimental Gerontology, 1999. **34**(7): p. 875-884.
161. Miller, T.D., et al., *Comparison of acute myocardial infarct size to two-year mortality in patients <65 to those  $\geq$ 65 years of age*. The American Journal of Cardiology, 1999. **84**(10): p. 1170-1175.
162. Shim, Y.H., *Cardioprotection and ageing*. Korean journal of anesthesiology, 2010. **58**(3): p. 223-230.
163. Franceschi, C., et al., *Inflamm-aging. An evolutionary perspective on immunosenescence*. Ann N Y Acad Sci, 2000. **908**: p. 244-54.

164. Franceschi, C. and J. Campisi, *Chronic Inflammation (Inflammaging) and Its Potential Contribution to Age-Associated Diseases*. The Journals of Gerontology: Series A, 2014. **69**(Suppl\_1): p. S4-S9.
165. Franceschi, C., et al., *Inflammaging: a new immune–metabolic viewpoint for age-related diseases*. Nature Reviews Endocrinology, 2018. **14**(10): p. 576-590.
166. Shaw, A.C., et al., *Aging of the innate immune system*. Current opinion in immunology, 2010. **22**(4): p. 507-513.
167. Mohebali, D., et al., *Alterations in platelet function during aging: clinical correlations with thromboinflammatory disease in older adults*. Journal of the American Geriatrics Society, 2014. **62**(3): p. 529-535.
168. Verschoor, C.P., et al., *Circulating TNF and mitochondrial DNA are major determinants of neutrophil phenotype in the advanced-age, frail elderly*. Molecular Immunology, 2015. **65**(1): p. 148-156.
169. Minciullo, P.L., et al., *Inflammaging and Anti-Inflammaging: The Role of Cytokines in Extreme Longevity*. Archivum Immunologiae et Therapiae Experimentalis, 2016. **64**(2): p. 111-126.
170. Nomellini, V., et al., *Dysregulation of neutrophil CXCR2 and pulmonary endothelial icam-1 promotes age-related pulmonary inflammation*. Aging and disease, 2012. **3**(3): p. 234-247.
171. Sapey, E., et al., *Phosphoinositide 3-kinase inhibition restores neutrophil accuracy in the elderly: toward targeted treatments for immunosenescence*. Blood, 2014. **123**(2): p. 239-248.
172. Sidney, S., et al., *Recent Trends in Cardiovascular Mortality in the United States and Public Health Goals*. JAMA Cardiology, 2016. **1**(5): p. 594-599.
173. Anand, S.S., et al., *Risk factors for myocardial infarction in women and men: insights from the INTERHEART study*. European Heart Journal, 2008. **29**(7): p. 932-940.
174. Fang, J., et al., *Acute Myocardial Infarction Hospitalization in the United States, 1979 to 2005*. The American Journal of Medicine, 2010. **123**(3): p. 259-266.
175. Benjamin, E.J., et al., *Heart Disease and Stroke Statistics&#x2014;2019 Update: A Report From the American Heart Association*. Circulation, 2019. **139**(10): p. e56-e528.
176. Vaccarino, V., et al., *Sex differences in mortality after acute myocardial infarction: changes from 1994 to 2006*. Archives of internal medicine, 2009. **169**(19): p. 1767-1774.
177. Prabhavathi, K., et al., *Role of biological sex in normal cardiac function and in its disease outcome - a review*. Journal of clinical and diagnostic research : JCDR, 2014. **8**(8): p. BE01-BE4.
178. Camper-Kirby, D., et al., *Myocardial Akt activation and gender: increased nuclear activity in females versus males*. Circ Res, 2001. **88**(10): p. 1020-7.
179. Patten, R.D., et al., *17beta-estradiol reduces cardiomyocyte apoptosis in vivo and in vitro via activation of phospho-inositide-3 kinase/Akt signaling*. Circ Res, 2004. **95**(7): p. 692-9.
180. Gabel, S.A., et al., *Estrogen receptor beta mediates gender differences in ischemia/reperfusion injury*. J Mol Cell Cardiol, 2005. **38**(2): p. 289-97.
181. Cavaasin, M.A., et al., *Estrogen and testosterone have opposing effects on chronic cardiac remodeling and function in mice with myocardial infarction*. Am J Physiol Heart Circ Physiol, 2003. **284**(5): p. H1560-9.
182. Sluijmer, A.V., et al., *Endocrine activity of the postmenopausal ovary: the effects of pituitary down-regulation and oophorectomy*. J Clin Endocrinol Metab, 1995. **80**(7): p. 2163-7.
183. Sullivan, M.L., et al., *The cardiac toxicity of anabolic steroids*. Prog Cardiovasc Dis, 1998. **41**(1): p. 1-15.
184. Abdullah, M., et al., *Gender effect on in vitro lymphocyte subset levels of healthy individuals*. Cell Immunol, 2012. **272**(2): p. 214-9.

185. Spitzer, J.A., *Gender differences in some host defense mechanisms*. *Lupus*, 1999. **8**(5): p. 380-3.
186. Aomatsu, M., et al., *Gender difference in tumor necrosis factor- $\alpha$  production in human neutrophils stimulated by lipopolysaccharide and interferon- $\gamma$* . *Biochem Biophys Res Commun*, 2013. **441**(1): p. 220-5.
187. Marriott, I., K.L. Bost, and Y.M. Huet-Hudson, *Sexual dimorphism in expression of receptors for bacterial lipopolysaccharides in murine macrophages: a possible mechanism for gender-based differences in endotoxic shock susceptibility*. *J Reprod Immunol*, 2006. **71**(1): p. 12-27.
188. Klein, S.L. and K.L. Flanagan, *Sex differences in immune responses*. *Nature Reviews Immunology*, 2016. **16**(10): p. 626-638.
189. Gavins, F.N. and B.E. Chatterjee, *Intravital microscopy for the study of mouse microcirculation in anti-inflammatory drug research: focus on the mesentery and cremaster preparations*. *J Pharmacol Toxicol Methods*, 2004. **49**(1): p. 1-14.
190. Kozhura, V.L., et al., *Reperfusion injury after critical intestinal ischemia and its correction with perfluorochemical emulsion "perftoran"*. *World J Gastroenterol*, 2005. **11**(45): p. 7084-90.
191. Yago, T., et al., *Blocking neutrophil integrin activation prevents ischemia-reperfusion injury*. *J Exp Med*, 2015. **212**(8): p. 1267-81.
192. Matsuura, R., et al., *Intravital imaging with two-photon microscopy reveals cellular dynamics in the ischemia-reperfused rat heart*. *Sci Rep*, 2018. **8**(1): p. 15991.
193. Pries, A.R. and B. Reglin, *Coronary microcirculatory pathophysiology: can we afford it to remain a black box?* *Eur Heart J*, 2016.
194. Yada, T., et al., *In vivo observation of subendocardial microvessels of the beating porcine heart using a needle-probe videomicroscope with a CCD camera*. *Circ Res*, 1993. **72**(5): p. 939-46.
195. Toyota, E., et al., *Dynamic changes in three-dimensional architecture and vascular volume of transmural coronary microvasculature between diastolic- and systolic-arrested rat hearts*. *Circulation*, 2002. **105**(5): p. 621-6.
196. Bujak, M., et al., *Interleukin-1 receptor type I signaling critically regulates infarct healing and cardiac remodeling*. *The American journal of pathology*, 2008. **173**(1): p. 57-67.
197. Abbate, A., et al., *Interleukin-1 Blockade With Anakinra to Prevent Adverse Cardiac Remodeling After Acute Myocardial Infarction (Virginia Commonwealth University Anakinra Remodeling Trial [VCU-ART] Pilot Study)*. *The American Journal of Cardiology*, 2010. **105**(10): p. 1371-1377.e1.
198. Ridker, P.M., et al., *Antiinflammatory Therapy with Canakinumab for Atherosclerotic Disease*. *New England Journal of Medicine*, 2017. **377**(12): p. 1119-1131.
199. Kleveland, O., et al., *Effect of a single dose of the interleukin-6 receptor antagonist tocilizumab on inflammation and troponin T release in patients with non-ST-elevation myocardial infarction: a double-blind, randomized, placebo-controlled phase 2 trial*. *European Heart Journal*, 2016. **37**(30): p. 2406-2413.
200. Padfield, G.J., et al., *Cardiovascular effects of tumour necrosis factor  $\alpha$  antagonism in patients with acute myocardial infarction: a first in human study*. *Heart*, 2013. **99**(18): p. 1330-1335.
201. Buhl, A.-L. and J. Wenzel, *Interleukin-36 in Infectious and Inflammatory Skin Diseases*. *Frontiers in Immunology*, 2019. **10**.
202. Boutet, M.A., et al., *Distinct expression of interleukin (IL)-36 $\alpha$ ,  $\beta$  and  $\gamma$ , their antagonist IL-36Ra and IL-38 in psoriasis, rheumatoid arthritis and Crohn's disease*. *Clinical & Experimental Immunology*, 2016. **184**(2): p. 159-173.

203. Luo, C., et al., *Deficiency of Interleukin-36 Receptor Protected Cardiomyocytes from Ischemia-Reperfusion Injury in Cardiopulmonary Bypass*. Medical Science Monitor, 2020. **26**.
204. Kavanagh, D.P.J., M.T. Gallagher, and N. Kalia, *Tify: A quality-based frame selection tool for improving the output of unstable biomedical imaging*. PLoS One, 2019. **14**(3): p. e0213162.
205. Brawn, W., *Stage I Norwood: The Birmingham Children's Hospital Approach*. Operative Techniques in Thoracic and Cardiovascular Surgery, 2005. **10**(4): p. 286-298.
206. d'Udekem, Y., et al., *Low risk of pulmonary valve implantation after a policy of transatrial repair of tetralogy of Fallot delayed beyond the neonatal period: the Melbourne experience over 25 years*. Journal of the American College of Cardiology, 2014. **63**(6): p. 563-568.
207. Hazekamp, M.G., et al., *Consensus document on optimal management of patients with common arterial trunk*. Eur J Cardiothorac Surg, 2021. **60**(1): p. 7-33.
208. Whitson, B.A., *Surgical implant techniques of left ventricular assist devices: an overview of acute and durable devices*. Journal of thoracic disease, 2015. **7**(12): p. 2097-2101.
209. Mahmood, T. and P.-C. Yang, *Western blot: technique, theory, and trouble shooting*. North American journal of medical sciences, 2012. **4**(9): p. 429-434.
210. Cromer, W., et al., *Murine rVEGF164b, an inhibitory VEGF reduces VEGF-A-dependent endothelial proliferation and barrier dysfunction*. Microcirculation (New York, N.Y. : 1994), 2010. **17**(7): p. 536-547.
211. Redfors, B., Y. Shao, and E. Omerovic, *Myocardial infarct size and area at risk assessment in mice*. Experimental and clinical cardiology, 2012. **17**(4): p. 268-272.
212. Kelly, D.J., et al., *Incidence and predictors of heart failure following percutaneous coronary intervention in ST-segment elevation myocardial infarction: the HORIZONS-AMI trial*. Am Heart J, 2011. **162**(4): p. 663-70.
213. Chandrasekaran, B. and A.S. Kurbaan, *Myocardial infarction with angiographically normal coronary arteries*. Journal of the Royal Society of Medicine, 2002. **95**(8): p. 398-400.
214. Niccoli, G., et al., *Coronary microvascular obstruction in acute myocardial infarction*. European Heart Journal, 2015. **37**(13): p. 1024-1033.
215. Lesnfsky, E.J., et al., *Aging increases ischemia-reperfusion injury in the isolated, buffer-perfused heart*. J Lab Clin Med, 1994. **124**(6): p. 843-51.
216. Mehta, R.H., et al., *Acute myocardial infarction in the elderly: differences by age*. J Am Coll Cardiol, 2001. **38**(3): p. 736-41.
217. Odden, M.C., et al., *The impact of the aging population on coronary heart disease in the United States*. Am J Med, 2011. **124**(9): p. 827-33.e5.
218. El Assar, M., et al., *Mechanisms involved in the aging-induced vascular dysfunction*. Frontiers in physiology, 2012. **3**: p. 132-132.
219. Gerhard, M., et al., *Aging progressively impairs endothelium-dependent vasodilation in forearm resistance vessels of humans*. Hypertension, 1996. **27**(4): p. 849-53.
220. Jenner, T.L., et al., *Age-related changes in cardiac adenosine receptor expression*. Mech Ageing Dev, 2004. **125**(3): p. 211-7.
221. Perskin, M.H. and B.N. Cronstein, *Age-related changes in neutrophil structure and function*. Mechanisms of Ageing and Development, 1992. **64**(3): p. 303-313.
222. Adrover, J.M., et al., *A Neutrophil Timer Coordinates Immune Defense and Vascular Protection*. Immunity, 2019. **50**(2): p. 390-402.e10.
223. Bullone, M. and J.-P. Lavoie, *The Contribution of Oxidative Stress and Inflamm-Aging in Human and Equine Asthma*. International journal of molecular sciences, 2017. **18**(12): p. 2612.

224. Barkaway, A., et al., *Age-related changes in the local milieu of inflamed tissues cause aberrant neutrophil trafficking and subsequent remote organ damage*. *Immunity*, 2021. **54**(7): p. 1494-1510.e7.
225. SABISTON, D.C. and D.E. GREGG, *Effect of Cardiac Contraction on Coronary Blood Flow*. *Circulation*, 1957. **15**(1): p. 14-20.
226. Panerai, R.B., J.H. Chamberlain, and B.M. Sayers, *Characterization of the extravascular component of coronary resistance by instantaneous pressure-flow relationships in the dog*. *Circ Res*, 1979. **45**(3): p. 378-90.
227. Sabbah, H.N., et al., *Coronary extravascular compression influences systolic coronary blood flow*. *Heart Vessels*, 1986. **2**(3): p. 140-6.
228. van de Hoef, T.P., et al., *Contribution of Age-Related Microvascular Dysfunction to Abnormal Coronary Hemodynamics in Patients With Ischemic Heart Disease*. *JACC Cardiovasc Interv*, 2020. **13**(1): p. 20-29.
229. Culmer, D.L., et al., *Circulating and vein wall P-selectin promote venous thrombogenesis during aging in a rodent model*. *Thrombosis Research*, 2013. **131**(1): p. 42-48.
230. Dayal, S., et al., *Hydrogen peroxide promotes aging-related platelet hyperactivation and thrombosis*. *Circulation*, 2013. **127**(12): p. 1308-1316.
231. Alavi, P., A.M. Rathod, and N. Jahroudi, *Age-Associated Increase in Thrombogenicity and Its Correlation with von Willebrand Factor*. *J Clin Med*, 2021. **10**(18).
232. Jin, K., *A Microcirculatory Theory of Aging*. *Aging and disease*, 2019. **10**(3): p. 676-683.
233. Olivetti, G., et al., *Gender differences and aging: effects on the human heart*. *J Am Coll Cardiol*, 1995. **26**(4): p. 1068-79.
234. Fleg, J.L. and J. Strait, *Age-associated changes in cardiovascular structure and function: a fertile milieu for future disease*. *Heart failure reviews*, 2012. **17**(4-5): p. 545-554.
235. Anversa, P., et al., *Myocyte cell loss and myocyte hypertrophy in the aging rat heart*. *J Am Coll Cardiol*, 1986. **8**(6): p. 1441-8.
236. Olivetti, G., et al., *Cardiomyopathy of the aging human heart. Myocyte loss and reactive cellular hypertrophy*. *Circ Res*, 1991. **68**(6): p. 1560-8.
237. Brown, W.R. and C.R. Thore, *Review: cerebral microvascular pathology in ageing and neurodegeneration*. *Neuropathology and applied neurobiology*, 2011. **37**(1): p. 56-74.
238. Shakeri, H., et al., *Cellular senescence links aging and diabetes in cardiovascular disease*. *Am J Physiol Heart Circ Physiol*, 2018. **315**(3): p. H448-h462.
239. Roubenoff, R., et al., *Monocyte cytokine production in an elderly population: effect of age and inflammation*. *J Gerontol A Biol Sci Med Sci*, 1998. **53**(1): p. M20-6.
240. Rizvi, F., et al., *Effects of Aging on Cardiac Oxidative Stress and Transcriptional Changes in Pathways of Reactive Oxygen Species Generation and Clearance*. *Journal of the American Heart Association*, 2021. **10**(16): p. e019948.
241. Kong, D.-H., et al., *Emerging Roles of Vascular Cell Adhesion Molecule-1 (VCAM-1) in Immunological Disorders and Cancer*. *International journal of molecular sciences*, 2018. **19**(4): p. 1057.
242. Zou, Y., et al., *Upregulation of Aortic Adhesion Molecules During Aging*. *The Journals of Gerontology: Series A*, 2006. **61**(3): p. 232-244.
243. Miller, S.J., et al., *Development of progressive aortic vasculopathy in a rat model of aging*. *American Journal of Physiology-Heart and Circulatory Physiology*, 2007. **293**(5): p. H2634-H2643.
244. Yousef, H., et al., *Aged blood impairs hippocampal neural precursor activity and activates microglia via brain endothelial cell VCAM1*. *Nat Med*, 2019. **25**(6): p. 988-1000.
245. Bowden, R.A., et al., *Role of  $\alpha 4$  Integrin and VCAM-1 in CD18-Independent Neutrophil Migration Across Mouse Cardiac Endothelium*. *Circulation Research*, 2002. **90**(5): p. 562-569.

246. Yellon, D.M. and D.J. Hausenloy, *Myocardial Reperfusion Injury*. New England Journal of Medicine, 2007. **357**(11): p. 1121-1135.
247. Jaffe, R., et al., *Microvascular Obstruction and the No-Reflow Phenomenon After Percutaneous Coronary Intervention*. Circulation, 2008. **117**(24): p. 3152-3156.
248. Vinten-Johansen, J., *Involvement of neutrophils in the pathogenesis of lethal myocardial reperfusion injury*. Cardiovascular Research, 2004. **61**(3): p. 481-497.
249. Worthen, G.S., et al., *Mechanics of stimulated neutrophils: cell stiffening induces retention in capillaries*. Science, 1989. **245**(4914): p. 183-6.
250. Ogawa, K., et al., *The association of elevated reactive oxygen species levels from neutrophils with low-grade inflammation in the elderly*. Immunity & ageing : I & A, 2008. **5**: p. 13-13.
251. Martinod, K., et al., *Peptidylarginine deiminase 4 promotes age-related organ fibrosis*. J Exp Med, 2017. **214**(2): p. 439-458.
252. Yamamoto, K., et al., *Aging and plasminogen activator inhibitor-1 (PAI-1) regulation: implication in the pathogenesis of thrombotic disorders in the elderly*. Cardiovasc Res, 2005. **66**(2): p. 276-85.
253. Le Blanc, J. and M. Lordkipanidzé, *Platelet Function in Aging*. Front Cardiovasc Med, 2019. **6**: p. 109.
254. El Amki, M., et al., *Neutrophils Obstructing Brain Capillaries Are a Major Cause of No-Reflow in Ischemic Stroke*. Cell Reports, 2020. **33**(2): p. 108260.
255. Willems, L., et al., *Age-related changes in ischemic tolerance in male and female mouse hearts*. Journal of Molecular and Cellular Cardiology, 2005. **38**(2): p. 245-256.
256. Ji, L.L., D. Dillon, and E. Wu, *Myocardial aging: antioxidant enzyme systems and related biochemical properties*. Am J Physiol, 1991. **261**(2 Pt 2): p. R386-92.
257. Bejma, J. and L.L. Ji, *Aging and acute exercise enhance free radical generation in rat skeletal muscle*. Journal of Applied Physiology, 1999. **87**(1): p. 465-470.
258. Rajiah, P., et al., *MR imaging of myocardial infarction*. Radiographics, 2013. **33**(5): p. 1383-412.
259. Huang, S. and N.G. Frangogiannis, *Anti-inflammatory therapies in myocardial infarction: failures, hopes and challenges*. Br J Pharmacol, 2018. **175**(9): p. 1377-1400.
260. Gaul, D.S., S. Stein, and C.M. Matter, *Neutrophils in cardiovascular disease*. European Heart Journal, 2017. **38**(22): p. 1702-1704.
261. Darbousset, R., et al., *Tissue factor-positive neutrophils bind to injured endothelial wall and initiate thrombus formation*. Blood, 2012. **120**(10): p. 2133-43.
262. Stakos, D.A., et al., *Expression of functional tissue factor by neutrophil extracellular traps in culprit artery of acute myocardial infarction*. Eur Heart J, 2015. **36**(22): p. 1405-14.
263. Baran, K.W., et al., *Double-Blind, Randomized Trial of an Anti-CD18 Antibody in Conjunction With Recombinant Tissue Plasminogen Activator for Acute Myocardial Infarction*. Circulation, 2001. **104**(23): p. 2778-2783.
264. Tardif, J.-C., et al., *Effects of the P-Selectin Antagonist Inclacumab on Myocardial Damage After Percutaneous Coronary Intervention for Non-ST-Segment Elevation Myocardial Infarction: Results of the SELECT-ACS Trial*. Journal of the American College of Cardiology, 2013. **61**(20): p. 2048-2055.
265. Kleveland, O., et al., *Effect of a single dose of the interleukin-6 receptor antagonist tocilizumab on inflammation and troponin T release in patients with non-ST-elevation myocardial infarction: a double-blind, randomized, placebo-controlled phase 2 trial†*. European Heart Journal, 2016. **37**(30): p. 2406-2413.
266. Marchant, D.J., et al., *Inflammation in myocardial diseases*. Circ Res, 2012. **110**(1): p. 126-44.
267. Ridker, P.M., *From C-Reactive Protein to Interleukin-6 to Interleukin-1*. Circulation Research, 2016. **118**(1): p. 145-156.

268. Moss, N.C., et al., *IKKbeta inhibition attenuates myocardial injury and dysfunction following acute ischemia-reperfusion injury*. Am J Physiol Heart Circ Physiol, 2007. **293**(4): p. H2248-53.
269. Zeng, M., et al., *Suppression of NF- $\kappa$ B Reduces Myocardial No-Reflow*. PLOS ONE, 2012. **7**(10): p. e47306.
270. Yi, G., et al., *Structural and Functional Attributes of the Interleukin-36 Receptor*. The Journal of biological chemistry, 2016. **291**(32): p. 16597-16609.
271. Fulop, T., et al., *Cytokine receptor signalling and aging*. Mech Ageing Dev, 2006. **127**(6): p. 526-37.
272. Towne, J.E., et al., *Interleukin (IL)-1F6, IL-1F8, and IL-1F9 signal through IL-1Rrp2 and IL-1RAcP to activate the pathway leading to NF- $\kappa$ B and MAPKs*. Journal of Biological Chemistry, 2004. **279**(14): p. 13677-13688.
273. Fulop, T., et al., *Signal transduction and functional changes in neutrophils with aging*. Aging Cell, 2004. **3**(4): p. 217-26.
274. Song, Y., et al., *Aging enhances the basal production of IL-6 and CCL2 in vascular smooth muscle cells*. Arterioscler Thromb Vasc Biol, 2012. **32**(1): p. 103-9.
275. Song, Y., et al., *Aging Enhances the Basal Production of IL-6 and CCL2 in Vascular Smooth Muscle Cells*. Arteriosclerosis, Thrombosis, and Vascular Biology, 2012. **32**(1): p. 103-109.
276. Nishikawa, H., et al., *Knockout of the interleukin-36 receptor protects against renal ischemia-reperfusion injury by reduction of proinflammatory cytokines*. Kidney Int, 2018. **93**(3): p. 599-614.
277. Ramadas, R.A., et al., *Interleukin-1 family member 9 stimulates chemokine production and neutrophil influx in mouse lungs*. Am J Respir Cell Mol Biol, 2011. **44**(2): p. 134-45.
278. Dal Lin, C., F. Tona, and E. Osto, *Coronary Microvascular Function and Beyond: The Crosstalk between Hormones, Cytokines, and Neurotransmitters*. International journal of endocrinology, 2015. **2015**: p. 312848-312848.
279. Maiellaro, K. and W.R. Taylor, *The role of the adventitia in vascular inflammation*. Cardiovasc Res, 2007. **75**(4): p. 640-8.
280. Koss, C.K., et al., *IL36 is a critical upstream amplifier of neutrophilic lung inflammation in mice*. Communications Biology, 2021. **4**(1): p. 172.
281. Butcher, S., H. Chahel, and J.M. Lord, *Review article: ageing and the neutrophil: no appetite for killing?* Immunology, 2000. **100**(4): p. 411-416.
282. Dangerfield, J.P., S. Wang, and S. Nourshargh, *Blockade of  $\alpha$ 6 integrin inhibits IL-16- but not TNF- $\alpha$ -induced neutrophil transmigration in vivo*. Journal of Leukocyte Biology, 2005. **77**(2): p. 159-165.
283. McNee, W. and C. Selby, *Neutrophil traffic in the lungs: role of haemodynamics, cell adhesion and deformability*. Thorax, 1993. **48**: p. 79-88.
284. Cruz Hernández, J.C., et al., *Neutrophil adhesion in brain capillaries reduces cortical blood flow and impairs memory function in Alzheimer's disease mouse models*. Nat Neurosci, 2019. **22**(3): p. 413-420.
285. Jones, C.I., *Platelet function and ageing*. Mammalian genome : official journal of the International Mammalian Genome Society, 2016. **27**(7-8): p. 358-366.
286. Sedlmayr, P., et al., *Platelets contain interleukin-1 alpha and beta which are detectable on the cell surface after activation*. Scand J Immunol, 1995. **42**(2): p. 209-14.
287. Medina-Contreras, O., et al., *Cutting Edge: IL-36 Receptor Promotes Resolution of Intestinal Damage*. The Journal of Immunology, 2016. **196**(1): p. 34-38.
288. Queen, D., C. Ediriweera, and L. Liu, *Function and Regulation of IL-36 Signaling in Inflammatory Diseases and Cancer Development*. Frontiers in Cell and Developmental Biology, 2019. **7**(317).

289. Cook-Mills, J.M., M.E. Marchese, and H. Abdala-Valencia, *Vascular cell adhesion molecule-1 expression and signaling during disease: regulation by reactive oxygen species and antioxidants*. Antioxidants & redox signaling, 2011. **15**(6): p. 1607-1638.
290. O'Donoghue, M.L., et al., *Effect of darapladib on major coronary events after an acute coronary syndrome: the SOLID-TIMI 52 randomized clinical trial*. Jama, 2014. **312**(10): p. 1006-15.
291. Matetic, A., et al., *Trends of Sex Differences in Clinical Outcomes After Myocardial Infarction in the United States*. CJC Open, 2021. **3**(12 Suppl): p. S19-s27.
292. Ramaekers, D., et al., *Heart rate variability and heart rate in healthy volunteers. Is the female autonomic nervous system cardioprotective?* Eur Heart J, 1998. **19**(9): p. 1334-41.
293. Gupta, S., et al., *Sex differences in neutrophil biology modulate response to type I interferons and immunometabolism*. Proceedings of the National Academy of Sciences, 2020. **117**(28): p. 16481-16491.
294. Lu, R.J., et al., *Multi-omic profiling of primary mouse neutrophils predicts a pattern of sex- and age-related functional regulation*. Nature Aging, 2021. **1**(8): p. 715-733.
295. Madalli, S., et al., *Sex-specific regulation of chemokine Cxcl5/6 controls neutrophil recruitment and tissue injury in acute inflammatory states*. Biology of sex differences, 2015. **6**: p. 27-27.
296. Gwak, M.S., et al., *Effects of gender on white blood cell populations and neutrophil-lymphocyte ratio following gastrectomy in patients with stomach cancer*. Journal of Korean medical science, 2007. **22 Suppl**(Suppl): p. S104-S108.
297. Butkiewicz, A.M., et al., *Platelet count, mean platelet volume and thrombocytopoietic indices in healthy women and men*. Thromb Res, 2006. **118**(2): p. 199-204.
298. Leng, X.H., et al., *Platelets of female mice are intrinsically more sensitive to agonists than are platelets of males*. Arterioscler Thromb Vasc Biol, 2004. **24**(2): p. 376-81.
299. Coleman, J.R., et al., *Female platelets have distinct functional activity compared with male platelets: Implications in transfusion practice and treatment of trauma-induced coagulopathy*. The journal of trauma and acute care surgery, 2019. **87**(5): p. 1052-1060.
300. Soo Kim, B., et al., *Sex-Specific Platelet Activation Through Protease-Activated Receptors Reverses in Myocardial Infarction*. Arteriosclerosis, thrombosis, and vascular biology, 2021. **41**(1): p. 390-400.
301. Nickander, J., et al., *Females have higher myocardial perfusion, blood volume and extracellular volume compared to males – an adenosine stress cardiovascular magnetic resonance study*. Scientific Reports, 2020. **10**(1): p. 10380.
302. Hou, X. and F. Pei, *Estradiol Inhibits Cytokine-Induced Expression of VCAM-1 and ICAM-1 in Cultured Human Endothelial Cells Via AMPK/PPAR $\alpha$  Activation*. Cell Biochem Biophys, 2015. **72**(3): p. 709-17.
303. Death, A.K., et al., *Dihydrotestosterone promotes vascular cell adhesion molecule-1 expression in male human endothelial cells via a nuclear factor-kappaB-dependent pathway*. Endocrinology, 2004. **145**(4): p. 1889-97.
304. Barp, J., et al., *Myocardial antioxidant and oxidative stress changes due to sex hormones*. Brazilian journal of medical and biological research = Revista brasileira de pesquisas médicas e biológicas / Sociedade Brasileira de Biofísica ... [et al.], 2002. **35**: p. 1075-81.
305. Ide, T., et al., *Greater oxidative stress in healthy young men compared with premenopausal women*. Arterioscler Thromb Vasc Biol, 2002. **22**(3): p. 438-42.
306. Loscalzo, J., *Oxidative stress in endothelial cell dysfunction and thrombosis*. Pathophysiol Haemost Thromb, 2002. **32**(5-6): p. 359-60.
307. InanlooRahatloo, K., et al., *Sex-based differences in myocardial gene expression in recently deceased organ donors with no prior cardiovascular disease*. PLoS One, 2017. **12**(8): p. e0183874.

308. Lynch, E.A., C.A. Dinarello, and J.G. Cannon, *Gender differences in IL-1 alpha, IL-1 beta, and IL-1 receptor antagonist secretion from mononuclear cells and urinary excretion*. The Journal of Immunology, 1994. **153**(1): p. 300-306.
309. Farkouh, A., et al., *Sex-Related Differences in Drugs with Anti-Inflammatory Properties*. Journal of clinical medicine, 2021. **10**(7): p. 1441.
310. Van Kerckhoven, R., et al., *Pharmacological therapy can increase capillary density in post-infarction remodeled rat hearts*. Cardiovascular Research, 2004. **61**(3): p. 620-629.
311. Stone, G.W., et al., *Relationship Between Infarct Size and Outcomes Following Primary PCI: Patient-Level Analysis From 10 Randomized Trials*. J Am Coll Cardiol, 2016. **67**(14): p. 1674-83.
312. van den Munckhof, I., et al., *Aging attenuates the protective effect of ischemic preconditioning against endothelial ischemia-reperfusion injury in humans*. Am J Physiol Heart Circ Physiol, 2013. **304**(12): p. H1727-32.
313. De Filippo, K. and S.M. Rankin, *The Secretive Life of Neutrophils Revealed by Intravital Microscopy*. Frontiers in Cell and Developmental Biology, 2020. **8**.
314. Singhal, A.K., et al., *Role of Endothelial Cells in Myocardial Ischemia-Reperfusion Injury*. Vasc Dis Prev, 2010. **7**: p. 1-14.
315. Li, T., et al., *Resveratrol alleviates hypoxia/reoxygenation injury-induced mitochondrial oxidative stress in cardiomyocytes*. Mol Med Rep, 2019. **19**(4): p. 2774-2780.
316. Takii, T., et al., *Interleukin-1 up-regulates transcription of its own receptor in a human fibroblast cell line TIG-1: role of endogenous PGE2 and cAMP*. European Journal of Immunology, 1992. **22**(5): p. 1221-1227.
317. FUJIOKA, S., et al., *Desensitization of NFkB for Overcoming Chemoresistance of Pancreatic Cancer Cells to TNF-α or Paclitaxel*. Anticancer Research, 2012. **32**(11): p. 4813-4821.
318. Iismaa, S.E., et al., *Cardiac hypertrophy limits infarct expansion after myocardial infarction in mice*. Scientific Reports, 2018. **8**(1): p. 6114.

# JCI insight

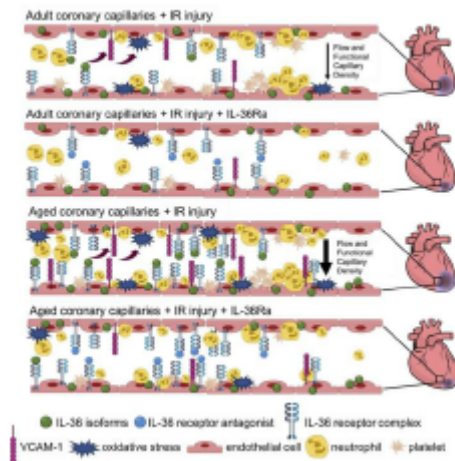
## Targeting IL-36 improves age-related coronary microcirculatory dysfunction and attenuates myocardial ischemia/reperfusion injury in mice

Juma El-Awaisi, ... , Nigel E. Drury, Neena Kalia

*JCI Insight*. 2022;7(5):e155236. <https://doi.org/10.1172/jci.insight.155236>.

Research Article Aging Inflammation

### Graphical abstract



Find the latest version:

<https://jci.me/155236/pdf>



# Targeting IL-36 improves age-related coronary microcirculatory dysfunction and attenuates myocardial ischemia/reperfusion injury in mice

Juma El-Awaisi,<sup>1</sup> Dean P.J. Kavanagh,<sup>1</sup> Marco R. Rink,<sup>2</sup> Chris J. Weston,<sup>2</sup> Nigel E. Drury,<sup>1</sup> and Neena Kalia<sup>1</sup>

<sup>1</sup>Microcirculation Research Group, Institute of Cardiovascular Sciences, and <sup>2</sup>Institute of Immunology and Immunotherapy, College of Medical and Dental Sciences, University of Birmingham, Birmingham, United Kingdom.

Following myocardial infarction (MI), elderly patients have a poorer prognosis than younger patients, which may be linked to increased coronary microvessel susceptibility to injury. Interleukin-36 (IL-36), a newly discovered proinflammatory member of the IL-1 superfamily, may mediate this injury, but its role in the injured heart is currently not known. We first demonstrated the presence of IL-36( $\alpha/\beta$ ) and its receptor (IL-36R) in ischemia/reperfusion-injured (IR-injured) mouse hearts and, interestingly, noted that expression of both increased with aging. An intravital model for imaging the adult and aged IR-injured beating heart in real time in vivo was used to demonstrate heightened basal and injury-induced neutrophil recruitment, and poorer blood flow, in the aged coronary microcirculation when compared with adult hearts. An IL-36R antagonist (IL-36Ra) decreased neutrophil recruitment, improved blood flow, and reduced infarct size in both adult and aged mice. This may be mechanistically explained by attenuated endothelial oxidative damage and VCAM-1 expression in IL-36Ra-treated mice. Our findings of an enhanced age-related coronary microcirculatory dysfunction in reperfused hearts may explain the poorer outcomes in elderly patients following MI. Since targeting the IL-36/IL-36R pathway was vasculoprotective in aged hearts, it may potentially be a therapy for treating MI in the elderly population.

## Introduction

Treatment of ST-elevation myocardial infarction (MI) focuses on rapidly reestablishing perfusion following blockage in one or more of the epicardial coronary arteries. This can be achieved by primary percutaneous coronary intervention (PCI) using a coronary stent to open the culprit artery. Despite these interventions, a substantial proportion of patients still incur extensive muscle damage and develop heart failure after MI (1). This is partly due to reperfusion paradoxically leading to additional tissue damage, a condition termed ischemia/reperfusion (IR) injury. Indeed, restoration of normal epicardial blood vessel flow, but with suboptimal myocardial perfusion, can be observed in up to 50% of patients following PCI, leading to worse outcomes than in patients with full perfusion recovery (2). This suggests tissue damage likely occurs subsequent to inadequate coronary microcirculatory perfusion (3, 4). Microvascular involvement is further highlighted by observations that patients may present with MI but with a normal coronary angiogram (4). Increased clinical recognition of the importance of the coronary microcirculation has meant strategies to improve potential perturbations within it have gained recent attention (3, 4). However, current clinical tools cannot resolve microvessels less than 200  $\mu$ m, and so little is known about the full range of cardiac microcirculatory responses to IR injury in vivo.

Age is a major risk factor for ischemic cardiovascular disease, increasing cardiac damage caused by IR injury, independent of "traditional" risk factors (5–7). Clinically, there is an increased incidence of heart failure, atrial fibrillation, and tachycardia in patients post-MI that increases with age (7). In experimental studies, coronary blood flow is much lower postreperfusion in senescent rats (8). Interestingly, the ability of the heart to respond to cardioprotective interventions is also lost with aging (8, 9). The term "inflammaging" describes the phenomenon of aging accompanied by a chronic low-grade, sterile inflammation

**Conflict of interest:** The authors have declared that no conflict of interest exists.

**Copyright:** © 2022, El-Awaisi et al. This is an open access article published under the terms of the Creative Commons Attribution 4.0 International License.

**Submitted:** September 23, 2021

**Accepted:** January 28, 2022

**Published:** March 8, 2022

**Reference information:** JCI insight. 2022;7(5):e155236.  
<https://doi.org/10.1172/jci.insight.155236>.

that persists in the absence of an overt inflammatory stimulus (10). It is characterized by raised levels of proinflammatory cytokines that contribute to gradual tissue damage as well as altered responses to acute inflammatory injuries. The drivers underlying this persistent inflammation appear to involve increased reactive oxygen species (ROS) production in the vasculature, decreased antioxidative ability, and changes in the number, structure, and function of immune cells (11). In particular, increased neutrophil presence is detected in otherwise healthy but aged tissues. Neutrophil chemotaxis is also impaired, with serious implications as adherent cells cannot exit or transigrate out of blood vessels (12). Here, they continue to release tissue-destructive proteases and ROS and cause vascular congestion as observed in aged, injured mouse lungs (13). Therefore, inflammaging may contribute to the enhanced age-related cardiovascular risk and poorer outcomes through actions on the local microcirculation. However, little is known *in vivo* about how age affects the coronary microcirculation in health and whether it increases the likelihood of microvascular disturbances after reperfusion injury.

The interleukin-1 family (IL-1F) consists of 11 known pro- and/or antiinflammatory cytokines, some of which have been studied extensively whereas others have received less attention (14). These are frequently the first and most upstream cytokines produced in response to injury and so are considered good targets for intervention (15). Since IL-1F members critically mediate sterile inflammation, they may be key mechanistic contributors causing myocardial microcirculatory disturbances postreperfusion (16). Indeed, the large-scale canakinumab antiinflammatory thrombosis outcomes study (CANTOS) trial provided exciting evidence that targeting this cytokine was beneficial in improving long-term outcomes post-MI in the absence of lipid lowering (17). In the last decade, genes encoding a novel cytokine cluster, namely interleukin-36 (IL-36), with structural and functional similarities to IL-1, were discovered (18, 19). IL-36, a collective name for 3 agonist ligands, IL-36 $\alpha$ , IL-36 $\beta$ , and IL-36 $\gamma$  (previously called IL-1F6, IL-1F8, and IL-1F9), is fast emerging as a novel player regulating both innate and adaptive immune responses in a number of acute and chronic disorders. As well as amplifying IL-1 effects, IL-36 is also a potent mediator of inflammation in its own right. Indeed, its critical role in psoriasis, equaling if not surpassing that of IL-1, is well established, with roles in Crohn's disease, airway infections, and rheumatoid arthritis recently identified (20–22).

IL-36 cytokines can be released from many sources, including epithelial cells, keratinocytes, fibroblasts, macrophages, monocytes, lymphocytes, and neurons, with neutrophils identified as an IL-36 source recently (18, 23–25). They signal through the IL-36 receptor (IL-36R), a heterodimer formed of IL-1Rrp2 and an accessory coreceptor protein, IL-1RacP (20). This receptor is also widely expressed at low levels in many organs and cell types, including leukocytes and vascular endothelial cells. Downstream intracellular signaling leads to NF- $\kappa$ B and MAPK activation and subsequent secretion of multiple potent proinflammatory mediators, including TNF- $\alpha$ , IL-1 $\beta$ , IL-6, and IL-8. The actions of the 3 agonists can be inhibited by a naturally occurring antagonist, namely the IL-36 receptor antagonist (IL-36Ra) (22–25). Although we know the IL-36/IL-36R pathway is highly proinflammatory in the skin and lungs, we are still at a very early stage in our current understanding of its *in vivo* biology, and no previous studies to our knowledge have investigated a role for this pathway in mediating inflammation in the IR-injured heart. Its downstream transcription factor, NF- $\kappa$ B, is a known mediator of coronary microvascular injury as inhibition of NF- $\kappa$ B in 2 independent rabbit models of myocardial IR injury reduced inflammation and the no-reflow area (26, 27). Therefore, the IL-36 signaling pathway is a potential target for cardioprotective interventions.

We have previously described an intravital imaging technique that allows the microcirculation of the anesthetized mouse beating heart to be imaged with cellular resolution *in vivo* (28). Using this technique, we have shown that despite deceptive hyperemic responses, increased microcirculatory flow heterogeneity, reduction in functional capillary density, and a marked thromboinflammatory infiltration were present within coronary capillaries immediately postreperfusion. The current study used this imaging model to determine whether the clinically observed age-related poorer outcomes post-MI were related to an increased susceptibility of the aged coronary microcirculation to myocardial IR injury. The presence of IL-36 and its receptor was investigated in the heart and the impact of age on their expression determined. To ascertain whether IL-36 could mediate coronary microcirculatory perturbations, the ability of IL-36 agonists to directly induce inflammation in the beating heart was imaged, and the effects of treatment with the IL-36Ra were determined. Mechanistic insights into how IL-36Ra may confer vasculoprotection via attenuating ROS-mediated endothelial oxidative damage and VCAM-1 expression are also presented.

## Results

*Age increases expression of IL-36R in healthy and IR-injured hearts, which was also induced in endothelial cells stimulated with TNF- $\alpha$  or IL-36 cytokines.* Immunofluorescence staining of frozen heart sections demonstrated very low constitutive expression of IL-36R in adult sham-injured hearts. This increased ( $P = 0.0146$ ) in response to IR injury in adult hearts. Basal expression of IL-36R was higher ( $P < 0.0001$ ) in aged sham hearts when compared with adult shams. This was further increased ( $P = 0.0003$ ) in aged injured hearts when compared with adult injured hearts (Figure 1, A and C). Western blot analysis showed similar stepwise increases in the presence of the IL-36R protein. The molecular weight of IL-36R is approximately 65 kDa, but it migrates to the position of approximately 85 kDa in denaturing protein gels (29). Hence, 2 bands were observed corresponding to a 65 kDa, active protein, due to cleavage of its signaling peptide, and an 85 kDa, less potent, glycosylated form (Figure 1B). Again, adult sham hearts expressed very low levels of IL-36R. This increased in adult injured hearts, which expressed the highest levels of the 85 kDa protein. However, significant increases ( $P < 0.0001$ ) in IL-36R protein were expressed in aged sham hearts when compared with adult sham hearts, particularly of the more potent 65 kDa protein. This expression increased ( $P = 0.001$ ) further in aged injured hearts, which exhibited the highest levels of the active 65 kDa IL-36R protein (Figure 1, B and D). To further confirm, at a more cellular level, the expression of IL-36R on coronary endothelial cells, hearts were collagenase digested and flow cytometrically analyzed. Very low basal levels of IL-36R were noted on adult sham coronary endothelial cells, but IL-36R was significantly ( $P < 0.05$ ) increased on endothelial cells from adult IR-injured hearts. Aged sham coronary endothelial cells again showed higher IL-36R than on adult sham endothelial cells, which was also significantly ( $P < 0.05$ ) increased with injury (Figure 1E). Interestingly, a similar pattern of IL-36R expression was noted flow cytometrically on cardiomyocytes (Figure 1F). To further identify whether IL-36R was expressed specifically on endothelial cells, murine vena cava endothelial cells (VCECs) were stained for IL-36R. Constitutive expression of IL-36R on unstimulated VCECs was very low. However, stimulation of VCECs with TNF- $\alpha$ , as well as IL-36 isoforms, significantly ( $P < 0.0001$ ) upregulated IL-36R expression, with no differences observed between cytokine treatments (Figure 1, G and H).

*Age increases expression of IL-36 $\alpha$ , IL-36 $\beta$ , and VCAM-1 in healthy and IR-injured hearts.* Immunofluorescence staining for IL-36 $\alpha$  and IL-36 $\beta$  revealed a similar pattern of expression in the heart to the IL-36R (Figure 2, A–C). Expression of the endothelial surface adhesion molecule, VCAM-1, was also investigated to better understand the impact of age on a well-established inflammatory marker. VCAM-1 was expressed on the larger vasculature of the heart rather than on coronary capillaries in all 4 groups and significantly increased in a stepwise manner with injury and age (Figure 2, D and E).

*Inducible expression of IL-36R and IL-36 cytokines occurs on coronary microvasculature.* Having demonstrated an increased vascular expression of IL-36R and IL-36 cytokines with IR injury and age, we further examined which component of the vascular network this increase occurred on by comparing the mean fluorescence intensity (MFI) between microvessels (capillaries) and macrovessels. Expression of IL-36R, IL-36 $\alpha$ , and IL-36 $\beta$  significantly increased with age and IR injury specifically on the microvasculature (Figure 3A). In contrast, expression on the macrovasculature remained relatively constant in all 4 groups (Figure 3B).

To further confirm that IL-36R expression was indeed present on blood vessels, heart sections were costained with an anti-CD31 antibody. IL-36R expression was intense within the wall of some of the larger blood vessels, particularly in the tunica adventitial layer, as well as on the coronary capillaries (Figure 3, C and D).

*Topical application of IL-36 is proinflammatory in adult and aged beating hearts in vivo.* To determine whether the IL-36R expressed in the heart was functional in vivo, intravital microscopy was used to directly visualize the ability of topical IL-36 to elicit an inflammatory response within the healthy adult and aged beating hearts. Intravital imaging of the beating heart was successfully achieved in anesthetized mice by attaching a 3D-printed stabilizer to the left ventricle (Figure 4, A–D). This reduced motion in the  $x$ - $y$  plane of a small region of the ventricle sufficiently enough to permit imaging. All 3 IL-36 agonists were able to increase neutrophil recruitment to a similar degree in healthy adult hearts, although IL-36 $\gamma$  was slightly more potent (Supplemental Video 1; supplemental material available online with this article; <https://doi.org/10.1172/jci.insight.155236DS1>). This proinflammatory response was rapid and increased with time until a plateau was reached at approximately 60 minutes. In addition to neutrophil adhesion within coronary capillaries, a remarkable involvement of more medium-sized blood vessels was also observed. Indeed, these vessels were not usually visible but were clearly identified when delineated with adherent neutrophils. Platelet aggregates were occasionally observed in some of these medium-sized vessels, particularly in response to IL-36 $\beta$  and IL-36 $\gamma$ . These were mostly present in

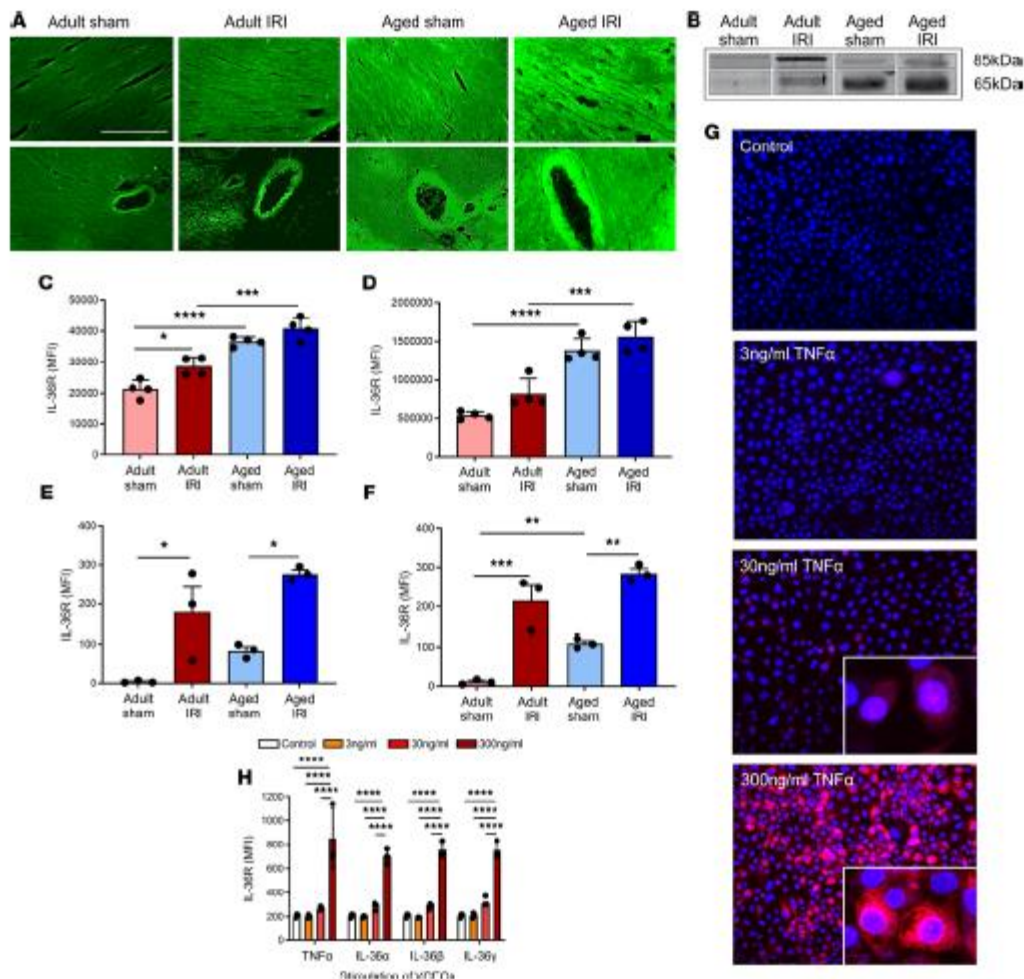


**Figure 1. Age increases expression of IL-36R in healthy and IR-injured hearts, and expression can also be induced in endothelial cells with TNF- $\alpha$  or IL-36 cytokine stimulation.** Hearts were assessed for IL-36R using immunostaining, Western blot analysis, and flow cytometry. Representative images of IL-36R (green) staining of (A) frozen heart sections and (B) Western blots. The molecular weight of IL-36R is about 65 kDa, but it migrates to the position of about 85 kDa in denaturing protein gels. Hence, 2 bands were observed corresponding to 65 kDa, the more active protein due to cleavage of its signaling peptide, and 85 kDa, the less potent glycosylated form. Quantitative analysis of the (C) immunofluorescence images (n = 4/group) and (D) Western blots (n = 4/group).  $P = 0.0146$  adult sham vs. adult IRI immunofluorescence.  $P = 0.0003$  aged sham vs. aged IRI immunofluorescence.  $P = 0.001$  aged sham vs. aged IRI Western blot. Hearts were also collagenase digested and analyzed flow cytometrically for IL-36R expression. Flow cytometry analysis confirmed that IRI injury and age induced a significant increase in IL-36R on (E) coronary endothelial cells and (F) cardiomyocytes (n = 3/group). (G and H) Murine vena cava endothelial cells (VCECs) were cultured and stimulated for 4 hours with experimental media (control), an IL-36 cytokine ( $\alpha$ ,  $\beta$ , or  $\gamma$ ), or TNF- $\alpha$ . (G) Representative images of IL-36R (red) expression on stimulated, nonpermeabilized cells (Hoechst 33342-stained nuclei in blue). (H) Quantitative analysis of IL-36R expression on VCECs following stimulation (n = 3/group). Scale bar indicates 200  $\mu$ m. \* $P < 0.05$ , \*\* $P < 0.01$ , \*\*\* $P < 0.001$ , \*\*\*\* $P < 0.0001$  as determined using a 1-way ANOVA followed by a Tukey's post hoc test.

vessels where extensive clusters of adherent neutrophils were observed (Figure 5, A, B, D, and E). A similar statistically significant proinflammatory response was also observed when cytokines were topically applied to the healthy aged hearts, although levels were slightly lower and the response slower than that observed in adult mice. However, unlike in adult hearts where the response plateaued, in aged hearts exposed to IL-36

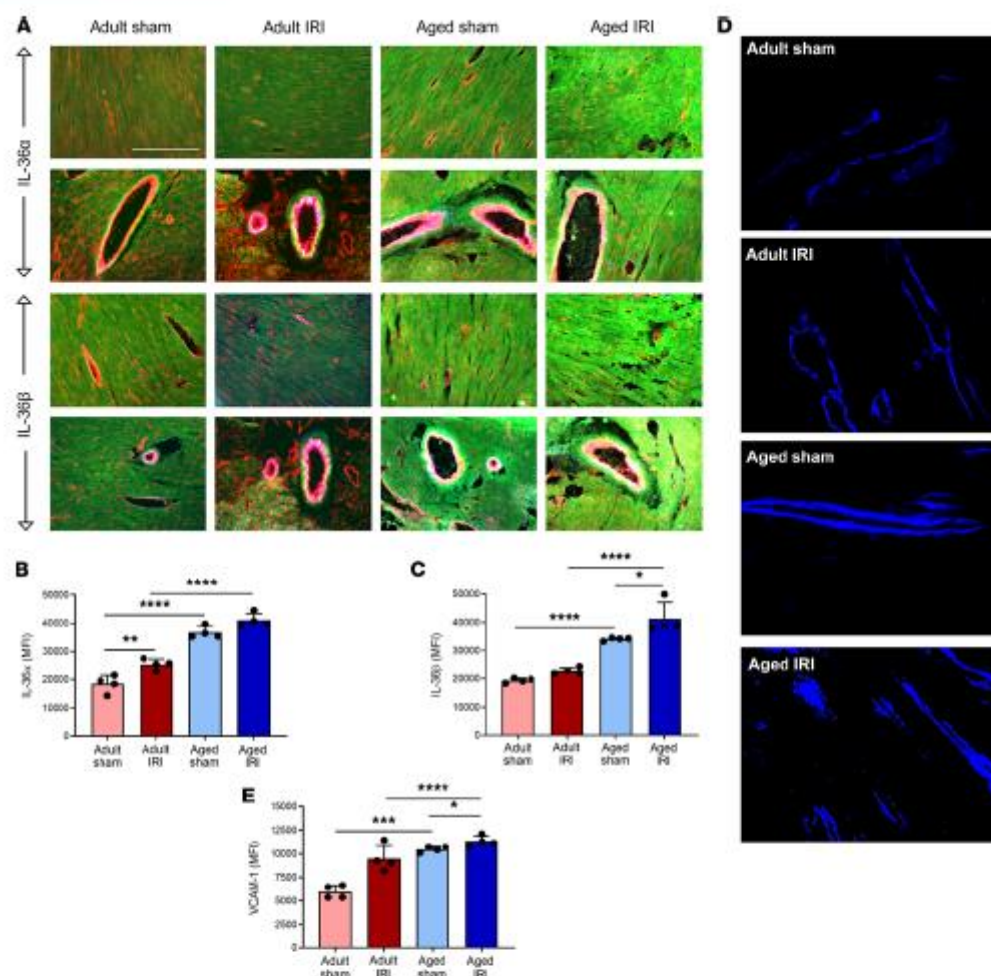


**Figure 2. Age increases expression of IL-36 $\alpha$ , IL-36 $\beta$ , and VCAM-1 in healthy and IR-injured hearts.** Hearts from adult and aged sham and IR-injured mice were immunostained with an anti-IL-36 $\alpha/\beta$ , anti-CD31, and anti-VCAM-1 antibody. (A) Representative images of IL-36 $\alpha$  (green; top 2 rows) and IL-36 $\beta$  (green; bottom 2 rows) staining of frozen heart sections costained with CD31 (red) and VCAM-1 (blue). The upper row of each cytokine panel shows coronary microvessels with the lower row selected to demonstrate staining of a large coronary blood vessel. Quantitative analysis of the immunofluorescence images for (B) IL-36 $\alpha$  and (C) IL-36 $\beta$  expression. \* $P = 0.0193$ , \*\* $P = 0.0054$ , \*\*\*\* $P < 0.0001$ . (D) Representative images of VCAM-1 (blue) staining of frozen heart sections. (E) Quantitative analysis of immunofluorescence images of VCAM-1 expression. \* $P = 0.0308$ , \*\*\* $P = 0.0002$ , \*\*\*\* $P < 0.0001$ . Scale bar indicates 200  $\mu\text{m}$ .  $n = 4/\text{group}$ .  $P$  values were determined using a 1-way ANOVA followed by a Tukey's post hoc test.

and IL-36 $\beta$ , neutrophil recruitment continued to rise. Platelet aggregates were again occasionally observed, but no significant differences were observed other than a decrease in their presence with IL-36 $\beta/\gamma$  (Figure 5, A and C–E). The number of free-flowing neutrophils generally decreased in response to all 3 IL-36 cytokine treatments in both adult and aged hearts (data not presented).

To ascertain whether thromboinflammatory events imaged intravitaly on the surface of the heart were also occurring in the deeper layers of the myocardium, multiphoton microscopy was used. A vibratome was used to precisely section the left ventricle wall into 4 sections of 300  $\mu\text{m}$  thickness from the outermost layer closest to the epicardium through to the inner layer closest to the endocardium. Multiphoton Z-stacks

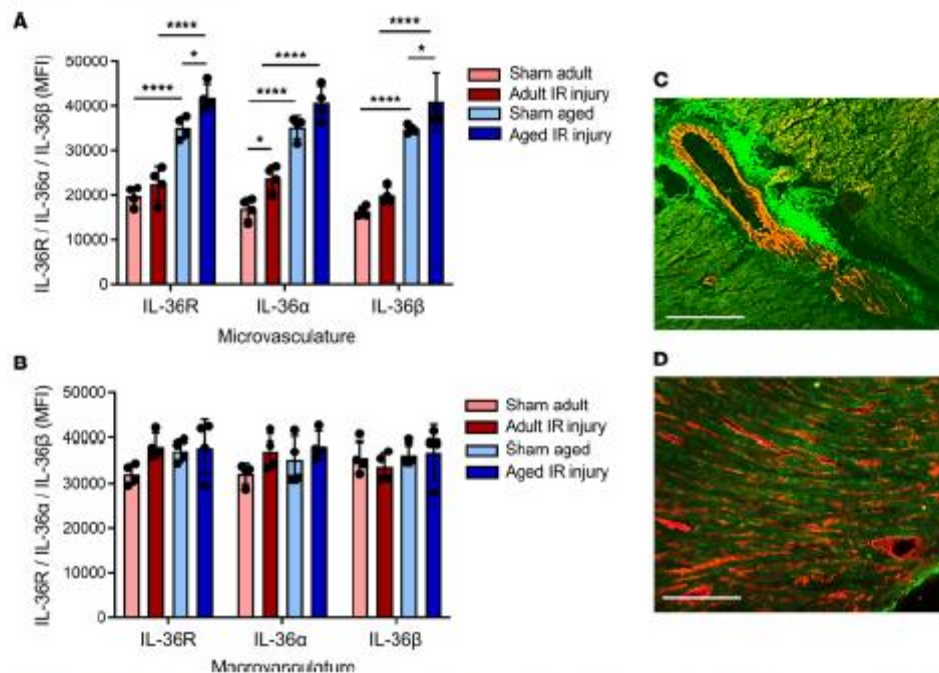


**Figure 3.** Changes in the expression of IL-36 cytokines and its receptor occur on the coronary microvasculature and not on the large blood vessels. Quantitative analysis of IL-36R, IL-36α, and IL-36β expression using immunofluorescence is shown for the (A) microvasculature and (B) macrovasculature of the adult and aged sham and IR-injured heart.  $n = 4/\text{group}$ . \* $P < 0.05$ , \*\*\*\* $P < 0.0001$  as determined using a 1-way ANOVA followed by a Tukey's post hoc test. To further determine whether IL-36R (green) expression was vascular in nature, heart sections were costained with an anti-CD31 antibody (red) and imaged using a multiphoton microscope. Representative image of (C) coronary macrovasculature and (D) microvasculature for an adult IR-injured mouse.

were taken from all 4 layers (Figure 4, E and F). The data obtained confirmed the ability of IL-36 cytokines to mediate a proinflammatory response in topically treated adult and aged hearts. However, this was only noted in the outermost layer of the heart muscle exposed to the topically applied cytokine and did not extend into the depths of the muscle wall, likely explained by the inability of the cytokine to permeate during the exposure period beyond the superficial myocardial layers. Multiphoton studies also detected a high basal presence of adherent neutrophils in aged mice throughout the muscle wall (Figure 5F).

*Age increases thromboinflammatory disturbances within healthy and IR-injured coronary microcirculation in vivo, which are prevented in both age groups by IL-36R inhibition.* Intravital imaging demonstrated an increase ( $P < 0.0001$ ) in adherent neutrophils, primarily within coronary capillaries, in response to IR injury in adult mice when compared with sham adult hearts (Supplemental Video 2). Basal neutrophil adhesion was also increased ( $P < 0.0001$ ) in aged sham hearts when compared with adult shams. Neutrophil recruitment was greatest in aged IR-injured hearts, which was higher ( $P < 0.0001$ ) than adult IR-injured hearts. This increase was noted at all time points postreperfusion and continued to rise. Individual neutrophils were often difficult to demarcate and appeared as clusters in aged injured hearts. Their presence was also noted in medium-sized coronary microvessels as well as in capillaries, something not observed in adult injured hearts (Figure 6, A–D). The number of free-flowing neutrophils decreased ( $P < 0.0001$ —data not presented) in all groups when compared with adult sham hearts with a concomitant and significant increase in the presence of small aggregates of platelets within coronary capillaries (Figure 6, A and E).

Intravital imaging further demonstrated the ability of exogenous IL-36Ra treatment to reduce neutrophil adhesion in both adult ( $P < 0.0001$ ) and aged IR-injured hearts ( $P < 0.0001$ ) when compared with their respective nontreated IR-injured groups (Figure 6, A–D). In some aged mice, neutrophil adhesion could

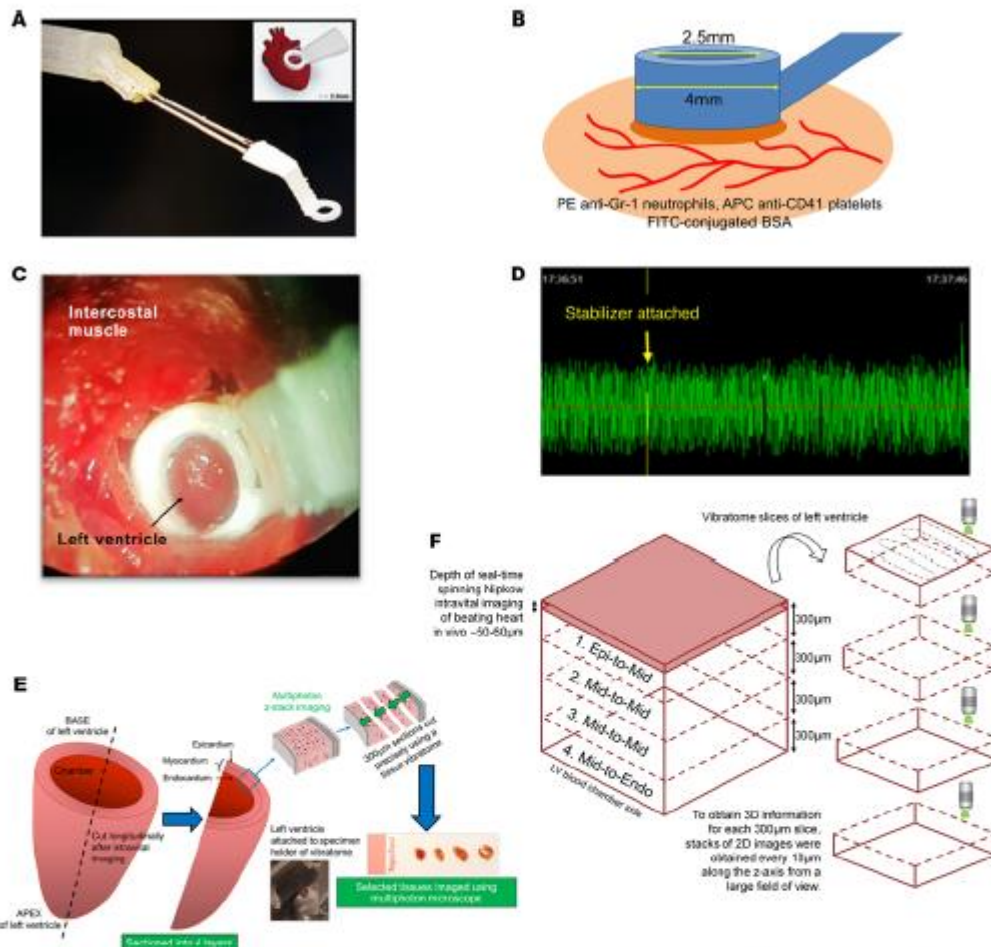


**Figure 4. Intravital imaging of the mouse beating heart microcirculation in vivo and multiphoton imaging of the heart ex vivo.** (A–C) An in-house-designed 3D-printed stabilizer is lowered onto the beating left ventricle, allowing confocal intravital imaging in its center. Only a small surface of the beating heart has its motion reduced enough to permit imaging. (D) No BP/heart rate changes were detected using this approach as determined by photoplethysmography in both adult and aged sham and IR-injured mice. The graph presented shows BP, which remains constant even after the stabilizer is attached. (E) To ascertain whether any thromboinflammatory and vasculoprotective events imaged intravital on the surface of the heart were also occurring in the deeper layers of the myocardium, multiphoton microscopy was used. The heart was cut in half longitudinally from the base to apex to expose the inner endocardial layer lining the left ventricle chamber. It was then placed on a specimen holder and attached to a tissue vibratome to precisely section the left ventricle wall into 4 × 300 μm thickness sections from the outermost layer closest to the epicardium, through to the inner layer closest to the endocardium. (F) Multiphoton Z-stacks were taken from all 4 layers, namely the (i) outermost layer closest to the epicardium – epi-to-mid (ii) outer myocardial layer – mid-to-mid (iii) inner myocardial layer – mid-to-mid, and (iv) innermost layer closest to the endocardium – mid-to-endo, avoiding the last section if it had “missing” myocardium due to sectioning through the actual ventricle chamber. Images from each layer were then rendered to form 3D stack images.

still occasionally be observed within the medium-sized coronary vessels, but this was much lower compared with nontreated groups (Figure 6A). There was no statistically significant impact of IL-36Ra treatment on the presence of platelet microthrombi within adult or aged IR-injured hearts (Figure 6E).

*Age increases neutrophil presence within the deeper layers of the healthy and IR-injured myocardium.* Minimal neutrophil presence was identified in adult sham hearts throughout the depth of the left ventricular wall when imaged

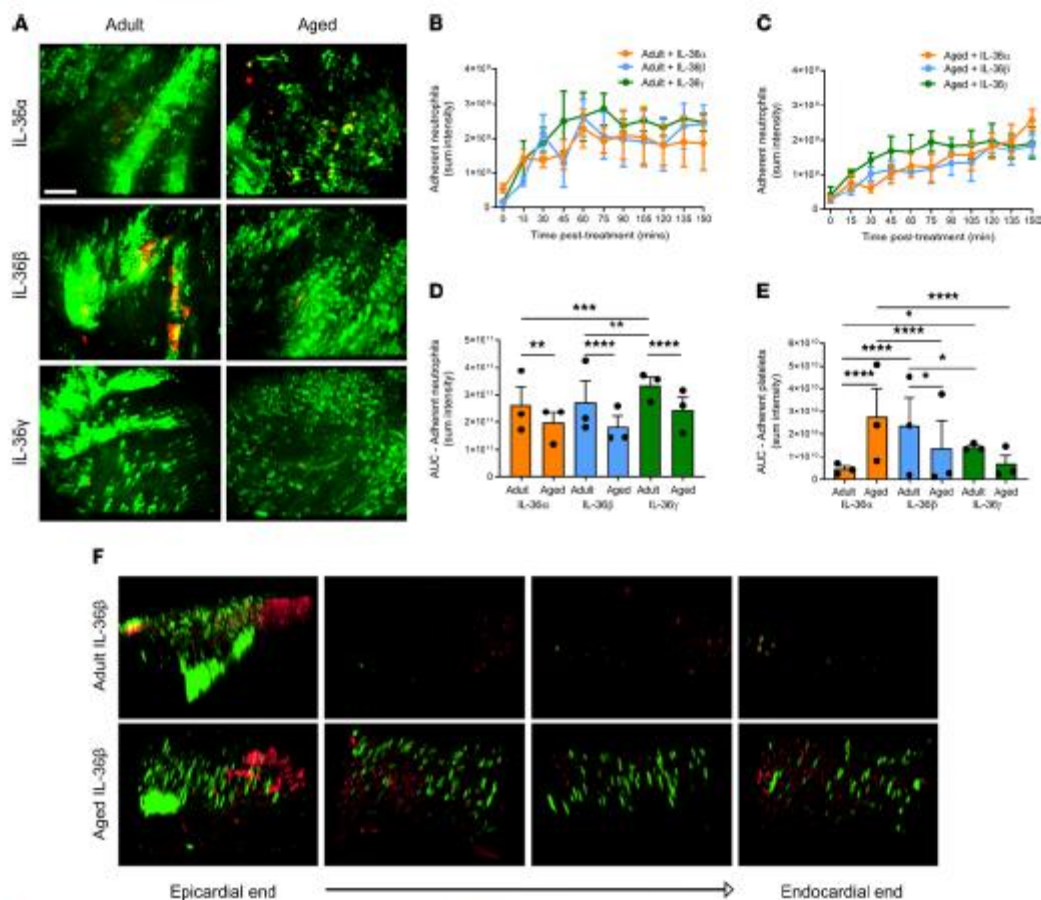


**Figure 5. Topically applied IL-36 is proinflammatory in the adult and aged beating heart in vivo.** IL-36 $\alpha$ , IL-36 $\beta$ , or IL-36 $\gamma$  (200 ng/mL) was topically applied to the healthy adult and aged beating heart left ventricle. (A) Representative intravital images of the beating heart showing adherent neutrophils (green) and platelets (red) in the coronary microcirculation at 120 minutes postapplication. Quantitative analysis of the intravital data for adherent neutrophils for the (B) adult and (C) aged groups and the area under the curve (AUC) for (D) adherent neutrophils and (E) platelets over a time course of 150 minutes. (F) Representative multiphoton images of neutrophils (green) and platelets (red) in all 4 layers of the left ventricle exposed to IL-36 $\beta$  in adult (top row) and aged (lower row) mice. Images are taken from the outermost layer closest to the epicardium, outer myocardial layer, inner myocardial layer, and innermost layer closest to the endocardium. Scale bar indicates 100  $\mu$ m.  $n = 3$ /group. \* $P < 0.05$ , \*\* $P < 0.01$ , \*\*\* $P < 0.001$ , \*\*\*\* $P < 0.0001$  as determined using a 1-way ANOVA followed by a Tukey's post hoc test.

*ex vivo* using multiphoton microscopy. However, in adult injured hearts, an increased ( $P = 0.035$ ) presence of neutrophils was observed in all 4 layers of the heart when compared with adult sham hearts (Supplemental Video 3). However, the largest neutrophil presence in response to injury occurred within the outermost 300  $\mu$ m layer. Basal neutrophil presence was also uniformly increased ( $P < 0.0001$ ) throughout all 4 layers of the ventricle in aged sham hearts when compared with adult sham hearts (also seen in Figure 5F). This was further increased ( $P < 0.0001$ ) in aged injured hearts when compared with adult injured hearts, with the greatest presence again noted within the outermost layer of the ventricle wall (Figure 7, A–C).

*IL-36R inhibition improved functional capillary density and reduced infarct size in vivo in adult and aged IR-injured hearts.* An extensive network of FITC-BSA-perfused capillaries was observed in both adult and aged sham mice, paralleling the arrangement of muscle fibers, with cross connections along their length. Focus-

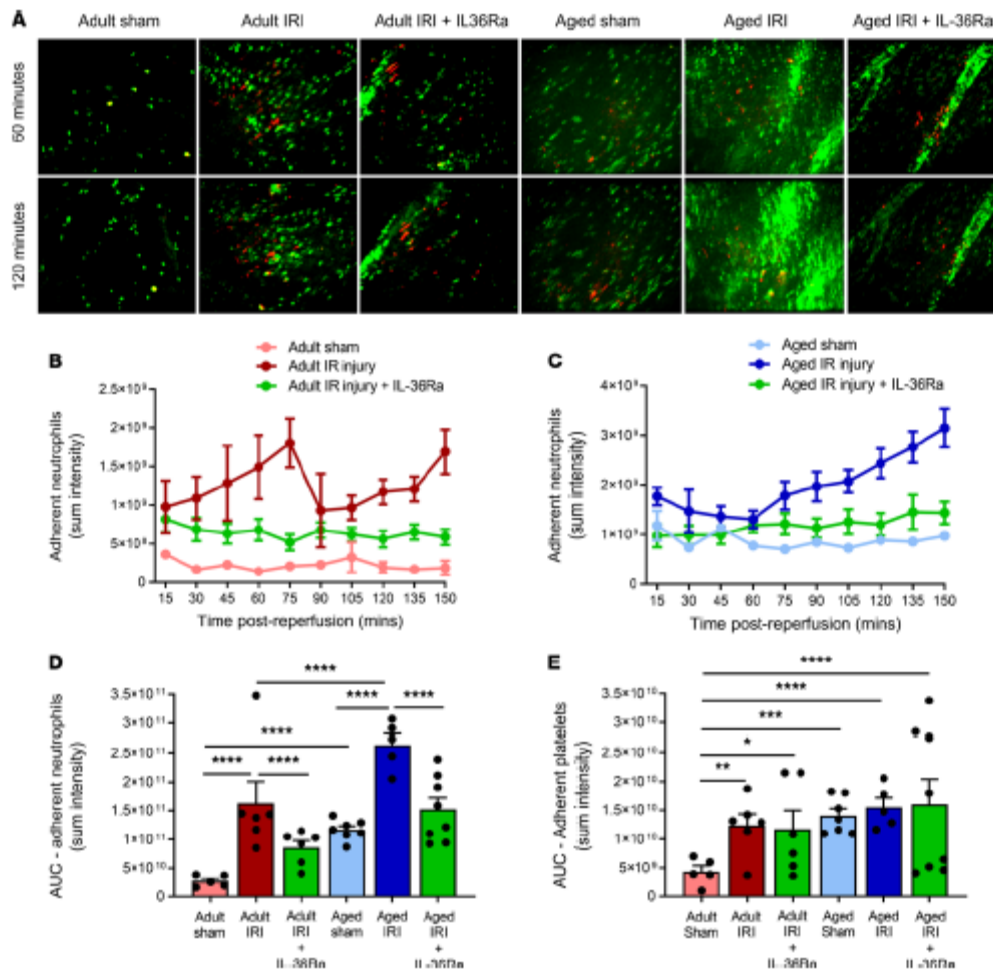


**Figure 6.** Age increases thromboinflammatory disturbances within the healthy and IR-injured beating heart coronary microcirculation in vivo, which can be prevented in both age groups by IL-36R inhibition. An IL-36Ra (15  $\mu$ g/mouse) was injected intra-arterially at 10 minutes prereperfusion and 60 minutes postreperfusion in adult and aged mice. **(A)** Representative intravital images of the beating heart showing adherent neutrophils (green) and platelets (red) in the coronary microcirculation at 60 and 120 minutes in sham hearts or 60 and 120 minutes postreperfusion in injured hearts. Adherent neutrophils (green) and platelet microthrombi (red) are primarily within coronary capillaries in injured hearts. Intensely fluorescent green areas in aged IR-injured hearts correspond to medium-sized blood vessels that have become delineated by the presence of a substantial number of adherent neutrophils. Quantitative analysis of the intravital data for adherent neutrophils in **(B)** adult and **(C)** aged IR-injured hearts and the AUC for **(D)** adherent neutrophils and **(E)** platelets over a time course of 150 minutes. Scale bar indicates 100  $\mu$ m. Adult sham –  $n = 5$ /group; adult IRI –  $n = 6$ /group; adult IRI + IL-36Ra –  $n = 5$ /group; aged sham –  $n = 7$ /group; aged IRI –  $n = 5$ /group; aged IRI + IL-36Ra –  $n = 8$ /group. \* $P = 0.0339$ , \*\* $P = 0.0014$ , \*\*\* $P = 0.0003$ , \*\*\*\* $P < 0.0001$  as determined using a 1-way ANOVA followed by a Tukey's post hoc test.

ing up and down on the field of view showed no areas devoid of perfused capillaries. Well-perfused medium-sized vessels were also visible in some fields of view. In contrast, IR injury of adult hearts was associated with multiple areas in which FITC-BSA did not perfuse. This resulted in patchy areas that appeared devoid of any microvasculature, indicating reduced functional capillary density. This was further reduced in aged IR-injured hearts. Indeed, in some fields of view, up to half of the imaged area appeared to lack perfusion. Of note, medium-sized vessels were still readily visible and well perfused in both adult and aged

injured hearts. The use of an IL-36Ra was able to improve functional capillary density in both adult and aged hearts, although some areas of no perfusion were still visible (Figure 8A).

Infarct size appeared slightly larger in aged mice when compared with adult mice, but this was not significant. However, a significant decrease in infarct size was observed in both adult ( $P < 0.0001$ ) and aged IR-injured hearts ( $P < 0.0001$ ) receiving IL-36Ra treatment when compared with their respective nontreated IR-injured groups. The area at risk (AAR) (and nonischemic area) was not significantly different across all 4 groups (Figure 8, B–D).

*IL-36R inhibition reduced endothelial and cardiomyocyte oxidative damage and VCAM-1 expression in the IR-injured adult and aged heart.* To determine whether IL-36Ra treatment conferred vasculoprotection via mechanisms involving attenuation of endothelial oxidative stress and VCAM-1 expression, flow cytometry of collagenase-digested adult and aged hearts and immunofluorescence on frozen adult and aged heart sections were performed. IR injury increased ROS-mediated oxidative damage on both adult ( $P < 0.05$ ) and aged ( $P < 0.01$ ) coronary endothelial cells and adult ( $P < 0.05$ ) and aged ( $P < 0.001$ ) cardiomyocytes when compared with appropriate age sham heart cells as determined by flow cytometry. The damage was significantly greater in IR-injured aged hearts compared with IR-injured adult hearts. However, this damage was significantly ( $P < 0.05$ ) reduced on both cell populations in all mice treated with the IL-36Ra regardless of age (Figure 9, A and B).

Significant oxidative damage in IR-injured adult ( $P < 0.05$ ) and aged ( $P < 0.001$ ) hearts was confirmed using immunofluorescence and was noted as punctate staining on both CD31<sup>+</sup> vascular and nonvascular structures (Figure 9C). Moreover, this damage was noticeably greater on aged IR-injured hearts. This was again reduced in all mice treated with the IL-36Ra regardless of age (Figure 9D). VCAM-1 was also increased in adult ( $P < 0.05$ ) IR-injured tissue, particularly around larger coronary blood vessels. In aged mice, basal VCAM-1 expression was high and did not increase further with IR injury. However, expression of this endothelial adhesion molecule decreased in both adult ( $P < 0.05$ ) and aged ( $P < 0.05$ ) hearts in IL-36Ra-treated mice (Figure 9, C–E).

## Discussion

By 2030, it is expected that 20% of the population will be over 65 years old, and cardiovascular disease is set to account for 40% of the deaths within this age group (30). Increased age is associated with a worse prognosis post-MI and may be explained by an increased microvascular susceptibility to reperfusion injury. Therefore, consideration of the effects of aging on the postischemic heart, particularly on the smallest blood vessels of the heart, is critical. This study provides original contributions on the architecture of the aged beating heart coronary microcirculation and how its response to myocardial IR injury differs from that of younger hearts in vivo. Aging is associated with a chronic low-grade inflammatory cell presence in otherwise healthy hearts as well as a heightened thromboinflammatory response in the immediate aftermath of reperfusion. Importantly, what we believe to be a new mechanistic role is identified for the IL-36/IL-36R pathway. Our data demonstrate that IL-36 and its receptor were present in the heart and that their expression increased, particularly on coronary microvessels, with age and injury. Not only is the receptor demonstrated for the first time, as far as we are aware, to be functional in the heart, but also, importantly, its antagonism is shown to markedly reduce microcirculatory perturbations and, consequently, infarct size in adult mice. By hyperactivating innate immunity, aging has been shown to reduce the therapeutic efficacy of both pharmacological and ischemic preconditioning interventions in the heart (31, 32). Indeed, preconditioning was unable to reduce infarct size even in middle-aged rat hearts (aged 12–13 months), demonstrating that the loss of cardioprotection manifests earlier and not only in senescence (32). Therefore, it was reassuring to observe that inhibiting IL-36R signaling remained vasculoprotective even in the highly inflamed aged injured heart.

The impact of age alone on the coronary microcirculation was not negligible. Indeed, an almost 5-fold increase in neutrophil adhesion within otherwise healthy coronary capillaries was demonstrated simply as a result of the mouse age increasing from approximately 3 to 18 months. This may be linked to the observed age-related upregulation of endothelial VCAM-1 in the heart or structural and functional changes in the neutrophils themselves (33, 34). Indeed, neutrophils in aged individuals have been shown to exist in a pre-activated state whereby they constitutively secrete more neutrophil elastase and ROS in close proximity to endothelium, which can lead to vascular damage and their subsequent adhesion (35). Although age-related capillary loss or rarefaction has also been described (36), no visible reduction in functional capillary density

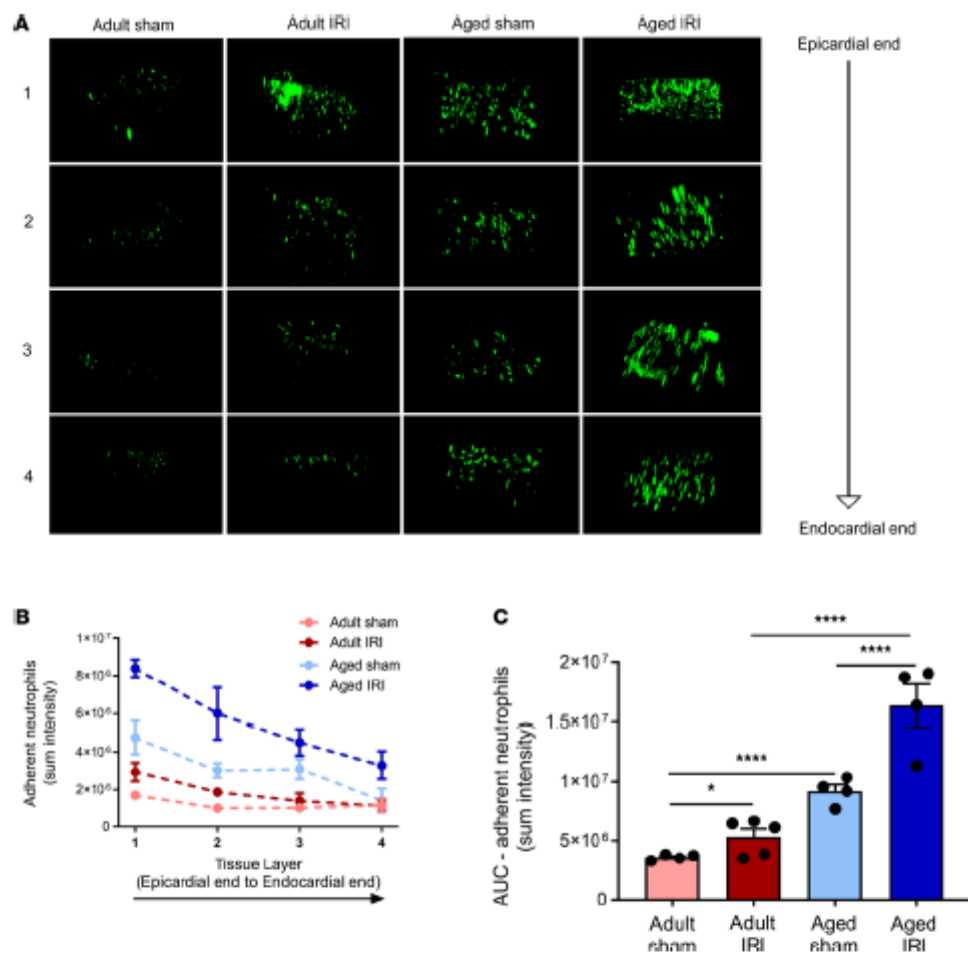


**Figure 7. Age increases neutrophil presence within the deeper layers of the healthy and IR-injured myocardium.** (A) The left ventricle was vibratome sectioned into four 300  $\mu$ m sections and imaged using a multiphoton microscope. Representative Z-stack multiphoton images of neutrophils (green) in the 4 layers of the left ventricle taken from the outermost layer closest to the epicardium (first row), outer myocardial layer (second row), inner myocardial layer (third row), and innermost layer closest to the endocardium (fourth row). Quantitative analysis of the multiphoton data at various depths for (B) adherent neutrophils and corresponding (C) AUC for adherent neutrophils. Adult sham –  $n = 4$ /group; adult IRI –  $n = 5$ /group; aged sham –  $n = 4$ /group; aged IRI –  $n = 4$ /group. \* $P = 0.0325$ , \*\*\*\* $P < 0.0001$  as determined using a 2-way ANOVA followed by a Tukey's post hoc test.

or increased vascular leakage was noted in noninjured aged hearts. Interestingly, a marked reduction in freely circulating neutrophils was observed, which may be linked to a possible decreased coronary blood flow in the aged heart (37). However, this would require further investigation. Furthermore, platelet aggregates were also visible in aged hearts and were sometimes occlusive as evidenced by the lack of circulating neutrophils passing through affected microvessels. Intravital microscopy therefore directly imaged the presence of a chronic low-grade inflammation in the aged heart but also alluded to a mildly prothrombotic state as well. These basal microcirculatory disturbances, when combined with an acute injurious insult, may create a more heightened thromboinflammatory effect in the presence of an aging comorbidity.

Indeed, this was the case in aged IR-injured hearts, where remarkable neutrophil adhesion was observed that surpassed that noted in adult injured hearts. Individual neutrophils were difficult to demarcate with

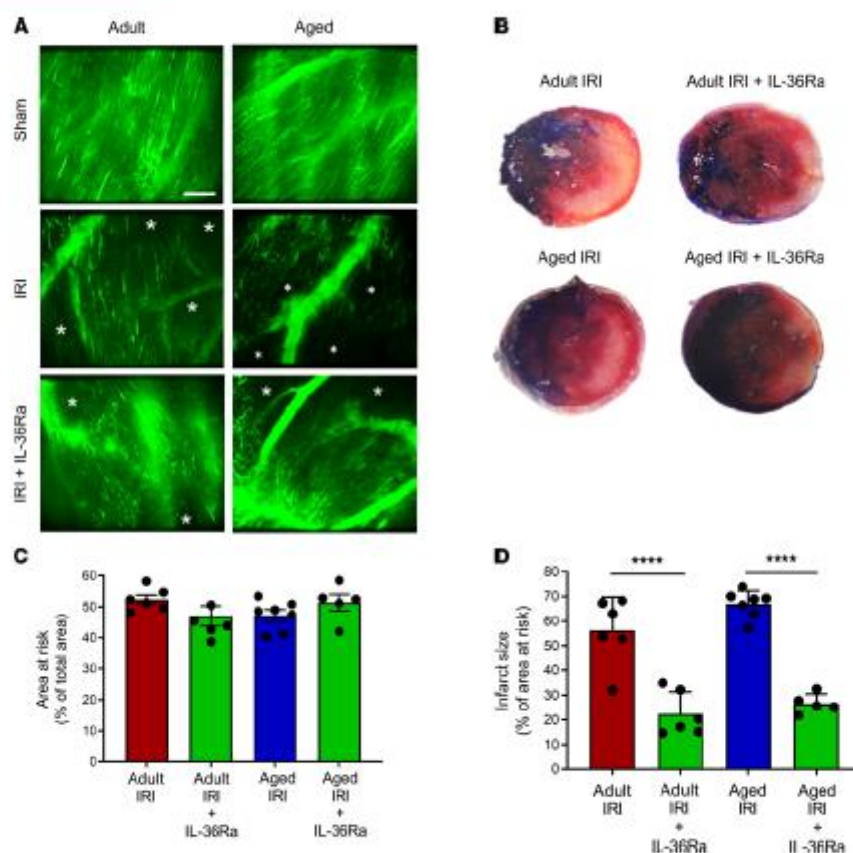


**Figure 8. IL-36R inhibition improves functional capillary density and reduces infarct size in vivo in the IR-injured adult and aged heart.** An IL-36Ra (15  $\mu$ g/mouse) was injected intra-arterially at 10 minutes preperfusion and 60 minutes postperfusion in adult and aged mice. (A) Representative intravital images of FITC-BSA-perfused (green) coronary microvessels at 150 minutes in sham hearts or 150 minutes postperfusion in injured hearts. \*Areas not perfused with FITC-BSA. Scale bar indicates 100  $\mu$ m. (B) Representative images of the TTC-stained infarct size in all 4 groups. (C) Quantitative analysis of the area at risk in all 4 groups. (D) Quantitative analysis of infarct size in all 4 groups.  $n = 6$ /group ( $n = 5$  for aged IRI + IL-36Ra group). \*\*\*\* $P < 0.0001$  as determined using a 1-way ANOVA followed by a Tukey's post hoc test. TTC, 2,3,5-triphenyltetrazolium chloride.

clusters observed occupying the full width of the capillaries. Activated neutrophils are well known to become stiffer, which contributes to their retention specifically within capillaries that have a smaller diameter than their own (38). However, larger coronary blood vessels, which we assume were postcapillary venules (PCVs), were also delineated with adherent neutrophils, something not noted in adult injured hearts. Although neutrophil recruitment plateaued in the adult hearts, this was not the case in injured aged hearts, where neutrophils continued to be recruited. Increased platelet presence was also noted, but this was not as remarkable as the effect on neutrophils. Consequently, these thromboinflammatory occlusive events resulted in the poorest coronary microcirculatory perfusion being noted in aged injured hearts, with multiple areas devoid of flow. We believe this to be the first real-time demonstration of a rapid and devastating impact of reperfusion on the smallest blood vessels of the aged heart in vivo. This may explain the reduced myocardial tolerance to IR injury previously demonstrated to occur as early as 12 months (middle age) in mice (39).

IL-36 is typically one of the most upstream and upregulated cytokines released upon tissue injury and cellular necrosis and critical in triggering subsequent synthesis and release of a multitude of inflammatory mediators (15). This study shows that IL-36R, IL-36 $\alpha$ , and IL-36 $\beta$  are constitutively expressed on vascular

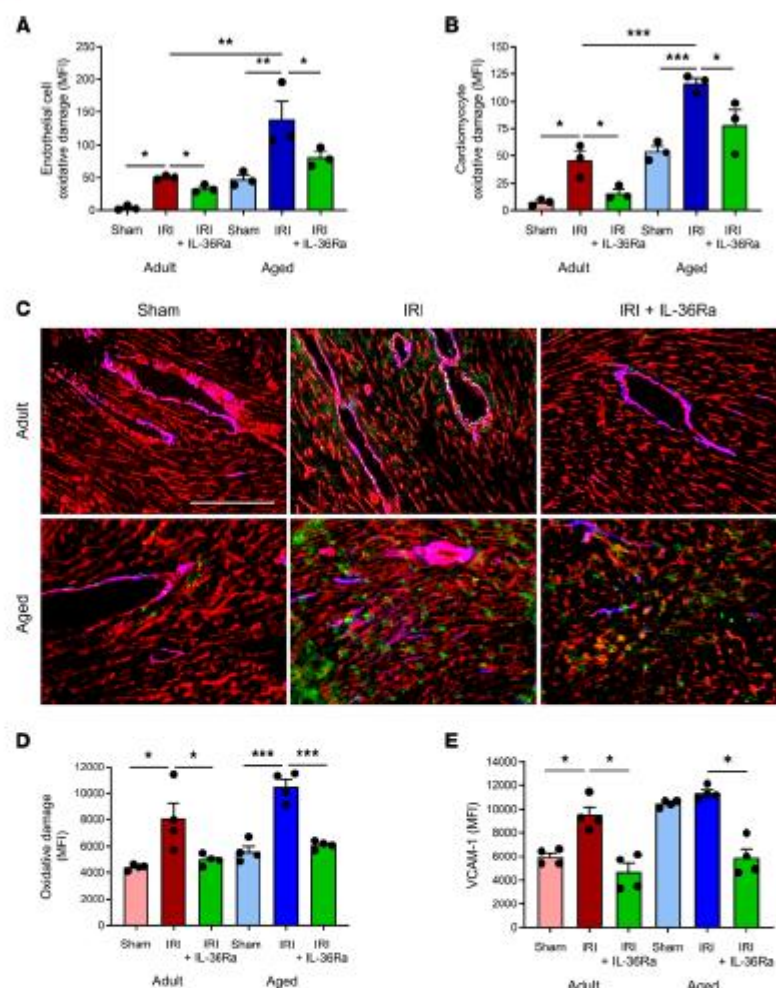


**Figure 9. IL-36R inhibition reduces endothelial and cardiomyocyte oxidative damage and VCAM-1 expression in the IR-injured adult and aged hearts.** Hearts from adult and aged sham, IRI-injured, and IRI-injured + IL-36Ra mice were either collagenase digested and analyzed flow cytometrically or sectioned and analyzed using immunofluorescence for oxidative damage and/or VCAM-1 expression. Flow cytometry analysis demonstrated that IRI injury increased oxidative damage of both (A) adult and aged coronary endothelial cells and (B) adult and aged cardiomyocytes when compared with appropriate age sham cells. This was reduced in both cell populations in adult and aged mice treated with the IL-36Ra.  $n = 3$ /group. (C) Representative immunofluorescence images of CD31 (red) costained with DNA/RNA oxidative damage (green) and VCAM-1 (blue) in sham, IRI-injured, and IL-36Ra-treated adult and aged mice. Quantitative analysis of the immunofluorescence images for myocardial (D) oxidative damage and (E) VCAM-1 expression. Scale bar indicates 200  $\mu$ m.  $n = 4$ /group. \* $P < 0.05$ , \*\* $P < 0.01$ , \*\*\* $P < 0.001$  as determined using a 1-way ANOVA followed by a Tukey's post hoc test.

and nonvascular cells, albeit at very low levels, in healthy adult murine hearts. A basal expression of IL-36R is also supported by Towne and colleagues, who used quantitative PCR to demonstrate low levels in human hearts (25). Although cytokine receptor changes have not been studied extensively with age, an enhanced age-related production of cytokines such as IL-6 has previously been demonstrated (40, 41). In the current study, our data demonstrated that expression of IL-36R, IL-36 $\alpha$ , and IL-36 $\beta$  increased with both age and

IR injury. Expression of IL-36 agonists have been shown to increase at both the mRNA and protein level in murine kidney tissue following renal IR injury (42). Additionally, IL-36 $\beta$  mRNA expression increased in lung homogenates 24 hours after allergic lung inflammation (43). Our study assessed IL-36 after a much shorter reperfusion injury duration, so the full extent of IL-36 upregulation was potentially not observed.

IL-36 and IL-36R expression were observed on the majority of coronary capillaries as evidenced by colocalization with CD31<sup>+</sup> endothelial cells. Moreover, it was only on microvessels that an age- and injury-related increase in cytokine and receptor expression was observed. This elevated age-related expression specifically on microvessels increases the likelihood of this signaling pathway exacerbating IR injury through targeting the coronary microcirculation in elderly patients with MI.

Immunofluorescence studies on VCECs confirmed expression of the IL-36R on endothelial cells. This was also recently shown on human umbilical vein and dermal lymphatic endothelial cells, where it was functionally important in mediating upregulation of ICAM-1/VCAM-1 and chemokine production in response to IL-36 stimulation (44). We further demonstrated that all 3 IL-36 agonists could upregulate endothelial surface expression of the IL-36 receptor. These data provide what we believe to be new insights into the fundamental biology of this cytokine. The ability of some cytokines to increase expression of their receptor is not new. Indeed, Takii and colleagues showed that IL-1 can enhance gene and surface expression of its own receptor in pulmonary fibroblast cells within 2 hours (45). Autoregulation forms a positive feedback loop that drives a strengthened activation of the signaling pathway of a given cytokine. Here, we show that IL-36 cytokines may also utilize this autoregulatory phenomenon to enhance their own activity.

Interestingly, intense IL-36/IL-36R staining was noted on the outer tunica adventitial layer of larger blood vessels. Inflammatory responses are generally considered to be initiated in an "inside-out" manner through capture of circulating leukocytes by the endothelial surface. However, growing evidence supports an "outside-in" model in which the adventitia, previously considered an inert layer that simply provides structural support, acts as an injury "sensor" within the vessel wall and subsequently directs responses to a wide array of stimuli, including ischemia. In this model, it is proposed that resident adventitial cells, such as fibroblasts, become activated and secrete inflammatory cyto/chemokines, which leads to expression of endothelial surface adhesion markers such as VCAM-1 and subsequent neutrophil recruitment to the intimal layer (46). Although recent studies have extended IL-36 and IL-36R expression to include stromal cells such as fibroblasts, further studies will be required to determine whether their presence in the adventitial vascular layer is of specific significance in mediating inflammatory responses in the heart after reperfusion injury.

A common finding in diseases where IL-36 cytokines contribute to pathology is the remarkable presence of neutrophils. Indirect evidence supporting the ability of IL-36 to recruit neutrophils has been obtained primarily from histological or flow cytometric studies in which inhibiting IL-36R signaling reduced recruitment in diseases such as psoriasis and colitis. Recent findings by Koss and colleagues pinpoint IL-36 as an early and upstream driver of acute and chronic pulmonary inflammation by promoting neutrophil recruitment and production of proinflammatory IL-1F cytokines and IL-6 (47). To directly demonstrate that IL-36 could be proinflammatory in the heart, we topically applied agonists within the center of the attached water-tight stabilizer ring. All isoforms were potentially proinflammatory, something not previously shown in vivo in any organ let alone the heart. Neutrophil recruitment was observed in both coronary capillaries and PCVs but, unexpectedly, was greater in adult rather than aged hearts, which could be due to reduced neutrophil responsiveness with age (48). The inflammatory response was rapid and appeared to plateau beyond 60 minutes in adult hearts. Although it was slower and less potent in aged hearts, neutrophil recruitment did continue to rise beyond 150 minutes. It is possible that with a more prolonged imaging period, this response may have reached similar, or exceeded, maximal levels observed in adult mice. It is also possible that our observed increases in the expression of IL-36R in aged mice may be associated with a concomitant increase in circulating levels of the endogenous antiinflammatory IL-36Ra. This would act to protect the balance of IL-36 pathway signaling in aged mice by inhibiting engagement of IL-36 cytokines with their receptor. This could also explain why the same dose of topical IL-36 was unable to elicit similar or greater inflammatory responses in aged compared to adult hearts. Indeed, this has been shown to be true for IL-1Ra, where higher circulating levels are detected in elderly patients, and has been suggested to play a role in the decline in the inflammatory response with age (49).

Interestingly, we also showed that topical application of IL-36 was more potent than similar doses of topical IL-1 $\beta$  and TNF- $\alpha$  at stimulating neutrophil recruitment in both adult and aged hearts (data not

presented). IL-36 also increased platelet microthrombi presence, although it is not known if this is driven through a direct response of IL-36 on platelets. It is possible that circulating platelets became trapped in vessels downstream of regions where substantial occlusive neutrophil adhesion occurred. Collectively, these studies provided a rationale for exploring the therapeutic potential of IL-36 signaling blockade to attenuate microcirculatory disturbances associated with injury.

The IL-36R is interesting in that it has 3 agonists but also 2 naturally occurring receptor antagonists, namely IL-36Ra and IL-38, which underpins the importance of careful endogenous management of the IL-36 pathway. Both competitively bind the IL-1Rrp2 component of the heterodimer receptor, preventing recruitment of the accessory coreceptor IL-1RAcP and thus inhibiting subsequent intracellular signaling (18). We tested the vasculoprotective effects of systemically injected IL-36Ra and observed a marked reduction in neutrophil recruitment in both adult and aged injured hearts. Although no antiplatelet effect was demonstrated, IL-36Ra treatment still led to a significant decrease in infarct size in both adult and aged mice. Since 1 dose of IL-36Ra was administered during the ischemic period, it is plausible that IL-36 could be targeted during PCI procedures and be therapeutically efficacious in a clinical setting.

ROS are implicated in the pathogenesis of various cardiac disorders, including MI and heart failure, and can promote the expression of endothelial adhesion molecules, such as ICAM-1 and VCAM-1, that are critical for neutrophil recruitment (50). Therefore, whether IL-36Ra mechanistically conferred vasculoprotection by limiting endothelial ROS damage and VCAM-1 expression was assessed in both adult and aged hearts. The anti-DNA/RNA antibody used in the study binds with high specificity and affinity to 8-hydroxy-2'-deoxyguanosine, 8-oxo-7,8-dihydroguanine, and 8-oxo-7,8-dihydroguanosine. These oxidative lesions serve as excellent markers for DNA and RNA damage produced specifically by ROS. Flow cytometric and immunofluorescence studies demonstrated a marked decrease in IR injury-mediated oxidative damage in the presence of the IL-36Ra. Importantly, this decrease was evident in both adult and more damaged aged hearts. Our data support the recent observation of reduced oxidative stress, measured using spectrophotometry of superoxide dismutase and malondialdehyde activity, in IL-36R-knockout rats undergoing cardiopulmonary bypass (51). However, we further detail that the antioxidant effects of IL-36Ra occur specifically on both coronary endothelial cells and cardiomyocytes. It has recently been shown that IL-36 can upregulate VCAM-1 and ICAM-1 on dermal endothelial cells in vitro and that this can be reversed by the presence of an IL-36Ra (44). However, we demonstrate the ability of IL-36Ra to decrease VCAM-1 expression in the IR-injured coronary microcirculation. Again, more importantly, this benefit was also observed in aged hearts where even basal VCAM-1 expression was high. Collectively, our data provide, we believe, novel mechanistic insights into how inhibition of IL-36/IL-36R signaling attenuates oxidative stress and VCAM-1 expression in adult and aged hearts, subsequently preventing excessive neutrophil recruitment in the coronary microcirculation, which ultimately leads to decreased infarct size postreperfusion.

**Concluding remarks.** New therapies need to be designed and optimized that are effective in improving the current poor prognosis of the aging population post-MI. We and others have recommended specific protection of the delicate coronary microcirculation from IR injury. Although studies on age-related changes of the inflammatory and immune system have gained momentum, this study is the first, as far as we know, to explore the impact of age on the coronary microcirculation in vivo both in health and postreperfusion injury. It is likely that the increased thromboinflammatory activation and microcirculatory perturbations that we have observed intravitaly in the aged injured heart may inhibit the therapeutic efficacy of existing and future cardiovascular drugs in the elderly. However, our finding that IL-36Ra not only was vasculoprotective but also, importantly, remained beneficial in the setting of an age-related heightened inflammation in the coronary microvessels makes it a candidate worth pursuing clinically in elderly patients undergoing PCI for MI. In support of this is the recent work by Luo and colleagues, who demonstrated experimentally that deficiency of IL-36R protected cardiomyocytes in the setting of cardiopulmonary bypass (51).

A number of antiinflammatories, shown to be successful in experimental studies, have met with translational failure when tested in patients with MI (52). The major outcome measured in such clinical trials (and indeed experimental studies) is usually a long-term one—namely the ability to prevent post-MI remodeling, a secondary nonfatal MI, or death. Whether these antiinflammatories can also protect and keep patent the coronary microcirculation in the immediate aftermath of PCI/reperfusion has received much less interest. However, a functioning microcirculation is imperative in order to improve long-term patient outcomes. It is therefore possible that translational failure is linked to a lack of early benefit at the level of the coronary microcirculation. Since we have shown multiple microcirculatory perturbations, ultimately resulting

in poor myocardial perfusion within minutes of reperfusion, it is also important that the design of an antiinflammatory therapy involves administration immediately before interventions designed to mediate reperfusion commence (e.g., PCI). However, not all clinical trials have delivered antiinflammatories prior to reperfusion, with some administered days later (53). Again, this may explain the lack of success of such compounds in clinical trials. Our data highlight a notable benefit to the coronary microcirculation and infarct size with early administration of IL-36Ra, which importantly is maintained in the presence of an aged comorbidity. This indicates that early intervention with an IL-36R inhibitor is worth considering for future clinical investigations.

## Methods

**Myocardial IR injury.** Experiments were conducted on female C57BL/6 adult (2–4 months) or aged (18–19 months) mice from Charles River in accordance with the Animals (Scientific Procedures) Act of 1986 (Project licence P552D4447). Anesthesia was induced by an intraperitoneal administration of ketamine hydrochloride (100 mg/kg) and medetomidine hydrochloride (100 mg/kg), confirmed by checking the pedal reflex every 15 minutes and maintained as required via intraperitoneal administration. Mice were intubated and ventilated with medical oxygen via a MiniVent rodent ventilator (stroke volume: 220  $\mu$ L, respiratory rate: 130 breaths/min; Biochrom Ltd. Harvard Apparatus). The carotid artery was cannulated to facilitate infusion of antibodies, dyes, saline, and IL-36Ra. IR injury was induced by ligating the left anterior descending (LAD) artery for 45 minutes and reperfusion allowed to proceed for 2 hours (tissue analysis), 2.5 hours (intravital observations), or 4 hours (infarct measurement). Sham surgery involved the same procedure but without LAD artery ligation. At the end of experiments, mice were euthanized by cervical dislocation, and euthanasia was confirmed by ensuring cessation of the circulation by making an incision in the carotid artery.

**Intravital imaging of the beating heart coronary microcirculation.** Real-time intravital observations were performed as previously described (28). Briefly, a 3D-printed stabilizer was permanently fixed to the left ventricle downstream of the ligation site (Figure 4, A–C). To simultaneously image endogenous neutrophils and platelets, PE anti-mouse Ly-6G (BioLegend clone RB6-8C5) and APC anti-mouse CD41 (BioLegend clone MWRed30) were injected 5 minutes prior to reperfusion. Intravital imaging was performed using a microscope (BX61WI, Olympus) equipped with a Nipkow spinning disk confocal head (Yokogawa CSU) and an Evolve EMCCD camera (Photometrics). The first 2-minute capture was performed at 15 minutes postreperfusion, followed by 2-minute captures every 15 minutes of the same area for 2.5 hours. In separate mice, FITC-BSA (Sigma) was injected at the end of a 2.5-hour reperfusion period to investigate overall vascular perfusion and functional capillary density.

For some studies, recombinant mouse IL-36Ra (15  $\mu$ g/mouse; Novus Biologicals) was injected intra-arterially at both 10 minutes prereperfusion and 60 minutes postreperfusion. One of the critical factors that limits the clinical success of previously tested antiinflammatory drugs is the time of intervention. Given the rapid development of microvascular no-reflow, the first hours, if not minutes, following reperfusion are critical. Our treatment strategy focused on introducing the antagonist during the ischemic phase to establish an effective circulating concentration to dampen the initial reperfusion-associated inflammatory response and maintain microvascular patency. The ability of IL-36 cytokines to directly mediate thromboinflammatory events *in vivo* was also assessed. After placing the stabilizer on the healthy heart, 20  $\mu$ L of recombinant mouse IL-36 cytokine ( $\alpha$ ,  $\beta$ , or  $\gamma$ ; 200 ng/mL) or PBS was topically applied to the heart surface within the water-tight stabilizer ring for 15 minutes and a 2-minute video recorded. This was replaced with fresh cytokine/PBS for 15 minutes and the process repeated 10 times for a total duration of 2.5 hours.

Data were captured, stored, and analyzed using Slidebook 6 software (Intelligent Imaging Innovations). Free-flowing neutrophils, which passed through the coronary microcirculation without making adhesive interactions, were counted manually over the 2-minute recorded capture. To analyze adherent neutrophil and platelet presence, captured videos were subjected to postacquisition image repair using in-house-designed software (Tif) in which out-of-focus frames were removed (54). Neutrophils and platelet aggregates/microthrombi were then quantitated by placing a mask around PE-Ly6G<sup>+</sup> and APC-CD41<sup>+</sup> areas, respectively. Integrated fluorescence density, which took into account size and fluorescence intensity, was then calculated using ImageJ (NIH).

**Multiphoton imaging of heart sections.** Intravital imaging captured microvascular events from the surface of the beating heart with a depth of approximately 50–60  $\mu$ m. To determine whether these events were mirrored throughout the thickness of the ventricular wall, multiphoton microscopy was performed on hearts harvested

at the end of intravital experimentation. The left ventricle was sectioned into 4 sections of 300  $\mu\text{m}$  using a tissue vibratome (Campden Instruments Limited) and imaged from the epicardial through to the endocardial end using a multiphoton microscope (FVMPE-RS Olympus). Z-stacks from the 4 layers were rendered to form 3D stack images, which were processed and displayed using ImageJ (Figure 4, E and F). The presence of neutrophils was analyzed as the sum fluorescence intensity for each section (ImageJ).

**Immunohistochemistry analysis of IL-36 cytokines and IL-36R.** Ten-micrometer sections of frozen heart tissue were incubated at room temperature with primary anti-IL-36R, anti-IL-36 $\alpha$ , anti-IL-36 $\beta$ , or IgG control antibodies (1:100 dilution; R&D Systems, polyclonal) and a secondary donkey anti-goat Alexa Fluor 488 antibody (1:100 dilution; Abcam, polyclonal). Sections were also incubated with a PE anti-mouse CD31 antibody (1:100 dilution, BioLegend, clone 390), an Alexa Fluor 647 anti-mouse CD106/VCAM-1 antibody (1:100 dilution, BioLegend, clone 429), or an anti-DNA/RNA damage antibody to detect oxidative damage (1:100 dilution, Abcam, clone 153A). Images were captured using an EVOS FL (Thermo Fisher Scientific) or multiphoton microscope (FVMPE-RS, Olympus). ImageJ was used to quantify the MFI of each image with additional analysis of MFI on regions containing only coronary capillaries or a large blood vessel.

**Western blotting analysis.** Total protein was extracted from harvested hearts using RIPA buffer and homogenization with beads. Lysates were normalized using a BCA protein assay kit (Thermo Fisher Scientific) to 2 mg/mL. Samples were run on an SDS-PAGE gel and then transferred onto a nitrocellulose membrane before being blocked for unspecific binding with 5% nonfat dried milk. The membrane was then incubated overnight at 4°C with the primary antibody for IL-36R (1:200 dilution) followed by incubation with the secondary antibody conjugated to Alexa Fluor 488 (1:1000 dilution). After washing, protein bands were visualized using a fluorescence detection system (ChemiDoc, Bio-Rad) and MFI was determined.

**Flow cytometric analysis of endothelial and cardiomyocyte oxidative stress.** Harvested adult and aged hearts were manually minced, added to 0.1% collagenase, and rotated in an incubator at 37°C for 15 minutes. The supernatant was removed, and the digestion process was repeated 2 times. The pellet was then centrifuged at 10000 rpm at 4°C for 10 minutes in the presence of ACK and MACS buffer to lyse red blood cells and stop enzymatic activity, respectively. The pellet was added to 20 mL media and run several times through a 70  $\mu\text{m}$  strainer. Cells were then incubated with an anti-DNA/RNA damage antibody to detect oxidative damage (1:100 dilution, Abcam, clone 153A), anti-IL-36R antibody to detect IL-36R expression (R&D Systems, polyclonal; Alexa Fluor 647 secondary, BioLegend, polyclonal; both at 1:100 dilution), anti-CD31 antibody to label endothelial cells (1:100 dilution, BioLegend, clone 390), anti-cTnT antibody to label cardiomyocytes (1:100 dilution, Miltenyi Biotec, clone REA400), Zombie to detect dead cells (1:500 dilution, BioLegend), and appropriate IgG controls (polyclonal). Cells were then fixed using 4% formalin for 10 minutes and washed with Dulbecco's PBS. Acquisition of cells was performed using a CyAn ADP (Beckman Coulter), and data analysis was performed using Summit 4.3 software (Beckman Coulter). For each sample, 250,000 events were captured and used in the analysis.

**Endothelial cell IL-36R expression analysis in vitro.** Immortalized murine VCECs were grown to confluence and stimulated for 4 hours with experimental media (vehicle control); recombinant mouse IL-36 $\alpha$ ,  $\beta$ , or  $\gamma$  (3, 30, or 300 ng/mL; R&D Systems); or recombinant mouse TNF- $\alpha$  (3, 30, or 300 ng/mL; Boster Biological Technology). Cells were then formalin-fixed and incubated overnight with a primary antibody against IL-36R (1:100 dilution), followed by incubation with a secondary antibody (1:100 dilution) and Hoechst 33342 dye (Thermo Fisher Scientific). Images were captured using a multiphoton microscope and MFI was determined (ImageJ).

**Myocardial infarct size analysis.** The LAD artery was religated 4 hours after reperfusion, and 0.5% Evans blue dye (Sigma) was infused via the carotid cannula to identify the AAR. The mouse was then sacrificed, and the harvested heart was cut into sequential slices and incubated with TTC (Sigma). Sections were imaged using a stereomicroscope, and analysis was performed using ImageJ to quantitate the infarct size (TTC-negative white regions) as a percentage of the AAR (TTC-positive red regions/Evans blue-negative).

**Data availability.** The authors confirm that the data supporting the findings of this study are available within the article and its supplemental materials. Raw data supporting the findings of this study are available from the corresponding author, NK, on request.

**Statistics.** All statistical analysis was performed using GraphPad 7.0 software (GraphPad Software Inc.). Multiple comparisons between 3 or more groups were performed by 1-way ANOVA, followed by a Tukey's post hoc test. For experiments that followed a time course, the AUC was also calculated and used

for subsequent analysis as a summation of the entire period. All data are presented as mean  $\pm$  SEM with statistical significance defined when  $P < 0.05$ .

**Study approval.** Experiments were conducted on mice in accordance with the Animals (Scientific Procedures) Act of 1986 (Project licence P552D4447 from Home Office, London, United Kingdom).

### Author contributions

JEA acquired, analyzed, and interpreted the data; drafted the work; and approved the submitted version. DPJK analyzed and interpreted the data and approved the submitted version. MRR provided material and approved the submitted version. CJW provided materials and approved the submitted version. NED approved the submitted version. NK obtained the funding, designed the experiments, interpreted the data, drafted the work, and approved the submitted version. All authors agreed to be personally accountable for contributions and to ensure that questions related to the accuracy or integrity of any part of the work are appropriately investigated and resolved, with the resolution documented in the literature.

### Acknowledgments

This work was supported by the British Heart Foundation (FS/18/45/33862).

Address correspondence to: Neena Kalia, Microcirculation Research Group, Institute of Cardiovascular Sciences, College of Medical and Dental Sciences, University of Birmingham, Birmingham B15 2TT, United Kingdom. Phone: 44.0.121.414.8818; Email: n.kalia@bham.ac.uk.

- Kelly DJ, et al. Incidence and predictors of heart failure following percutaneous coronary intervention in ST-segment elevation myocardial infarction: the HORIZONS-AMI trial. *Am Heart J*. 2011;162(4):1626-1633.
- Hausenloy DJ, Yellon DM. Myocardial ischemia-reperfusion injury: a neglected therapeutic target. *J Clin Invest*. 2013;123(1):92-100.
- Camillet PG, Crea F. Coronary microvascular dysfunction. *N Engl J Med*. 2007;356(8):830-840.
- Chandrasekaran B, Kutubun AS. Myocardial infarction with angiographically normal coronary arteries. *J R Soc Med*. 2002;95(8):398-400.
- Odden MC, et al. The impact of the aging population on coronary heart disease in the United States. *Am J Med*. 2011;124(9):827-833.
- Lemeshy EJ, et al. Aging increases ischemia-reperfusion injury in the isolated, buffer-perfused heart. *J Lab Clin Med*. 1994;6(6):843-851.
- Mehta RH, et al. Acute myocardial infarction in the elderly: differences by age. *J Am Coll Cardiol*. 2001;38(3):736-741.
- Besse S, et al. Cardioprotection with cariporide, a sodium-proton exchanger inhibitor, after prolonged ischemia and reperfusion in senescent rats. *Exp Gerontol*. 2004;39(9):1307-1314.
- Van Den Munckhof, et al. Aging attenuates the protective effect of ischemic preconditioning against endothelial ischemia-reperfusion injury in humans. *Am J Physiol Heart Circ Physiol*. 2013;304(12):H1727-H1732.
- Franceschi C, et al. Inflamm-aging: An evolutionary perspective on immunosenescence. *Ann NY Acad Sci*. 2000;908:244-254.
- Shaw AC, et al. Aging of the innate immune system. *Curr Opin Immunol*. 2010;22(4):507-513.
- Sapey E, et al. Phosphoinositide 3-kinase inhibition restores neutrophil accuracy in the elderly: toward targeted treatments for immunosenescence. *Blood*. 2014;123(2):239-248.
- Nomellini V, et al. Dysregulation of neutrophil CXCR2 and pulmonary endothelial ICAM-1 promotes age-related pulmonary inflammation. *Aging Dis*. 2012;3(3):234-247.
- Akdis M, et al. Interleukins, from 1 to 37, and interferon- $\gamma$ : receptors, functions, and roles in diseases. *J Allergy Clin Immunol*. 2011;127(3):701-721.
- Ridker PM. From C reactive protein to Interleukin-6 to Interleukin-1: moving upstream to identify novel targets for atheroprotection. *Circ Res*. 2016;118(1):145-156.
- Marchant DJ, et al. Inflammation in myocardial diseases. *Circ Res*. 2012;111(1):126-144.
- Ridker PM, et al. Antiinflammatory therapy with canakinumab for atherosclerotic disease. *N Engl J Med*. 2017;377(12):1119-1131.
- Gresnigt MS, Van De Veenendaal FL. Biology of IL-36 cytokines and their role in disease. *Semin Immunol*. 2013;25(6):458-465.
- Cahay C, Towne JE. Regulation and function of interleukin-36 cytokines in homeostasis and pathological conditions. *J Leukoc Biol*. 2015;97(4):645-652.
- Ainscough JS, et al. Cathelicidin is the major activator of the psoriasis-associated proinflammatory cytokine IL-36 $\gamma$ . *Proc Natl Acad Sci U S A*. 2017;114(13):E2748-E2757.
- Hahn M, et al. The novel interleukin-1 cytokine family members in inflammatory diseases. *Curr Opin Rheumatol*. 2017;29(2):208-213.
- Johnston A, et al. IL-1 and IL-36 are dominant cytokines in generalized pustular psoriasis. *J Allergy Clin Immunol*. 2017;140(1):109-120.
- Martin U, et al. Externalization of the leaderless cytokine IL-1F6 occurs in response to lipopolysaccharide/ATP activation of transduced bone marrow macrophages. *J Immunol*. 2009;182(6):4021-4030.
- Kovach MA, et al. IL-36 $\gamma$  is secreted in microparticles and exosomes by lung macrophages in response to bacteria and bacterial components. *J Leukoc Biol*. 2016;100(2):413-421.

25. Towne JE, et al. Interleukin (IL)-1P6, IL-1P8, and IL-1P9 signal through IL-1Rrp2 and IL-1RAcP to activate the pathway leading to NF-kappaB and MAPKs. *J Biol Chem*. 2004;279(14):13677–13688.
26. Moss NC, et al. IKKbeta inhibition attenuates myocardial injury and dysfunction following acute ischemia-reperfusion injury. *Am J Physiol Heart Circ Physiol*. 2007;293(4):2248–2253.
27. Zeng M, et al. Suppression of NF-kB reduces myocardial no-reflow. *PLoS One*. 2012;7(10):e47306.
28. Kavanagh DPJ, et al. Imaging the injured beating heart intravitaly and the vasculoprotection afforded by haematopoietic stem cells. *Cardiovasc Res*. 2019;115(13):1918–1932.
29. Yi C, et al. Structural and functional attributes of the interleukin-36 receptor. *J Biol Chem*. 2016;291(32):16597–16609.
30. North BJ, Sinclair DA. The intersection between aging and cardiovascular disease. *Circ Res*. 2012;8(8):1097–1108.
31. Sanuki R, et al. Normal aging hyperactivates innate immunity and reduces the medical efficacy of minocycline in brain injury. *Brain Behav Immun*. 2019;80:427–438.
32. Boengler K, et al. Loss of cardioprotection with ageing. *Cardiovasc Res*. 2009;83(2):247–261.
33. Perskin MH, Cronstein BN. Age-related changes in neutrophil structure and function. *Mech Ageing Dev*. 1992;64(3):303–313.
34. Yousef H, et al. Aged blood impairs hippocampal neural precursor activity and activates microglia via brain endothelial cell VCAM1. *Nat Med*. 2019;25(6):988–1000.
35. Nogueira-Neto J, et al. Basal neutrophil function in human aging: implication in endothelial cell adhesion. *Cell Bio Int*. 2016;4(7):796–802.
36. Jin K. A microcirculatory theory of aging. *Ageing Dis*. 2019;10(3):676–683.
37. Van De Hoef TP, et al. Contribution of age-related microvascular dysfunction to abnormal coronary hemodynamics in patients with ischemic heart disease. *JACC Cardiovasc Interv*. 2020;13(1):20–29.
38. Worthen GS, et al. Mechanics of stimulated neutrophils: cell stiffening induces retention in capillaries. *Science*. 1989;245(4914):183–186.
39. Willems L, et al. Age-related changes in ischemic tolerance in male and female mouse hearts. *J Mol Cell Cardiol*. 2005;38(2):245–256.
40. Fulop T, et al. Cytokine receptor signalling and aging. *Mech Ageing Dev*. 2006;127(6):526–537.
41. Song Y, et al. Aging enhances the basal production of IL-6 and CCL2 in vascular smooth muscle cells. *Arterioscler Thromb Vasc Biol*. 2012;32(1):103–109.
42. Nishikawa H, et al. Knockout of the interleukin-36 receptor protects against renal ischemia-reperfusion injury by reduction of proinflammatory cytokines. *Kidney Int*. 2018;93(3):599–614.
43. Ramadas RA, et al. Interleukin-1 family member 9 stimulates chemokine production and neutrophil influx in mouse lungs. *Am J Respir Cell Mol Biol*. 2011;44(2):134–145.
44. Bridgwood C, et al. IL-36γ has proinflammatory effects on human endothelial cells. *Exp Dermatol*. 2017;26(5):402–408.
45. Takai T, et al. Interleukin-1 up-regulates transcription of its own receptor in a human fibroblast cell line TIG-1: role of endogenous PGE2 and cAMP. *Eur J Immunol*. 1992;22(5):1221–1227.
46. Matellaro K, Taylor WR. The role of the adventitia in vascular inflammation. *Cardiovasc Res*. 2007;75(4):640–648.
47. Koss CK, et al. IL-36 is a critical upstream amplifier of neutrophilic lung inflammation in mice. *Commun Biol*. 2021;4(1):172.
48. Butcher S, et al. Review article: ageing and the neutrophil: no appetite for killing? *Immunology*. 2000;100(4):411–416.
49. Roubenoff R, et al. Monocyte cytokine production in an elderly population: effect of age and inflammation. *J Gerontol A Biol Sci Med Sci*. 1998;53(1):M20–M26.
50. Cook-Mills JM, et al. Vascular cell adhesion molecule-1 expression and signaling during disease: regulation by reactive oxygen species and antioxidants. *Antioxid Redox Signal*. 2011;15(6):1607–1638.
51. Luo C, et al. Deficiency of interleukin-36 receptor protected cardiomyocytes from ischemia-reperfusion injury in cardiopulmonary bypass. *Med Sci Monit*. 2020;26:e918933.
52. Huang S, Frangogiannis NC. Anti-inflammatory therapies in myocardial infarction: failures, hopes and challenges. *Br J Pharmacol*. 2018;175(9):1377–1400.
53. O'Donoghue ML, et al. Effect of darapladib on major coronary events after an acute coronary syndrome: the SOLID-TIMI 52 randomized clinical trial. *JAMA*. 2014;312(10):1006–1015.
54. Kavanagh DPJ, et al. Tiffy: a quality-based frame selection tool for improving the output of unstable biomedical imaging. *PLoS One*. 2019;14(3):e0213162.